Journal of Inorganic & Nuclear Chemistry

VOLUME 22 1961

VOL.
22
1961

EDITORS

JOSEPH J. KATZ, Argonne · A. G. MADDOCK, Cambridge · L. E. J. ROBERTS, Harwell · E. J. W. VERWEY, Eindhoven

EDITORIAL ADVISORY BOARD

U.K. and Commonwealth: J. S. ANDERSON, F.R.S., Teddington · C. C. ADDISON, Nottingham · C. B. AMPHLETT, Harwell · F. M. BREWER, Oxford · G. E. COATES, Durham · J. F. DUNCAN, Melbourne · H. J. EMELÉUS, F.R.S., Cambridge · F. FAIRBROTHER, Manchester · J. H. GREEN, Kensington, N.S.W. · H. M. N. H. IRVING, Leeds · L. E. ORGEL, Cambridge · A. R. POWELL, F.R.S., Wembley · P. L. ROBINSON, Newcastle-upon-Tyne · R. SPENCE, Harwell · H. G. THODE, F.R.S., Hamilton · L. YAFFE, Montreal

U.S.A.: L. F. AUDRIETH and JOHN C. BAILAR JR., Univ. of Illinois · F. BASOLO, Northwestern Univ. · E. O. BRIMM, Linde Air Products · HERBERT C. BROWN, Purdue · ANTON B. BURG, Univ. South Calif. · CHARLES D. CORYELL, M.I.T. · R. W. DODSON, Brookhaven · W. CONARD FERNELIUS, Koppers Company, Penn. · WARREN C. JOHNSON, Chicago · H. B. JONASSEN, Tulane Univ. · JACOB KLEINBERG, Univ. of Kansas · K. A. KRAUS, Oak Ridge · W. F. LIBBY, Los Angeles · W. M. MANNING, Argonne · THERALD MOELLER, Univ. of Illinois · EARL L. MUETTERTIES, Wilmington, Delaware · EUGENE G. ROCHOW, Harvard · GLENN T. SEABORG, Univ. of California · P. W. SELWOOD, Evanston · F. H. SPEDDING, Ames · R. W. STOUGHTON, Oak Ridge · J. R. VAN WAZER, Missouri · DON M. YOST, Pasadena, Calif. · W. H. ZACHARIASEN, Chicago · R. A. PENNEMAN and B. B. CUNNINGHAM, Univ. of California · H. TAUBE, Chicago

Austria: E. BRODA, Vienna · BERTHA KARLIK, Vienna · V. GUTMANN, Vienna
Denmark: J. BJERRUM, Copenhagen
France: J. BÉNARD, Paris · J. CHÉDIN, Paris · J. GUÉRON, Paris · M. MAGAT, Paris
Germany: W. HIEBER, Munich · G. JANDER, Berlin · A. MUENSTER, Frankfurt
Netherlands: A. E. VAN ARKEL, Leiden · A. H. W. ATEN JR., Amsterdam · J. H. DE BOER, Geleen · J. H. VAN SANTEN, Eindhoven
Israel: M. BOBTELSKY, Jerusalem · *Italy:* V. CAGLIOTI, Rome
Norway: H. HARALDSEN, Oslo · ODD HASSEL, Oslo
Persia: H. A. C. McKAY, Tehran
Sweden: G. HÄGG, Uppsala · L. G. SILLÉN, Stockholm
Switzerland: G. SCHWARZENBACH, Zürich

Copyright © 1961 Pergamon Press Ltd.

PERGAMON PRESS OXFORD · LONDON · NEW YORK · PARIS

JOURNAL OF INORGANIC AND NUCLEAR CHEMISTRY

Editors:

JOSEPH J. KATZ: *Argonne National Laboratory, 9700 South Cass Avenue, Argonne, Illinois, U.S.A.*
A. G. MADDOCK: *University Chemical Laboratory, Lensfield Road, Cambridge, England*
L. E. J. ROBERTS: *Atomic Energy Research Establishment, Harwell, Didcot, Berks, England*
E. J. W. VERWEY: *Philips Research Laboratories, Eindhoven, The Netherlands*

NOTES FOR CONTRIBUTORS

I. General

1. Papers should, in general, be concerned with original work in the field of inorganic and nuclear chemistry. They should be submitted to the Editors, Dr. A. G. MADDOCK, Dr. L. E. J. ROBERTS, or Dr. J. J. KATZ, or, in the case of papers not in the English language, to Dr. E. J. W. VERWEY. The addresses are given above.

2. Fifty free reprints of each paper are supplied. Additional copies can be supplied at a reasonable cost if ordered at the time when the first proofs are returned. A reprint order form will accompany proofs.

II. Script Requirements

1. Scripts should be submitted in duplicate. They must be typewritten, and double-spaced. Authors are requested to make clear any Greek characters which may be confused with ordinary letters or with other characters. Authors will receive proofs for correction when their contribution is first set, but there is rarely time for page proofs also to be sent for checking. This will be done, however, where the amount of alteration makes it advisable.

2. Illustrations should be placed at the end of the manuscript, and legends should be typed on a separate sheet. It is requested that photographs should be kept to the minimum necessary. Line drawings or good photo-prints may be provided. Line drawings must include all relevant details: if they are already well drawn it may be possible to reproduce them direct from the original. It is not possible to reproduce from "dye-line" prints, or from prints with weak lines. Illustrations for reproduction should normally be about twice the final size required. Any lettering on diagrams—other than Greek letters, symbols, etc.—should be stencilled and should be sufficiently large and bold to permit reproduction when the diagram has been reduced to a size suitable for inclusion in the journal.

3. References should be clearly indicated in the text by superior numbers. Full references should be given in numbered footnotes containing author's name, initials, title of paper (where desired), abbreviated title of journal, year, volume number, and page number.

4. The text of articles submitted must be concise and in a readily understandable style. The technical description of the methods used should only be given in detail when such methods are new. The essential contents of each paper should be briefly recapitulated in an abstract. French and German papers should be submitted with English abstracts. **Four copies of the English abstracts are required with all papers, including those in the English language.**

5. To conserve space, authors are requested to mark less important portions of the paper (such as description of methods, record of experimental results, etc.) for printing in smaller type.

PERGAMON PRESS LTD.

HEADINGTON HILL HALL, OXFORD 122 EAST 55TH STREET, NEW YORK 22, N.Y

LIST OF CONTENTS

VOL.
22
1961

NUMBERS 1/2

D. G. VALLIS and J. L. PERKIN: Yttrium-96 and strontium-93: new nuclear data . . . 1
J. H. WOLFE and J. P. HUMMEL: Decay properties of the ^{117}In isomers 7
W. D. JOHNSTON: Crystal structures in the $OsTe_{2-x}Sb_x$ system 13
K. MOEDRITZER: The structure of dialkyl and diaryl phosphonates 19
A. V. GROSSE: The temperature range of liquid metals and an estimate of their critical constants 23
A. D. KIRSHENBAUM, J. A. CAHILL and A. V. GROSSE: The density of liquid lead from the melting point to the normal boiling point 33
A. GLASNER and M. STEINBERG: Thermal decomposition of the light rare earth oxalates . 39
G. W. WATT and W. A. BAKER JR.: The reduction of zirconium(IV) iodide 49
R. H. LINNELL: Kinetics of precipitation of aluminium 8-quinolinolate from basic aluminium chloride 55
G. E. COATES and C. PARKIN: Ethynyl-copper(I) complexes with tertiary phosphines . . 59
R. G. CHARLES and S. BARNARTT: Reactions of decammino-μ-peroxo-dicobalt(III) sulphate with aqueous sulphuric acid 69
W. W. WENDLANDT and J. L. BEAR: The thermal deaquation of some aquopentammine-chromium(III) complexes 77
D. P. GRADDON: The absorption spectra of complex salts—V. Structures of copper(II) N:aryl-glycinates 85
G. R. CHOPPIN and J. A. CHOPOORIAN: Complexes of the lanthanide elements with α-hydroxy carboxylate ligands 97
W. L. MARSHALL and J. S. GILL: Aqueous systems at high temperature—III. Investigations on the system UO_3–CuO–NiO–SO_3–H_2O at 300°C 115
T. C. ICHNIOWSKI and A. F. CLIFFORD: A polarographic study of chromium(III) in ammonia solvents (Divers' liquids) 133
Y. MARCUS and I. ABRAHAMER: Anion exchange of metal complexes—VII. The lanthanides-nitrate system 141
Notes:
D. COHEN and L. B. TAYLOR: Some Observation of Np(VI) in chloride solutions . . 151
C. EDEN, H. FEILCHENFELD and D. ZEHAVI: The reduction of titanium tetrachloride by sodium dispersed on alumina 153
E. M. MAGEE: The product of reaction of BF_3 with B_2O_3 155
A. GLASNER and M. STEINBERG: The thermal decomposition of erbium and lutetium oxalates 156

NUMBERS 3/4

U. L. VALLINDER and A. C. PAPPAS: The mass distribution in fission of lead induced by 54 MeV protons 161
I. MÁDI: Absonderung radioaktiver Atomarten in trägerfreiem Zustande mit Hilfe eine elektrochromatographischen Verfahrens. 169
D. W. BARUM: Electronic absorption spectra of acetylacetonato complexes—II. Hückel LACO-MO calculations for complexes with trivalent transition metal ions 183
N. A. DAUGHERTY and C. H. BRUBAKER, JR: The complexes of some 5-substituted tetrazoles with nickel(II) 193
K. JOHN and T. MOELLER: Phosphonitrilic bromides 199
D. B. SOWERBY: The preparation and properties of some inorganic isothiocyanates . . 205
L. E. J. ROBERTS and A. J. WALTER: Equilibrium pressures and phase relations in the uranium oxide system 213
M. W. NATHANS: A differential thermal analysis study of the rare earth ethyl sulphates . . 231
BADAR-UD-DIN and J. C. BAILAR, JR: Observations on the oxidation and reduction of platinum(II) nitro complexes 241
J. KRTIL: Exchange properties of ammonium salts of 12-heteropolyacids—III. The sorption of strontium and yttrium on ammonium phosphotungstate and their separation from caesium 247
C. HEITNER-WIRGUIN and J. KENDY: An ion exchange study of copper pyro-phosphate complexes in solution 253

G. H. NANCOLLAS and R. PATTERSON: The kinetics of ion exchange on zirconium phosphate and hydrated thoria 259
J. KENNEDY, J. MARRIOT and V. J. WHEELER: The adsorption of monovalent and divalent cations by diallyl phosphate and styrene methylene phosphonate polymers 269
I. V. NELSON, R. C. LARSON and R. T. IWAMOTO: Polarographic evidence for the stability of copper(I) ion in some non-complexing nonaqueous solvents 279
J. R. FERRARO, G. W. MASON and D. F. PEPPARD: Molecular weight studies of several organophosphorus acids 285
M. M. MARKOWITZ, R. K. HARRIS and W. N. HAWLEY: Liquidus relations in the system lithium metaphosphate-lithium pyrophosphate 293
K. MOEDRITZER and R. R. IRANI: Synthesis and properties of mono- and poly-methylenediphosphonic acids and esters 297
W. Z. HELDT: Reactions of co-ordinated ligands—II. Preparation of a new class of iron isonitrile complexes, $(RCH_2NC)_5Fe^{II}CNX$ 305

AUTHOR INDEX

ABRAHAMER, I. p. 141
BADAR-UD-DIN. p. 241
BAILAR, J. C., JR. p. 241
BAKER, W. A., JR. p. 49
BARNARTT, S. p. 69
BARNUM, D. W. p. 193
BEAR, J. L. p. 77
BRUBAKER, C. H., JR. p. 193
CAHILL, J. A. p. 33
CHARLES, R. G. p. 69
CHOPOORIAN, J. A. p. 97
CHOPPIN, G. R. p. 97
CLIFFORD, A. F. p. 133
COATES, G. E. p. 59
COHEN, D. p. 151
DAUGHERTY, N. A. p. 193
EDEN, C. p. 153
FEILCHENFELD, H. p. 153
FERRARO, J. R. p. 285
GILL, J. S. p. 115
GLASNER, A. p. 39, 156
GRADDON, D. P. p. 85
GROSSE, A. V. pp. 23, 33
HARRIS, R. F. p. 293
HAWLEY, W. N. p. 293
HEITNER-WIRGUIN, C. p. 253
HELDT, W. Z. p. 305
HUMMEL, J. P. p. 7
ICHNIOWSKI, T. C. p. 133
IRANI, R. R. p. 297
IWAMOTO, R. T. p. 279
JOHN, K. p. 199
JOHNSTON, W. D. p. 13
KENDY, J. p. 253
KENNEDY, J. p. 269
KIRSHENBAUM, A. D. p. 33
KRTIL, J. p. 247
LARSON, R. C. p. 279
LINNELL, R. H. p. 55
MÁDI, I. p. 169
MAGEE, E. M. p. 155
MARCUS, Y. p. 141
MARKOWITZ, M. M. p. 293
MARRIOT, J. p. 259
MARSHALL, W. L. p. 115
MASON, G. W. p. 285
MOEDRITZER, K. pp. 19, 297
MOELLER, T. p. 199
NANCOLLAS, G. H. p. 259
NATHANS, M. W. p. 231
NELSON, I. V. p. 279
PAPPAS, A. C. p. 161
PARKIN, C. p. 59
PATTERSON, R. p. 259
PEPPARD, D. F. p. 285
PERKIN, J. L. p. 1.
ROBERTS, L. E. J. p. 213
SOWERBY, D. B. p. 205
STEINBERG, M. pp. 139, 156
TAYLOR, B. p. 151
VALLINDER, U. L. p. 161
VALLIS, D. G. p. 1
WALTER, A. J. p. 213
WATT, G. W. p. 49
WENDLANDT, W. W. p. 77
WHEELER, V. J. p. 269
WOLFE, J. H. p. 7.
ZEHAVI, D. p. 153

J. Inorg. Nucl. Chem., 1961, Vol. 22, pp. 1 to 5. Pergamon Press Ltd. Printed in Northern Ireland

YTTRIUM-96 AND STRONTIUM-93: NEW NUCLEAR DATA

D. G. VALLIS and J. L. PERKIN
Atomic Weapons Research Establishment, Aldermaston, Berks.

(*Received* 8 *February* 1961)

Abstract—Targets of ^{96}Zr have been irradiated with 14·5 MeV neutrons and the decay of the resultant β-particle and γ-ray activity has been found to have two components with half-lives of 2·3 and 8·3 min. Only the shorter lived component was present in yttrium fractions chemically separated from the targets. This activity has been assigned to the previously unreported isotope ^{96}Y produced by the reaction ^{96}Zr $(n,p)^{96}$Y. The longer-lived component was due to the (n,a) product ^{93}Sr whose half-life has been reported previously. Other details are as follows:

^{96}Y: $T_{\frac{1}{2}}$ 2·3 ± 0·1 min; $E\beta$ max 3·5 MeV; $E\gamma$ 0–2·5 MeV, resolved peaks at 0·7 and 1·0 MeV.
^{93}Sr: $T_{\frac{1}{2}}$ 8·3 ± 0·5 min; $E\beta$ max 2·0 MeV; $E\gamma$ 0–2 MeV, resolved peaks at 0·6 and 2·0 MeV.

The short-lived ^{96}Y was chemically separated from other activation products using an automatically controlled centrifuge. As the apparatus has some novel features and may be employed for other rapid chemical separations, it is described in detail.

VOL. 22 1961

THERE does not appear to be any published data concerning the decay of ^{96}Y and only the half-life of ^{93}Sr has been reported previously. In the present work these two nuclides were made by irradiating zirconium with 14·5 MeV neutrons, the reactions being ^{96}Zr$(n,p)^{96}$Y and ^{96}Zr$(n,\alpha)^{93}$Sr. In order to identify ^{96}Y, a fast chemical separation was carried out using apparatus which is described in some detail as it is of more general interest.

Neutron irradiation and counting

Samples containing about 5 mg of enriched ^{96}Zr,* having the following isotopic composition: ^{90}Zr, 3·22; ^{91}Zr, 0·94; ^{92}Zr, 1·79; ^{94}Zr 4·66; ^{96}Zr, 89·4%; were irradiated in a 14·5 MeV neutron flux of about 2×10^9 sec^{-1} cm^{-2}. These neutrons were produced by bombarding a zirconium tritide target with 300 keV deuterons accelerated by the Aldermaston 3MV Van de Graaff.

When a chemical separation of yttrium was to be performed the zirconium was irradiated in a nitric acid solution in a shallow cylindrical cavity (16 mm × 1·5 mm) in a thin-walled Perspex cell. At other times targets of the enriched zirconium and of natural zirconium were irradiated as the oxide and counted without prior chemical treatment. These targets had been chemically purified before irradiation by the method described later to prevent activation of impurity elements.

The γ-rays from the reaction products were detected with a cylindrical sodium iodide crystal (5·7 cm × 5·7 cm). β-particles were detected with a plastic scintillator (Pamelon, supplied by Isotopes Development Limited) of similar size. In addition to counting the total number of pulses from these detectors, the pulse height distributions were recorded every few minutes on a 100-channel analyser. The data from the analyser were printed out automatically.

When no chemical separations were performed on the irradiated zirconium samples, these were transferred manually to the detectors. When yttrium was separated from the enriched zirconium, it was transferred automatically as a solution by suction via a 12 ft length of 1 mm bore plastic tubing to a 3 ml capacity thin walled Perspex cell in contact with the detectors. Several feet of concrete shielding was used to prevent high counter backgrounds due to neutron activation.

* Obtained from A.E.R.E. Harwell, Berks.

1

Chemical procedure

The enriched zirconium sample was originally 99 per cent pure, the impurities, shown by spectrochemical analysis, being mainly antimony (0·4 per cent) and silicon (0·3 per cent). The sample was purified by absorbing the zirconium from 10 M HCl solution on an 80 × 5 mm column of Amberlite CG 400 anion-exchange resin. After washing the column with 10 ml of 10 M HCl the zirconium was eluted with 10 ml of an 0·5 HF–4 M HCl mixture. The distribution coefficients for Sb(III) and Sb(V) for this eluting medium and this resin are about 100 so that antimony was retained by the column. The solution was collected in a platinum dish and, to ensure the removal of silica, twice evaporated nearly to dryness after the addition of a few drops of 70 per cent perchloric acid. The residue was dissolved in 6 M HNO_3 and zirconium hydroxide was precipitated by bubbling ammonia gas through the solution. After the precipitate had been centrifuged and washed with water, it was re-dissolved in 6 M HNO_3. A chemical treatment similar to the above was used to recover the enriched ^{96}Zr after each neutron irradiation.

Immediately at the end of an irradiation, usually of 3 min duration, the irradiated zirconium solution was transferred pneumatically to an apparatus which performed automatically, and to a preset schedule, a fast separation of yttrium activity. The irradiated solution was first added to 2 mg of yttrium carrier and 50 μg of strontium carrier dissolved in 0·5 ml of 6 M HNO_3 contained in the centrifuge cup of the automatic chemistry apparatus described later. 1 ml of 12% NH_4F solution was added with vigorous stirring and yttrium fluoride precipitated. The supernatant liquid containing zirconium was centrifuged out of this vessel and, with continued centrifuging, the yttrium fluoride precipitate was washed first with 2 ml of 0·5% NH_4F solution and then with three successive 2 ml amounts of water. As the solubility of strontium fluoride in water is 100 μg/ml, this washing leached out nearly all the strontium carrier and accompanying ^{91}Sr and ^{93}Sr produced by Zr (n,α) reactions. The washes also removed 7·4 sec ^{16}N formed by the irradiation of oxygen in water and nitric acid with 14 MeV neutrons. The yttrium fluoride was then quickly re-dissolved, with vigorous stirring, in 3 ml of a 1:1 concentrated HCl–saturated HBO_3 solution and transferred to the counting cell. The total time required for these operations from the end of the irradiation to the commencement of counting was 40 sec.

Chemical separation apparatus

The basic part, the centrifuge cup, shown in Fig. 1 consists of a thistle-shaped Pyrex glass vessel (A) in the upper, open end of which is sealed an annular 3 cm o.d. filter of sintered glass (B). The vessel is supported in the chuck (*C*) of an inverted electric stirrer motor. Another similar motor (not shown in the diagram) is placed above the centrifuge cup, its stirring rod (*D*) entering the cup through the stainless steel tube-guide (*E*) and the hole in the sintered glass filter. The cup is surrounded by a spray receiver (*F*) also made of Pyrex which collects the liquid flung from the periphery of the sintered-glass filter. Seven polythene tubes of 1 mm bore are held in position by the tube-guide clamped centrally in the opening in the sintered glass to give clearance for rotation of the centrifuge cup. One of these tubes is used to deliver the irradiated liquid to the cup and is therefore connected to the irradiation cell. Five other tubes are each connected to separate 5 ml capacity reagent reservoirs. The seventh tube reaches the bottom of the cup and is used for transferring, by suction, liquid from the cup to the counting cell which in turn connected to a vacuum pump. Alternatively, in other applications of the apparatus, liquid may be removed from the spray receiver by applying suction to the side-arm (*H*). The irradiation cell and the reagent reservoirs are each connected in turn to a magnetically-operated compressed air valve, a pressure gauge, a needle valve and a common compressed air supply.

The combined effect of centrifugation and filtration obtained when the centrifuge cup spins at a speed of up to 5000 rev/min permits extremely fast separation of liquid and solid phases. The solid phase, trapped behind the sintered glass, may be re-dissolved, as in the case of the Zr/Y separation described above, by nearly filling the stationary cup with a suitable solvent and stirring vigorously.

It is of interest to note here that the scope of chemical separations which this apparatus will perform has been considerably extended by its use for the separation of immiscible aqueous and organic phases*. Above 800 rev/min, pure aqueous or pure organic liquid leave the centrifuge. When both are present the water leaves the centrifuge as before, but the organic solvent does not break through the surface tension 'barrier' of the residual water in the sintered glass until about 3000 rev/min

* Patent Applied for. U.K. Patent Application No. 42279/60.

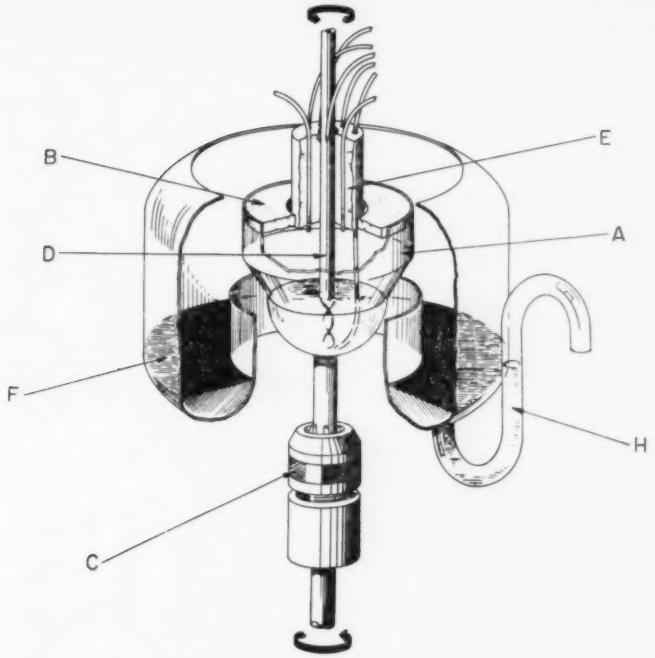

FIG. 1.—Apparatus for fast chemical separation.

is reached. If the sintered glass is treated with a 25 per cent solution of dimethyl-dichlorosilane in CCl_4, and subsequently dried at 100°C, its water-repellent behaviour then permits the opposite phenomenon, i.e. organic solvent will leave the cup at speeds greater than 800 rev/min, whereas aqueous solution is not ejected below about 3000 rev/min. In both cases, satisfactory separations can be obtained when the two phases are intimately dispersed prior to the acceleration of the cup from rest.

The speeds quoted above vary slightly according to the aqueous solution and organic solvent used but there is always a wide range of speed in which quantitative separation is possible. Using this phenomenon, single-step separations by specific solvent extraction procedures may be carried out automatically in less than 1 min.

Each part of the apparatus (motors, vacuum pump and magnetic valves) is controlled by two relays. The timing of operation of these parts is obtained by energizing these relays by means of a uniselector. The time for one complete revolution of the wiper-arm of the uniselector can be varied to suit the overall time required for chemical separation. The timing, sequence and repetition of the operation of each part of the apparatus is determined simply by the order and spacing of the connexions of the relays around the contact bank of the uniselector.

RESULTS

Decay curves for the β-particle activity observed are shown in Fig. 2. Similar curves were obtained for the γ-ray activity. The chemically separated 2·3 min yttrium activity can be assigned to ^{96}Y for the following reasons. Firstly, all the other yttrium isotopes that could be formed by reactions with 14·5 MeV neutrons and any zirconium isotopes have known half-lives quite different from that found. Secondly, by irradiating a sample of natural zirconium and comparing the activity observed with that for the enriched sample, it was found that the yield of the 2·3 min activity was proportional to the abundance of ^{96}Zr present. This activity can therefore be assigned to the ^{96}Zr(n,p) product: ^{96}Y.

VOL. 22 1961

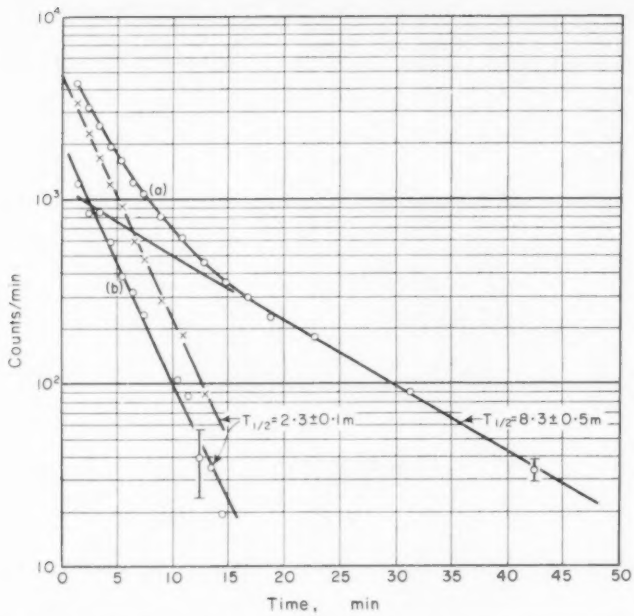

FIG. 2.—Beta particle decay of a sample of ^{96}Zr after a 3 min irradiation with 14·5 MeV neutrons. (a) total decay curve and its resolved 2·3 min activity (points denoted by crosses), (b) decay of chemically separated yttrium activity.

COCHRAN and REED[1] have measured the (n,p) cross-sections at 14·1 MeV for the zirconium isotopes with mass numbers 90, 91, 92 and 94. These cross-sections lie on a smooth curve when plotted against the mass number. The extrapolated value of this curve for the ^{96}Zr$(n,p)^{96}$Y reaction is about 5–10 mbarns. This is in fair agreement with the value of 13 $\pm$ 4 mbarns found for this cross-section in the present work. The method used was to compare the ^{96}Y activity produced by neutron irradiation with that of ^{27}Mg from the ^{27}Al$(n,p)^{27}$Mg reaction in an aluminium foil irradiated in the same neutron flux. The value of 70 $\pm$ 10 mbarns for ^{27}Al$(n,p)^{27}$Mg reaction cross-section at 14·5 MeV was taken from the work of MANI *et al.*[2]

The 8·3 min activity was not observed in the chemically separated yttrium activity and must therefore be due to a zirconium isotope produced by an $(n,2n)$, $(n,3n)$ or (n,γ) reaction or a strontium isotope produced by an (n,α) reaction. From the published nuclear data this activity can be assigned to ^{93}Sr the half-life of which has been previously quoted[3] to be 8 min.

The β-particle spectra observed had well defined high energy end-points at 3·5 MeV for the 2·3 min activity and 2·0 MeV for 8·3 min activity. A detailed analysis of the spectra was not made as the thickness of the final sources for counting was sufficient to distort the spectrum below about 1 MeV.

Gamma ray spectra from the decay of ^{96}Y and ^{93}Sr are shown in Fig. 3. The spectrum for ^{93}Sr was obtained from an enriched ^{96}Zr sample on which no chemical

[1] D. R. F. COCHRAN and C. H. REED, Los Alomos Scientific Laboratory. Private communication. To be published.
[2] G. S. MANI, G. J. MCCALLUM and A. T. G. FERGUSON. *Nucl. Phys.* **30**, 535 (1960).
[3] D. STROMINGER, J. M. HOLLANDER and G. T. SEABORG, *Rev. Mod. Phys.* **30**, (part 2), 660 (1958).

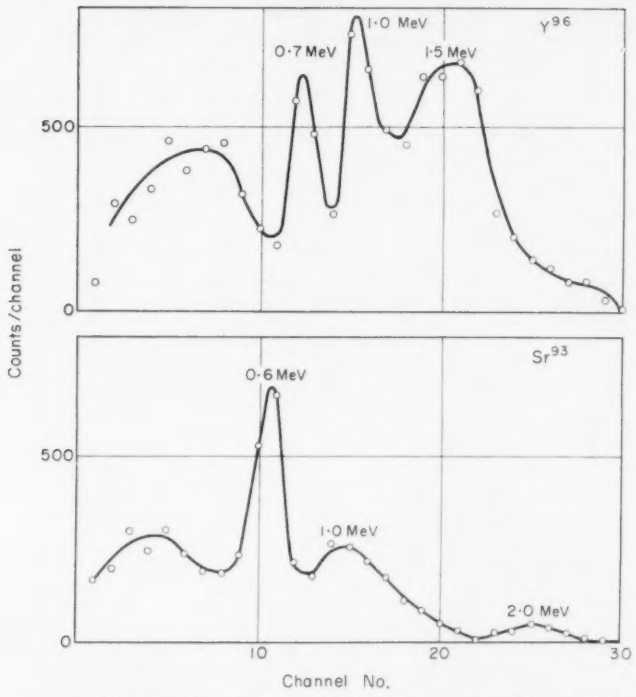

FIG. 3.—Sodium iodide γ-ray pulse height spectra from the decay of ^{96}Y and ^{93}Sr.

separations had been performed and after sufficient time had elapsed for the ^{96}Y formed to have decayed. The ^{96}Y spectrum was obtained with the same sample by subtracting the ^{93}Sr spectrum from that observed immediately after the neutron irradiation. The statistical accuracy of the spectrum obtained by this indirect method was greater than that measured directly from the chemically separated yttrium activity because of the rather low yields in these experiments.

The data obtained may be summarized as follows:

^{96}Y: $T_{\frac{1}{2}}$ 2·3 $\pm$ 0·1 min; $E\beta$ max 3·5: $E\gamma$ complex 0–2·5 MeV resolved peaks at 0·7 and 1·0 MeV.

^{93}Sr: $T_{\frac{1}{2}}$ 8·3 $\pm$ 0·5 min; $E\beta$ max 2·0 MeV: $E\gamma$ complex 0–2·0 MeV resolved peaks at 0·6 and 2·0 MeV.

VOL. 22 1961

J. Inorg. Nucl. Chem., 1961, Vol. 22, pp. 7 to 11. Pergamon Press Ltd. Printed in Northern Ireland

DECAY PROPERTIES OF THE ^{117}In ISOMERS*

J. H. WOLFE and J. P. HUMMEL
Department of Chemistry and Chemical Engineering and Department of Physics,
University of Illinois, Urbana, Illinois

(*Received* 2 *March* 1961; *in revised form* 8 *May* 1961)

Abstract—Samples of $^{117-117m}$In were produced by the ^{121}Sb(γ,α) reaction and studied by gamma ray spectroscopy techniques. The analysis of the decay curves for the various photopeaks gives a 1·9 ± 0·1 hr half-life for ^{117m}In which agrees with the previous value and 43 ± 4 min for ^{117}In which is shorter than the previous value. An analysis of the intensities of the γ-rays gives the following intensities for the various decay branches in ^{117m}In: 28% 311 keV isomeric transition, 21% 1·616 meV β-transition, and 51% 1·772 meV β-transition. This gives slightly more isomeric transition than previously reported.

VOL. 22 1961

THIS paper reports the results of some recent scintillation spectroscopy studies on the decay of the ^{117}In isomers. This has lead to some modifications of the decay schemes for ^{117}In and ^{117m}In that were proposed by MCGINNIS[1] in 1955. (MCGINNIS' decay schemes are shown in Fig. 1.) The modifications are not extensive enough to require changes in the previous spin assignments for the various nuclear levels involved. However, they are serious enough to significantly affect any experimental determination of the relative numbers of the ^{117}In and ^{117m}In nuclei present in a sample when the determination is made by beta or gamma ray counting. Since the ^{117}In isomers are convenient products for the study of the relative rates of production of different spin states (determination of the so-called isomer ratio) in several different nuclear reactions, we consider it important to report these decay scheme modifications. The important changes involve a new value for the half-life of ^{117}In and new values for the branching ratios in the decay of ^{117m}In.

The $^{117-117m}$In samples for the present study were produced by irradiating solutions of antimony trichloride for 90 min in the external bremsstrahlung beam of the University of Illinois 22 MeV betatron. The $^{117-117m}$In was produced by the ^{121}Sb (γ, α) reaction. This reaction and the ^{123}Sb(γ,α)$^{119-119m}$In reaction are expected to be the only important reactions that produce indium isotopes with the bremsstrahlung energies available with the 22 MeV betatron. Since the half-lives and decay properties of the ^{119}In isomers are quite different from those of the ^{117}In isomers,[2] the presence of the $^{119-119m}$In does not interfere with the study of the ^{117}In isomers. After the addition of indium carrier, an indium fraction was chemically separated by precipitating the indium with 8-hydroxyquinoline from a basic solution after the antimony had been precipitated as antimony oxychloride from a neutral solution.†

* The work was supported by the Office of Naval Research.

† The pH adjustment that allows the complete precipitation of antimony as the oxychloride without the precipitation of the indium-8-hydroxyquinolate complex was achieved by using the yellow colour of the indium complex as an indicator. The pH was adjusted to a point just prior to that at which the indium complex precipitates, and the antimony oxychloride was removed. Then ammonium hydroxide was added, and the indium complex precipitated.

[1] C. L. MCGINNIS, *Phys. Rev.* **97**, 93 (1955).
[2] D. STROMINGER, J. HOLLANDER and G. T. SEABORG, *Revs. Modern Phys*, **30**, 585 (1958).

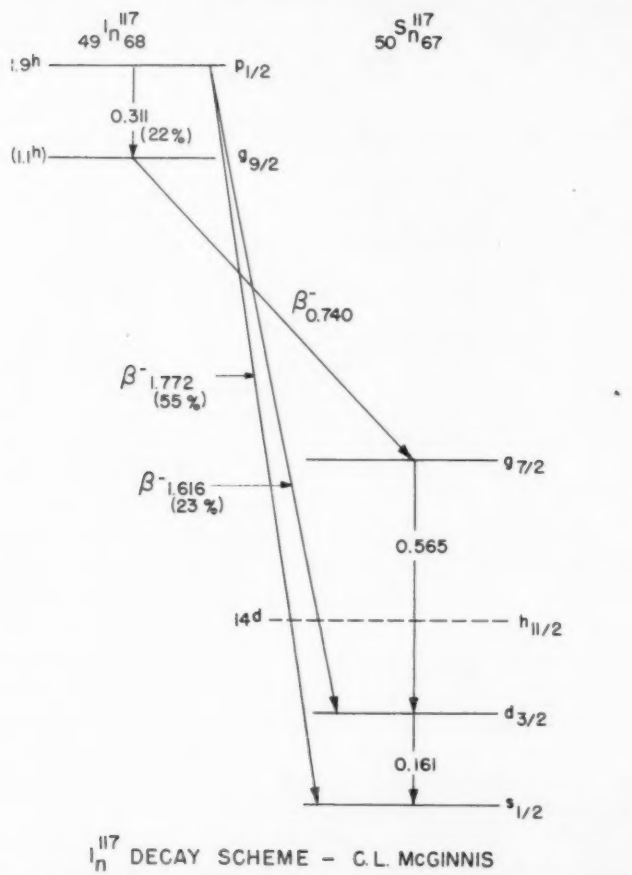

FIG. 1.—$^{117-117m}$In decay scheme reported by MCGINNIS (reference 1). The items in parentheses (the ground state half-life and the branching intensities in the decay of the isomer) are those quantities for which new values are proposed as a result of the present study. Our proposed new values are 43 min for the ground state half-life, 28 per cent for the intensity of the isomeric transition, 51 per cent for the intensity of the 1·772 MeV β-transition, and 21 per cent for the intensity of the 1·616-MeV beta transition.

The chemical separation and mounting of the sample for counting generally required about one hour.

The γ-ray spectra of the indium samples were then studied with a scintillation spectrometer system incorporating a $1\frac{1}{2}$ in. diameter by $1\frac{1}{2}$ in. long NaI(Tl) crystal and a 100-channel pulse-height analyser. Two different counting procedures were followed. For studies of the half-lives involved, short counts of 5–15 min duration were taken over times of up to 14 hr. For studies of the γ-ray intensities, three long counts, each of 55 min duration were made on each sample.

A typical γ-ray spectrum is shown in Fig. 2. The energies of the various photopeaks were determined by calibrating the 100-channel analyser with several known γ-rays. The energies agree well with those reported by MCGINNIS. The origin of the various γ-rays can be seen by referring to MCGINNIS' decay scheme in Fig. 1. The 161 keV peak arises from both ground state and isomer decay; the 311 keV peak is due only to

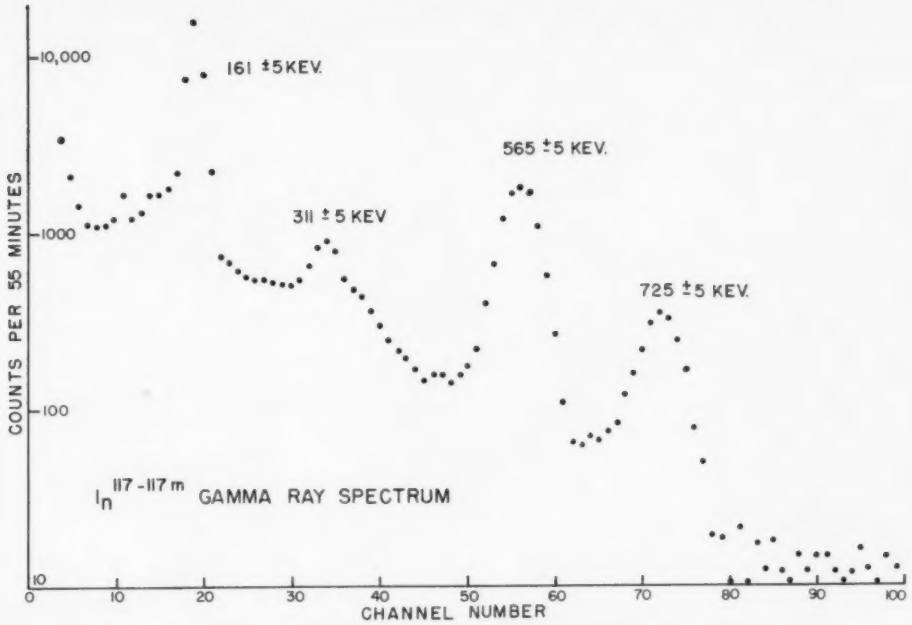

FIG. 2.—Typical γ-ray spectrum of $^{117-117m}$In.

the isomer decay; the 565 keV peak is due only to the ground state decay; and the 725 keV peak is due to coincidence summing of 161 keV and 565 keV photons in the ground-state decay.

A decay curve for the 161-keV photopeak is shown in Fig. 3. It is seen that the decay curve is complex and can be resolved into two components. The 565 keV photopeak decay showed the same complexity. Least squares analyses were made on the 161 and 565 keV photopeak decay curves for two samples. These gave 1·9 $\pm$ 0·1 hr and 43 $\pm$ 4 min for the half-lives of the two components. The decay of the 311 keV photopeak showed only a 1·9 hr component. The 725 keV peak decay was complex, showing both 1·9 hr and 43 min components. The value of 1·9 hr agrees with that reported by McGINNIS for the half-life of ^{117m}In. However, the value of 43 min is significantly shorter than the 1·1 hr value reported by McGINNIS for the ground state half-life. His ground state half-life was determined by following the decay of the 161 and 565 keV photopeaks in a sample prepared by separating ^{117}In that had grown into ^{117}Cd. Any branching to the isomer could have distorted his decay curve and lead to a higher value for the half-life. DUDEY and SUGIHARA[3] have recently repeated McGINNIS' experiment. They found a significant 1·93 hr component by following the decay for longer periods. After subtracting the 1·93 hr component, they obtained a value of 38·0 $\pm$ 1·3 min for the ground state half-life. This ground state half-life is slightly shorter than our result, but the two values are not considered to be in disagreement with each other.

The relative intensities of the various branches in the decay of ^{117m}In can be deduced from our observed γ-ray intensities providing that we use some of the results

[3] N. D. DUDEY and T. T. SUGIHARA. Private communication (1961).

VOL. 22 1961

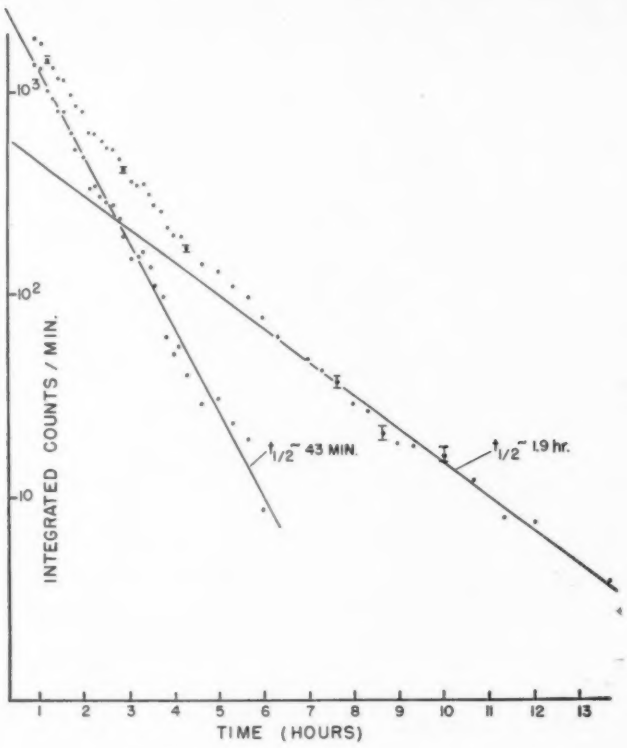

FIG. 3.—Decay curve for the 161 keV photopeak.

of MCGINNIS' magnetic lens β-spectroscopy studies. The results that we adopt are only those that were determined directly from the β-spectrum and did not involve any assumption about the half-lives involved. These are the ratio of the 1·616 and 1·772 MeV β-transitions in the decay of the isomer and the conversion coefficients of the 161 and 565 keV γ-rays. The analysis proceeds as follows. The number of 565 keV transitions observed in any two counts on a sample can be used along with standard decay and growth equations to determine the number of ground state nuclei present at the end of the irradiation and k times the number of isomer nuclei present at the end of the irradiation where k is the fraction of isomer decays that proceeds by the isomeric transition to the ground state. This then allows the calculation of the number of isomeric transitions (311 keV transitions) that occurred during any one count on the sample. Next, we note that the number of 565 keV transitions during any one count is also the same as the number of 161 keV transitions that were due to the decay of ground state nuclei during that count. This can then be subtracted from the total number of 161 keV transitions observed during the count to get the number of 161 keV transitions arising from isomer decays. This is the same as the number of 1·616 MeV β-transitions that occurred during that count. Thus, the ratio of the number of 311 keV isomeric transitions and the number of 1·616 MeV beta transitions is obtained. This can be combined with the ratio of the intensities of the two beta

groups to obtain the relative intensities of the three branches in the decay of the isomer. In this analysis corrections were made for the geometry of the system, the photopeak counting efficiencies,* absorption in the crystal housing,[5] and for the fact that the primary γ-ray spectrum is modified by the coincidence summing of 161 and 565 keV photons in the ground state decay.[6] The analysis of the data taken on thirteen samples gave the following results: 28% 311 keV isomeric transition, 21% 1·616 MeV β-transition, and 51% 1·772 MeV β-transition. It is estimated that the uncertainty in the intensity of the isomeric transition is such that the intensity should be quoted as 28 ± 3 per cent indicating a slightly larger amount of isomeric transition than reported by McGinnis.

It is also possible to obtain the conversion coefficient of the 311 keV γ-ray by utilizing the calculated number of isomeric transitions occurring during any count and the observed number of 311 keV γ-rays. We obtain a value of $1{\cdot}50 \pm 0{\cdot}10$ for the total conversion coefficient which agrees with the value of $1{\cdot}66 \pm 0{\cdot}20$ given by McGinnis.

The new decay scheme information is summarized in the caption for Fig. 1.

VOL. 22 1961

* The photopeak counting efficiency was taken as the product of the total intrinsic efficiency and a photopeak to total ratio. The total efficiencies were taken from Stanford and Rivers[4], The peak to total ratios were taken from reference[5].

[4] A. L. Stanford Jr. and W. K. Rivers Jr, *Rev. Sci. Instrums.* **29**, 406 (1958).
[5] L. T. Dillman. Ph.D. thesis, University of Illinois (1958) (Unpublished).
[6] N. H. Lazar and E. D. Klema, *Phys. Rev.* **98**, 710 (1955).

J. Inorg. Nucl. Chem., 1961, Vol. 22, pp. 13 to 18. Pergamon Press Ltd. Printed in Northern Ireland

CRYSTAL STRUCTURES IN THE $OsTe_{2-x}Sb_x$ SYSTEM

W. D. JOHNSTON
Westinghouse Research Laboratories, Pittsburgh 35, Pennsylvania

(*Received* 23 *March* 1961)

Abstract—The $OsTe_{2-x}Sb_x$ system has been examined by X-ray diffraction techniques. Three of the phases present have been indexed. $OsTe_2$ has the pyrite structure, $OsTe_{1.9}Sb_{0.1}$ has the marcasite structure, and $OsSb_2$ has the löllingite structure.

VOL. 22 1961

As a part of an investigation of the electrical properties of heavy metal tellurides and antimonides the system $OsTe_{2-x}Sb_x$ was surveyed. This particular system was of interest since both end members are semiconductors of moderately high electrical conductivity. Of more direct interest is the fact that several new phases have been found and have been identified crystallographically.

RESULTS AND DISCUSSION

The crystal structure of $OsTe_2$ is pyrite with the cell edge $a = 6{\cdot}3974$ Å which is in agreement with the earlier findings of MEIJER[1] and THOMASSEN[2] who reported $a = 6{\cdot}3985$ and $a = 6{\cdot}382$ Å respectively. The pyrite structure may be considered to be a NaCl cubic structure with Os in the Na position and Te_2 pairs in the Cl position. Tellurium pairs are directed along all body diagonals.

$OsSb_2$ has not been previously reported. The X-ray data for this material are given in Table 1. The structure is of the löllingite type, the X-ray pattern being somewhat similar in the front reflection to $FeSb_2$ which also has this structure. The löllingite structure may be formed from the pyrite structure by shortening the pyrite cube along one face diagonal and lengthening it along a second face diagonal. The nonmetal pairs are rotated out of the direction of the shortening and lie nearly parallel to the two remaining pyrite body diagonals. Half of the shortened diagonal is the orthorhombic *c*-axis, half the lengthened diagonal is the orthorhombic *b*-axis. The precursor of the orthorhombic *a*-axis is the pyrite cube edge and, as can be seen from the data, they are quite close together in size. The löllingites occur when the nonmetal pair are from Group V of the periodic table[3,4] (see also ROSENQUIST[5]) and their ratio of b/c which indicates the degree of distortion from cubic is typically 1·76–1·86. For a pyrite this ratio would be unity. This ratio for $OsSb_2$ is 1·850.

If antimony is substituted for tellurium in $OsTe_2$ giving, for example, $OsTe_{1.9}Sb_{0.1}$ the structure formed is marcasite as shown in Table 2. This is the structure of $FeTe_2$. Marcasite structures have the same distortions of the pyrite structure as has löllingite, but the distortions are much less severe, b/c 1·31–1·39.[4] For $OsTe_{1.9}Sb_{0.1}$ this ratio is 1·305.

[1] W. O. J. GROENWELD MEIJER, *Amer. Min.*, 646 (1955).
[2] L. THOMASSEN, *Z. Phys. Chem.* **48**, 277 (1929).
[3] M. J. BUERGER, *Amer. Min.* **22**, 48 (1937).
[4] J. HARALDSEN, Anhandl Norski Videnskaps Akad Oslo I Mat.–Natur Klasse **4**, 1 (1949).
[5] T. ROSENQUIST, *Acta Met.* **1**, 761 (1953).

TABLE 1.—$OsSb_2$
$a = 6{\cdot}684$ $b = 5{\cdot}937$ $c = 3{\cdot}210$ Å
$\lambda CoK_\alpha = 1{\cdot}79021$ Å
d X-ray $= 11{\cdot}306$ g/cm³
d found $11{\cdot}12 \pm 0{\cdot}2$

I	$\sin^2\theta$ obs. all corrected to λK_α	hkl	$\sin^2\theta$ calc.	$\sin^2\theta$ calc. corrected for absorption
s	0·0407	110	0·0406	0·0414
w	0·0716	200	0·0717	0·0726
vs	0·0956	210	0·0944	0·0955
		101	0·0957	0·0968
vs	0·1016	011	0·1005	0·1016
m	0·1098	120	0·1088	0·1099
s	0·1196	111	0·1184	0·1195
s	0·1643	220	0·1626	0·1639
m	0·1736	211	0·1722	0·1735
vvs	0·1857	310	0·1841	0·1854
vvs	0·1881	121	0·1866	0·1879
m	0·2239	130	0·2224	0·2238
vs	0·2408	301	0·2392	0·2406
		221	0·2404	0·2418
vvw	0·2532	320	0·2523	0·2538
vw	0·2631	311	0·2619	0·2634
m	0·3123	002	0·3110	0·3125
m	0·3553	231	0·3540	0·3555
m	0·3793	420	0·3779	0·3793
vw	0·3833 double	140	0·3815	0·3829
		202	0·3927	0·3841
w	0·4065	212	0·4054	0·4068
vw	0·4211	122	0·4198	0·4212
vw	0·4372	240	0·4353	0·4367
m	0·4606	141	0·4393	0·4607
m	0·4747	222	0·4736	0·4750
m	0·4933	430	0·4915	0·4929
m	0·5145	241	0·5131	0·5145
vw	0·5274	501	0·5262	0·5276
m	0·5344	132	0·5334	0·5348
w	0·5504	511	0·5489	0·5503
s	0·5705	431	0·5693	0·5706
s	0·6476	600	0·6457	0·6468
		051	0·6460	0·6471
vvw	0·6658	151	0·6639	0·6647
m	0·6900	422	0·6889	0·6899
vw	0·7185	251	0·7177	0·7186
		103	0·7177	0·7186
vw	0·7233	013	0·7225	0·7233
w	0·7304	531	0·7307	0·7315
		441	0·7284	0·7292
vvw	0·7412	113	0·7404	0·7412
m	0·7469	611	0·7462	0·7470
		242	0·7463	0·7471
vw	0·7828	512	0·7821	0·7829
vvw	0·7950	213	0·7942	0·7950

Table 1 (*cont'd*)

I	$\sin^2\theta$ obs. all corrected to λK_α	*hkl*	$\sin^2\theta$ calc.	$\sin^2\theta$ calc. corrected for absorption
m	0·8093	123	0·8086	0·8093
w	0·8188	060	0·8182	0·8189
vvw	0·8369	160	0·8361	0·8366
		342	0·8360	0·8365
w	0·8507	522	0·8503	0·8508
		630	0·8502	0·8507
m	0·8617	303	0·8612	0·8617
vvw	0·8844	313	0·8839	0·8843
w	0·8900	541	0·8898	0·8901
		260	0.8899	0·8902
w	0·9511	252	0·9509	0·9511
m	0·9564	602	0·9567	0·9568
m	0·9612	442	0·9616	0·9617
vvw	0·9673	261	0·9677	0·9678
m	0·9759	233	0·9760	0·9761

VOL. 22 1961

The transformation from pyrite to marcasite apparently occurs near the composition $OsTe_{1\cdot95}Sb_{0\cdot05}$ since duplicate preparations of this composition have yielded either structure or both simultaneously. The structural transformation is probably not controlled by a change in the metal to nonmetal ratio since according to electrical data discussed later the phase field of $OsTe_2$ is probably quite narrow. As further evidence of a narrow phase field preparations of the nominal compositions $OsTe_{2\cdot05}$ and $OsTe_{1\cdot95}$ both have the pyrite structure with essentially identical lattice parameters.

The central region between $OsTe_{1\cdot9}Sb_{0\cdot1}$ and $OsSb_2$ gives extremely complicated X-ray patterns and as a result has not been investigated. In addition to the very obvious presence of multiple phase regions it is probable that an intermediate of the monoclinic arsenopyrite type may be present. It should be pointed out, however, that single phase marcasite and löllingite structures are found respectively at $OsTe_{1\cdot8}Sb_{0\cdot2}$ and $OsSb_{1\cdot95}Te_{0\cdot05}$ and thus their phase fields have some width.

These results suggested that the difference between the naturally occurring pyrite and marcasite forms of FeS_2 might be due to both temperature[6] and the presence of a group V impurity, such as As. Our experiments have shown that this is not the case. Preparations of $FeS_{2-x}As_x$ where $x = 0\cdot01$ and $0\cdot1$ followed by annealing at various temperatures give only the pyrite structure. Chemical analysis of naturally occurring minerals for arsenic show no systematic behaviour. Thus the $OsTe_{2-x}Sb_x$ system remains unique in that the pyrite-marcasite transformation may be achieved entirely by chemical means.

EXPERIMENTAL

Starting materials were American Smelting & Refining Co. 99·999% Te, A. D. Mackay 99·999% Sb, and Englehardt 99·99% Os. The osmium was extremely grassy and was flamed out at dull red heat under vacuum immediately prior to use. The −100 mesh powders were weighed, mixed and compacted and placed in Vycor containers which were evacuated and sealed off. After firing to 700° for 20 hr the sample was reground to −100 mesh, repressed, and refired a second time. In view of the previously mentioned phase transformation it is interesting to note that $OsTe_2$ and $OsTe_{1\cdot98}Sb_{0\cdot02}$,

[6] J. E. Hiller and K. Probsthain, *Geologie* (Berlin) **5**, 607 (1956).

TABLE 2.—$OsTe_{1.9}Sb_{0.1}$

$a = 6{\cdot}404$ $b = 5{\cdot}281$ $c = 4{\cdot}046$ Å

$\lambda CoK_\alpha = 1{\cdot}79021$ Å d X-ray 10·79 g/cm³ d found 10·58 ± 0·2

I	$\sin^2\theta$ obs. all corrected to λK_α	hkl	$\sin^2\theta$ calc.	$\sin^2\theta$ calc. corrected for absorption
m	0·0495	110	0·0482	0·0490
s	0·0792	200	0·0781	0·0793
		011	0·0776	0·0788
m	0·0989	111	0·0971	0·0987
m	0·1085	210	0·1068	0·1084
vw	0·1360	120	0·1344	0·1361
vw	0·1444	Os		
m	0·1578	211	0·1557	0·1575
vvs	0·1853	121	0·1833	0·1852
w	0·1882	Os		
m	0·1948	220	0·1930	0·1950
m	0·1976	002	0·1958	0·1978
m	0·2068	310	0·2045	0·2065
vs	0·2269	301	0·2247	0·2267
m	0·2457	112	0·2240	0·2461
m	0·2560	311	0·2534	0·2555
m	0·2763	202	0·2739	0·2760
m	0·2804	130	0·2781	0·2802
m	0·3047	212	0·3026	0·3048
vw	0·3167	Os		
m	0·3291	131	0·3270	0·3292
m	0·3387	230	0·3367	0·3389
m	0·3871	231	0·3856	0·3877
m	0·3916	222	0·3888	0·3909
		411	0·3902	0·3923
m	0·4024	312	0·4003	0·4024
s	0·4298	420	0·4275	0·4296
m	0·4613	040	0·4597	0·4617
		103	0·4600	0·4620
vw	0·4707	013	0·4692	0·4718
m	0·4754	132	0·4739	0·4759
vw	0·4853	331	0·4833	0·4853
m	0·4907	113	0·4887	0·4907
m	0·5195	510	0·5171	0·5191
vw	0·5300	141	0·5281	0·5300
m	0·5338	232	0·5325	0·5344
m	0·5396	240	0·5378	0·5397
		501	0·5373	0·5392
m	0·5492	213	0·5473	0·5492
m	0·5685	511	0·5660	0·5678
s	0·5770	123	0·5749	0·5764
m	0·5878	241	0·5867	0·5884
m	0·6022			
m	0·6173	303	0·6163	0·6180
m	0·6213	431	0·6201	0·6218
s	0·6245	422	0·6233	0·6250
vw	0·6352	225	0·6335	0·6351

Table 2 (*cont'd*).

I	$\sin^2\theta$ obs. all corrected to λK_α	*hkl*	$\sin^2\theta$ calc.	$\sin^2\theta$ calc. corrected for absorption
vw	0·6462	313	0·6450	0·6466
m	0·6572	042	0·6555	0·6571
m	0·6863	341	0·6844	0·6869
w	0·7041	600	0·7033	0·7047
w	0·7138	512	0·7129	0·7143
vw	0·7181	133	0·7186	0·7200
w	0·7347	242	0·7336	0·7349
m	0·7687	432	0·7670	0·7682
		051	0·7671	0·7683
m	0·7785	233	0·7772	0·7783
	0·7838	413	0·7818	0·7829
		004	0·7831	0·7842
m	0·7975	531	0·7959	0·7969
		250	0·7963	0·7973
m	0·8323	342	0·8313	0·8321
		114	0·8313	0·8321
m	0·8462	251	0·8452	0·8460
w	0·8617	204	0·8612	0·8619
w	0·8759	333	0·8749	0·8755
m	0·8909	214	0·8999	0·8904
m	0·8999	043	0·9002	0·9007
		602	0·8991	0·8996
vs	0·9294	503	0·9289	0·9292
		612	0·9278	0·9281
m	0·9440	532	0·9428	0·9430
		351	0·9429	0·9431
s	0·9585	007	0·9573	0·9575
		513	0·9576	0·9578
m	0·9626	630	0·9619	0·9621
m	0·9762	224	0·9761	0·9762
m	0·9786	243	0·9783	0·9784

which are both of the pyrite structure, give extremely weak pellets while the other compositions studied were all rather strong mechanically.

X-rays taken with cobalt radiations $\lambda K_\alpha = 1{\cdot}97021$, $\lambda K_{\alpha_1} = 1{\cdot}78892$, $\lambda K_{\alpha_2} = 1{\cdot}79278$ were generally clean and sharp. The initial attempts at indexing $OsSb_2$ and $OsTe_{1\cdot9}Sb_{0\cdot1}$ were facilitated by referrring to the data for $FeSb_2$ and $FeTe_2$. The lattice parameters reported were obtained by extrapolating calculated values of the parameter vs. $(\cos^2\theta/\sin\theta + \cos^2\theta/\theta)/2$.[7] The samples were quite strongly absorbing, so in order to compare values of $\sin^2\theta$ calculated and observed over the entire range of θ the absorption function of TAYLOR and FLOYD[8] was used.

Densities were determined pyenometrically using alcohol. The error due to weighing makes the measurement of density uncertain to ± 2 per cent. The results in Tables 1 and 2 are within this limit of error.

Thermoelectric power measurements were made on many of these samples. $OsTe_2$ consistently has a thermoelectric power, α, of about $-70\ \mu V/°C$ regardless of whether it is made with excess osmium or tellurium, suggesting that the $OsTe_2$ phase has a very small range of composition containing a slight excess of Os. On the other hand $OsTe_{1\cdot9}Sb_{0\cdot1}$ has a consistent thermoelectric power of about

[7] A. TAYLOR and H. SINCLAIR, *Proc. Phys. Soc.* **57**, 126 (1954).
[8] A. TAYLOR and R. W. FLOYD, *Acta Cryst.* **3**, 285 (1950).

VOL. 22 1961

+105 μV/°C indicating that antimony additions have taken place causing *p*-type conduction as would be expected since antimony substitution results in a deficit of electrons. At the composition $OsTe_{1\cdot95}Sb_{0\cdot05}$ where the transformation is taking place, the results of thermoelectric measurements were rather erratic. In the case of $OsSb_2$ the sample is *n*-type with $\alpha = -115$ μV/°C. It might be pointed out in passing that attempts to change the sign or magnitude of conduction in $OsTe_2$ by substituting for the Os such elements as Li, Al or Ga were ineffective.

Arsenic was determined in the FeS_2 mineral samples by the colourimetric silver diethyldithiocarbamate method.[9] Thr percent arsenic found were: marcasite 0·023 per cent, two different pyrite samples 0·0065 and 0·056 ± 0·002.

Acknowledgements—Mr. D. E. SESTRICH has contributed to a number of aspects of this work. The chemical analyses were performed by Dr. R. J. NADALIN.

[9] V. VASAK and V. SEDIVEC, *Chem. Listy* **46**, 341 (1052).

J. Inorg. Nucl. Chem., 1961, Vol. 22, pp. 19 to 21. Pergamon Press Ltd. Printed in Northern Ireland

THE STRUCTURE OF DIALYKL AND DIARYL PHOSPHONATES*

K. MOEDRITZER
Monsanto Chemical Co., Inorganic Chemicals Division, Research Department,
St. Louis, Missouri

(*Received* 19 *April* 1961)

Abstract—Nuclear magnetic resonance (n.m.r) studies of the ^{31}P nucleus in alkali metal salts of dialkyl and diaryl phosphonates dissolved in diglyme demonstrate that the phosphorus in such salts exists in the trivalent form. Acid base studies show that the salts of dialkyl phosphonates resemble to alcoholates with respect to their base strength.

VOL.
22
1961

THE structure of the dialkyl phosphonates as well as that of the parent acid was a subject of considerable controversy in the early days of phosphorus chemistry. The question as to which of the two tautomeric forms

$$\underset{\text{I}}{(RO)_2P(OH)} \rightleftharpoons \underset{\text{II}}{(RO)_2P(H)O} \qquad (1)$$

predominates, has been decided in favour of form II[1], on the basis of physical measurements alone. Phosphorus n.m.r. measurements[2] on dialkyl phosphonates have unequivocally confirmed the generally accepted structure (II) and have provided no evidence for the existence of the phosphite form (I). Indirect spin spin splitting by the hydrogen attached directly to the phosphorus atom and the absence of other detectable peaks at field strengths where resonance is observed for the trisubstituted phosphites (Table 1) proves that approximately 95 per cent or more of the dialkyl phosphonate is present in form (II). Proton magnetic resonance measurements on dialkyl phosphonates[3] are in complete agreement with the conclusions reached in the ^{31}P studies.

Dialkyl phosphonates in organic solvents react with alkali metals with evolution of hydrogen and the formation of the corresponding salts. An investigation of the infra-red spectra of the lithium, sodium, potassium and silver salts of several dialkyl phosphonates[4] revealed that in the majority of the salts studied there was a complete absence of the phosphoryl frequency. The slight absorption found in a few cases was attributed to hydrolysis by atmospheric moisture during transfer of the sample. All salts investigated showed strong absorption bands at 1050 cm^{-1} which is characteristic for both the P—O^- and the P—O—R group. Therefore, although the phosphonate structure could be ruled out, no direct evidence for the structure

* This research was supported in part by the Air Research and Development Command, United States Air Force, under contract AF 33(616)–6950, monitored by the Materials Laboratory Wright Air Development Centre, Wright Patterson Air Force Base, Ohio.

(1) G. O. DOAK and L. D. FREEDMAN, *Chem. Rev.* **61**, 31 (1961).
(2) C. F. CALLIS, J. R. VAN WAZER, J. N. SHOOLERY and W. A. ANDERSON, *J. Amer. Chem. Soc.* **79**, 2719 (1957).
(3) G. MAVEL, *C. R. Acad. Sci., Paris* **248**, 3699 (1959).
(4) L. W. DAASCH, *J. Amer. Chem. Soc.* **80**, 5301 (1958).

$(RO)_2P—O^-\ M^+$ was obtained. Based on the infra-red spectra and the remarkable solubility of the alkali metal salts of dialkyl phosphonates in non polar solvents, such as the solubility of dibutyl phosphonate in petroleum ether, the same author postulated a structure containing an oxygen metal bond with a calculated covalent bond character of 70–75 per cent.

In this connexion it was of interest to study the ^{31}P n.m.r. spectra of the alkali metal salts of dialkyl and diaryl phosphonates. The ^{31}P n.m.r. spectrum of the

TABLE 1.—^{31}P CHEMICAL SHIFTS OF ALKALI METAL SALTS OF DIALKYL AND DIARYL PHOSPHONATES, DIALKYL AND DIARYL PHOSPHONATES AND TRIALKYL AND TRIARYL PHOSPHITES, IN P.P.M. RELATIVE TO 85% H_3PO_4*

$LiOP(OC_2H_5)_2$	−145	$HPO(OCH_3)_2$	−11†
$NaOP(OC_2H_5)_2$	−153	$HPO(OC_2H_5)_2$	−8†
$KOP(OC_2H_5)_2$	−152	$HPO(OC_4H_9)_2$	−8†
		$HPO(OC_6H_5)_2$	0†
$LiOP(OC_4H_9)_2$	−145	$P(OCH_3)_3$	−141
$NaOP(OC_4H_9)_2$	−152	$P(OC_2H_5)_3$	−139
$KOP(OC_4H_9)_2$	−153	$P(OC_4H_9)_3$	−139
		$P(OC_6H_5)_3$	−128
$LiOP(OC_6H_5)_2$	−142		
$NaOP(OC_6H_5)_2$	−148		
$KOP(OC_6H_5)_2$	−139		

* The alkali metal salts of the dialkyl and diaryl phosphonates were measured in solution in bis (2-methoxyethyl) ether (diglyme), the dialkyl and diaryl phosphonates as well as the trialkyl and triaryl phosphites as pure liquids. The reported shifts are to within ±1 p.p.m. confidence.

† 1–1 spin spin splitting, the splitting in cps. in $HPO(OR)_2$ is for R=CH_3: 715, C_2H_5: 686, C_4H_9: 690, C_6H_5: 746.

lithium, sodium and potassium salts of dialkyl and diaryl phosphonates show a single peak with a chemical shift in a region where only triply connected phosphorus compounds were found to resonate. These shifts were definitely out of the region of signals of quadruply connected phosphorus compounds.

The close agreement of the values of the chemical shifts of the salts of the dialkyl and diaryl phosphonates with those of the triply connected trialkyl and triaryl phosphites (Table 1) is evidence for a triply connected structure $(RO)_2P—O—M$ (M = Li, Na or K). Although the n.m.r. spectrum does not give any information about the character of the metal oxygen linkage, a predominantly covalent bond seems to describe the state of bonding most closely due to reasons discussed above.

The now known ^{31}P chemical shift of the alkali metal salts of dialkyl phosphonates suggested a semi-quantitative study of the basicity of the dialkyl phosphonate anion. This study should yield further information about the nature of the oxygen–metal bond in the salts of dialkyl phosphonates. The equilibrium reaction

$$MY + HPO(OR)_2 \rightleftharpoons MOP(OR)_2 + HY \qquad (2)$$

(M = alkali metal, Y = anion) was investigated by adding MY (diglyme-insoluble substances in slight excess, diglyme-soluble substances in equivalent amounts) to solutions of dibutyl phosphonate in diglyme. The n.m.r. spectrum of the resulting

solutions showed that for MY = $LiNH_2$, LiH, NaH, $NaCH_2COONa$, $BrMgCH_3$,* $BrMgC_6H_5$* LiC_6H_5* equation (2) is shifted to the extent of more than 95 per cent to the right, forming the salt of the dialkyl phosphonate and the respective HY (NH_3, H_2, H_2, CH_3COONa, CH_4, C_6H_6, C_6H_6). This clearly indicates the stronger basicity of the anions NH_2^-, H^-, $NaOOCCH_2^-$, CH_3^-, $C_6H_5^-$ as compared with $(RO)_2PO^-$.

Reaction (2) reaches an equilibrium state for MY = $NaOC_2H_5$ (addition of an equivalent amount of $NaOC_2H_5$ to a solution of dibutyl phosphonate in diglyme) represented by the coexistence of about 30% $NaOP(OR')_2$ and 70% $HPO(OR')_2$ ($R' = C_4H_9$). The addition of an equivalent amount of C_2H_5OH (HY in equation 2) to this solution shifts, in accordance with the mass action law, the equilibrium to the extent of more than 95 per cent to the left, as signalled by the disappearance of the $NaOP(OR)_2$ peak in the n.m.r. spectrum. The influence of this equilibrium upon the yield of Michaelis Becker-type reactions has been pointed out by KOSOLAPOFF[5].

These observations suggest a similarity in bond character of the oxygen–metal bond in alkali metal alcoholates and alkali metal salts of dialkyl phosphonates.

VOL. 22 1961

* In order to prevent side reactions of the type $(RO)_2OPH + 2R'MgBr \rightarrow R_2'(O)PH + 2MgBr(OR)$ these reagents were added to dibutyl phosphonate solutions kept at −78°C.

[5] G. M. KOSOLAPOFF, *J. Amer. Chem. Soc.* **68**, 1103 (1946).

VOL
22
196

J. Inorg. Nucl. Chem., 1961, Vol. 22, pp. 23 to 31. Pergamon Press Ltd. Printed in Northern Ireland

THE TEMPERATURE RANGE OF LIQUID METALS AND AN ESTIMATE OF THEIR CRITICAL CONSTANTS

A. V. GROSSE
The Research Institute of Temple University, Philadephia

(*Received* 16 *March* 1961)

Abstract—It is shown that the temperature range of liquid metals extends in the case of the "refractory" metals, tungsten, tantalum and rhenium, to over 20,000°K. Methods are described that show how, based on the law of rectilinear diameter, and available experimental data, such as density vs. temperature, and vapour-pressures, heats and entropies of vaporization, liquid temperature diagrams for various metals, may be constructed. Estimates for the critical temperature, pressure and density of various metals, for example, sodium, lead and tin, have been made.

VOL.
22
1961

THE strength of even the strongest chemical bonds is not sufficient to hold atoms together in molecules at temperatures above 5000–6000°K. Even such thermally stable molecules as carbon monoxide and nitrogen, which exist in the atmosphere of the sun are atomized above 6000°K. Thus chemical substances, as they are known in inorganic and physical chemistry, cease to exist above this temperature range. As will be shown in this paper[1] exceptions are the liquid metals. The temperature range of the liquid state of metals extends in the case of the so-called refractory metals, such as tungsten, rhenium and tantalum, to over 20,000°K. In comparison, the solid metal state ranges from absolute zero to a maximum of 3650°K, i.e., the melting point of the highest melting metal—tungsten. Thus the liquid range is about six times greater!

Since the metals are *elementary monatomic* substances they are not subject to chemical decomposition or dissociation at extremely high temperatures. Even above 20,000°K the only possible change is ionization to positive ions and electrons. The amount of ionization in the saturated vapour of the metal can be readily calculated by the use of Saha's equation or the TOLMAN[2] procedure since the ionization potentials of most metals are accurately known.[3] The amount of this ionization is small, of the order of a few per cent, particularly in view of the high saturated vapour-pressure.

In the liquid (as well as the solid) metal the present-day quantum-mechanical theory assumes that *all the metal atoms are ionized*, i.e., present as cations, and the electrons are moving freely between the ions, thus accounting for most of the characteristic metallic properties. Thus an increase in temperature does not change the basic chemical nature of the liquid metal.

The limits of the liquid state or the critical temperature of a large number of chemical substances investigated are usually about one and one-half times their absolute boiling points. This is true for ideal liquids such as argon, for example, most homopolar inorganic compounds typified by water, carbon dioxide and carbon tetrachloride and most organic substances such as methane and benzene; the forces among the above molecules are the *weak Van der Waals forces*. It does not seem to be true for metals, however, although so far only one metal, namely, mercury, has

[1] A. V. GROSSE, *The Liquid Range of Metals and Some of Their Physical Properties at High Temperature*. The Research Institute of Temple University (1960).
[2] R. C. TOLMAN, *J. Amer. Chem. Soc.* **43**, 1630–32 (1921).
[3] See, for example, *Handbook of Chemistry and Physics* (40th Ed.), pp. 2546–47. (1959).

been investigated experimentally. This is to be anticipated because in metals we have the characteristic *metallic bond*[4] as distinguished from the homopolar bond as in the case of the inorganic and organic substances mentioned above, or the ionic bond as it exists in typical salts such as sodium chloride or calcium fluoride. Theoretically, the liquid state is the least understood state of matter, as compared to our knowledge of solids or gases. Of all liquids the liquid metal should represent, from the theoretical point of view, a particularly simple case since all metals are monatomic.

In the last two years particularly, advances in the theory of liquids have been made by EYRING and his associates[5–9] in this country, and by BERNAL[10] in England. Theoreticians, however, still need some arbitrary parameters to adjust the theory to experimentally available data. The main advantage is that they give a deeper insight into the structural, geometric, molecular and atomic factors involved and will give a much deeper understanding as to what makes a liquid liquid.

We will proceed on a semiempirical basis. A sufficiently accurate estimate of critical temperatures, pressures and densities can be made by using well established empirical relationships as well as presently available experimental data on liquid densities and vapour pressures and their temperature dependence.

Of special assistance for the evaluation of the liquid range or estimation of critical constants is the *empirical* law of Cailletet and Mathias, or the law of rectilinear diameter which states that "the average density or half the sum of the densities of a liquid and its saturated vapour decrease linearly with temperature; at the critical point the densities of liquid and saturated vapour are equal."

This law has been tested experimentally on a large variety of *thermally stable* organic and inorganic liquids. Examples are hydrocarbons, such as benzene, methane, pentane, ethyl ether, inorganic compounds such as water, sulphur dioxide, carbon dioxide, carbon tetrachloride, carbon monoxide and elements such as argon, krypton, xenon, nitrogen, oxygen, hydrogen and even such quantum liquids as helium-4 and helium-3. The early and very precise work of Young showed extremely small deviations from additivity and linearity in the case of some hydrocarbons near the critical region; even these deviations, in our opinion, may be due to thermal decomposition and/or impurities. Although about 80 per cent of the chemical elements are metals, only *one*, namely, *mercury*, has been heated to the critical point. Liquid and vapour densities, as well as vapour-pressure data, are available and, as we shall see, the law of Cailletet and Mathias is fulfilled for mercury. For these reasons a detailed summary of all data on liquid mercury will be discussed here.

Temperature range of liquid mercury and its critical data

The critical point of mercury was determined for the first and only time by BIRCH[11] in Bridgman's laboratory at Harvard, by measuring the electrical resistance of liquid mercury, under pressure, up to about 1800°K. He found the critical temperature to $= 1733°K$ ($\pm$ 50°) and the critical pressure to $= 1587$ ($\pm$ 50) atm. This is the only

[4] See L. PAULING, *The Nature of the Chemical Bond*, (3rd Ed.) Chap. 11. Cornell Univ. Press (1960).
[5] H. EYRING, T. REE and N. HIRAI, *Proc. Natl. Acad. Sci.* **44**, 683 (1958).
[6] E. J. FULLER, T. REE and H. EYRING, *Proc. Natl. Acad. Sci.* **45**, 1594 (1959).
[7] C. M. CARLSON, H. EYRING and T. REE, *Proc. Natl. Acad. Sci.* **46**, 333 (1960).
[8] T. R. THOMSON, H. EYRING and T. REE, *Proc. Natl. Acad. Sci.* **46**, 336 (1960).
[9] C. M. CARLSON, H. EYRING and T. REE, *Proc. Natl. Acad. Sci.* **46**, 649 (1960).
[10] J. D. BERNAL, *Proc. Royal Inst. of Gt. Britain* **37**, 380 (1959).
[11] F. BIRCH, *Phys. Rev.* **41**, 641–48 (1952).

direct determination of the critical data of a metal. In view of their importance and because mercury is the lowest boiling metal and thus the easier with which to experiment, these measurements should be repeated to insure maximum reliability.

The *complete* range of saturated vapour-pressures of liquid mercury, over the whole range from the melting point to the critical point, is a straight line on a logarithmic plot,[1] over a 10^{12}-fold increase in pressure from $1{\cdot}91 \times 10^{-9}$ atm at the melting point, i.e., 234·3°K, to 1587 $\pm$ 50 atm at the critical point (1733°K).

The vapour-pressures from the melting point to about 2 atm are known with great precision.[12] Two sets of data are available for the range of 2–140 atm.; the older data are due to CAILLETET[13], and the more recent to BERNHARDT[14]. The latter extended his measurement to 1708°K, and to a pressure of 1955 atm. Both CAILLETET and BERNHARDT observed the actual boiling of the mercury in a pressure vessel; the measurements became progressively more difficult and less accurate at the higher pressures and temperatures.

VOL. 22 1961

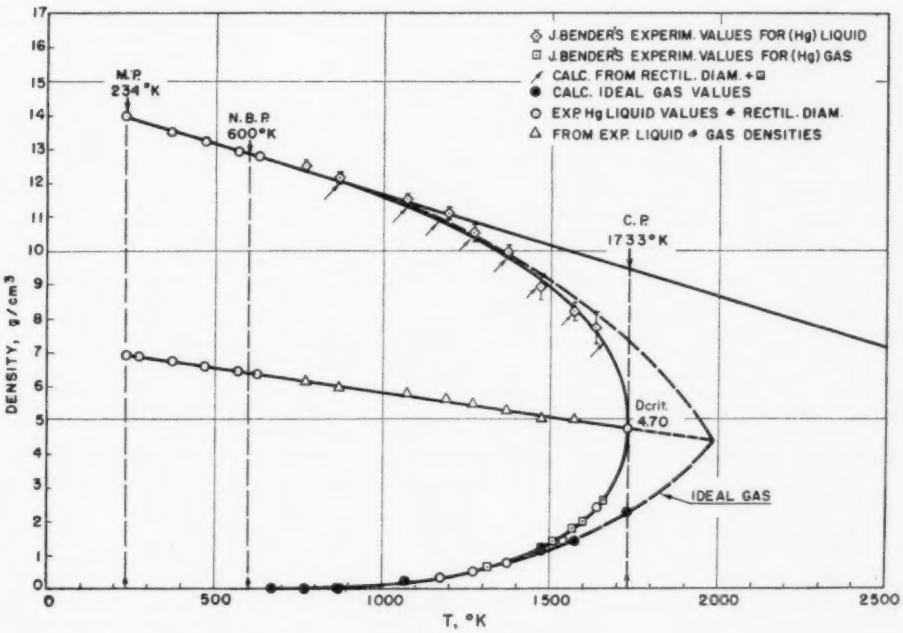

FIG. 1.

The liquid and saturated vapour density of mercury over the whole liquid temperature range

Fig. 1 shows a summary of mercury data on the density of both liquid and vapour and demonstrates that the law of rectilinear diameter is fulfilled. Because of the importance of these data they will be discussed in detail. They are due to the observations of BENDER[15,16] who measured the density of both liquid and saturated vapour

[12] See, for example, *Handbook of Chemistry and Physics*, (40th Ed.), p. 2331. (1959).
[13] CAILLETET, COLARDEAU and RIVIERE, *C.R. Acad. Sci., Paris* **130,** 1585 (1900).
[14] F. BERNHARDT, *Phys. Z*, **26,** 265–275 (1925).
[15] J. BENDER, *Phys. Z.* **16,** 246–247 (1915).
[16] J. BENDER, *Phys. Z.* **19,** 410–414 (1918).

in the range of 500–1380°C, i.e., up to 60°C of the critical point, in sealed quartz vessels. The liquid densities from the melting point to the normal boiling point are known[17] with great accuracy and were also used in Fig. 1; they are indicated by ⊙; BENDER's values for the saturated vapour are shown by ●, while the liquid densities together with their error range are indicated by ⊡. The calculated values for the vapour density, assuming ideal gas laws and the vapour-pressure of mercury, are shown as ⊡; up to about 1200°C there is no significant deviation between the ideal and actual values.

Values for the liquid density, calculated from this law and the experimental vapour density, are indicated with ↗ on the liquid curve; values for $\frac{1}{2}(D_{\text{liq.}} + D_{\text{vap.}})$, calculated from the experimental data, are shown in triangles △ on the rectilinear diameter. The vapour densities, because of their lower absolute values, can be determined with greater accuracy; the liquid values show appreciable scatter because of experimental difficulties.

Using BENDER's smoothed values, we obtain for the equation of mercury's rectilinear diameter, the expression:

$$D_{\text{rec.}}\ ♂ = 6{\cdot}7978 - 14{\cdot}30 \times 10^{-4}\ T\ (°\text{C}).$$

Based on this equation the critical density of mercury, at 1460°C., equals 4·70 g/cm³, whereas BIRCH[11] estimated a value of 5 g/cm.³

We see further, from Fig. 1, that the two legs of the Cailletet–Mathias curve have two envelopes, (shown in dotted lines). The *first envelope* is the curve of the *ideal gas density*, the latter being always *less* than the actual saturated vapour density. The *second envelope* of the liquid leg is obtained by deducting the ideal saturated vapour density, in line with the rectilinear law, from the straight liquid density line. The two envelopes meet at a point which sets *an upper limit for the critical temperature;* in the case of mercury this limit is about 2000°K (see Fig. 1.)

Since the rectilinear diameter law is fulfilled for liquid mercury, as the only metal among many other liquids, *we will assume* it to hold for other metals also. It would be highly desirable if critical data for other metals were obtained so that the experimental evidence for the validity of the law can be put on as broad a foundation as possible.

THE TEMPERATURE RANGE OF OTHER LIQUID METALS

We are now interested in estimating, even if only approximately, the temperature range of other liquid metals. Usually, for most homopolar compounds, as has been mentioned, the normal boiling point corresponds to approximately two-thirds of the critical temperature.

As can be seen, this is not the case for the only known metal, mercury, where the ratio of the critical point to the normal boiling point

$$1733°\text{K}/629{\cdot}9°\text{K} = 2{\cdot}75$$

In order to estimate critical temperatures it is best to choose those physical properties which equal zero at the critical temperature and apply the principle of

[17] Data of THIESSEN and SCHEEL, *Handbook of Chemistry and Physics*, (40th Ed.) p. 2115. (1959).

corresponding states. Such properties are, for example, heat of vaporization, *entropy of vaporization* or surface tension.

The principle of corresponding states[18] requires that the molar entropies of vaporization of various liquids should be equal at corresponding temperatures and vice versa.

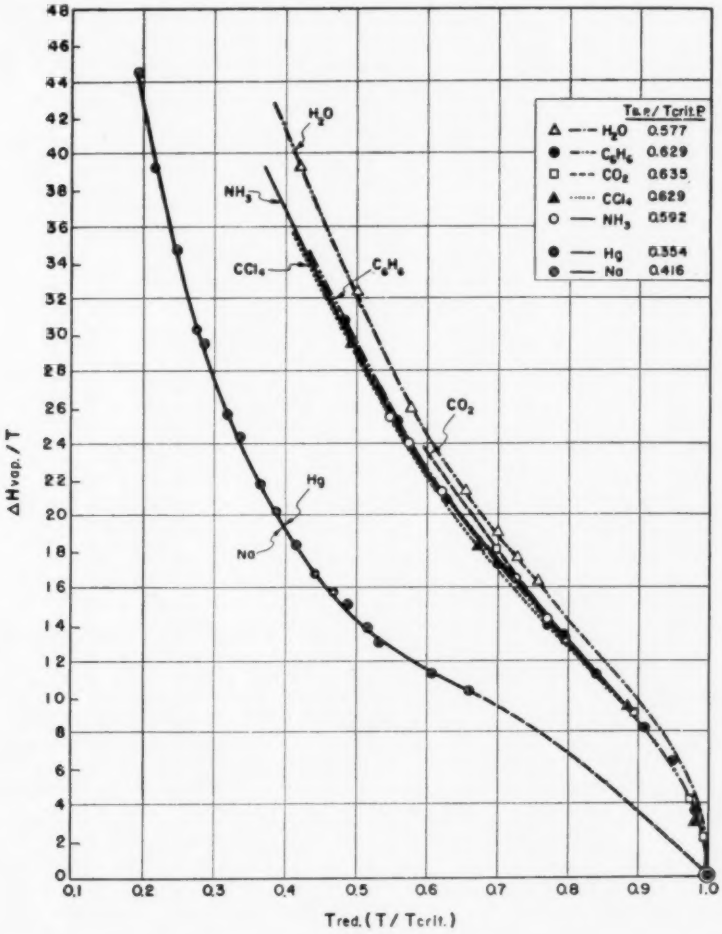

FIG. 2.

The heat of vaporization of mercury, $\Delta H_{\text{vap.}}$, is known over an appreciable range and can be readily extrapolated to the critical temperature; the same applies to the entropy, $\Delta S_{\text{vap.}} = \Delta H_{\text{vap.}}/T$. Fig. 2 shows the *entropy curve of mercury* and compares it with a number of well known normal liquids, such as carbon dioxide, carbon tetrachloride, ammonia, benzene and water. It will be noticed that mercury, the only known metal, shows a markedly different behaviour. We will assume for the present that other metals will behave in the same manner. By assuming the principle of corresponding states to be valid for other metals and using the experimentally

[18] For example, E. A. GUGGENHEIM, *J. Chem. Phys.* **13**, 253–261 (1945).

determined entropy of vaporization of other metals, for example, at their normal boiling points, we can, by using Fig. 2, arrive at their *reduced temperatures* and thus also at their approximate critical temperatures. Table 1 contains a summary of critical temperatures of a number of metals, arranged in ascending order from 1733°K, for mercury up to 23,000°K for tungsten. These critical temperatures (see last column of Table 2), were estimated, based on $\Delta S_{vap.}$ only at the boiling point.

TABLE 1.—CRITICAL TEMPERATURES, HEATS OF VAPORIZATION AND ENTROPIES AT NORMAL BOILING POINTS FOR VARIOUS METALS[21]

Metal	Boiling point at 1 atm. (°K)	$\Delta H_{vap.}$ (cal/g atom)	$\Delta S_{vap.}$ (cal/g atom °K)	$T_{red.}$ from Hg-curve Fig. 2	$T_{crit.}$ °K
Cs	958	15,750	16·95	0·445	2150
Rb	974	16,540	16·99	0·445	2190
K	1039	18,530	17·88	0·425	2440
Na	1163	21,280	18·40	0·415	2800
Bi	1832	36,200	19·75	0·397	4620
Pb	2024	42,880	21·15	0·375	5400
Ga	2510	61,200	24·40	0·330	7620
Sn	2960	69,400	23·42	0·340	8720
Fe	3160	83,900	26·55	0·305	10,000
U	4200	101,000	24·05	0·333	12,500
Mo	5100	142,000	27·85	0·295	17,000
Re	5900	169,000	28·63	0·287	20,500
Ta	5700	180,000	31·60	0·260	22,000
W	5800	191,000	32·90	0·250	23,000

Data on liquid sodium[19,20] have recently become available which gives $\Delta H_{vap.}$ and $\Delta S_{vap.}$ over the whole range from 800° (445°K) to 3000°R (1667°K). Thus in the case of liquid sodium a close fit to the mercury curve can be obtained only if the critical point of sodium is assumed to equal 2800°K (see Fig. 2 data for sodium).

The most interesting point revealed by the data of Table 1 is the wide temperature range of the liquid state of metals. Such metals as molybdenum, tantalum and tungsten will exist as liquids well over 10,000°K.

Vapour and critical pressures

Mercury is the only metal for which saturated vapour-pressures have been measured all the way to the critical point (see p. 25). For sodium and lead experimental data are available up to 15 and 12 atm, respectively.[1] For most other metals vapour-pressures have been measured below 1 atm. They have been critically evaluated in the well known contribution of KELLEY[22]. The vapour-pressure data on all elements have been brought up to date and published by STULL and SINKE[21]. As a first approximation, however, it can be assumed that the logarithm of the vapour-pressure is a straight line function of the reciprocal absolute temperature. Thus from the estimated critical

[19] C. T. EWING, J. P. STONE and R. R. MILLER, Report NRL 1069 (1960).
[20] M. MAKANSI, W. A. SELKE and C. F. BONILLA, *J. Chem. Engng. Soc. Imp. Coll. Data*, **5**, 441–452 (1960).
[21] All data on normal boiling points and $\Delta H_{vap.}$ taken from D. R. STULL and G. C. SINKE, *Thermodynamic Properties of the Elements, Advances in Chemistry Series, Vol.* 19. American Chemical Society, (1956).
[22] K. K. KELLEY, *U.S. Bur. Min. Bull.* **383** (1935).

temperatures from the preceding section we can obtain the critical pressure by extrapolation of the logarithmic vapour-pressure line.

Our estimates[1] of the critical pressures are as follows:

Sodium	490 atm
Lead	850 atm
Tin	2100 atm
Tungsten	> 10000 atm

Liquid range diagrams of typical metals

We have constructed liquid range diagrams of typical metals in analogy to mercury (Fig. 1) based on the estimates of critical temperatures and pressures given in the preceding sections. In addition, experimental data on the densities of liquid metals are available. We have selected such metals for which liquid density measurements have been made over as wide a temperature range as possible. In addition to mercury, these metals are *sodium*, *gallium*, *lead* and *tin*. The available data on these metals, particularly their liquid densities, temperature coefficients and the experimental temperature ranges where they have been determined, are all given in Table 2.

VOL. 22 1961

TABLE 2.—EXPERIMENTAL DENSITIES OF LIQUID METALS AT VARIOUS TEMPERATURES

Metal	Reference	Melting point (°K)	Normal boiling point (°K)	D at normal boiling point (estimate) (g/cm³)	Experimental range of D-measurements (°C)	Experimental $-dD/dt$, (g/cm³ °K)	$D_{crit.}$ (estimate) (g/cm³)	$D_{b.p.}/D_{crit.}$
Hg	This paper 23	234·3	629·9	12·7374	−39–480	$28{\cdot}6 \cdot 10^{-4}$	4·70	2·72
Na	24	371·0	1163	0·740	97·8–800	$2{\cdot}43 \cdot 10^{-4}$	0·18	4·1
Ga	25	303·1	2510	4·55	29·9–1100	$6{\cdot}07 \cdot 10^{-4}$	0·95	4·8
Pb	26	600·6	2024	8·85	327–850	$11{\cdot}62 \cdot 10^{-4}$	2·1	4·2
Sn	26	505·1	2960	5·55	232–1600	$6{\cdot}05 \cdot 10^{-4}$	1·3	4·3

In the case of mercury (see Fig. 1), we see that the actual vapour density *begins to differ* appreciably from the ideal gas density only above a $T_{red.} = 0{\cdot}8$, i.e., above 80 per cent of the liquid range, in contrast to most inorganic and organic compounds. Knowing the vapour-pressure of the metal we can readily calculate the ideal density of the saturated vapour as a function of temperature and correct the liquid density in line with the rectilinear diameter law, up to about $T_{red.} = 0{\cdot}8$. Thus, if the vapour density of the metal, $D_{vap.}$ is expressed as a function of the type:

$$D_{vap.} = c + aT + bT^2 + cT^3 + \ldots,$$

while the liquid density, $D^{(0)}_{liq.}$, in the range where $D_{vap.}$ is 0 or negligible, is given by:

$$D^{(0)}_{liq.} = M + nt$$

[23] Data of THIESEN and SCHEEL, *Handbook of Chemistry and Physics*, (40th Ed.), p. 2115. (1959). *International Critical Tables*, Vol. 2 p. 456. (1928).

[24] C. E. JACKSON, *Liquid–Metals Handbook*, *Sodium*–NaK *Supplement*, p. 26. (Editor-in-Chief) Sponsored by The Atomic Energy Commission and The Bureau of Ships Department of the Navy, Washington, D.C. (1955).

[25] W. H. HOATHER, *Proc. Roy. Soc.* **48**, 699 (1936).

[26] DAY, SOSMAN and HOSTETTER, *Amer. J. Sci.* **37**, 1 (1914).

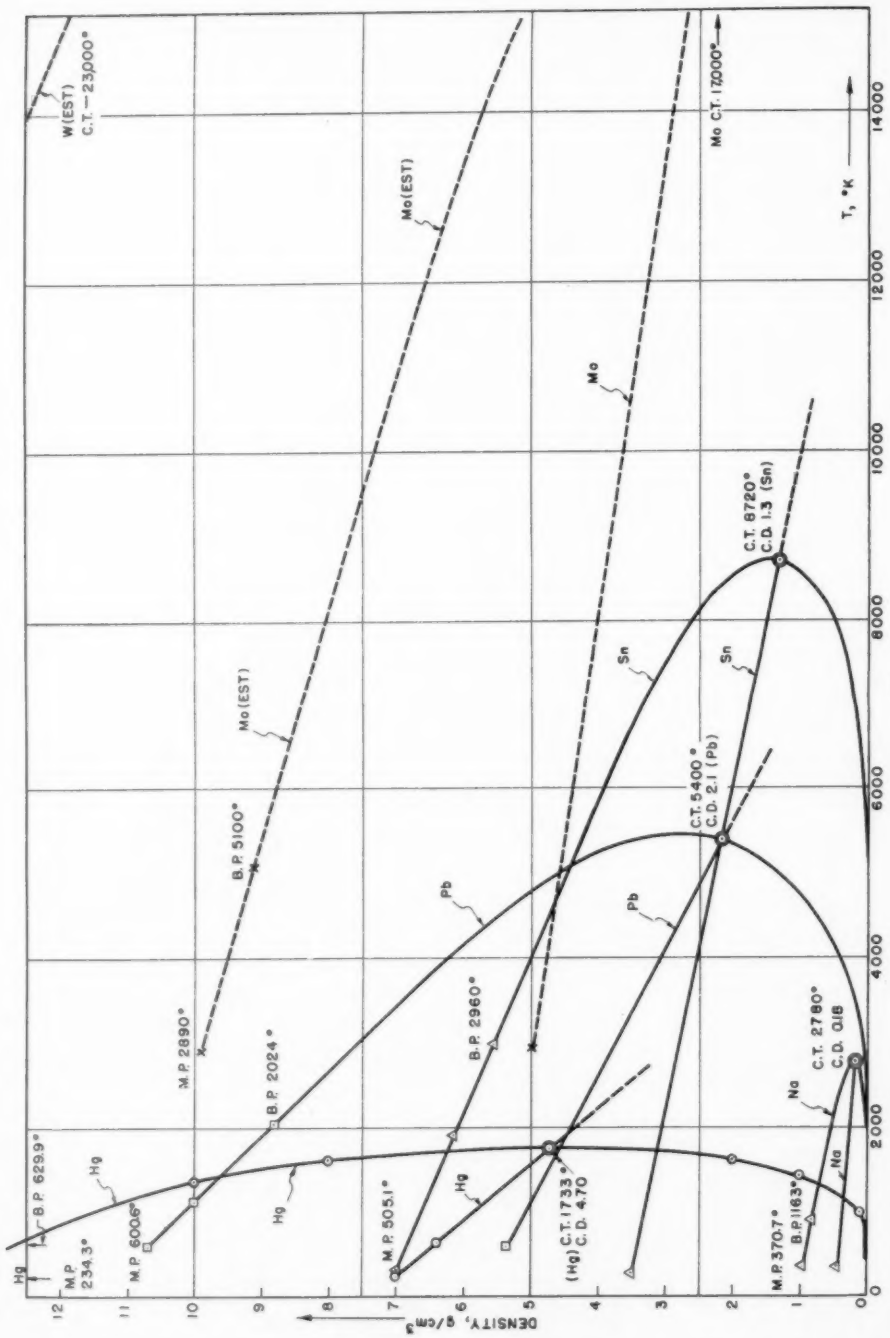
W(EST)
C.T. — 23000°
Mo(EST)
Mo C.T. 12000°
T, °K
Mo
Mo(EST)
B.P. 5100°
M.P. 2890°
B.P. 2024°
C.T. 8720°
C.D. 1.3 (Sn)
Sn
Sn
C.T. 5400°
C.D. 2.1 (Pb)
Pb
Pb
B.P. 2960°
C.T. 2780°
C.D. 0.18
Na
Na
Na
B.P. 629.9°
Hg
M.P. 234.3°
Hg
M.P. 60.06°
Hg
Hg
M.P. 505.1°
Hg
C.T. 1733°
(Hg) C.D. 4.70
M.P. 370.7°
B.P. 1163°
DENSITY, g/cm³

FIG. 3.

the correct density of the liquid metal, $D_{\text{liq.}}$, *up to about* 80 *per cent of the critical temperature*, will be given by the equation:

$$D_{\text{liq.}} = D^{(0)}_{\text{liq.}} - D_{\text{vap.}} = M - K + (n - a)T - bT^2 - cT^3 - \ldots$$

The liquid range diagrams of the above metals were constructed using the above data (Table 2) together with the law of rectilinear diameter. They are shown in Fig. 3, where the density (in g/cm^3) of both liquid and saturated vapour, in equilibrium with it, are plotted against temperature.

A study of this figure shows that for all these metals the density vs. temperature is a straight line function, at least up to the normal boiling point of the metal.

Fig. 3 shows strikingly the wide difference in the liquid state of metals (compare, for example, sodium vs. tin and molybdenum).

The *experimental slope* of the $D_{\text{liq.}}$ vs. temperature line, i.e., dD/dT, immediately establishes the rectilinear diameter with an accuracy corresponding to the error of the density measurement at the highest temperature.

VOL. 22 1961

The critical density for any metal can be roughly estimated since it equals one-fourth to one-fifth of the density at the normal boiling point—see Table 2. In conjunction with the estimated critical temperature (see Table 1) one can now deduce, approximately, the liquid density of any metal in the temperature range where its $D_{\text{vap.}}$ can be neglected. It follows directly from the rectilinear diameter law that the liquid density at the absolute temperature, T, or

$$D_T = D_{\text{c.p.}} \frac{(D_{\text{m.p.}}/D_{\text{c.p.}} - 2)}{(T_{\text{c.p.}} - T_{\text{m.p.}})} (T_{\text{c.p.}} - T) + 2\, D_{\text{c.p.}}$$

where $T_{\text{c.p.}}$ and $T_{\text{m.p.}}$ are the critical and melting points, respectively in °K, and $D_{\text{c.p.}}$ and $D_{\text{m.p.}}$ the liquid densities at these points.

VOL
22
196

J. Inorg. Nucl. Chem., 1961, Vol. 22, pp. 33 to 38. Pergamon Press Ltd. Printed in Northern Ireland

THE DENSITY OF LIQUID LEAD FROM THE MELTING POINT TO THE NORMAL BOILING POINT*

A. D. KIRSHENBAUM, J. A. CAHILL and A. V. GROSSE
Research Institute of Temple University, Philadelphia, Penn.

(*Received* 6 *March* 1961; *in revised form* 11 *May* 1961)

Abstract—The density of liquid lead was determined, by using the Archimedean principle, from its melting point to its normal boiling point. It can be expressed by the equation:

$$D(\text{g/cm}^3) = 10{\cdot}678 - 13{\cdot}174 \times 10^{-4}(T - 600{\cdot}6^\circ),$$

where T is in °K. The density of liquid lead is 10·678 g/cm³ at its melting point (600·6°K), and 8·803 g/cm³ at its boiling point (2024°K).

VOL. 22 1961

IN the pursuit of the Institute's programme of physical-chemical measurements at high temperatures, the densities of liquid oxides (Al_2O_3)[1] and fluorides,[2] CaF_2, LaF_3, etc., have been measured up to 2600°K. Recently the densities of liquid metals, namely, iron[3] and copper[4] have been determined up to 2500°K.

The liquid metal density measurements have now been extended to cover the whole temperature range from the melting point to the normal boiling point.

The two metals:

Lead, m.p. = 600·6°K; normal b.p. = 2024°K,
and Silver, m.p. = 1234·0°K; normal b.p. = 2450°K,

were chosen because (1) their normal boiling points can be readily attained in simple apparatus and (2) a suitable container material, namely, graphite, is available. Graphite is chemically inert and practically insoluble at high temperatures. This paper covers the results obtained on liquid lead. The results on liquid silver, upon completion, will be submitted in a subsequent paper.

The density of lead has been determined with an average probable error of about 0·03 per cent up to its boiling point. It is hoped that eventually its density can be extended, under pressure, to about 3500°K by using either an areometer type sinker or a null balance electrical system in a high pressure boiler apparatus, as described by GREENWOOD.[5]

EXPERIMENTAL

A. *Experimental procedure*

The density of liquid lead was measured from about 360°C to its boiling point by the immersed sinker method, by using a graphite crucible, reflux condenser and sinker. The source of heat in these studies was the carbon tube furnace (i.d. = 7·0 cm), with argon atmosphere, described previously.[6]

* This research was sponsored by the National Science Foundation under Grants 6277 and 15540.

[1] A. D. KIRSHENBAUM and J. A. CAHILL, *J. Inorg. Nucl. Chem.* **14**, 283–287 (1960).
[2] A. D. KIRSHENBAUM, J. A. CAHILL and C. S. STOKES, *J. Inorg. Nucl. Chem.* **15**, 297–304 (1960).
[3] A. D. KIRSHENBAUM and J. A. CAHILL, *Trans. Met. Soc. of AIME*. "Density of Liquid Iron from melting point to 2500°K." In press.
[4] A. D. KIRSHENBAUM, "*Second Annual Report on High Temperature Inorganic Chemistry to the National Science Foundation*," Research Grant NSF–G6278, The Research Institute of Temple University, Dec. 15, (1960).
[5] H. C. GREENWOOD, *Proc. Roy. Soc.* **83 A**, 483–491 (1910).
[6] A. D. KIRSHENBAUM and J. A. CAHILL, *J. Inorg. Nucl. Chem.* **14**, 283 (1960).

The liquid lead was heated or boiled in a cylindrical *graphite crucible* or *boiler* (i.d. = 5·7 cm, height = 7·0 cm, and volume = 180 cm³), with a tight graphite cover, containing three graphite tubes. The centre tube (i.d., = 2·0 cm, length = 20·0 cm), was the reflux condenser. One side tube served as the housing for the adjustable and insulated graphite rod to measure the liquid lead level. The second tube, closed at the bottom and protruding 1·5 cm into the boiler, was the black body source in our temperature readings. The amount of lead used was 1275 g; the loss due to leak and diffusion during about 4 hr of operation was about 3 per cent. The sinker was immersed into the liquid lead through the centre tube and the lead refluxed at atmospheric pressure for ½–1 hr in order to remove all entrapped and dissolved gases. The temperature of the lead was then dropped below its boiling point in approximately 50°K intervals and the density measurements made from the loss in weight and volume of the sinker.

The *sinker* was a *graphite* cylinder 2·0 cm long and 1·3 cm in diameter with 60° angle cones at each end. The upper cone tapered into a graphite rod (0·20 cm in diameter). A counter weight was attached to the graphite rod. The volume of the sinker was 3·596 cm³ at 20°C (293°K). The volume of the sinker at 20°C was determined by the loss in weight of the sinker when immersed in mercury, corrected for surface tension. The density of the mercury at 20°C is 13·5462 g/cm³ and the surface tension 465 dyne/cm with a contact angle of 140°. The volume of the sinker was corrected to the operating temperature using the thermal expansion data reported by GOLDSMITH, *et al.*,[7] together with the data known for the graphite used. The graphite used as the sinker was Dixon* E-821, which is a fine grain petroleum coke base stock with a transverse linear coefficient of expansion from 100 to 600°C of 35×10^{-7} and a parallel expansion of $20{\cdot}8 \times 10^{-7}$.

The volumes calculated for the various temperatures, were as follows:

°C	Volume (cm³)
20	1·0000
1000	1·0121
1500	1·0183
2000	1·0244

The volume of the sinker depended upon its depth of immersion in the liquid lead. This was determined by the difference between the depth of the liquid lead and the distance of the sinker from the crucible base. The distance of the sinker from the base of the crucible was determined by adjusting the sinker to a known distance from the base of the crucible by means of a micrometer screw incorporated as part of the suspension wires. The depth of the liquid lead was then obtained by reading the height of an adjustable graphite rod with a cathetometer when the rod was on the crucible base and at the point of electrical contact (6 V) of the rod with the surface of the liquid lead observed by means of a voltmeter.

The losses in weights were corrected for surface tension. The value used at the boiling point of lead (330 dyne/cm), was obtained by extrapolating the data reported by DRATH and SAUERWALD.[8] A contact angle of 140° was assumed in these calculations. The correction at the boiling point was −0·184 g (= 0·56 per cent of total weight loss).

Although good density values of lead from the melting point to about 700°C are available, the density at the boiling point of mercury was redetermined in this laboratory. The sinker used at the boiling point of lead was also used in this measurement. This determination was carried out in the usual manner by using a total refluxing mercury bath at atmospheric pressure. A correction was made for barometric pressure.

B. *Temperature measurements*

The temperature readings were made by an optical pyrometer. The pyrometer was calibrated by measuring the melting points of platinum (2043° ± 0·9°K)[9] and silver (1234·0° ± 0·1°K) and the

* J. Dixon Crucible Co., Jersey City, N.J.

[7] A. GOLDSMITH, T. E. WATERMAN and H. J. HIRSCHHORN, "Thermophysical Properties of Solid Materials, *Vol.* 1, *WADC Technical Report* 58–476, Aug. 1960 p. 59–158.

[8] G. DRATH and F. SAUERWALD, *Z. Anorg. Chem.* **162**, 301 (1927).

[9] F. HENNING and H. T. WENSEL, *Bur. Stand. J. Res., Wash.* **10**, 809 (1933).

boiling points of lead (2024°K) and silver (2450°K)[10]. The probable average deviation for our temperature measurements was ±5°K.

C. *Purity of lead*

The lead used in these studies was Mallinckrodt lead metal, analytical reagent, and had the following analysis:

Lead	99·9 wt. % min.
Antimony and tin	0·005
Arsenic	0·0001
Bismuth	0·001
Copper	0·003
Iron	0·001
Nickel	0·001
Silver	0·0002
Total known metal impurities	0·0077 wt. %

The remaining impurity was lead oxide. Since the measurements were performed in graphite crucibles at elevated temperatures, the lead oxide was reduced to lead. Thus the purity was 99·99+ per cent lead.

After each experiment the sinker was cleaned free of external lead and then analysed for absorbed lead by treating with dilute nitric acid. Less than 10 mg of lead was absorbed. The sinker was then washed free of acid, dried and reweighed. There was no loss in weight of the graphite sinker, this proved that the lead was saturated with graphite from the boiler *before* immersion of the sinker. The solubility of carbon in liquid lead was measured by RUFF[11] and found to be as follows:

°K	C (%)
1643	0·024
1890	0·046
2024 (b.p.)	0·094

Thus a correction of +0·006 g/cm³ in the density was required at the boiling point and proportionately less at lower temperatures.

RESULTS

Density of $(Pb)_{liq}$ *at b.p. of* Hg. The density was determined in a glass apparatus under reflux of boiling mercury at atmospheric pressure. The same sinker was used as in the high temperature experiments. The density = 10·635 at 629·88°K or = 10·678 g/cm³ at the melting point (600·6°K; 327·4°C).

Density at high temperature. The values obtained for lead at temperatures up to its boiling point are presented in Table 1.

Density equation. The final results were treated by the method of least mean squares. From the equation obtained below, it was evident that the density of lead was a linear function of the temperature.

$$D(g/cm^3) = 10{\cdot}678 - 13{\cdot}174 \times 10^{-4}\,(T - 600{\cdot}6),\ (T \text{ in } °K.).$$

Any deviations from linearity were within experimental error. The average probable error of our measurements was ±0·0027 g/cm³.

The values calculated from the above equation are correlated with the experimental values in Table 1. The atomic volumes and the volume coefficients of expansion are tabulated in Table 2.

[10] D. R. STULL and G. C. SINKE, *Thermodynamic Properties of the Elements, Advances in Chemistry Series* Volume 19. Amer. Chem. Soc. (1956).
[11] O. RUFF and B. BERGDAHL, *Z. Anorg. Chem.* **106,** 91 (1919).

VOL. 22 1961

TABLE 1.—DENSITIES OF LIQUID LEAD

Temperature (°K)	Density (g/cm³)		Exp. − Calc.
	Exp.	Calc.	
1601	9·382	9·362	+0·020
1709	9·216	9·218	−0·002
1807	9·089	9·089	0·000
1840	9·040	9·045	−0·005
1923	8·928	8·936	−0·008
1958	8·872	8·890	−0·018
1961	8·881	8·886	−0·005
1973	8·885	8·870	+0·015

TABLE 2.—ATOMIC VOLUMES AND VOLUME COEFFICIENTS OF EXPANSION OF LIQUID LEAD

T(°K)	D(g/cm³)	Specific volume (cm³/g)	Atomic volume cm³/g-atom	Volume coefficient of expansion $\times 10^6$(°K^{-1}) (cm³/g-atom)
600·6 = m.p.	10 678	0·09365	19·405	123·4
800	10·415	0·09602	19·895	126·5
1000	10·152	0·09850	20·411	129·8
1200	9·888	0·10115	20·956	133·2
1400	9·625	0·10390	21·528	136·9
1600	9·361	0·10683	22·135	140·7
1800	9·098	0·10991	22·775	144·8
2000	8·834	0·11320	23·456	149·1
2024 = N.B.P.	8·803	0·11360	23·539	149·7

DISCUSSION OF LITERATURE DATA AND COMPARISON WITH OUR VALUES

A complete literature survey of the data on liquid lead is given in Table 3 and also in Fig. 1. In the Table the densities are all compared at the melting point. The temperature coefficients are also given; the error in dD/dt depends to a large extent on the temperature range investigated. For purposes of comparison it was assumed that the error in density at the melting point is $\pm 0{\cdot}001$ and at the high temperature end point $\pm 0{\cdot}02$ g/cm³.

Four independent methods were used, i.e., (1) the Archimidean principle, by most observers, (2) the U-tube pressure method (HOGNESS)[16], (3) the maximum bubble pressure,[19,21,22], and (4) the centrifugal casting method (KNAPPWOST[20]). The first two methods are reliable and have a long experimental background. The maximum bubble pressure method was introduced for the density determination of metals by GREENAWAY[19] and gave low values (see Fig. 1); further and more precise measurements by SCHNEIDER and associates,[21,22] over a wider temperature range brought them in agreement with the other good measurements. The latest method, namely, of centrifugally casting a liquid metal into a mold (and determining the weight of metal and volume of cast on cooling) at present gives highly scattered values (see Fig. 1) and will require further study. It will not be included in our averaging procedure.

TABLE 3.—COMPLETE LITERATURE DATA ON THE DENSITY OF LIQUID LEAD (ARRANGED IN CHRONOLOGICAL ORDER)

Authors	Year	Temperature range (°C)		Density at m.p. (g/cm³) = 327·4°C	$-dD/dt \times 10^4$	Error in $-dD/dt \times 10^4$	Method used
VICENTINI[12]	1887–1890	327	0	10·64	—	—	—
PASCAL and JOUNIAUX[13]	1914	327–969	640	10·875	Curve!	—	Archimedean principle
DAY, *et al.*[14]	1914	327–850	525	10·685	11·61	±0·39	Archimedean principle
PLUSS[15]	1915	340	0	10·913	—	—	—
HOGNESS[16]	1921	366–522	155	10·71	13·90	±1·32	U-tube pressure
MATSUYAMA[17]	1929	410–700	290	10·70	13·10	±0·70	
SAEGER[18]	1932	400	0	10·66	—	—	
GREENAWAY[19]	1947	340–440	100	10·55	14·00	—	Maximum bubble pressure
KNAPPWOST[20]	1954	370–490	120	10·785	14·10	(Large scatter	Centrifugal casting
SCHNEIDER[21,22]	1954–1956	400–710	310	10·66	13·26	±0·68	Maximum bubble pressure
This paper	1961	357–1700	1350	10·674	13·17	±0·15	Archimedean principle
Solid[23]				11·079	10·57		

The agreement between most investigators is good not only (1) in the value at the melting point but also (2) in the fact that the density is a straight-line function of temperature. The *slope of the line* of all observers is also in good agreement within the experimental error.

The *only values* in *definite disagreement* are those of PASCAL and JOUNIAUX.[13] They obtained *a curve* (see Fig. 1) with higher density values than those of all of the other investigators; for example, about 4 per cent higher at 600°C. The crude manner with which they heated their lead, namely, a gas burner, may have caused poor temperature control and account for the nonlinear relationship; not enough details are given in their paper, however, to judge this and other error possibilities. JOUNIAUX[24], using the same apparatus many years later to determine the density of liquid

[12] G. VICENTINI and OMODEI, *Atti accad. nazion. dei Lincei* 3 I, 235, 294, 321 (1887); 4 II, 19 39, 75 (1888); 611, 152 (1890).
[13] M. P. PASCAL and A. JOUNIAUX, *C.R. Acad. Sci., Paris* **158,** 414–416 (1914).
[14] A. L. DAY, R. B. SOSMAN and J. C. HOSTETTER, *Amer. J. Sci.* **37,** 1 (1914).
[15] M. PLUSS, *Z. Anorg. Chem.* **93,** 1–45 (1915).
[16] T. R. HOGNESS, *J. Amer. Chem. Soc.* **43,** 1621 (1921).
[17] Y. MATSUYAMA, *Sci. Rep. Töhoku Univ.* 18, 19, 737 (1929).
[18] C. M. SAEGER, *Bur. Stand. J. Res.* **8,** 37 (1932).
[19] H. T. GREENAWAY, *J. Inst. Met.* **74,** 133 (1947).
[20] A. KNAPPWOST and H. RESTLE, *Z. Elektrochem.* **58,** 112–118 (1954).
[21] A. SCHNEIDER, A. STAUFFER and G. HEYMER, *Naturwissenschaften* **41,** 326–7 (1954).
[22] A. SCHNEIDER and G. HEYMER, *Z. Anorg. Chem.* **286,** 118–135 (1956).
[23] *U.S. Bur. Stand. Circ.* 447, Washington, D.C. (1943).
[24] A. JOUNIAUX, *Bull. Soc. Chim. France,* **51,** 677–81 (1932).

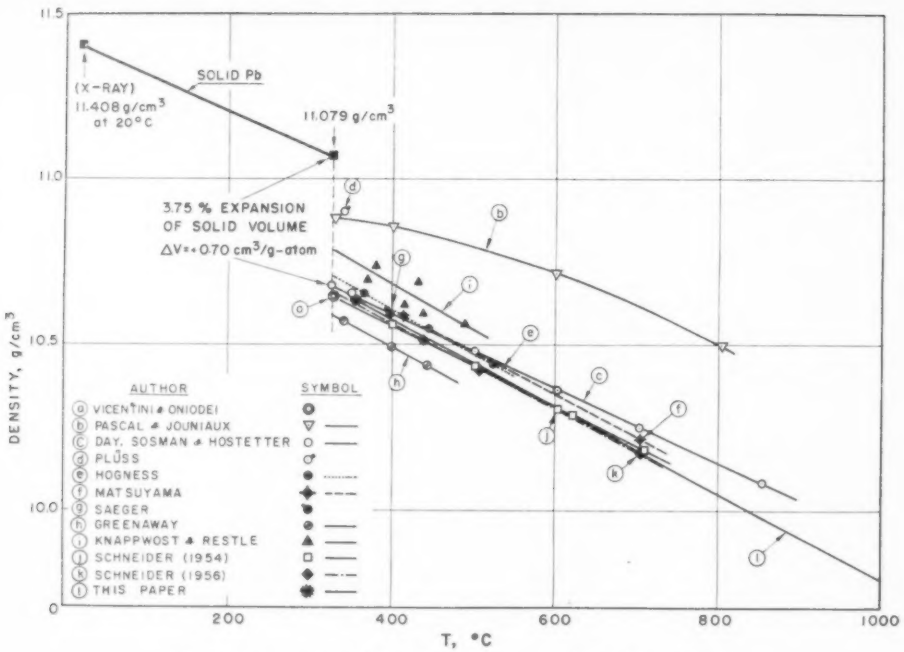

FIG. 1.—Comparison of literature data on densities of liquid lead.

bismuth, obtained a straight-line relationship between 420–1100°C, in complete agreement with HOGNESS,[16] while *a curve* was obtained from 420°C down to the melting point.

The average of all the density values of liquid lead at the melting point given in Table 3, excluding only the single value of PLUSS and the data of GREENAWAY and PASCAL, for reasons given above, is $10{\cdot}678 \pm 0{\cdot}021$ g/cm³. This is in excellent agreement with our value of 10·674.

The average value of the temperature coefficient, of particular interest to us, is $-12{\cdot}97\ (\pm 0{\cdot}77) \times 10^{-4}$ g/cm³ . °K. This value is also in good agreement with our value of $-13{\cdot}17\ (\pm 0{\cdot}15) \times 10^{-4}$ which was obtained over a temperature range from the melting point to the normal boiling point, when an absolute error of $\pm 0{\cdot}02$ g/cm² at the normal boiling point was assumed.

Acknowledgement—The authors wish to thank Mr. W. J. LIDDELL for his help with the design and construction of the apparatus.

J. Inorg. Nucl. Chem., 1961, Vol. 22, pp. 39 to 48. Pergamon Press Ltd. Printed in Northern Ireland

THERMAL DECOMPOSITION OF THE LIGHT RARE EARTH OXALATES

A. GLASNER and M. STEINBERG
Department of Inorganic and Analytical Chemistry,
The Hebrew University of Jerusalem, Israel

(*Received* 31 *January* 1961; *in revised form* 9 *April* 1961)

Abstract—The thermal decomposition of the light rare earth oxalates was studied in vacuum in the temperature range 340–440°C. The behaviour of the whole group (with the exception of europium oxalate) was analogous to that of lanthanum oxalate.[1] The relative order of stability, as well as that of the intermediate normal and basic carbonates, is: Gd > Sm > Nd > La > Pr > Ce.

The carbon monoxide, initially formed by the decomposition of the oxalates, underwent disproportionation. The degree of disproportionation was highest in the case of cerous oxalate (72 per cent), and lowest in the case of gadolinium oxalate (58 per cent), decreasing in reverse of the order of stability, with lanthanum and praseodymium changing places.

VOL. 22 1961

THE thermal decomposition of lanthanum oxalate was described in a previous article.[1] When heated in vacuum, the light rare earth oxalates, except for europium oxalate, behaved similarly. In air, cerous oxalate also differed from the other members of the group, decomposing at a much lower temperature,[2,3] while being oxidized simultaneously to CeO_2. A study of the thermal decomposition of erbium and lutetium oxalates[4] revealed that the normal carbonates of these elements are less stable than the carbonates of the lighter rare earths, thereby complicating the interpretation of the gasometric measurements. The behaviour of ytterbium(III) oxalate is similar to that of europium oxalate,[4] both cations being reduced (in vacuum) to the divalent state

This article reports and compares results obtained with the light rare earth oxalates (except europium); well-defined regular variations of properties from member to member in the group are shown.

EXPERIMENTAL

The various oxalates were prepared by precipitation[5,6] from solutions of the oxide, or a salt (Lindsay, 99·9 per cent) in dilute nitric acid. The precipitate consisted of fine grains of the order of 5 μ diameter, as measured on a magnified photoprint (×360). In some experiments the original Lindsay rare earth oxalate powders were used.

Dehydration was effected by heating in vacuum at 300°C, for a few hours.[2] Continued heating for 24 hr resulted, in some cases, in a faint colouring and a small increase of pressure in the vacuum apparatus. In the following experiments care was taken to use only such samples as did not show an initial decomposition. Lindsay oxalates gave identical results with our own preparations.

Samples of the dehydrated oxalates weighing 6–12 mg were heated in vacuum (about one μ initial pressure) at a constant temperature (320–440°C), and the increasing pressure was recorded at

[1] A. GLASNER and M. STEINBERG, *J. Inorg. Nucl. Chem.* **16**, 279 (1961).
[2] A. GLASNER and M. STEINBERG, *Bull. Res. Council, Israel* **8 A**, 174 (1959).
[3] P. CARO and J. LORRIERS, *J. Rech.* No. **39**, 107 (1957).
[4] A. GLASNER, M. STEINBERG and E. LEVY. Unpublished data.
[5] A. GLASNER, M. STEINBERG and E. LEVY, *Chem. Analyt.* **48** 37 (1959).
[6] V. GILPIN and W. C. MCCRANE, *Analyt. Chem.* **24**, 225 (1952).

frequent intervals, until the evolution of gases ceased. One or two hours later, the partial pressure of the carbon dioxide was determined by condensing it in liquid air traps. Lastly, the silver crucible with the solid residue was removed from the reaction vessel and reweighed. The observed loss of weight could be compared to the calculated weight of the evolved gases. The correspondence was mostly quite satisfactory, within 0·1 mg, but occasionally larger deviations were observed. These might have been caused by accident; for example, a speck of grease, from the ground glass, might have adhered to the silver crucible on its removal from the reaction vessel.

Infra-red spectra of a large number of the solid residues were taken by the potassium bromide disk method, whereby the presence or absence of oxalate or carbonate ions was observed.

All residues were coloured more or less dark brown, by dispersed carbon formed during the thermal decomposition.

The vacuum apparatus and the various techniques employed have already been described.[1]

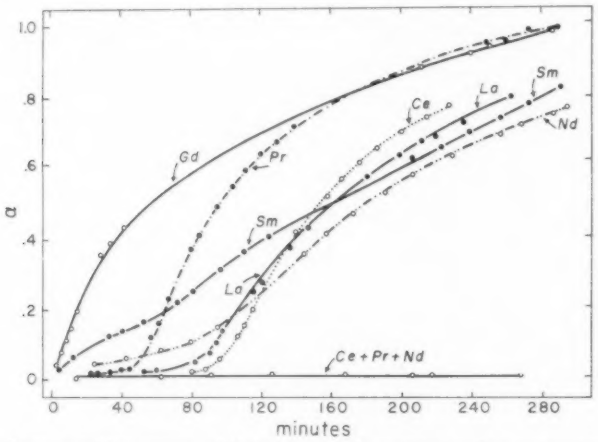

FIG. 1.—Decomposition curves of light rare earth oxalates at low temperatures showing induction periods. La, Ce, Pr and Nd at 340°C; Sm at 360°C; Gd at 375°C. Curve parallel to abscissa indicates "no decomposition" with experiments at 320°C.

RESULTS

Decomposition curves and induction periods

None of the light rare earth oxalates showed any appreciable decomposition when heated in vacuum at 320°C, for 6 hr or more. As a rule, decomposition started at 340°C after an induction period, most prolonged in the case of the cerium oxalate (90 min). The length of the induction period decreased as the atomic number of the rare earth element increased, as well as with rise of temperature. This is shown in Fig. 1, which presents fraction α of the final pressure at time t min. Indeed, with neodymium oxalate the induction period converted into a rather slow initial reaction, and with gadolinium oxalate, it could not be observed at all. The decomposition curve of samarium oxalate at the lowest temperature observed (360°C) is somewhat irregular. There is circumstantial evidence of the length of the induction periods being connected with traces of water retained by the various oxalates, decomposition starting only after these have been driven off. The evolution of the last traces of water could occasionally be observed on the pressure gauge, which indicated a temporary rise of pressure before the water vapour was condensed by the dry-ice-acetone traps. This was often the case with the cerous oxalate samples, as may be seen on the curve presenting a run at 375°C (see inset, Fig. 2).

The rates of decomposition decreased the greater the atomic number, thus causing intersection of the decomposition curves. The lowest temperature at which gadolinium oxalate decomposed was 375°C. Clearly, the light rare earth oxalates, from cerium to gadolinium, are the more stable the higher their atomic number. This is also illustrated in Fig. 2, giving a collection of typical decomposition curves to the respective carbonates. The stability of lanthanum oxalate, for which decomposition curves have already been given[1] in the 340–420° temperature range, is between that of praseodymium and neodymium.

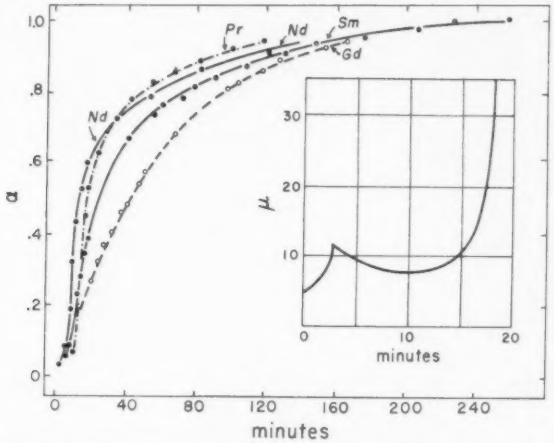

FIG. 2.—Decomposition curves of light rare earth oxalates at intermediate temperatures. Pr at 375°C; Nd, Sm and Gd at 391°C.
Inset shows temporary rise of pressure μ caused by presence of residual water in $Ce_2(Ox)_3$, 375°C.

Composition of the solid residues and the evolved gases

Tables 1–5 give experimental data and some of the conclusions arrived at. For the sake of easy comparison, the partial pressures actually measured were converted into pressures corresponding to samples of *standard* weight, i.e. mole per cent of

TABLE 1.—FINAL COMPOSITION OF GASES AND SOLID RESIDUE OBTAINED ON HEATING $Ce_2(C_2O_4)_3$ IN VACUUM

°C	Wt. of sample	Mole % of gases evolved		*R*	Comp.	Loss of wt. (mg)	
		CO	CO_2			Exp.	Calc.
341	6·62	26·0	34·1	1·31	B	1·00	0·80
360	8·53	26·5	42·7	1·39	B	1·57	1·22
375	6·24	28·0	58·0	1·30	C	1·15	1·13
391	12·84	30·0	57·0	1·17	C	2·61	2·33
410	10·18	26·7	51·6	1·38	C	2·44	1·66
420	8·58	30·2	68·2	1·16	D	2·36	1·79

4·30 mg $Ce_2(C_2O_4)_3$ + 3% aq ≡ 100 μ CO
B = $Ce_2(CO_3)_3$; C = $Ce_2O_{0\cdot6}(CO_3)_{2\cdot4}$; D = $Ce_2O(CO_3)_2$

TABLE 2.—FINAL COMPOSITION OF GASES AND SOLID RESIDUE OBTAINED ON HEATING $Pr_2(C_2O_4)_3$ IN VACUUM

°C	Wt. of sample	Mole % of gases evolved		*R*	Comp.	Loss of wt. (mg)	
		CO	CO_2			Exp.	Calc.
340	8·38	23·0	21·1	0·92	A	0·74	0·73
360	9·27	32·5	38·0	1·04	B	1·10	1·19
375	5·86	28·6	44·4	1·25	B	0·90	0·91
391	8·86	33·6	52·1	1·00	C	1·8	1·6

4·20 mg $Pr_2Ox_3 \equiv 100\ \mu$ CO

A = $Pr_2(C_2O_4)(CO_3)_2$; B = $Pr_2(CO_3)_3$; C = $Pr_2O_{0\cdot6}(CO_3)_{2\cdot4}$

TABLE 3.—FINAL COMPOSITION OF GASES AND SOLID RESIDUE OBTAINED ON HEATING $Nd_2(C_2O_4)_3$ IN VACUUM

°C	Wt. of sample	Mole % of gases evolved		*R*	Comp.	Loss of wt. (mg)	
		CO	CO_2			Exp.	Calc.
340	9·31	14·35	12·30	0·86	A_0	0·45	0·486
360	8·76	25·58	23·75	0·93	A	0·75	0·853
375	4·93	24·28	20·65	0·85	A	—	—
391	6·83	30·45	41·94	1·14	B	0·82	1·015
420	10·10	36·98	50·84	0·85	C	2·64	1·9

4·24 mg $Nd_2Ox_3 \equiv 100\ \mu$ CO

A_0 = $Nd_2(C_2O_4)_{1\cdot8}(CO_3)_{1\cdot2}$; A = $Nd_2(C_2O_4)(CO_3)_2$; B = $Nd_2(CO_2)_3$; C = $Nd_2O_{0\cdot6}(CO_3)_{2\cdot4}$

TABLE 4.—FINAL COMPOSITION OF GASES AND SOLID RESIDUE OBTAINED ON HEATING Sm_2Ox_3 IN VACUUM

°C	Wt. of sample	Mole % of gases evolved		*R*	Comp.	Loss of wt. (mg)	
		CO	CO_2			Exp.	Calc.
360	14·50	23·93	17·95	0·75	A	1·03	1·148
375	5·70	32·80	39·58	1·02	B	0·70	0·819
391	11·69	40·06	26·34	0·66	B	1·56	1·450
400	9·18	34·49	38·26	0·95	B	1·30	1·314
420	8·83	42·25	48·63	0·70	C	1·58	1·63
440	7·14	37·06	58·33	0·85	D	1·39	1·385

4·34 mg $Sm_2Ox_3 \equiv 100\ \mu$ CO

A = $Sm_2(C_2O_4)_{1\cdot2}(CO_3)_{1\cdot8}$; B = $Sm_2(CO_3)_3$; C = $Sm_2O_{0\cdot6}(CO_3)_{2\cdot4}$

D = $Sm_2O(CO_3)_2$

gases evolved. This was done by assuming that decomposition proceeded according to the simple equations (a) and (b):

$$M_2(C_2O_4)_3 \rightarrow M_2(CO_3)_3 + 3CO \quad \text{(a)}$$

$$M_2(CO_3)_3 \rightarrow M_2O_3 + 3CO_2 \quad \text{(b)}$$

TABLE 5.—FINAL COMPOSITION OF GASES AND SOLID RESIDUE OBTAINED ON HEATING Gd_2Ox_3 IN VACUUM

°C	Wt. of sample	Mole % of gases evolved		R	Comp.	Loss of wt. (mg)	
		CO	CO_2			exp.	Calc.
375	5·32	33·3	33·4	1·00	B	0·56	0·67
391	13·20	38·7	27·3	0·71	B	1·73	1·59
400	9·02	43·3	36·9	0·65	B	—	1·315
420	6·10	40·0	41·5	0·75	C	1·30	0·95
440	3·00	40·0	58·5	0·75	D	0·60	0·585

4·44 mg $Gd_2Ox_3 \equiv 100\ \mu$ CO

B = $Gd_2(CO_3)_3$; C = $Gd_2O_{0.6}(CO_3)_{2.4}$; D = $Gd_2O(CO_3)_2$

and the *standard* weight for each oxalate was calculated to yield 100 μ of carbon monoxide and of carbon dioxide with the vacuum apparatus at room temperature. The reader may revert to the actually measured values by simple calculation: for example, if the mole per cent of CO from $Ce_2(Ox)_3$ at 341° is recorded as 26·0, the actual partial pressure measured was this value multiplied by the weight of the sample and divided by the standard weight for $Ce_2(Ox)_3$, i.e. $(26{\cdot}0 \times 6{\cdot}62)/4{\cdot}30 = 40{\cdot}0\ \mu$. Similarly, the measured partial pressure of CO_2 was: $(34{\cdot}1 \times 6{\cdot}62)/4{\cdot}30 = 52{\cdot}5\ \mu$.

The pressure of carbon monoxide was higher than that of carbon dioxide in the case of the cerium oxalate, and also in the case of the other four rare earth oxalates, in runs made at higher temperatures. Hence, the source of the carbon dioxide could not be reaction (b) *only*, but, as already proved in the case of lanthanum oxalate,[1] it originated from a disproportionation of the carbon monoxide formed in reaction (a):

$$2CO \rightarrow CO_2 + C \qquad (c)$$

This conclusion is corroborated by: (1) the low percentage of carbon monoxide obtained in any one of the runs (25–40 per cent), (2) infra-red absorption spectra characteristic of the presence of carbonates, (3) the brown colour of the solid residues due to dispersed carbon.

The columns headed by R in Tables 1–5 give the ratio of the partial pressure of carbon dioxide from the Boudouard reaction (c) to that of the remaining carbon monoxide. The column headed "Comp." gives the best approximate composition of the solid residues.

(a) *Cerous oxalate.* The percentage of carbon monoxide obtained over the whole range of temperatures is almost constant (26–30 per cent); the percentage of carbon dioxide, on the other hand, increases in definite steps with the rise of temperature (see Table 1). Clearly, 74–70 per cent of the carbon monoxide originally formed is converted into 37–35 per cent of carbon dioxide by disproportionation. The solid residues obtained at 341° and 360°C are therefore assumed to be the normal carbonate $Ce_2(CO_3)_3$: the reaction is not quite complete at the lower temperature, but the percentage of carbon dioxide at 360°C indicates a slight decomposition of the carbonate, too.

In the 375–410°C temperature range, the carbon dioxide evolved amounts to an

additional 20 per cent, and at 420°C to about 33 per cent more. Hence, the composition of the solid residues at the above temperatures should be: $Ce_2O_{0\cdot6}(CO_3)_{2\cdot4}$ and $Ce_2O(CO_3)_2$ respectively, the first being typical for the intermediary decomposition products of all the light rare earth oxalates.

In the case of cerous oxalate, the experimentally ascertained loss of weight was inadvertently greater than that calculated. This was due to traces of water tenaciously retained by the dehydrated salt, estimated at 3 per cent by weight.

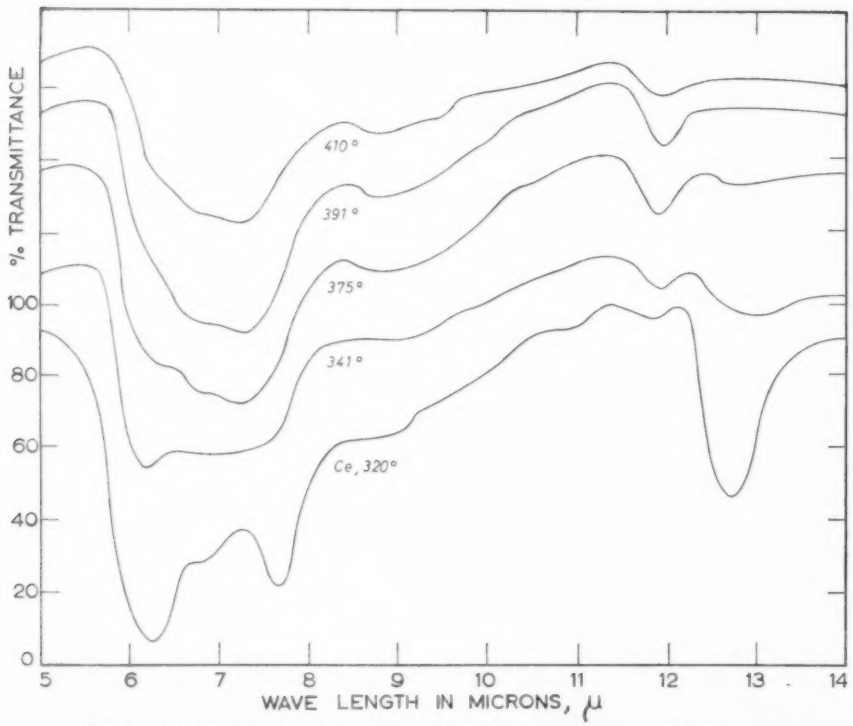

FIG. 3.—Infra-red spectra of $Ce_2(Ox)_3$ residues obtained at the temperatures indicated.
The absorption due to an oxalate is transformed into that due to a carbonate with rise of temperature.
The scale on the ordinate has been shifted upwards for each successive spectrum.

Fig. 3 shows a series of infra-red absorption spectra of the solid residues obtained at various temperatures. The sample heated at 320° gives three distinct absorption bands at $\lambda = 6{\cdot}25$, $7{\cdot}65$ and $12{\cdot}7\ \mu$, characteristic of an oxalate.[7] The spectrum of the 341° sample is somewhat blurred, indicating the presence of residual oxalate ions. The spectra of the 375°, 391° and 410° samples, on the other hand, show a broad band peaking at about $7{\cdot}3\ \mu$ and another one at $11{\cdot}9\ \mu$, indicating the absence of oxalate, and the presence of carbonate ions. The infra-red spectra are thus seen to be in complete accord with the interpretation of the results presented in Table 1. The topmost curve in Fig. 4 is that of a calcium carbonate[7] sample, obtained by heating

[7] J. M. HUNT, M. P. WISHERD and L. C. BONHAM, *Analyt. Chem.* **22**, 1478 (1950); F. A. MILLER and C. A. WILKINS, *Ibid.* **24**. 1253 (1952).

calcium oxalate at 440°C in vacuum. The calcium carbonate residue was also brown and the ratio R was equal to 0·4.

(b) *Praseodymium oxalate.* As shown in Table 2, praseodymium, at 340°C, gives a mixed oxalate–carbonate of the approximate composition: $Pr_2(C_2O_4)(CO_3)_2$. The normal carbonate is formed at 360° and 375°C, and the basic carbonate $Pr_2O_{0·6}(CO_3)_{2·4}$ at 391°C. About two thirds of the primarily formed carbon monoxide undergoes disproportionation. Results with praseodymium oxalate at 400–420°C are not

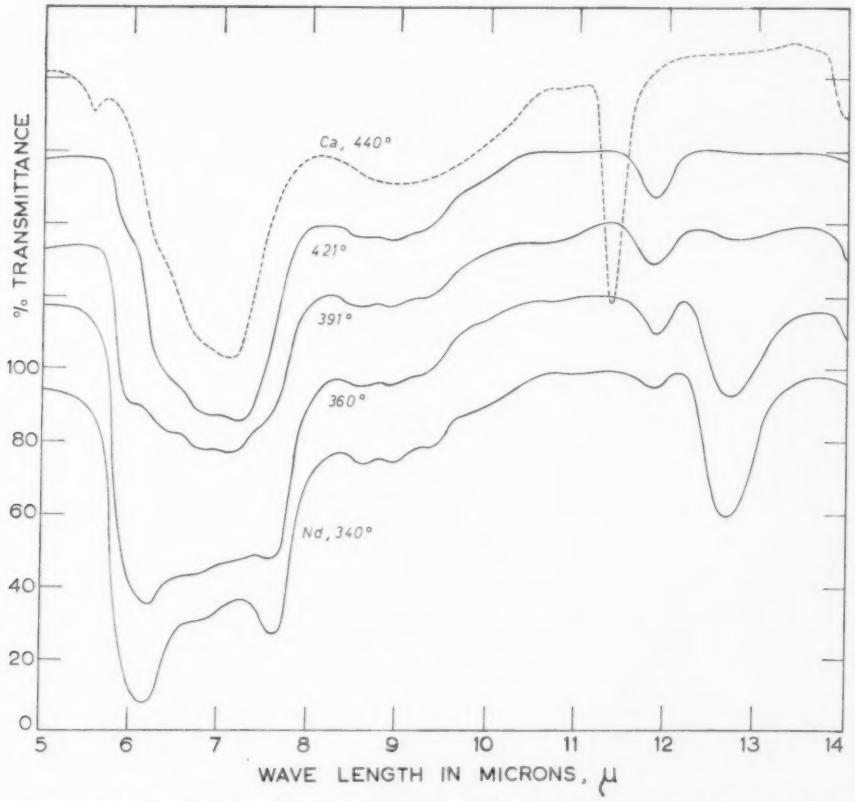

FIG. 4.—Infra-red spectra of $Nd_2(Ox)_3$ residues obtained at the temperatures indicated. The topmost spectrum in that of a $CaCO_3$ obtained by heating CaOx in vacuum at 440°C. The scale on the ordinate has been shifted upwards for each successive spectrum.

recorded in the Table, as many of the experiments were spoiled by spitting, making a quantitative evaluation impossible.

(c) *Neodymium oxalate.* Neodymium gives partly decomposed oxalate–carbonate intermediates up to 375°C (Table 3), and the first basic carbonate $Nd_2O_{0·6}(CO_3)_{2·4}$ is obtained at 420°C. About 63·5 per cent of the carbon monoxide undergoes disproportionation. The composition of the intermediates, derived from the gasometric measurements, were confirmed by the infra-red spectra of the solid residues (see Fig. 4).

It should be remarked that GÜNTHER and REHAAG[8], on heating neodymium

[8] P. L. GÜNTHER and H. REHAAG, *Ber. Dtsch Chem. Ges.* **71 B**, 1771 (1938).

oxalate at 340°C, obtained a brown residue to which they attributed the formula $Nd_2(O_2)(C_2O_4)_2$, containing peroxidic oxygen. Although their interpretation of the constitution of the residue is incorrect,[1] the stoichiometric combination is the same as the oxalate–carbonate intermediate obtained by us at 360–375°C.

(d) *Samarium oxalate*. Samarium oxalate seems to be somewhat more stable than its antecedents and decomposition sets in at 360°C (Table 4), yielding a mixed oxalate–carbonate. The percentage of carbon monoxide obtained fluctuates in a wider range (33–42 per cent) than in the case of the other oxalates studied. Taking the mean value of $R = 0{\cdot}82$, one would expect the evolution of 38 per cent carbon monoxide and 31 per cent carbon dioxide when $Sm_2(CO_3)_3$ is formed. The best approximation for the composition of the various intermediates is therefore that given in Table 4. It should, however, be remarked that the infra-red spectrum of the solid residue obtained at 391° indicates the presence of some traces of oxalate.

(e) *Gadolinium oxalate*. No decomposition of gadolinium oxalate could be observed at 360°, or at lower temperatures. The solid residues obtained in the range 375–440°C appear to have similar compositions to those of samarium oxalate, but disproportionation of the carbon monoxide is somewhat less, the ratio R being 0·72.

DISCUSSION

The results presented here indicate the behaviour and stability of the light rare earth oxalates and the intermediate carbonates into which they decompose, in a critical range of temperatures; it was shown that they exhibit small quantitative but regular changes of properties. The lowest temperature at which decomposition was observed was 340°C in the case of most of the oxalates studied, but the minimum temperature rose gradually to 375°C in the case of gadolinium oxalate. Generally speaking, this is in agreement with published observations obtained by the thermogravimetric method,[9,10,11] but Duval as well as Wendlandt have occasionally recorded higher temperatures for the beginning of decomposition for one or other rare earth oxalate. The discrepancies in the thermogravimetric observations are evidently due to the continuous rise of temperature, which overrides the induction periods. This characteristic of the thermogravimetric method also renders it unsuitable for the discovery of intermediates, which are stable in narrow temperature ranges; the only indication of these intermediates is an occasional change in the slopes of the thermograms.

In this work, a whole array of intermediates was obtained, in addition to the basic carbonate with the general formula $M_2O_2(CO_3)$ indicated in the literature. Furthermore, cerous oxalate was shown to decompose in vacuum in similar fashion to the other light rare earths, whilst in air CeO_2 is obtained at a rather low temperature.[2,12] Yet it is interesting to note that the oxidizability of cerium and praseodymium makes the oxalates of these elements the least stable in the group, when even heated in vacuum.

The compositions of the intermediates were calculated from the partial pressures (and percentages) of carbon monoxide and carbon dioxide given in Tables 1–5, and

[9] C. DUVAL, *Inorganic Thermogravimetric Analysis*, pp. 400–416. Elsevier, Amsterdam (1953).
[10] W. W. WENDLANDT, *Analyt. Chem.* **30**, 58 (1958); **31**, 408 (1959).
[11] V. M. PADMANAHHAN, S. C. SARAIYA and A. K. SUNDARAM, *J. Inorg. Nucl. Chem.* **12**, 356 (1960).
[12] R. P. AGARWALA and M. C. NAIK, *Anal. Chim. Acta* **24**, 128 (1961).

confirmed qualitatively by the infra-red spectra of the solid residues. These calculations were based on the observation that the ratio R (representing the extent of carbon monoxide disproportionation) is very nearly constant for each rare earth oxalate. For example, in the case of cerous oxalate the extreme values of R were 1·16–1·39, corresponding to a disproportionation of 70–73·6 per cent of the carbon monoxide. In some cases regular deviations may be observed. Of these, the greater percentage of CO_2 obtained with samples of a smaller weight than with those of a larger sample should be mentioned. (Compare: Table 1, 375° and 391°; Table 2, 360° and 375°; Table 4, 375° and 391°; Table 5, 375° and 391°). However, the conclusion that the pressure of CO_2 in the system affects either the disproportionation of the CO, or the

TABLE 6.—TEMPERATURES, °C, AT WHICH THE STABLE INTERMEDIATES WERE PRODUCED, AND THE RATIO R

	A	B	C	D	R
La	340	360–391	410	420	1·20
Ce	—	340–360	375–410	420	1·30
Pr	340	360–375	391	—	1·05
Nd	340–375	391	420	—	0·93
Sm	360	375–400	420	440	0·82
Gd	—	375–400	420	440	0·77

$A = M_2(C_2O_4)(CO_3)_2$; $B = M_2(CO_3)_3$; $C = M_2O_{0\cdot6}(CO_3)_{2\cdot4}$; $D = M_2O(CO_3)_2$; $R = \frac{\mu CO_2}{\mu CO}$

decomposition of the carbonate, is not altogether justified in view of the inherent errors in pressure measurement as well as accidental incomplete condensations of CO_2 from the CO/CO_2 mixtures. Such errors are often made evident by comparing the calculated loss of weight with that actually observed, the former being larger when the partial pressure of CO_2 appears to be too great (for example Table 3, 391°; and Tables 4–5, 375°) and vice versa (for example, Table 1, 391° and 420°; Tables 4–5, 391°). Thus, quite often the "loss of weight" reveals that the deviations in either R or "Composition" are due to an experimental error in the gasometric measurements.

Table 6 lists the temperatures at which the various intermediates were obtained, together with mean R values (including results from experiments with lanthanum oxalate). As a rule the order of variations is the same whichever property is considered, namely: Gd → Sm → Nd → La → Pr → Ce.

The relative stability of the oxalates. This may be judged by the lowest temperature at which decomposition begins, or the highest temperature at which a mixed oxalate–carbonate intermediate is obtained. No such intermediate was observed in the case of cerium, which decomposed at 340°C into the normal carbonate, and also in the case of gadolinium, which did not decompose at a temperature below 375°C. The extreme stability of neodymium oxalate–carbonate is somewhat exceptional.

The relative stability of the carbonates. The normal carbonates are stable about 30°C above the temperature of complete decomposition of the oxalates, the temperatures of decomposition decreasing in the order given above. This is in agreement with data recently published by Russian investigators[13] on the thermal decomposition

[13] M. N. AMBROZHII, E. F. LUCHNIKOVA and M. I. SIDORAVA, *Zh. Neorg. Khim.* **5**, 366 (1960).

of the light rare earth carbonates. The same authors also indicate that intermediate basic carbonates are stable up to 570–670°C.

In the present work two basic carbonates, $M_2O_{0\cdot6}(CO_3)_{2\cdot4}$ and $M_2O(CO_3)_2$ (not recorded in the literature) were obtained. The first of these is remarkable for its recurrence with each of the six members of the group.

The stabilities of the oxalates, as well as the carbonates, are thus seen to increase with decreasing radii, with the exception of cerium and praseodymium, which tend to pass to a higher valency. Hence a partial covalency between the tervalent rare earths and the oxy-anions is indicated.

The extent of disproportionation of carbon monoxide. The *R* values giving the ratio of carbon dioxide to carbon monoxide increase in the same order as the stabilities decrease, except that praseodymium and lanthanum change places. No reason for this correlation is suggested for the time being.

Acknowledgements—The authors wish to espress their thanks to Dr. L. BEN-DOR and Mrs. H. FEILCHENFELD for recording the infra-red spectra. They are also indebted to Messrs. Lindsay Chemical Co. for a supply of some of the rare earth oxides.

J. Inorg. Nucl. Chem., 1961, Vol. 22, pp. 49 to 54. Pergamon Press Ltd. Printed in Northern Ireland

THE REDUCTION OF ZIRCONIUM(IV) IODIDE*

G. W. WATT and W. A. BAKER, JR.
Department of Chemistry, The University of Texas, Austin 12, Texas

(*Received* 17 *January* 1961; *in revised form* 22 *May* 1961)

Abstract—The reduction of ZrI_4 with Al to ZrI_3 in high yields and high purity under conditions that essentially eliminate product contamination with Al is described; limited evidence for reduction to ZrI_2 is included. Similar reduction with other metals that form volatile iodides (Fe, Ge, Hg) is also described. The reduction of ZrI_4 to Zr or conversion of ZrI_4 to ZrO_2 in electrodeless discharges in different gaseous atmospheres is described and the results are compared with those from related work.

VOL. 22 1961

RECENT evidence of continued interest in the lower iodides of zirconium[1,2] prompts us to report some results of experiments carried out several years ago and concerned with the reduction of zirconium(IV) iodide under a rather wide variety of conditions. Although these studies were discontinued following publication of work[3] that either duplicated or anticipated our experiments, we nevertheless report here results that were obtained under novel conditions or that relate to methods previously employed in the reduction of zirconium halides other than the iodide.

EXPERIMENTAL

Materials

Unless otherwise indicated, all chemicals employed in this work were reagent grade materials that were dried thoroughly prior to use.

Zirconium(IV) iodide. Attempts to prepare ZrI_4 from ZrO_2, C, and I_2, i.e., a procedure analogous to that used by HONIGSCHMIDT[4] and by RUFF and WALLSTEIN[5] in the synthesis of the corresponding bromide and chloride, were unsuccessful despite variation of reactant mole ratios, temperature, and pressure over wide ranges.

The iodide was prepared in high yield and high purity as follows. Approximately 1·5 g of Zr powder was supported on a fritted glass disc in a vertical 25 mm i.d. Pyrex tube, the top of which was attached to a series of traps connected by ball-joints and vacuum stopcocks. The tube was heated by resistance wire and iodine carried in dry helium was admitted at the bottom of the tube. Although reaction was observed at temperatures as low as 150°, more rapid conversion occurred at 400°† and a pressure of ca. 25 mm. The product was sublimed into the traps by heating the connecting tube with a burner flame; the total reaction time was $\leqslant$4 hr. After all of the zirconium was consumed, the traps were heated to 50° at 10^{-2} mm for 1 hr to remove excess iodine, the connecting stopcocks were closed and the traps (under reduced pressure) were transferred to the dry-box for removal of the product in a dry helium atmosphere. (Found: Zr, 15·3; I, 84·9. Calc. for ZrI_4: Zr, 15·2; I, 84·8%). The yields ranged from 90 to 95 per cent based on Zr used and the product consisted of orange-red or yellow powder, depending upon particle size. The X-ray diffraction data for this product were in all respects identical with those for HfI_4.[6,7]

* This work was supported in part by the U.S. Atomic Energy Commission, Contract AT-(40-1)-1639.

† The same reactants were used by LARSEN and LEDDY[3] at 500° and by NEWNHAM and WATTS[4] at 750°. In neither case however are other details of the synthesis reported.

(1) F. I. BUSOL, *Zh. Fiz. Khim.* **33,** 799 (1959).
(2) I. E. NEWNHAM and J. A. WATTS, *J. Amer. Chem. Soc.* **82,** 2113 (1960); cf., I. E. NEWNHAM, *Proc. Australian Atomic Energy Symposium*, 128 (1958).
(3) E. M. LARSEN and J. J. LEDDY, *J. Amer. Chem. Soc.* **78,** 5983 (1956).
(4) O. HONIGSCHMIDT, *Z. Anorg. Chem.* **139,** 293 (1924).
(5) O. RUFF and R. WALLSTEIN, *Z. Anorg. Chem.* **128,** 96 (1923).
(6) B. KRAUSE, A. B. HOOK, F. WAWNER and H. ROSENWASSER, *Analyt. Chem.* **32,** 1210 (1960).
(7) W. KLEMM, E. HOLZE and W. BASUALDO, Congr. intern. chim. pure et appl., 16e, Paris 1957, Mém. sect. chim. minerale, 43 (1958).

Tin(II) iodide. This compound was prepared as described by LISTER and SUTTON.[8]

p-Chloromandelic acid. This reagent, used in the quantitative determination of zirconium, was prepared by the method of JENKINS.[9]

Analytical methods

With one exception, standard methods were employed.

Several methods for the determination of zirconium were examined and the following modification of the procedure of KLINGENBERG and PAPUCCI[10] was found to give the best precision and accuracy.

The solution containing zirconium was evaporated to dryness, the residue was warmed with concentrated hydrochloric acid until dissolution was complete, and cooled to room temperature. An aqueous 0·160 N solution of p-chloromandelic acid (29 g/l.) was added to the extent of 20 ml/100 mg of (estimated) zirconium present plus 35 ml in excess. The resulting precipitate was digested for 30–45 min on a steam bath, cooled to 20°, filtered, dried and ignited in a silica crucible at 800° and weighed as ZrO_2.

Electrodeless discharge equipment

Reactions of ZrI_4 in a variety of gaseous atmospheres were studied using a horizontal Pyrex discharge tube (20 mm × 12 in) each end of which was fitted with standard taper joints and stopcocks so that the tube could be removed to the dry-box for removal of reaction products in an inert atmosphere. A U-shaped side arm, one end of which terminated in a bulb of about 5 ml capacity was sealed to the discharge tube near one end and served as a container for ZrI_4. This side arm was wrapped with nichrome wire and asbestos and was provided with a thermocouple. At the upstream end of the discharge tube, buoyancy type flow-meters were provided to control gas flow-rates. The downstream end was connected to a series of product collection traps, vacuum pumps and a McLeod gauge. Product traps were designed for removal to the dry-box and, during operation, were cooled with ice, isopropanol–dry-ice mixtures, and liquid air.

The discharge tube was placed inside the output coil of a simple radio frequency oscillator that supplied the energy for the discharge and consisted of a self-driven 813 tube and inductance feedback. The plate voltage was furnished by a 500 W power supply and controlled by means of a variac; the screen voltage of 300 V was fed off the same supply through a dropping resistor. The output coil was made removable so that the frequency could be easily changed by changing coils. Most of the experiments were done at 12·2 mc/s and a plate voltage of 1500 V. At this voltage the 813 tube has a rated output of 175 W, and the power input to the gas during the discharge process was determined to be 35 ± 5 W.

The procedure for use of this equipment was as follows. The gas flow system was maintained at 10^{-3} mm, the discharge tube was degassed by heating with a burner flame, filled with dry helium and removed to the dry-box where a weighed sample of ZrI_4 was charged to the side arm bulb. The discharge tube was reconnected, evacuated and the particular gas to be used in the experiment was allowed to flow through the entire system. The flow rate and pressure were adjusted until an intense and steady discharge was maintained in the substrate gas. Thereupon, the side arm bulb containing the ZrI_4 was heated to a temperature just sufficient to maintain a steady flow of ZrI_4 gas into the discharge tube. The time required for the transfer of a few hundred milligrams of ZrI_4 ranged from 4 to 8 hr.

Reduction with metals that form volatile iodides

Aluminium. In a typical case, 6·1087 g of ZrI_4 and 0·0500 g of Al (ZrI_4/Al = 5·5/1 were placed in a thoroughly degassed heavy wall 8 mm i.d. Pyrex tube. After reducing the pressure in the tube to 10^{-3} mm it was sealed and heated in a furnace at 300° for four weeks, with intermittent agitation of the reaction mixture. The tube was opened in the dry-box and the contents transferred to another tube for sublimation at 325° and 10^{-3} mm. X-ray diffraction data established that the sublimate consisted of (only) ZrI_4 and AlI_3. The red-brown solid residue (1·0717 g) was treated with water and 21·9 cm^3 of resultant hydrogen was collected. The grey water-insoluble solid product (0·0341 g) was removed by filtration and identified as aluminium by its X-ray diffraction pattern. The filtrate and

[8] M. W. LISTER and L. E. SUTTON, *Trans. Faraday Soc.* **37**, 406 (1941).
[9] S. S. JENKINS, *J. Amer. Chem. Soc.* **53**, 2341 (1931).
[10] J. J. KLINGENBERG and R. A. PAPUCCI, *Analyt. Chem.* **24**, 1861 (1952); cf. **25**, 1758 (1953); **27**, 835 (1955).

washings was analysed for zirconium and iodine. (Found: Zr, 19·1; I, 81·1%; (I/Zr = 3·07/1). Calc. for ZrI_3: Zr, 19·3; I, 80·7%). Assuming the reaction: $3ZrI_4 + Al \rightarrow 3ZrI_3 + AlI_3$, the yield of ZrI_3 was 31·3 per cent and the anticipated volume of hydrogen upon reaction of the sublimation residue with water was 24·6 cm^3. X-ray diffraction data from a pattern obtained for the original sublimation residue are given (less lines attributable to Al) in Table 1. These data are in good agreement with data obtained from LARSEN.[11] In two strictly analogous experiments employing initial ZrI_4/Al ratios of 3/1 and reaction times of 3 and 5 weeks, the I/Zr ratios found were 2·99/1 and 3·10/1; the yields of ZrI_3 were 19·1 and 25·3 per cent, respectively.

TABLE 1.—X-RAY DIFFRACTION DATA FOR ZIRCONIUM(III) IODIDE*

d (Å)	I/I_0	d (Å)	I/I_0	d (Å)	I/I_0
10·6	0·05	1·94	0·05	1·31	0·20
6·32	0·40	1·89	0·35	1·28	0·05
3·63	0·10	1·78	0·20	1·26	0·05
3·19	1·00	1·76	0·20	1·22	0·05
2·93	0·05	1·67	0·10	1·18	0·05
2·46	0·50	1·60	0·10	1·08	0·05
2·28	0·10	1·41	0·10	1·00	0·05
2·10	0·40	1·35	0·20	0·98	0·05

† All patterns were obtained using CuKα radiation (Ni filter), tube voltage of 35 kV, filament current of 15 mA, and exposure times of 6–12 hr. Relative intensities were estimated visually.

In an effort to obtain ZrI_3 free of Al, 5·1298 g of ZrI_4 and 0·0359 g of Al (ZrI_4/Al = 9/1) were treated as described above except that the total reaction time was ten weeks. Sublimation yielded a non-volatile residue (in 87·8 per cent yield based on Al) that gave an X-ray diffraction pattern attributable to (only) ZrI_3 and that included no lines characteristic of Al. Upon dissolving samples for analysis, only traces of insoluble material were observed. (Found: Zr, 19·0; I, 81·3. Calc. for ZrI_3: Zr, 19·3; I, 80·7%).

In an attempt to reduce Zr(IV) to Zr(<III), a reaction employing ZrI_4/Al = 3/2 was carried out as described above over a period of four weeks. The sublimation residue was black (possibly owing to the presence of ZrI_2); the X-ray diffraction pattern was characteristic of ZrI_3 but included also lines corresponding to *d*-spacings of 5·13 and 2·38 Å. (Found: Zr, 21·7; I, 77·3; soluble Al, 0·9 (I/Zr = 2·55/1)). The presence of Al is believed due to incomplete sublimation of AlI_3. Efforts to separate ZrI_2 and ZrI_3 by selective dissolution in liquid ammonia and by selective disproportionation were both unrewarding.

Iron. The only experiments reported here employed ZrI_4/Fe ratios of 2/1, initial reaction temperatures of 325°, reaction times of three weeks, and procedures otherwise as described above. In preliminary experiments however, it was found that complete sublimation of volatile iron required heating at 400° for 12 hr and that this resulted in some disproportionation of ZrI_3 and resultant low I/Zr ratios in the non-volatile sublimation residues. Accordingly, the sublimation procedure was modified by placing the tube in a near vertical position, heating the lower end to 400° while maintaining the upper end at 200°. After several days, the latter was cooled to room temperature for 3 hr and the tube removed from the furnace. The red-brown residue gave an X-ray diffraction pattern which (after correction for the presence of unreacted iron) gave data substantially identical with those in Table 1. A sample of the residue was dissolved in water (unreacted iron was removed by filtration) and analysed. (Found: Zr, 19·4; I, 81·0% (I/Zr = 3·03/1); a qualitative test for iron was negative. Calc. for ZrI_3: Zr, 19·3; I, 80·7%).

It was assumed that, in the sublimation, iron was volatilized as FeI_2; this was substantiated by analysing the sublimate for Zr, Fe and I, and correcting for volatile Zr as ZrI_4. (Found: Fe, 17·5; I, 82·8. Calc. for FeI_2: Fe, 18·0; I, 82·0%).

Germanium. Analogous reactions involving ZrI_4/Ge ratios of 4/1 at 350° for four weeks yielded gross reaction products that contained ZrI_3, as evidenced by X-ray diffraction data. Following

[11] E. M. LARSEN. Private communication (1958).

VOL. 22 1961

sublimation however, the only products that could be identified were Zr and Ge in the residue and ZrI_4 and GeI_4 in the sublimate. Analytical data for these fractions were inconclusive.

Mercury. After heating the reactants (ZrI_4/Hg = 1/1) as described above for five weeks at 325°, the presence of much unreacted Hg was clearly evident. The reaction mixture was therefore heated for an additional six weeks at 300° prior to separation by sublimation at 325°. The sublimate consisted of ZrI_4, HgI_2 (identified by X-ray diffraction patterns) and Hg. The residue consisted of ZrI_3 (24·3 per cent yield based on ZrI_4) which gave the usual characteristic X-ray diffraction pattern. (Found: Zr, 19·1; I, 81·4. Calc. for ZrI_3: Zr, 19·3; I, 80·7%).

Tin(II) iodide. Over a period of six weeks at 325° there was no evidence of reaction between ZrI_4 and SnI_2 (2/1); an X-ray diffraction pattern showed only the presence of the starting materials.

Reactions with ternary hydrides

Treatment of ZrI_4 with excess $NaBH_4$ or $LiAlH_4$ under the following conditions failed to provide evidence for reduction of ZrI_4: (a) In tetrahydrofuran or bis(2-methoxyethyl) ether at or below their boiling points, (b) in tetrahydrofuran under pressure at 80–90° for two weeks, and (c) in the absence of solvent for as long as two weeks in sealed tubes at 200°. The only evidence for reaction consisted of the detection (by X-ray diffraction patterns) of sodium iodide.

Reactions in the electrodeless discharge

By preliminary experiments it was established that ZrI_4 could be transferred without decomposition from the side arm container to the discharge tube by heating the former at 125–150° both without and with an electrical discharge in the tube. Similarly, it was found that with a discharge in a helium atmosphere, decomposition of ZrI_4 induced in the discharge zone was negligible.

For reactions in all gaseous atmospheres other than hydrogen and helium, elemental Zr or ZrO_2 (identified by analysis, X-ray diffraction patterns, or both) were produced in the discharge tube; iodine and (in most cases) unreacted ZrI_4 were found in the downstream traps. Other products identified (by X-ray diffraction patterns unless otherwise indicated) are listed under the following headings which include the gaseous atmosphere followed by flow rate, pressure, and reaction time (or the range of these variables investigated).

Hydrogen (100–900 cm³/hr, 0·1–1·5 mm, 4–8 hr). Trace quantities of a light yellow solid were deposited on the wall of the discharge tube.

Ethylene (200 cm³/hr, 0·5 mm, 3·5 hr). The solid deposited in the discharge tube included Zr together with mixtures of C_2H_4 polymers and iodine-containing organic products. With C_2H_4 alone in the discharge zone, white polymeric products were formed; with C_2H_4 and I_2, a black organic product containing 38·5 per cent iodine was produced.

Acetylene (300 cm³/hr, 0·5 mm, 4 hr). The results were similar to those observed with ZrI_4 and ethylene.

Carbon monoxide (600 cm³/hr, 0·9 mm, 3 hr). There was no evidence of reaction.

Sulphur dioxide (400 cm³/hr, 0·4 mm, 2 hr). Of the total ZrI_4 fed to the discharge zone, 87 per cent was converted to a white solid that was deposited on the walls of the discharge tube and which gave an X-ray diffraction pattern characteristic of ZrO_2. (Found: Zr, 73·6. Calc. for ZrO_2: Zr, 74·0%). Sulphur and iodine were condensed in a downstream trap at 0°, iodine in a trap at −78°, and a dark red solid in a trap at −196°; this latter product exhibited all of the properties characteristic of sulphur monoxide.[12] Separate experiments with SO_2 alone in the discharge produced elemental sulphur but not sulphur monoxide.

Nitric oxide (300 cm³/hr, 0·6 mm, 6 hr). In the successive downstream traps at 0°, −78° and −196°, I_2, I_2 and NO_2, and NO, respectively, were collected. In the discharge tube, solid products were deposited in two distinct zones. A white solid deposited near the ZrI_4 inlet point gave an X-ray diffraction pattern for ZrO_2; this accounted for 81 per cent of the Zr fed to the discharge zone as ZrI_4. (Found: Zr, 73·3. Calc. for ZrO_2: Zr, 74·0%). Near the exit end of the discharge tube a pale pink solid was deposited. This solid was hydroscopic, soluble in water, and did not contain either Zr or iodine as I^-. This substance was shown, by analysis to consist of I_2O_5 in 99·6 per cent purity; X-ray diffraction data were in sufficiently good agreement with published values[13] to constitute identification.

[12] P. W. SCHENK, *Z. Anorg. Chem.* **233**, 385 (1937).
[13] J. D. HANAWALT, H. W. RINN and L. K. FREVEL, *Industr. Engng. Chem. Analyt. Ed.* **10**, 457 (1938).

DISCUSSION

The results reported above show that the method previously used to form zirconium(III) chloride[5] and bromide,[14] i.e., reduction with aluminium, is also applicable to the reduction of ZrI_4 to ZrI_3 in yields as high as 87 per cent. Contamination of the lower iodide product with aluminium was virtually eliminated by the use of high ZrI_4/Al ratios. Use of an appropriately low ratio led to products that apparently consisted of about equimolar quantities of ZrI_3 and ZrI_2; efforts to separate these two products however were unsuccessful. Reduction with iron,[14] germanium and mercury has also been demonstrated but the yields and purity of product were less satisfactory in these cases.

Except for the qualitative identification of sodium iodide as a reaction product, treatment of ZrI_4 with $NaBH_4$ or $LiAlH_4$ did not provide evidence for reaction of any kind. This was surprising in view of the known reduction by ternary hydrides of Ti(IV),[15] Ce(IV), Cr(VI), Hg(II) and Fe(III).[16]

VOL. 22 1961

Enough work has now been done on the use of various types of electrical discharges in the reduction of volatile halides to establish the generality of application of this type of procedure.[2,17–20] Unfortunately, however, the information published is not sufficiently detailed in some cases to permit any correlation of the results obtained with the specific characteristics of the electrical discharges employed. It is quite clear however that the reactions that occur are largely determined by the nature of the discharge, the gaseous atmosphere present, and/or the exact physical arrangement of the equipment (i.e., in addition to the usual variables of pressure, discharge tube wall temperature, tube geometry, etc.). Thus NEWNHAM and WATTS[2] found that the particular equipment used by INGRAHAM *et al.*[20] for the reduction of $TiCl_4$ was inapplicable to the reduction of the tetrahalides of zirconium. NEWNHAM and WATTS used hydrogen in a glow discharge generated between recessed tungsten electrodes to reduct ZrI_4 to ZrI_3 whereas in the present work the use of an electrodeless discharge did not provide the lower iodide.

Electrodeless discharges of the type used in this work are characterized by high electron densities in the discharge zone. Thus, DEAKINS[21] showed that in neon at pressures from 10^{-2} to 30 mm, the density is reasonably constant at ca. $10^{10} e^-/cm^3$. It was felt in the present studies that, despite unfavourable thermodynamics, reduction of ZrI_4 might be accomplished owing to the great variety of radicals and ions that could be generated by electron impact[22–24] in the various gaseous atmospheres. Thus there could be formed species that would act as acceptors for iodine atoms formed by the dissociation of activated ZrI_4 molecules, or that would abstract iodine upon collision in the gas phase.

The results reported above show that reactions of these types in all probability did occur, but speculation as to mechanism is unwarranted in view of the limited

[14] R. C. YOUNG and W. C. SCHUMB, *J. Amer. Chem. Soc.* **53,** 2148 (1931).
[15] H. R. HOEKSTRA and J. J. KATZ, *J. Amer. Chem. Soc.* **71,** 2488 (1949).
[16] N. G. GAYLORD, *Reduction with Complex Metal Hydrides*, p. 60. Interscience, New York (1956).
[17] W. C. SCHUMB and H. H. ROGERS, *J. Amer. Chem. Soc.* **73,** 5806 (1951).
[18] V. GUTMANN, H. NOWOTNY, and F. OFNER, *Z. Anorg. Chem.* **278,** 78 (1955).
[19] V. GUTMANN and H. TANNENBERGER, *Monatsh.* **87,** 769 (1956).
[20] T. R. INGRAHAM, K. W. DOWNES, and P. MARIER, *Canad. J. Chem.* **35,** 850 (1957).
[21] G. DEAKINS. Dissertation, The University of Texas (1956).
[22] O. TUXEN, *Z. Physik*, **103,** 463 (1936).
[23] J. DELFOSSE and W. BLEAKNEY, *Phys. Rev.* **56,** 208 (1939).
[24] J. A. HIPPLE, JR., *Phys. Rev.* **53,** 530 (1938).

information available and the complexity of the systems involved. The formation of ZrO_2, SO, and S from ZrI_4 and SO_2 in the discharge zone appears to be reasonably straightforward and the products can be accounted for on the basis of a variety of mechanisms that are too obvious for elaboration here. The same is true for the formation of ZrO_2, NO_2, and I_2O_5[25,26] from ZrI_4 and NO.

[25] M. GUICHARD, *Ann. chim.* (Paris), [9], **7**, 28 (1917).
[26] E. MOLES and A. P. VITORIA, *Z. Physik. Chem.*, Bodenstein Festschrift, 583 (1931).

J. Inorg. Nucl. Chem., 1961, Vol. 22, pp. 55 to 58. Pergamon Press Ltd. Printed in Northern Ireland

KINETICS OF PRECIPITATION OF ALUMINIUM 8-QUINOLINOLATE FROM BASIC ALUMINIUM CHLORIDE

R. H. LINNELL
Chemistry Department, University of Vermont, Burlington, Vermont

(*Received* 9 *February* 1961; *in revised form* 10 *April* 1961)

Abstract—$AlCl_3$ precipitates quantitatively as Al(8-quinolinolate)$_3$ at 20° in 0·5 hr, whereas the amount of aluminium precipitating from $Al_2(OH)_5Cl$ (5/6 basic) as 8-quinolinolate depends on time and temperature with an apparent activation energy of 27·9 ± 1·4 kcal. This behaviour is interpreted as due to equilibria between polynuclear aluminium cations in the 5/6 basic solution.

VOL. 22 1961

QUANTITATIVE, gravimetric analysis of aluminium as the 8-quinolinolate was first developed by KOLTHOFF and SANDELL[1]. Their procedure calls for precipitation with a 2 N HOAc solution of 8-quinolinol from a slightly acid solution of aluminium, buffering by NH_4OAc, digestion at 50–60°, filtering, washing with cold water, drying at 120–140°, and weighing as $Al(C_9H_6ON)_3$.

When the above procedure was used on basic aluminium chloride of Al:Cl of 2:1 (5/6 basic) low and erratic results were obtained for total aluminium. A preliminary nitric acid digestion prior to precipitation yields consistently good results.[2]

This work was undertaken to determine the conditions of precipitation of aluminium chloride, 5/6 basic, as 8-quinolinolate, and hence to deduce more about the nature of the aluminium species present in these solutions.

EXPERIMENTAL

Reagents

8-Quinolinol (Eastman No. 794) was used without further purification; 12·5 g + 30 ml C.P. HOAc (glacial) was diluted to 250 ml volume with distilled water. A fresh solution was prepared every 2 weeks. Alcoa atomized aluminium powder 99·4% Al was dissolved in reagent HCl to make $AlCl_3$ solution. The 5/6 basic aluminium chloride (Chlorhydrol) was supplied by Reheis Company, Berkeley Heights, New Jersey, and was of high purity (12·4–12·5% Al, 8·3–8·5% Cl, less than 20 p.p.m. Fe, less than 5 p.p.m. heavy metals as Pb). Reagent NH_4OAc, 154 g was made to 1 l. with distilled water. Dilute HOAc contained 1·0 ml glacial + 9·0 ml distilled water. All other reagents were analytical grade.

Procedure

A stock solution of $AlCl_3$, $1{\cdot}63 \times 10^{-3}$ mole Al/ml was analysed for Al by conventional 8-quinolinolate precipitation and gravimetric AgCl method yielding Al:Cl of 1·00:2·85. 10·00 ml of this solution was made to 25·00 ml and 1·00 ml used for each analysis. The stock 5/6 basic aluminium chloride solution contained 3 g of Chlorhydrol/100 ml and 5·00 ml was used for each analysis.

For prior acid digestion, 5·00 ml of the 5/6 basic solution was placed in a 250 ml beaker, 5 ml conc. HNO_3 and 125 ml water added, and the mixture boiled one-half hour. The conventional procedure then followed. This involves cooling, addition of aqueous NH_3 to the first sign of precipitation, addition of 5·00 ml dilute HOAc plus water to 100 ml, heating to 70–90° for 5–10 min,

[1] I. M. KOLTOFF and E. B. SANDELL, *J. Amer. Chem. Soc.* **50**, 1900 (1929).
[2] Reheis Co., Inc., Berkeley Heights, N.J. "Analysis Procedure, Chlorhydrol 50% Solution" (a pure 5/6 basic aluminum chloride).

addition of 18 ml 8-quinolinol solution, addition of NH_4OAc solution until a precipitate appears plus 25 ml excess, and finally digestion at 70–90° until a clear supernatant appears. After cooling, the precipitate is filtered on a Gooch sintered glass, medium porosity (Coors No. 3), washed thoroughly with water, dried 3 hr at 130–140°, cooled and weighed.

Kinetic experiments were run as above with omission of the HNO_3 treatment and holding the samples in a thermostat controlled to ±0·1°C for the specified time during precipitation with immediate filtration and washing. In the low temperature where relatively small percentages of total aluminium were precipitated, the quantity of 8-quinolinol reagent was reduced to about a 25 per cent excess (determined by previous experiment) to avoid error by crystallization of the excess reagent.

TABLE 1.—PER CENT ALUMINIUM PRECIPITATED BY 8-QUINOLINATE

Al	Time (hr)	Temperatures (°C)			
		10	20	30	40
$Al_{1\cdot00}Cl_{2\cdot85}$	½	—	100·2 ± 0·2	101·1 ± 0·4	—
$Al_{1\cdot94}Cl_{1\cdot00}$	½	4·7 ± 1·0	21·5 ± 0·1	42·5 ± 1·4	74·4 ± 1·2
$Al_{1\cdot94}Cl_{1\cdot00}$	1	7·2	—	51·6 ± 0·3	82·7 ± 0·3
$Al_{1\cdot94}Cl_{1\cdot00}$	1½	8·7	45·4 ± 1·6	68·1 ± 0·5	83·6 ± 2·3
$Al_{1\cdot94}Cl_{1\cdot00}$	3	16·6 ± 0·3	62·7 ± 0·4	76·7 ± 3·0	88·5 ± 0·4
$Al_{1\cdot94}Cl_{1\cdot00}$	6	29·3	66·6 ± 0·1	79·5 ± 0·2	99·6 ± 0·2
$Al_{1\cdot94}Cl_{1\cdot00}$	16	—	87·6 ± 2·0	99·9 ± 0·2	
$Al_{1\cdot94}Cl_{1\cdot00}$	64	—	99·4 ± 0·4	—	—

Uncertainties given are average deviations of triplicate determinations. Some difficulty in control of filtration time and in transfer of precipitate accounts for large uncertainties.

The composition of the Al–8-quinolinate precipitates is assumed to be $Al(C_9H_6ON)_3$. The evidence for this is that $CHCl_3$ solutions of these precipitates have the same absorbancies at 390 mμ as $CHCl_3$ solutions of known $Al(C_9H_6ON)_3$ of the same concentration.

RESULTS AND DISCUSSION

Preliminary experiments were done to determine if the age of the diluted 5/6 basic aluminium chloride solution, prepared for analysis, would affect per cent aluminium precipitated. All experiments in this series were precipitated 1 hr at 20° yielding the following results (% Al precipitated, time after dilution): 15·0 ± 0·5, 0 hr; 21·3 ± 0·5, 24 hr; 23·8 ± 0·8, 72 hr; 23·9 ± 0·7, 168 hr; 22·7 ± 0·1, 36 days. From these results it is concluded that equilibrium is obtained after 24 hr so all studies in Table 1 were made on solutions that were diluted and aged 24 hr or more.

A concentrated solution of 5/6 basic aluminium chloride (12·45% Al, 8·22% Cl; Al:Cl atomic ratio 2·00:1·00) was refluxed for 2 hr at 90–100°. An unrefluxed sample was diluted and analysed at once by precipitation for 1 hr at 20° and 16·7 ± 1·1 per cent of the total Al precipitated compared to 24·2 ± 0·5 per cent for the refluxed sample. The refluxed material was stored 41 days and then a freshly diluted sample analysed at 20° for 1 hr, yielding 14·7 ± 0·6 per cent of total Al precipitated.

The results here indicate polymers in 5/6 basic aluminium chloride solutions which cannot be precipitated by 8-quinolinol. We assume the precipitating reagent

can only react with monomeric aluminium (footnote to Table 1). It appears that polymeric aluminium species slowly break down to monomers, which are then precipitated by the reagent; the rate of this breakdown is strongly temperature dependent. Even at low temperatures all the aluminium can be precipitated at sufficiently long times. Since $AlCl_3$ is quantitatively precipitated in one half hour at 20°, this further supports the idea that the 8-quinolinol reacts rapidly with aluminium monomers.

It seems reasonable to assume that the rate controlling step in these precipitations is the decomposition of polynuclear aluminium species, ultimately to monomeric species which are precipitated immediately in our experiments. If we let C_{Al} = concentration of Al not yet precipitated at any time, t, and plot log c_{Al} vs. t, we do not obtain a straight line. Tangents drawn at $t = 0$ for these plots yield initial rates, and an Arrhenius plot of these rates yields an activation energy (least squares) of 27·9 $\pm$ 1·4 kcal (probable error). Recent Russian work[3] on the kinetics of decomposition of 5/6 basic aluminium chloride by HCl at 25–55° yields first order kinetics and an activation energy of 30 kcal. It would appear that we are dealing with strong Al–OH bonds which must be broken in both the reaction with HCl and with 8-quinolinol, and that an energy of about 30 kcal is to be associated with these bonds.

VOL. 22 1961

A study by KENTTÄMAA[4] using cryscopic and potentiometric methods indicates that 5/6 basic aluminium chloride solutions contain species of the general formula $[Al_2(OH)_5]_n^{n+}$ with perhaps dominance of species with $n = 2$–3. There is probably little or no monomeric aluminium in the 5/6 basic aluminium chloride solution. Our initial rates of precipitation therefore probably correspond to the following reaction:

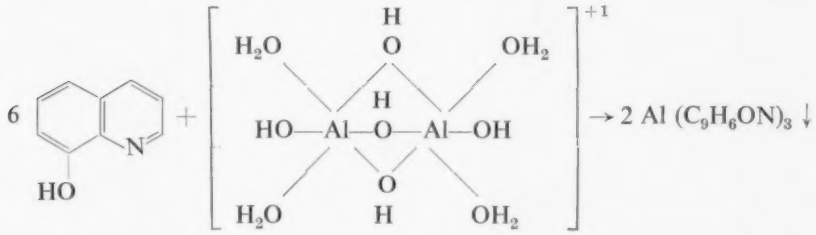

A series of equilibria involving higher aluminium polymeric cations is then all displaced toward the dimer represented above, as shown below:

$$[Al_8(OH)_{20}(H_2O)_7]^{4+} \overset{H_2O}{\rightleftharpoons} [Al_6(OH)_{15}(H_2O)_6]^{3+} + [Al_2(OH)_5(H_2O)_4]^{+}$$

$$[Al_6(OH)_{15}(H_2O)_6]^{3+} \overset{H_2O}{\rightleftharpoons} [Al_4(OH)_{10}(H_2O)_5]^{2+} + [Al_2(OH)_5(H_2O)_4]^{+}$$

$$[Al_4(OH)_{10}(H_2O)_5]^{2+} \overset{H_2O}{\rightleftharpoons} 2\,[Al_2(OH)_5(H_2O)_4]^{+}$$

These general ideas are consistent with the earlier work of KOHLSCHUTTER and HANTELMANN[5] whose cryoscopic values indicate an average of 6-Al per polymer unit; diffusion experiments by DENK and ALT[6] indicate ionic weights of 5/6 basic

[3] M. E. SHISHNIASHUILI and A. L. BATSANDZE, *Trudy Inst. Khim. im.* P. G. MELIKISHUILI, *Akad. Nauk Gruzin.* S.S.R., **B**, 61–6 (1957). *Chem. Abstr.* **53**, 4871a (1959).
[4] J. KENTTÄMAA, *Ann. Acad. Sci. Fennicae Ser.* A, 11, **67**, 7 (1955) (in English). *Chem. Abstr.* **50**, 15307 h. (1956).
[5] H. W. KOHLSCHUTTER and P. HANTELMANN, *Z. Anorg. Chem.* **248**, 319 (1941).
[6] G. DENK and J. ALT, *Z. Anorg. Chem.* **269**, 244 (1952).

aluminium chloride of about 350–400. Work by BROSSET[7] and by SILLEN[8] also indicates equilibria involving polynuclear complexes in these basic solutions. Ion exchange studies show all chloride to be anionic and the aluminium uptake on cation resins to be dependent on resin cross-linking, temperature, and contact time[9] so that chloride-containing complexes do not appear to be important.

By developing more refined experimental techniques, it should be possible to study the kinetics of organic basic metal ion species reaction, and gain more insight into the nature of the basic species present.

Acknowledgements—The author thanks the Reheis Company, Inc., for financial support of this work. Thanks are also due to Mr. T. PHILLIPS and Mr. F. RAAB, who carried out this work as undergraduate research participants.

[7] C. BROSSET, *Acta Chem. Scand.* **6**, 910 (1952).
[8] L. SILLÉN, *Acta Chem. Scand.* **8**, 299 (1954).
[9] R. H. LINNELL and B. NOBLE, *J. Inorg. Nucl. Chem.* To be published.

J. Inorg. Nucl. Chem., 1961, Vol. 22, pp. 59 to 67. Pergamon Press Ltd. Printed in Northern Ireland

ETHYNYL-COPPER(I) COMPLEXES WITH TERTIARY PHOSPHINES

G. E. COATES and C. PARKIN
Chemistry Department, University of Durham, Durham

(*Received* 2 *March* 1961)

Abstract—Ethynyl (tertiary phosphine) copper(I) complexes, $RC{:}CCu(PR'_3)_n$, are dimeric in nitrobenzene and rather more associated in benzene when $n = 1$; they are monomeric when $n = 2$. One unstable complex with $n = 3$ was also prepared. Infra-red spectra indicate strong interaction between metal and acetylenic orbitals in all the complexes, though not so strong as in the polymers $(RC{:}CCu)_x$.

Some diacetylenic complexes $PhC{:}C{\cdot}C{:}CCu(PR'_3)$: are also described, and crystalline $(PhC{:}C{\cdot}C{:}CCu)_2(PEt_3)_3$ probably has a structure closely related to that of $(PhC{:}CCuPMe_3)_4$ which was shown to contain a chain of four linked copper atoms.

VOL. 22 1961

A FEW ethynyl–copper(I) and –silver(I) complexes of the type $R{\cdot}C{:}CCu(Ag){\cdot}P(As)Et_3$ (R = Ph, Me), have been reported in a preliminary note.[1] Those complexes which were sufficiently stable for cryoscopic measurements were found to be associated, and it was suggested that in the dimeric complexes, for example, the ethynyl group acts as donor towards the metal, as indicated in (I).

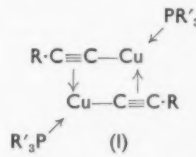

(I)

Analogous compounds of gold(I), e.g. $PhC{:}CAuPEt_3$, are monomeric,[2] since gold(I) has a relatively low tendency to raise its co-ordination number above two, in contrast to copper(I) and silver(I).

An unstable ammonia complex $(PhC{:}CCuNH_3)_x$ has previously been prepared by reactions in liquid ammonia. It reverts to polymeric $PhC{:}CCu$ in a stream of nitrogen and its molecular complexity is not known.[3] Phenylethynylcopper in liquid ammonia absorbs carbon monoxide but the carbonyl thus formed reverts to $PhC{:}CCu$ when solvent is removed;[4] a colourless four co-ordinate isocyanide complex $PhC{:}CCu(CNp\text{-}tolyl)_3$, dec. 100° has been described.[5] We find that phenylethynyl copper can itself be slowly extracted (in a Soxhlet apparatus) by isopropylamine; though it comes out of solution in crystalline form, the crystals so far obtained have unfortunately been too small for detailed crystallographic study.

We now describe further studies on ethynyl copper(I) complexes, with the three principal objects,

[1] D. BLAKE, G. CALVIN and G. E. COATES, *Proc. Chem. Soc.* 396 (1959).
[2] G. CALVIN, G. E. COATES and P. DIXON, *Chem. and Industr.* 1628 (1959).
[3] R. NAST and W. PFAB, *Ber. Dtsch. Chem. Ger.* **89**, 415 (1956).
[4] R. NAST and C. SCHULTZE, *Z. Anorg. Chem.* **307**, 15 (1960).
[5] F. KLAGES, K. MÖNKEMEYER and R. HEINLE, *Ber. Dtsch. Chem. Ger.* **85**, 109 (1952).

(a) to find out whether more than one molecule of tertiary phosphine would co-ordinate to each copper atom,
(b) to obtain more extensive molecular weight data, and
(c) to investigate the infra-red absorption of the ethynyl groups in these compounds.

Difficulties due to the inconveniently high solubilities of the triethylphosphine complexes reported earlier have largely been overcome by the use of trimethylphosphine (the more symmetrical molecule usually resulting in higher melting points and lower solubilities).

Complexes were normally prepared by the addition of the tertiary phosphine to a suspension of the insoluble ethynyl compound in an organic solvent, followed by filtration and crystallization. Their properties are summarized in Table 1, which includes analytical and cryoscopic data. The association of the monophosphine complexes, $RC{:}CCuPR'_3$, is confirmed, but compound (X) in Table 1 is exceptional in being dimeric in benzene and monomeric in nitrobenzene. The nitrobenzene solutions of monophosphine complexes may well contain dimer molecules of structure (I), in which case the copper atoms have the co-ordination number *three*, but we cannot exclude the possibility that the solvent acts as donor as well as ethynyl groups thus allowing the more usual four-co-ordination. The higher degrees of association observed in benzene are interpreted later.

In agreement with the view that ethynyl–copper(I) compounds are co-ordination polymers, and that the polymerization is reduced (to structures like (I)) by tertiary phosphines successfully competing with ethynyl groups as ligands,[1] we find that when two phosphorus atoms are co-ordinated to each copper the resulting complexes, (III) and (VI), are monomeric. The bisphosphine complexes are more difficult to purify; (III) evidently dissociates in nitrobenzene solution, though partial replacement of phosphine by nitrobenzene would give the same cryoscopic result. Dissociation is probably also responsible for the bis-, and the one trisphosphine complex prepared, melting over a range of several degrees.

Progressive addition of tertiary phosphine causes a marked lightening of colour. For example, tertiary butylethynyl–copper(I), which is octameric in benzene solution, both cryoscopically[6] and ebullioscopically* is orange-red, while its dimeric mono-(trimethyl phosphine) complex is yellow-green, and its monomeric bisphosphine complex is colourless.

We cannot explain satisfactorily the observation that the *para*-nitrophenylethynyl complex (X) is monomeric in nitrobenzene and dimeric in benzene. It would be surprising if nitrobenzene could behave as a donor molecule of sufficient strength to split the dimer (formula (I), $R = p\text{-}NO_2C_6H_4$, $R' = Ph$) by co-ordination to copper. When orange crystals of (X), obtained from benzene–hexane solution, are allowed to stand in contact with ethanol, in which it is insoluble, it turns into a bright red powdery material (m.p. and analysis unchanged). This red form of (X) dissolves in benzene giving an orange solution, and in which it has a dimeric constitution, and from which the orange crystalline form can be recovered. Similarly the orange form gives a *red* solution in nitrobenzene.

* Found: M, 1140, 1161, 1177 in 0·73, 1·48 and 2·95 per cent benzene solution. Calc. for $(C_6H_9Cu)_8$, M, 1157.

[6] L. FAVORSKI and A. MOREV, *J. Russ. Phys. Chem. Soc.* **50**, 571 (1920); BLAKE and COATES, Unpublished work. (1956).

TABLE 1.

Complex	Colour	m.p.	Found (%)	Formula	Required (%)	Degree of association, cryoscopically			
						Benzene		Nitrobenzene	
						Wt. %	*n*	Wt. %	*n*
$Bu^tC{:}\,C{\cdot}CuPMe_3$ (II)	Yellow-green	105–106°[a]	C, 48·9 H, 8·45 Cu, 28·8	$C_9H_{18}CuP$	C, 49·0 H, 8·2 Cu, 28·8	2·78 3·35 3·84 4·20	2·67 2·79 2·73 2·74	1·65 1·94 2·29 2·49	2·01 2·04 1·99 2·05
$Bu^tC{:}\,C{\cdot}Cu(PMe_3)_2$ (III)	Colourless	95–98[a]	C, 46·4 H, 9·1 Cu, 21·2	$C_{12}H_{27}CuP_2$	C, 48·55 H, 9·2 Cu, 21·4	0·31 0·71 1·41 1·85	1·00 0·98 0·98 0·98	0·18 0·62 1·13 1·47	0·43 0·75 0·88 0·84
$CH_2{:}CMeC{:}\,C{\cdot}CuPMe_3$ (IV)	Yellow	82–82·5[a]	C, 46·8 H, 6·9 Cu, 30·8 30·9	$C_8H_{14}CuP$	C, 47·0 H, 6·9 Cu, 31·0	1·77 2·18 2·49 2·66	3·34 3·28 3·37 3·39	1·23 1·90 2·34 2·64 2·85	2·12 2·31 2·24 2·16 2·40
$PhC{:}\,C{\cdot}CuPMe_3$ (V)	Yellow	116–117[f]	C, 54·8 H, 6·1 Cu, 26·1	$C_{11}H_{14}CuP$	C, 54·9 H, 5·9 Cu, 26·4	0·91 1·81 2·41 2·97 3·07 6·36	2·60 2·75 2·80 2·79 2·70 2·70	0·41 0·61 0·73 0·99 1·39 1·53	1·99 2·06 1·88 2·05 1·94 2·04
$PhC{:}\,C{\cdot}Cu(PMe_3)_2$ (VI)	Yellow-green	94–96[b]	C, 52·9 H, 7·0 Cu, 20·1, 20·0	$C_{14}H_{23}CuP_2$	C, 53·1 H, 7·3 Cu, 20·05	0·63 0·86 1·17 1·71	0·98 1·12 1·35 1·37	0·53 0·78 1·09 1·34	0·93 1·00 0·95 0·98
$PhC{:}\,C{\cdot}Cu(PMe_3)_3$ (VII)	Pale cream	88–93[b]	C, 51·5 H, 7·4 Cu, 16·3, 16·4	$C_{17}H_{32}CuP_3$	C, 52·0 H, 8·2 Cu, 16·2	Unstable			
$PhC{:}\,C{\cdot}CuPEt_3$* (VIII)	Yellow	139·5[a]	C, 59·6 H, 7·3 Cu, 22·2	$C_{14}H_{20}CuP$	C, 59·5 H, 7·1 Cu, 22·5	0·68 1·16 1·27 2·00 2·63	2·93 2·70 2·54 2·64 2·70	0·44 0·97 1·50 2·05	2·00 2·02 1·89 2·03

Table 1 (continued)

Complex	Colour	m.p.	Found (%)	Formula	Required (%)	Degree of association, cryoscopically			
						Benzene		Nitrobenzene	
						Wt. %	*n*	Wt. %	*n*
PhC:C·CuPPh$_3$ (IX)	Yellow-green	212–214[e] (decomp.)	C, 73·2 H, 4·8 Cu, 14·4, 14·8	$C_{26}H_{20}CuP$	C, 73·2 H, 4·7 Cu, 14·9	Too sparingly soluble			
p-NO$_2$C$_6$H$_4$C:C·CuPPh$_3$ (X)	Orange	222–224[e] (decomp.)	C, 66·0 H, 4·3 Cu, 13·7	$C_{26}H_{19}CuNO_2P$	C, 66·2 H, 4·1 Cu, 13·5	1·14 1·77 2·18 2·44	2·10 2·07 2·02 1·96	0·39 0·49 0·64 0·76	1·12 0·94 0·92 1·14
p-NO$_2$C$_6$H$_4$C:C·Cu-(PPhEt$_2$)$_2$ (XI)	Deep red	75[e]	C, 61·6 H, 6·6 Cu, 11·7	$C_{28}H_{34}$-$CuNO_2P_2$	C, 62·0 H, 6·3 Cu, 11·7	Unstable			
PhC:C·C:CCuPMe$_3$ (XII)	Yellow	decomp.[e] >140	C, 58·5 H, 5·5 Cu, 23·9, 23·6	$C_{13}H_{14}CuP$	C, 58·95 H, 5·3 Cu, 24·0	Too sparingly soluble			
PhC:C·C:CCuPEt$_3$ (XIII)	Yellow	155–156[g] (decomp.)	C, 62·3 H, 6·7 Cu, 20·5, 20·8	$C_{16}H_{20}CuP$	C, 62·6 H, 6·6 Cu, 20·7	1·10 1·40 1·71 1·77	3·27 3·29 3·05 3·23	1·13 1·75 2·15 2·43	1·97 2·04 2·11 2·13
(PhC:C·C:C·Cu)$_2$(PEt$_3$)$_3$ (XIV)	Pale-yellow	95–96[a]	C, 62·4 H, 7·7 Cu, 17·4, 17·8	$C_{38}H_{55}Cu_2P_3$	C, 62·4 H, 7·6 Cu, 17·4	0·91 1·31 1·64 1·82	0·71 0·51 0·63 0·69	0·57 0·99 1·49 1·87	0 91 1·03 0·95 0·96
PhC:C·C:CCuPPr$^n_3$ (XV)	Yellow	87[g]	C, 65·2 H, 7·8 Cu, 18·3, 18·3	$C_{19}H_{26}CuP$	C, 65·4 H, 7·5 Cu, 18·2	2·52 3·78 4·54 5·09	3·36 3·19 3·11 3·01	1·05 1·40 1·68 2·11	2·00 2·00 2·04 1·95

Crystallized from "n-hexane described previously" [as in MS.]

Copper(I) derivatives of alkylacetylenes (with the exception of tertiary butylacetylene) did not readily yield isolable tertiary phosphine complexes. Propynyl-(triethylphosphine)–copper(I), for example, at once gives a yellow precipitate of insoluble propynyl–copper(I) when added to benzene; the precipitate dissolves again if excess triethylphosphine is added.

Some diacetylene complexes $PhC{:}C{\cdot}C{:}C{\cdot}CuPR_3$ (R = Me, Et, Pr^n) were also prepared and unexpectedly found to be more stable to decomposition in the air than the mono-acetylenic conpounds discussed earlier. In contrast the diacetylenes (e.g. $PhC{:}C{\cdot}C{:}CH$) are very much less stable than the mono-acetylenes. Whereas $PhC{:}CCuPEt_3$ reverted to yellow amorphous PhC:CCu after exposure to air for a day or two, the corresponding butadiynyl complex was unchanged after a week's exposure. The complex (XIV) with a Cu:P ratio 2:3 loses triethylphosphine when it stands in the air, or is heated in propanol, giving the monophosphine complex.

In general the silver analogues, $RC{:}C{\cdot}AgPR'_3$, are less easy to prepare and purify than the copper compounds, and they decompose more readily on exposure to air and also to light. Since preliminary investigations[1] had shown that the copper and silver complexes are rather similar, the latter were not further studied (with the exception of the preparation of $PhC{:}C{\cdot}AgPMe_3$, which was found to be dimeric in boiling benzene).

VOL. 22 1961

Infra-red spectra. Disubstituted acetylenes absorb light in the range[7] 2190–2260 cm^{-1}. Co-ordination between acetylenic groups and metal atoms should result in a reduction of the stretching frequency because of electron flow from the occupied π_u-bonding orbitals to the metal and from occupied metal *d*-orbitals to unoccupied π_g-antibonding orbitals of the acetylene. Both these effects should reduce the acetylenic bond order, and hence reduce the stretching frequency. For example, the acetylenic stretching frequency of ditertiary butyl acetylene is reduced by about 200 cm^{-1} when it becomes π-bonded to platinum (II),[8] and similar effects have been found in heavy metal complexes of olefins.[9]

In agreement with our view that alkyl- and aryl-ethynyl–copper(I) compounds (RC:CCu) are co-ordination polymers in which there is substantial back co-ordination from filled copper 3*d*-orbitals to the acetylenic antibonding orbitals, we find that these compounds absorb in the region 1920–1960 cm^{-1} which is 270–300 cm^{-1} lower than the range characteristic of disubstituted acetylenes. This effect is less marked in corresponding silver compounds (see Table 2), whose acetylenic frequencies are in the range 2020–2060 cm^{-1}, a reduction of only 150–200 cm^{-1}. The acetylenic frequencies of some ethynylmercury (II) compounds are included in Table 2 for comparison as examples of disubstituted acetylenes containing ethynyl–metal bonds. Any decrease of acetylenic stretching frequency below that found in mercury derivatives should indicate some substantial electronic effect. Table 2 shows that the decrease in $\nu(C{:}C)$ on substituting copper and silver for mercury is about 200 and 100 cm^{-1} respectively. No absorption that could be due to an acetylenic vibration could be detected in tertiary butylethynyl–copper(I), either in a potassium bromide disk or in solution in tetrachlorethylene; this may be connected with the mass of a copper atom being fairly near that of a butyl group.

[7] L. J. Bellamy, *The Infra-red Spectra of Complex Molecules.* Methuen, London (1958); N. Sheppard and D. M. Simpson, *Quart. Rev.* **6**, 1 (1952).
[8] J. Chatt, L. A. Duncanson and R. G. Guy, *Chem. and Industr.* 430 (1959).
[9] J. Chatt and L. A. Duncanson, *J.* 2939 (1953).

Table 2.—Infra-red stretching frequencies[a] of the acetylenic group in RC:CM

R·	M = ½ Hg	Cu	Ag
Me	2156	1955	2061
Et	2165	1952	ca. 2040[a,c]
Pr^n	2164[a], 2175[b]	1942	2045
Bu^t	2180, 2146 2188, 2154[b]	absent	2055
Ph	2149	1933	2055
p-$NO_2C_6H_4$	absent[a,c]	1929	2042
Mesityl	2142	1933[c] (*v.w.*)	2026
p-BrC_6H_4	2160	1942	2048[c]
PhC:C	2204, 2098	2180[a,c]	2190

measured in [a]KBr disc, [b]benzene solution, [c]Nujol mull.

Table 3.—Effect of P:Cu ratio on ν(C:C) of benzene solutions of RC:CCu$(PMe_3)_n$

R	$n = 1$	$n = 2$	$n = 3$	$n = 4$
Ph·	2025 (*m*)	2042 (*m*)	2041 (*s*)	2035 (*s*)
	2053 (*m*)		2061 (*sh*)	2061 (*s*)
	2086 (*w*)	2087 (*w*)	2087 (*w*)	2086 (*w*)
CH_2CMe·	*2013 (*m*)	†2021 (*m*)	‡2017 (*m*)	‡2017 (*m*)
	2035 (*m*)		2039 (*m*)	2039 (*s*)
	2063 (*w*)	2064 (*m*)	2062 (*m*)	2062 (*s*)
	2089 (*w*)	2089 (*w*)		

Colour of solution: * yellow, † pale yellow, ‡ colourless, *w*, weak; *m*, medium; *s*, strong; (*sh*) shoulder.

Complex formation with a tertiary phosphine raises ν(C:C) by nearly 100 cm^{-1} from that observed in the corresponding ethynyl–copper(I) compounds $(RC:CCu)_x$. It is remarkable that the frequency of the acetylenic absorption is much the same whether the complex contains one, two or more mols of phosphine. Table 3 shows ν(C:C) for two series of complexes RC:CCu$(PMe_3)_n$, (R = Ph· and CH_2:CMe·) measured in benzene solution. Solutions containing the higher P:Cu ratios were obtained by dissolving the 1:1 complex in benzene and adding the appropriate amount of trimethylphosphine. Extinction co-efficients are not given since it is very likely that the solutions contain mixtures of more than one complex. It is relevant to note that in the isopropenyl series solutions for which the P:Cu ratios were three and four

were quite colourless, and hence could not contain appreciable amounts of the bright yellow 1:1 complex.

Two or more ν(C⋮C) bands were also observed in the spectra of some of the solid complexes pressed in a potassium bromide disc. These data are collected in Table 4. It is worth noting that ν(C⋮C) increases in the series PhC⋮CMPR$_3$ in the sense M = Cu < Ag < Au, and that the change from (RC⋮CCu)$_x$ to RC⋮CCuPR$_3$ (about 100 cm^{-1}) is much greater than that from (RC⋮CAg)$_x$ to RC⋮CAgPR$_3$ (about 20 cm^{-1}).

TABLE 4.—ETHYNYL COMPLEXES, ν(C⋮C)*

Bu^{t}C⋮CCuPMe$_3$	2050 cm^{-1} (*vw*)
†PhC⋮CCuPMe$_3$	2019 (*w*), 2045 (*m*)
PhC⋮CCu(PMe$_3$)$_2$	2035 (*m*), 2048 (*m*)
PhC⋮CCu(PMe$_3$)$_3$	2034 (*s*), 2051 (*vw*)
PhC⋮CCuPEt$_3$	2018 (*s*), [a]2020 (*s*), 2048 (*m*)
PhC⋮CCuPPh$_3$	2043 (*m*)
p-NO$_2$C$_6$H$_4$C⋮CCuPPh$_3$	2015 (*s*)
p-NO$_2$C$_6$H$_4$C⋮CCu(PPhEt$_2$)$_2$	2025 (*s*)
PhC⋮C·C⋮C·CuPMe$_3$	2161 (*s*), 1981 (*m*)
PhC⋮C·C⋮C·CuPEt$_3$	2159 (*s*) 1988 (*m*)
PhC⋮C·C⋮C·CuPEt$_3$	[b]2167 (*s*), 1988 (*m*)
(PhC⋮C·C⋮C·Cu)$_2$(PEt$_3$)$_3$	2165 (*s*), 2008 (*m*)
(PhC⋮C·C⋮C·Cu)$_2$(PEt$_3$)$_3$	[a]2171 (*s*), 2009 (*m*)
PhC⋮C·C⋮C·CuPPr$^n_3$	2164 (*s*), 1984 (*m*)
PhC⋮C·C⋮C·CuPPr$^n_3$	[b]2166 (*s*), 1986 (*m*).

* Spectra measured in KBr disk, except [a] in benzene, [b] in tetrachlorethylene;
† PhC⋮CAgPMe$_3$ 2075 (*w*)

The observations that need explanation are the cryoscopic data, particularly the apparent degree of association 2·5–3·5 for monophosphine complexes in benzene, and the number of distinct acetylenic infra-red bands. The monophosphine complex PhC⋮CCuPMe$_3$ has been examined crystallographically by Dr. H. M. M. SHEARER and Mr. P. W. R. CORFIELD of this Department, and the structure (Fig. 1) will be discussed in detail elsewhere. The complex contains tetrameric units (PhC⋮CCuPMe$_3$)$_4$, each with a zig-zag chain of four copper atoms; two phosphine molecules are bound to each of the terminal copper atoms, the central two copper atoms not being co-ordinated to phosphorus. Two of the four acetylene groups have a different environment from the other two. Apart from the phosphine groups (methyls not shown) which lie above and below the plane of the paper, the structure is nearly flat. Carbon atoms 4 and 5 are about 0·2 Å out of the *xy*-plane of the diagram, C$_7$, C$_8$, C$_{15}$ and C$_{16}$ each being about 0·3 Å away from the *xy*-plane. The average *z* co-ordinate of the other atoms (i.e. excluding the phosphine groups and the carbon atoms mentioned) is 0·06 Å ($\Sigma |z| / n$, n = number of atoms). The benzene rings are only slightly twisted out of the *xy*-plane. The copper–copper distances (Cu$_1$–Cu$_1$ = 2·7 Å, Cu$_1$–Cu$_2$ = 2·45 Å) are close to those in metallic copper (2·56 Å). The acetylene groups are bent, particularly those (C$_9$ and C$_{10}$) which evidently form "broadside-on" π bonds to copper (angle C$_9$C$_{10}$C$_{11}$ = 154°). The other kind of acetylene group (C$_1$ and C$_2$) is clearly σ-bonded to Cu$_1$ and is no doubt "end-on" π bonded with it. The environment of Cu$_2$ is roughly trigonal with respect to the

VOL. 22 1961

phosphines and Cu_1 (angle P–Cu–P = 124°), and tetrahedral with respect to the phosphines and C_1 and C_9. $Copper_1$ appears to have five ligands in a plane, regarding C_6 and C_{10} as one ligand. If, in spite of the Cu–Cu distances, copper-to-copper bonding is ignored, then it would be possible to regard Cu_1 as trigonally co-ordinated (C_1, C_9 and C_9–C_{10}), and Cu_2 as tetrahedral (C_1, C_9 and the phosphines).

The anomalous cryoscopic results are evidently due to the presence in *solution* of both tetramer and less associated species. The infra-red bands are clearly due to the different types of acetylene present in the tetramer, and again to equilibria in solution between the tetrameric and less associated species.

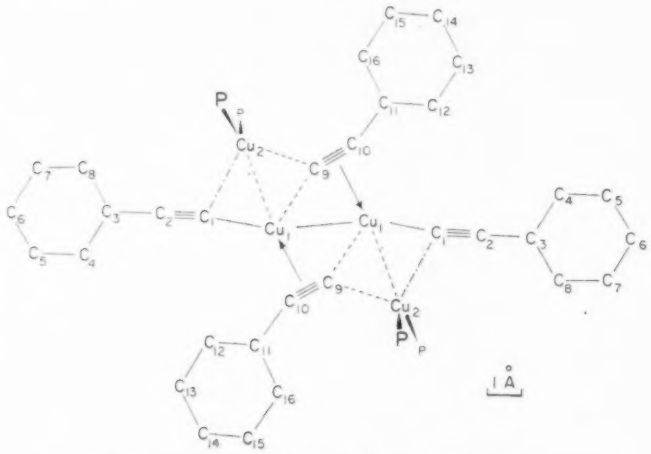

FIG. 1.—The phenylethynyl (trimethyl phosphine)-copper(I) tetramer (after CORFIELD and SHEARER).

The mercury compound $(PhC{:}C{\cdot}C{:}C)_2Hg$, has acetylenic absorptions at 2204 and 2098 cm^{-1} (KBr disk), the copper(I) and silver derivatives having single absorptions at 2180 and 2190 cm^{-1} (Table 2). Since the monophosphine complexes, $PhC{:}C{\cdot}C{:}C{\cdot}CuPR_3$, have two frequencies in the range 2159–2165 and 1981–1988 cm^{-1} (Table 4), it seems clear that only one of the two acetylene groups is involved to any large extent in π-bonding to copper.

Dr. Shearer and Mr. Corfield report as follows on the complex $(PhC{:}C{\cdot}C{:}CCu)_2(PEt_3)_3$ (XIV):—"The space group *P bca*, $a = 14{\cdot}85$, $b = 20{\cdot}8$, $c = 26{\cdot}7$ Å, $\alpha = \beta = \gamma = 90°$, is similar to that of $PhC{:}CCuPMe_3$. From these data and the observed density (1·182) the unit cell contains sixteen copper atoms. These data are consistent with a structure different from that of $PhC{:}CCuPMe_3$ only in that three instead of two phosphine groups are bound to the terminal copper atoms of the Cu_4 chain". In nitrobenzene this complex evidently dissolves as dimer (two Cu atoms), and there must be extensive dissociation in benzene (see Table 1).

EXPERIMENTAL

Micro-analyses were by Miss V. CONWAY of this department. Melting points are corrected. All preparations were carried out in a nitrogen atmosphere, and all the compounds except the triphenylphosphine complexes were to varying degrees sensitive to air-oxidation.

Difficulties in obtaining reproducible results using nitrobenzene as a cryoscopic solvent have been reported, due to variable water content. We find that these difficulties can be overcome by the addition

of a little Linde "Molecular Sieve"(5)a. Biphenyl was used as a standard for molecular weight measurements in benzene, and p-nitrotoluene for nitrobenzene.

Copper was determined gravimetrically as thiocyanate, silver by potentiometric titration with potassium bromide.

Infra-red spectra were recorded with a Grubb-Parsons GS2A grating instrument. Spectra of substances in solution were measured in a 1 mm cell, at a concentration of about 10 mg/ml. A similar cell containing solvent only was placed in the reference beam. Though benzene absorbs quite appreciably near 2000 cm^{-1}, better results were obtained (with slow scanning) than with the use of tetrachlorethylene, which, though more transparent, slowly reacts with some of the aliphatic tertiary phosphines.

Since all the complexes were prepared by rather similar methods, only one representative preparation is described here.

Phenylethynyl (trimethylphosphine)–copper(I), (PhC⋮C·CuPMe_3). A phenylethynylcopper(I) (10 g, 0·061 mole) and benzene (30 ml) was placed in one limb of a double Schlenck tube[10] which had been flushed out with nitrogen. Trimethylphosphine (6 ml, 0·063 mole) was added by means of a hypodermic syringe, and the reaction mixture was shaken until the solid had dissolved. The benzene was pumped off and the residue dissolved in hot toluene. The solution was filtered into the other limb of the Schlenck tube through a sintered disk, and allowed to crystallize. A second crystallization from toluene yielded the *complex* as yellow needles, 12 g, 69 per cent.

The following complexes, prepared by similar methods, are not described in the preceding text *Phenylethynyl(trimethylphosphine–silver*, [PhC⋮C·AgPMe_3], decomp. 130–140° from acetone (Found: C, 46·5; H, 5·3; Ag, 37·7. Calc. for $C_{11}H_{14}AgP$ C, 46·3; H, 5·0; Ag, 37·9%). The degree of association ebullioscopically in 2·07, 2·99 and 3·82% benzene was 2·21, 1·82 and 2·00. *Phenylethynyl (triethyl phosphine)silver* [PhC⋮C·AgPEt_3), colourless needles m.p. 77·5–78·5° from hexane–toluene (Found: Ag, 32·1, 32·3. Calc. for $C_{14}H_{20}AgP$: Ag, 33·0%). *Phenylethynyl(triethylarsine)silver*,* [PhC⋮C·Ag$AsEt_3$], colourless needles m.p. 89° from toluene containing 30 per cent triethylarsine (Found: C, 45·1; H, 5·5; Ag, 27·9. Calc. for $C_{14}H_{20}AgAs$: C, 45·3; H, 5·4; Ag, 29·1%). This compound turns pink quickly in sunlight. *Propynyl(triethylphosphine)copper*,* [MeC⋮C·CuPEt_3], yellow needles from hexane (Found: C, 48·1; H, 8·2; Cu, 28·9. Calc. for $C_9H_{18}CuP$: C, 49·0; H, 8·2; Cu, 28·8%). This compound is very air sensitive and it dissociates readily.

Acknowledgement—The authors wish to thank the Ethyl Corporation for a research grant.

* These compounds were prepared by Dr. D. Blake.

[10] E. O. Fischer, W. Hafner and H. O. Stahl, *Z. Anorg. Chem.* **282**, 47 (1959).

VOL. 22 1961

VO
2
19

J. Inorg. Nucl. Chem., 1961, Vol. 22, pp. 69 to 76. Pergamon Press Ltd. Printed in Northern Ireland

REACTIONS OF DECAMMINO-μ-PEROXO-DICOBALT(III) SULPHATE WITH AQUEOUS SULPHURIC ACID

R. G. CHARLES and S. BARNARTT
Westinghouse Research Laboratories, Pittsburgh 35, Pennsylvania

(*Received* 3 *April* 1961; *in revised form* 3 *May* 1961)

Abstract—The complex salt $[(NH_3)_5CoOOCo(NH_3)_5](SO_4)_2.3H_2O$ decomposes irreversibly in dilute aqueous H_2SO_4 solutions with the evolution of approximately one half of the peroxo oxygen content as oxygen gas. Simultaneously at least eight cobalt species are produced. Four of these have been identified as Co^{2+}, $[(NH_3)_5Co(H_2O)]^{3+}$, $[(NH_3)_6Co]^{3+}$ and $[(NH_3)_5CoOOCo(NH_3)_5]^{5+}$. A reaction mechanism is postulated which accounts quantitatively for the identified products and for the H_2SO_4 consumed, and which predicts the formation of one or more cobalt(III) complexes containing H_2O_2.

VOL. 22 1961

AMMONIACAL aqueous Co(II) solutions react readily with molecular oxygen to form the decammino-μ-peroxo-dicobalt(III) ion (formula II),[1]

$$[(NH_3)_5CoOOCo(NH_3)_5](SO_4)_2\cdot 3H_2O \qquad [(NH_3)_5CoOOCo(NH_3)_5]^{4+}$$
$$\text{I} \qquad\qquad\qquad\qquad \text{II}$$

Such solutions can be made to give up most of the peroxo oxygen as oxygen gas, with the regeneration of Co(II) ions.[2] Salts containing the ion II are sufficiently stable, however, to be isolated in the solid form; and a number of such salts have been reported in the literature.[3] When added to water (in the absence of excess ammonia) or to acid these salts are known to decompose irreversibly with the evolution of oxygen gas.[2,3] There appears to have been no detailed study, however, of the mode of decomposition or of the products formed, aside from oxygen. We have now carried out an investigation of the reactions of one such salt, decammino-μ-peroxo-dicobalt(III) sulphate trihydrate (compound I), with aqueous sulphuric acid solutions at room temperature.

RESULTS AND DISCUSSION

Sulphuric acid consumed

The number of moles H_2SO_4 which react with 1 mole of compound I in aqueous solution was determined from pH measurements. Fig. 1 shows the data obtained by dissolving 0·0010 mole of I in 10 ml water or in 10 ml of aqueous H_2SO_4 solution, each point on the curve representing a new solution. In pure water the brown compound yields a reddish brown solution, pH 9·5, containing free ammonia, and a small amount of red precipitate. As the H_2SO_4 concentration is raised to a molar ratio above three the solution becomes violet and no precipitation occurs. From Fig. 1 it can be concluded that one mole of compound I reacts with 2·9 H_2SO_4, this proportion being unaffected by the presence of $(NH_4)_2SO_4$ in the solution.

[1] J. C. BAILAR, JR., (Editor) *The Chemistry of the Co-ordination Compounds*, p. 26. Reinhold, New York (1956).
[2] W. GLUUD, K. KELLER and H. NORDT, *Ber. Ges. Kohlentech., Halle* **4**, 210 (1933).
[3] GMELIN'S *Handbuch der anorganischen Chemie, Kobalt, Teil B.* Verlag Chemie, Berlin (1930).

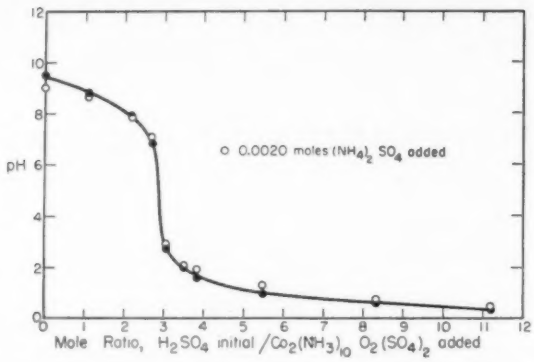

FIG. 1.—pH of solutions made by adding 0·0010 mole $[(NH_3)_5CoOOCo(NH_3)_5](SO_4)_2$ to 10 ml aqueous H_2SO_4, with and without the addition of $(NH_4)_2$ SO_4, 30·2°C.

Oxygen gas evolved

The reaction of I with aqueous H_2SO_4 is accompanied by vigorous gas evolution. Mass spectrometric analysis of the gas evolved indicated essentially pure oxygen, which probably originated from the peroxo oxygen in the compound. The percentage of the peroxo oxygen evolved from H_2SO_4 solutions at 30°C was determined volumetrically, Fig. 2. Provided sufficient acid was present in the solution to react with all the compound added, $H_2SO_4/I > 2·9$, about one-half of the peroxo oxygen was liberated as oxygen gas, this fraction remaining essentially constant up to a molar ratio of 35. In more concentrated acid the oxygen evolution decreased again.

Cobalt-containing compounds produced

Ion-exchange chromatography, utilizing a resin of the sulphonic acid type, was employed to separate cobalt-containing compounds produced by the reaction of I with aqueous H_2SO_4. This separation yielded eight different cobalt-containing species.

The visible absorption spectrum of each coloured band eluted from the resin was

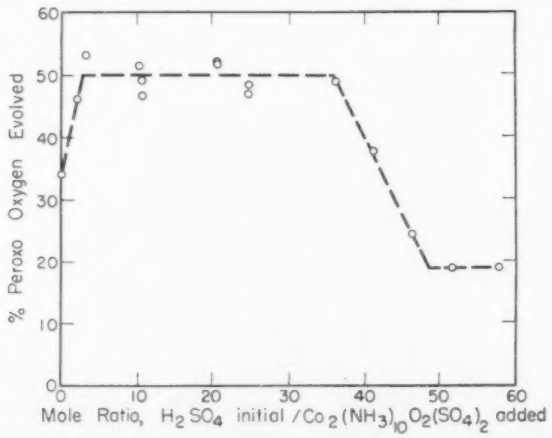

FIG. 2.—Oxygen evolution from solutions made by adding 2×10^{-6} mole $[(NH_3)_5CoOOCo(NH_3)_5]$ $(SO_4)_2$ to 2 ml of aqueous H_2SO_4, 30·2°C.

found to have a peak within the wavelength range 4750–5300 Å (Fig. 4). Hence absorption at 5000 Å was used to follow the separation, measurements being made on successive 35 ml samples of eluate. The results, given in Fig. 3, show that seven coloured fractions, *A* to *G*, were eluted from the column. A green fraction, *H*, remained on the column. The relatively large sample volume (35 ml) used prevented optimum delineation of fractions *A* and *B*; their separation on the column was clearly visible, although a tailing of fraction *A* into *B* was evident.

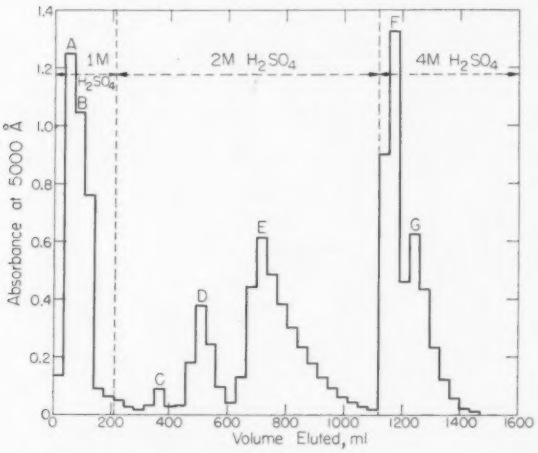

FIG. 3.—Ion-exchange separation of cobalt species from the reaction of $[(NH_3)_5CoOOCo(NH_3)_5](SO_4)_2$ with aqueous H_2SO_4.

In a second experiment a more precise separation of the seven eluted species was carried out by collecting each as a single fraction, using the best visual estimate of the end point. Each fraction was analysed for total cobalt, by fuming a portion to dryness with H_2SO_4 and weighing as $CoSO_4$. Visible absorption spectra of the fractions, determined in 10 cm cells, are shown in Fig. 4. The optical densities plotted have been recalculated to a fraction volume of 500 ml in each case. Fig. 5

TABLE 1.—COBALT-CONTAINING IONS IN ACID SOLUTION OF $[(NH_3)_5CoOOCo(NH_3)_5](SO_4)_2$, SEPARATED BY ION-EXCHANGE

Fraction	Colour	% of original Co taken	Ion identified
A	Red	4·0	
B	Red	53·6*	Co^{2+}
C	Red	2·7	
D	Red	4·0	
E	Red	6·0	
F	Red	7·9	$[(NH_3)_5Co(H_2O)]^{3+}$
G	Yellow	7·9	$[Co(NH_3)_6]^{3+}$
H	Green	6·4	$[(NH_3)_5CoOOCo(NH_3)_5]^{5+}$
TOTAL		92·5	

* 50·9% as Co^{2+}, 2·7% as ion of fraction *A*.

presents the spectrum of the original reaction solution (0·100 M I, 1·00 M H_2SO_4), as well as spectra for solutions of pure cobalt compounds identified as present in one of the fractions. The data are summarized in Table 1.

The absorption spectrum of fraction B required correction for the presence of *A*,

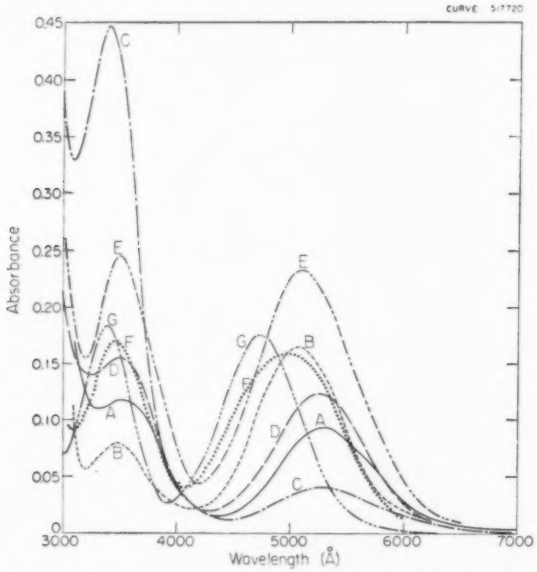

FIG. 4.—Absorption spectra of eluted fractions from ion-exchange separation of cobalt species resulting from the reaction of $[(NH_3)_5CoOOCo(NH_3)_5](SO_4)_2$ with aqueous H_2SO_4.

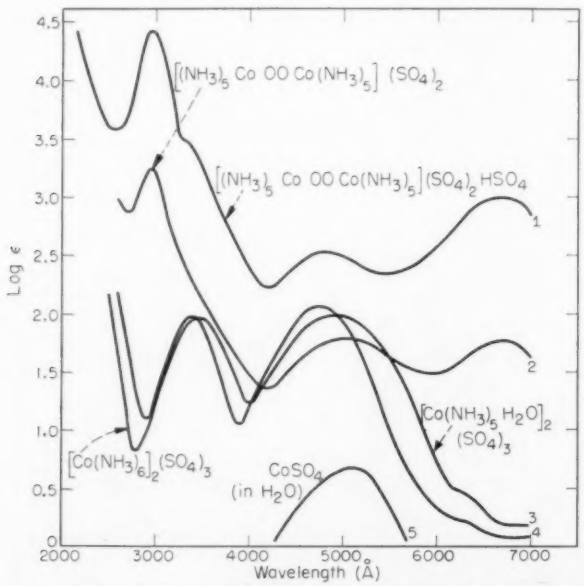

FIG. 5.—Ultra-violet and visible spectra of cobalt complexes in 1 M H_2SO_4.

the contribution of which was determined from the 3500 Å peak, and the corrected spectrum was in good agreement with that for $CoSO_4$. Confirmation of Co^{2+} ion was obtained by magnetic susceptibility measurements on the original solution of I in 1 M H_2SO_4. These measurements were corrected for the presence of the paramagnetic $[(NH_3)_5CoOOCo(NH_3)_5]^{5+}$ ion, the susceptibility of which is known;[4] it was assumed that this was the only other paramagnetic ion present. The results showed approximately one-half of the cobalt present in the solution as Co^{2+}, in agreement with the spectrophotometric data. It was inferred from this agreement that essentially all of the compound I reacted irreversibly and none remained as such in the reaction mixture, for any remaining compound would have decomposed further during the ion-exchange separation, thus increasing the Co^{2+} yield. Additional evidence for the production of Co^{2+}, as well as for free NH_4^+, was obtained by adding acetone to the reaction mixture of I with 1 M H_2SO_4. An X-ray diffraction powder pattern of the precipitated solid showed the presence of the double salt

$$CoSO_4 \cdot (NH_4)_2SO_4 \cdot 6H_2O.$$

VOL. 22 1961

The identification of fraction *F* was made by an ion-exchange separation of the original solution to which $[(NH_3)_5Co(H_2O)]_2(SO_4)_3 \cdot 3H_2O$ was added. It was found that the added compound eluted out quantitatively with *F*. The presence of this compound was demonstrated also by treating the original reaction mixture (without the added aquo compound) with 8-hydroxyquinoline and ammonia to precipitate the Co(II) fraction, then adding acetone and H_2SO_4 to the filtrate to precipitate out Co(III) salts. The latter precipitate was shown by X-ray diffraction to contain $[(NH_3)_5Co(H_2O)]_2(SO_4)_3 \cdot 3H_2O$ as the major crystalline component.

Identification of fraction *G* as the hexammino cobalt(III) salt was confirmed by addition of this salt to the ion-exchange column; it eluted out quantitatively with *G*.

Fraction *H* had the characteristic green colour of

$$[(NH_3)_5CoOOCo(NH_3)_5](SO_4)_2\ HSO_4.$$

III

Its identification as compound III was provided by absorption spectra, curves 1 and 2 of Fig. 5, since this compound exhibited two distinctive absorption peaks at 6750 and 2960 Å. From these peaks, the reaction mixture of I in H_2SO_4 (curve 2) has 6·2 per cent of the total cobalt as compound III, is good agreement with the value found by chemical analysis of separated fraction *H* (Table 1). As shown in the Experimental section below, the starting compound contains III as an impurity. The quantity found in the reaction mixture, however, is appreciably larger, hence compound III is also a reaction product.

The unidentified fractions *A*, *C*, *D* and *E* contain red compounds all having spectra which exhibit two absorption peaks, one near 5000 Å and one near 3500 Å. This type of spectrum is characteristic of Co(III) complexes (curves 3 and 4, Fig. 5). It was anticipated that the sulphato-pentammino Co(III) salt, $[(NH_3)_5Co(SO_4)]_2\ SO_4$, would be formed in the reaction solution, since it can exist in equilibrium with the aquo-pentammino salt in sulphate solutions.[5,6] The monovalent ion: $[(NH_3)_5Co$

[4] V. K. Gleu and K. Rehm, *Z. Anorg. Chem.* **237**, 79 (1938).
[5] H. Taube and F. A. Posey, *J. Amer. Chem. Soc.* **75**, 1463 (1953).
[6] M. Mori and R. Tsuchiya, *Bull. Chem. Soc. Japan* **33**, 841 (1960).

$(SO_4)]^+$ would tend to pass through the column more readily than ions with greater charge, and might be expected in fraction *A*. It was found, however, by addition of this compound to the original solution and subsequent passage through the ion exchange column, that this ion moved distinctly more slowly than fraction *A* and more rapidly than *C*. It is possible that a trace of the sulphato compound was present in the reaction solution and was eluted with fraction *B*.

Hydrogen peroxide as a reaction product

It was anticipated that hydrogen peroxide, if formed in the reaction mixture, would elute out of the ion exchange column before fraction *A*. Portions of the initial eluate, up to the time that the first red band reached the bottom of the column, were each tested with a drop of dilute $KMnO_4$. The latter was not decolourized, hence there was no free H_2O_2 in the eluate. A direct quantitative measurement on the original reaction solution (0·10 M compound I, 1·00 M H_2SO_4) was made by preparing the latter in a closed system and measuring the oxygen evolved; then $KMnO_4$ was added and the increase in oxygen (from oxidation of H_2O_2) determined. This test, capable of detecting 0·3 per cent conversion of peroxo-oxygen to H_2O_2, was negative. Polarograms of the original reaction solution diluted tenfold also showed no detectable wave corresponding to H_2O_2, although a recent paper[7] indicates that the presence of Co(III) complexes in the solution might interfere. It was concluded that H_2O_2, if present as a reaction product, must be complexed with one or more cobalt-containing species.

Reaction mechanism

The results described above demonstrate that compound I decomposes entirely and irreversibly in aqueous sulphuric acid. The multitude of reaction products precludes any single, simple reaction path. Nevertheless one can postulate a straightforward reaction scheme, as described below, which is in essential agreement with all of the known facts and provides reasonable predictions concerning the unidentified products.

The primary reaction of the ion II in acid is assumed to be the addition of H^+ to form the intermediate ion IV:

$$\underset{\text{II}}{[(NH_3)_5CoOOCo(NH_3)_5]^{4+}} + H^+ \rightarrow \underset{\text{IV}}{[(NH_3)_5CoOOCo(NH_3)_5]^{5+}} \qquad (1)$$
$$\qquad\qquad\qquad

Ion VI, containing uncharged HO_2, would be very reactive towards other species present in the solution. The probable reactions with H_2O, NH_4^+ and undissociated ion IV are:

$$2VI + H_2O \rightarrow O_2 + [(NH_3)_5Co(H_2O)]^{3+} + [(NH_3)_5Co(H_2O_2)]^{3+} \quad (4)$$
VII

$$2VI + NH_4^+ \rightarrow O_2 + [(NH_3)_6Co]^{3+} + [(NH_3)_5Co(H_2O_2)]^{3+} + H^+ \quad (5)$$

$$VI + IV \rightarrow [(NH_3)_5CoOOCo(NH_3)_5]^{5+} + [(NH_3)_5Co(H_2O_2)]^{3+} \quad (6)$$

Further interaction of ion VI with other species, particularly with VII, would undoubtedly occur to produce the unidentified products found as fractions *A*, *C*, *D* and *E*. It is probable that one of the latter fractions contains VII. There is no direct evidence for the existence of Co(III) complexes containing H_2O_2, such as VII, but evidence for the corresponding Fe(III) complex has been reported recently.[8]

If it is assumed that reaction (5) accounts for all of the $[(NH_3)_6Co]^{3+}$ ion actually found (0·16 mole per mole of I reacted), and that $[(NH_3)_5CoOOCo(NH_3)_5]^{5+}$ ion (0·03 mole per mole I) is generated by reaction (6), the above equations predict the following numbers of moles per mole of compound I reacting:

Calculated: H_2SO_4 reacted, 2·9; Co^{2+} produced, 1·00; O_2 evolved, 0·47.

Found: H_2SO_4, 2·9; Co^{2+}, 1·05; O_2, 0·5.

Thus the proposed mechanism is in good agreement with the experimental facts.

EXPERIMENTAL

Decammino-μ-peroxo-dicobalt(III) sulphate trihydrate (compound I)

The method of preparation was a modification of that described by VORTMANN.[9] Ammonium sulphate (13·2 g or 0·1 mole) and $CoSO_4 \cdot 7H_2O$ (28·1 g or 0·1 mole) were dissolved in 100 ml water, and 100 ml of concentrated NH_4OH added. Oxygen was bubbled through the filtered solution at room temperature for 2 hr at a rate of 100 ml/min. The solution was refrigerated in a stoppered flask overnight, during which time a precipitate formed. The latter was filtered off and washed with 50 ml of 7 M NH_4OH. The dark brown solid was dried over $CaCl_2$ for 72 hr. It was stored in a refrigerator in a tightly capped jar. The yield was 18·5 g. (Found: Co, 21·0; SO_4, 34·4; Calc. for $Co_2(NH_3)_{10}O_2(SO_4)_2 \cdot 3H_2O$: Co, 20·81; SO_4, 33·93%).

By magnetic susceptibility measurements the solid was found to be diamagnetic, as expected for a dicobalt (III) ammino compound; the corresponding nitrate has been reported to be diamagnetic.[10] Paramagnetic resonance measurements, however, showed the presence of a small amount of a paramagnetic impurity. The paramagnetic ion was identified as $[(NH_3)_5CoOOCo(NH_3)_5]^{5+}$ by comparison with resonance data on compound III diluted with the compound $[(NH_3)_5Co(H_2O)]_2(SO_4)_3 \cdot 3H_2O$. The results showed that this paramagnetic ion contained 3·1% of the total cobalt in the material. Since no method of further purification was found, the material was used in this form.

Other cobalt compounds used in the investigation were prepared by standard methods.[3,4]

Oxygen evolution measurements

The volume of oxygen evolved when compound I was dissolved in aqueous solutions was measured at constant pressure and 30·2°C. The apparatus used consisted of a Pyrex reaction tube connected to a 5 ml glass syringe, equipped with a micrometer driver, and to a differential metal Bourdon gauge. The internal volume of the system was about 60 ml. A small tube containing a plastic-covered magnet and $2{\cdot}00 \times 10^{-4}$ mole of I was suspended magnetically above 2·00 ml of solution, at a fixed pressure

[8] M. L. HAGGETT, P. JONES and W. F. K. WYNNE-JONES, *Discussions Faraday Soc.* **29**, 153 (1960).
[9] G. VORTMANN, *Monatsch. Chem.* **6**, 404 (1885).
[10] E. FEYTIS, *C. R. Acad. Sci., Paris* **152**, 710 (1911).

VOL. 22 1961

near atmospheric. The compound was then dropped into the solution and the mixture stirred magnetically. The pressure was restored to its original value by means of the micrometer syringe and the change in volume measured. Visible gas evolution terminated within a few minutes, and steady state volume readings usually were reached within an hour.

Ion-exchange fractionation

The resin used was Dowex AG 50 W-X8 in the hydrogen form, 100–200 mesh (Bio Rad Laboratories, Richmond, California). A column of 25 ml of the resin in a standard 50 ml burette (1 cm i.d.) was washed with 100 ml of water, followed by 100 ml of 1 M H_2SO_4. The mixture to be resolved was prepared by dissolving $1{\cdot}00 \times 10^{-3}$ mole of I in 10·0 ml of 1·00 M H_2SO_4. This was allowed to stand for 2 hr. It was then drawn into the column, at which time collection of the first fraction was initiated, and this was followed by 10 ml of 1 M H_2SO_4 wash solution. Elution was then continued with 1 M, 2 M, or 4 M H_2SO_4 (refer Fig. 3).

Chemical separation of reaction products

(a) Acetone was added to a solution of 0·1 M compound I in 1 M H_2SO_4. A precipitate formed, which was filtered off and washed with acetone. An X-ray powder diffraction pattern of this solid showed the presence of the double salt $CoSO_4{\cdot}(NH_4)_2SO_4{\cdot}6H_2O$ as the principal component.

(b) A solution of 0·1 M compound I in 0·3 M H_2SO_4 was treated with a slight excess of 8-hydroxyquinoline, followed by ammonia to pH 5·0, to precipitate out Co(II) 8-hydroxyquinolate.[4] The filtrate was extracted with benzene to remove the excess 8-hydroxyquinoline. The aqueous layer was concentrated in a stream of oxygen, after which acetone was added to form two liquid layers. The upper, nearly colourless, layer which contained $(NH_4)_2SO_4$ was discarded. The lower red solution was treated with 0·001 M H_2SO_4 and additional acetone, again forming two layers of which the upper was discarded. This process was repeated until a red crystalline solid precipitated. The X-ray powder diffraction pattern of the air-dried solid showed $[Co(NH_3)_5H_2O]_2(SO_4)_3{\cdot}3H_2O$ as the only crystalline component. Chemical analysis, however, showed that at least one other (amorphous) component must have been present. (Found: Co, 12·2; SO_4, 47·0; Calc. for $[Co(NH_3)_5H_2O]_2(SO_4)_3{\cdot}3H_2O$: Co, 17·66; SO_4, 43·25%).

Other procedures

Ultra-violet and visible absorption spectra were recorded with a Cary model 14 spectrophotometer Quartz cells of path length 0·20, 0·50, 1·00 or 10·0 cm were used as required. The fractions from the ion exchange separation were diluted quantitatively to give peak absorbance (optical density) values in the range 0·5–1·0. For purposes of comparison in Fig. 4 the observed absorbance values were all recalculated to a volume of 500 ml.

A glass–calomel pair was used for all of the pH measurements. Magnetic susceptibility measurements on either solids or solutions were made at room temperature by the Faraday method.[11] The paramagnetic resonance of compound III was observed at 9×10 c/s and 77°K.

Acknowledgement—The writers are grateful to Mr. P. PIOTROWSKI for the magnetic susceptibility measurements, to Dr. J. CASTLE for paramagnetic resonance measurements, to Mrs. M. A. DOLAN and Miss A. PERROTTO for the syntheses of some of the cobalt complexes, and to Mr. E. W. BEITER for some of the analyses.

[11] P. W. SELWOOD, *Magnetochemistry*, (2nd Ed.) p. 11. Interscience, New York (1956).

VOL. 22 1961

J. Inorg. Nucl. Chem., 1961, Vol. 22, pp. 77 to 85. Pergamon Press Ltd. Printed in Northern Ireland

THE THERMAL DEAQUATION OF SOME AQUOPENTAMMINE-CHROMIUM (III)COMPLEXES†

W. W. WENDLANDT and J. L. BEAR‡
Department of Chemistry, Texas Technological College, Lubbock, Texas

(*Received* 28 *March* 1961; *in revised form* 24 *April* 1961)

Abstract—The thermal deaquation of aquopentamminechromium(III) chloride, bromide, iodide and nitrate was studied by the techniques of DTA and TGA. The deaquation reaction was found to take place between 50 and 150°. The rate of deaquation was determined by following the increase in water vapour-pressure as a function of time at constant temperature. The deaquation reactions appeared to be first order with E^* values ranging from 16 ± 2 to 31 ± 3 kcal. An attempt was made to determine the heat of deaquation by quantitative DTA. The heats of deaquation found were 6·1 ± 0·5, 7·8 ± 0·6 and 6·3 ± 0·5 kcal mole^{-1}, for the chloride, bromide and iodide complexes, respectively.

JORGENSEN[1] was the first to observe that the aquopentamminechromium(III) complexes, $[Cr(NH_3)_5H_2O]X_3$, where X^- is Cl^-, Br^-, I^- and NO_3^-, lost the co-ordinated water when heated to 100°, according to the reaction:

$$[Cr(NH_3)_5H_2O]X_3(s) \xrightarrow{100°} [Cr(NH_3)_5X]X_2(s) + H_2O(g) \quad (1)$$

Since this time, few studies have been reported on the deaquation of other aquochromium(III) complexes, except perhaps from a synthesis viewpoint. The thermogravimetric analysis (TGA) of the $CrCl_3 \cdot 6H_2O$ hydration isomers has been reported[2] as well as a study by differential thermal analysis (DTA).[3] A TGA and DTA study has been reported on *cis*- and *trans*-$K[Cr(C_2O_4)_2(H_2O)_2]$.[4] Because of the limited amount of information available on the thermal deaquation of the aquopentamminechromium(III) complexes, the complexes, $[Cr(NH_3)_5H_2O]X_3$, where X^- is Cl^-, Br^-, I^- and NO_3^-, were prepared and subjected to TGA, DTA, and deaquation rate studies.

EXPERIMENTAL

Thermobalance

The automatic recording thermobalance and its modification has been described previously.[5] Sample sizes ranged in weight from 50 to 100 mg and were decomposed in an air atmosphere. The furnace heating rate was approximately linear with time at about 5° per min. All samples were studied in duplicate or triplicate with an agreement between the resultant pyrolysis curves of about ±3 per cent. Particle sizes of the samples ranged between 200 and 400 mesh. No attempt was made to determine the effect of particle size on the minimum decomposition temperatures.

† Taken in part from the Ph.D. thesis of J. L. BEAR, Texas Technological College, Lubbock, Texas, 1960.
‡ Present address: Dept. of Chemistry, Florida State Univ., Tallahassee, Florida.

[1] S. M. JORGENSEN, *J. Prakt. Chem.* **18**, 209 (1878).
[2] D. KIRÁLY, K. ZALATNAI and M. T. BECK, *J. Inorg. Chem.* **11**, 170 (1959). In Press
[3] A. V. PAMFILOV and N. N. GUMENYUK, *Zh. Obshchei Khim.* **23** 1065 (1953).
[4] W. W. WENDLANDT, T. D. GEORGE and K. V. KRISHNAMURTY, *J. Inorg. Nucl. Chem.* In press.
[5] W. W. WENDLANDT, *Analyt. Chem.* **30**, 56 (1958); **32**, 848 (1960).

Differential thermal analysis apparatus

The DTA apparatus consisted of a furnace and sample holder similar to that previously described[6,7] and a strip-chart microvolt recorder.[8] The differential temperatures, ΔT, were detected by chromel–alumel thermocouples, symmetrically located in the centre of the ceramic sample chambers. Sample sizes ranged in weight from 100 to 150 mg and were packed in the sample chamber using a "sandwich" type packing with α-alumina. The reference chamber packing consisted of previously ignited α-alumina. The heating rate of the furnace was approximately linear with time at about 6° per min with an air atmosphere maintained in the furnace during the thermal decomposition reaction. Duplicate studies were made on each compound with a resultant agreement between peak maxima temperatures of about ±2 per cent.

Rate studies

The rates of deaquation of the aquopentamminechromium complexes were determined by means of a modified Smith-Menzies isoteniscope.[9] The isoteniscope was placed in an oil bath, the temperature of which was controlled to ±0·1°. Sample sizes ranged in weight from 25 to 50 mg, with a sample particle size between 200 and 400 mesh. The pressure of the system was measured either with a 0·1–10 mm McLeod gauge or a mercury manometer and cathetometer, depending upon the pressure range being studied.

DTA *Heat of deaquation studies*

The apparatus and technique have been described previously.[10]

Preparation of the complexes

The aquopentamminechromium(III) complexes were prepared from $[Cr(NH_3)_5H_2O](NO_3)_3 \cdot NH_4NO_3$ as previously described.[11]

The nitrato- and halopentamminechromium(III) complexes were prepared from the corresponding aquo- complexes by treatment with an appropriate mineral acid.[11]

The aquo-complexes were studied by the various techniques immediately after preparation and analysis since they are unstable with respect to the deaquation reaction even at room temperature. The complexes were analysed for anion content (except the nitrate ion) by an argentimetric titration; for water content by weight-loss at 100–110°; and for chromium content by a complexometric titration.[12]

RESULTS AND DISCUSSION

TGA *studies*

The results of the TGA studies are given in Fig. 1. Although data for only the aquopentamminechromium(III) complexes are given, the corresponding anionopentammine complexes were also studied. However, the curves for these complexes were similar to those of the aquopentammine complexes, after the deaquation reaction. All of the complexes began to lose co-ordinated water in the 55°–100° temperature range, the process being completed in the 100°–145° temperature region. Above 140°–200°, the resulting anionopentammine complexes decomposed to give Cr_2O_3 or possibly mixed oxides as the thermal decomposition product.

If the minimum deaquation temperature can be taken as a measure of the stability of the aquopentammine complexes, the order of decreasing stability of the complexes may be listed as: $[Cr(NH_3)_5H_2O]Cl_3 < [Cr(NH_3)_5H_2O](NO_3)_3 < [Cr(NH_3)_5H_2O]Br_3 < [Cr(NH_3)_5H_2O]I_3$. A more pronounced difference in the thermal stability was

[6] W. LODDING and L. HAMMEL, *Rev. Sci. Instrum.* **30**, 885 (1959).
[7] W. LODDING and L. HAMMEL, *Analyt. Chem.* **32**, 657 (1960).
[8] W. W. WENDLANDT, *J. Chem. Educ.* **37**, 94 (1960).
[9] G.W. THOMSON, *Physical Methods of Organic Chemistry*, (Edited by A. WEISSBERGER) Vol. 1, p. 175. Interscience, New York, (1949).
[10] W. W. WENDLANDT and J. L. BEAR, *J. Phys. Chem.* In press
[11] M. MORI, *Inorganic Syntheses*, (Edited by T. MOELLER) Vol. 5, p. 132. McGraw-Hill, New York (1957).
[12] H. L. SCHLAEFER and O. KLING, *Z. Anorg. Chem.* **302**, 1 (1959).

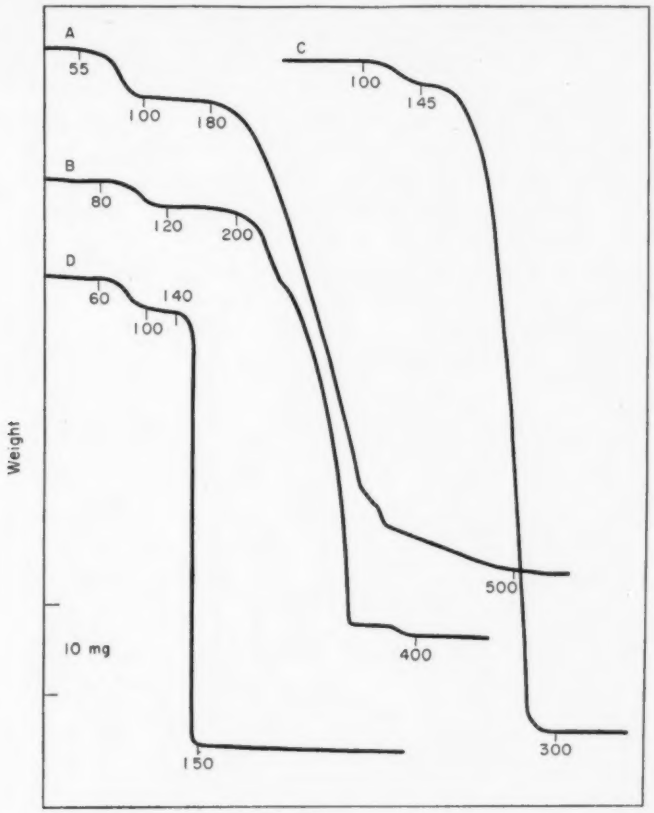

FIG. 1.—TGA curves of the aquopentamminechromium(III) complexes.
A, $[Cr(NH_3)_5H_2O]Cl_3$; *B*, $[Cr(NH_3)_5H_2O]Br_3$;
C, $[Cr(NH_3)_5H_2O](NO_3)_3$; *D*, $[Cr(NH_3)_5H_2O]I_3$.

TABLE 1.—FIRST ORDER RATE CONSTANTS AND ACTIVATION ENERGIES FOR THE AQUOPENTAMMINE-CHROMIUM(III) COMPLEXES

Compound	Temperature (°C)	$-\log k$	Order	E^* (kcal)
$[Cr(NH_3)_5H_2O]Cl_3$	85·2	3·00	1	18 ± 2
	90·2	2·85		
	94·2	2·74		
$[Cr(NH_3)_5H_2O]Br_3$	83·6	3·73	1	31 ± 3
	87·7	3·50		
	92·7	3·37		
$[Cr(NH_3)_5H_2O]I_3$	86·2	3·45	1	18 ± 2
	90	3·35		
	94·5	3·23		
$[Cr(NH_3)_5H_2O](NO_3)_3$	58·1	3·73	1	16 ± 2
	62·5	3·59		
	65·6	3·50		

observed in the case of the anionopentammine complexes, where the order of decreasing stability was: $[Cr(NH_3)_5NO_3](NO_3)_2 < [Cr(NH_3)_5I]I_2 < [Cr(NH_3)_5Cl]Cl_2 < [Cr(NH_3)_5Br]Br_2$. The lower thermal stability of the nitratopentammine complex was not unexpected in view of the oxidizing nature of the nitrate ion; in fact, the complex exploded at about 150°. With the halopentammine complexes, no distinction was made between thermal stability, i.e., pyrolysis of the complex, and ease of oxidation of the complex by oxygen. Perhaps both reactions occur at the minimum decomposition temperatures. The iodopentammine complex released voluminous amounts of free iodine; a fact which may account for its low thermal stability in comparison with that of the other halopentammine complexes.

DTA *studies*

The DTA thermograms of the aquo- and anionopentammine complexes are given in Figs. 2 and 3.

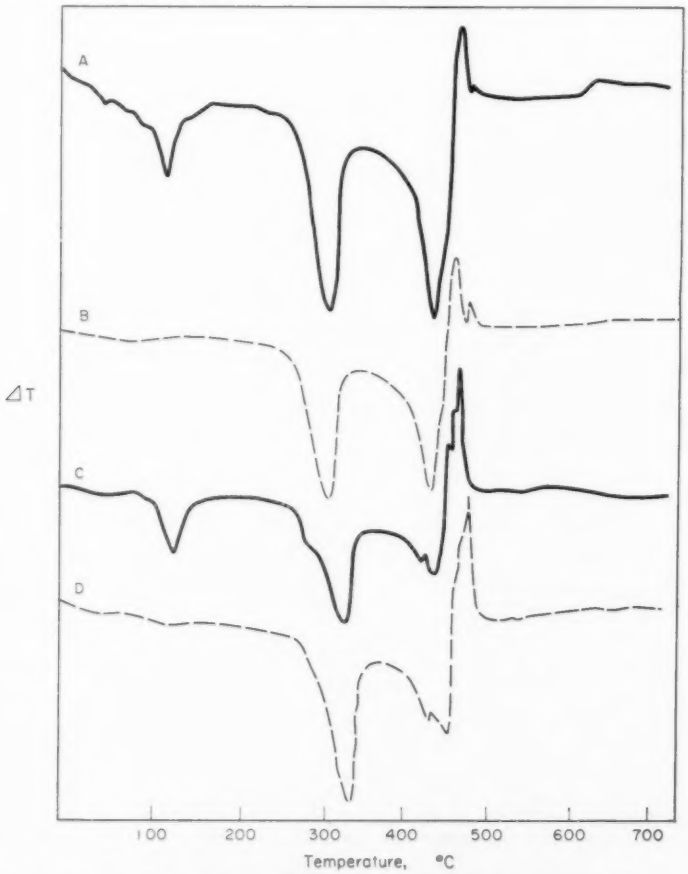

FIG. 2.—DTA curves of aquo- and anionopentamminechromium(III) complexes.
A, $[Cr(NH_3)_5H_2O]Cl_3$; *B*, $[Cr(NH_3)_5Cl]Cl_2$;
C, $[Cr(NH_3)_5H_2O]Br_3$; *D*, $[Cr(NH_3)_5Br]Br_2$.

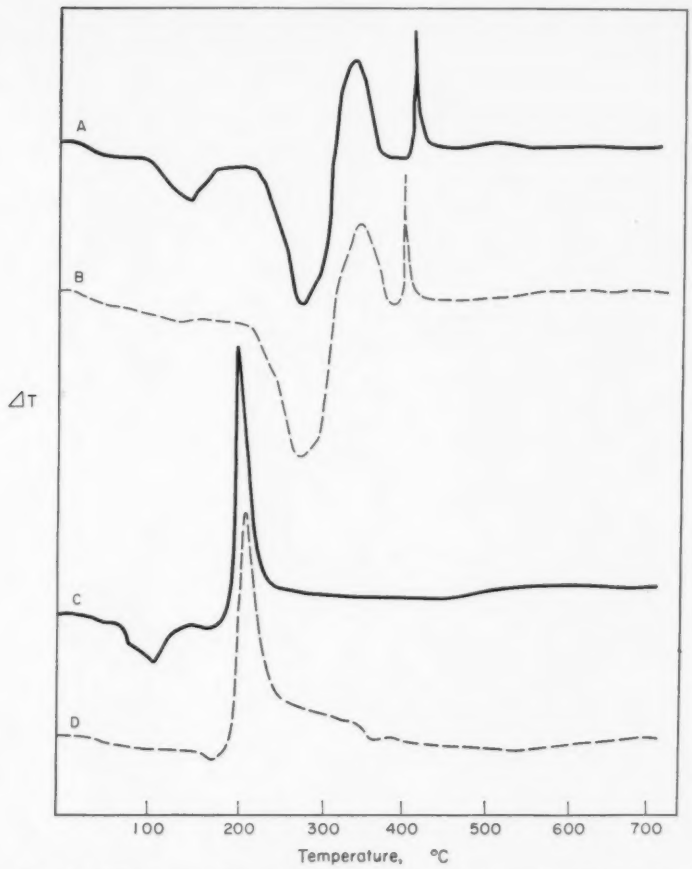

FIG. 3.—DTA curves of aquo- and anionopentamminechromium(III) complexes.
A, $[Cr(NH_3)_5H_2O]I_3$; *B*, $[Cr(NH_3)_5I]I_2$;
C, $[Cr(NH_3)_5H_2O](NO_3)_3$; *D*, $[Cr(NH_3)_5NO_3](NO_3)_2$.

For the aquopentammine complexes, endothermic peaks, with peak maximas in the 104°–138° temperature range, were observed for the deaquation reaction. This peak was followed by a series of endothermic and exothermic peaks which were the result of further decomposition of the complex. However, it was not possible to assign definite transitions to these peaks due to the complex nature of the reactions involved and also to the lack of other confirming data such as X-ray diffraction.

The thermogram for $[Cr(NH_3)_5H_2O]Cl_3$ showed three endothermic peaks at 115°, 302° and 440°, respectively, and a sharp exothermic peak with a maxima at 460°. In the case of $[Cr(NH_3)_5Cl]Cl_2$, all of these peaks were present except the 115° peak. Thus, this latter peak is assigned to the deaquation reaction as shown in equation (1). The 302° peak was probably caused by the primary disruption of the chloropentammine complex followed by further decomposition and oxidation to give Cr_2O_3 as the terminal product.

A similar interpretation may be pursued with the bromide and iodide aquopentammine complexes. The deaquation peaks were centred at 215° and 138°,

respectively, followed by decomposition peaks in the higher temperature range. The halopentammine thermograms gave peaks at the same temperature maximas as were found in the aquopentammine curves, after the deaquation reaction. The extremely sharp exothermic peak at 400° and 410° for the iodo- and aquopentammine iodide complexes should be noted. Such a peak could be caused by some type of a phase transition.

The exothermic nature of the decomposition of the aquo- and nitratopentammine nitrate complexes was well illustrated in the thermograms for these two compounds. In the case of the aquo-complex, the deaquation reaction gave an endothermic peak

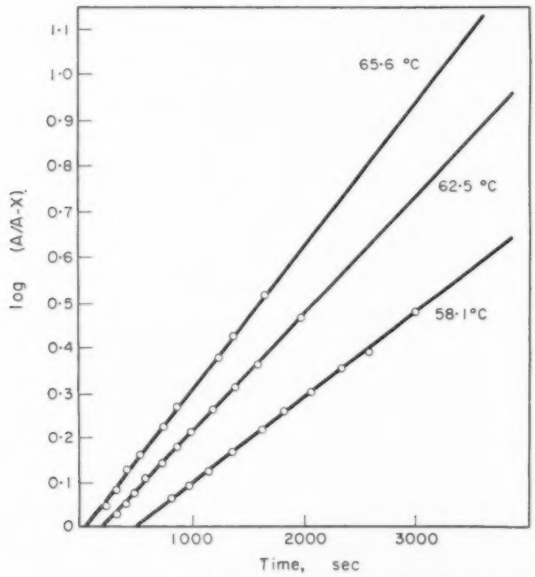

FIG. 4.—First order rate plots for $[Cr(NH_3)_5H_2O](NO_3)_3$.

centered at about 104°, followed by a large exothermic peak at 200°. This latter peak was caused by the decomposition of the complex. Similarly, the nitrato-complex gave the same exothermic peak.

Rate of deaquation studies

The rate of the deaquation reaction, as illustrated by equation (1), was determined at three different temperatures by following the pressure increase in the isoteniscope due to the liberation of gaseous water. It was assumed that the number of moles of gaseous water produced upon the completion of the reaction was equal to the number of moles of reactant initially present. Thus, the final pressure, a, represented the number of moles of complex at the beginning of the reaction, and x, the pressure at time t, represented the number of moles of water produced up to time t. A plot of $a/(a - x)$ vs. t was made for each complex.

Such a plot is illustrated in Fig. 4 for $[Cr(NH_3)_5H_2O](NO_3)_3$. As may be observed, straight lines were obtained for each temperature indicating that all of the deaquation reactions followed a first order rate law. From the first order rate constants obtained

at various temperatures, the activation energies, E^*, were evaluated using an Arrhenius plot. Such a plot is shown in Fig. 5 for $[Cr(NH_3)_5H_2O](NO_3)_3$. The other complexes yielded similar plots.

The activation energies for the deaquation reaction were all very similar to each other except in the case of $[Cr(NH_3)_5H_2O]Br_3$. The E^* for this complex was roughly twice that for the others. An explanation for this is not known at the present time. Perhaps this anomaly may be due to a different distribution of particle sizes present in the two different samples.

Heat of deaquation studies

The heats of deaquation of the complexes, ΔH, as represented in equation (1),

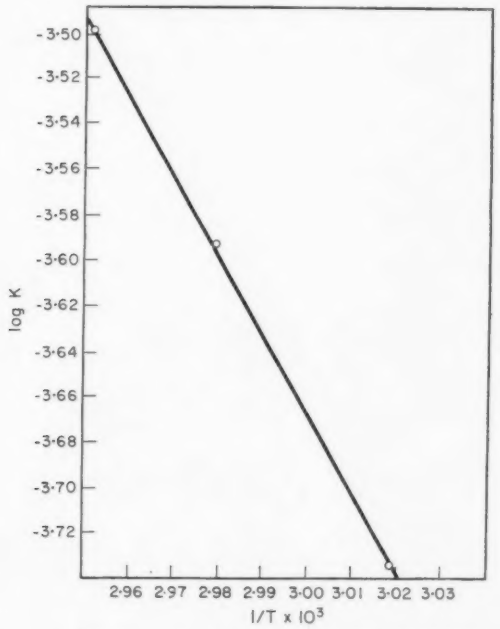

FIG. 5.—Arrhenius plot for $[Cr(NH_3)_5H_2O](NO_3)_3$.

were determined by quantitative DTA. The ΔH of the reaction was obtained by integration of the peak areas obtained for the deaquation reaction. From the various theories on quantitative DTA,[13–15] that of SPEIL *et al.*[13] states that the peak area is equal to

$$\text{peak area} = \int_{t_1}^{t_2} \theta \, dt = \frac{\Delta H M}{g\lambda}$$

where t_1 and t_2 are the time at the beginning and end of the peak, θ is the differential temperature, ΔH is the heat of reaction involved in the deaquation reaction, M is the mass of reactive sample present, λ is the thermal conductivity of the sample, and g is

[13] S. SPIEL, L. H. BERKELHAMER, J. A. PASK and B. DAVIS, *U.S. Bur. Min. Tech. Paper* **664**, (1945).
[14] M. J. VOLD, *Analyt. Chem.* **21**, 683 (1949).
[15] S. L. BOERSMA, *J. Amer. Ceram. Soc.* **38**, 281 (1955).

a constant dependent on the furnace and sample holder geometry. To determine the above constants, g and λ, the instrument was calibrated with compounds of known thermal properties.

The heats of deaquation of the aquopentamminechromium(III) chloride, bromide and iodide complexes, was $6{\cdot}1 \pm 0{\cdot}5$, $7{\cdot}8 \pm 0{\cdot}6$ and $6{\cdot}3 \pm 0{\cdot}5$ kcal mole^{-1}, respectively. However, no great accuracy is claimed for these results due to the number of variables involved in their determination.

Acknowledgements—The helpful assistance of T. D. GEORGE, W. ROBINSON and P. KUHN is gratefully acknowledged. This work was supported in part by the Robert A. Welch Foundation of Houston, Texas.

J. Inorg. Nucl. Chem., 1961, Vol. 22, pp. 85 to 95. Pergamon Press Ltd. Printed in Northern Ireland

THE ABSORPTION SPECTRA OF COMPLEX SALTS—V

STRUCTURES OF COPPER(II) N:ARYL-GLYCINATES

D. P. GRADDON
Inorganic Chemistry Department, University of New South Wales, Sydney, Australia

(*Received* 26 *April* 1961)

Abstract—In aqueous solution copper(II) N:aryl-glycinates appear to be of two types:—copper(II) N:(4:methyl-phenyl)glycinate, N:(4:ethoxy-phenyl)glycinate and N:(4:chloro-phenyl)glycinate are highly stable, react with excess aryl-glycinate ion and have a single absorption band in the visible region at about 730 mμ; they are thought to have the usual chelate amino-acid type of structure (I).

Copper(II) N:phenyl-glycinate, N:(2:methyl-phenyl)glycinate, N:(2:methoxy-phenyl)glycinate, N:(2:chloro-phenyl)glycinate, N:(2:4:dimethyl-phenyl)glycinate, N:methyl-N:phenyl-glycinate and N:(4:fluoro-phenyl)glycinate are much less stable in solution, do not react with excess aryl-glycinate ion and have two overlapping absorption bands in the visible region at about 670 mμ and 870 mμ; these compounds are thought to have the copper(II) alkanoate type of structure (II), in which the nitrogen atom no longer acts as donor. Factors are discussed which could account for the favouring of the suggested structures in each case.

VOL. 22 1961

IN the course of studies on the absorption spectra of copper(II) complexes it became apparent that the copper(II) N:aryl-glycinates were of two distinct types, depending upon the nature of the aryl residue. Whereas continuous variation studies showed that in aqueous solution the stable species were always of empirical formula (ArNH.$CH_2CO_2)_2Cu$, plots of colour intensity versus anion concentration for a fixed copper(II) concentration showed that two types of compound could be formed of widely different stabilities; these differences were reflected in different reactions of the neutral species with excess anion, in different behaviour towards acids and in different absorption spectra, and lead to the conclusion that the two groups of neutral species are of structurally different types.

1. *Reaction of N:aryl-glycinate ions with copper(II) ions in aqueous solution*

The addition of copper(II) sulphate solution to aqueous solutions of sodium N:aryl-glycinates produced an intense green colour, shown by continuous variation studies to be characteristic of the neutral species $(ArNH{\cdot}CH_2CO_2)_2Cu$.

The stability of neutral copper(II) N:phenyl-glycinate in aqueous solution was not very high and the intensity of colour continued to increase indefinitely with increasing anion concentration, formation of the neutral species being about 80 per cent complete at a copper(II) concentration of 0·002 g-ion per litre and N:phenyl-glycinate concentration 0·004 g-ion per litre. Parallel results were obtained for the ortho-substituted aryl-glycinates N:(2:methyl-phenyl)glycinate, N:(2:methoxy-phenyl)glycinate and N:(2:chloro-phenyl)glycinate, for the N:methyl-N:phenyl-glycinate and for the N:(4:fluoro-phenyl) glycinate (Fig. 1).

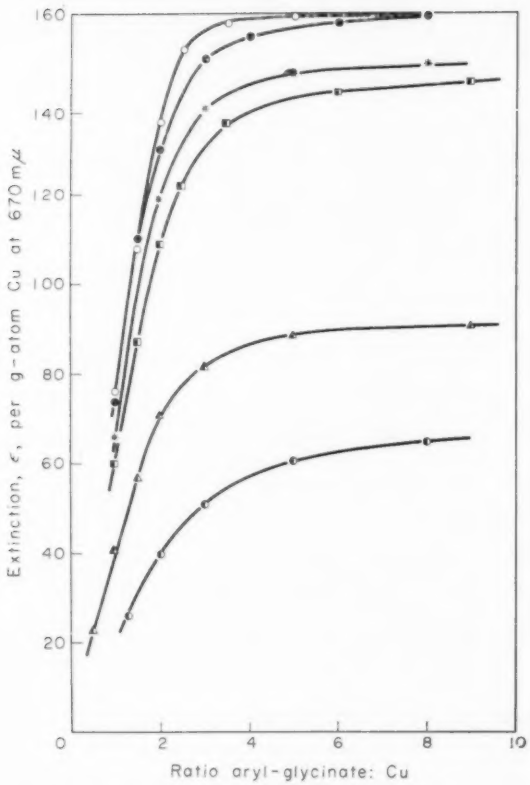

FIG. 1.—Extinction/composition curves for aqueous solutions of copper(II) sulphate (0·002 g-ion Cu per litre) and sodium N:phenyl-glycinate ●, N:(2:methyl-phenyl)glycinate ◧, N:(2:methoxy-phenyl)glycinate ▲, N:(2:chloro-phenyl)glycinate ◐, N:methyl-N:phenyl-glycinate ○, and N:(4:fluoro-phenyl)glycinate .*

Fig. 2 shows corresponding intensity-composition curves for the para-substituted aryl-glycinates N:(4:methyl-phenyl)glycinate, N:(4:ethoxy-phenyl)glycinate and N:(4:chloro-phenyl)glycinate, the intensity of absorption in each case reaching a maximum with an anion:cation ratio of 2:1 and decreasing slightly with further excess of anion. Similar behaviour is observed with glycinate ions* and suggests that the neutral species first formed, $(ArNH{\cdot}CH_2CO_2)_2Cu$, is highly stable, but reacts with excess aryl-glycinate ion to form an unstable complex anion, $[(ArNH.CH_2CO_2)_3Cu]^-$, as occurs with glycinate.[1] While most other open-chain amino-acid anions show little tendency to form complex anions of this type with copper(II) ions in aqueous solution, the composition-intensity curves always show a sharp break at an anion:cation ratio of 2:1, indicating a high stability for the neutral complex, as exemplified in Fig. 2. by the N:methyl-glycinate (sarcosinate).

The N:(4:methyl-phenyl)glycinate ion and the other two ions in this group thus react with copper(II) ions in a way characteristic of α-amino-acid anions, and we

* With glycinate ions the extinction remains constant in presence of excess anion, but there is a reversal in the composition/wavelength curve.

[1] H. L. RILEY and V. GALLAFENT, *J. Chem. Soc.* 2029 (1931).

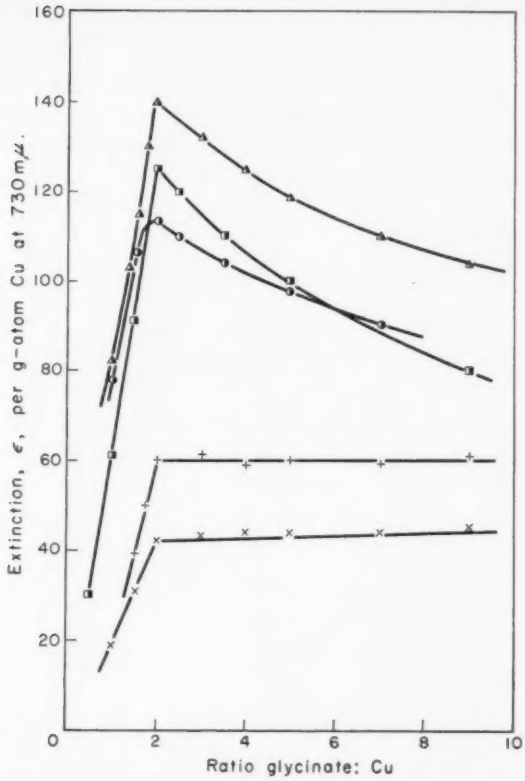

FIG. 2.—Extinction/composition curves for aqueous solutions of copper(II) sulphate (0·002 g-ion Cu per litre) and sodium N:(4:methyl-phenyl) glycinate ◨, N:(4:ethoxy-phenyl)glycinate ▲, N:(4:chloro-phenyl)glycinate ◑, glycinate ×, and N:methyl-glycinate +.

conclude that the neutral complex formed has the normal amino-acid chelate type of structure (I)

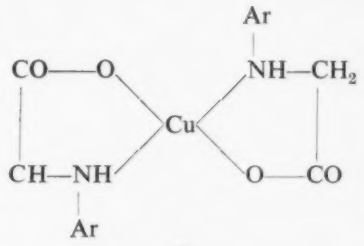

(I)

probably with additional water molecules co-ordinated along the axis normal to the molecular plane.

Since it is difficult to conceive of any reason why copper(II) N:phenyl-glycinate and other compounds of that group, if they also had this structure, should be very much less stable than the corresponding N:(4:methyl-phenyl)glycinate etc., it seemed probable that the copper compounds of the N:phenyl-glycinate group should have some other structure.

2. *Effect of acid on solutions containing excess aryl-glycinate*

Addition of acid to solutions of copper(II) N:(4:methyl-phenyl)glycinate, and to other compounds of this group containing excess aryl-glycinate anion, caused an intensification of colour until the extinction was restored to that of the neutral species, whereafter further addition of acid caused a decrease in intensity (Fig. 3). The amount of acid required to produce the maximum intensity was exactly equivalent to the amount of aryl-glycinate anion in excess of the neutral species, in conformity with the series of equilibria:

$$MA_2 + A^- \rightleftharpoons MA_3^-$$

$$MA_3^- + H^+ \rightleftharpoons MA_2 + HA$$

$$MA_2 + H^+ \rightleftharpoons MA^+ + HA$$

(where M represents the copper(II) ion and A the aryl-glycine ion).

Addition of acid to corresponding solutions of copper(II) N:phenyl-glycinate, and to other compounds of that group containing excess of aryl-glycinate anion,

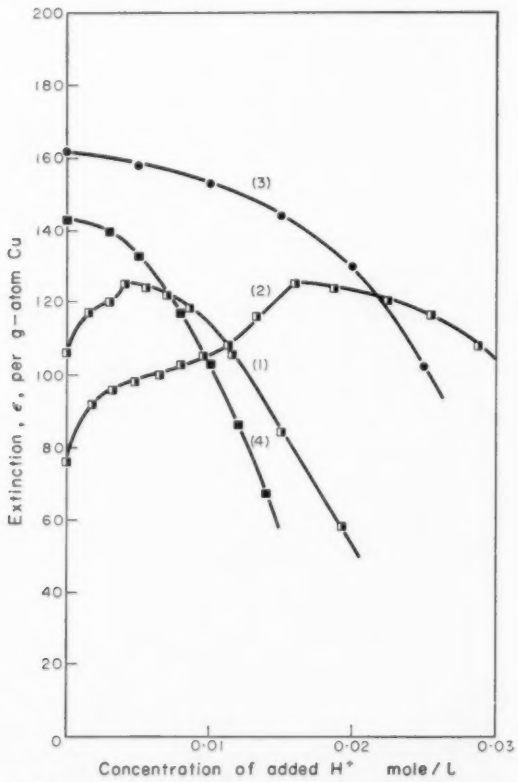

FIG. 3.—Effect of adding acid to aqueous solutions of copper-(II) N:aryl-glycinates containing excess N:aryl-glycinate ion. Copper(II) N:aryl-glycinate concentrations 0·002 g-ion Cu per litre; excess concentrations of N:aryl-glycinate ions:— N:(4:methyl-phenyl)glycinate 0·004 g-ion per litre (1), 0·016 g-ion per litre (2), N:phenyl-glycinate 0·012 g-ion per litre (3), N:(2:methyl-phenyl)glycinate 0·008 g-ion per litre (4).

caused only a decrease in extinction corresponding to a disturbance of the equilibria:

$$MA^+ + A^- \rightleftharpoons MA_2$$
$$MA_2 + H^+ \rightleftharpoons MA^+ + HA$$

thus confirming the non-formation of complex anions of the type MA_3^- in compounds of this group, the structure of copper(II) N:phenyl-glycinate etc. being such that formation of these complex anions does not readily occur.

3. *Absorption spectra of neutral complexes*

In addition to differences in the stability of the neutral species and their reactions with excess aryl-glycinate ions, the two types of species were found to have distinctive absorption spectra in the visible region. Copper(II) N:phenyl-glycinate and those of its derivatives which formed comparatively unstable neutral compounds had an absorption maximum in the visible region about 670 mμ. A similar absorption maximum was observed for copper(II) N:(2:4:dimethyl-phenyl)glycinate, the stability of which was too low to permit observation of composition-intensity data. Copper(II) N:(4:methyl-phenyl)glycinate and other compounds of this group had an absorption maximum about 730 mμ. Analysis of these absorption curves (Fig. 4) showed that whereas those with maxima about 730 mμ (frequency about 1·37 μ^{-1}) were of almost perfect Gaussian shape, those with maxima about 670 mμ could be resolved into two Gaussian components with maxima about 1·50 μ^{-1} (667 mμ) and 1·15 μ^{-1} (870 mμ). Parameters for all of these bands are shown in Table 1.

TABLE 1.—PARAMETERS OF VISIBLE-REGION ABSORPTION BANDS OF AQUEOUS SOLUTIONS OF COPPER(II) N:ARYL-GLYCINATES

Glycinate	ν_1 (μ^{-1})	ε_1	width (μ^{-1})	ν_2 (μ^{-1})	ε_2	width (μ^{-1})
N:phenyl	1·15	46	0·37	1·50	170	0·50
N:methyl-N:phenyl	1·17	71	0·33	1·52	178	0·45
N:(2:methyl-phenyl)	1·10	36	0·40	1·50	157	0·55
N:(2:methoxy-phenyl)	1·23	14	0·40	1·57	95	0·45
N:(2:chloro-phenyl)	1·14	18	0·32	1·45	70	0·50
N:(2:4:dimethyl-phenyl)	1·10	27	0·38	1·51	163	0·55
N:(4:fluoro-phenyl)	1·10	22	0·32	1·50	155	0·55
N:(4:methyl-phenyl)	1·38	125	0·55			
N:(4:ethoxy-phenyl)	1·38	140	0·55			
N:(4:chloro-phenyl)	1·36	113	0·50			

In the solid state the difference between these two types of absorption was evident in the colour of the compounds, copper(II) N:(4:methyl-phenyl)glycinate, for example, being bright green, whereas the N:phenyl-glycinate and N:(2:methyl-phenyl)glycinate were very dark green, and when seen in bulk almost black.

The appearance of a single absorption band in the visible region is characteristic of copper(II) complexes in which the formal co-ordination number of four is presumably extended to six by further co-ordination of solvent molecules along the axis normal to the plane of four:co-ordination, and in terms of ligand-field theory is consistent with an octahedral environment of the copper atom. The slight elongation

of the octahedron commonly observed in solid copper(II) compounds,[2] and presumably persisting in solution, can then allow the symmetry of the external ligand field to match the internal symmetry of the d^9 copper(II) ion.

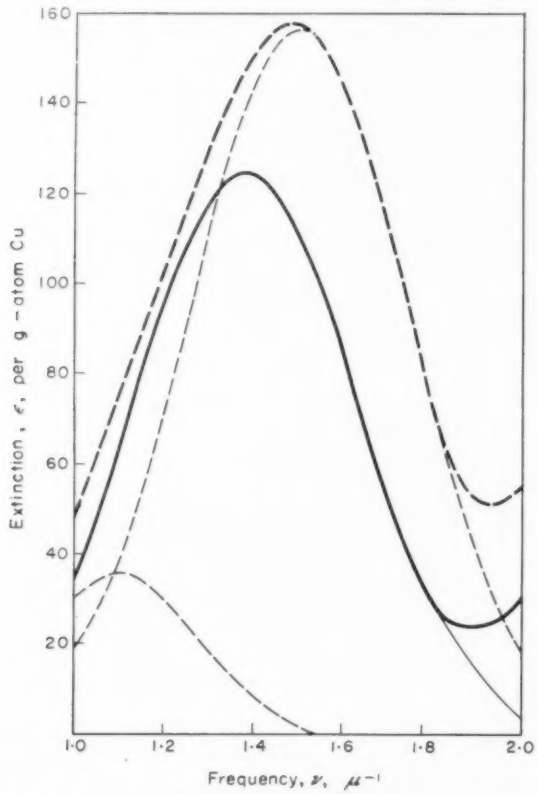

FIG. 4.—Analysis of visible-region absorption spectra of copper(II) N:(4:methyl-phenyl) glycinate ————, and N:(2:methyl-phenyl)glycinate – – – –, in aqueous solution. Gaussian components are shown as thin lines, experimental curves as thick lines.

The visible-region absorption spectra of copper(II) N:(4:methyl-phenyl)glycinate and the corresponding 4:ethoxy- and 4:chloro- compounds in aqueous solution are thus consistent with the normal amino-acid chelate structure (I) already suggested. The visible-region absorption spectra of copper(II) N:phenyl-glycinate and the other compounds in that group, which can be resolved into two bands with absorption maxima near 1·15 and 1·50 μ^{-1}, are not consistent with this structure, but rather suggest, by analogy with the visible-region absorption spectra of the copper(II) alkanoates[3] and the heterocyclic base adducts of the copper(II) β-diketonates,[4],[5] that in this group of copper(II) N:aryl-glycinates the copper atom is 5:co-ordinated. Table 2 shows the parameters of the visible-region absorption bands of a typical member of each series of compounds.

[2] A. F. WELLS, *Structural Inorganic Chemistry*, (2nd. Ed.), p. 618. Oxford University Press (1950).
[3] D. P. GRADDON, *J. Inorg. Nucl. Chem.* **17**, 222 (1961)
[4] R. C. BELFORD, M. CALVIN and G. BELFORD, *J. Chem. Phys.* **26**, 1165 (1957).
[5] D. P. GRADDON, *J. Inorg. Nucl. Chem.* **14**, 161 (1960).

TABLE 2.—PARAMETERS OF VISIBLE-REGION ABSORPTION BANDS OF A TYPICAL COPPER(II) N:ARYL-GLYCINATE, ALKANOATE AND β-DIKETONATE-HETEROCYCLIC BASE ADDUCT.

Copper(II) compound	ν_1 (μ^{-1})	ε_1	width (μ^{-1})	ν_2 (μ^{-1})	ε_2	width (μ^{-1})
Acetate–acetic acid solvate $[(CH_3CO_2)_4Cu_2(CH_3CO_2H)_2]$	1·16	21	0·30	1·47	182	0·34
$[(CH_3CO{\cdot}CH{\cdot}CO_2C_2H_5)_2Cu{\cdot}C_5H_5N]$	1·12	43	0·36	1·44	70	0·40
N:phenyl-glycinate	1·15	46	0·37	1·50	170	0·50

A characteristic of the absorption spectra of the alkanoates and the β-diketonate adducts is the occurrence of a third ligand-field band in the near ultra-violet region about 2·7 μ^{-1} (370 mμ). A band at this frequency was observed for copper(II) N:phenyl-glycinate as expected, but a band at this frequency was also observed for copper(II) N:(4:methyl-phenyl)glycinate, which we suppose to have a normal amino-acid type of chelate structure (I) and would thus not expect to have a ligand-field band in this region (Fig. 5). The parameters of these bands are shown in Table 3.

VOL. 22 1961

TABLE 3.—PARAMETERS OF NEAR ULTRA-VIOLET ABSORPTION BANDS

Copper(II) compound	ν (μ^{-1})	ε	width (μ^{-1})
Acetate–acetic acid solvate	2·67	45	0·52
$[(CH_3CO{\cdot}CH{\cdot}CO_2C_2H_5)_2Cu{\cdot}C_5H_5N]$	2·64	220	0·64
N:phenyl-glycinate	2·64	1730	0·48
N:(4:methyl-phenyl)glycinate	2·63	830	0·52

It is thus necessary to seek some other explanation for these bands in the near ultra-violet absorption of the copper(II) aryl-glycinates, particularly as their extinctions are much greater than would be expected for ligand-field bands. The absorption spectrum of ethyl-N:phenylglycinate was therefore examined, seeking for low-intensity absorption in the near ultra-violet region, attributable to non-equivalence of the carboxyl oxygen atoms (*R*-bands). Fig. 5 shows the absorption curves of aqueous sodium N:phenyl-glycinate, which does not absorb at frequencies below about 3·1 mμ (320 mμ) and of the ethyl ester, showing an absorption band of very low intensity (ε about 2·5) at about 2·8–2·9 μ^{-1} (350 mμ). It seems possible that in the presence of the copper(II) ion the transition responsible for this band could lead to a much more intense absorption band at a slightly lower frequency, in the same way that the low-intensity absorption band of the covalently bound oxalate group at 246 mμ (4·06 μ^{-1}) leads to a band of high intensity (ε about 2400) at 252 mμ (3·97 μ^{-1}) in the complex bis(oxalato)-cuprate-(II) ion,[6] though the nature of these bands of higher intensity is not known.

[6] D. P. GRADDON, *J. Inorg. Nucl. Chem.* **3**, 308 (1956).

4. *Structures of copper(II) N:aryl-glycinates*

On the basis of the high stability of the neutral species in aqueous solution, the reaction with excess anion and the single absorption band in the visible region, it is concluded that copper(II) N:(4:methyl-phenyl)glycinate and the corresponding 4:ethoxy- and 4:chloro-compounds have structures of the usual chelate amino-acid

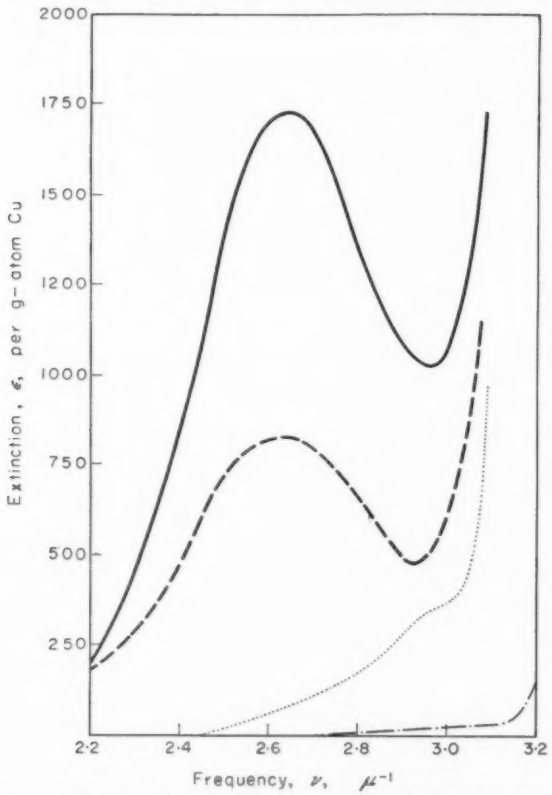

FIG. 5.—Near ultra-violet absorption spectra of copper(II) N:phenyl-glycinate ————, copper(II) N:(4:methyl-phenyl)glycinate – – – –, sodium N:phenyl-glycinate (extinction × 100) —·—·—·—, all in aqueous solution and ethyl N:phenyl-glycinate (extinction × 100) · · · · · · · , in ethanol.

type (I). The appearance of the visible-region absorption band at about 730 mμ indicates that the ligand field due to the co-ordinated aromatic amino-group is considerably smaller than that due to aliphatic amino-groups (absorption maximum of copper(II) glycinate and homologues about 620 mμ), as might be expected, and is about the same as that due to co-ordinated carboxylate anions (absorption maximum of bis-oxalato-cuprate ion and homologues about 700 mμ).

From the visible-region absorption spectra it is concluded that copper(II) N:phenyl-glycinate and the other compounds of that group have structures in which the copper atoms are 5:co-ordinated, and as their much lower stability is hardly consistent with chelation of the amino-acid type, it seems probable that these compounds have structures of the copper(II) alkanoate type (II), the aromatic nitrogen atoms being non-donors.

In compounds with this structure the copper(II) ions usually have an anomalously low magnetic moment. The moments of the copper atoms in copper(II) N:phenyl-glycinate, N:(2:methyl-phenyl)glycinate and N:(4:methyl-phenyl)glycinate were therefore determined and found to be normal (1·8–1·9 β) in every case at room temperature, as shown in Table 4.

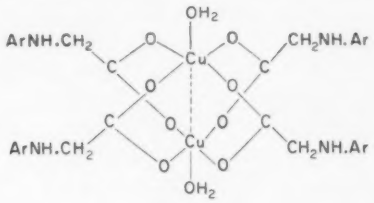

II

While these results would appear to disagree with the copper(II) alkanoate structure proposed for the N:phenyl-glycinate and the N:(2:methyl-phenyl)glycinate, it has been found in other cases that if aryl groups form part of the structure the

TABLE 4.—MAGNETIC PROPERTIES OF COPPER(II) N:ARYL-GLYCINATES

Aryl-glycinate	Temp. (°K)	$10^6\chi$	$10^6\chi_M$	$10^6\chi_M'$	$\mu_{eff}(\beta)$
N:phenyl, anhydrous	291	3·46	1260	1443	1·84
N:(2:methyl-phenyl), $4H_2O$	291	3·16	1311	1544	1·90
N:(4:methyl-phenyl), $2H_2O$	290	2·74	1272	1531	1·89

moments are no longer anomalous at room temperatures.[7] It is therefore concluded that whereas the copper(II) compounds of some N:aryl-glycines have normal chelate amino-acid structures, those of others have structures of the copper(II) alkanoate type, and factors which may affect the change from one structure to the other will now be discussed.

The essential difference between the two structures is that in the amino-acid structure (I) the aromatic nitrogen atom and one of the carboxyl oxygen atoms act as donors (IV), but in the alkanoate structure (II) both oxygen atoms act as donors and the nitrogen atom is a non-donor (III)

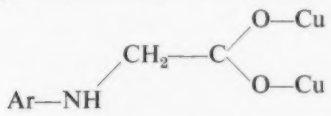

(III)

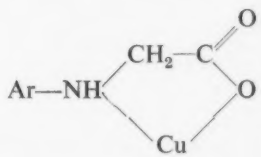

(IV)

The type of structure adopted thus depends upon the relative donor power of the nitrogen and oxygen atoms and upon any additional stabilizing energy that may be available; since the position of the single absorption band of copper(II) N:(4:methyl-phenyl)glycinate etc. shows that the ligand fields of the aromatic nitrogen and carboxyl oxygen atoms are nearly equal, we may expect that very small changes in the nature of the anions could bring about a change in structure of the copper complexes.

[7] E. KOKOT, Thesis, University of New South Wales (1961).

Our spectroscopic evidence suggests that copper(II) N:phenyl-glycinate has the alkanoate structure, in which the nitrogen atom is a non-donor. Substitution in the 4:position could be expected to increase the donor power of the nitrogen atom by either inductive or mesomeric effects, thus leading to the amino-acid structure observed in the N:(4:methyl-phenyl)glycinate, N:(4:ethoxy-phenyl)glycinate and N:(4:chloro-phenyl)glycinate, but where neither of these effects operates, as in the N:(4:fluoro-phenyl)glycinate, there is no increased donor power at the nitrogen atom and the alkanoate structure persists.

The effect on the nitrogen atom of substitution in the 2:position should parallel that of 4:substitution, but in no case did 2:substitution produce the expected change in structure of the copper(II) compounds; furthermore, when substitution occurred in both the 2: and 4:positions, the absorption spectrum corresponded to the alkanoate structure (copper(II) N:(2:4:dimethyl-phenyl)glycinate). Apparently substitution in the 2:position prevents the change in structure usually brought about by substitution in the 4:position, suggesting that 2:substitution of the aromatic ring introduced a steric destabilization of the chelate amino-acid structure. When space-filling models were built it was found that, although there was no difficulty in making a 4:co-ordinated model of chelate amino-acid structure with 2:substituted N:aryl-glycinates, the substituents blocked access to the fifth and sixth co-ordination positions of the copper(II) ion and also restricted the free rotation of the aryl group. We can guess from the crystal structures of formally 4:co-ordinated copper(II) compounds[2] that further co-ordination along the axis normal to the plane of 4:co-ordination is an important stabilizing factor and we also know that mesomeric electronic effects are sensitive to restrictions of rotation; the combination of these effects is evidently sufficient to destabilize the chelate amino-acid structure (IV) in favour of the alkanoate structure (III).

EXPERIMENTAL

Preparation of N:aryl-glycines

Pure sodium N:phenyl-glycinate was obtained by repeated recrystallization of the commercial material from hot water. Substituted N:aryl-glycines were obtained by reaction of sodium chloracetate with the appropriate arylamine in aqueous alcoholic solution and purified by crystallization from benzene or aqueous alocohol. Analyses of the purified products are given below:

N:(4:methyl-phenyl)glycine	Found:	C, 65·59;	H, 6·72;	N, 8·51%.
$C_9H_{11}O_2N$ requires:		65·44;	6·71;	8·49%.
N:(4:ethoxy-phenyl)glycine	Found:	C, 61·83;	H, 6·68;	N, 7·29%.
$C_{10}H_{13}O_3N$ requires:		61·53;	6·71;	7·18%.
N:(2:4:dimethyl-phenyl)glycine	Found:	C, 67·35;	H, 7·28;	N, 8·11%.
$C_{10}H_{13}O_2N$ requires:		67·01;	7·31;	7·82%.
N:(2:methyl-phenyl)glycine	Found:	C, 65·17;	H, 6·56;	N, 8·50%.
$C_9H_{11}O_2N$ requires:		65·44;	6·71;	8·49%.
N:(2:methoxy-phenyl)glycine	Found:	C, 59·53;	H, 6·14;	N, 7·71%.
$C_9H_{11}O_3N$ requires:		59·66;	6·12;	7·73%.
N:methyl-N:phenyl-glycine	Found:	C, 65·78;	H, 6·82;	N, 8·56%.
$C_9H_{11}O_2N$ requires:		65·44;	6·71;	8·49%.
N:(4:fluoro-phenyl)glycine	Found:	C, 56·97;	H, 4·52;	N, 8·27%.
$C_8H_8O_2NF$ requires:		56·80;	4·77;	8·28%.
N:(4:chloro-phenyl)glycine	Found:	C, 52·03;	H, 4·31;	N, 7·31%.
$C_8H_8O_2NCl$ requires:		51·76;	4·34;	7·55%.
N:(2:chloro-phenyl)glycine	Found:	C, 51·78;	H, 4·46;	N, 7·43%.
$C_8H_8O_2NCl$ requires:		51·76;	4·34;	7·55%.

Preparation of crystalline copper N:aryl-glycinates

Solid copper(II) N:phenyl-glycinate, N:(2:methyl-phenyl)glycinate and N:(4:methyl-phenyl)-glycinate were prepared by adding hot aqueous copper(II) sulphate solution to a hot solution of the sodium salt of the N:aryl-glycine and allowing the deep green solution so formed to cool, when crystals of the copper(II) salts were produced, filtered and washed with cold water. The copper salts thus obtained were of low solubility and decomposed slightly on heating in water or when the cold solutions were allowed to stand for a long time; purification by recrystallization was not practicable. Analyses of the copper(II) salts were as follows:

N:phenyl-glycinate, anhydrous	Found:	C, 52·34;	H, 4·50;	N, 7·76;	Cu, 17·1%.
$C_{16}H_{16}O_4N_2Cu$ requires:		52·61;	4·43;	7·70;	17·5%.
N:(2:methyl-phenyl)glycinate tetrahydrate	Found:	C, 46·07;	H, 5·56;	N, 5·64;	Cu, 13·9%.
$C_{18}H_{28}O_8N_2Cu$ requires:		46·60;	6·08;	6·04;	13·7%.
N:(4:methyl-phenyl)glycinate dihydrate	Found:	C, 49·05;	H, 5·51;	N, 6·53;	Cu, 15·1%.
$C_{18}H_{24}O_6N_2Cu$ requires:		50·52;	5·65;	6·55;	14·9%.

Optical measurements

All optical measurements were obtained on a Unicam SP500 spectrophotometer using quartz cells. Solutions of sodium N:aryl-glycinates were obtained by dissolving theoretical quantities of N:aryl-glycines and sodium bicarbonate in hot water and making the cooled solutions up to volume. Resolution of absorption spectra into Gaussian components was done by trial and error.

VOL. 22 1961

J. Inorg. Nucl. Chem., 1961, Vol. 22, pp. 97 to 113. Pergamon Press Ltd. Printed in Northern Ireland

COMPLEXES OF THE LANTHANIDE ELEMENTS WITH α-HYDROXY CARBOXYLATE LIGANDS

G. R. CHOPPIN and J. A. CHOPOORIAN*
Department of Chemistry, Florida State University, Tallahassee, Florida

(*Received* 17 *March* 1961)

Abstract—The successive formation constants have been determined for the α-hydroxy-isobutyrate, lactate and glycolate complexes of nine lanthanide elements and yttrium by potentiometric titration. The formation constants increase as a function of atomic number for each ligand system with some irregularity in the trend in the Sm–Eu–Gd region. For a given lanthanide the order of complex stability is α-hydroxy isobutyrate > lactate > glycolate. This order and the values of ΔH and ΔS for the formation of the monocomplex of Ce(III) and Gd(III) indicate that the relative order of complex stability is governed by an inductive effect of the ligand. For all the metal ions, including Y(III), the average ligand number exceeds a value of three indicating the formation of the complex ML_4^- (M = trivalent metal ion, L = organic ligand).

VOL. 22 1961

THE separation of the trivalent transplutonium elements is accomplished by elution from a bed of cation exchange resin using solutions of the ammonium salt of glycolic,[1] lactic,[1,2] or α-hydroxy-isobutyric[3] acid as eluant. The principal chemical proof of the identity of a new actinide element is the correspondence of the elution position in these systems with that predicted from analogy with the elution position of the lanthanide ions.[4] Solutions of these same organic ligands (i.e. glycolate, lactate and isobutyrate) are also very commonly used to separate mixtures of lanthanide ions by ion exchange elution when amounts of less than a gram of these elements are involved.[1,5]

The efficiency of the separation of the lanthanides and of the actinides with the solutions of these three organic ligands increases in the order

glycolate < lactate < isobutyrate.

However, previous to this investigation insufficient information existed concerning the stabilities of the complexes involved in these systems to allow explanation of the above order. Recently, SONESSON[6] reported values for the stability constants for the acetate and glycolate complexes of a number of the lanthanide elements. This work indicates that glycolate, at least in the formation of the first complex, ML^{2+}, functions as a bidentate chelating agent. Other investigations[7,8] involving glycolate studied only a limited range of lanthanide elements and stressed the comparison of

* This paper is abstracted from the Ph.D. dissertation of J. A. CHOPOORIAN, Florida State University (1960).

[1] D. C. STEWART, *Proceedings of the International Conference on the Peaceful Uses of Atomic Energy, Geneva* 1955, Vol. 7, Paper 837, United Nations (1956).
[2] S. G. THOMPSON, B. G. HARVEY, G. R. CHOPPIN and G. T. SEABORG, *J. Amer. Chem. Soc.* **76**, 6229 (1954).
[3] G. R. CHOPPIN, B. G. HARVEY and S. G. THOMPSON, *J. Inorg. Nucl. Chem.*, **2**, 66 (1956).
[4] J. J. KATZ, and G. T. SEABORG, "The Chemistry of the Actinide Elements," John Wiley and Sons, New York (1957).
[5] G. R. CHOPPIN and R. J. SILVA, *J. Inorg. Nucl. Chem.*, **3**, 153 (1956).
[6] A. SONESSON, *Acta Chem. Scand.* **12**, 165 (1958); **12**, 1937 (1958); **13**, 998 (1959).
[7] R. C. VICKERY, *J. Mol. Spectroscopy*, **2**, 308 (1958).
[8] P. GENTILE, private communication.

many types of ligand structure. Two recent studies[9,10] provided evidence that glycolate, lactate and isobutyrate form uninegative tetra-ligand complexes with both the lanthanide and actinide elements; i.e. ML_4^-.

In this investigation, the stepwise stability constants of a number of lanthanide ions have been determined with glycolate, lactate and isobutyrate ligands by a potentiometric titration technique. Such data for a system of cations which are very similar chemically and of ligands which are closely related could provide information on factors important in complex formation which are obscured in systems chemically more dissimilar.

Determination of stability constants

If only mononuclear complexes $ML_1, ML_2, \ldots ML_N$ are formed in a given system, the consecutive equilibria and the corresponding equilibrium constants are described by the following generalized equations.

$$M + L = ML \qquad K_1 = \frac{[ML]}{[M]\,[L]}$$

$$ML + L = ML_2 \qquad K_2 = \frac{[ML_2]}{[ML]\,[L]}$$

$$\vdots \qquad\qquad \vdots$$

$$ML_{N-1} + L = ML_N \qquad K_N = \frac{[ML_N]}{[ML_{N-1}]\,[L]}$$

Here, as throughout the paper, ionic charges are neglected; they are easily calculated for the trivalent metal ions and univalent anions.

The method of BJERRUM was used to arrive at the values of K_N, the stability or formation constants. The underlying principle of this method is found in the unambiguous relationship between the average number of ligands bound to a metal ion in an equilibrium mixture, $\bar{n}$ and the total equilibrium concentration of anionic ligand [L]. $\bar{n}$ can be expressed by the quotient of the total bound ligand concentration to the total metal concentration; i.e.

$$\bar{n} = \frac{[ML] + 2[ML_2] + \ldots N[ML_N]}{[M] + [ML] + [ML_2] + \ldots [ML_N]} \tag{2}$$

By substituting in this equation for the concentrations of the various metal-ligand complexes their equivalents derived from the stability constant equations and eliminating [M] from both numerator and denominator, equation (3) is obtained.

$$\bar{n} = \frac{(K_1[L]) + 2(K_1K_2[L]^2) + \ldots N(K_1K_2 \ldots K_N[L]^N)}{1 + (K_1[L]) + (K_1K_2[L]^2) + \ldots (K_1K_2 \ldots K_N[L]^N)} \tag{3}$$

Using the complex product β, defined as

$$\beta_N = \frac{[ML_N]}{[M]\,[L]^N} = \prod_{i=1}^{N} K_i \tag{4}$$

[9] A. SONESSON, *Acta Chem. Scand.* **13**, 1437 (1959).

[10] G. R. CHOPPIN, D. MOY and L. HOLM, *I.A.E.A. Conference on Uses of Radioisotopes in the Physical Sciences and Industry*, Paper 282, Copenhagen (1960). L. HOLM, G. R. CHOPPIN and D. MOY, *J. Inorg. Nucl. Chem.* In Press.

the formation function (equation 3) can be written in a more concise form.

$$\bar{n} = \frac{\sum_{n=1}^{N} n\beta_n[\mathrm{L}]^n}{1 + \sum_{n=1}^{N} \beta_n[\mathrm{L}]^n} \tag{5}$$

Theoretically, it should be possible to solve equation 5 for the desired constants with only N pairs of $\bar{n}$ and [L] data. However, if the constants are to be accurate, it is necessary in practice to use considerably more than N pairs of $\bar{n}$ and [L] over a sufficiently large range of [L].

Two methods of solving equation 5 were used. One method involving a least squares treatment of $\bar{n}$ and [L] by an IBM 650 digital computer was developed during the course of this investigation.[11] Concurrently, another group[12] has described a similar computation method. The use of such computer programmes greatly simplifies the calculation burden of these investigations and represents a considerable saving of time.

VOL. 22 1961

The second method used to calculate the stability constants was developed by FRONAEUS[13] from the earlier studies of BJERRUM[14]. This method was used to check the values obtained by the computer method.

Dividing equation (5) by [L] gives:

$$\frac{\bar{n}}{[\mathrm{L}]} = \frac{\sum_{n=1}^{N} n\beta_n[\mathrm{L}]^{n-1}}{1 + \sum_{n=1}^{N} \beta_n[\mathrm{L}]^n} \tag{6}$$

It is seen that the numerator of this equation,

$$X' = \sum_{n=1}^{N} n\beta_n\,[\mathrm{L}]^{n-1}$$

is the derivative of the denominator,

$$X = 1 + \sum_{n=1}^{N} \beta_n[\mathrm{L}]^n.$$

Equation (6) is simply expressed as

$$\frac{\bar{n}}{[\mathrm{L}]} = \frac{X'}{X} \tag{7}$$

and integration yields

$$\ln X([\mathrm{L}]_j) = \int_0^{(\mathrm{L})_j} \frac{\bar{n}}{[\mathrm{L}]}\, d[\mathrm{L}]. \tag{8}$$

Numerical or graphical integration of equation (8) gives the corresponding values of

[11] J. A. CHOPOORIAN, G. R. CHOPPIN, H. C. GRIFFITH and R. CHANDLER, *J. Inorg. Nucl. Chem.* In Press.
[12] J. C. SULLIVAN, J. RYDBERG and W. F. MILLER, *Acta Chem. Scand.*, **13**, 2033 (1959).
[13] S. FRONAEUS, *Doctoral Dissertation*, Lund, Sweden (1948).
[14] J. BJERRUM, "Metal Ammine Formation in Aqueous Solution," P. Haase and Son, Copenhagen (1941).

X and [L]. The complex products $\beta_1, \beta_2, \ldots \beta_N$ can be calculated by extrapolation to [L] = 0 for the functions $X_1, X_2, \ldots X_N$ when these latter are defined as

$$X = 1 + \beta_1[\mathrm{L}] + \ldots \beta_N[\mathrm{L}]^N,$$

$$X_1 = \frac{X - 1}{[\mathrm{L}]} = \beta_1 + \beta_2[\mathrm{L}] + \ldots \beta_N[\mathrm{L}]^{N-1}$$

$$X_2 = \frac{X_1 - \beta_1}{[\mathrm{L}]} = \beta_2 + \beta_3[\mathrm{L}] + \ldots \beta_N[\mathrm{L}]^{N-2}$$

$$X_{N-1} = \frac{X_{N-1} - \beta_{N-2}}{[\mathrm{L}]} = \beta_{N-1} + \beta_N[\mathrm{L}]$$

Inspection of equation (6) shows that the first stability constant K_1 (i.e. β_1) is also obtainable from the intercept of a plot of $\frac{\bar{n}}{[\mathrm{L}]}$ vs. [L]. Furthermore, the area under the curve in such a plot between the limits [L] = 0 and [L] = $[\mathrm{L}]_j$ equals ln $X([\mathrm{L}]_j)$.

The calculation of $\bar{n}$ and [L]

The concentration of a given α-hydroxy carboxylate ion was calculated from hydrogen ion measurements in concentration cells, using a quinhydrone electrode.[15]

For a buffer solution of these organic acids, designating the stoichiometric concentration of the protolysed ligand by C_{HL}' and that of the sodium salt of the organic anion by C_{L}', the acid equilibrium constant may be expressed as

$$K_A = \frac{[\mathrm{H}]'(C_{\mathrm{L}}' + [\mathrm{H}]')}{C_{\mathrm{HL}}' - [\mathrm{H}]'} \tag{8}$$

Where [H]′ is the hydrogen ion concentration of the buffer solution. When lanthanide ions are added to this buffer solution, the acid constant expression becomes

$$K_A = \frac{[\mathrm{H}]\,[\mathrm{L}]}{C_{\mathrm{HL}}' + C_{\mathrm{H}} - [\mathrm{H}]} \tag{9}$$

C_{H} is a correction to account for any free acid—e.g. $HClO_4$—introduced into the buffer solution along with the lanthanide ions; [H] is the hydrogen ion concentration for the solution containing metal ion; [L] is the concentration of anionic ligand. If $C_{\mathrm{HL}}'/C_{\mathrm{L}}' \equiv \delta$, combination of equations (8) and (9) gives

$$[\mathrm{L}] = \frac{[\mathrm{H}]'}{[\mathrm{H}]}\left(C_{\mathrm{L}}' + \frac{C_{\mathrm{H}} - [\mathrm{H}] + (1 + \delta)[\mathrm{H}]'}{\delta}\right). \tag{10}$$

The total concentration of anionic ligand in the solution is equal to $C_{\mathrm{L}}' + [\mathrm{H}] - C_{\mathrm{H}}$. The concentration of complexed ligand is the difference between this and the free ligand concentration [L]. Consequently,

$$\bar{n} = \frac{C_{\mathrm{L}}' + [\mathrm{H}] - C_{\mathrm{H}} - [\mathrm{L}]}{C_{\mathrm{M}}} \tag{11}$$

where C_{M} is the total metal concentration.

[15] S. FRONAEUS, *Acta Chem. Scand.*, **6**, 100 (1952).

By measuring [H] and [H]′ as the acid buffer solution is added to a lanthanide salt solution, the values of $\bar{n}$ and [L] may be calculated if C_L', C_H and C_{HL}' are known.

EXPERIMENTAL

Reagents

Lanthanide perchlorate solutions. These were prepared from the lanthanide chlorides (Lindsay Chemical Co., 99·9 per cent). The chloride was evaporated with perchloric acid (using a heat lamp) until a negative test for chloride resulted. Most of the excess perchloric acid was removed in the evaporation and the small residual amount determined by titration.

The concentrations of the lanthanide perchlorate solutions (of the order of 20–25 mM) were determined by gravimetric analysis, using the oxalic acid method and the oxide weighing form.[16] Upon examination with a Cary Spectrophotometer, these solutions showed an absence of impurities and colloidal suspensions. The spectral intensity of colloidal solutions show an inverse fourth power dependence on the wave-length.[17] True solutions give no absorption except for the characteristic solute and solvent bands.

Sodium perchlorate. G. F. Smith Co., anhydrous reagent grade was used as obtained in adjusting the ionic strength of the various solutions to 2·0 M.

Organic acid buffer solutions. Aqueous solutions of α-hydroxy isobutyric acid (Eastman Organic Chemicals), glycolic acid (Fisher Scientific Co., purified), and lactic acid (Baker and Adams Co., reagent grade) were standardized against sodium hydroxide. Before standardization the α-hydroxy isobutyric acid was passed through a hydrogen form cation exchange resin (Dowex-50) for removal of coloured impurities.

The buffer solutions of α-hydroxy isobutyric and glycolic acid were made by partially neutralizing the standard solutions with sodium hydroxide. Lactic acid was completely neutralized, then partially hydrolysed with perchloric acid to give the desired buffering. This alteration in the buffering procedure for the lactic acid was necessary to dedimerize the lactone form of lactic acid present to some degree in the stock solution.[5]

In each case, the buffer ratio δ was close to unity, and C_L' varied from 0·5 to 1·0 M.

Equipment

The quinhydrone electrode. The quinhydrone used was a grade specially made by the Fisher Scientific Company for pH determination. Approximately 25 mg of quinhydrone were used for every 10 ml of solution being measured. Bright pieces of freshly ignited pure platinum wire were used as the electrodes.

The salt bridge. The salt bridge, of simple U-tube construction, made electrical contact between the half-cell and the bridge solutions by means of asbestos fibres imbedded at the ends of the bridge.

The potentiometer. A Leeds-Northrup Student Potentiometer was used. A Weston Cell was employed as the standard battery, and two 1·5 V Ever Ready Dry Cells connected in series were used as the working battery.

Procedure

The experimental arrangement is a modification of that used by FRONAEUS.[15] The description of the composition of each half-cell compartment is given in equation (12) where $M(ClO_4)_3$ is the lanthanide perchlorate, L, the complexing ligand, and μ, the ionic strength.

A		B		C	
Pt, Quinhydrone [H]° mM $HClO_4$ $NaClO_4$ to $\mu = 2$ M	2 M $NaClO_4$	Pt, Quinhydrone C_M mM $M(ClO_4)_3$ C_H mM $HClO_4$ C_L' mM NaL $C_{HL}' = \delta C_L'$ mM HL $NaClO_4$ to $\mu = 2$M	2 M $NaClO_4$	Pt, Quinhydrone $C_M = 0$ $C_H = 0$ C_L' mM NaL $C_{HL}' = \delta C_L'$ mM HL $NaClO_4$ to $\mu = 2$ M	(12)

[16] W. F. HILLEBRAND, *et al.*, "Applied Inorganic Analysis," John Wiley and Sons, Inc., New York (1953) pp. 547–563.

[17] D. C. PEASLEE and H. MUELLER, "Elements of Atomic Physics," Prentice-Hall, Inc., New York (1955) p. 94.

VOL. 22 1961

Compartment A in equation (12) contained a reference solution of known perchloric acid concentration [H]°. The value of [H]° in all titration series did not differ appreciably from 11·0 mM. Compartment B was prepared by adding increasing amounts of acid buffer solution to 10 ml of rare earth perchlorate solution. Compartment C was correspondingly prepared by adding the acid buffer to 10 ml of 2·0 M sodium perchlorate. The initial composition of the rare earth perchlorate solution is given in equation (13), and the composition of the acid buffer solution is given in equation (14).

$$C_M^\circ \text{ mM } M(ClO_4)_3;\ C_H^\circ \text{ mM } HClO_4;\ (2{,}000 - 6C_M^\circ) \text{ mM } NaClO_4 \tag{13}$$

$$C_L^\circ \text{ mM acid anion};\ \delta C_L^\circ \text{ mM acid (i.e. } C_{HL}^\circ);\ (2{,}000 - C_L^\circ) \text{ mM } NaClO_4 \tag{14}$$

Micropipettes fitted with syringes were used to deliver the titrant. The solutions were mixed with magnetic stirrers which were turned off during e.m.f. readings.

As the titration proceeded, the stoichiometric concentrations of C_L' and C_{HL}' in compartments B and C were equivalent, and a difference in hydrogen ion concentration between the two compartments resulted from the presence of complex formation in B. Also, the solution compositions were such that except for very small changes due to complex formation in compartment B, the ionic strength of each half-cell compartment remained at 2·0 M throughout the course of a titration. The e.m.f. values were later corrected for the change in ionic strength upon complexation.[6]

For the hydrogen ion concentration cells in equation (12), the e.m.f. expressions are

$$E_{AB}(\text{mV}) = 59{\cdot}15 \log \frac{[H]^\circ}{[H]} \text{ at } 25^\circ \tag{15}$$

$$E_{BC}(\text{mV}) = 59{\cdot}15 \log \frac{[H]}{[H]'} \text{ at } 25^\circ\text{C} \tag{16}$$

Since [H]° is known, the measured e.m.f. values may be used to calculate [H], [H]′ and [H]′/[H] as a function of acid buffer solution added. The e.m.f. values were stable and reproducible within 0·2–0·3 mV except in the instances where precipitation of the lanthanide complex occurred.

The titration cells were jacketed so that water could be circulated to maintain a constant temperature during titration. Temperature of 0·5 ± 0·3, 25·0 ± 0·1, 40·0 ± 0·2, and 62·8 ± 0·3°C were used in this study.

Since these complexes were not exceptionally strong and the ligands were charged, it was considered better not to attempt evaluation of thermodynamically valid stability constants. Instead, stoichiometric constants were determined in solutions of relatively high and constant (2·0 M) ionic strength. Although ideal conditions were not met, the stability constants are thought to be sufficiently good approximations for the purposes of this investigation.

RESULTS

Tables 1(a–d) present some examples of the experimental data and the calculated values of [L] and $\bar{n}$/[L]. The complete tabulation of experimental data may be found elsewhere.[18] Fig. 1 shows the graphs of $\bar{n}$/[L] vs. [L] for the examples in Tables 1 (a–d).

The values of $\bar{n}$ and [L] were used to calculate the successive stability constants by an iterative least squares treatment of equation (5) with an IBM 650 computer. These values are listed in Table 2. To check the computer values, the stability constants were determined by graphical integration in some cases and typical results are given in Table 3. In addition, the values of K_1 obtained from the ordinate intercepts of $\bar{n}$/[L] vs. [L] graphs confirmed the computer values in all cases. Considering the difference in temperature and the experimental error, there is generally good agreement between the lanthanide–glycolate stability constants reported by SONESSON[6b] and those in Table 2.

[18] J. A. CHOPOORIAN, "The Complex Stabilities of the Lanthanides with a Series of α-Hydroxy Carboxylate Ligands," Dissertation, Florida State University (1960).

TABLE 1.—DETERMINATION OF [L] AND $\bar{n}/[L]$ FROM EXPERIMENTAL DATA

(a) CERIUM–GLYCOLATE SYSTEM

$C_H^\circ = 3{\cdot}39$ mM $\quad C_L^\circ = 1200$ mM

$C_M^\circ = 25{\cdot}98$ mM $\quad \delta = 1{\cdot}000$

Initial volume = 10 ml

Volume of titrant (ml)	E_{BC}(mV)	E_{AB}(mV)	[L](mM)	$\frac{\bar{n}}{[L]}$ (M^{-1})
0·100	51·5	52·9	1·92	162
0·200	44·1	59·9	4·72	138
0·300	39·0	64·8	8·33	115
0·400	34·9	69·1	12·7	97·4
0·500	31·4	72·7	17·9	83·0
0·600	28·2	75·8	23·9	70·7
0·800	23·5	80·8	37·2	54·7
1·00	19·9	84·1	52·3	43·9
1·25	16·7	87·2	72·0	35·3
1·50	14·5	89·5	91·8	29·9
2·00	11·4	93·0	132	23·1
2·50	9·5	94·5	170	19·3

(b) CERIUM-α-HYDROXYISOBUTYRATE SYSTEM

$C_H^\circ = 3{\cdot}39$ mM $\quad C_L^\circ = 955{\cdot}2$ mM

$C_M^\circ = 25{\cdot}98$ mM $\quad \delta = 1{\cdot}072$

Initial volume = 10 ml

Volume of titrant (ml)	E_{BC}(mV)	E_{AB}(mV)	[L](mM)	$\frac{\bar{n}}{[L]}$ (M^{-1})
0·250	50·7	63·8	3·60	190
0·500	38·9	75·4	10·7	122
0·750	30·8	83·4	21·1	83·7
1·00	25·1	89·1	34·1	62·0
1·25	21·1	93·1	48·5	49·1
1·50	18·7	96·0	62·2	42·5
2·00	15·0	99·9	91·3	33·0
2·50	12·3	102·7	121	26·7
3·50	9·1	105·9	177	19·9
4·50	7·2	107·8	228	16·3

VOL. 22 1961

TABLE 1. (Cont'd)—DETERMINATION OF [L] AND $\bar{n}/[L]$ FROM EXPERIMENTAL DATA

(c) HOLMIUM–LACTATE SYSTEM

$C_H^\circ = 1{\cdot}72$ mM $\quad C_L^\circ = 574{\cdot}0$ mM

$C_M^\circ = 26{\cdot}80$ mM $\quad \delta = 0{\cdot}8394$

Initial volume = 10 ml

Volume of titrant (ml)	E_{BC}(mV)	E_{AB}(mV)	[L](mM)	$\frac{\bar{n}}{[L]}$ (M^{-1})
0·100	64·1	41·5	0·453	477
0·200	63·6	41·2	0·929	445
0·300	62·6	42·2	1·45	416
0·400	60·8	44·0	2·08	379
0·600	56·5	48·4	3·67	312
0·800	51·6	53·2	5·84	252
1·00	47·0	58·0	8·60	206
1·25	41·6	63·4	13·0	162
1·50	37·2	68·0	18·1	133
2·00	29·2	75·8	31·5	89·9
2·50	22·5	82·4	49·0	61·7
3·00	17·4	87·4	68·8	44·2

(d) YTTERBIUM–LACTATE SYSTEM

$C_H^\circ = 0{\cdot}70$ mM $\quad C_L^\circ = 574{\cdot}0$ mM

$C_M^\circ = 22{\cdot}72$ mM $\quad \delta = 0{\cdot}8394$

Initial volume = 10 ml

Volume of titrant (ml)	E_{BC}(mV)	E_{AB}(mV)	[L](mM)	$\frac{\bar{n}}{[L]}$ (M^{-1})
0·100	60·0	44·5	0·444	651
0·200	61·7	42·0	0·902	589
0·300	61·6	41·9	1·40	543
0·400	60·2	43·6	2·02	486
0·600	55·6	48·1	3·66	380
0·800	50·2	53·6	6·01	294
1·00	44·3	59·1	9·37	224
1·25	39·5	63·6	13·9	179
1·50	35·8	67·2	18·8	151
2·00	25·0	77·8	36·7	84·7
3·00	15·8	85·2	72·7	47·0

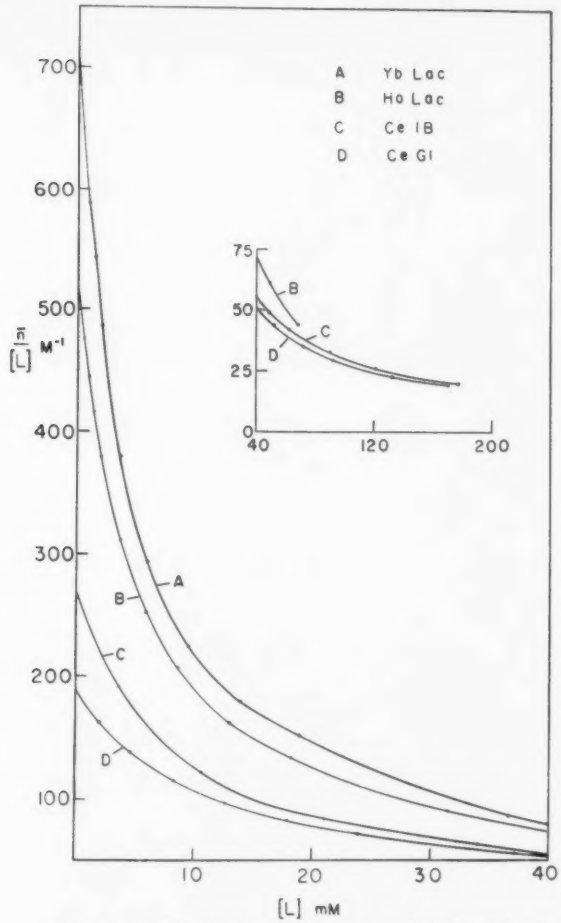

FIG. 1.—$\bar{n}$/[L] vs [L] curves for systems listed in Table 1.

Sets of $\bar{n}$ and [L] values which differed within the determinate error were used to calculate error limits for the stability constants. These errors were of the order of $\pm$ 5 per cent for K_1, $\pm$ 10 per cent for K_2, and $\pm$ 20 per cent for K_3.

The experimental value of $\bar{n}$ exceeded three in all but a few titrations, indicating the formation of a fourth complex, ML_4^-. However, random computational errors gave such large fluctuations in the values of K_4 that no values are reported for the fourth constant.

Titrations were performed at two metal ion concentrations with both lactate and isobutyrate using Sm(III). FRONAEUS has shown[13] that when formation of complexes of the type $M_yL_n(y > 1)$ occurs, $\bar{n}$/[L] increases as C_M increases. From Fig. 2, the conclusion may be drawn that such polynuclear complexes are not present in any notable concentration. This agrees with a similar observation for the glycolate complexes.[6]

Analyses of crystals of the tris-glycolato metal complexes isolated from ammonium and sodium glycolate solutions have shown the composition to be ML_3. In addition,

TABLE 2.—STABILITY CONSTANTS OF THE VARIOUS LANTHANIDE AND YTTRIUM COMPLEX SYSTEMS AT 25·0°C.

α-Hydroxyisobutyrate

	Ce	Nd	Sm	Eu	Gd	Tb	Y	Ho	Er	Yb
K_1	270	420	560	503	660	673	730	1127	1168	1400
K_2	77	111	141	174	213	261	380	392	453	715
K_3	10	25	38	38	42	60	72	106	117	132
K_1/K_2	3·5	3·8	3·9	2·8	3·0	2·6	2·0	2·8	2·6	2·0
K_2/K_3	7·7	4·5	3·6	4·7	5·0	4·4	5·2	3·9	3·9	5·4

Lactate

	Ce	Nd	Sm	Eu	Gd	Tb	Y	Ho	Er	Yb
K_1	214	292	366	337	337	403	341	511	590	706
K_2	59	80	105	117	125	131	149	183	218	265
K_3	13	17	21	19	19	19	26	38	39	49
K_1/K_2	3·7	3·7	3·5	2·9	2·7	3·1	2·3	2·8	2·7	2·6
K_2/K_3	4·6	4·7	4·9	6·3	6·8	7·0	5·6	4·8	5·6	5·4

Glycolate

	Ce	Sm	Eu	Gd	Ho	Yb	Y
K_1	186	291	285	287	308	420	239
K_2	55	88	92	74	109	158	94
K_3	13	29	23	36	24	25	18
K_1/K_2	3·4	3·3	3·1	3·8	2·9	2·7	2·5
K_2/K_3	4·3	3·0	4·0	2·1	4·5	6·0	5·0

TABLE 3.—A COMPARISON OF THE COMPUTED AND GRAPHICALLY CALCULATED STABILITY CONSTANTS FOR THE α-HYDROXYISOBUTYRATE AND LACTATE SYSTEMS OF SAMARIUM

Stability constant	Sm-α-hydroxyisobutyrate		Sm-lactate	
	Graphical	Computer	Graphical	Computer
K_1	555	560	362	366
K_2	151	141	115	105
K_3	41	38	18	21
K_1/K_2	3·7	3·9	3·2	3·5
K_2/K_3	3·7	3·6	6·3	5·0

the complex ML_4 has been shown to be uninegative.[9,10] From these facts it is reasonable to assume that α-hydroxy group of these ligands probably does not ionize upon chelation.

Values for K_1 were determined by titration for the Ce(III) and Gd(III) systems at 0·5, 40·0 and 62·8°C as well as at 25·0°C. The results of these experiments are shown in Figs. 3 and 4 as graphs of log K_1 vs. $1/T$. Least squares analysis of the slopes of these curves provided enthalpy of complex formation values for the species

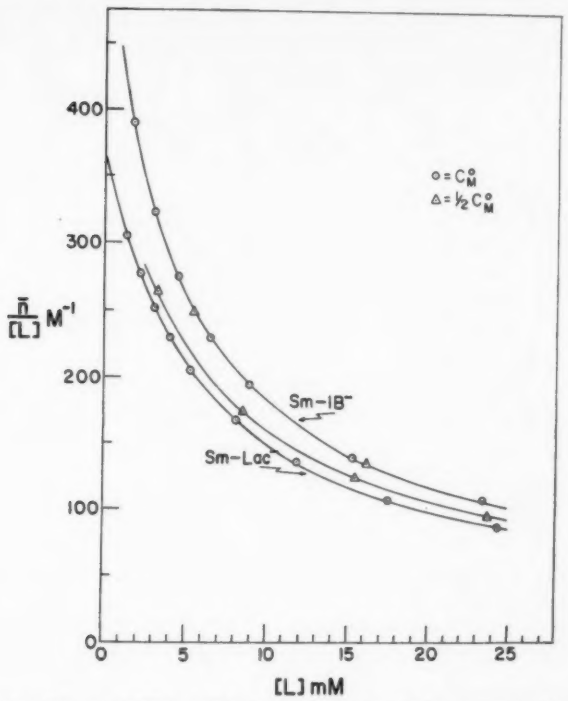

FIG. 2.—Curves of $\bar{n}/[L]$ vs. [L] at two different metal ion concentrations for Sm(III).

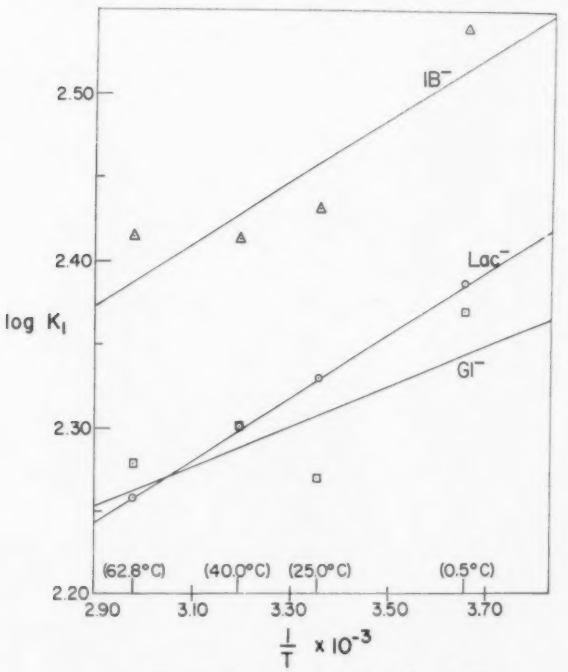

FIG. 3.—Plot of log K_1 vs $1/T$ for Ce(III).

VOL. 22 1961

TABLE 4.—ΔH_1 AND ΔS_1 FOR THE FORMATION OF ML_1, WHERE M IS Ce AND Gd, AND L IS α-HYDROXYISOBUTYRATE (IB^-), LACTATE (Lac^-), AND GLYCOLATE (Gl^-).

M	L	ΔH_1(kCal/mole)	ΔS_1(e.u./mole)
Ce	IB^-	-0.83 ± 0.41	8.4 ± 1.2
	Lac^-	-0.83 ± 0.41	7.9 ± 1.1
	Gl^-	-0.44 ± 0.22	8.9 ± 1.3
Gd	IB^-	-0.89 ± 0.45	9.9 ± 1.4
	Lac^-	-0.54 ± 0.27	9.8 ± 1.4
	Gl^-	-0.40 ± 0.20	9.9 ± 1.4

ML^{2+}. Table 4 gives these values of ΔH as well as the corresponding ΔS values for 25·0°C. The large random and determinate errors in this experimental technique limit severely its utility.

DISCUSSION

The stability constants K_1, K_2 and K_3 of the systems investigated at 25·0°C are plotted in Figs. 5, 6 and 7 as a function of lanthanide ion atomic number. The order of stability isobutyrate > lactate > glycolate holds for each complex formation step and is interpreted to mean that the inductive effect arising from methyl group substitution in the α-carbon position is more important than possible steric effects from this same substitution. Consequently, as the lanthanide cationic radius decreases

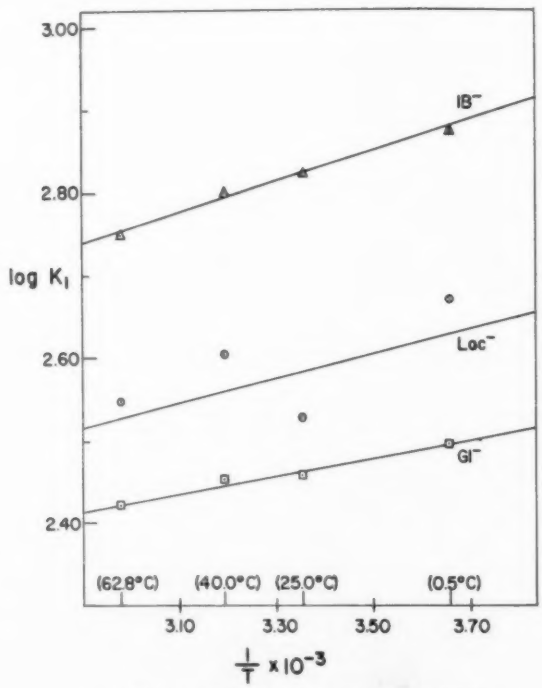

FIG. 4.—Plot of log K_1 vs $1/T$ for Gd(III).

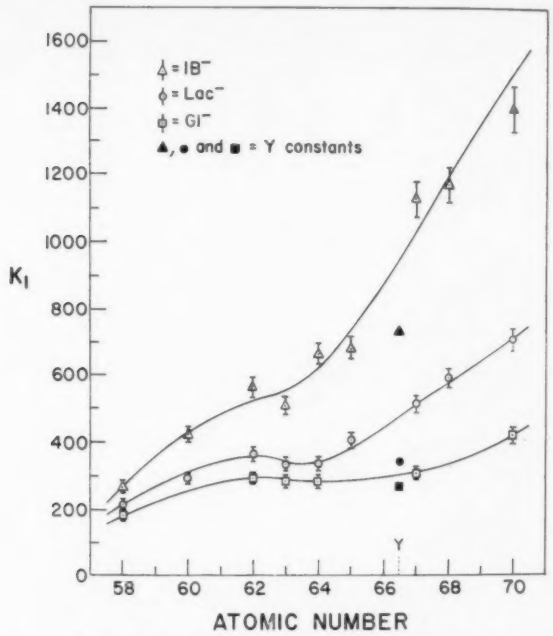

FIG. 5.—K_1 for the lanthanide ions and glycolate, lactate and isobutyrate anions.

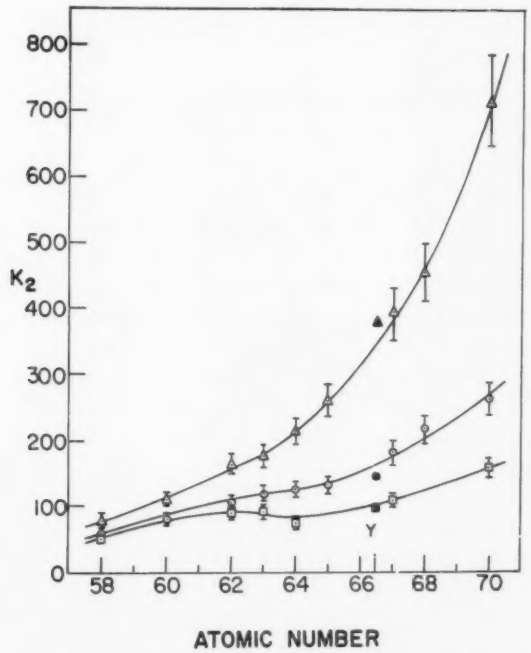

FIG. 6.—K_2 for the lanthanide ions and glycolate, lactate and isobutyrate anions.

VOL. 22 1961

(with increasing atomic number) the metal ions can more effectively exploit the differences in basicities of the glycolate, lactate and isobutyrate ligands. The result is the increasing differences in the slopes of the graphs of Figs. 5, 6 and 7. The rather constant values for the ratios of successive stability constants (Table 2) is also evidence

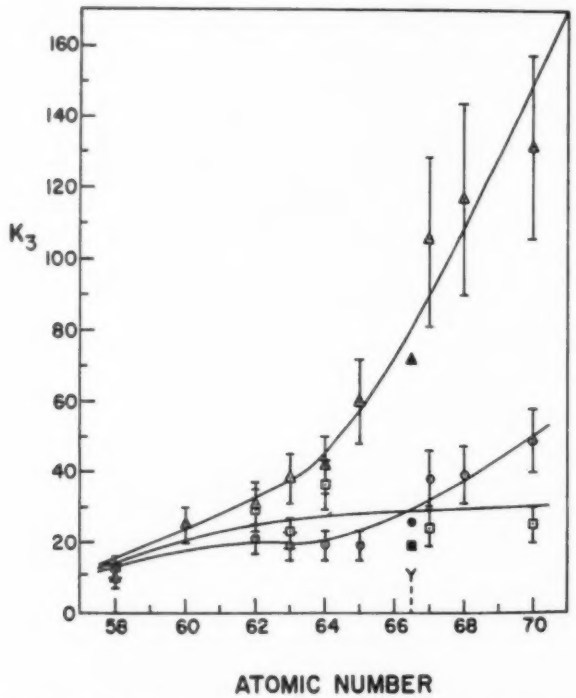

FIG. 7.—K_3 for the lanthanide ions and glycolate, lactate and isobutyrate anions.

for the lack of a steric effect by the α-substituted methyl groups since steric hindrance would be expected to result in an increase in these ratios in the order glycolate < lactate < isobutyrate.[19]

If the trends in the values of β_3 for the lanthanide ions with these three ligands are compared with the relative ion exchange elution behaviour for the same systems, a striking similarity is obvious. This is confirmation that complex stability is the most important factor in determining the cation exchange elution behaviour of the lanthanide systems. It is reasonable to believe that this is also true for the analogous actinide systems. The increased separability of these ions upon elution with isobutyrate solution is a result of the increase in complex stability due to the greater inductive effect in isobutyrate relative to glycolate and lactate.

The existence of the anionic species ML_4^- has been confirmed by this research, as $\bar{n}$ consistently exceeds a value of three. These data suggest that perhaps four organic ligands, each functioning as a bidentate chelating agent, are fulfilling a co-ordination number of eight. A number of earlier papers have speculated on this

[19] F. J. C. ROSSOTTI, Chapter 1, *Modern Co-ordination Chemistry*, Interscience Publishers, Inc., New York (1960)

co-ordination number and its possible steric configurations.[20–25] However, the fact that $\bar{n}$ also exceeds three with yttrium (Fig. 8) weakens the argument for a co-ordination number of eight. As a transition element yttrium is most likely to have a co-ordination number of six; and on this basis it is suspected that all of the complexes ML_4^- are actually of octahedral structure with two ligands functioning as bidentate groups and two as monodentate.

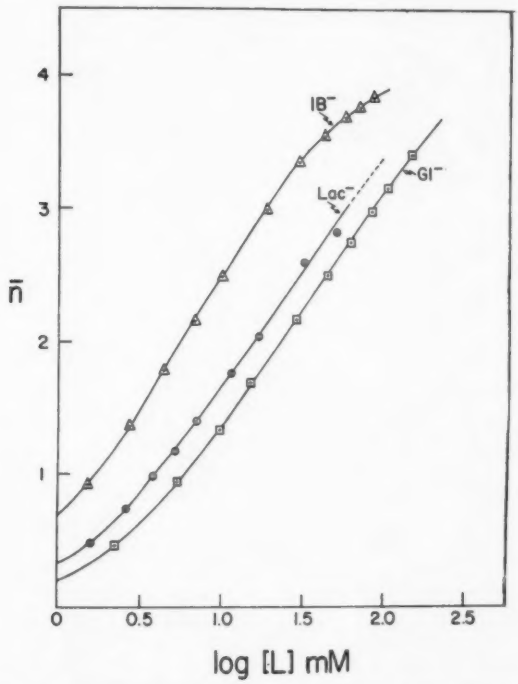

FIG. 8.—Average ligand number, $\bar{n}$, plotted as a function of ligand concentration, [L].

While a co-ordination number of six seems more plausible, it is not possible from the available data to rule out a co-ordination number of eight. In either case the fact that the values of $\log(K_n/K_{n+1})$ are positive and less than unity indicates that there is probably no change in stereochemistry as $\bar{n}$ proceeds from 1 to 4 (this is also indicative of a lack of any strong π bonding in these systems).

The enthalpy values listed in Table 4 are indicative that these complexes are ionic. The entropy values are considerably lower than those reported for the malonate[26] and EDTA[27] complexes. However, since the latter investigations were conducted

[20] R. S. NYHOLM, *Progress in Stereochemistry*, Vol. 1, Butterworth Scientific Publications, London (1954) p. 1954.
[21] T. D. O'BRIEN, Chapter 10, *Chemistry of the Co-ordination Compounds*, Reinhold Publishing Corp., New York (1956) p. 394.
[22] C. DUCULOT, *Compt. rend.*, **245**, 692 (1957).
[23] J. C. EISENSTEIN, *J. Chem. Phys.*, **25**, 142 (1956).
[24] L. E. ORGEL, *J. Chem. Soc.*, 4186 (1958).
[25] L. E. MARCHI, W. C. FERNELIUS, and J. P. MCREYNOLDS, *J. Amer. Chem. Soc.*, **65**, 329 (1943).
[26] E. GELLES and G. H. NANCOLLAS, *Trans. Faraday Soc.*, **52**, 680 (1956).
[27] J. K. FOREMAN and T. D. SMITH, *J. Chem. Soc.*, **1957**, 1752.

at lower ionic strengths, the sensitivity of the entropy change to the magnitude of the ionic strength[28] may render a comparison meaningless.

Several recent papers have suggested that the interruption at Gd(III) in a monotonic progression in many chemical properties of the lanthanide elements as a function of atomic number is a result of crystal field effects.[29,30,31]. According to these authors the characteristic elution pattern of the actinide and lanthanide ions may be a reflection

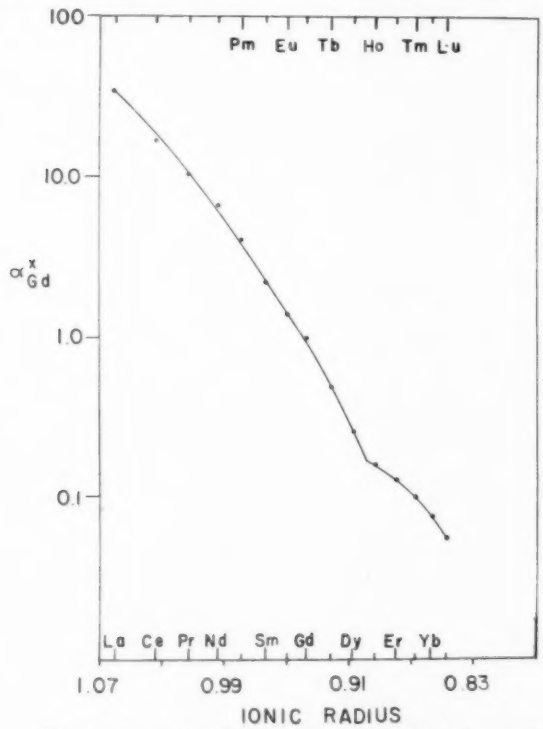

FIG. 9.—Separation factors from Dowex-50 relative to Gd(III) for elution with α-hydroxy isobutyrate solution.

of this effect. Crystal field stabilization effects should be larger for the actinide series than for the lanthanide series, but are expected to be much smaller in both than for the ions of the transition elements. The fact that the monoligand complex for yttrium is less stable than expected from the cationic radius could be attributed to the absence of crystal field stabilization for yttrium complexes. An approximation to the amount of stabilization present in dysprosium and holmium complexes can be obtained by assuming that the difference between the measured and expected values in yttrium are a valid indication of crystal field stabilization. Thus for isobutyrate $\Delta(\Delta F) = RT \ln K_1 \text{ (expected)}/K_1 \text{ (actual)} \approx 145$ calories

$$\% \text{ Stabilization} \approx \frac{\Delta(\Delta F)}{\Delta F} \approx \frac{145}{3900} \times 100 = 3{\cdot}7\%$$

[28] K. B. YATSIMIRSKII and V. P. VASIL'EV, *Instability Constants of Complex Compounds*, English Translation, Consultants Bureau, New York (1960) p. 69.
[29] P. GEORGE, D. S. MCCLURE, J. S. GRIFFITH and L. E. ORGEL, *J. Chem. Phys.*, **24**, 1269 (1956).
[30] N. S. HUSH, *Disc. Faraday Soc.*, **26**, 145 (1958).
[31] L. A. K. STAVELEY and T. RANDALL, *Disc. Farday Soc.*, **26**, 157 (1958).

This amount of stabilization is consistent with that expected for the lanthanide ions of $f^{10} - f^{11}$ configuration. If crystal field effects are the only source of the differences in stabilities for yttrium and dysprosium complexes, a stability correlation between gadolinium and yttrium due solely to ionic size is to be expected as crystal field effects should be absent or at a minimum for these two ions (assuming a weak ligand field). In Table 2, it is seen that the order of stability as measured by K_1 is yttrium slightly less than gadolinium for glycolate and yttrium increasingly greater than gadolinium going from lactate to isobutyrate. Moreover, no correlation is evident based on relative size for aminopolycarboxylic acid systems, where yttrium complexes are often significantly lower in stability than the analogous gadolinium complexes.[32] It must be emphasized, however, that these arguments are based on the premise that no effects are present in Y(III) such that a correlation between that ion and the lanthanide ions based solely on ionic radius would be invalid.

The evidence from ion exchange studies for crystal field effects in these systems is also not definitive. Assuming a weak ligand field, maximum effects would be expected in the ions of f^3 or f^4 configurations with a second but smaller maximum for f^{10} or f^{11} ions; f^0, f^7 and f^{14} ions should show no or minimum crystal field effects. In many systems, increased stability is seen for dysprosium ($4f^9$) and californium ($5f^9$).[2] As an example, in Fig. 9 the elution volumes relative to gadolinium using isobutyrate and Dowex-50 are plotted against the ionic radius of the lanthanides, showing this extra stability for the elements in the region of Dy–Ho. An expected corresponding minimum in the Pr–Pm region is not seen nor is any significant decrease in stability evident for La, Gd or Lu. Strong field and/or entropy effects could be responsible for this behaviour. In addition, for isobutyrate, the elution data indicates that the transcurium actinides show greater stability relative to curium than their lanthanide analogues show relative to gadolinium, but for citrate, the reverse is true.[4] Consequently, although it is tempting to use stability constant and ion exchange data to confirm the existence of crystal field stabilization in complexes of the actinide and lanthanide ions, caution must be exercised that all of the expected manifestations of this effect be checked and not just a "break" at gadolinium.

Acknowledgement—The authors wish to thank Mr. H. G. FRIEDMAN and Mr. J. TATUM for their technical assistance. We are also indebted to Mr. R. CHANDLER for his help with the IBM computations. This research has been supported by the U.S. Atomic Energy Commission.

[32] F. J. C. ROSSOTTI, *Disc. Faraday Soc.*, **26**, 190 (1958).

VOL. 22 1961

J. Inorg. Nucl. Chem., 1961, Vol. 22, pp. 115 to 132. Pergamon Press Ltd. Printed in Northern Ireland

AQUEOUS SYSTEMS AT HIGH TEMPERATURE—III INVESTIGATIONS ON THE SYSTEM UO_3–CuO–NiO–SO_3–H_2O AT 300°C*†

WILLIAM L. MARSHALL and JAMES S. GILL
Reactor Chemistry Division, Oak Ridge National Laboratory
Oak Ridge, Tennessee

(*Received* 28 *December* 1960; *in revised form* 2 *May* 1961)

Abstract—Solubility relationships at 300°C in the five-component system UO_3–CuO–NiO–SO_3–H_2O, and its included aqueous four- and three-component systems, have been investigated. Also reported are a few data on the analogous D_2O system. In order to gain over-all information in a relatively short period of time, the experimental program consisted in determining ternary $L + S$, quaternary $L + 2S$, and quinary $L + 3S$ curves at constant temperature for which, by definition, one, two and three solid phases, respectively, were in equilibrium with a liquid phase. For any set of experiments containing the same solid phases the SO_3 concentration was varied in order to give a solubility curve as a function of this variable. Accordingly, skeletal solubility data, obtained for the five-component system and its accessory four- and three-component systems, gave an over-all description of the solubility equilibria at 300° in the condensed system.

Comments are made regarding the nature of the species in solution, the general shape of some of the solubility curves, the correlation of solid–liquid with liquid–liquid equilibria, and a specific application to aqueous homogeneous reactor fuels.

VOL. 22 1961

DILUTE solutions of uranyl sulphate and sulphuric acid in water (or heavy water) under relatively high pressures and at temperatures above 250° serve as fuels for aqueous homogeneous reactors.[2] Copper sulphate is incorporated to catalyse the recombination of H_2 and O_2 from radiolysis of the water and $NiSO_4$ appears in solution as a consequence of corrosion of the stainless steel reactor system. A knowledge of the phase behaviour of the five-component system UO_3–CuO–NiO–SO_3–H_2O and of its D_2O counterpart at elevated temperatures is, accordingly, clearly necessary.

Detailed definition of phase behaviour in a five-component system is a difficult experimental feat at best. Study of this system is further complicated by the high vapour-pressure of the system (ca 83 atm at 300°), and by the occurrence of a second liquid phase over a wide range of compositions. The following experimental programme has been conducted to obtain a general description of the solubility equilibria in this system. Solubility relationships have been determined after equilibration at 300° of solution and solid mixtures of chosen composition in the presence of saturated vapour using pressure vessels of titanium. Compositions of the solutions were obtained by chemical analysis for the components SO_3, UO_3, CuO and NiO of

* This paper was presented at the 137th National Meeting of the American Chemical Society, Cleveland, Ohio, April, 1960, and is based upon work performed at Oak Ridge National Laboratory, which is operated by Union Carbide Corporation for the Atomic Energy Commission.

† Previous Paper in Series: BARTON, *et al. Liquid–Liquid Immiscibility in the System* UO_3–SO_3–N_2O_5–H_2O *Above* 300°.[1]

[1] C. J. BARTON, G. M. HEBERT and W. L. MARSHALL, *J. Inorg. Nucl. Chem.* **21**, 141 (1961).

[2] H. F. MCDUFFIE, *Fluid Fuel Reactors*, Edited by J. A. LANE, H. G. MACPHERSON, F. MASLAN Chap. 3, p 85–127. Addison–Wesley, Reading, Mass. (1958).

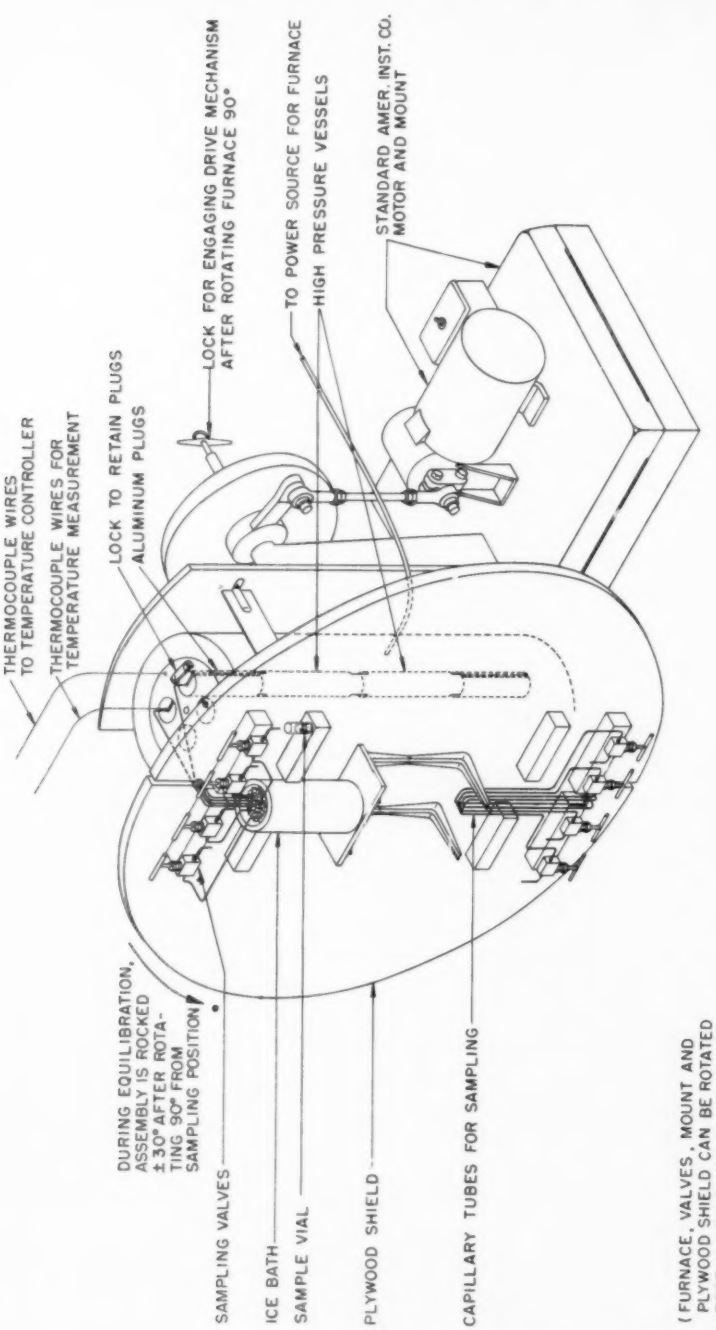
THERMOCOUPLE WIRES TO TEMPERATURE CONTROLLER
THERMOCOUPLE WIRES FOR TEMPERATURE MEASUREMENT
LOCK TO RETAIN PLUGS ALUMINUM PLUGS
LOCK FOR ENGAGING DRIVE MECHANISM AFTER ROTATING FURNACE 90°
TO POWER SOURCE FOR FURNACE HIGH PRESSURE VESSELS
STANDARD AMER. INST. CO. MOTOR AND MOUNT
DURING EQUILIBRATION, ASSEMBLY IS ROCKED ±30° AFTER ROTATING 90° FROM SAMPLING POSITION
SAMPLING VALVES
ICE BATH
SAMPLE VIAL
PLYWOOD SHIELD
CAPILLARY TUBES FOR SAMPLING
(FURNACE, VALVES, MOUNT AND PLYWOOD SHIELD CAN BE ROTATED FREELY OR LOCKED IN POSITION FOR EQUILIBRATION.)

FIG. 1.—Furnace, rocker, and sampling assembly for solubility studies at high temperature and pressure (shown in sampling position).

samples drawn at equilibrium; solids were examined at the conclusion of each experiment to ascertain the number and identity of the solid phases. By proper choice of materials loaded into the bombs, the compositions of solutions in equilibrium at 300° with one, two or three solid phases of known identity were defined. In separate experiments, concentrations of metallic oxide components in solution at equilibrium with each phase or phases were also examined as a function of SO_3 concentration. From the resulting data a general description of solubility equilibria at 300° was obtained for a portion of the five-component system and its included quaternary and ternary systems.

EXPERIMENTAL

Reagents. Solutions were prepared by use of distilled H_2O or of heavy water containing at least 98 per cent of D_2O. For light-water experiments, H_2SO_4 was diluted with distilled water and was used to dissolve the solid components. To prepare heavy-water solutions, H_2SO_4 was repeatedly diluted with D_2O and concentrated by evaporation; solutions so prepared contained less than 3 per cent of H_2SO_4 and H_2O determined by mass spectrographic analysis.

Uranium trioxide monohydrate, obtained from Mallinckrodt Chemical Company and containing less than 0·03 per cent nitrate after several water washings at 100° and less than 0·01 per cent metallic impurities, NiO, $Ni(OH)_2$, $NiSO_4 \cdot H_2O$ and $CuSO_4 \cdot 5H_2O$, all of C.p. purity or equivalent, were used. These materials were converted to their D_2O counterparts when necessary by addition of D_2O to the dehydrated compounds.

Antlerite ($2CuO \cdot CuSO_4 \cdot 2H_2O$) was prepared in gramme quantities by refluxing overnight a sulphuric acid solution initially containing sufficient C.p. $CuCO_3$ to equal 3 moles of CuO for each mole of SO_3. The solid, $2CuO \cdot CuSO_4 \cdot 2H_2O$, resulted. In making the D_2O hydrate, D_2SO_4 in D_2O was substituted for H_2SO_4 in H_2O and was used in an analogous procedure.

Apparatus. A representation of the constant temperature furnace, rocker and sampling assembly is shown in Fig. 1. The sampling system, procedure and schematic diagram of a generally similar pressure vessel was described previously.[3]

The present furnace was fabricated from a 20·3 cm diameter cylindrical block of aluminium alloy. Four 3·8 cm holes machined through the cylinder provided spaces for eight pressure vessels, four inserted from each end. An aluminium plug, 13·6 cm in length, fitted into the hole above each pressure vessel and aided in maintaining uniform temperature. Nichrome wire insulated with ceramic beads was wound in a spiral groove machined in the outer wall of the block to serve as the heater while a layer of asbestos 3 cm in thickness served to insulate the block. The assembly was rocked ±30 degrees from the horizontal position by means of a standard autoclave rocker to provide agitation.

As temperature coefficients of solubility were relatively low for all solid phases under investigation, control and measurement of sample temperatures to ±1° was, accordingly, sufficient for this study. Constant temperature of the furnace was achieved by use of a Leeds and Northrup controller activated by an iron–constantan thermocouple in the aluminium-alloy block. Temperature measurements were made with an iron–constantan thermocouple and a modified Brown recording potentiometer having a suppressed zero and a full-scale reading of 5·0 mV. The thermocouple was precalibrated against a platinum: platinum rhodium thermocouple, and the recording potentiometer was checked periodically against a portable potentiometer to observe any drift in calibration. By the use of this arrangement, the instrumental precision was found to be within approximately ±0·3°. Temperature gradients within the furnace were shown to be less than ±1° in repeated experiments.

The pressure vessels, of 50 cm^3 capacity and 3·5 cm o.d. by 15 cm in length, were fabricated from titanium cylinders. Closure was effected by use of a plug with machined threads matching those on the pressure vessel. A seal was obtained by means of a Teflon gasket between flat surfaces of titanium. A length of flexible titanium capillary dip tube (1·14 mm o.d., 0·51 mm i.d.) inserted through the top plug terminated within the solution volume. Outside the pressure vessel this capillary tube, 1 m in length, was partially immersed in an ice-bath, and was fitted to a "midget" high pressure valve of

[3] W. L. MARSHALL, *Analyt. Chem.* **27**, 1923 (1955).

stainless steel. When the valve was slowly opened in service the high pressure within the vessel forced solution through the capillary tube; the solution was cooled below room temperature by the ice bath and was collected in a sample vial for subsequent analysis.

Experimental procedure. The following procedure was used after preliminary experimentation permitted definition of the solid phase or phases to be encountered in various portions of the system.

A pressure vessel was loaded with a predetermined quantity of solid or solids, 25 ml of H_2SO_4–H_2O (or D_2SO_4–D_2O) with or without additional components in solution and 2 ml of 30% H_2O_2. In the case of the D_2SO_4–D_2O solutions, dilution with H_2O_2 reduced the concentration of D_2O from approximately 98 to 93 per cent. The solid or solids and other soluble components were in amounts which would yield after equilibration the desired number and type of solid phases. The H_2O_2 decomposed at elevated temperatures to produce an overpressure of O_2 which served to prevent both reduction of solution components and corrosion of the titanium vessel. Any UO_4 produced upon the addition of H_2O_2 to uranyl solutions would be expected[4] and was found to decompose rapidly at 300°.

Eight pressure vessels so loaded were placed in the furnace. The temperature was raised to 300° and the furnace was rocked at this temperature for 3–72 hr before sampling the solution phase. To sample the solutions, the rocker was stopped, the cylindrical furnace was placed in a vertical position, and the solid phases in the four vessels in the upper section of the furnace were allowed to settle for 15 min after which sampling, preceded by removal of a holdup volume, was accomplished. The furnace was turned upside down and the other four solutions were sampled in a similar manner.

Samples taken after 72 hr yielded data very near those obtained after 3–4 hr. While considerable supersaturation was observed in previous studies at 190° for solutions which did not contain solid phases initially,[5] no evidence of supersaturation was observed in this study. This difference in behaviour is not unexpected since virtually all solutions examined in this present program were initially in contact with solids. Moreover, rates of attainment of equilibrium were expected to be considerably more rapid at 300° than at 200°. If new solid phases had to form for the attainment of equilibrium, then these anticipations may not apply.

Virtually all analyses for uranium, copper and nickel were performed by controlled-potential coulometric titration.[6,7] The SO_3 was determined by titration with a standard NaOH solution after removal of cations by means of Dowex-50 cation exchange resin.[8]

Results from all wet chemical analyses were reported on a molarity basis. Since molar concentrations are dependent on temperature, the analytical values were converted to molal units by making use of density-concentration curves for separate two-component solutions, i.e., for UO_2SO_4 in H_2O, $CuSO_4$ in H_2O, $NiSO_4$ in H_2O and H_2SO_4 in H_2O. The analogous D_2O system was treated in the same manner. The separate correction factors for a particular solution were summed in order to arrive at a correction factor for conversion from molarities to molalities.

The variables of particular interest in this study were not the actual concentrations but rather the saturation molal or molar ratios, R, defined specifically as R_U, R_{Cu}, and R_{Ni} for m_{UO_3}: m_{SO_3}, m_{CuO}: m_{SO_3}, and m_{NiO}: m_{SO_3}, respectively. For the most part, these were found to change slowly as the concentrations of solution components changed. For example, a 10 per cent change in the SO_3 concentration between 0·01 and 0·1 m SO_3 (Fig. 2) changed R_U by only 1 per cent.

After a run the pressure vessels were cooled from high temperature by removing each of them from the furnace and placing them in a crushed-ice–water mixture. This procedure cooled the vessels and contents to low temperature within several minutes; the solids were then removed and dried between sheets of filter paper within 15 min. Some of the solids were identified by chemical analyses but most were identified by X-ray diffraction and optical petrography. The chemical analyses were performed by methods similar to those described above for the solutions.

In a special set of experiments the solubilities of UO_3 hydrates were determined at 150°, 225° and 300° in water solutions from 0·001 to 0·1 molal in total SO_3 (Table 1). Mixtures were equilibrated for 16 hr at each temperature before sampling the solution phases. After the solubility determinations at 300° the solid phases were removed from many of the vessels and identified by X-ray diffraction

[4] M. D. SILVERMAN, G. M. WATSON and H. F. MCDUFFIE, *Industr. Engng. Chem.* **48,** 1238 (1956).
[5] C. H. SECOY and J. S. GILL. Unpublished work (1956).
[6] M. T. KELLY, H. C. JONES and D. J. FISHER, *Analyt. Chem.* **31,** 488 (1959).
[7] W. D. SHULTS and P. F. THOMASON, *Analyt. Chem.* **31,** 492 (1959).
[8] H. O. DAY, J. S. GILL, E. V. JONES and W. L. MARSHALL, *Analyt. Chem.* **26,** 611 (1954).

In another set of experiments solubilities of UO_3 hydrates in H_2SO_4–H_2O solutions were determined from liquid-phase samples obtained in less than an hour at 225 and 300° and after 18 hr at 150, 225 and 300° (Table 1). A pair of vessels was removed after each 18 hr sampling. The solid phases were dried between sheets of filter paper within 10 min after removal from a vessel and were identified by X-ray diffraction within 2 hr after drying. A second pair of vessels was also removed and opened after 30 min at 300° in order to identify the solid phases after a short length of time.

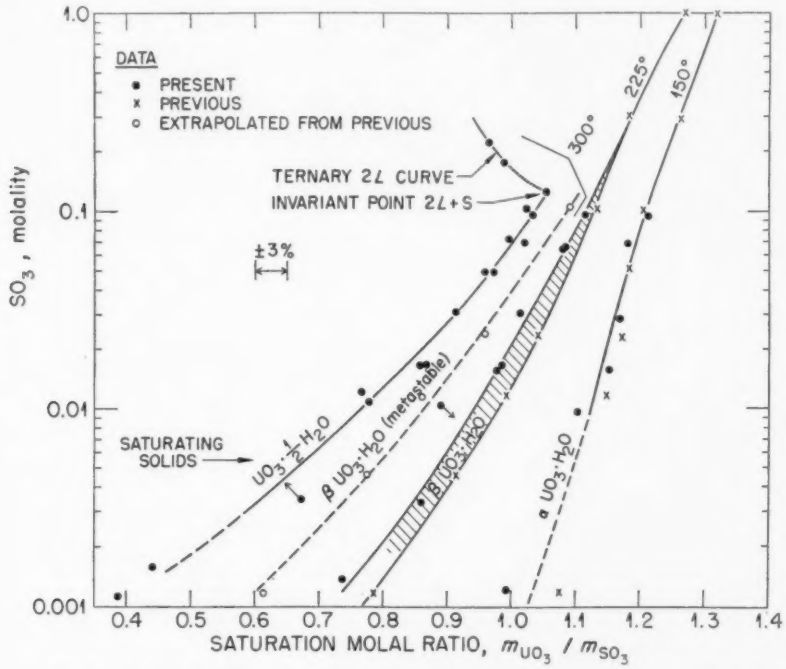

FIG. 2.—Saturation molal ratios at 150, 225 and 300° for the solubility of UO_3 hydrates in H_2SO_4–H_2O solutions. ($\alpha UO_3 \cdot H_2O$ = DAWSON'S *et al.*, $UO_3 \cdot 0{\cdot}8H_2O$; $\beta UO_3 \cdot H_2O$ = DAWSON'S *et al.*, $UO_3 \cdot 1 \cdot H_2O$)

RESULTS AND DISCUSSION

The data

The solubility data are given in Tables 1–9. This investigation involves the study of several subsidiary ternary and quaternary systems in addition to the over-all quinary system UO_3–CuO–NiO–SO_3–H_2O. These are the three ternary systems UO_3–SO_3–H_2O, CuO–SO_3–H_2O and NiO–SO_3–H_2O (Tables 1, 2 and 3, Figs. 2, 3 and 4) and the three quaternary systems UO_3–CuO–SO_3–H_2O, UO_3–NiO–SO_3–H_2O and CuO–NiO–SO_3–H_2O (Tables 4, 5, 6 and 7, Figs. 5, 6, 7 and 8). For each class of systems the tables and figures give data for isothermally univariant condensed equilibria, $L + 1S$ for three components, $L + 2S$ for four components, and $L + 3S$ for five components. The reported data for the system NiO–SO_3–H_2O at 300°, obtained with SLUSHER of this Laboratory, were selected from over-all results for this system.[9]

The concentration of each component in one sample was determined in duplicate.

[9] W. L. MARSHALL, J. S. GILL and R. SLUSHER. Presented at the 138th National Meeting of the American Chemical Society, New York, N.Y., September, 1960.

TABLE 1.—SOLUBILITIES AT 150, 225 AND 300° OF UO_3 HYDRATES IN H_2SO_4–H_2O SOLUTIONS

Time at temperature, (hr)	SO_3, (m)	UO_3, (m)	Ratio, $\frac{\text{Molar (at 25°)}}{\text{Molal}}$	Solid phases§
At 150° (Stable Solid = $\alpha UO_3 \cdot H_2O$)				
16·	0·0954	0·1157	0·992	
18·	0·0704	0·0834	0·993	A
16·	0·0295	0·0345	0·995	
18·	0·01589	0·01829	0·996	A + D*
16·	0·00964	0·01063	0·997	
16·	0·00120	0·00119	0·997	
At 225° (Stable Solid = $\beta UO_3 \cdot H_2O$)				
16·	0·0967	0·1077	0·992	
0·25	0·0677	0·0730	0·993	
18·	0·0689	0·0741	0·993	B + A*
16·	0·0303	0·0307	0·995	
0·25	0·01583	0·01549	0·996	
18·	0·01614	0·01590	0·996	B + A*
16·	0·01039	0·00913	0·997	
16·	0·00324	0·00279	0·997	
16·	0·00134	0·00098	0·997	
At 300° (Stable Solid = $UO_3 \cdot \frac{1}{2}H_2O$)				
16·	0·2204†	0·2125	0·990	
16·	0·1758†	0·1731	0·990	
16·	0·1248‡	0·1314	0·992	
16·	0·1031	0·1053	0·992	C
16·	0·0974	0·0974	0·992	
16·	0·0969	0·1000	0·992	
0·50	0·0697	0·0712	0·993	C + B* + A*
0·50	0·0677	0·0696	0·993	C + B* + A*
18·	0·0736	0·0729	0·993	C
16·	0·0491	0·0477	0·995	
16·	0·0490	0·0470	0·995	
16·	0·0312	0·0284	0·995	C
0·50	0·01584	0·01417	0·996	B* + A*
0·50	0·01675	0·01450	0·996	B* + A*
18·	0·01691	0·01450	0·996	C
16·	0·01208	0·00922	0·997	
16·	0·01092	0·00847	0·997	C
16·	0·00347	0·00233	0·997	C
16·	0·00155	0·00068	0·997	C
16·	0·00113	0·00044	0·997	C

Where A = $\alpha UO_3 \cdot H_2O$, B = $\beta UO_3 \cdot H_2O$, C = $UO_3 \cdot \frac{1}{2}H_2O$, D = $UO_4 \cdot 2H_2O$:

* Metastable Solids—Decomposing.
† Points on Ternary 2L curve (no solid phase present).
‡ Isothermal invariant point $S + 2L$.
§ Established by comparison of X-ray diffraction patterns.

TABLE 2.—SOLUBILITY AT 300° OF $2CuO \cdot CuSO_4 \cdot 2H_2O$ IN H_2SO_4–H_2O SOLUTIONS

SO_3 (*m*)	CuO (*m*)	Ratio, $\frac{\text{Molar (at 25°)}}{\text{Molal}}$
1·89	1·54	0·98
1·16	0·849	0·99
0·844	0·590	0·990
0·282	0·177	0·995
0·0759	0·0436	0·997
0·0254	0·0133	0·997
0·00730	0·00325	0·997
0·00256	0·00970	0·997

TABLE 3.—SOLUBILITY AT 300° OF $NiSO_4 \cdot H_2O$ IN H_2SO_4–H_2O SOLUTIONS[9]

SO_3 (*m*)	NiO (*m*)	Ratio, $\frac{\text{Molar (at 25°)}}{\text{Molal}}$
0·403	0·129	0·992
0·375	0·130	0·993
0·196	0·0662	0·995
0·193	0·0683	0·995
0·191	0·0702	0·995
0·101	0·0392	0·996
0·0989	0·0381	0·996
0·0963	0·0360	0·996
0·0501	0·0205	0·997
0·0500	0·0205	0·997
0·0291	0·0130	0·997
0·0134	0·00642	0·997

TABLE 4.—SIMULTANEOUS SOLUBILITIES AT 300° OF $2CuO \cdot CuSO_4 \cdot 2H_2O$, $CuO \cdot 3UO_3$ AND $CuO \cdot 2UO_2SO_4 \cdot 7H_2O$ IN H_2SO_4–H_2O SOLUTIONS

SO_3 (*m*)	UO_3 (*m*)	CuO (*m*)	Ratio, $\frac{\text{Molar (at 25°)}}{\text{Molal}}$
0·323	0·1530	0·1379	0·989
0·221	0·1271	0·0759	0·991
0·1950	0·1180	0·0604	0·991
0·1849	0·1179	0·0561	0·991
0·1803	0·1156	0·0531	0·991
0·1800	0·1171	0·0571	0·991
0·1769	0·1143	0·0538	0·991
0·1643	0·0997	0·0538	0·992
0·1596	0·1024	0·0490	0·992
0·1257	0·0769	0·0389	0·993
0·1068	0·0616	0·0323	0·994
0·1058	0·0630	0·0314	0·994
0·0851	0·0478	0·0258	0·995
0·0668	0·0364	0·0206	0·995
0·0619	0·0321	0·0192	0·995

Solid phases:
Below 0·18 m SO_3: $2CuO \cdot CuSO_4 \cdot 2H_2O + CuO \cdot 3UO_3$.
Above 0·18 m SO_3: $2CuO \cdot CuSO_4 \cdot 2H_2O + CuO \cdot 2UO_2SO_4 \cdot 7H_2O$.

VOL. 22 1961

TABLE 5.—SIMULTANEOUS SOLUBILITIES AT 300° OF $CuO{\cdot}3UO_3$, $UO_3{\cdot}\frac{1}{2}H_2O$ AND HEAVY-LIQUID PHASE IN H_2SO_4–H_2O SOLUTIONS

SO_3 (*m*)	UO_3 (*m*)	CuO (*m*)	Ratio, $\frac{\text{Molar (at 25°)}}{\text{Molal}}$
0·455	0·295	0·0823	0·981
0·1668	0·1253	0·0321	0·990
0·1659	0·1232	0·0327	0·990
0·1577	0·1334	0·01774	0·990
0·1528	0·1372	0·01045	0·990
0·1507	0·1392	0·00851	0·990
0·1411	0·1264	0·01031	0·991
0·1350	0·1288	0·00377	0·991
0·1204	0·1246	0·00075	0·991
0·1111	0·1125	0·00069	0·991
0·1107	0·1125	0·00072	0·991
0·1104	0·1118	0·00068	0·991
0·1104	0·1125	0·00068	0·991
0·1102	0·1107	0·00068	0·991
0·1100	0·1130	0·00072	0·991
0·0940	0·0958	0·00054	0·992
0·0771	0·0769	0·00041	0·993
0·0500	0·0476	0·00024	0·994
0·0157	0·0131	0·00010	0·996

Solid and heavy-liquid phases:
Below 0·11 m SO_3: $CuO{\cdot}3UO_3 + UO_3{\cdot}\frac{1}{2}H_2O$.
Above 0·11 m SO_3: $CuO{\cdot}3UO_3$ + Heavy-liquid phase.

TABLE 6.—SIMULTANEOUS SOLUBILITIES AT 300° OF $UO_3{\cdot}UO_2SO_4{\cdot}5H_2O$ AND $NiSO_4{\cdot}H_2O$ IN H_2SO_4–H_2O SOLUTIONS

SO_3 (*m*)	UO_3 (*m*)	NiO (*m*)	Ratio, $\frac{\text{Molar (at 25°)}}{\text{Molal}}$
0·272	0·1737	0·0721	0·988
0·1952	0·1330	0·0507	0·990
0·1879	0·1268	0·0505	0·991
0·1564	0·1022	0·0423	0·992
0·1281	0·0830	0·0342	0·993
0·1031	0·0616	0·0318	0·994
0·0734	0·0402	0·0215	0·995
0·0517	0·0261	0·0154	0·996

These duplicate analyses agreed within ± 0·5–3 per cent, depending upon the total concentration of the component. They were averaged and the variation of these averages between successive samples was approximately ± 2–4 per cent. Each datum listed in Tables 1–9 represents usually the average value of two to three separate samples. The number of significant figures of the data is greater than is indicated by the over-all precision but is consistent with the best expected precision of the analytical methods. This reporting procedure is followed in order to retain usefulness of the data for statistical treatment.

TABLE 7.—SIMULTANEOUS SOLUBILITIES AT 300° OF $2CuO{\cdot}CuSO_4{\cdot}2H_2O$ AND $NiSO_4{\cdot}H_2O$ IN H_2SO_4–H_2O SOLUTIONS

SO_3 (*m*)	CuO (*m*)	NiO (*m*)	Ratio, $\frac{\text{Molar (at 25°)}}{\text{Molal}}$
0·306	0·1632	0·0343	0·995
0·217	0·1076	0·0281	0·995
0·1922	0·0920	0·0268	0·996
0·1281	0·0533	0·0209	0·996
0·1075	0·0396	0·0191	0·996
0·0819	0·0299	0·0174	0·997
0·0696	0·0238	0·0151	0·997
0·0513	0·0152	0·0118	0·997

TABLE 8.—SIMULTANEOUS SOLUBILITIES AT 300° OF $UO_3{\cdot}UO_2SO_4{\cdot}5H_2O$, $NiSO_4{\cdot}H_2O$ AND $2CuO{\cdot}CuSO_4{\cdot}2H_2O$ IN H_2SO_4–H_2O SOLUTIONS

SO_3 (*m*)	UO_3 (*m*)	CuO (*m*)	NiO (*m*)	Ratio, $\frac{\text{Molar (at 25°)}}{\text{Molal}}$
0·999	0·207	0·537	0·0857	0·984
0·556	0·189	0·218	0·0730	0·988
0·356	0·129	0·118	0·0524	0·990
0·207	0·107	0·0388	0·0394	0·991
0·0942	0·0437	0·0167	0·0216	0·995
0·0561	0·0227	0·0086	0·0142	0·996
0·0457	0·0173	0·0071	0·0122	0·996
0·0450	0·0170	0·0065	0·0119	0·996

TABLE 9.—SIMULTANEOUS SOLUBILITIES AT 300° OF $UO_3{\cdot}UO_2SO_4{\cdot}5D_2O$, $NiSO_4{\cdot}D_2O$ AND $2CuO{\cdot}CuSO_4{\cdot}2H_2O$ IN D_2SO_4–D_2O SOLUTIONS

SO_3 (*m*)	UO_3 (*m*)	CuO (*m*)	NiO (*m*)	Ratio, $\frac{\text{Molar (at 25°)}}{\text{Molal}}$
0·525	0·0920	0·282	0·0376	1·095
0·231	0·0536	0·0945	0·0269	1·100
0·090	0·0441	0·0163	0·0183	1·102
0·0609	0·0272	0·0103	0·0135	1·102
0·0603	0·0262	0·00996	0·0130	1·102
0·0449	0·0175	0·00700	0·0117	1·103
0·039		0·00612	0·00988	1·103
0·0390	0·0142	0·00555	0·00988	1·103
0·0376		0·00545	0·0104	1·103

The solubility data are shown graphically in Figs. 2–10, plotted in each case as R_U, R_{Cu} or R_{Ni} against the logarithm of the total SO_3 concentration. This type of plot allows a wide coverage of SO_3 concentrations and reveals the precision of data somewhat better than a linear plot of molalities of the components. In order to determine the saturation concentration of one of the metallic oxide components such as CuO, the saturation molal ratio is multiplied by the corresponding or indicated concentration of SO_3.

VOL. 22 1961

Saturation molal ratios, $m_{UO_3}:m_{SO_3}$, obtained by extrapolation from 290 to 300° of previous data[3] for the system UO_3–SO_3–H_2O yielded ratios approximately 10 per cent higher than those reported here. In the present study of the system UO_3–SO_3–H_2O most solution–solid mixtures were rocked at 300° for a minimum of 16 hr. Previously, although experimental data were reproducible after 15 min at one temperature, an entire run—at several temperatures—was usually finished in 10 hr. The

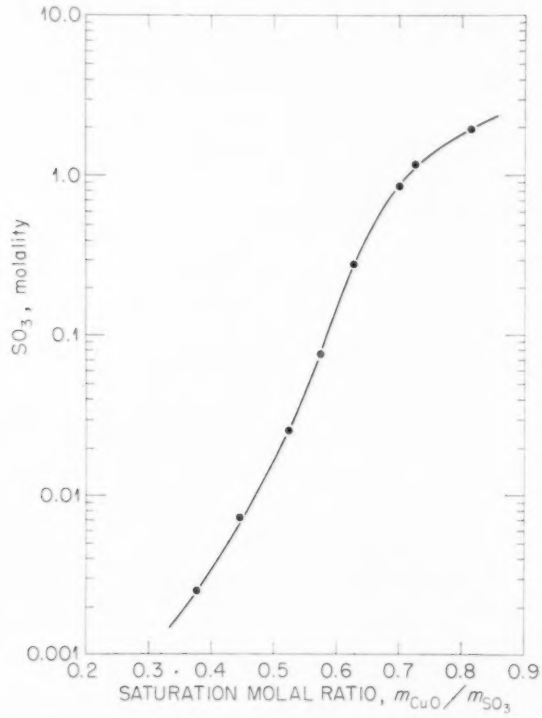

FIG. 3.—Saturation molal ratios at 300° for the solubility of $2CuO{\cdot}CuSO_4{\cdot}2H_2O$ in H_2SO_4–H_2O solutions.

stable solid phase at 300° in the current investigation was identified as the hemihydrate, $UO_3{\cdot}\frac{1}{2}H_2O$, by the use of an accepted X-ray diffraction pattern for this solid.[10] However, in the earlier investigation up to 290°, UO_3 monohydrate was stated to be the solid phase. In pure water under a saturation vapour-pressure the exact temperature for a transition from DAWSON'S *et al.*, $UO_3{\cdot}1{\cdot}OH_2O$ orthorhombic II phase, in this paper designated $\beta UO_3{\cdot}H_2O$, to $UO_3{\cdot}\frac{1}{2}H_2O$ is in doubt but is reported to be between 280° and 325°.[10]

In view of the disagreement at 300°, further solubilities were determined at 150, 225 and 300°; these are included in Table 1 and Fig. 2. After 15 min at 150° attempts to obtain clear samples of two solution phases, approximately 0·016 and 0·07 molal in SO_3, produced a lemon-white and a yellow solid suspended in the samples. These solids presumably were a UO_4 hydrate formed upon the addition at 25° of H_2O_2 and a UO_3 hydrate, respectively. The two vessels containing these solution and solid

[10] J. K. DAWSON, E. WAIT, K. ALCOCK and D. R. CHILTON, *J. Chem. Soc.* 3531 (1956).

VOL.
22
1961

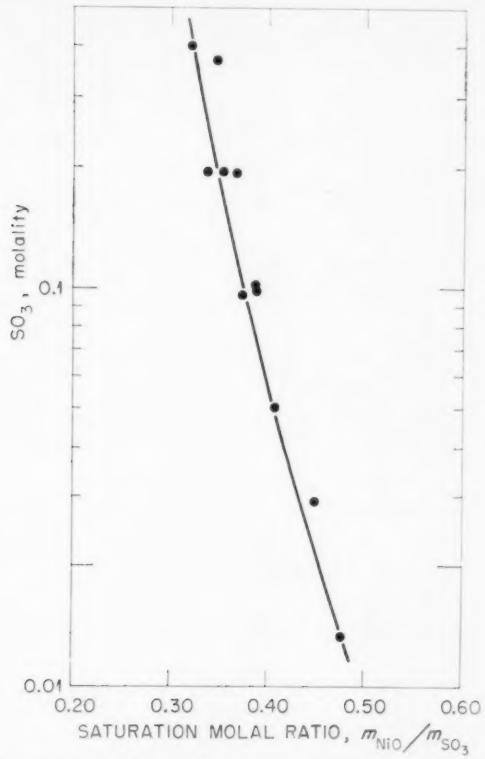

FIG. 4.—Saturation molal ratios at 300° for the solubility of $NiSO_4 \cdot H_2O$ in H_2SO_4–H_2O solutions.

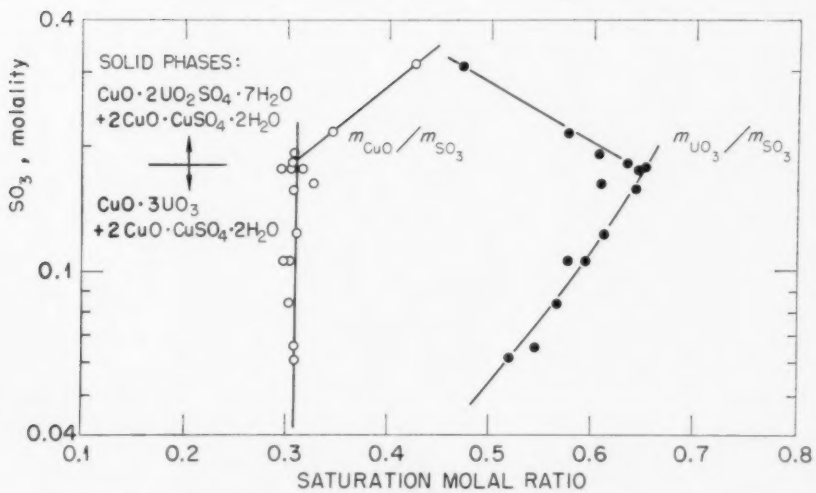

FIG. 5.—Saturation molal ratios at 300° for the simultaneous solubilities of $CuO \cdot 3UO_3$ and $2CuO \cdot CuSO_4 \cdot 2H_2O$, and of $CuO \cdot 3UO_3$ and $CuO \cdot 2UO_2SO_4 \cdot 7H_2O$ in $H_2SO_4 \cdot H_2O$ solutions.

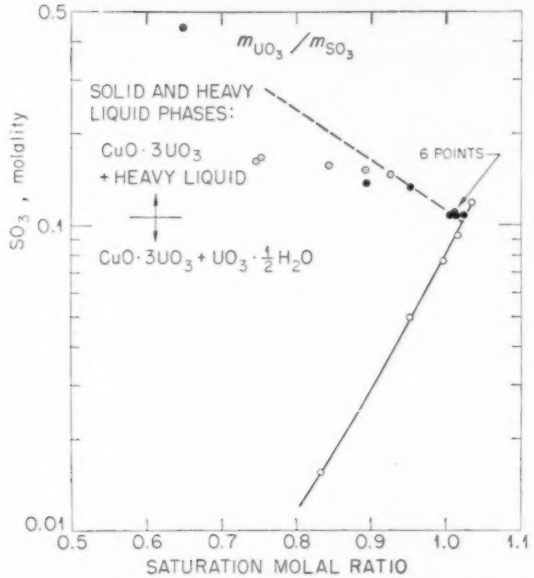

FIG. 6a.—Saturation molal ratios for the simultaneous solubilities of $CuO \cdot 3UO_3$ and $UO_3 \cdot \frac{1}{2}H_2O$, and of $CuO \cdot 3UO_3$ and heavy-liquid phase in H_2SO_4–H_2O solutions.

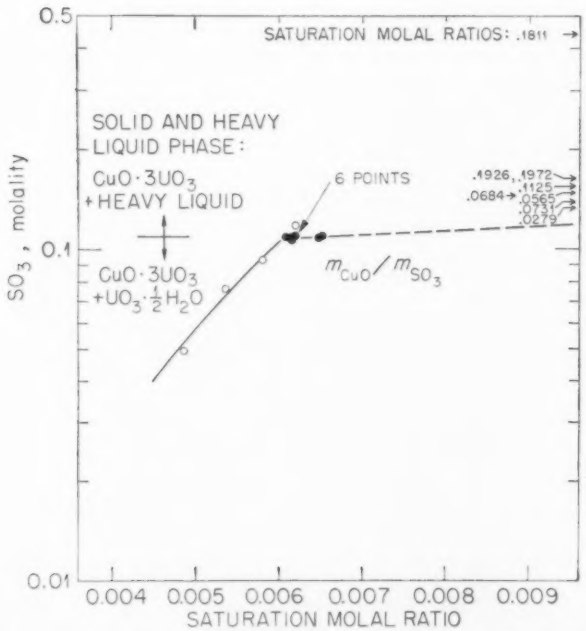

FIG. 6b.—Saturation molal ratios for the simultaneous solubilities of $CuO \cdot 3UO_3$ and $UO_3 \cdot \frac{1}{2}H_2O$, and of $CuO \cdot 3UO_3$ and heavy-liquid phase in H_2SO_4–H_2O solutions.

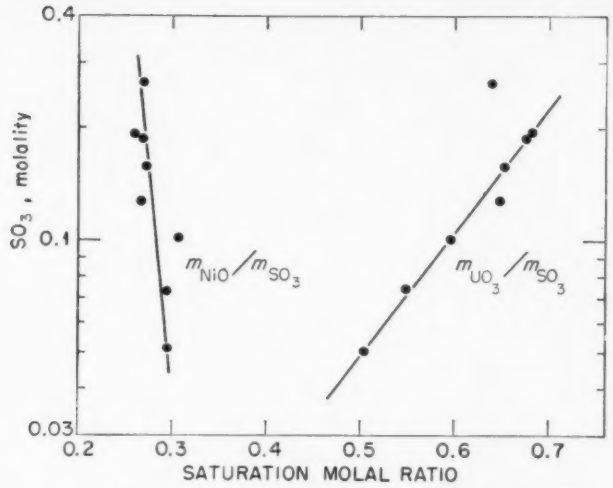

FIG. 7.—Saturation molal ratios for the simultaneous solubilities of $UO_3 \cdot UO_2SO_4 \cdot 5H_2O$ and $NiSO_4 \cdot H_2O$ in H_2SO_4–H_2O solutions.

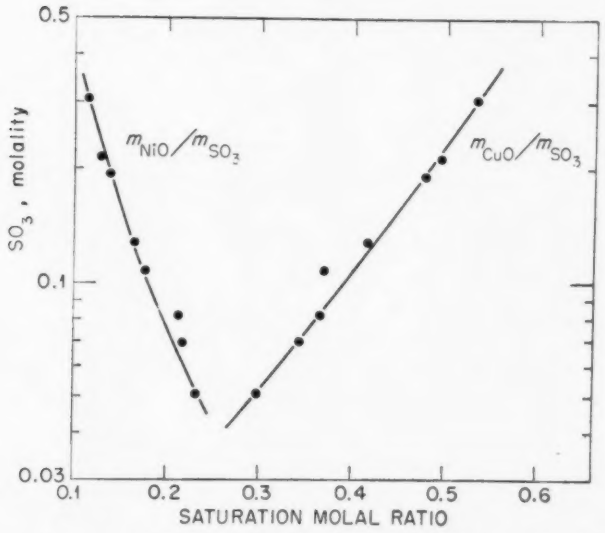

FIG. 8.—Saturation molal ratios for the simultaneous solubilities of $2CuO \cdot CuSO_4 \cdot 2H_2O$ and $NiSO_4 \cdot H_2O$ in H_2SO_4–H_2O solutions.

mixtures were opened after 18 hr at 150°. Only the yellow solid was found in the vessel containing 0·07 m SO_3 solution, but both the yellow solid and a small amount of the lemon-white solid were found in the vessel containing 0·016 m SO_3. The X-ray diffraction pattern for the yellow solid was that for DAWSON's, *et al.*, $UO_3 \cdot 0{\cdot}8H_2O$ orthorhombic I phase,[10] in this paper designated $\alpha UO_3 \cdot H_2O$. The pattern for the lemon-white solid was that for $UO_4 \cdot 2H_2O$ identified by WATT *et al.*, found in contact

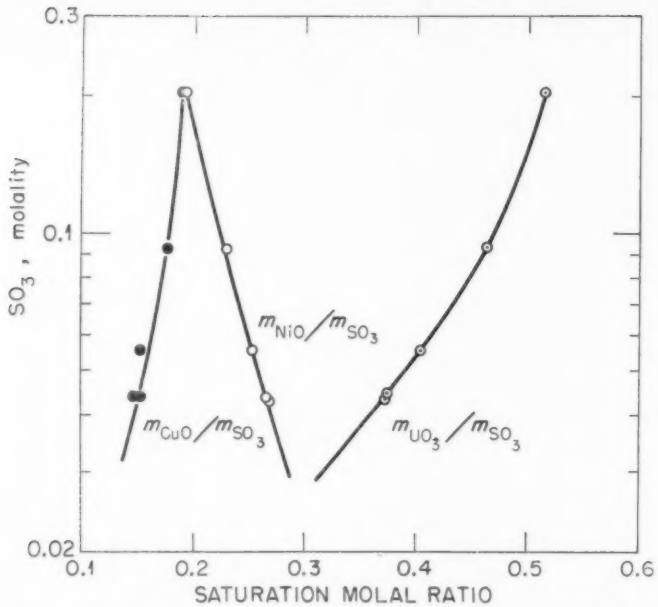

FIG. 9.—Saturation molal ratios for the simultaneous solubilities of $UO_3 \cdot UO_2SO_4 \cdot 5H_2O$, $2CuO \cdot CuSO_4 \cdot 2H_2O$ and $NiSO_4 \cdot H_2O$ in H_2SO_4–H_2O solutions.

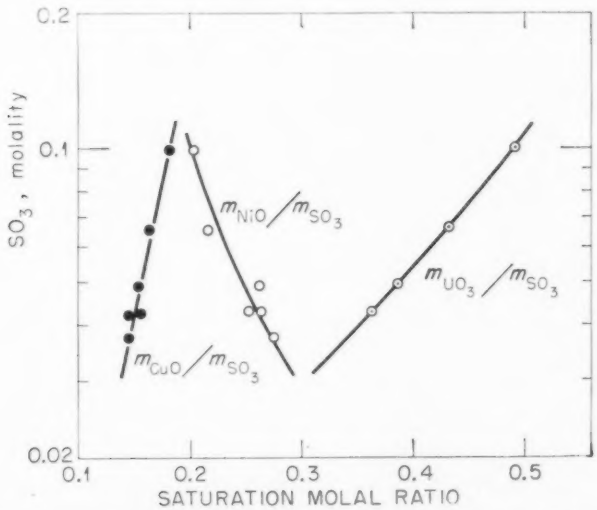

FIG. 10.—Saturation molal ratios for the simultaneous solubilities of $UO_3 \cdot UO_2SO_4 \cdot 5D_2O$, $2CuO \cdot CuSO_4 \cdot 2D_2O$ and $NiSO_4 \cdot D_2O$ in D_2SO_4–D_2O solutions.

with aqueous solutions above 64° by GILPATRICK and MCDUFFIE and confirmed by SILVERMAN and SALLACH.[11]

[11] G. W. WATT, S. L. ACHORN and J. L. MARLEY, *J. Amer. Chem. Soc.* **72,** 3341 (1950); L. O. GILPATRICK and H. F. MCDUFFIE, Report ORNL–2931, TID–4500, p. 125 (1960), Office of Technical Services, Dept. of Commerce, Washington, D.C., U.S.A.; L. SILVERMAN and R. A. SALLACH, *J. Phys. Chem.* **65,** 370 (1961).

Decreased acidity of a solution phase containing dissolved UO_4 will reduce the solubility of UO_4 hydrate and lower its rate of decomposition.[4] The acidity of an SO_3 solution is lowered by saturating it with UO_3;[3] thus the rate of decomposition of dissolved UO_4 is reduced. At the higher temperatures all UO_4 hydrate was decomposed, leaving only the UO_3 hydrates.

Results in Table 1 where indicated show that $\alpha UO_3 \cdot H_2O$ is a stable solid phase at 150°, presumably $\beta UO_3 \cdot H_2O$ at 225° and $UO_3 \cdot \frac{1}{2}H_2O$ at 300°. If at any temperature a metastable solid is present but is converting to the stable solid, the observed solubility should be that for the metastable solid which has the higher solubility. The previous data at 270° and 290°, and the extrapolated data at 300° (Fig. 2) should be those for the solubility of $\beta UO_3 \cdot H_2O$ which at least at 300° is metastable. In Fig. 2 even the previous data at 225° may represent the solubility of metastable $\alpha UO_3 \cdot H_2O$ while the present data at 225° are for the solubility of stable $\beta UO_3 \cdot H_2O$. Two curves at this temperature are drawn although there is at most only a 5 per cent difference in molal ratio between the two sets of data. A low heat of transition between the three solid hydrates of UO_3 may be expected and therefore it appears that metastability by one or the other could very easily occur in the above range of temperature.

VOL. 22 1961

Solubilities in D_2O *media.* Solubilities at 300° in D_2O media along the quinary $L + 3S$ curve for $UO_3 \cdot UO_2SO_4 \cdot 5D_2O$, $2CuO \cdot CuSO_4 \cdot 2D_2O$ and $NiSO_4 \cdot D_2O$ as stable solid phases are presented in Table 9 and Fig. 10. These data do not indicate large differences from comparative solubilities in H_2O at least in this range of concentration. As an approximation, solubilities of solids in the H_2O system therefore have been applied to the estimation of solubilities in D_2O media.

Isothermal invariant points. The system UO_3–CuO–SO_3–H_2O exhibits two isothermal invariant points at 300° in the range of concentration investigated and for the particular solid phases. One of these is shown in Fig. 5 and occurs at 0·18 m SO_3, at which concentration there are three solids, $CuO \cdot 3UO_3$,* $2CuO \cdot CuSO_4 \cdot 2H_2O$ and $CuO \cdot 2UO_2SO_4 \cdot 7H_2O$, in equilibrium with the solution phase. There are three solubility curves which intersect at this isothermal invariant point along which (1) $2CuO \cdot CuSO_4 \cdot 2H_2O$ and $CuO \cdot 3UO_3$, (2) $2CuO \cdot CuSO_4 \cdot 2H_2O$ and $CuO \cdot 2UO_2SO_4 \cdot 7H_2O$, and (3) $CuO \cdot 3UO_3$ and $CuO \cdot 2UO_2SO_4 \cdot 7H_2O$ are saturating solids, respectively. Experimental data to define part of curves (1) and (2) are presented in Fig. 5.

The second isothermal invariant point found for the system UO_3–CuO–SO_3–H_2O occurs at 0·11 m SO_3 (Figs. 6a and 6b) at which $CuO \cdot 3UO_3$, $UO_3 \cdot \frac{1}{2}H_2O$, and two liquid phases are at equilibrium. This invariant point of the system was established by the identical analytical composition of saturated light-liquid phases from six experimental runs. The concentrations of the starting mixtures, assuming 100 per cent dissolution of all solids, were varied from 0·12 to 0·33 m SO_3, from 0·44 to 1·0 m UO_3 and from 0·07 to 0·18 m CuO. Moreover, the light-liquid phases, which were obtained from six runs by sampling the saturated solution at 300°, were heated in sealed silica tubes in order to observe any phase changes. The second liquid phase was observed to appear at 300° in each solution and to increase in amount above 300°, thus indicating that the light-liquid phase was in equilibrium with heavy liquid

* A new compound described by GILL and MARSHALL.[12]

[12] J. S. GILL and W. L. MARSHALL, *J. Inorg. Nucl. Chem.* **20**, 85 (1961).

as well as solid phases at 300°. This observation substantiates the existence at equilibrium of a second liquid phase in addition to $CuO{\cdot}3UO_3$ and $UO_3{\cdot}\frac{1}{2}H_2O$ solids at the isothermal invariant point. The second liquid phase formed in the pressure vessels, however, was not observed after cooling the vessels to room temperature and opening. It is expected that this heavy-liquid phase dissolved in the residual light-liquid phase upon cooling and therefore was not seen.

In the system UO_3–SO_3–H_2O an isothermal invariant point was found at 0·1248 m SO_3 at a saturation molal ratio, $m_{UO_3}:m_{SO_3}$, of 1·053. To obtain this point an excess of $UO_3{\cdot}H_2O$ was added to a 0·25 m UO_2SO_4 solution to serve as a starting mixture. At 300° two liquid phases and $UO_3{\cdot}\frac{1}{2}H_2O$ solid were in equilibrium.

Comparative changes of R *with sulphate concentration.* Upon inspection of Figs. 2–4 it is apparent that the saturation molal ratio, *R*, decreases for saturating solids $UO_3{\cdot}\frac{1}{2}H_2O$ and $2CuO{\cdot}CuSO_4{\cdot}2H_2O$ and increases for $NiSO_4{\cdot}H_2O$ as the SO_3 concentration decreases. These saturation molal ratios must ultimately reach infinity, 3 and 1, the values for *R* at either the true or the hypothetical solubilities in water for the three solids, respectively. In either a real or hypothetical sense, values of *R* for saturating solids, $UO_3{\cdot}\frac{1}{2}H_2O$ and $2CuO{\cdot}CuSO_4{\cdot}2H_2O$ must go through a minimum as the SO_3 concentration decreases whereas in the case of $NiSO_4{\cdot}H_2O$, *R* is already approaching one, its value at the hypothetical solubility point for $NiSO_4{\cdot}H_2O$ in H_2O. This value of one in the system NiO–SO_3–H_2O is not realized since hydrolytic decomposition of $NiSO_4{\cdot}H_2O$ occurs at 0·013 m SO_3 to produce a nickel–oxy-sulphate solid phase.[9]

Skeletal representation of five-component systems. The curves shown in Figs. 2–10 are reference curves and are used for deriving skeletal descriptions of the five-component system UO_3–CuO–NiO–SO_3–H_2O. In order to show visually the simultaneous variations in saturation concentrations of all components in solutions, some of the variables must of necessity be restricted. Temperature is accordingly held constant, the pressure is the saturation vapour-pressure of the system, and saturation concentrations are selected at the same SO_3 concentration from Figs. 2 to 10. Three-dimensional models were constructed to show variations in solubility under the above restrictions for various selected values of m_{SO_3}. One of these for the system at 0·1 m SO_3 in H_2O solution is shown in Fig. 11; the three orthogonal axes represent concentrations of components UO_3, CuO and NiO, respectively. The compositions of the saturating solid phases cannot be plotted within the model but their identities have been determined and are designated. The model shows surfaces of saturation for particular solid phases the boundaries of which are determined from the reference curves; the included volume represents unsaturated solution. From a set of these models the concentrations at saturation can be estimated.

Several isothermal quaternary and quinary curves over which SO_3 concentration is the only variable are as yet not determined or fully established. Points on these curves at 0·1 molal SO_3 are indicated in Fig. 11. The point at constant SO_3 at which $CuO{\cdot}3UO_3$, $2CuO{\cdot}CuSO_4{\cdot}2H_2O$, and $UO_3{\cdot}UO_2SO_4{\cdot}5H_2O$ are saturating solids is difficult to obtain since nickel is present only in solution. Some approximate data obtained for the variation of NiO and SO_3 on the quinary surface of liquid saturated with the two solids $CuO{\cdot}3UO_3$ and $2CuO{\cdot}CuSO_4{\cdot}2H_2O$ indicate the general direction of the boundary curve shown in Fig. 11. The direction thereby establishes an approximate intersectional position for this point. The positions for the point involving the

VOL.
22
1961

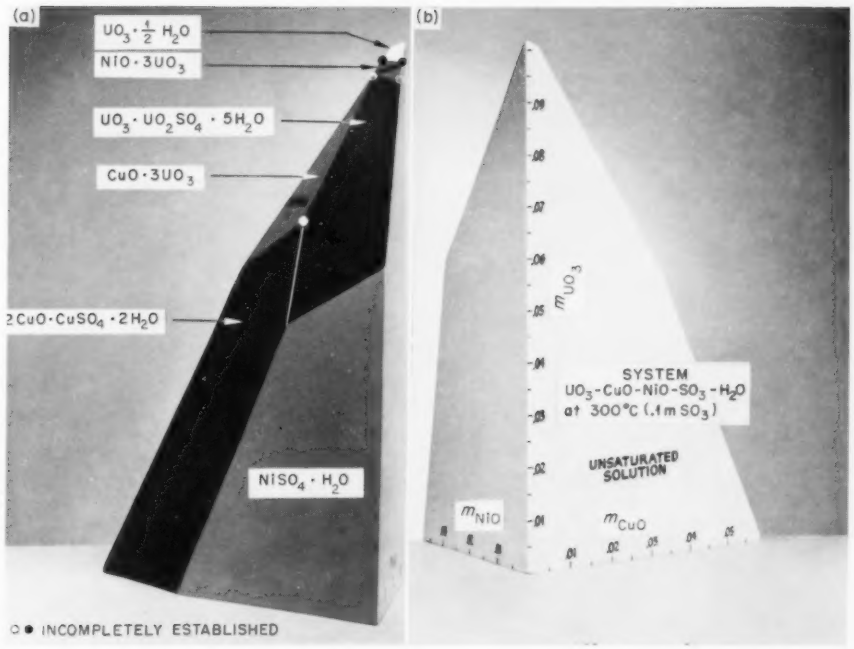

FIG. 11.—Three-dimensional model representing system UO_3–CuO–NiO–SO_3–H_2O at 300°C; 0·1 molal in total SO_3.

VO
2
19

solids $NiO{\cdot}3UO_3$* and $UO_3{\cdot}UO_2SO_4{\cdot}5H_2O$ in the quaternary system UO_3–NiO–SO_3–H_2O, and for the quinary point involving the solid $CuO{\cdot}3UO_3$ in addition, are believed to be approximately correct based on a few experimental data in this region. The quaternary and quinary curves over which $UO_3{\cdot}\frac{1}{2}H_2O$ is one of the solid phases gave saturation molal ratios, $m_{UO_3}:m_{SO_3}$, from 0·83 to 1·02, $m_{CuO}:m_{SO_3}$ from 0·006 to 0·009 and $m_{NiO}:m_{SO_3}$ from 0·026 to 0·023 as the SO_3 concentration was varied from 0·02 to 0·1 m. On the model these points, estimated at 0·1 m SO_3 from the data, were expanded from the UO_3 apex for clarity of presentation.

In order to present a complete picture of a surface of saturation at constant SO_3 concentration, many additional experimental runs should be made. Nevertheless, the skeletal approach produces approximate surfaces of saturation and specifies, in addition, the stable solid phases and their regions of stability.

Specific application. A series of three-dimensional models is useful for visualizing the phase boundaries of a system in order to select compositions for aqueous homogeneous reactor fuels over a wide range of SO_3 concentration. As one example, the initial composition of fuel solution would be specified on the front face of the model (Fig. 11b), showing the isothermal phase relationships at 0·1 m SO_3. As corrosion of the stainless steel container material progresses and nickel dissolves into the solution, the composition moves into the volume representing unsaturated solution and, depending upon the initial composition, any one of several solids will be the first to appear at the saturation limit.

There is also a need for an equation to estimate solubility limits. On the model shown in Fig. 11 the combined surfaces of saturation are observed to approximate a plane which cuts the three orthogonal axes. This plane can be defined by the geometrical equation

$$m'_{UO_3}/m_{UO_3} + m'_{CuO}/m'_{CuO} + m'_{NiO}/m'_{NiO} = 1$$

where m_{UO_3}, m_{CuO} and m_{NiO} are saturation concentrations for the isolated three-component systems and m'_{UO_3}, m'_{CuO} and m'_{NiO} are saturation concentrations for compositions which may contain all five components. Values for m_{UO_3}, m_{CuO} and m_{NiO} at the same sulphate concentration are obtained from Figs. 2, 3 and 4. In application a composition not violating the saturation limits expressed by the equation is estimated to be phase stable at least to 300° for homogeneous reactor fuels, 0·05–0·2 m in SO_3.

Theoretical postulates. To attempt to calculate precisely the effect of variable solution compositions on solubility, which must include the identification of solid or solids in stable equilibrium with a particular solution composition, is a formidable task. Many additional data are needed to provide assurance that a method of calculation would be successful. Nevertheless, a few comments are in order which may suggest an over-all approach to the problem for this system. At 300° it is likely that HSO_4^- is a predominant anionic species or complexing agent in solution and that UO_2^{2+} may hydrolyse to form the dimeric ion, $U_2O_5^{2+}$, or may form the undissociated species, UO_2SO_4. Investigations of the sulphate–bisulphate equilibria between 25 and 50° have indicated that HSO_4^- may be the predominant anionic species in aqueous

* The composition, $NiO{\cdot}3UO_3$, was established by preliminary analyses which indicate that it is a new compound, analogous to $CuO{\cdot}3UO_3$.[12]

VOL. 22 1961

media at higher temperatures on the basis of T. F. YOUNG's equation.* Investigations at room temperature by SUTTON,[14] AHRLAND,[15] and many others[16] were interpreted to show that UO_2^{2+} can be polymerized to a dimer, a trimer, or even higher polymers, as the acidity of the solution decreases. Since the solutions considered in this investigation are saturated for the most part with oxides or oxy-sulphates, the relative acidity should be low, a condition which would favour hydrolytic polymerization of UO_2^{2+}. The other possibility, that undissociated UO_2SO_4 is a predominant species, may be valid at these temperatures. This latter proposition is suggested by LIETZKE and STOUGHTON'S[13] results which show that UO_2SO_4 (undissociated) appears to be a major species of aqueous uranyl sulphate solution up to 240°. If either UO_2SO_4 or $U_2O_5(HSO_4)_2$ (undissociated or as $U_2O_5^{2+} + 2HSO_4^{2-}$) exists in high concentrations, then the saturation molal ratio, $m_{UO_3} : m_{SO_3}$, in the system UO_3–SO_3–H_2O should be near unity. Extensive formation of the complex, $UO_2(SO_4)_2^{2-}$, substantiated by others at lower temperatures,[17] or of $UO_2(HSO_4)_2$ should yield saturation molal ratios, $m_{UO_3} : m_{SO_3}$, near 0·5.

The solubility data presented are not inconsistent with these propositions at least in the 0·02–0·1 m range of SO_3 concentration. The sum of the saturation molal ratios expressed as $\frac{1}{2}R_U + R_{Cu} + R_{Ni}$ for each set of curves shown in Figs. 3 and 5–9 varies from 0·50 ± 0·05 at 0·02 m SO_3 to 0·60 ± 0·05 at 0·1 m SO_3, thus implying that HSO_4^{1-}, Cu^{2+}, Ni^{2+} and either $U_2O_5^{2+}$, $U_2O_5(HSO_4)_2$ or UO_2SO_4 (undissociated) may bepredominant species in solution in this concentration range. The saturation molal ratio, R, for the systems NiO–SO_3–H_2O and UO_3–SO_3–H_2O do not fall within these limits but are close.

Boundary curves between solid-liquid and liquid-liquid equilibria. Considerable experimental data above 300° in the two-liquid-phase regions of the systems UO_3–SO_3–H_2O, UO_3–CuO–SO_3–H_2O and UO_3–NiO–SO_3–H_2O have been obtained previously[2] but as yet over-all knowledge of the connection to solid–liquid boundaries is incomplete. In this study at 300°, a second liquid phase was found for SO_3 concentrations above approximately 0·12 molal (Figs. 2, 6a and 6b) and therefore must also be considered in representing the five-component system. On the basis of the behaviour of two-liquid-phase regions at and above 300° in the systems UO_3–SO_3–H_2O[2] and UO_3–CuO–SO_3–H_2O[2,18] it is believed that liquid–liquid immiscibility regions for the five-component system UO_3–CuO–NiO–SO_3–H_2O and the analogous D_2O system will engulf a larger portion of the solid–liquid regions as temperatures extend higher than 300°.

Acknowledgements—It is a pleasure to acknowledge the continual advice and encouragement of Professor J. E. Ricci New York University, during the course of this research. Many of the chemical analysis were performed by W. R. LAING and his group, ORNL. Identification of solid phases by X-ray diffraction was performed by R. L. SHERMAN, ORNL.

* Equation for dissociation of HSO_4^- as a function of temperature reported in LIETZKE and STOUGHTON's paper,[13] and derived by Young for use at much lower temperatures.

[13] M. H. LIETZKE and R. W. STOUGHTON, *J. Amer. Chem. Soc.* **64**, 816 (1960).
[14] J. SUTTON, *J. Inorg. Nucl. Chem.* **1**, 68 (1955); *J. Chem. Soc.* S275 (1949).
[15] S. AHRLAND, *Acta Chem. Scand.* **8**, 1907 (1954).
[16] K. A. KRAUS. *Proceedings of International Conference on Peaceful Uses of Atomic Energy, Geneva*, 1955. Vol. 7, pp. 245–257, United Nations, New York (1956).
[17] Anion Exchange Studies of Metal Complexes, Chapter 23, K. A. KRAUS and F. NELSON *The Structure of Electrolytic Solutions*, (Edited by W. J. HAMER) p. 348. J. Wiley, New York (1959).
[18] F. E. CLARK, J. S. GILL, R. S. SLUSHER and C. H. SECOY, *J. Chem. Engng. Data* **4**, 12–15 (1959).

J. Inorg. Nucl. Chem., 1961, Vol. 22, pp. 133 to 139. Pergamon Press Ltd. Printed in Northern Ireland

A POLAROGRAPHIC STUDY OF CHROMIUM(III) IN AMMONIA SOLVENTS (DIVERS' LIQUIDS)*

T. C. ICHNIOWSKI† and A. F. CLIFFORD
Department of Chemistry, Purdue University, West Lafayette, Indiana

(*Received* 7 *February* 1961; *in revised form* 23 *April* 1961)

Abstract—Chromium(III) is shown to catalyse the electrolytic reduction of nitrate ion in Divers' liquids containing nitrate ion. The use of Divers' liquids as polarographic solvents is extended to include the ammonia–ammonium thiocyanate system. The half-wave potentials and diffusion currents for several chromium(III) salts in this solvent are reported.

VOL. 22 1961

DIVERS[1] reported that a clear liquid was formed at room temperature when gaseous NH_3 was passed over dry NH_4NO_3. At 0° this liquid has a mole ratio of NH_3 to NH_4NO_3 of approximately two to three, and its formation has been described as being primarily a deliquescence phenomenon.[1,2] This liquid is a good conductor of electricity[1] and will dissolve both organic and inorganic substances.[1–4]

SELLERS[2] has shown that a variety of salts (e.g., NH_4Br, NH_4I, NH_4SCN, as well as NH_4ClO_4,[5] and NH_4BF_4[5]) can be used to form liquids with similar properties. For this study, the liquids formed from gaseous NH_3 and NH_4NO_3, $LiNO_3$, and NH_4SCN were used. Some of the physical properties of these liquids are listed in Table 1.

TABLE 1.—SOME PHYSICAL PROPERTIES OF DIVERS' LIQUIDS

Solid constituent	Temperature at which $P_{NH_3} = 1$ Atm[2] (°C)	Solubility, g per 100 g of NH_3 at 25°	Moles of NH_3 per mole of salt at 0°
NH_4NO_3	26	390[6]	1·59[2]
$LiNO_3$	80	243·7[7]	3·89‡
NH_4SCN	64	321[6]	2·00[2]

‡ This work, obtained by the method of reference (2).

The NH_3–NH_4NO_3[3,4] and the NH_3–NaI[2] systems have been used previously for polarographic studies. In addition to their general interest as non-aqueous

* This work was supported in part by the Office of Ordnance Research, Contract No. DA-33-008-ORD-1233 with Purdue University.

† Taken in part from a thesis submitted by T. C. ICHNIOWSKI to the faculty of Purdue University in partial fulfilment of the requirements for the degree of Master of Science.

[1] E. DIVERS, *Phil. Trans.* **163,** 368 (1874). *Proc. Roy. Soc.* **21,** 109 (1875).
[2] D. E. SELLERS Ph.D. Thesis, Kansas State College of Agriculture and Applied Science, Manhattan, Kansas (1958).
[3] E. VECCHI, *R.C. Acad. Lincei* **14,** 290–93 (1953).
[4] G. W. LEONARD, JR. and D. E. SELLERS, *J. Electrochem. Soc.* **102,** 95–7 (1955).
[5] A. F. CLIFFORD and R. A. SANFORD. Unpublished results, (1957).
[6] H. HUNT, *J. Amer. Chem. Soc.* **54,** 3509–12 (1932).
[7] H. HUNT and L. BONCZYK, *J. Amer. Chem. Soc.* **55,** 3528–30 (1955).

solvents, these liquids possess the following desirable properties, for use as polarographic solvents, as compared with liquid ammonia:[3]

(1) Because their vapour pressures are lower they do not require the use of high pressures and low temperatures.
(2) They can be used at temperatures above the freezing point of mercury without special equipment.
(3) The supporting electrolyte is a component of the solvents and its concentration therefore is only temperature dependent.

The polarographic reduction of chromium(III) salts was investigated in three of these systems, NH_3–NH_4NO_3, NH_3–$LiNO_3$, and NH_3–NH_4SCN. In nitrate-containing solvents, the solvent discharge wave appeared in the presence of chromium salts at lower potentials than in their absence, whereas in NH_4SCN it was unaffected. This effect was attributed to a catalytic action of chromium on the reduction of the nitrate ion. Since the thiocyanate ion was not reduced under similar conditions, NH_3–NH_4SCN Divers' liquid proved to be a convenient medium in which to study the reduction of a variety of chromium(III) compounds.

EXPERIMENTAL

Equipment and procedure

A Sargent Model XXI automatic recording polarograph was used throughout the study. The voltmeters of this instrument were calibrated by using a Leeds and Northrup voltage divider and a Pyrotest potentiometer. The cell used for all polarographic determinations was the Sargent two-piece polarographic vessel which was designed for use with an internal reference electrode. The polarographic cell was calibrated for volume in order to facilitate the transfer of the solvent. A dropping mercury electrode was assembled in the usual manner (The height of the reservoir varied from 60 cm to 70 cm) and the capillary characteristic, m, and drop time, t, were determined by the method suggested by MEITES.[8] Half-wave potentials were determined from plots of voltage versus log $(id - i)/i$ at the point where log $(id-i)/i=0$. Voltages were read directly from the recorder record; half-wave potentials were corrected from the calibration curves. The values for the diffusion currents were obtained by the method recommended by Sargent and Co.[9] The voltage at which the solvent discharge wave crossed the "100" co-ordinate on the current axis of the recorder chart was referred to as the solvent decomposition potential. This method of estimating the decomposition potential was deemed accurate enough in view of the fact that the same decomposition was obtained in NH_3–NH_4SCN regardless of the amount of chromium present (Fig. 2). Gelatin was added as needed to suppress maxima. Polarographic data were taken at 0°C.

The reference electrode, a mercury pool anode,[10] was found to give reproducible half-wave potentials in concurrence with VECCHI's observation. The results reported in Table 4 indicated that there was no change in the half-wave potential with time. Therefore, the use of an external reference electrode[2,4] was not considered necessary.*

When the experiment required a solution of known concentration, the following procedure was used: The polarographic cell was kept at 0° while anhydrous gaseous ammonia was passed through it. A known volume of the DIVERS' liquid was transferred from the collection vessel to the calibrated cell by a positive pressure of ammonia. Mercury and a weighed amount of the salt were added, and the solution was stirred by a current of ammonia.

Preparation of Divers' liquids

Anhydrous gaseous ammonia was passed into a collection vessel (a 500 ml, three-necked flask which was fitted with inlet and outlet tubes) containing the appropriate dry solid. The collection vessel was immersed in an ice-bath in a Dewar flask. (This method was also used for storage of the

* The referee has suggested that the mercury salt formed at the anode may be so insoluble "that equilibration occurs essentially instantly."

[8] L. MEITES, *Polarographic Techniques*, p. 31–37. Interscience Publishers, New York (1955).
[9] E. H. SARGENT and Co., Instruction Manual : Sargent Model XXI Recording Polarograph, p. 20.
[10] H. A. LAITINEN and C. E. SHOEMAKER, *J. Amer. Chem. Soc.* **72**, 663–5 (1950.)

Divers' liquid.) The ammonia was passed through the solid until a clear liquid formed and then for an additional hour to insure equilibration.

Materials and compounds

Commercial ammonia was distilled directly from the cylinder. Ammonium nitrate and lithium nitrate were Mallinckrodt AR Grade Reagent; ammonium thiocyanate was Baker's "Analysed" Grade Reagent. The solids were dried prior to use by keeping them *in vacuo* for 24 hr.

The compounds which were used in this study were synthesized by the methods indicated: $[Cr(NH_3)_6](NO_3)_3$,[11] $[Cr(NH_3)_6]I_3$,[12] $[Cr(NH_3)_5(NO_3)](NO_3)_2$,[13] $[Cr(NH_3)_5Cl]Cl_2$,[14] $[Cr(NH_3)_5(SCN)](NO_3)_2$,[15] $[Cr(NH_3)_5(SCN)]I_2$,[16] $(NH_4)[Cr(NH_3)_2(SCN)_4]$[17] $K_3[Cr(SCN)_6]\cdot 4H_2O$,[18] $[Co(NH_3)_6](NO_3)_3$,[19] $[Co(NH_3)_6]I_3$.[20]

RESULTS AND DISCUSSION

Catalytic decomposition of nitrate ion

The polarograms of the various chromium(III) salts which were taken in NH_3–NH_4NO_3 Divers' liquid possessed the same characteristics. A one-electron reduction wave of chromium(III) was obtained and was superimposed on the solvent discharge wave. As the concentration of the chromium(III) species increased, the two waves became indistinguishable. Also, as the concentration of the chromium(III) species increased, the solvent decomposition potential shifted from the determined value of $-1{\cdot}19 \pm 0{\cdot}02$ V to more positive values (Fig. 1). When a cobalt(III) salt was studied, the shifting of the solvent decomposition potential was not observed, indicating that chromium, but not cobalt, was acting catalytically to cause the observed shifts. Table 2 summarizes the polarographic data obtained with the solvent NH_3–NH_4NO_3 Divers' liquid.

In order to determine which constituent of the solvent was being reduced, similar studies were conducted in NH_3–$LiNO_3$ and NH_3–NH_4SCN Divers' liquids. The solvent decomposition potential of the NH_3–$LiNO_3$ system was shifted from $-1{\cdot}466 \pm 0{\cdot}006$ V to $-1{\cdot}280$ V by saturated solutions of $[(Cr(NH_3)_6]I_3$ and $[(Cr(NH_3)_5Cl]Cl_2$. However, the solvent decomposition potential, $-1{\cdot}466 \pm 0{\cdot}007$ V, of the NH_3–NH_4SCN system (Fig. 2) was not shifted by the presence of chromium(III) species. Obviously, it was the reduction of nitrate ion rather than ammonium ion which was catalysed by chromium(III) in these solvents. A similar type of catalytic behaviour of chromium(III) for nitrate decomposition has been observed previously. GUIOCHON and JACQUE[21] have reported that the thermal decomposition of NH_4NO_3 was accelerated by chromium(III). Also, lanthanum(III), cerium(III) and uranium(III) have been

[11] L. F. AUDRIETH (Editor), *Inorganic Synthesis*, Vol. 3, p. 153 McGraw-Hill, New York (1950).
[12] J. N. FRIEND, *A Textbook of Inorganic Chemistry*, Vol. 10, *The Metal Ammines*, p. 82. Griffin, London (1928); S. M. JORGENSEN, *J. Prakt. Chem.* **30**, 22 (1884).
[13] T. MOELLER (Editor), *Inorganic Synthesis*, Vol. 5, p. 131–33. McGraw-Hill, New York (1955).
[14] W. R. LANG and C. M. CARSON, *J. Amer. Chem. Soc.* **26**, 414 (1904).
[15] J. N. FRIEND, *A Text book of Inorganic Chemistry*, Vol. 10, *The Metal Ammines*, p. 94. Griffin, London (1928); A. WERNER and J. VON HALBAN, *Ber. Dtsch. Chem. Ges.* **39**, 3671 (1906).
[16] J. N. FRIEND, *A Text book of Inorganic Chemistry*, Vol. 10, *The Metal Ammines*, p. 96. Griffin, London (1928); A. WERNER and J. VON HALBAN, *Ber. Dtsch. Chem. Ges.* **39**, 2668 (1906).
[17] A. KING, *Inorganic Preparations*, p. 108. Van Nostrand, New York (1936).
[18] W. G. PALMER, *Experimental Inorganic Chemistry*, p 391. Cambridge Press (1954).
[19] W. G. FERNELIUS (Editor), *Inorganic Synthesis* Vol. 2, p. 218. McGraw-Hill, New York (1946).
[20] J. W. MELLOR, *Comprehensive Treatise of Inorganic Chemistry*, Vol. 14, p. 742. Longmans, Green, London (1935).
[21] G. GUIOCHON and L. JACQUE, *C.R. Acad. Sci., Paris* **245**, 163–66 (1957).

VOL. 22 1961

reported to catalyse the polarographic reduction of nitrate ion in aqueous solution.[22]

The mechanism for the observed catalytic decomposition of nitrate-containing Divers' liquids may be analogous to that described by BENNETT *et al.*[23] for aluminium. They postulated, based on their results obtained from the anodic oxidation of aluminium in liquid ammonia, that aluminium(I) was formed as part of the primary

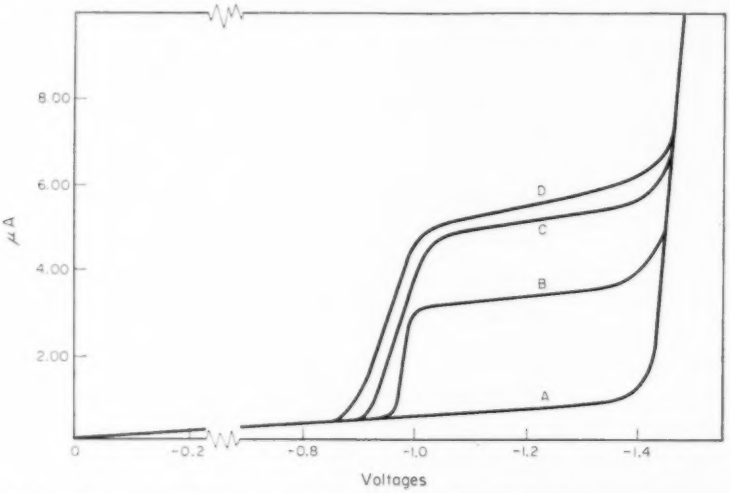

FIG. 1.—Changes in reduction wave character in NH_3–NH_4NO_3 with changes in concentration of chromium and cobalt complexes. (*A*)NH_3–NH_4NO_3 only; (*B*) 2×10^{-3} $[Cr(NH_3)_5Cl]Cl_2$; (*C*) 3×10^{-3} M$[Cr(NH_3)_5Cl]Cl_2$; (*D*) 2×10^{-3} M$[Co(NH_3)_6](NO_3)_3$.

electrode process and, further, that the aluminium(I) was oxidized by nitrate ion to the +3 oxidation state. Since the primary electrode process in this study was a one-electron reduction of chromium(III), the observed catalytic decomposition of

TABLE 2.—SUMMARY OF POLAROGRAPHIC DATA IN AMMONIUM NITRATE DIVERS' LIQUID

Compound	$E_{\frac{1}{2}}$ (Estimated) (V)	Solvent decomposition potential* (V)	Remarks
$[Cr(NH_3)_6](NO_3)_3$	—	−1·152	Very slightly soluble
$[Cr(NH_3)_6]I_3$	−0·931	−1·100	—
$[Cr(NH_3)_5Cl]Cl_2$	−0·902	−1·107	—
$[Cr(NH_3)_5(SCN)](NO_3)_2$	—	−1·170	Very slightly soluble
$[Cr(NH_3)_5(NO_3)](NO_3)_2$	−0·926	−1·120	—
$[Co(NH_3)_6](NO_3)_3$	−0·184	−1·19	—

* These values are for saturated solutions.

[22] J. W. COLLAT and J. J. LINGANE, *J. Amer. Chem. Soc.* **76**, 4214–18, (1954).
[23] W. E. BENNETT, A. W. DAVIDSON and J. KLEINBERG, *J. Amer. Chem. Soc.* **74**, 732–35 (1952).

nitrate ion could be assumed to be a reduction of the nitrate ion by chromium(II). This assumption is further substantiated by the fact that chromium in the +3 and +2 oxidation states can be detected chemically in considerable amount when chromium metal is anodically oxidized in NH_3–NH_4NO_3 Divers' liquid.[24]

Divers' liquids as polarographic solvents

The applicability of NH_3–NH_4NO_3 Divers' liquid as a polarographic solvent has been shown by VECCHI[3] and LEONARD and SELLERS.[4] In this study, its use was complicated by the catalytic reduction of the nitrate ion.

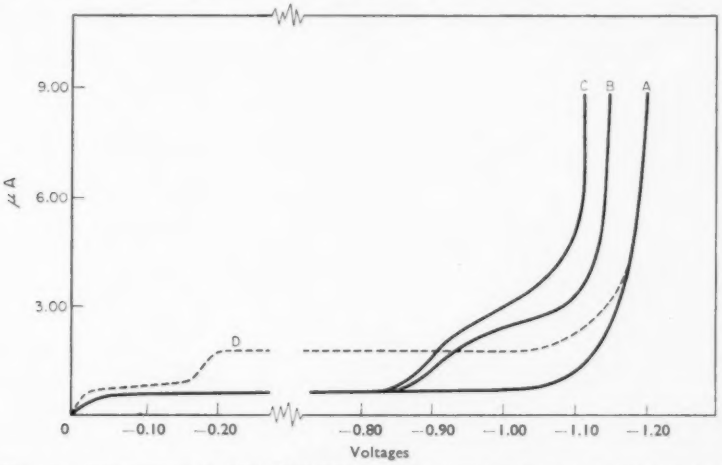

FIG. 2.—Polarograms in NH_3–NH_4SCN Divers' liquid with (A) 0, (B) $1{\cdot}89 \times 10^{-3}$ M, (C) $2{\cdot}01 \times 10^{-3}$ M, 8, (D) $3{\cdot}54 \times 10^{-3}$ M $[Cr(NH_3)_6]I_3$.

Ammonia–lithium nitrate Divers' liquid was the poorest solvent of the group which was studied. In general, the salts studied were, at best, only slightly soluble in this medium and the waves obtained were small. Observed maxima which were associated with the solvent discharge wave could be suppressed by the addition of small quantities of gelatin.

In the NH_3–NH_4SCN system, well-defined waves were obtained for the chromium(III) salts which were studied (Fig. 2). The wave heights varied linearly with the concentration of salt. Salts which contained anionic nitrate ion gave maxima which could be suppressed using gelatin. These data are summarized in Table 3. The analysis of these data, i.e. the slope of the plot of log $[(id - i)/i]$ versus voltage, indicated that a one electron, reversible reduction of chromium(III) occurred (Fig. 3); the values of the slope varied by $\pm 1{\cdot}00$ slope units from the theoretical value of 18·25 (Table 4).

In order to verify further the reversibility of the system, a study of the values of the half-wave potentials was made with two calibrated capillaries of different drop time.[25] A time study was also made as a means of proving that exchanges of the type

$$[Cr(NH_3)_6]^{3+} + x\ SCN^- \rightarrow [Cr(NH_3)_{(6-x)}\ (SCN)_x]^{(3-x)+} + x\ NH_3$$

and

$$[Cr(NH_2)_2(SCN)_4]^- + y NH_3 \rightarrow [Cr(NH_3)_{(2+y)}\ (SCN)_{(4-y)}]^{(1+y)-} + y\ SCN^-$$

[24] R. A. SANFORD, T. C. ICHNIOWSKI and A. F. CLIFFORD. Unpublished results (1958).
[25] P. KIVALO, K. B. OLDHAM and H. A. LAITINEN, *J. Amer. Chem. Soc.* **75**, 4148–52 (1953).

VOL. 22 1961

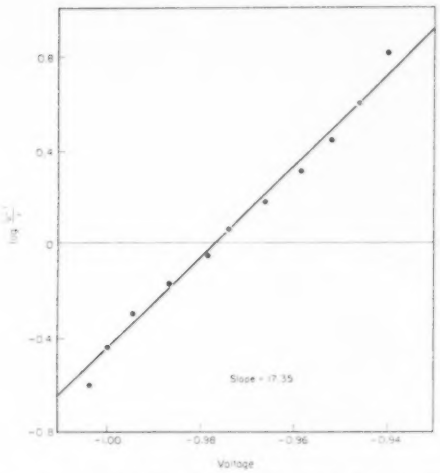

FIG. 3.—Analysis of polarographic data for a $2{\cdot}01 \times 10^{-3}$ M solution of $[Cr(NH_3)_6]I_3$ in NH_3–NH_4SCN Divers' liquid.

TABLE 3.—SUMMARY OF POLAROGRAPHIC DATA IN AMMONIUM THIOCYANATE DIVERS' LIQUID

Compound	Concentration (M)	$E_{\frac{1}{2}}$ (V)	i_d* (μA)	Slope of log $(id - i/i)$ vs. V plots
$[Cr(NH_3)_6]I_3$	$2{\cdot}01 \times 10^{-3}$	−0·972 (±0·005)	4·20 (±0·10)	17·35
$[Cr(NH_3)_5(SCN)]I_2$	$2{\cdot}47 \times 10^{-3}$	−0·991 (±0·010)	6·20 (±0·63)	18·73
$(NH_4)[Cr(NH_3)_2(SCN)_4]$	$6{\cdot}45 \times 10^{-3}$	−0·993 (±0·003)	11·85 (±0·29)	17·50
$K_3[Cr(SCN)_6]{\cdot}4H_2O$	$4{\cdot}80 \times 10^{-3}$	−0·967 (±0·006)	5·43 (±0·10)	17·25

* $m = 1{\cdot}68$ mg sec^{-1}, 77 cm column of Hg. $t = 3{\cdot}75(\pm 0{\cdot}01)$ sec

TABLE 4.—SUMMARY OF A TIME STUDY ON $[Cr(NH_3)_6]I_3$ IN AMMONIUM THIOCYANATE DIVERS' LIQUID WITH TWO CAPILLARIES

$E_{\frac{1}{2}}$ Values	Time (min)			
	0·00	70·0	300	540
Cap I*	−0·963 V	−0·964 V	−0·969 V	−0·963 V
Cap II†	−0·961 V	−0·966 V	−0·965 V	−0·965 V

* Cap I — $m = 1{\cdot}68 \pm 0{\cdot}02$ mg sec^{-1}, $t = 3{\cdot}75 \pm 0{\cdot}01$ sec.
† Cap II — $m = 0{\cdot}530 \pm 0{\cdot}02$ mg sec^{-1}, $t = 8{\cdot}37 \pm 0{\cdot}21$ sec.

were not occurring. As the data summarized in Table 4 show, the values for the half-wave potentials did not vary with drop time or with elapsed time, indicating a reversible system.

Attempts to obtain anodic waves resulted in almost immediate solvent decomposition. This is perhaps to be expected for liquid ammonia, which has a very low overvoltage for N_2 liberation.[26]

The effect of water on the half-wave potential of a $6{\cdot}75 \times 10^{-3}$ M solution of $(NH_4)[Cr(NH_3)_2(SCN)_4]$ was tested as a means of verifying the half-wave potential of $K_3[Cr(SCN)_6]{\cdot}4H_2O$ (Table 3). Measured quantities of water were added to the solution of $(NH_4)[Cr(NH_3)_2(SCN)_4]$. The results, summarized in Table 5, show that the value of the half-wave potential shifts to more negative values with the addition of water. Therefore, the value of the half-wave potential of $K_3[Cr(SCN)_6]$ may be somewhat more positive than that of $K_3[Cr(SCN)_6]{\cdot}4H_2O$ by perhaps 0·01 V.

TABLE 5.—CHANGES IN THE HALF-WAVE POTENTIAL OF $NH_4[Cr(NH_3)_2(SCN)_4]$ WITH THE ADDITION OF WATER

Amount of H_2O (ml)	$E_{\frac{1}{2}}$ (V)
0·00 ml	$-0{\cdot}993 \pm 0{\cdot}003$
0·50 ml*	$-1{\cdot}001 \pm 0{\cdot}006$
4·00 ml	$-1{\cdot}031 \pm 0{\cdot}006$

* This corresponds to an ammonia solution of a salt of the formula $(NH_3)[Cr(NH_3)_2(SCN)_4]{\cdot}4H_2O$.

[26] See, for example, A. F. CLIFFORD and M. GIMENEZ-HUGUET, *J. Amer. Chem. Soc.* **82**, 1024 (1960).

VOL. 22 1961

J. Inorg. Nucl. Chem., 1961, Vol. 22, pp. 141 to 150. Pergamon Press Ltd. Printed in Northern Ireland

ANION EXCHANGE OF METAL COMPLEXES—VII

THE LANTHANIDES–NITRATE SYSTEM[1]

Y. MARCUS and I. ABRAHAMER
Israel Atomic Energy Commission Laboratories, Rehovoth

(*Received* 7 *March* 1961; *in revised form* 17 *May* 1961)

Abstract—Previous results for the distribution of the lighter lanthanides between nitrate solutions and a strongly basic anion exchanger are extended by data for the heavier lanthanides. An odd-even *Z* effect, previously observed in solvent extraction studies, is also found in this work. The extraction of the lanthanides by a long chain amine is described briefly. The results are interpreted in terms of nitrate complex formation and changes in the hydration of the lanthanides in nitrate solutions.

VOL.
22
1961

A STUDY of the distribution of a number of the rare earth nitrates between lithium nitrate solutions and a strongly basic anion exchanger was presented in a previous paper.[2] The work was later extended[3] to include some of the heavier lanthanides. These results showed that, whereas for the lighter lanthanides the distribution coefficient D is a monotonically decreasing function of the atomic number Z, this is not the case for the heavier ones. A detailed study was therefore made of the dependence of D on Z and on the nitrate concentration for the heavier lanthanides and yttrium. A fairly complete picture of the anion exchange behaviour of the tervalent lanthanides and the analogous elements yttrium, actinium[4] and americium in nitric acid[5] and other nitrate solutions is now available.

The anion exchange results, together with other pertinent data, were examined for evidence of complex formation between lanthanide cations and nitrate anions. Previous work on this subject is not extensive and deals almost exclusively with the lightest lanthanides. RYABCHIKOV and TERENT'EVA[6], TERENT'EVA[7] and GARNER[8] explain the behaviour of the lanthanides in nitrate solutions in terms of complex formation. CONNICK and MAYER[9], MATTERN[10] and FOMIN *et al.*[11] calculated the stability of the first nitrate complexes of La^{3+} and Ce^{3+} and found only weak complexing. The formation of anionic nitrate complexes was, however, indicated for

[1] Previous papers in this series: V. The Silver-Thiosulphate System, *Acta Chem. Scand.* **11** (1957); VI. The Uranium (VI)–Phosphate System, *Proceedings of the 2nd. International Conference on the Peaceful Uses of Atomic Energy, United Nations, Geneva* 1958. Vol. 3. p. 465 United Nations (1958). IAEC report No. IA–608.
[2] Y. MARCUS, and F. NELSON, *J. Phys. Chem.* **63,** 77 (1959).
[3] Y. MARCUS, Israel Atomic Energy Commission Report R-20 (1959); XVIIth *International Union of Pure and Applied Chemistry Congress*, Munich, August–September 1959.
[4] J. DANON, *J. Inorg. Nucl. Chem.* **7,** 422 (1958)
[5] R. F. BUCHANAN and J. P. FARIS *Conference on the use of Radioisotopes in the Physical Sciences and Industry*. Paper RICC-173 Copenhagen, September 1960.
[6] D. I. RYABCHIKOV and E. A. TERENT'EVA, *Izvest Akad. Nauk. SSSR. Otdel. Khim. Nauk*, 44 (1949).
[7] E. A. TERENT'EVA, *Uspechki Khim.* **26,** 1010 (1957).
[8] C. S. GARNER, *The Rare Earth Elements and their Compounds* (Edited by D. M. YOST, H. RUSSELL and C. S. GARNER) p. 61. J. Wiley and Sons, New York (1949).
[9] R. E. CONNICK and S. W. MAYER, *J. Amer. Chem. Soc.* **73,** 1176 (1951).
[10] K. L. MATTERN, *U.S.A.E.C. Report* UCRL-1407 (1951).
[11] V. V. FOMIN, R. E. KARTUSHOVA and I. I. RUDENKO, *Zh. Neorg. Khim.* **3,** 2117 (1958).

Am^{3+} in nitric acid above 2 M by electromigration experiments.[12] The most extensive studies of the behaviour of the lanthanides in concentrated nitrate solutions have been made by solvent extraction methods, in particular with the use of tributyl phosphate. The most comprehensive and recent of these investigations is that of HESFORD *et al.*[13]

Anion exchange data have been shown in other studies to be interpretable in terms of the complex species formed in solutions. A knowledge of the predominant, or average species in the resin phase is essential for this purpose, but is difficult to obtain. However one way to go about this, is to assume that the predominant species found in the organic phase in long-chain amine extraction experiments is also the one predominant in the anion exchange resin. This approach has previously been found reasonable.[14] Amine extraction experiments have therefore been performed, to supplement the anion exchange studies.

EXPERIMENTAL

The anion exchange distribution experiments were performed under conditions similar to those used previously.[2] Preliminary experiments showed that the slight changes made (use of 8% DVB Dowex-1 resin, 200–400 mesh size and 87°C) did not basically affect the results. The acidity of the lithium nitrate was within the "pH" range 2–5, as measured with a glass-electrode pH meter calibrated with a standard buffer. Neutral lithium nitrate solutions from 2 to 8 M, which were made 0·002 M in the nitric acid, showed a "pH" of around 2·5. The acidity was thus in a range where it had little effect on the distribution coefficient.[2]

Distribution coefficients were obtained by the column technique. The eluates were passed through a γ-well type scintillation counter, or through a flowtype plastic β-scintillation counter (No. NE801 of nuclear Enterprises Ltd.). The coefficients were calculated from the volume required to elute the peak, subtracting the volume of the tubes from column to counter (approx. 0·5 column volume) and one free column volume (approx. 0·4 column volume). The precision of the results was determined by the accuracy of measuring the volume of the column, the position of the peak in the elution curve and the free volume. It was within ± 15 per cent at $D_v = 3$ and ± 8 per cent at $D_v = 20$ at the 95 per cent confidence level. The results are expressed as volume distribution coefficients, D_v, as function of the nitrate ion molality of the eluting solutions ($m_{NO_3^-}$) and the atomic number Z. The molality of nitrate ions was used rather the salt molarity, M, because salts of various valencies were used and the experiments were compared at various temperatures. For the connexion between molality and molarity, the relationship for lithium nitrate

$$M = m(d_0 - 0{\cdot}031\ m + 0{\cdot}0008\ m^2) \qquad (1)$$

$$d_0 = 0{\cdot}997$$

was determined experimentally to be valid to within $\pm 0{\cdot}5$ per cent between 25° and 32°C, up to 10 m.[15]

The following radioactive isotopes were used in this work, the data included in the parenthesis being the type of emission, the half-life and the source. ^{90}Sr–Y(β, 29 years and 65, hr, Amersham), ^{91}Y ($\beta\gamma$, 58 days, Amersham), ^{140}La ($\beta\gamma$, 40·2 hr., Israel Research Reactor), ^{144}Ce–Pr ($\beta\gamma$, 285 days and 17 min, Amersham), ^{152,154}Eu ($\beta\gamma$, 13 years and 16 years, Amersham), ^{153}Gd (EC, 236 days, Amersham), ^{160}Tb ($\beta\gamma$, 72 days, Amersham), ^{165}Dy ($\beta\gamma$, 2·3 hr, I.R.R.), ^{166}Ho ($\beta\gamma$, 27 hr and 30 years, Amersham), ^{169}Er (β, 9·4 days, Amersham), ^{170}Tm ($\beta\gamma$, 129 days, Amersham), ^{177}Lu ($\beta\gamma$, 6·8 days, I.R.R.) and ^{241}Am (α, 470 years, O.R.N.L.). The concentration of tagged lanthanides was always below 10^{-4} M.

The amine used in the extraction experiments was tri-iso-octyl amine, kindly supplied by the Inorganic Chemistry Department of the Hebrew University, Jerusalem. The equivalent weight of

[12] G. N. YAKOVLEV and V. N. KOSYAKOV, *Proceedings of the International Conference on the Peaceful Uses of Atomic Energy, United Nations, Geneva*, 1955 Vol. 7. p. 363. United Nations (1956).
[13] E. HESFORD, E. E. JACKSON and H. A. C. MCKAY, *J. Inorg. Nucl. Chem.* **9**, 279 (1959).
[14] U. SCHINDEWOLF, *Z. Electrochem.* **62**, 335 (1958); Y. MARCUS, *Bull. Res. Council Israel*, **8** A 17 (1959).
[15] Compare H. S. HARNED and B. B. OWEN, *The Physical Chemistry of Electrolytic Solutions* (3rd Ed.) p. 725. Reinhold, New York (1958).

this material was determined by titration, and was found to be 345($(C_8H_{17})_3NH^+$ = 354). The amine was diluted with xylene or nitrobenzene, neutralized with nitric acid and washed with water and lithium nitrate solution. The organic phase was then equilibrated at 30 ± 1°C with lithium nitrate solutions containing the radioisotopes. Aliquots from both phases were counted in order to determine the distribution coefficients, and material balance was always within 5 per cent. The free amine showed distribution coefficients much lower than the amine salt, and in some cases precipitation of the rare earth was observed. Preliminary experiments with the liquid anion exchanger Amberlite LA-1 yielded negligible extraction ($D < 10^{-2}$) even with concentrated lithium nitrate solutions.

Electromigration experiments were performed in a cell with five compartments. The lantanide tracer was introduced into the middle compartment with a lithium nitrate solution made 1 M with respect to nitric acid. This was separated by sintered glass discs from the adjacent compartments, which were connected to the cathode and anode compartments via salt bridges. The three interior compartments were thermostatically controlled at 25°C, and samples were taken from the penultimate compartments after the passage of a constant current of the order of 50 mA for a few hours to determine the direction of migration.

TABLE 1.—ANION EXCHANGE DISTRIBUTION COEFFICIENTS IN LITHIUM NITRATE SOLUTIONS

Ce		Pm		Eu		Gd		Tb		Dy	
m_{LiNO_3}	log D_v	m_{LiNO_3}	log D_v	m_{LiNO_3}	log D_v	m_{LiNO_3}	log D_v	m_{LiNO_3}	log D_v	m_{LiNO_3}	log D_v
1·0	−0·1	2·7	0·3	2·1	0·2	2·7	−0·1	2·1	0·3	4·4	0·45
2·1	0·3	3·7	0·55	3·3	0·3	4·0	0·2	3·7	0·4	7·0	0·85
3·2	0·65	4·5	0·65	4·5	0·40	5·2	0·45	6·7	0·80	9·1	1·00
3·7	0·85	5·2	0·75	6·7	0·65	7·5	0·70	8·0	1·00	9·8	1·10
4·5	1·25	7·5	1·40	7·3	0·90	9·1	1·00	9·5	1·25		
5·6	1·60			8·0	1·10						
				9·5	1·40						

Ho		Er		Tm		Lu		Y		Am*	
m_{LiNO_3}	log D_v	m_{LiNO_3}	log D_v	m_{LiNO_3}	log D_v	m_{LiNO_3}	log D_v	m_{LiNO_3}	log D_v	m_{LiNO_3}	log D_v
5·2	0·0	4·3	0·60	2·8	−0·1	5·5	0·40	4·3	0·3	2·0	0·55
6·2	0·35	5·5	0·70	4·1	0·1	6·2	0·45	6·2	0·55	3·0	0·85
7·5	0·50	7·1	0·85	5·2	0·15	7·0	0·50	7·1	0·75	4·5	1·10
9·2	1·05	8·9	1·00	7·5	0·45	9·1	0·85	8·9	0·80	6·0	1·45
		11·7	1·20	9·3	0·90	9·7	0·90	11·7	0·90	7·5	1·80
										9·0	2·00

* The values for Am were calculated from data obtained by batch equilibration at room temperature, taking into account the specific volume of the resin.

RESULTS

A careful study of D_v as function of m_{LiNO_3} revealed an interesting odd-even effect of Z, which was not observed in the previous incomplete investigation. The results are shown in Table 1 and some of the data are replotted as log $D_v(m_{LiNO_3})_Z$ curves in Fig. 1, to exemplify various types of behaviour. The curves in Fig. 2 showing the relationship log $D_v(Z)_{mLiNO_3}$ have been constructed from these data.

One of the outstanding features in the figure is that the curves for the different heavy lanthanides cross over; this does not occur for the light lanthanides. The success of separating the latter[2] follows from this, together with the impossibility of obtaining a sequential separation of the former by gradually changing the lithium nitrate concentration. This does not, however, preclude the successful separation of a

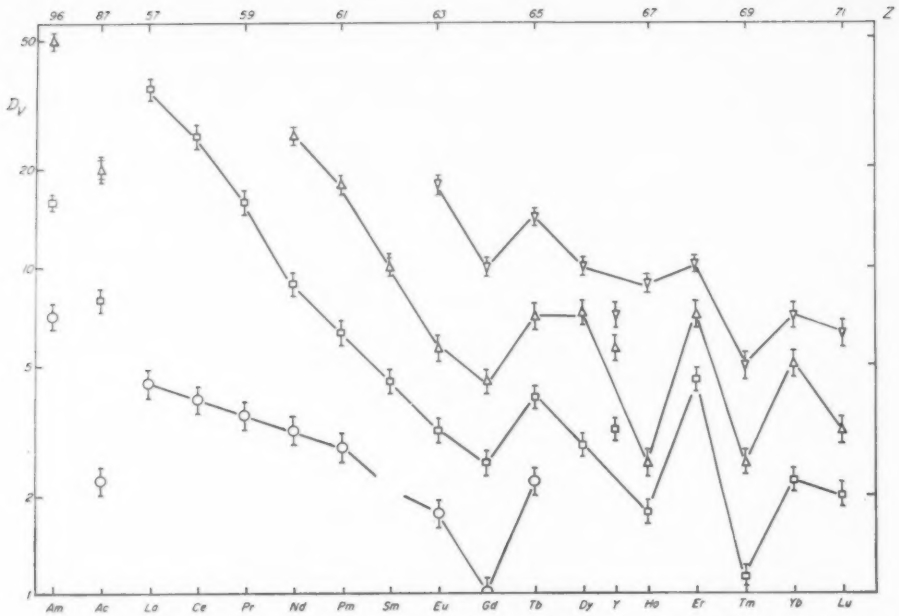

FIG. 1.—Volume distribution coefficients (log D_v) between Dowex-1 and lithium nitrate solutions as function of molality of nitrate for Er^{3+}, Ce^{3+}, Eu^{3+} and Tm^{3+}. For Am^{3+} the weight distribution coefficient (log D) is shown.

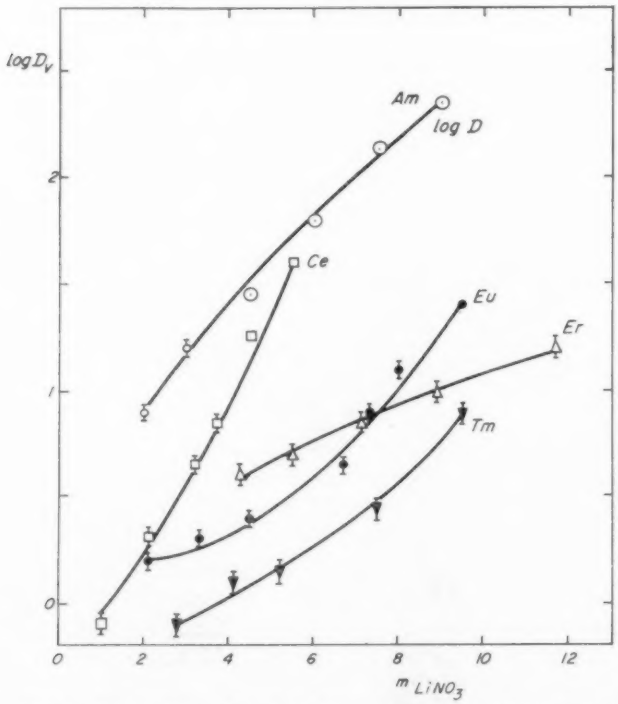

FIG. 2.—Volume distribution coefficients D_v between Dowex-1 and lithium nitrate solutions as function of atomic number Z of the lanthanides. Lithium nitrate molalities: ○ 3 m, □ 5 m, △ 7 m and ▽ 9 m, 95 per cent confidence limits for D_v being shown.

limited number of the heavier rare earth—and yttrium—by elution with lithium nitrate. The separation of europium and terbium is shown in Fig. 3 while the separation of the radioactive mother-daughter pair ^{90}Sr–^{90}Y is shown in Fig. 4.

Series of experiments which were performed to demonstrate the effect of the bulk cation on the distribution coefficient of tracer lanthanides, are shown in Fig. 5 as

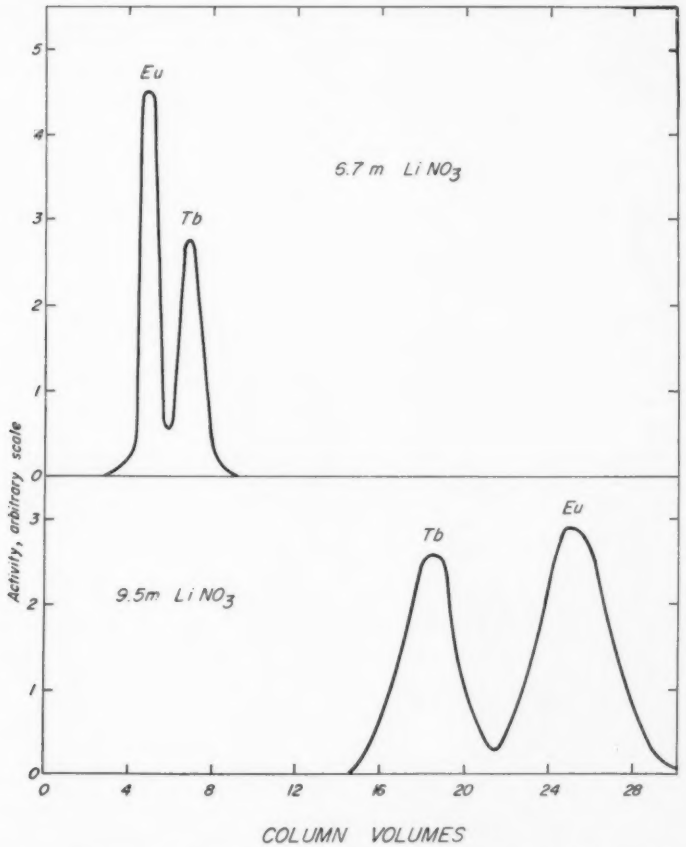

FIG. 3.—Elution curves for the separation of Tb^{3+} and Eu^{3+} tracers on a column of Dowex-1 (0·25 cm² × 6 cm, 87°C, 1 cm/min flow-rate) with 6·7 and 9·5 m lithium nitrate. Note inversion of peak positions.

log $D_v(m_{NO_3^-})$ curves. Anionic nitrate complexes of the lanthanides are formed (see below), thus the concentration of the nitrate ligand should be of primary importance in determining the distribution coefficients. Therefore the various nitrate salts should be compared at given nitrate ion, not salt or cation, concentrations. For the light lanthanides the order of decreasing effectiveness, in causing absorption by the resin is: lithium, aluminium, calcium, ammonium and hydrogen. This is similar to the order found by DANON[4] using salt molarity as basis, except for the position of lithium, which is the most effective on the basis of nitrate ion concentration. Efforts to improve the separability of the lanthanides by substituting another cation for lithium were unsuccessful.

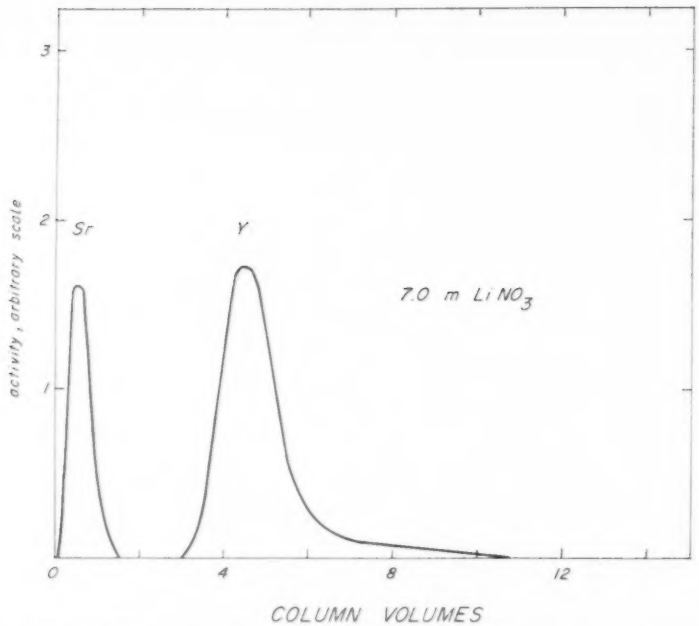

FIG. 4.—Elution curve for the separation of Sr^{2+} and Y^{3+} tracers on a column of Dowex-1 as in Fig. 3 with 7·0 m lithium nitrate.

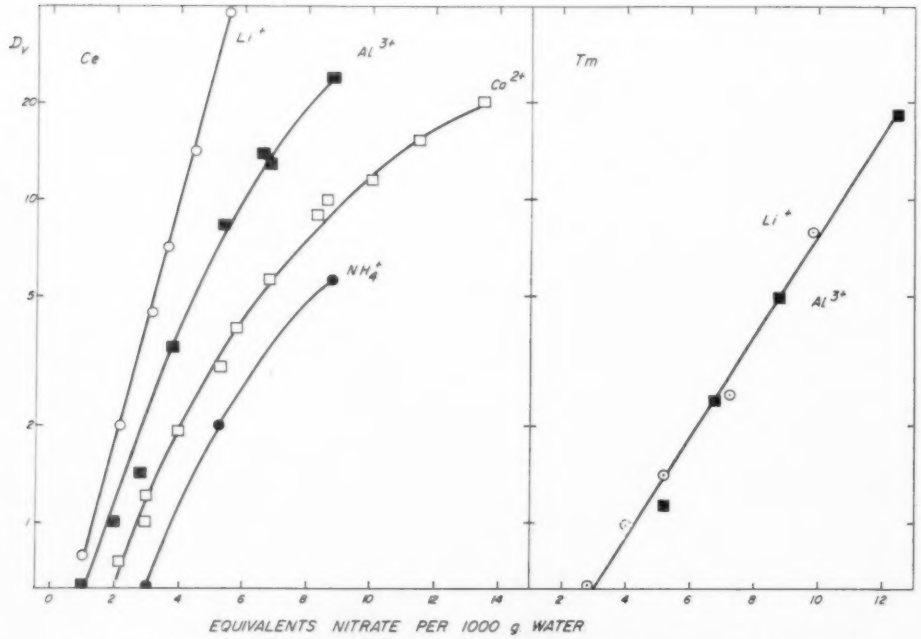

FIG. 5.—Volume distribution coefficients D_v for Ce^{3+} and Tm^{3+} between Dowex-1 and various nitrate solutions as function of nitrate ion molality $m_{NO_3^-}$. Nitrates are: ○ Li^+, ■ Al^{3+}, □ Ca^{2+} and ● NH_4^+.

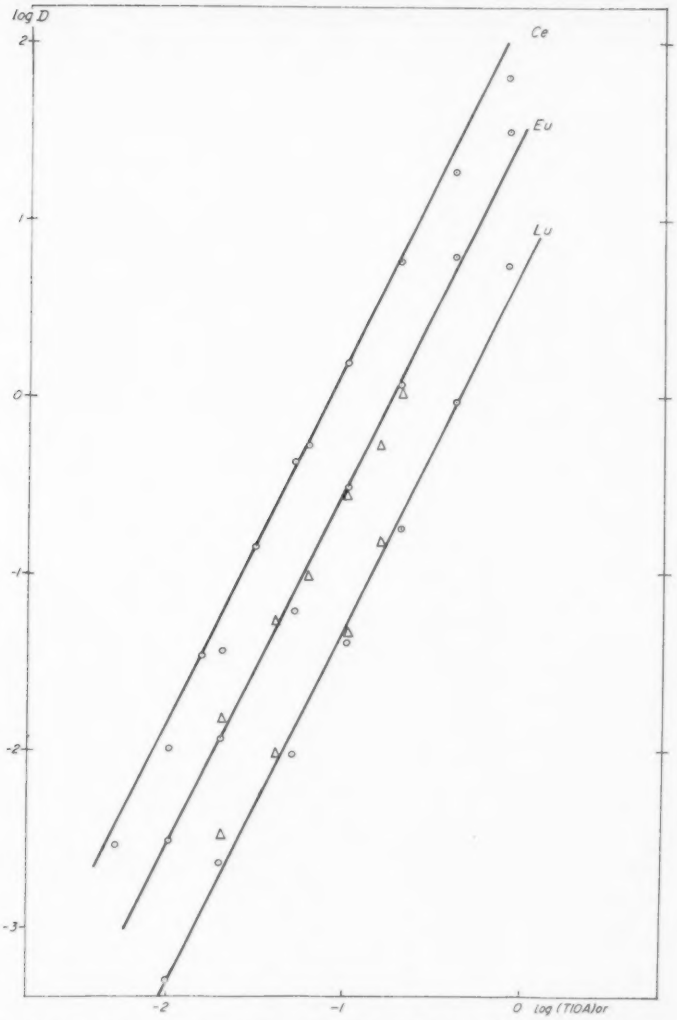

FIG. 6.—Distribution coefficients (log D) for Ce^{3+}, Eu^{3+} and Lu^{3+} between triisooctylamine (TIOA) in xylene (○) or nitrobenzene (△) and 7·5 m lithium nitrate solutions, as function of amine concentration ($\log(TIOA)_{or}$). Straight lines have slope 2·00.

As was previously mentioned, an indication of the species absorbed by the anion exchange resin may be obtained by experiments using a long-chain amine diluted with an inert diluent. This is done by measuring the slopes s of log $D(\log m_{R^+})$ plots, provided the systems behave approximately ideally. This should occur in dilute solutions of the monomeric tertiary amines. Over the range where a slope s is obtained the predominant reaction is

$$M(NO_3)_3\,(aq) + s\,RNO_3(org) \rightleftharpoons R_s\,M(NO_3)_{3+s}(org) \qquad (2)$$

where M^{3+} denotes a lanthanide cation, and R^+ the tri-iso-octyl ammonium ion. A number of such plots, for different values of Z and m_{LiNO_3} and two different diluents are shown in Figs. 6 and 7. Straight lines with slopes $s = 2$ were drawn and found

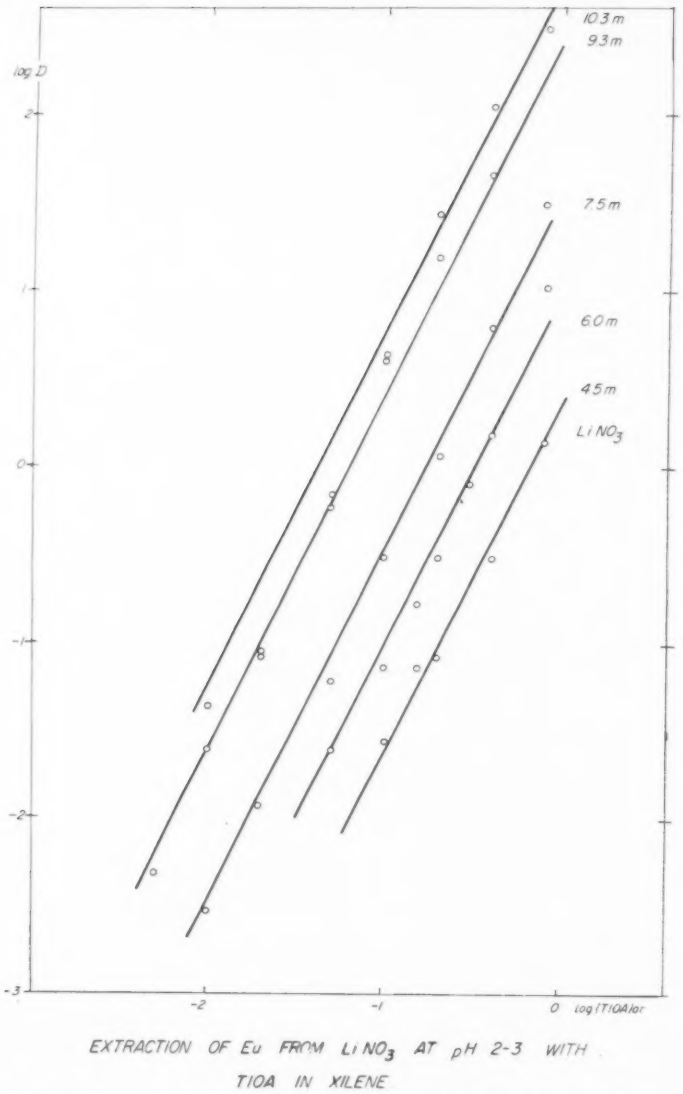

FIG. 7.—Distribution coefficients (log D) of Eu^{3+} between TIOA in xylene and lithium nitrate solutions of various concentrations as function of amine concentration ($\log(TIOA)_{or}$). Straight lines have slope 2·00.

to fit the experimental points fairly well, so that the presence of the anionic species $M(NO_3)_5^{2-}$ in the organic phase is indicated.

The electromigration experiments showed unequivocally that cerium and europium tracers migrate towards the anode in 10 m nitrate solutions, while less definite anodic migration also occurs in 6 m solutions. In 3 m nitrate cerium migrates towards the cathode. It may be concluded that under suitable conditions, anionic nitrate complexes of the lanthanides are formed.

DISCUSSION

In order to interpret the data presented in Figs. 1, 2 and 5, it is necessary to take into account the hydration of the ions. Since the crystal radius decreases with Z, i.e. from La to Lu, the average hydration should increase in this order, similar to the effect observed with the alkaline metals, where hydration decreases from Li to Cs. In this case, the electrostatic interaction of the hydrated ion with nitrate ions may weaken from La to Lu analogous to the decreasing affinity between hydrated alkaline metals and the sulfonic group in cation exchangers from Cs to Li. There should be little difference between the intrinsic adsorbabilities of lanthanide nitrate complexes of similar structure and size. The distribution coefficients therefore reflect the easier complexing of the lighter lanthanides which occurs at lower nitrate concentrations.

A secondary effect, which is responsible for the odd-even fluctuations is superimposed over this general trend. Similar fluctuations have already been observed by HESFORD *et al.*[13] in the distribution of lanthanides between nitric acid and TBP, and by SURLS[16] in their distribution between dilute perchloric acid and the sulfonic acid groups of the cation exchanger Dowex 50. The anion exchange and TBP extraction phenomena are so similar that even the details of the fluctuation are the same although they are different from those of the cation exchange results.[16] (The similarity is shown by gadolinium, which has a relatively lower distribution coefficient than the other even Z elements, and the two zig-zags, one from europium to dysprosium with higher D for odd Z, and one from holmium to lutecium, with higher D for even Z.) This difference in the fluctuations might be attributed to a specific effect of the nitrate anions. The present authors agree with the conclusion of HESFORD *et al.*[13] "an odd even effect would arise if, in building up the 4*f* shell, every second electron paired with the previous electron, but it is not believed that the shell builds up in this way". Nevertheless, perhaps it does build up like this under the influence of the ligand field due to the nitrate ions in the complex.

The variation of the distribution coefficients with the lithium nitrate concentration is caused by two factors. One is the increase in nitrate concentration with the attendant complexing of the lanthanide, which causes a lowering of the net charge, and easier penetration into the anion exchanger. The other is the dehydrating effect of the lithium ion, which may cause partial stripping of the hydration sheath of the lanthanide ion, and thereby enhance complexation. This dehydration should be stronger with the light lanthanides than with the heavy ones, which hold on to their hydration sheath more tenaciously. This could be the explanation of the negligible effect on the distribution coefficient of Tm when 1/3 Al^{3+} is substituted for Li^+, compared with the large effect obtained with Ce (Fig. 5). A measure of the relative dehydrating effect of Li^+, NH_4^+, Ca^{2+} and Al^{3+} ions is the osmotic coefficient of their nitrate solutions.[17] With the exception of aluminium it is of the same order as the cation effect on the anion exchange distribution coefficients at least for concentrations above 1 m. The aluminium ion appears to have a stronger dehydrating effect above 3·5 m than lithium, but the association of the trivalent cations with nitrate anions would decrease the effective nitrate concentration. This may account for the fact that aluminium also shows a lower cation effect than lithium in concentrated solutions. That aluminium and cerium (III) ions associate with nitrate ions to a much larger

[16] J. P. SURLS, U.S.A.E.C. Report UCRL-3209 (1956).
[17] R. A. ROBINSON and R. H. STOKES, *Electrolyte Solutions*, *Appendix* 8.10, *Butterworths*, London (1955).

VOL. 22 1961

extent than lithium or calcium ions is also concluded from the presence of shifted Raman lines in concentrated solutions of the former and not the latter.[18] These shifts indicate the presence of nitrate ions differing from those present in dilute solution, and they may be taken to be those associated with the cations.

The results of the electromigration experiments are evidence that under certain conditions nitrate complex formation of the lanthanides proceeds so far as to produce anionic species. These species are expected to show an affinity for the anion exchange resin, and it is probable that the predominant form of the lanthanides in the resin is an anionic complex. This argument is strengthened by the results of the amine extraction experiments, which show that fairly stable species $M(NO_3)_5^{2-}$ are extracted and combine with the ammonium groups in the organic phase. Since the same slope $s = 2$, is obtained with xylene diluent (dielectric constant 2·4) as with nitrobenzene (dielectric constant 35), it is concluded that the anion $M(NO_3)_5^{2-}$ is stable both associated with cations, as in the former diluent, and partially dissociated, as it probably is in the latter. It should then also be stable when extracted by the benzyl trimetyl ammonium groups into the aqueous–organic environment of the resin.

A co-ordination of five nitrate groups round the lanthanide cation seems rather unusual. Reference may, however, be made to the stable double salts $(NH_4)_2M(NO_3)_5 \cdot 4\,H_2O$ where M is a lanthanide from lanthanum to dysprosium[19] and to the complexes $R_2M(NO_3)_5$, where M is lanthanum, cerium, prasaeodymium or neodymium, and R is $[(C_6H_5)_3PC_6H_4OH]^+$ or $[(C_6H_5)_3AsC_6H_4OH]^+$, which may be isolated and dissolved unchanged in ethanol.[20] In all these cases a molecule of the solvent probably occupies the sixth co-ordination place. Five nitrate groups and a water molecule are also said to be co-ordinated with Ce (IV) in the acido-complex extracted by ether from nitric acid solutions.[21]

The results obtained so far are insufficient to describe in detail the complex formation in nitrate solutions of the lanthanides. It is expected that with more information concerning the activities in the anion exchanger in equilibrium with nitrate solutions, and particularly at elevated temperatures, the distribution curves for the lanthanides may be analysed fully.

At the present the work may be summarized as follows. Anionic nitrate complexes of the lanthanides indeed form as shown by electromigration. The complex in the anion exchange resin is probably $R_2M(NO_3)_5$, as shown by extraction experiments. Nitrate complexing increases, while hydration decreases, with increasing atomic number Z, except for an unexplained odd-even effect. Association of nitrate ions occurs with the hydrated cations, and any cause that influences this hydration has a corresponding effect on the complex formation.

Acknowledgements—The authors thank Mr. G. FELBERT and Mrs. N. BAUMAN for technical help in carrying out the experiments and Drs. M. GIVON and A. HELLER for helpful discussion of the work. Dr. M. PEISSACH and the staff of the Israel Research Reactor are thanked for carrying out the irradiations.

[18] J. P. MATHIEU and M. LOUNSBURY, *Disc. Faraday Soc.* **9**, 196 (1950).
[19] R. C. VICKERY, *Chemistry of the Lanthanons*, p. 115. Butterworths London (1953).
[20] G. V. MEDOCKS, *Zh. Obshchei Khim.* **26**, 382 (1956).
[21] A. W. WYLIE, *J. Chem. Soc.* 1474 (1951).

J. Inorg. Nucl. Chem., 1961, Vol. 22, pp. 151 to 159. Pergamon Press Ltd. Printed in Northern Ireland

VOL. 22 1961

NOTES

Some observations of Np(VI) in chloride solutions*

(*Received* 19 *June* 1961; *in revised form* 18 *July* 1961)

REPORTS on the early work on the solution chemistry of neptunium[1,3] contain reference to the instability of aqueous solutions of Np(VI) in the presence of Cl^- owing to the reaction

$$2NpO_2^{+2} + 2Cl^- \rightarrow 2NpO_2^+ + Cl_2. \quad (1)$$

Although this reaction was stated to be slow at room temperature, no satisfactory absorption spectra of Np(VI) in HCl could be obtained in the near U.V. region[1] and this was interpreted as being due to the absorption of Cl_2(aq) liberated by reaction (1).[2] Additional evidence apparently supporting reaction (1) was obtained from measurements of the Np(V)–Np(VI) couple in chloride media.[3] The potentials were unstable in the presence of both gold and platinum electrodes, drifting to more positive values. This was again attributed to reduction by chloride ions, though the possibility that the metal electrode might be the reductant was mentioned.[1] The present study shows that the reduction of Np(VI) in chloride media is very slow at room temperature, not differing greatly from that expected from auto-reduction, and that a satisfactory absorption spectrum can be obtained. The accelerated reduction observed in the presence of platinum is shown not to be due to a catalytic effect but to reduction by the platinum itself.

Spectrophotometry was used to investigate this system. Since the major Np(VI) peak is in the near infrared, 12,240 Å, the Np(VI) was prepared in DCl and $DClO_4$ solutions in D_2O. The Np(VI) was prepared by ozone oxidation of Np(V). Solutions of Np(VI) are pink in 2 M $DClO_4$ and straw yellow in 2 M DCl. All spectral measurements were made with a Cary Recording Spectrophotometer Model 14 at room temperature. The spectra of Np(VI) in both DCl and $DClO_4$ solutions were measured over a period of seven weeks. After 32 days the 2 M $DClO_4$ solution contained 1·5 per cent of the neptunium in the (V) state, while the 2 M DCl solution contained 2·5 per cent of the (V) state. These slow changes produced no significant change in the near U.V. spectra. From the data on the auto-reduction of Np(VI) in perchlorate media,[4] it is calculated that 1 per cent should take place in this period. Thus the reduction of Np(VI) is a little faster in both $DClO_4$ and DCl than in $HClO_4$ but still very slow. It is possible that the nature of the ions present would affect the rate of auto-reduction. Earlier observations in HCl rather than DCl solutions are in general agreement with the above and in addition showed that heating these solutions to 50–60°C had no significant effect on the rate of reduction.[5] The spectra of Np(VI) in both 2 M $DClO_4$ and 2 M DCl are given in Figs. 1 and 2. The major peak occurs at a longer wavelength in 2 M DCl than in 2 M $DClO_4$ and its molar extinction coefficient is increased from 46 in 2 M $DClO_4$ to 54 in 2 M DCl.

The formal potential of the Np(V)–Np(VI) couple in 1 M HCl is −1·135 V.[3] while the standard oxidation reduction potential of the Cl^-–Cl_2 couple is −1·36 V.[6] An approximate calculation shows

* Based on work performed under the auspices of the U.S. Atomic Energy Commission.

[1] L. B. MAGNUSSON, J. C. HINDMAN and T. J. LA CHAPELLE, paper 15.11, "*The Transuranium Elements*," edited by G. T. SEABORG, J. J. KATZ and W. M. MANNING, National Nuclear Energy Series, Division IV, Vol. 14B, McGraw-Hill Book Co., Inc., New York, N.Y., 1949.
[2] J. C. HINDMAN, L. B. MAGNUSSON and T. J. LA CHAPELLE, paper 15.2 *Ibid.*
[3] L. B. MAGNUSSON, J. C. HINDMAN and T. J. LA CHAPELLE, paper 15.4, *Ibid.*
[4] A. J. ZIELEN, J. C. SULLIVAN and D. COHEN, *J. Inorg. Nucl. Chem.* 7, 378 (1958).
[5] B. L. TAYLOR, Thesis, University of London (1959).
[6] W. M. LATIMER, "*The Oxidation States of the Elements and Their Potentials in Aqueous Solutions*," 2nd Ed., Prentice-Hall, Inc., New York, N.Y., 1952).

that at equilibrium in a closed system, reduction of Np(VI) by chloride ion would be the order of 1 per cent in our solutions. Even if this amount of reduction did take place, the extinction coefficients of the species involved[7] are such that no change in the near U.V. spectrum would be detected. The difficulties encountered by earlier workers in obtaining satisfactory spectra remains unexplained.

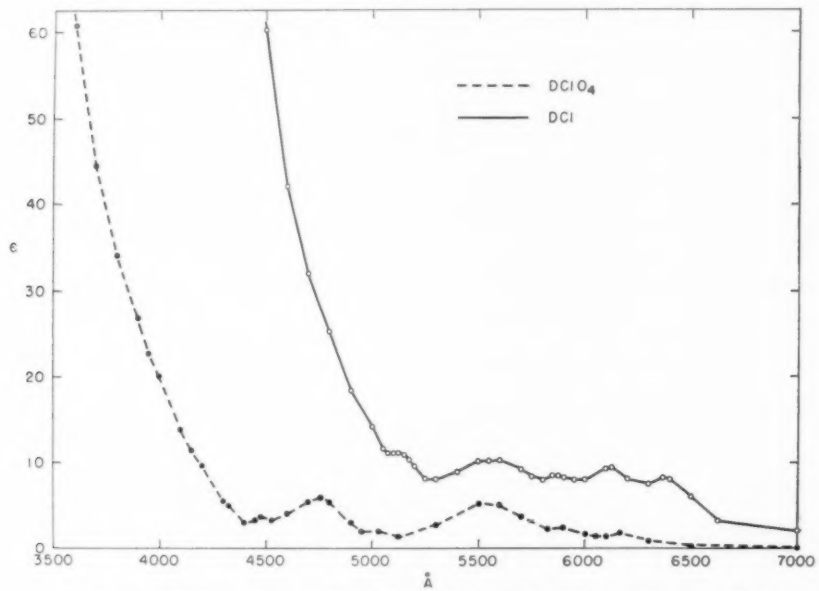

FIG. 1.—Visible spectra of 0·02 M Np(VI) in 2 M DCl and 2 M $DClO_4$ at 25°C.

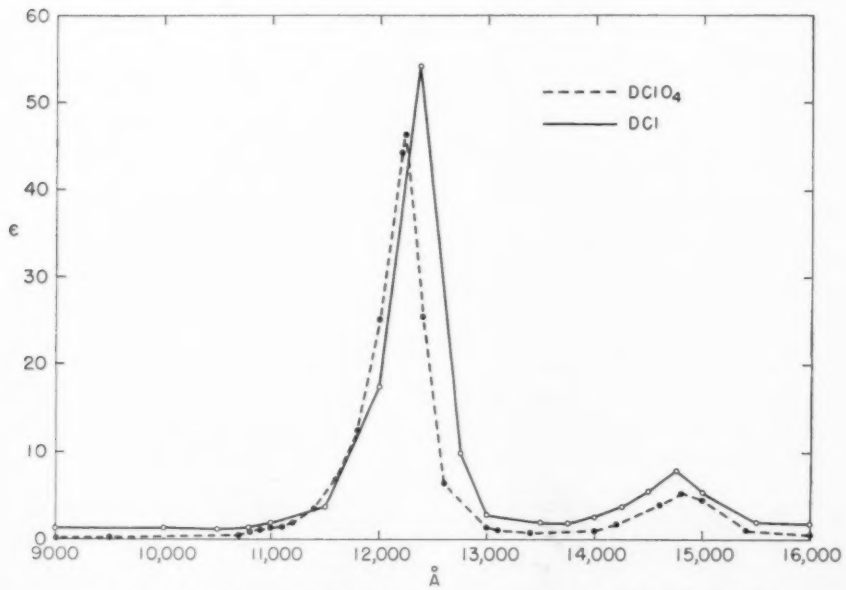

FIG. 2.—Infrared spectra of 0·02 M Np(VI) in 2 M DCl and 2 M $DClO_4$ at 25°C.

[7] G. ZIMMERMAN and F. C. STRONG, *J. Amer. Chem. Soc.* **79**, 2063 (1957).

The accelerated reduction of Np(VI) in chloride media in the presence of platinum that was observed by earlier workers[3] was confirmed by us. The potential of the couple

$$Pt + 6Cl^- \rightleftarrows PtCl_6^{2-} + 2e$$

is $-0{\cdot}73$ V[6] which is sufficiently positive for reduction of Np(VI) to the (V) and (IV) states. An analysis by emission spectroscopy of a solution resulting from the addition of a piece of Pt wire to a Np(VI) solution in HCl, showed the presence of platinum in solution. The absorption spectrum of this solution showed that some Np(IV) was present in addition to Np(V) and a large absorption peak occurred in the U.V. at 262·5 mμ; $PtCl_6^{2-}$(aq) is reported to have an absorption maximum at 262 mμ.[8] As a further test on the mechanism of reduction in the presence of platinum, a piece of carefully cleaned platinum wire was weighed on a micro balance and then placed in contact with a $2{\cdot}15 \times 10^{-2}$ M Np(VI) solution in 2 M HCl. After one week the platinum was removed, washed and reweighed; the concentrations of Np(V) and Np(IV) in the solution were determined spectrophotometrically as $1{\cdot}80 \times 10^{-2}$ M Np(V) and $0{\cdot}30 \times 10^{-2}$ M Np(IV). A simple calculation shows that 2·81 mg of Pt would be required for this reduction. The loss of weight of the Pt wire was measured to be 2·77 mg. This agreement is well within the experimental errors. It would be of interest to repeat these observations using gold metal. It is therefore concluded that the reduction in the presence of Pt is not due to catalysis of the Cl^- reduction but to reduction by platinum itself. There is no evidence from our work that reduction of Np(VI) by chloride takes place to any significant extent, either in the presence or absence of platinum.

DONALD COHEN
BRIAN TAYLOR†

Chemistry Division
Argonne National Laboratory
Argonne, Illinois

† Present address, Chemistry Division, AERE, Harwell, England.

[8] J. J. KIRKLAND and J. H. YOE, *Anal. Chim. Acta.* **9**, 441 (1953).

VOL. 22 1961

The reduction of titanium tetrachloride by sodium dispersed on alumina

(*Received* 24 *May* 1961; *in revised form* 17 *July* 1961)

IT IS known that $TiCl_4$ can be reduced to metallic Ti by the action of sodium.[1] To obtain a highly active product it has been recommended to use a sodium dispersion prepared by impregnating alumina or sodium chloride with molten sodium.[2] Indeed, on reacting liquid $TiCl_4$ with such a dispersion, a black product was obtained. It is specifically stated that the reaction temperature should be held between 125–200°C. When this precaution was not taken, ignition occurred, the reaction being highly exothermic.

On using a lithium dispersion instead of a sodium dispersion violet $TiCl_3$ was obtained.

It is surprising that the relatively small difference in the net electronegativity of Na and Li should cause the reduction of Ti^{IV} by three additional oxidation states. Indeed, very early,[3] doubts were raised whether the reduction product obtained under relatively mild conditions was not $TiCl_2$ rather than Ti. Since the product from the reaction of $TiCl_4$ with finely dispersed Na shows catalytic properties, it has been thought necessary to check its identity.

The analysis of the mixture, which in addition to alumina possibly contains Ti°, $TiCl_2$, Na and NaCl, is not straightforward. It is however possible to distinguish between $TiCl_2$ + 2Na and Ti° by first decomposing the $TiCl_2$ and Na with hot NaOH solution. Any metallic Ti present will not react.[4] Both $TiCl_2$ and $TiCl_3$ will be oxidized to Ti^{IV} under evolution of hydrogen.[5] The metallic

[1] F. C. ROBINSON and C. C. HUTCHINS, *J. Amer. Chem. Soc.* **6**, 74 (1884). M. A. HUNTER, *J. Amer. Chem. Soc.* **32**, 330 (1910). D. LEVY and L. HAMBURGER, *Z. Anorg. Chem.* **87**, 209 (1914).
[2] High Surface Sodium, National Distillers Chemical Co. Ashtabula, Ohio, 1953.
[3] O.V.D. PFORDTEN, *Ann. Phys.* **237**, 201 (1887).
[4] L. WEISS and H. KAISER, *Z. Anorg. Chem.* **65**, 345 (1910).
[5] EBELMAN, *Ann. chim. phys.* **20**, 385 (1847).

Ti can then be determined by dissolving it in hot hydrochloric acid, measuring the amount of hydrogen evolved and titrating the Ti^{III} with Fe^{III}.[6] This method is complicated by the fact that some of the nascent hydrogen reduces Ti^{IV} formed in the primary decomposition with NaOH, thereby increasing the amount of Ti^{III} and decreasing the amount of hydrogen evolved.[7]

Preparation of the Reduction Product

Alumina ("ALCOA" grade F-10) was first crushed to pass 120 mesh and then heated for 3 hr at 500°C in a muffle furnace. It was then transferred to the reaction vessel and kept for a further six hours *in vacuo* at 450°C. It was then allowed to cool to 150°C and mixed with molten sodium. The mixture was stirred *in vacuo* for about 15 min and a greyish black dispersion was obtained. The dispersion was allowed to cool and $TiCl_4$ was injected through a rubber gasket using a hypodermic syringe. The dispersion was stirred vigorously both during the addition of the $TiCl_4$ and while the mixture cooled. The colour of the dispersion changed to jet black. The dispersion thus obtained could be filled into separate ampoules for testing and analysing or all of the dispersion could be used.

Analysis of the Reduction Product

The black reduction product was decomposed by the addition of 10 ml of *ca.* 40 per cent aqueous NaOH solution *in vacuo*. The solution was heated for about 30 min. Under these conditions both $TiCl_2$ and $TiCl_3$ are oxidized to Ti^{IV} liberating a corresponding amount of hydrogen. Any residual Na is also decomposed. Only metallic titanium is not attacked. The vessel was then cooled by immersion in liquid air and all the gases were pumped off. The vessel was allowed to warm to room temperature and concentrated hydrochloric acid was added in excess. On heating, the metallic titanium dissolved evolving hydrogen and leaving the titanium in the trivalent state. The vessel was then cooled again in liquid air and the amount of hydrogen evolved was measured. The vacuum was then broken and the Ti^{III} was rapidly titrated with Fe^{III} using NH_4CNS as an indicator.

If a is the number of moles of hydrogen evolved by the action of HCl and b is the number of moles of Ti^{III} titrated, then the quantity of metallic titanium originally present is $c = \frac{2a + b}{4}$ gm-atoms.

The method was checked by analysing a synthetic mixture containing 0·64-gm-atoms Ti° (crushed sponge Ti metal "B.D.H." laboratory reagent), 0·97 mmole $TiCl_2$ and 40 gm-atoms Na by the method outlined above.

The results were: $a = 0{\cdot}67$; $b = 1{\cdot}15$; thence $c = 0{\cdot}62$ gm-atoms Ti°.

The results are shown in the Table. It will be seen that the highest percentage of Ti° found was 8·8%. Obviously most of the $TiCl_4$ was not reduced below $TiCl_2$.

TABLE

Used			Received		
Al_2O_3 (ml)	Na (mg-atom)	$TiCl_4$ (mmole)	Na : $TiCl_4$	Ti° (mg-atom)	Ti° : Ti
15	90	4·5	20	0·11	2·4
15	90	9·0	10	0·26	2·9
15	90	18·0	5	0·23	1·3
15	90	22·5	4	0·33	1·5
15	90	36·0	2·5	0·66	1·8
7·5	45	9·0	5	0·79	8·8
7·5	45	13·5	3·33	0·69	5·1
7·5	45	27	1·67	0·72	2·7

[6] E. KNECHT and E. HIBBERT, *Ber. dtsch. Chem. Ges.* **36**, 1549 (1903).
[7] G. PATSCHEKE and W. SCHALLER, *Z. Anorg. Chem.* **235**, 257 (1938).

Actually the success of the reduction to Ti° depends on the temperature reached, which is not uniform. The appearance of a flame shows that at least locally temperatures above 500°C were reached. This is also borne out by the observed sublimation of a little violet $TiCl_3$. Stirring during the injection was not sufficient to result in uniform temperature and the surface of the mass was hotter than the bulk. Therefore a comparison of the results at the same ratio $Na:TiCl_4$ shows consistently higher yields of Ti° when smaller quantities were used. If the reaction is carried out under mild conditions, the temperature being kept below 200°C, no metallic Ti was formed.

To verify the effect of temperature a dispersion prepared in the usual way was divided into two parts; the first was analysed without further treatment and the other heated for 3 hr at about 500°C. On heating the yield of Ti° had risen from 1·5 per cent to 5·1 per cent. It is quite possible that the Ti° is not formed through the reduction by Na but by decomposition of $TiCl_2$. SCHUMB and SUNDSTROM[8] obtained 5 per cent decomposition when $TiCl_2$ was heated *in vacuo* to 475°C.

It follows that ordinarily even finely divided Na does not reduce $TiCl_4$ below $TiCl_3$.

Petrochemical Laboratory of the National Council for Research and Development and of the Physical Chemistry Department Hebrew University, Jerusalem

C. EDEN
H. FEILCHENFELD
D. ZEHAVI

VOL. 22 1961

[8] W. C. SCHUMB and R. F. SUNDSTROM, *J. Amer. Chem. Soc.* **55**, 596 (1933).

The product of reaction of BF_3 with B_2O_3*

THE FORMATION of trifluoroboroxine, $(BOF)_3$, was first reported by BAUMGARTEN and BRUNS[1,2,3]. The material was reported as a product of reaction of BF_3 with a number of oxides including B_2O_3 and SiO_2.

Recently a report suggests that trifluoroboroxine is stable only below $-130°$ and decomposes rapidly above this temperature to give BF_3 and B_2O_3[4,5]. This leads us to feel that a report of our experiments and observations on the product (hereafter written as *product*) of the BF_3–B_2O_3 reaction is warranted.

Boron trifluoride was allowed to react with B_2O_3 and SiO_2 in a flow system at 450° in the manner outlined in Ref. 1. The white solid product, collected in a cool portion of the system at room temperature, was used in further studies.

The product was stable for days at room temperature but melted at about 80° with decomposition to B_2O_3 and BF_3. As found by BAUMGARTEN and BRUNS, the material contained B, O and F, but always more B_2O_3 than BF_3. A typical analysis showed the ratio of B_2O_3 to BF_3 to be 2·19.

An attempt was made to measure the equilibrium constant between BF_3 and the tacky mixture of B_2O_3 and product at 80°. However, the reverse reaction, $B_2O_3(s) + BF_3 \rightarrow$ product was very slow at 80° and the results were not completely definitive.

The heat of formation of the product was determined by measuring its heat of solution in both water and CH_3OH after correcting for the heat of solution of the excess B_2O_3. Assuming that the product was trifluoroboroxine, the entropy of the material was calculated. The following table gives a summary of the properties observed, calculated and estimated for $(BOF)_3$.

Until a definite proof of the structure for the product is established, important conclusions from these results should not be drawn. If the material is shown indeed to be trifluoroboroxine, then the

* This work was carried out under Government Contract No. DA-30-069-ORD-2487.

[1] P. BAUMGARTEN and W. BRUNS, *Ber.* **72B**, 1753 (1939); 1232 (1941).
[2] T. MOELLER, "*Inorganic Chemistry*," John Wiley and Sons, Inc., New York 1952, p. 751.
[3] N. V. SIDGWICK, "*The Chemical Elements and Their Compounds, Vol. I*" Oxford University Press, London, 1950, p. 396.
[4] H. D. FISHER and I. SHAPIRO, Abstracts of Papers, 138th Meeting American Chemical Society, p. 39N, 1960.
[5] H. D. FISHER, W. J. LEHMANN and I. SHAPIRO, *J. Phys. Chem.* **65**, 1166 (1961).

lack of appreciable resonance stabilization (as shown by the closeness of the measured ΔH_f° and that calculated from bond strengths) would be interesting since Burg concludes that resonance exists in methyl boric anhydride.[6]

Whether or not the product is $(BOF)_3$, it must be concluded that a relatively stable material is produced when BF_3 reacts with B_2O_3 or SiO_2.

E. M. Magee

Special Projects Unit
Esso Research and Engineering Company
Linden, New Jersey

[6] A. Burg, *J. Amer. Chem. Soc.* **62**, 2228 (1940).

Table—Summary of thermodynamic properties[a]

Property	Compound		
	B_2O_3 [g/s]	BF_3 [g]	$(BOF)_3$ [g]
ΔH_f° (25°C) kcal/mole	−300·98	−266·9	−587·6[b] −582·3[c] −585·0[d] −574·8[e] −589[f]
ΔH soln. (H_2O) kcal/mole	−7·596	−25·3	−13·1[g]
ΔH soln. (CH_3OH) kcal/mole	−8·83[g]	−23·5	−17·9[g]
ΔH vaporization kcal/mole			11·8[h]
ΔH fusion kcal/mole			3·1[i]
S° (solid), (25°), cal deg.$^{-1}$ mole^{-1}	19·03		52[j] 63[e]
S° (gas), (25°), cal deg^{-1} mole^{-1}		60·72	85·3[j]
ΔS fusion, cal deg^{-1} mole^{-1}			8·8[k]
ΔS vaporization, cal deg^{-1} mole^{-1}			21[l]
M.P. °C			80[m]
B.P. °C			288[n]

[a] Unless otherwise noted, values are from W. H. Evans, D. D. Wagman and E. J. Prosen, "*Thermodynamic Properties of Some Boron Compounds*," National Bureau of Standards Report No. 4943, 8/31/56.
[b] From ΔHs in H_2O.
[c] From ΔHs in CH_3OH.
[d] Average of (a) and (b).
[e] Equilibrium studies.
[f] From bond strengths.
[g] From present work.
[h] From ΔS vaporization and B.P.
[i] Average of B_2O_3 and BF_3.
[j] Calculated.
[k] From ΔH fusion and M.P.
[l] Trouton's Rule.
[m] Approximate—observed.
[n] Assumed.

The thermal decomposition of erbium and lutetium oxalates

(*Received* 29 *May* 1961; *in revised form* 23 *August* 1961)

In the course of a study of the thermal decomposition of the rare earth oxalates, it became evident that the behaviour of erbium and lutetium oxalates differs in many ways from that of the light rare earth group.[1,2]

(a) Whilst the light rare earth oxalates (with the exception of cerous oxalate) were more or less completely dehydrated on heating in vacuum at 300°C, the erbium and lutetium salts retained, under these conditions, more than 25 per cent of their water of crystallization.

[1] A. Glasner and M. Steinberg, *J. Inorg. Nucl. Chem.* **16**, 279 (1961).
[2] A. Glasner and M. Steinberg, *J. Inorg. Nucl. Chem.* In press.

For example, a representative sample of lutetium oxalate, precipitated at 60°C, was shown by analysis to have the composition Lu_2O_{z3} . 6·05H_2O (15·06% H_2O). 0·14675 g of this sample lost only 0·01567 g in weight on prolonged heating in vacuum at 300°C, retaining 1·76 M H_2O per formula weight (4·9%). Samples similarly dried were used in the decomposition experiments at higher temperatures.

In these experiments, too, the actual loss of weight of the solid sample, after decomposition, was always greater than that calculated from the partial pressures of carbon oxides evolved, indicating the presence of about 5 per cent moisture.

In a short study of the thermal decomposition of the heavy rare earth oxalates,[3] apparently the only one reported in the literature, WENDLANDT also notes the exceptional stability of the di-hydrates, to temperatures over 300°C.

(b) The partly dehydrated powders, when heated at 340°–360°, exhibited lengthy induction periods (see Figs. 1 and 2). At higher temperatures, the decomposition was always preceded by a high pressure "kick", owing to the lag in the condensation of water vapour in the dry ice-acetone traps. Evidently, the retained water stabilizes the oxalate, which decomposes as soon as this is driven off.

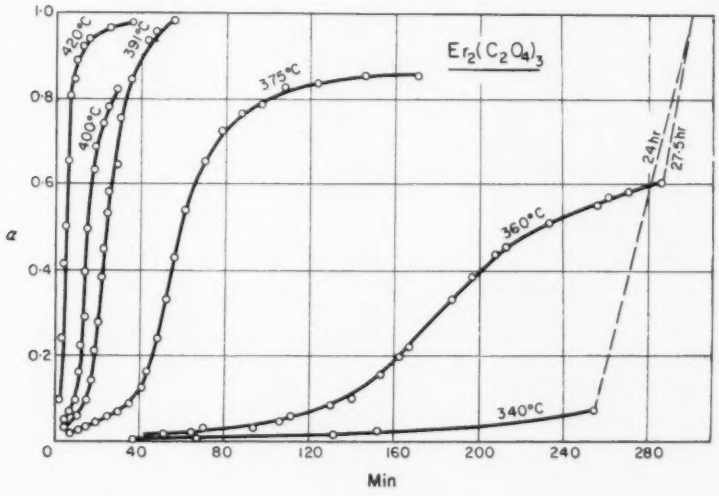

FIG. 1.

(c) The decomposition curves (Figs. 1 and 2) are often irregular and show distinct steps, especially on their upper halves. This leaves doubt as to the termination of the reaction.

(d) The amount of carbon monoxide evolved, expressed in mole per cent of the reaction:

$$M_2(C_2O_4)_3 \rightarrow M_2(CO_3)_3 + 3CO \qquad (1)$$

is up to 65 per cent with erbium and 86 per cent with lutetium (see Tables 1 and 2), as compared to 30–45 per cent with the light rare earth oxalates.

This indicates that disproportionation:

$$2CO \rightarrow CO_2 + C \qquad (2)$$

proceeds only to a small extent, a conclusion confirmed qualitatively by the slight brown coloration of the residues.

On the other hand, the variations in the mole % of carbon monoxide evolved in several runs (shown in Tables 1 and 2), as well as the relative amounts of carbon monoxide and carbon dioxide, are puzzling, giving the impression of an irregular reaction.

[3] W. W. WENDLANDT, *Anal. Chem.* **31**, 408 (1959).

TABLE 1.—COMPOSITION OF GASES EVOLVED ON HEATING Er_2Ox_3 IN VACUUM, AND I.R. SPECTRA OF RESIDUES

°C	Wt. of sample (mg)	Mole % of gases		% I_t at charact. w.l.	
		CO	CO_2	6·1 μ	7·1 μ
340	7·39	45·44	43·48	39	52(—)
360	3·76	65·53	79·82	77(—)	69
375	10·57	57·60	48·00	48	53
391	11·05	59·64	49·42	46	49
391	3·28	61·86	79·54	—	—
400	5·27	60·32	68·76	—	—
420	12·87	64·93	45·80	52(—)	33

4·83 mg Er_2Ox_3 (+4·9% H_2O) ≡ 100 μ CO

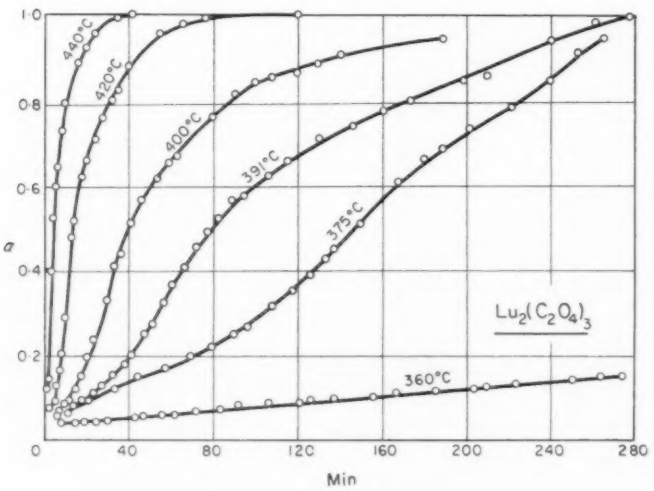

FIG. 2.

TABLE 2.—COMPOSITION OF GASES EVOLVED ON HEATING Lu_2Ox_3 IN VACUUM

°C	Wt. of sample (mg)	Mole per cent of gases	
		CO	CO_2
360	6·73	65·49	68·51
375	10·73	48·51	36·50
391	9·53	73·88	52·53
400	6·89	86·00	70·52
420	6·07	81·07	71·87
440	6·88	79·61	76·75

(e) The infra-red spectra of the residues indicate in all cases the presence of carbonate as well as oxalate. This is illustrated in Table 1, by the percentage of transmitted light I_t at the most characteristic absorption peaks (6·1 μ for the oxalate, and 7·1 μ for the carbonate; (—) indicates the absence of a well-defined peak); KBr disks were used, containing in each case 1 mg of the solid residue. Here again, the irregular variation of the transmission values with temperature is conspicuous. On the other hand it was observed that the less the transmitted light at 6·1 μ, the smaller the mole % of CO evolved. Both measurements show a higher percentage of undecomposed oxalate in the residue. Taking into consideration the disproportionation of a small fraction of CO, it was found that there was good accord between the estimated amount of carbonate and the relative transmittance at 7·1 μ.

An important observation was that small sample weights yielded high molar percentages of carbon dioxide, whilst larger samples, even at higher temperatures, evolved relatively small amounts of CO_2. Hence it may be concluded that the accumulated pressure of CO_2 hinders the further decomposition of the carbonate. Judging by the observed stability of the mixed oxalate-carbonates of some of the light rare earths, it seems that the decomposition of the oxalate itself is also regulated, indirectly, by the CO_2 pressure; a mixed salt of composition $M_2(Ox)_{3/2}(CO_3)_{3/2}$ or $M_2Ox(CO_3)_2$, is first formed, which after the conversion of the carbonate into the oxide, becomes unstable and continues to evolve CO, causing the appearance of the observed steps on the decomposition curves. Considering experiments with small sample weights, in which the percentage of CO_2 evolved is greater than that of CO, and correlating gasometric results with the infra-red measurements, the authors estimate that about $\frac{1}{8}$th of the carbon dioxide evolved from erbium oxalate undergoes disproportionation, but only about 6% from the lutetium oxalate.

An attempt to prepare erbium carbonate under a pressure of CO_2 succeeded only partially. A sample of the original hydrate (53% Er_2O_3) weighing about 0·7 g was heated in a current of CO_2 at 420°C for 24 hr. A dark residue was obtained which, according to chemical analysis, is thought to have the composition [$(ErO)_2CO_3$ + C]. If 17 per cent of CO underwent decomposition, the % wt. of the residue should have been 59·94%, while that actually found was 61·48%; hence about 4·2 per cent of the oxalate remained undecomposed.

The thermal decomposition and properties of erbium and lutetium oxalate may be summarized as follows:

1. Both salts tenaciously retain a part of their water of crystallization.
2. The last traces of water stabilizes the oxalates; decomposition in vacuum begins at 340°–360°C, as with the light rare earth oxalates, but only after a long induction period.
3. Initially carbonates are formed, and the CO disproportionates only to a small extent, about 17 per cent with erbium oxalate and about 6 per cent with lutetium oxalate.
4. The carbonates are unstable and decomposition to the oxides follows soon. This reaction has an unstabilizing effect on eventual oxalato-carbonate intermediates.
5. The regularities in the stability of the oxalates and in the disproportionation of CO, observed in the case of the light rare earths, are thus seen to extend also to the heavy rare earths.

Acknowledgement—The authors wish to thank Messrs. Lindsay Chemical Co. for donating several rare earth oxides.

ABRAHAM GLASNER
MENACHEM STEINBERG

Department of Inorganic & Analytical Chemistry
The Hebrew University
Jerusalem Israel

VOL. 22 1961

VO
2
19

J. Inorg. Nucl. Chem., 1961, Vol. 22, pp. 161 to 167. Pergamon Press Ltd. Printed in Northern Ireland

THE MASS DISTRIBUTION IN FISSION OF LEAD INDUCED BY 54 MeV PROTONS

U. L. VALLINDER and A. C. PAPPAS*
The Gustaf Werner Institute for Nuclear Chemistry,
University of Uppsala, Sweden

(*Received* 24 *May* 1961)

Abstract—The mass distribution in fission of natural lead induced by 54 MeV protons has been studied. The yield mass curve seems nearly symmetric in character around mass number 102. It has a width of about 28 mass units at half the maximum yield. The fission cross section is 13 ± 4 mbarns, i.e. the same as for bismuth under comparable conditions.

VOL.
22
1961

THE increase in fissionability with increasing atomic number is very pronounced in the elements from lead to thorium. Thus, while the fission cross section for low energy particles is of the order of millibarns in the elements around lead[1] it reaches a thousand-fold value in thorium under similar conditions.[2] This change in fission probability is followed by a typical change from symmetric to asymmetric division of the fissioning nucleus. Another characteristic feature of fission induced in the elements lighter than thorium is the rapid increase with energy in fission width to total width, at least up to 40 MeV.[3,4]

Elements beyond thorium show a high fission cross section and at low irradiation energies asymmetric division is typical and overshadows the symmetric division. With increasing energy, however, a gradual change from asymmetric to symmetric fission is observed in all these elements.

These observations seem to suggest that fission in the elements lighter than thorium is different from fission in the heavier elements. Fission studies of elements lighter than thorium have therefore during the past years drawn a considerable interest.

The only element with atomic number between bismuth and thorium that is available to fission mass distribution studies is radium. Radium, however, lies closer to the heavier elements than to the elements in the region of bismuth. JENSEN and FAIRHALL[5] determined the yield mass distribution in proton induced fission of radium. With 11 MeV protons they found the distributions due to the symmetric and asymmetric fission modes distinctly separated. The yield mass curve shows three peaks of about equal heights. The narrow one in the centre corresponds to symmetric fission while the two on either side correspond to asymmetric fission. These findings support the idea of TURKEVICH and NIDAY[6] that the yield mass distributions observed are composites of one distribution due to symmetric fission and another due to asymmetric

* Permanent address: Department of Chemistry, University of Oslo, Blindern, Norway.

[1] J. ROESMER and T. T. SUGIHARA, Annual Progress Report, Clark University NYO–7759 (1959).
[2] H. A. TEWES and R. A. JAMES, *Phys. Rev.* **88**, 860 (1952).
[3] A. W. FAIRHALL, R. C. JENSEN and E. F. NEUZIL, *Proceedings of the Second International Conference on the Peaceful Uses of Atomic Energy, Geneva*, 1958, Vol. 15, 452, United Nations (1958).
[4] A. W. FAIRHALL and E. F. NEUZIL, Annual Progress Report, University of Washington (1959).
[5] R. C. JENSEN and A. W. FAIRHALL, *Phys. Rev.* **109**, 942 (1958).
[6] A. TURKEVICH and J. B. NIDAY, *Phys. Rev.* **84**, 52 (1951).

fission. The symmetric fission is assumed[5] to take place in the compound nucleus ^{227}Ac formed with an excitation energy of about 16 MeV and the asymmetric fission in ^{226}Ac formed by a (p, n) reaction and thus excited only to 7–8 MeV.

Furthermore, FAIRHALL *et al.*[3] conclude from their studies of fission induced in elements lighter than thorium that the asymmetric fission mode is associated with nuclei of low excitation energy, whereas nuclei with higher excitation energy would fission symmetrically. In accordance with this JENSEN and FAIRHALL[7] found qualitative evidence that prompt fission is symmetric in character.

The elements below the region of radium have a very low fission cross-section and fission studies with low energy protons were not available until quite recently. By irradiation of bismuth with 36 MeV protons ROESMER and SUGIHARA[1] found a symmetric mass distribution and indications of a very low contribution from asymmetric fission (about 0·3 per cent of the symmetric fission).

Further fission studies of elements in the region around lead should be of interest in the discusssion of the two different modes of fission. The present paper gives the yield mass distribution of fission induced in natural lead by 54 MeV protons. The use of an appreciable lower energy would be of interest, but was not feasible under our conditions due to the large spread in proton energy. Nevertheless it is hoped that the results presented in this paper may contribute to our understanding of the fission process in these elements.

EXPERIMENTAL

The irradiations (0·5–2 hr) were carried out at a maximum proton energy of 65 MeV. This corresponds to a maximum intensity of the ion beam at 54 MeV, and an energy width at half the maximum of about 13 MeV. The maximum energy loss for protons in the target was not more than about 3 MeV.

Spectroscopically pure lead metal or lead nitrate was used as target material. The impurities present (less than 5 p.p.m.) would not interfere with the measurements. Lead nitrate packed in aluminium foil was used only when the dissolution of lead metal would result in loss of the fission product of interest.

Carrier (10 mg) isotopic with the fission product element to be separated was added to the solvent, usually before the target was dissolved. As the ^{89}Sr was used as internal monitor, strontium carrier was also added to the target solution. After isolation and purification the nuclides of interest were identified through half-life and β-energy determinations (Feather analysis).

The counting was performed with Geiger-Mueller counters according to the techniques of absolute β-counting, after which the observed activities were converted to absolute disintegration rates in a standard way.[8]

The available radiochemical procedures[9,10,11] were applicable only after some modifications and additional steps were introduced due to the specific properties of the target material. The procedures used are outlined in the Appendix. A few comments are, however, necessary.

In the first determinations of ruthenium the target was dissolved in nitric acid. This resulted in low and irreproducible values, probably due to incomplete exchange between fission product ruthenium and the added carrier. It is very likely that the reason for this is the formation of strong nitroso complexes of ruthenium[12] which prevent the exchange between carrier and added tracer. But if glacial acetic acid containing hydrogen peroxide was used to dissolve the target the fission yields obtained for the ruthenium isotopes were higher and also reproducible.

[7] R. C. JENSEN and A. W. FAIRHALL, *Phys. Rev.* **118,** 771 (1960).
[8] A. C. PAPPAS, Report AECU-2806, LNS-MIT-63 (1953); (Inaugural Dissertation, University of Oslo).
[9] C. D. CORYELL and N. SUGARMAN (Editors), *Radiochemical Studies: The Fission Products, NNES.*, Div. IV, Vol. 9, McGraw-Hill, New York (1951).
[10] J. KLEINBERG *et al.*, Report LA 1721 (1958).
[11] W. W. MEINKE, Report UCRL-432 (1949) and later additions.
[12] O. E. ZVYAGINTSEV, *Proceedings of the International Conference on the Peaceful Uses of Atomic Energy, Geneva,* 1955, Vol. 7, 169, United Nations (1956).

The internal monitor strontium was in most of the separations first precipitated as hydroxide from strongly alkaline solution before the other elements were separated.

Zirconium was precipitated as m-nitrobenzoate[13] before a further purification was performed according to a method by HUME.[10]

The absolute cross-section of the monitor ^{89}Sr was determined by comparison with the formation cross-section of ^{24}Na in the reaction of protons with natural magnesium. According to the excitation function as given by RUDSTAM[14] on the basis of earlier work[15,16] the cross-section for this reaction is 7·5 mbarns at 54 MeV. The normalization was in the present experiments carried out by the sandwich method, i.e. the lead foil was inserted between magnesium foils, three on each side. The foils were aligned to ensure that the same ion current passed through all the foils. The second magnesium foil of the three was the monitoring foil, while the rest were guard and compensating foils. The lead foil was thick enough to ensure that the fission recoil losses could be neglected.

RESULTS

The fission yields given in Table 1 are averages of three or four determinations. The limits listed are mean deviations or are larger if errors involved in the measurements themselves so require. The measured cross-sections are plotted versus mass number in Fig. 1.

VOL. 22 1961

TABLE 1.—ABSOLUTE FORMATION CROSS-SECTION FOR PRODUCTS FROM 54-MEV PROTON INDUCED FISSION OF NATURAL LEAD

Nuclide	Fission yield (mbarns)	Fission yield (%)
^{76}As (shielded)	(0·2–0·7) × 10^{-2}	0·015–0·05
^{77}As	0·074 ± 0·008	0·57 ± 0·06
^{89}Sr	0·53 ± 0·02	4·1 ± 0·15
^{95}Zr	$0·74 \begin{matrix} \pm 0·08 \\ - 0·21 \end{matrix}$	$5·7 \begin{matrix} \pm 0·6 \\ - 1·6 \end{matrix}$
^{97}Zr	0·80 ± 0·08	6·2 ± 0·6
^{99}Mo	0·86 ± 0·05	6·6 ± 0·4
^{103}Ru	0·87 ± 0·09	6·7 ± 0·7
^{105}Ru	0·95 ± 0·14	7·3 ± 1·1
^{106}Ru	0·85 ± 0·09	6·5 ± 0·7
^{110m}Ag (shielded)	(0·3–0·7) × 10^{-2}	0·02–0·05
^{111}Ag	0·72 ± 0·07	5·6 ± 0·5
^{115m}Cd	0·09 ± 0·01	0·72 ± 0·08
^{115}Cd	0·36 ± 0·04	2·7 ± 0·3
$^{115+115m}$Cd	0·44 ± 0·05	3·4 ± 0·4
^{126}I (shielded)	~0·5 × 10^{-2}	~0·04
^{131}I	0·013 ± 0·002	0·10 ± 0·02
^{140}Ba	<0·16 × 10^{-2}	<0·012

DISCUSSION

In order to get an idea to what extent the cumulative yields in Table 1 really represent the total yields of the corresponding mass chains the maxima Z_P of the (isobaric) charge distribution curves should be estimated. According to FAIRHALL *et al.*[3] most of the fissions observed for nuclei in the mass region around lead take place before neutrons are evaporated, at least up to an excitation energy of 30–40 MeV.

[13] R. BELCHER and C. L. WILSON, *New Methods in Analytical Chemistry*. Chapman and Hall, London (1955).
[14] G. RUDSTAM, Inaugural Dissertation, University of Uppsala (1956).
[15] J. W. MEADOWS and R. B. HOLT, *Phys. Rev.* **83**, 47 (1951).
[16] W. E. CRANDALL, G. P. MILBURN, R. V. PYLE and W. BIRNBAUM, *Phys. Rev.* **101**, 329 (1956).

Moreover in these elements symmetric fission seems to be associated with high excitation energy and to occur rapidly. In the present study therefore the majority of fissions may be assumed to occur before neutron evaporation. It seems also reasonable that the hypothesis of unchanged charge distribution[17] should be preferred to a hypothesis that requires a redistribution of charge before fission[8] for estimating Z_P.

Due to the different lead isotopes involved there is in reality a spread in mass number of the most probable fissioning nuclide. Nevertheless, it is assumed that the compound nucleus ^{208}Bi (weighted average of the compound nuclei involved) may be

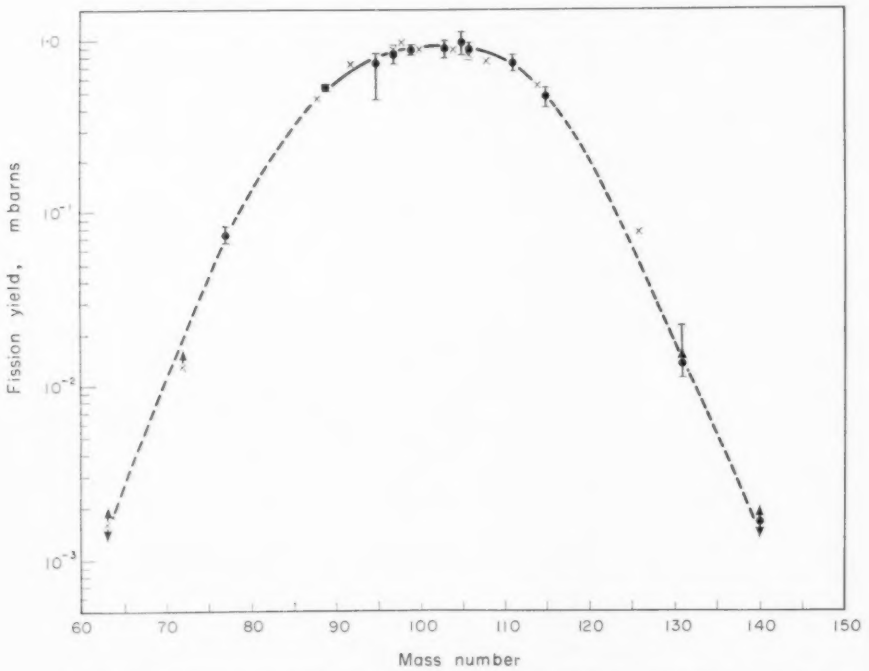

FIG. 1.—Yield mass curve for fission of lead induced by 54 MeV protons (drawn through the measured points only).
● measured yields, x reflected yields assuming $A_1 + A_H = 203$.

taken as a good representative of the "most probable fissioning nucleus". In accordance with the yield mass distribution observed five neutrons are assumed evaporated from the fission fragments (to give the apparent fissioning nucleus ^{203}Bi).

Fig. 2 shows the β-stability lines,[18] the line of Z_P computed on the basis of an apparent neutron to proton ratio of 1·45 and the position of nuclides the yields of which have been determined. According to this figure, most of the yields in Table 1 must be regarded as lower limits but presumably quite close to the total yields of the corresponding mass chains. This conclusion is supported by the fact that the yields of the shielded nuclides ^{76}As and ^{126}I are considerably lower than the yields of neighbouring non shielded nuclides and that the yields of ^{103}Ru, ^{105}Ru and ^{106}Ru, representing cumulative yields of the mass chains 103, 105 and 106, are about the same.

[17] R. H. GOECKERMAN and I. PERLMAN, *Phys. Rev.* **76**, 628 (1949).
[18] C. D. CORYELL, *Ann. Rev. Nucl. Sci.* **2**, 305 (1953).

The charge distribution curve found in fission of bismuth induced by 340 MeV protons[19] is narrow when compared to that found for the symmetric fission mode in fission of uranium under the same conditions.[20] Moreover, it has been observed that the charge distribution curve for the symmetric fission modes in thorium[21] and uranium[22] broadens with increasing energy of the irradiating particle.

Thus the charge distribution curve in fission of elements with as low atomic numbers as that of lead should be expected to be rather narrow at low energies. This seems to be supported by the observations in the present paper.

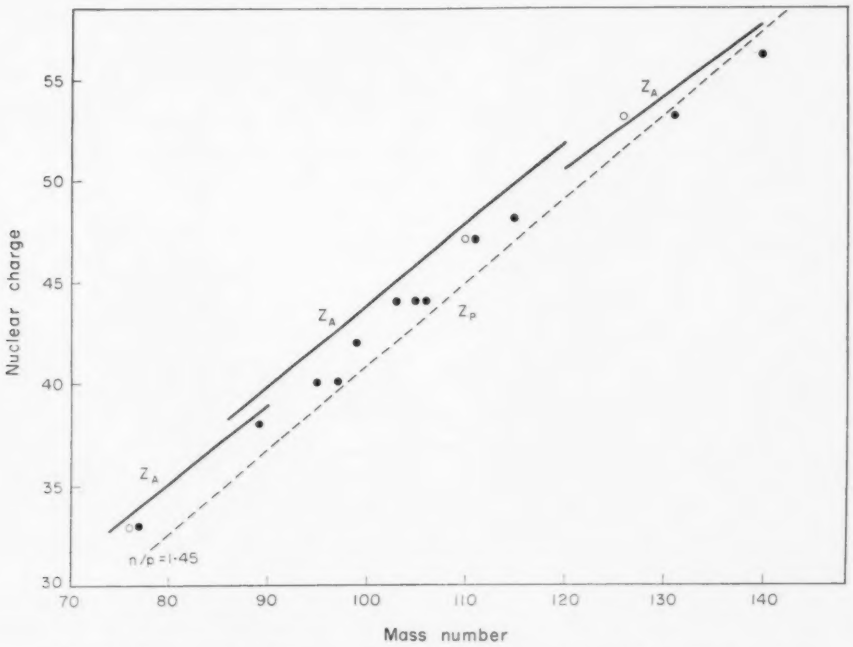

FIG. 2.—Position of nuclides studied in fission of lead induced by 54 MeV protons. ———lines of maximum stability, - - - - -maxima assumed for charge distribution curves, ● nuclides representing cumulative yields, ○ shielded nuclides.

On this basis the measured points in Fig. 1 are considered to represent the total chain yields in fission of lead induced by 54 MeV protons. The curve is drawn through the measured points only. The reflected points (assuming five nucleons evaporated) lie close to this curve thus suggesting the possibility of a yield mass distribution not far from symmetric around mass numbers 101–102. This gives mass number 202–204 for the apparent fissioning nuclide. The curve has a width at half maximum of about 28 mass units. By graphical integration of the yield mass curve a fission cross section of 13 ± 4 mbarns is obtained. The limit given includes a standard deviation of 15 per cent in the absolute cross-section of the monitor reaction.

[19] W. F. BILLER, Report UCRL-2067 (1953).
[20] R. L. FOLGER, P. C. STEVENSON and G. T. SEABORG, *Phys. Rev.* **98**, 107 (1955).
[21] B. D. PATE, J. S. FOSTER and L. YAFFE, *Canad. J. Chem.* **36**, 1691 (1958).
[22] A. C. PAPPAS and J. ALSTAD, *J. Inorg. Nucl. Chem.* **17**, 195, (1961).

It is not clear to what degree the different lead isotopes contribute to the total fission cross-section. FAIRHALL *et al.*[3] have recently found that in the case of lead isotopes the cross section for fission induced by helium ions of various energies up to 42 MeV seems to be only slightly dependent on mass number.

The general character of the mass distribution curve for fission of lead with 54 MeV protons is the same as for fission of bismuth at moderate energies, i.e. the yield mass curve is single-humped and rather narrow. With 36 MeV and 58 MeV protons[1] the mass distribution of bismuth has a half-width of about 20 mass units. In 54 MeV proton induced fission of lead the yield curve at half maximum is about 8 mass units broader, i.e. 28 mass units, but one has to take into account that the target material extends over five mass numbers.* Correcting for this one should conclude that fission of natural lead leads to a somewhat broader distribution than fission of bismuth under the same conditions. This view supports the observations made by FAIRHALL and NEUZIL[4] that the mass distribution becomes broader with decreasing atomic number of the target for otherwise identical irradiation conditions. Concerning the fission cross section of lead it is the same as found for bismuth (14 mbarns[1]) under comparable conditions.

FAIRHALL *et al.*[3,7] have, as mentioned before, suggested that it is meaningful to discuss the mass distribution in fission of elements below thorium in terms of two different types of mass division, asymmetric fission associated with low excitation energy of the fissioning nucleus and the symmetric fission associated with higher energy. The probability of symmetric fission seems to be a strongly increasing function of the excitation energy up to at least 30–40 MeV and furthermore its mass distribution becomes broader at higher energies. There are indications that the probability of asymmetric fission is not very sensitive to energy, but it is apparent that it drops off as the atomic number of the target decreases.[3] These circumstances together would explain why no evidence of appreciable departure from the symmetric fission mode was observed in proton induced fission of lead at the irradiation energy used in the present study.

Acknowledgements—The authors wish to express their gratitude to Professor T. SVEDBERG, director of the Gustaf Werner Institute for Nuclear Chemistry, for his interest in this work and the excellent working conditions given. The work has been supported by the Swedish Atomic Energy Commission and by the Royal Norwegian Council for Scientific and Industrial Research.

APPENDIX

For each element investigated, the essential steps of the chemical procedure are summarized. The steps listed were usually repeated several times in cycles. The targets were dissolved in HNO_3 unless stated otherwise.

Arsenic. From the target solution of $Pb(NO_3)_2$ dissolved in water, As was distilled off as $AsCl_3$ and precipitated as sulphide. Volatile chlorides and oxides were fumed off from a strongly oxidizing solution (conc. HCl + conc. HNO_3 + 70% $HClO_4$). As was then extracted as AsI_3 into chloroform and finally reduced to As° by $CrCl_2$ solution.

Strontium. Sr was precipitated as $Sr(NO_3)_2$ with fuming HNO_3. $Fe(OH)_3$ scavengings were used as well as purifications by precipitations of CdS and $BaCrO_4$. Sr was finally weighed as $SrCO_3$.

Zirconium. Zr was precipitated with m-nitrobenzoic acid and as $BaZrF_6$. After LaF_3 scavengings Zr was precipitated as hydroxide and finally as Zr-*m*-nitrobenzoate, which was ignited to oxide before weighing.

* 1·4% ^{204}Pb, 25·2% ^{206}Pb, 21·7% ^{207}Pb and 51·7% ^{208}Pb.

Molybdenum. The target solution was made strongly alkaline and the precipitated $Sr(OH)_2$ separated. Pb was separated as PbS and the solution made acidic with conc. HCl to precipitate Mo sulphides. The sulphides were dissolved in hot conc. HNO_3 after which HNO_3 was destroyed by means of $KMnO_4 + H_2SO_4$. Oxidation with Br_2 was performed before extraction of Mo from 6 N HCl into ether saturated with 6 N HCl. Mo was then precipitated with α-benzoinoxime from 1·5 N HNO_3 containing $H_2C_2O_4$, and dissolved. Following $Fe(OH)_3$ scavengings, Mo was finally precipitated with 8-hydroxyquinoline and ignited to MoO_3 before weighing.

Ruthenium. The target was dissolved in glacial acetic acid $+H_2O_2$. OsO_4 was fumed off from a solution 6 N in HNO_3. Ru was distilled as RuO_4 into 6 N NaOH from a solution containing 70% $HClO_4$, H_3PO_4 and $NaBiO_3$, and Br, I and Mo carriers. Ru was then precipitated as a lower oxide by ethyl alcohol and reduced to Ru^0 from HCl solution by Mg powder.

Silver. Ag was precipitated as AgCl and Ag_2S using $Fe(OH)_3$ scavengings in between. Ag was weighed as AgCl.

Cadmium. Cd was precipitated as $Cd(OH)_2$ together with Sr, then as CdS from HCl and from NH_4OH. Scavengings with PdS, basic Fe(III) acetate and $La(OH)_3$ were used as well as separation of $In(OH)_3$. Cd was finally precipitated as $CdNH_4PO_4 \cdot H_2O$.

Iodine. I was distilled off from HNO_3 into $NaHSO_3$ solution and extracted as I_2 into CCl_4 after oxidation with $NaNO_2$. I was weighed as AgI.

Barium. Ba was precipitated as $Ba(NO_3)_2$ with fuming HNO_3 and as $BaCrO_4$ with $Fe(OH)_3$ scavengings in between. Ba was finally precipitated as $BaCl_2 \cdot H_2O$ with ether–HCl mixture.

VOL. 22 1961

J. Inorg. Nucl. Chem., 1961, Vol. 22, pp. 169 to 181. Pergamon Press Ltd. Printed in Northern Ireland

ABSONDERUNG RADIOAKTIVER ATOMARTEN IN TRÄGERFREIEM ZUSTANDE MIT HILFE EINES ELEKTROCHROMATOGRAPHISCHEN VERFAHRENS

I. MÁDI
Institut für Physikalische Chemie, L. Kossuth Universität, Debrecen

(*Received* 17 *March* 1961; *in revised form* 16 *June* 1961)

Abstract—By our electrochromatographic method there were various kinds of radioactive atoms separated in a carrier-free state. By a cathodically polarized platinum powder column, for instance, we separated the radioactive kind of atom Y-90 from its parent element, the Sr-90, and the La-140 from the Ba-140, respectively. By an anodically polarized platinum powder column we separated the Pm-147 from the Ce-144, and the natural radioactive kind of atom Bi-212 from its parent element, the Pb-212, respectively.

VOL. 22 1961

AUS IMRES[1,2] neuesten Untersuchungen bezüglich der Elektrolyse trägerfreier radioaktiver Stoffe liess sich erweisen, dass unter Anwendung asymmetrischer Elektrodensysteme und mit Hilfe eines richtigen theoretischen Bildes über die Reduktions-, beziehungsweise Oxydationsvorgänge, die sich auf den Elektroden abspielen,[3] die Methode der Elektrolyse zur Absonderung trägerfreier radioaktiver Atomarten in vielen Fällen erfolgreich angewandt werden kann. Gestützt auf diese grundlegenden Untersuchungen haben wir zur Absonderung trägerfreier radioaktiver Atomarten ein mit Elektrolyse verbundenes, kolonnenchromatographisches Verfahren ausgearbeitet, das bis jetzt in zahlreichen Fällen mit vollem Erfolg angewendet werden konnte.

Wie darüber schon in unserer vorhergegangenen Mitteilung[4] berichtet wurde, lässt sich das Wesen unseres Verfahrens dadurch kennzeichnen, dass man in den elektrolysierenden Stromkreis als Kathode oder als Anode eine Platinpulverkolonne (eingefüllt in ein, unten mit Hahn verschlossenes Glasrohr von 5 mm Durchmesser und 15 cm Länge) einschaltet, während ihr gegenüber als Anode, beziehungsweise als Kathode eine Platinnadel eingeschaltet wird, (je nachdem man die bezügliche radioaktive Atomart kathodisch oder anodisch abscheiden will). Eine schematische Abbildung der Apparatur findet man in Abbild. 1. Bei bestimmter Klemmspannung lässt man die Lösung, welche die abzusondernden Atomarten enthält (und deren Gesamtionenstärke mindestens etwa 0,001 norm. betrug, um bei der gegebenen Spannung mit konstanter Stromintensität arbeiten zu können) durch diese Platinpulverkolonne durchfliessen, indem sich an ihr die entsprechenden radioaktiven Atomarten elektrolytisch ausfallen. Mit Hilfe einer geeigneten Elutionsflüssigkeit löst man dann die einzelnen radioaktiven Atomarten—voneinander getrennt—von der Platinpulverkolonne ab. Im folgenden wollen wir die Brauchbarkeit der Methode durch Darlegung einiger Versuchsergebnisse vorführen.

(1) L. IMRE u. G. FEJES, *Acta Univ. Debr.* **3**, 176 (1955).
(2) L. IMRE u. G. FEJES, *Acta Univ. Debr.* (im Druch)
(3) L. IMRE, *KFKI Közlem.* **7**, 3, (1959).
(4) I. MÁDI, *Naturwisenschaften* **48**, 155 (1961).

1. *Absonderung trägerfreier radioaktiver Atomarten mit Hilfe von kathodisch polarisierter Platinpulverkolonne*

Als experimentelle Grundlage des Verfahrens dienen solche Versuche, die sich auf zeitlichen Ablauf elektrolytischer Ausscheidung radioaktiver Stoffe an asymmetrisch angeordneten, indifferenten Elektroden beziehen. Diese Messungen wurden folgendermassen ausgeführt: in 20 ml der Lösung, welche die entsprechende radioaktive

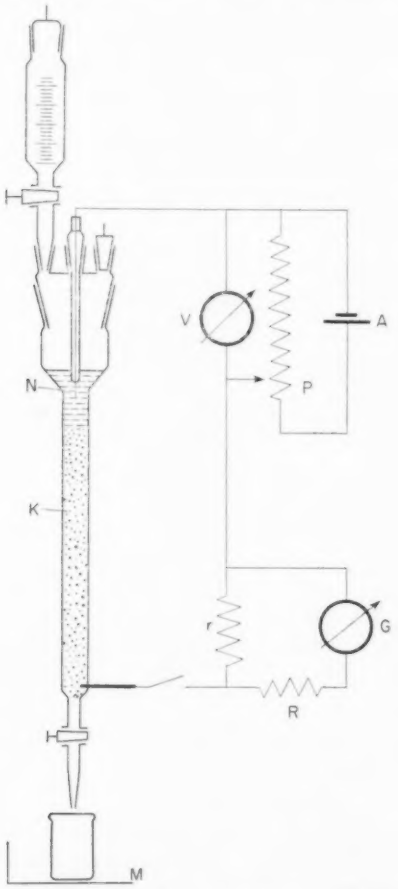

ABB. 1.—Schematische Zeichnung der elektrochromatographischen Einrichtung. *A*: Stromquelle, *P*: Potentiometer, *V*: Voltmeter, *G*: Galvanometer, *r*: Nachschluss, *R*: Vorwiderstand, *K*: Elektrochromatographische Kolonne, *N*: Platinnadelelektrode, *M*: Automatischer Probewechsel.

Ionenart enthielt (und—um die Bildung Radiokolloide zu vermeiden—auch 0·001 norm. stark salpetersauer war), tauchte man unter der vorausgesehenen Klemmspannung eine vorher ausgeglühte und an der einen Seite paraffinierte Platinkathode von 3·14 cm^2 Oberfläche und eine hundertmal kleinere Platinnadelanode ein. Unter intensiver Umrührung belastete man die Elektroden mit der entsprechenden Klemmspannung für die gewünschte Zeit und nachher hebte man sie aus der Lösung (doch vorerst noch ohne Unterbrechung der Klemmspannung). Die Aktivität des auf die

Elektrode ausgefällten Stoffes wurde üblicherweise (mit G.M.-Zählrohr) unmittelbar gemessen. Die Lösung selbst wurde in jedem Falle verdampft, und zwar in einem Platinschälchen, dessen Grundfläche der Oberfläche der Elektrode gleich war; im übrigen wurde die Aktivität jeder einzelnen Lösung unter denselben geometrischen Verhältnissen wie die der Elektroden gemessen. Die radioaktive Stoffmenge, die sich im Laufe der Elektrolyse während der jeweilig vorgesehenen Zeitdauer (t) an der Kathode absonderte, wurde in Bruchteilen der im ganzen System anwesenden Stoffmenge ausgedrückt und als Funktion der Zeit (t) auch graphisch dargestellt. In Abbild. 2a sind z.B. diejenigen Versuchsdaten angeführt, die bezüglich der unter 70 V Klemmspannung ausgeführten Elektrolyse von Y-90 gewonnen worden sind. Die Angaben dieses Abbildes zeigen, dass der Vorgang der elektrolytischen Ausfällung des Y-90 zu einem Gleichgewichtszustande führt. Dieser Gleichgewichtszustand ist dynamischer Natur, und lässt sich dadurch kennzeichnen, dass in der Zeiteinheit ebensoviele Ionen an der Oberfläche der Elektrode sich ausscheiden, wie sich davon zurücklösen. Falls die an der Elektrode befindliche Stoffmenge mindestens eine monoatomare Schicht ausmacht, ist die Anzahl der sich zurücklösenden Atome (auf die Flächen- und Zeiteinheit gerechnet) unabhängig von der schon an der Elektrode abgeschiedenen Menge, d.h. es darf in diesem Falle die chemische Aktivität des abgeschiedenen Stoffes als Konstant betrachtet und mit der Einheit gleichgesetzt werden. Unter solchen Bedingungen kann der Zahlenwert des Elektrodpotentials (E) folgenderweise ausgedrückt werden (wenn man anstatt der Ionenaktivitäten die Konzentrationen einsetzt und sich in bezug auf Symbolik an die Lewis-Randallsche Konvention hält):

$$E = E_0 - \frac{RT}{\nu F} \ln c_{ox} \tag{1}$$

wo E_0 das Normalpotential, c_{ox} aber die Konzentration der in gelöstem Zustande anwesenden Ionen bedeutet.

Bei unseren Untersuchungen war jeweils nur eine Tracer-Menge der abzuscheidenden Stoffart in der Lösung befindlich, deshalb konnte an der Oberfläche der indifferenten Elektrode eine vollständige monoatomare Schicht nicht zustandekommen. Unter solchen Umständen ist nun aber die Wahrscheinlichkeit der Umwandlung der schon abgeschiedenen Atome in einen Ionenzustand proportional der Menge des schon an der Elektrode abgeschiedenen Stoffes. Dies gelangt im Herzfeldschen Prinzip[5] zum Ausdruck, laut dessen der Wert des Gleichgewichtspotentials bezüglich der kathodischen Ausfällung mit Hilfe der folgenden Gleichung dürfte ausgedrückt werden:

$$E = E^0 + \frac{RT}{\nu F} \ln \frac{c_{red}}{c_0 - c_{red}} \tag{2}$$

wo c_0 die Konzentration der am Anfang der Elektrolyse in gelöstem Zustande anwesenden radioaktiven Ionen, c_{red} die Konzentration der an der Oberfläche der Elektrode abgeschiedenen (im Reduktionszustande befindlichen) Ionen und $c_0 - c_{red} = c_{ox}$ die Konzentration der im Gleichgewichtszustande (in der Lösung) befindlichen Ionen bedeutet.

Enthält die Lösung zwei Arten von radioaktiven Stoffen, so hängt das Konzentrationverhältnis der schon abgeschiedenen radioaktiven Stoffe—im Sinne der

[5] K. HERZFELD, *Physik. Zeit.* **14**, 29 (1913).

VOL. 22 1961

Herzfeldschen Konzeption—vom Potential folgendermassen ab:

$$\frac{c_{\mathrm{red}(1)}}{c_{\mathrm{red}(2)}} = \frac{c_{0(1)}}{c_{0(2)}} \left\{ \frac{1 + \exp\left[\frac{(E - E_2^0)vF}{RT}\right]}{1 + \exp\left[\frac{(E - E_1^0)vF}{RT}\right]} \right\} \tag{3}$$

wo $c_{\mathrm{red}}(1)/c_{\mathrm{red}}(2)$ das Konzentrationverhältnis der an der Kathode—beim Potential E—abgeschiedenen Ionen, $c_0(1)/c_0(2)$ das Konzentrationverhältnis der anfänglich gegenwärtigen Atomarten, E_1^0 und E_2^0 aber die entsprechenden Normalpotentiale bedeuten. Im Sinne des Zusammenhanges ändert sich der Zahlenwert des Verteilungskoeffizienten (für die Verteilung zwischen der Kathode und der Lösung) mit dem Elektrodenpotential etwa folgendermassen:

$$\frac{y_\infty}{x_\infty} = \text{const} \,.\, \exp - \left(\frac{EvF}{RT}\right) \tag{2a}$$

(x_∞ bedeutet die Höchstmenge des auf die Elektrode ausgefällten radioaktiven Stoffes und y_∞ die Menge des in der Lösung verbliebenen radioaktiven Stoffes, beide im Prozent der gesamten radioaktiven Stoffmenge des Systems ausgedrückt). Die im Laufe befindlichen Untersuchungen unseres Institutes lassen uns wohl den Schluss zu, dass diese Gleichung (obwohl sie nicht *völlig* den Erfahrungen entspricht, die wir bei der Elektrolyse radioaktiver Stoffe haben gewinnen können) hinsichtlich des Problems, das in dieser Arbeit behandelt wird, als geeignet betrachtet werden kann.

Auf Grund dieser Gleichung kann geschlossen werden, dass eine als Elektrode geschaltete Platinpulverkolonne zur Absonderung radioaktiver Atomarten gebraucht werden mag, sofern man jene vom System gebotene Möglichkeit benützt, dass sich die verschiedenen Ionen an der Platinpulverkolonne bei bestimmten Elektrodenpotentialen in einer ihren Normalpotentialen entsprechenden Reihenfolge ausscheiden. Steigert man den Grad dieser Absonderung noch unter Zuziehung von geeigneten Elutionslösungen, so kann die Methode auch zur Absonderung einander nahestehender Ionen gebraucht, und in der Trennung eine ausserordentlich grosse radiochemische Reinheit erreicht werden, insoferne für die Reinheit der Elutionslösung in genügendem Masse gesorgt worden war.

Eine direkte Folge der in Abbild. 2a dargestellten Versuchsangaben ist z.B., dass aus der die Atomarten Sr-90 und Y-90 enthaltenden Lösung das radioaktive Y-90 quantitativ in *einem* Schritte abgesondert werden kann, da sich das Sr-90 an der als Kathode eingeschalteten Platinpulverkolonne elektrolytisch nicht ausscheidet, während sich das Y-90 bei der angegebenen Klemmspannung ausfällt. Wir haben einfach so verfahren, dass wir durch die als Kathode eingeschaltete Platinpulverkolonne—unter 70 V Klemmspannung—eine solche (0·001 norm. salpetersaure) Lösung durchfliessen liessen, in der das Y-90 mit dem Sr-90 in radioaktivem Gleichgewicht stand. Das Y-90 liess sich an der Platinpulverkathode elektrolytisch niederschlagen, die durch den Hahn gewonnene Lösung enthielt nur die Atomart Sr-90. Nachher wurde die Platinpulverkolonne unter Spannung mit 0·001 norm. Salpetersäurelösung längere Zeit gewaschen, um dann (nach Ausschaltung der Spannung) die radioaktive Atomart Y-90 mit 0·1 norm. Salpetersäurelösung zu eluieren. Unsere Messungsangaben sind in Abbild. 3a angeführt, wo die Aktivität der durch die Kolonne durchflossenen Flüssigkeit als Funktion der Ausströmungszeit dargestellt ist. (Ausströmungsgeschwindigkeit: 0·5 ml/min).

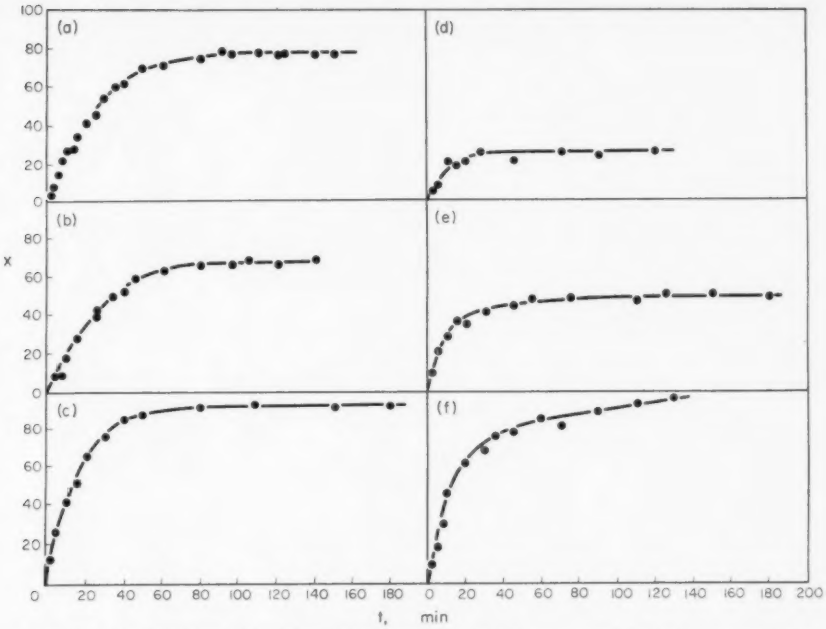

Abb. 2.—(a) Zeitlicher Ablauf der Elektrolyse des Y-90 (Klemmspannung 70 V; Stromdichte 5·0 mA/cm²).
(b) Zeitlicher Ablauf der Elektrolyse des La-140. (Klemmspannung 70 V; Stromdichte 5·05 mA/cm²).
(c) Zeitlicher Ablauf der anodischen Elektrolyse des Ce-144. (Klemmspannung 3 V; Stromdichte 0·12 mA/cm²).
(d) Zeitlicher Ablauf der Adsorption des Tl-204 auf einer passivierten Platin-Oberfläche.
(e) Zeitlicher Ablauf der anodischen Ausscheidung des Pm-147. (Klemmspannung 3 V; Stromdichte 0·13 mA/cm²).
(f) Zeitlicher Ablauf der anodischen Ausscheidung des Pb-212. (Klemmspannung 3 V; Stromdichte 0·13 mA/cm²).*

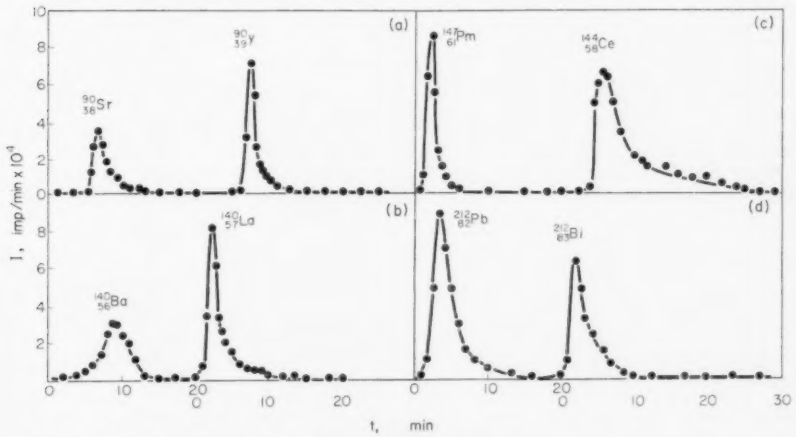

Abb. 3.—(a) Absonderung des Y-90 von der Atomart Sr-90.
(b) Absonderung des La-140 von seinem Mutterelement, dem Ba-140.
(c) Absonderung des Pm-147 von der Atomart Ce-144.
(d) Absonderung des Bi-212 von seinem Mutterelement, dem Pb-212.

* Unter "Stromdichte" versteht man die Stromdichte unmittelbar an der Kathode bzw. an der Anode.

VOL. 22 1961

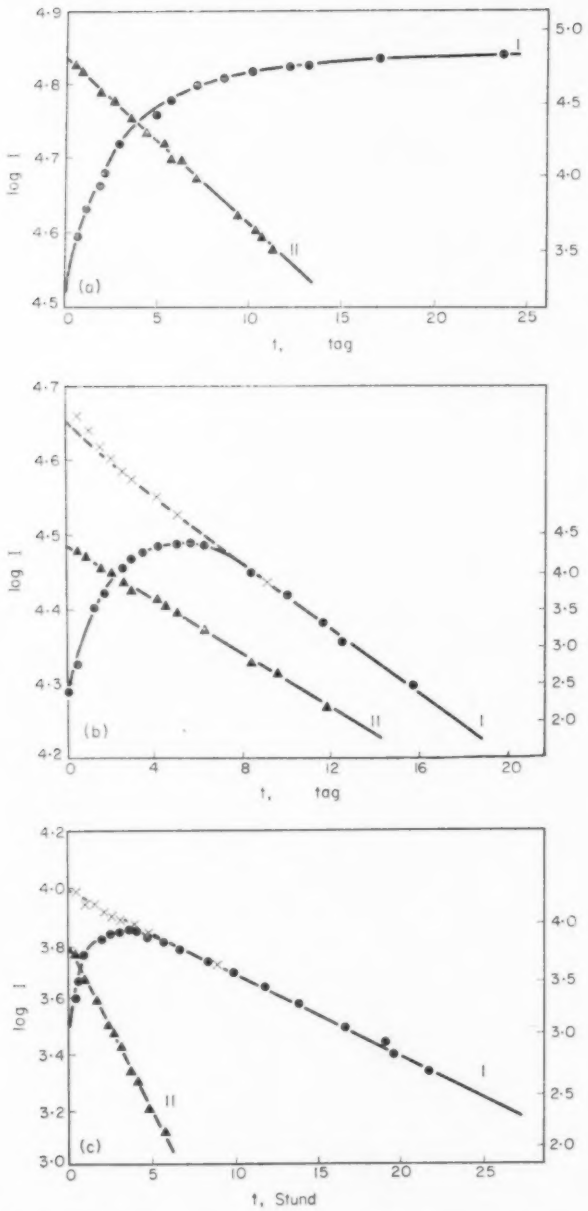

ABB. 4.—(a) I. Zunahme der Aktivität der die Atomart Sr-90 enthaltneden Fraktion nach der Absonderung
II. Zeitliche Abnahme der Aktivität des abgesonderten Y-90.
(b) I. Zunahme der Aktivität der die Atomart Ba-140 enthaltenden Fraktion nach der Trennung. (Mit der Strichellinie haben wir die theoretische Kurve dargestellt).
II. Zeitliche Abnahme der Aktivität des abgesonderten La-140.
(c) I. Zunahme der Aktivität der die Atomart Pb-212 enthaltenden Fraktion nach der Absonderung.
II. Zeitliche Abnahme der Aktivität der abgesonderten Fraktion Bi-212.

Den Gehalt der einzelnen Fraktionen an der betr. radioaktiven Substanz haben wir durch Aktivitäts-Messungen festgestellt. Wir bestimmten z.B. die zeitliche Zunahme der β-Aktivität der Sr-90 Fraktion, d.h. ihre Anreicherung am Y-90. Aus Abbild. 4aI ist wohl ersichtlich, dass die Aktivität dieser Fraktion mit der Zeit zunimmt, bis zur Erreichung des radioaktiven stationären Zustandes. Was die Reinheit der Fraktion von Y-90 anbelangt, diese wurde derart geprüft, dass man die Zerfallsgeschwindigkeit untersuchte. Die Halbwertzeit ergab sich (nach den Angaben des Abbilds 4aII zu 63·2 Stunden; eine nenneswerte Verunreinigung von Sr-90 konnte also in der Y-90 Fraktion nicht nachgewiesen werden.

Den zeitlichen Ablauf der Elektrolyse der in unendlich geringer Konzentration anwesenden Atomart La-140 (ebenfalls unter 70 V Klemmspannung) sieht man an Abbild. 2b. Unter den gegebenen Bedingungen liess sich das Mutterelement Ba-140 elektrolytisch an der Kathode nicht ausfällen. Demzufolge ist es möglich, das Tochterelement La-140 quantitativ abzusondern, u.z. in der Weise, dass man die (0·001 norm. salpetersäurige) Lösung (die das Ba-140 in Gleichgewicht mit dem La-140 enthält) unter 70 V Klemmspannung durch die als Kathode eingeschaltete Platinpulverkolonne durchfliessen lässt: das La-140 scheidet sich elektrolytisch aus, und die ausfliessende Lösung enthält nur das Ba-140. Die Kolonne, die nur die Atomart La-140 enthält, wird mit norm. Salpetersäure eluiert. Die Versuchsangaben sind im Abbild. 3b aufgezeichnet. Die Reinheit der die Atomart La-140 enthaltenden Fraktion wurde derart geprüft, dass man die Zerfallsgeschwindigkeit des La-140 bestimmte. Die Halbwertzeit ergab sich (nach den Angaben des Abbilds 4bII.) zu 40·8 Stunden. Auch die Angaben des Abbildes 4bI liefern den Beweis, dass es uns gelang, das La-140 von seinem Mutterelement quantitativ abzusondern. Es stellte sich klar heraus, dass die Aktivität der Ba-140-Fraktion nach der Absonderung des La-140 vorerst zunimmt, um einen Höchswert zu überschreiten und nachher abzunehmen.

Der Wert der jeweiligen relativen Strahlintensität vom Ba-140 und La-140 (I) lässt sich mit Hilfe der folgenden Gleichung auszudrücken:

$$I = e^{-\lambda_1 t} + k \frac{\lambda_2}{\lambda_2 - \lambda_1} e^{-\lambda_1 t} [1 - e^{-(\lambda_2 - \lambda_1)t}] \tag{4}$$

wo $k = k_1/k_2$ das Verhältnis der Ionisierungsfähigkeiten der β-Strahlen des La-140, beziehungsweise des Ba-140 bedeutet, dessen Wert von den Versuchsangaben des Abbilds 4bI. folgendermassen hergeleitet werden kann:

$$k = \frac{\lambda_1}{\lambda_2} I_{\max} e^{\lambda_2 t_{\max}} \tag{5}$$

(λ_1 bedeutet die Zerfallskonstante des Ba-140, λ_2 die des La-140, $I_{\max}$ den im Zeitpunkt $t_{\max}$ erreichten Höchstwert der relativen Strahlintensität. Aus den Versuchsangaben ergab sich der Zahlenwert: $k = 1{\cdot}90$.)

Wenn schon das laufende Gleichgewicht sich eingestellt hat, dann verschwindet der Faktor $\exp[-(\lambda_2 - \lambda_1)t]$, deshalb kann der Wert der relativen Strahlintensität folgendermassen ausgedrückt werden:

$$I^* = e^{-\lambda_1 t}\left(1 + k \frac{\lambda_2}{\lambda_2 - \lambda_1}\right) = e^{-\lambda_1 t}\left(\frac{\lambda_2 - \lambda_1 + k\lambda_2}{\lambda_2 - \lambda_1}\right) \tag{4a}$$

VOL. 22 1961

Durch Vergleich der Gleichungen (4) und (4a) bekommt man folgendes:

$$\frac{I^*}{I} = \frac{\lambda_2 - \lambda_1 + k\lambda_2}{\lambda_2 - \lambda_1 + k\lambda_2[1 - e^{-(\lambda_2 - \lambda_1)t}]} = q$$

und schliesslich:

$$I^* = qI = \text{konstans} \,.\, e^{-\lambda_1 t} \tag{4b}$$

wo

$$\text{konstans} = 1 + \frac{k\lambda_2}{\lambda_2 - \lambda_1}$$

Das heisst: multipliziert man den Wert der jeweiligen relativen Strahlungsintensität mit dem jeweiligen Faktor q, so erhält man eine solche Folge von Zahlenwerten (in Abbild. 4bI gestrichelt dargestellt), deren Logarithmen eine der Zerfallsperiode des Ba-140 entsprechende Gerade ergeben.

Die Angaben, die zur Berechnung der gestrichelten Linie nach Gl.(4b) nötig waren, sind in Tabelle 1 enthalten. ($\lambda_1 = 0{\cdot}0022$ Stunde^{-1}, $\lambda_2 = 0{\cdot}0173$ Stunde^{-1}, $k = 1{\cdot}90$.)

TABELLE 1.—ANGABEN ZUR BERECHNUNG DER THEORETISCHEN KURVE

t_{Tag}	$k\lambda_2\{1 - \exp[-(\lambda_2 - \lambda_1)t]\}$	q	$\log qI$
0·5	0·00544	2·3	4·6730
1·0	0·00997	1·9	4·6434
1·5	0·01506	1·6	4·6232
2·0	0·01693	1·5	4·6170
2·5	0·01958	1·4	4·5963
3·0	0·02180	1·3	4·5852
4·0	0·02527	1·19	4·5550
5·0	0·02758	1·12	4·5405
6·0	0·02860	1·08	4·5152
9·0	0·03173	1·02	4·4315

Nach Abbild. 4bI lässt sich folgern, dass die Ba-140 Fraktion am Anfang nur eine Minimalmenge der Atomart La-140 enthielt, trotzdem dürfte die Trennung der beiden Atomarten als beinahe quantitativ erscheinen.

2. *Absonderung trägerfreier radioaktiver Atomarten mit Hilfe von anodisch polarisierten Platinpulverkolonnen*

Zahlreiche Forscher, die sich mit der Untersuchung der elektrolytischen Ausfällung radioaktiver Stoffe beschäftigen, haben schon früher bemerkt,[6–8] dass bei der Elektrolyse von Po, ThB, Pa u.a. eine gewisse Aktivität auch an der Anode erscheint, dass also diese radioaktiven Ionenarten sich teilweise auch an der Anode ausscheiden. Es wurde angenommen, dass sich diese Elemente in Form ihrer Oxyde oder Peroxyde ausscheiden, wie dies auch bei der Elektrolyse einer Makromenge von Blei beobachtet wird. Von unseren Untersuchungen, die mit Hilfe des L. Imreschen Verfahrens asymmetrischer Elektrodensysteme ausgeführt wurden, stellte sich heraus, dass nicht

[6] G. HEVESY u. F. PANETH, *Monatsh.* **36**, 75, (1915).
[7] O. ERBACHER u. K. PHILIPP, *Z. Phys.* **51**, 311, (1928).
[8] H. EMMANUEL u. M. HAISSINSKY, *C.R. Acad. Sci., Paris* **206**, 1102. (1934).

nur die obenerwähnten radioaktiven Atomarten, sondern auch das Ce-144 sowie das Pm-147 sich an der Anode abscheiden lässt. Unsere Versuche zeigten, dass die Menge des Ceriums, die sich an der Anode bei geeigneten Klemmspannungen niederschlägt, mit der Zeit der Elektrolyse zunahm, um nach einer bestimmten Zeit einen definierten Gleichgewichtszustand zu erreichen. Deshalb dürfte sich nach ROGERS[9] auch zur Beschreibung der anodischen Ausfällung solcher Ionenarten das Herzfeldsche Prinzip anwenden lassen, laut dessen der Wert des für die anodische Ausfällung charakteristischen Gleichgewichtspotentials mit der folgenden Gleichung ausgedrückt werden kann:

$$E = E^0 + \frac{RT}{\nu F} \ln \frac{c_0 - c_{ox}}{c_{ox}} \tag{6}$$

wo E^0 das Normalpotential der Redoxyelektrode, c_0 die gesamte Konzentration der vor der Elektrolyse anwesenden Ionen, schliesslich c_{ox} die Konzentration der an der Elektrode abgeschiedenen Ionen bedeuten. Drückt man die an der Anode ausgeschiedene Stoffmenge in Prozenten der im ganzen System befindlichen radioaktiven Stoffmenge, so ergibt sich folgendes:

$$E = E^0 + \frac{RT}{\nu F} \ln \frac{y_\infty}{x_\infty} \tag{6a}$$

(x_∞ bedeutet die relative Menge der an der Anode ausgeschiedenen, y_∞ aber die der in der Lösung verbliebenen entsprechenden Ionen). Aus dieser Gleichung ist ersichtlich, dass auch im Falle der anodischen Ausfällung (sofern die ausgeschiedene Stoffmenge *höchstens* je eine monomolekuläre Schicht zustandebringt) der Verteilungskoeffizient (in bezug auf die Gleichgewichts-Verteilung zwischen der Anode und der Lösung) ähnlich der Gleichung (2a), sich mit dem Elektrodenpotential folgendermassen ändert:

$$\frac{y_\infty}{x_\infty} = \text{Konst} \,.\, e^{\frac{E\nu F}{RT}} \tag{7}$$

Obwohl diese Gleichung den Zusammenhang der Faktoren, die auf die anodische Ausscheidung Einfluss ausüben, nur annähernd ausdrükt, darf sie bezüglich des hier behandelten Problems als erste Annäherung wohl angewendet werden. Demgemäss tritt auch bei der anodischen Ausfällung ein Gleichgewichtszustand ein, wie dies durch unsere Versuchsangaben nach Abbild. 2c ebenfalls bewiesen wird. Diese Angaben beziehen sich auf die Elektrolyse von je 20 ml 0·001 norm. salpetersäurigen Ce-144 Lösungen unter 3 V Klemmspannung.

Schon früher waren die Forscher darin einverstanden, dass im Zustandekommen der Oxyd- und Peroxydprodukte der an der Anode elektrolytisch ausgeschiedene nascente Sauerstoff eine grosse Rolle spielt, doch wurden jene neueren Beobachtungen ausser Acht gelassen, die auf eine anodische Passivierung des Platins hindeuten.[10] An der Oberfläche des Platins entsteht bei der Elektrolyse der verdünnten salpetersäurigen Lösung eine Oxydschicht und die in dieser Schicht befindlichen Sauerstoffatome bilden eine Brücke zwischen der Platinoberfläche und den Oxydprodukten des radioaktiven Stoffes.

Aus den neuesten Beobachtungen bezüglich der Verdrängungswirkung, welche die durch anodische Elektrolyse entstandenen Oxydschichten auf die Adsorption der

[9] L. B. ROGERS u. A. F. STEHNEY, *J. Electrochem. Soc.* **95**, 33 (1949).
[10] A. FRUMKIN u. E. AIKASJAN: *Ber. Akad. Wiss. Ud. S.S.R.* **100**, 315 (1955).

VOL. 22 1961

Anionen ausüben, wurde auch festgestellt,[11] dass die auf der Platinoberfläche entstandenen Oxyde solche Dipole bilden, deren negative Teile sich gegen die Lösung orientieren. Dieses Verhalten suchten wir in der Weise nachzuweisen, dass wir die 0·001 norm. salpetersäurige Lösung—unter den obenerwähnten Bedingungen—ohne Anwesenheit irgendwelcher radioaktiven Atomart elektrolysierten. Der nascente Sauerstoff, der bei der Elektrolyse der verdünnten salpetersäurigen Lösung entsteht, passiviert die Oberfläche des Platins. Nach einer Elektrolyse von 10 Minuten unterbrachen wir den Stromkreis und gaben der Lösung eine entsprechende Menge radioaktiven Stoffes zu. Den Zeitpunkt, im dem der radioaktive Stoff zugesetzt wurde, haben wir folgerichtig als kinetischen Nullpunkt ($t = 0$) angenommen. Zum Beispiel lassen sich die Tl-204-Ionen an der Oberfläche des Platinblechs, die wir auf die erwähnte Weise polarisiert haben auch ohne Elektrolyse ausscheiden, dieser Ausscheidungsprozess führt jedoch, wie dies die Angaben des Abbildes. 2d zeigen, zu einem Gleichgewichtszustande. Das ist keine elektrolytische Ausfällung (denn es wurde ja der Stromkreis vor der Beimengung des Tl-204 ausgeschaltet), sondern eine Adsorption der Tl-204-Ionen auf der passivierten Platin-Oberfläche. Da unter den erwähnten Bedingungen an einer nichtpassivierten Platinoberfläche keine Adsorption des Tl-204 beobachtet werden konnte, dürfte unser Versuchsergebnis darauf zurückzuführen sein, dass die Platinoxyd-Dipole die adsorptive Bindung des Tl-204 bewirkten.

Unter ähnlichen Umständen haben wir eine Lösung mit Pm-147 Gehalt bei 3 V Klemmspannung elektrolysiert. Es ergaben sich die Versuchsangaben, die in Abbild. 2e angeführt worden sind. Daraus lässt sich klar erkennen, dass die relative Menge des Pm-147, die sich an der Oberfläche der Platinanode abscheiden liess, trotz der gleichen Versuchsbedingungen, wesentlich geringer ist, als die entsprechende Menge des Ce-144. Dies erscheint zu beweisen, dass sich das Ce-144 in Anbetracht der anodischen Ausscheidung wesentlich anders verhält, als das Pm-147. Lässt man also eine Lösung, die die radioaktiven Atomarten Ce-144 und Pm-147 enthält (ungefähr mit 0·2 ml/min. Ausströmungsgeschwindigkeit) durch eine solche Platinpulverkolonne durchfliessen, die unter 3 V Klemmspannung als Anode eingeschaltet wurde, dann wird sich sowohl das Ce-144 wie das Pm-147 an der Oberfläche der Anode niederschlagen. Weil aber das Ce-144 zur anodischen Ausfällung wesentlich mehr geneigt ist, wird es sich dabei vom Pm-147 absondern. Den Grad der Absonderung kann man unter Anwendung einer geeigneten Elutionslösung sogar noch steigern. Unsere Versuche, deren Ergebnisse in Abbild. 3c dargestellt sind, haben bewiesen, dass eine vollständige Abtrennung zu erreichen ist, wenn man von der Oberfläche der Platinanode die Atomart Pm-147 mit 0·1 norm. salpetersäuriger Lösung, und nachher das Ce-144 mit 1 norm. salpetersäuriger Lösung eluiert. Die Reinheit der Fraktion, die die radioaktive Atomart Pm-147 enthielt, wurde in der Weise geprüft, dass man mit Hilfe von Absorptionsmessungen (unter Anwendung von Aluminiumfolien als Absorbentien) die Dicke der Halbierungsschicht bestimmte. Diese Messungsangaben sind in Abbild. 5 angeführt. Nach der Angaben des Abbildes ergibt sich für den maximalen Energiewert der β-Strahlen 0·230 MeV, in guter Ubereinstimmung mit anderweitig bestimmten Werten. Was aber die Reinheit der Ce-144-Fraktion betrifft, diese wurde derart geprüft, dass man diese Fraktion mehrmals durch die Platinpulverkolonne fliessen liess: es liessen sich dabei keinerlei nennenswerten Spuren von Pm-147 nachweisen. (Die Aktivität sowohl des Pm-147 wie des Ce-144 wurde etwa

[11] N. BALASCHOWA: *Ber. Akad. Wiss. Ud.S.S.R.* **103**, 639 (1955).

in 170 Minuten nach der Beendigung der Abtrennung gemessen, damit die Aktivität des Pr-144, das anfänglich in der Pm-147-Fraktion enthalten war, vollkommen abklingt, beziehungsweise das Ce-144 mit dem Pr-144 in radioaktives Gleichgewicht gelangt).

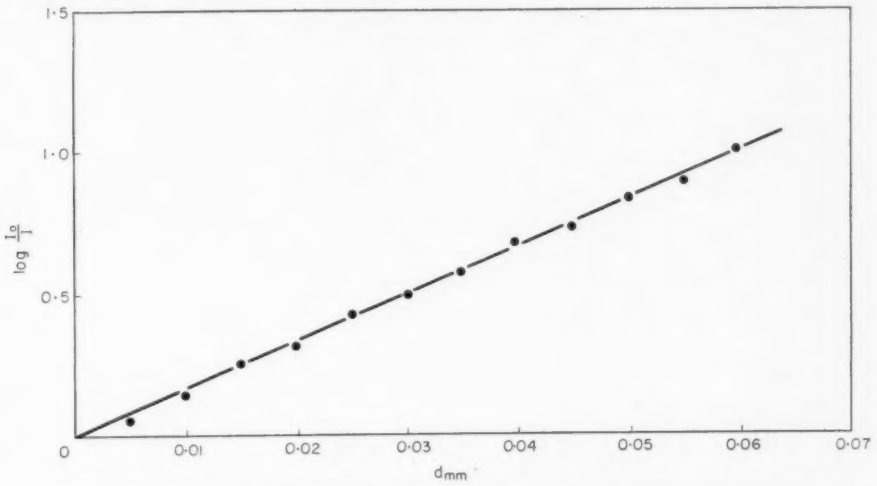

Abb. 5.—Absorption der β-Strahlen der abgesonderten Fraktion Pm-147 in Aluminium.

Es lässt sich auch theoretisch erklären, warum das Ce-144, das sich aus 0·001 norm. salpetersäuriger Lösung an der Platinpulveranode abgeschieden hat, durch eine stärkere Säure in Lösung gebracht wird. Es findet nämlich im Anodenraume der folgende Oxydationsprozess statt:

$$Ce^{3+} + 2H_2O \rightleftharpoons CeO_2 + 4H^+ + e^-$$

Der Wert des für den Prozess bezeichnenden Gleichgewichtspotentials kann mit Hilfe der folgenden Gleichung angegeben werden:

$$E = E^0 - \frac{RT}{\nu F} \ln (a_{H^+})^4 + \frac{RT}{\nu F} \ln \frac{y_\infty}{x_\infty} \qquad (8)$$

wo a_{H^+} die Aktivität der Wasserstoffionen bedeutet. Auch die Versuchsergebnisse, die wir in Abbild. 6 angeführt haben, bestätigen diesen Zusammenhang: es ersieht sich, dass die Logarithmen der Zahlenwerte des Verteilungskoeffizienten mit den p_H-Werten sich linear ändern, wie dies die Gleichung (8) erfordert. (Die ziemlich beträchtliche Abweichung, die sich im 0·1 norm. salpetersäurigen Mittel bemerkbar macht, dürfte man darauf zurückführen können, dass in solchen Lösungen von höherer Konzentration der Zahlenwert des Aktivitätskoeffizienten von der Einheit abweicht.)

Mit diesem elektrochromatographischen Verfahren konnten wir auch einige Glieder der natürlichen radioaktiven Reihen in trägerfreiem Zustande absondern. Die Absonderung des Bi-212 vom Pb-212—zum Beispiel—ist ebenfalls möglich, wenn man die Platinpulverkolonne als Anode einschaltet. Wird nämlich die 0·001 norm. salpetersäurige Lösung von Pb-212 unter 3 V Klemmspannung anodisch elektrolysiert (mit den asymmetrisch angeordneten Platinelektroden, die wir in Verbindung mit der Elektrolyse des Ce-144 bekanntgemacht haben), dann nimmt die Aktivität der Platinanode zeitlich den Angaben des Abbildes 2f gemäss zu. Es scheint in der Elektrolyse

des Pb-212 kein eigentliches Gleichgewicht vorzuliegen; soviel kann sich aber doch feststellen, dass je mehr sich die von aussen angelegte Potential vom Abscheidungspotential unterscheidet, um so vollständiger ist die elektrolytische Abscheidung der Mikrokomponente. Obwohl nun demzufolge die obenerwähnten Formeln (für die Verteilungskoeffizienten) ungültig sind, ergibt sich doch aus der Tatsache, dass sich das Pb-212 an der Anode abscheiden lässt, doch eine Hoffnung, dass es vom Bi-212

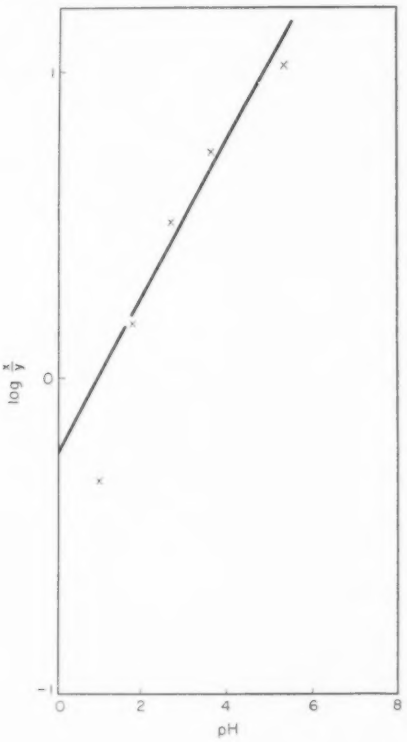

ABB. 6.—Wirkung der Wasserstoffionkonzentration auf die anodischeAusfällung der Ce-144

abgesondert werden kann. Die Versuchsangaben in Abbild. 3d zeigen tatsächlich, dass unter Anwendung von zweckmässig erwählten, geeigneten Elutionslösungen die Absonderung erfolgreich durchgeführt werden kann. Es wurde folgendermassen vorgegangen: eine 0·1 norm. salpetersäurige Lösung, die das Pb-212 (in radioaktivem Gleichgewicht mit Bi-212) enthielt, liessen wir unter 3 V Klemmspannung durch die Platinpulverkolonne fliessen. Sowohl das Pb-212 wie das Bi-212 liess sich an der Anodenfläche elektrolytisch ausscheiden. (Es ist nicht wahrscheinlich, dass in einer 0·1 norm. salpetersäurigen Lösung nur die gewöhnliche Adsorption hätte stattfinden können). Nachher eluierten wir das Pb-212 mit 1 norm. Salpetersäure, dann das Bi-212 mit 5 norm. Salpetersäure. Die Reinheit der beiden Fraktionen wurde durch Aktivitäts-Messungen geprüft. In Abbild. 4cII ist die Zerfallskurve des so abgetrennten Bi-212 dargestellt; es lässt sich erkennen, dass keine Pb-212-Verunreinigung vorhanden war. Die mit gestrichelter Linie dargestellte theoretische Kurve in Abbild. 4cI haben wir auf Grund der Gleichungen (5) und (4b) berechnet. Das Verhältnis der Ionisierungsfähigkeiten nach der Gleichung (5) hatte den Wert:

$k = 2{\cdot}24$; $\lambda_1 = 0{\cdot}0654$ Stunde^{-1}, $\lambda_2 = 0{\cdot}692$ Stunde^{-1}. Die Angaben, die zur Berechnung des in der Gleichung (4b) befindliche Faktors q nötig sind, enthält die Tabelle 2.

Aus dem Verlaufe der theoretischen Kurve wird man wohl schliessen können, dass die Pb-212-Fraktion unmittelbar nach der Trennung überhaupt keine nachweisbaren Spuren von Bi-212 enthielt.

Es ist wohl zu hoffen, dass das hier beschriebene elektrochromatographische Verfahren unter Anwendung einer längeren Platinpulverkolonne auch in verwickelteren Systemen erfolgreich gebraucht werden kann, in erster Linie zur Herstellung trägerfreier radioaktiver Präparate. Über diesbezügliche Untersuchungen soll in weiteren Mitteilungen berichtet werden.

TABELLE 2.—DIE ANGABEN ZUR BERECHNUNG DES FAKTORS q

t_{Stund}	$k\lambda_2\{1 - \exp[-(\lambda_2 - \lambda_1)t]\}$	q	$\log qI$
0·5	0·411	2·07	3·9960
1·0	0·709	1·54	3·9479
1·5	0·929	1·40	3·9364
2·0	1·086	1·26	3·9105
2·5	1·202	1·17	3·8881
3·0	1·289	1·12	3·8796
4·0	1·396	1·06	3·8578
5·0	1·407	1·05	3·8413
9·0	1·512	1·005	3·7240

VOL. 22 1961

Zusammenfassung

Es wurde ein neuartiges elektrochromatographisches Verfahren beschrieben, welches sich geeignet erwies radioaktive Atomarten in trägerfreiem Zustande gegeneinander abzugrenzen. Das Wesen der Methode besteht darin, dass man in den elektrolysierenden Stromkreis eine Platinpulverkolonne als Kathode bzw. als Anode (ihr gegenüber aber eine Platinnadel als Anode bzw. als Kathode) einschaltet, je nachdem man die bezüglichen Atomarten kathodisch oder anodisch absondern will. Unter Anwendung geeingeter Klemmspennungen wird die Lösung, die die abzusondernden radioaktiven Atomarten enthält, durch diese Platinpulverkolonne durchfliessen gelassen: dabei werden die vorgesehenen radioaktiven Atomarten an der Platinpulverkolonne elektrolytisch ausgefällt. Mit Hilfe von geeigneten Elutionslösungen werden nun die einzelnen radioaktiven Atomarten nacheinander von der Platinpulverkolonne abegelöst. Die Reinheit der abgesonderten radioaktiven Atomarten wurde mit Hilfe von Aktivitäts Messungen geprüft.

Mit Hilfe dieses Verfahrens wurde u.a. die radioaktive Atomart Y-90 von ihrer Muttersubstanz Sr-90 und das La-140 von der radioaktiven Atomart Ba-140 abgesondert. Unter Einschaltung der Platinpulverkolonne als Anode konnten solche radioaktiven Ionen, die zum Redozprozess geneigt sind, von anderweitigen Ionenarten abgetrennt werden. Es konnte u.a. das Pm-147 von der Atomart Ce-144, die natürlich-radioaktive Atomart Bi-212 von dem Pb-212 abgesondert werden.

Anerkennungen—Zuletzt möchte ich hier die Gelegenheit ergreifen, Herrn Prof. Dr. L. IMRE für die Hilfe, die er mir im Laufe dieser Arbeit zu gewähren gefällig war, meinen besten Dank auszudrücken.

J. Inorg. Nucl. Chem., 1961, Vol. 22, pp. 183 to 191. Pergamon Press Ltd. Printed in Northern Ireland

ELECTRONIC ABSORPTION SPECTRA OF ACETYLACETONATO COMPLEXES—II

HÜCKEL LCAO-MO CALCULATIONS FOR COMPLEXES WITH TRIVALENT TRANSITION METAL IONS

D. W. BARNUM
Shell Development Co., Emeryville, California

(*Received* 28 *February* 1961; *in revised form* 5 *June* 1961)

VOL. 22 1961

Abstract—Hückel LCAO-MO calculations were used to estimate the effect of metal–ligand π-bonding on the electronic transition energies in a series of acetylacetonato complexes with trivalent transition metal ions. Coulomb and exchange integrals were estimated respectively from electronegativities and bond energy data, except for the exchange integral for the metal–oxygen π-bond which was left as a variable parameter. The results allow most of the ultra-violet absorption bands to be assigned to specific transitions. Very good agreement between calculated and observed energies was obtained.

Metal–ligand π-bonding, which increases throughout the series $Ti(acac)_3$, $V(acac)_3$, $Cr(acac)_3$, $Mn(acac)_3$, $Fe(acac)_3$, and $Co(acac)_3$, causes the $\pi_3 \rightarrow \pi_4$ transition to split into four bands. One band, which is less intense, is independent of π-bonding whereas the other three shift to higher energy. The $d_\varepsilon \rightarrow \pi_4$ transition is split into three bands by π-bonding. One less intense band shifts to lower energy with increasing metal–ligand π-interaction. The other two overlap and are nearly independent of π-bonding.

IN a previous paper[1] simple LCAO–MO calculations were used to help interpret the absorption spectra of a series of acetylacetonato complexes with trivalent transition metal ions. Since then, slightly better calculations have been carried out which allow a much more complete interpretation of the spectra, including rough estimates of the energy of metal–oxygen π-bonding. The purpose of the present paper is to describe the calculations, present the results, and assign observed absorption bands to specific transitions.

One of the main difficulties with the Hückel LCAO-MO model is in estimating the relative values of the Coulomb integrals and exchange integrals when atoms other than carbon are present. The difficulty becomes greater the further apart the electronegativities of the different atoms are. In a chelate we have the two extremes of very electronegative atoms on the ligand and an electropositive metal ion. A common practice in treating organic molecules is to leave these as variable parameters that can be chosen to give the best fit with some experimentally determined quantity such as the position of an absorption band or the resonance energy. However, in the present work, the exchange integrals were estimated from bond energies and the Coulomb integrals were estimated from absolute electronegativities. This has the advantage that it eliminates adjustable parameters. The same general procedure has been used to calculate the energy levels of several enolate ions of β-diketones with good results.[2]

[1] D. W. BARNUM, *J. Inorg. Nucl. Chem.* **21**, 221–237 (1961).
[2] D. W. BARNUM, π-Energy Levels and Absorption Spectra of Some Enolate Ions, in preparation.

BELFORD *et al.*[3] made a similar calculation for the acetylacetonate ion. For the copper chelate however, they treated the metal as a point positive charge rather than including the metal orbitals. The effect of the positive charge has been discussed in detail elsewhere.[1,4] In the present treatment the metal *d*-orbitals are included. This makes it possible to estimate the energies of the electron transfer absorption bands and to determine the effect of metal–ligand π-bonding on the energy levels.

METHOD OF CALCULATION

For the details of the Hückel LCAO-MO model, the reader is referred to the original literature[5] or any recent textbook on quantum chemistry.[6,7] The result of the mathematical development is that the energy levels are given by the following determinant:

$$\det |H_{ij} - S_{ij}E| = 0,$$

where E is the energy and the H_{ij} are defined in the following section. Since the ϕ_i have been normalized, we have, when $i = j$:

$$S_{ij} = S_{ii} = \int \phi_i^2 \, dv = 1.$$

The *overlap integral* is $S_{ij} = \int \phi_i \phi_j$ where $i \neq j$. As is customary in Hückel LCAO-MO calculations, all overlap integrals were set equal to zero, even when atoms i and j are adjacent.

Usually, the energy levels are expressed in terms of the H_{ij}, however, in the present work, values were estimated semi-empirically.

ESTIMATION OF PARAMETERS

The *exchange integral* is $H_{ij} = \int \phi_i H \phi_j dv = \beta_{ij}$, where $i \neq j$. Since this integral represents the energy of interaction between two π-type orbitals, ϕ_i and ϕ_j, it was assumed to be equal to the energy of a double bond between atoms i and j minus the energy of a single bond. Thus $\beta_{ij} = -[U(\text{C=C}) - U(\text{C—C})]$. Of course, if atoms i and j are not adjacent, then $\beta_{ij} = 0$. Bond energies taken from the recent compilation by COTTRELL[8] give the following values of β_{ij}:

$$U(\text{C=C}) - U(\text{C—C}) = 145{\cdot}8 - 82{\cdot}6 = 63{\cdot}2 \text{ kcal} = -\beta_{CC}$$

$$\beta_{CC} = -22{,}100 \text{ cm}^{-1}{}_{CC}$$

$$U(\text{C=O}) - U(\text{C—O}) = 179 - 85{\cdot}5 = 94 \text{ kcal} = -\beta_{CO}$$

$$\beta_{CO} = -32{,}900 \text{ cm}^{-1}$$

The value of β_{MO} for the metal–oxygen bond was left as a variable parameter, since there is no independent way to evaluate it without assuming explicit forms of the atomic wave functions and a Hamiltonian.

If $i = j$ then the *Coulomb integral* is $H_{ij} = H_{ii} = \int \phi_i H \phi_i \, dv = \alpha_i$. This is the energy of an electron in the orbital ϕ_i, and is related to the absolute electronegativity of the atom. MULLIKEN[9,10] has defined electronegativity as the average of the ionization potential, I, and the electron affinity, E_e:

$$\chi_M = \frac{E_e + I}{2}$$

That is, it is the average of the energy required to remove an electron from atom i and the energy liberated when an electron is added. This average was taken to be a measure of the energy of the lowest occupied atomic orbital (neglecting the difference between spectroscopic ground states that sometimes occurs). After correction for the inductive effect and for the splitting of the *d*-orbital degeneracy by the ligand field, this value was set equal to α_i. Most electronegativity values are expressed on Pauling's scale, but these are related to Mulliken's absolute scale in the following way:

$$\chi_{\text{Mulliken}} \text{ (eV)} = 2{\cdot}82 \, \chi_{\text{Pauling}}$$

[3] R. L. BELFORD, A. E. MARTELL and M. CALVIN, *J. Inorg. Nucl. Chem.* **2**, 11–31 (1956).
[4] R. H. HOLM and F. A. COTTON, *J. Amer. Chem. Soc.* **80**, 5658 (1958).
[5] E. HÜCKEL, *Z. physik.* **70**, 204 (1931).
[6] C. A. COULSON, *Valence*. Oxford (1952).
[7] K. S. PITZER *Quantum Chemistry*. Prentice-Hall, New York (1953).
[8] T. L. COTTRELL, *The Strengths of Chemical Bonds*, (2nd Ed.). Butterworth London (1958).
[9] R. S. MULLIKEN, *J. Chem. Phys.* **3**, 573 (1935).
[10] R. S. MULLIKEN, *J. Chem. Phys.* **2**, 782 (1934).

The following values of $\chi_{Pauling}$ that were used in this work were taken from the work of ALLRED and ROCHOW:[11] C = 2·50, O = 3·50, V = 1·45, Cr = 1·56, Mn = 1·60, Fe = 1·64, Co = 1·70. Also, H = 2·10[12]. Electronegativities of the uncharged atoms were used since, according to Pauling's electroneutrality principle, the charge on the central metal ion in a complex compound is very close to zero.

When two atoms with different electronegativities are brought together in a compound, there is a partial shift of electrons toward the more electronegative atom. Hence, the electronegativities are different in a compound than in the free atom. In the present case, the electronegativity difference between the central metal ion and the surrounding oxygen atoms is very large and a correction for this becomes much more important than in organic molecules with the more common hetero atoms. The inductive parameter, δ, was set equal to 1/3 for adjacent atoms, 1/9 for two atoms separated by a third, 1/27 when separated by two atoms, etc. Although some workers have used slightly different values, these seem to be the most widely used. Hydrogen atoms were ignored and only one chelate ring was considered. Thus, the central metal ion is treated as though it were bound to only two oxygen atoms rather than six. Although there is no positive justification for this, it may be stated that δ = 1/3, 1/9, 1/27, etc. refers to induction along a chain and for an atom surrounded by six others the inductive parameter is probably different. Since it is not known what value should be used, it is necessary to resort to some arbitrary devise. Values of the electronegativity that have been corrected for the inductive effect have been labelled χ_i'

VOL. 22 1961

TABLE 1.—VALUES OF COULOMB INTEGRALS AND OF Δ USED IN THE CALCULATIONS

	$Ti(acac)_3$ (cm^{-1})	$V(acac)_3$ (cm^{-1})	$Cr(acac)_3$ (cm^{-1})	$Mn(acac)_3$ (cm^{-1})	$Fe(acac)_3$ (cm^{-1})	$Co(acac)_3$ (cm^{-1})
α_P*	−59200	−59940	−60800	−62700	−60180	−63000
α_A*	−65200	−65600	−66100	−66100	−66300	−66500
α_B*	−59200	−59500	−59700	−59700	−59700	−60400
α_C*	−58600	−59000	−59000	−59000	−59000	−59300
Δ	20300	18600	17400	21000	13700	19100

* Subscripts refer to Fig. 1.

An additional correction must be applied to the electronegativity of the central metal ion in order to take the ligand field splitting of the *d*-orbitals into account. This correction was made after the electronegativities were corrected for the inductive effect. In a free gaseous metal ion all five *d*-orbitals have the same energy, but in an octahedral complex they are split into three orbitals of lower energy and two of higher energy.[13] The energy difference between these two sets is denoted Δ, the three d_ε-orbitals being lower by 0·4 Δ and the two $d\gamma$-orbitals higher by 0·6 Δ. Since the electronegativity refers to the free ion, −0·4 Δ is added to χ'_{metal} (which is also negative if equated to the Coulomb integral) in order to obtain the Coulomb integral for the central metal ion. This gives the energy of the d_ε-orbitals which are the ones that participate in π-bonding with the ligands. The value of Δ may be estimated from the positions of the $d \rightarrow d$ absorption bands of the complex for which the calculation is being made, but in the present work, the values given by JORGENSEN[14] for the hexaaquo ions of the various metals were used. This is justified on the grounds that water and acetylacetone lie very close to one another in the spectrochemical series[15] and it allows the calculation to be made without prior knowledge of the spectrum. Table 1 summarizes the values of Coulomb integrals that were finally used in the calculations.

In order to determine the π-energy levels of a complex of the type $M(acac)_3$, one must solve an 18 × 18 determinant. This can be factored into smaller determinants by taking advantage of the D_3 symmetry and standard methods of group theory. In this manner, the following sets of normalized

[11] A. L. ALLRED and E. G. ROCHOW, *J. Inorg. Nuclear Chem.* **5**, 264–8 (1958).
[12] L. PAULING, *Nature of the Chemical Bond*, (3rd Ed). Cornell Univ. Press, Ithaca, New York (1960).
[13] R. S. NYHOLM, *Quelques Problèmes de Chimie Minérale*, Tenth Solvay Conference, Inst. International de Chimie Solvay, pp. 225–287 (1956).
[14] C. K. JORGENSEN, *Quelques Problèmes de Chimie Minérale*, Tenth Solvay Conference, Inst. International de Chimie Solvay, pp. 355–81 (1955).
[15] Y. SHIMURA and R. TSUCHIDA, *Bull. Chem. Soc. Japan*, **29**, 311–16 (1956).

and mutually orthogonal symmetry orbitals were obtained. Individual atoms are labelled according to Fig. 1:

$$A_1: \quad \Phi_1 = \frac{1}{\sqrt{3}}(\phi_{d_{xy}} + \phi_{d_{yz}} + \phi_{d_{xz}})$$

$$\Phi_2 = \frac{1}{\sqrt{6}}(\phi_A + \phi_F + \phi_K - \phi_E - \phi_O - \phi_J)$$

$$\Phi_3 = \frac{1}{\sqrt{6}}(\phi_B + \phi_G + \phi_L - \phi_D - \phi_N - \phi_I)$$

$$A_2: \quad \Phi_4 = \frac{1}{\sqrt{6}}(\phi_A + \phi_F + \phi_K + \phi_E + \phi_O + \phi_J)$$

$$\Phi_5 = \frac{1}{\sqrt{6}}(\phi_B + \phi_G + \phi_L + \phi_D + \phi_N + \phi_I)$$

$$\Phi_6 = \frac{1}{\sqrt{3}}(\phi_C + \phi_H + \phi_M)$$

$$E: \quad \Phi_7 = \frac{1}{\sqrt{6}}(2\phi_{d_{xy}} - \phi_{d_{yz}} - \phi_{d_{xz}}$$

$$\Phi_8 = \frac{1}{\sqrt{6}}(2\phi_A - \phi_F - \phi_K)$$

$$\Phi_9 = \frac{1}{\sqrt{6}}(2\phi_B - \phi_G - \phi_L)$$

$$\Phi_{10} = \frac{1}{\sqrt{6}}(2\phi_C - \phi_H - \phi_M)$$

$$\Phi_{11} = \frac{1}{\sqrt{6}}(2\phi_D - \phi_I - \phi_N)$$

$$\Phi_{12} = \frac{1}{\sqrt{6}}(2\phi_E - \phi_J - \phi_O)$$

In these equations, ϕ_X represents an atomic orbital on atom **X** which has the correct symmetry properties in order to combine with neighbouring orbitals that contribute to the overall conjugated system.

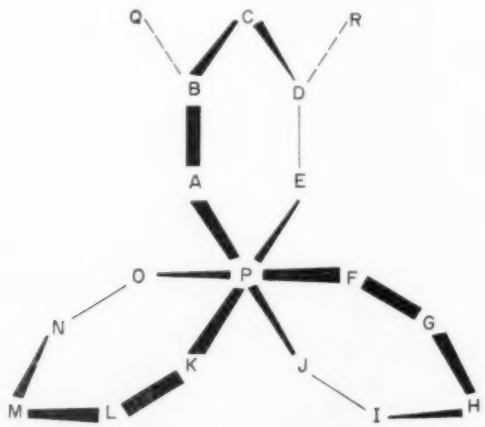

FIG. 1.—Labelling of atoms in a $M(acac)_3$ complex.

RESULTS AND DISCUSSION

Calculations of the π-energy levels in $Ti(acac)_3$, $V(acac)_3$, $Cr(acac)_3$, $Mn(acac)_3$, $Fe(acac)_3$, and $Co(acac)_3$ were carried out for the following values of the energy of the metal–oxygen π-bond: $\beta_{MO} = 0$, 6000, 10000, 20000 and 30000 cm^{-1}. These results are illustrated in Figs. 2 and 3.

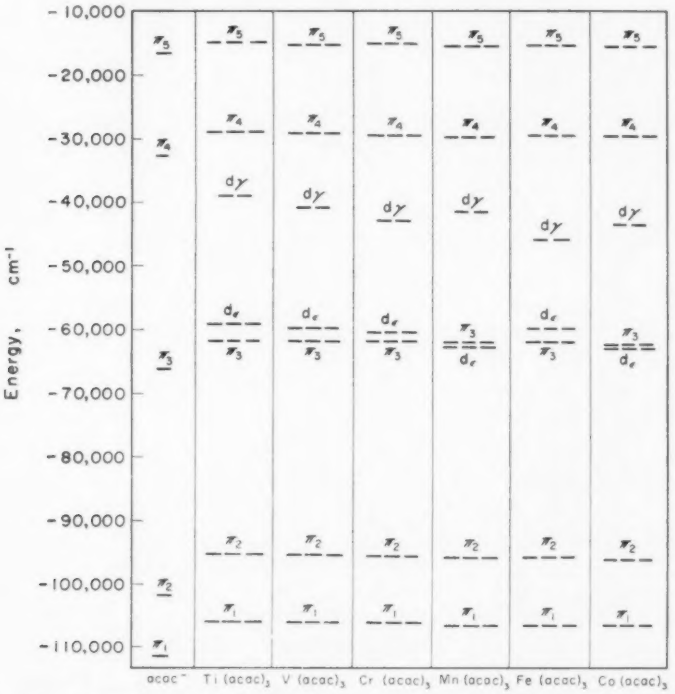

FIG. 2.—π-Energy levels in some acetylacetone complexes. Metal–ligand π-bonding neglected.

Energy levels in the absence of π-bonding

The energy levels of the free acetylacetonate ion and of the six metal chelates, in the absence of metal–ligand π-bonding, are presented in Fig. 2. The levels of the enolate ion were calculated by a comparable procedure to that described in this report.[2] Each $acac^-$ ion has six π-electrons which occupy the π_1, π_2, and π_3-orbitals. In the metal complexes there are from one to six electrons in the 3*d*-orbitals. These are distributed among the d_ε and d_γ-orbitals as indicated in Table 2.

Chemical observations show that these energy levels are at least qualitatively correct, except in the case of $Mn(acac)_3$ and probably $Co(acac)_3$. According to Hund's rules, if partly filled d_ε-orbitals were to lie below the filled π_3-orbitals, electrons would spontaneously fall into the lower energy vacancies. Therefore, according to the calculated energy levels in $Mn(acac)_3$, the Mn^{3+} ion should be reduced by acetylacetone. Since this does not occur the d_ε-orbital must lie above the π_3-orbital. This is no cause for concern however, because the margin of error in the calculations is large enough that the order of these two levels could easily be reversed. The same argument cannot be applied to $Co(acac)_3$ because the d_ε-orbitals are completely filled. By a similar

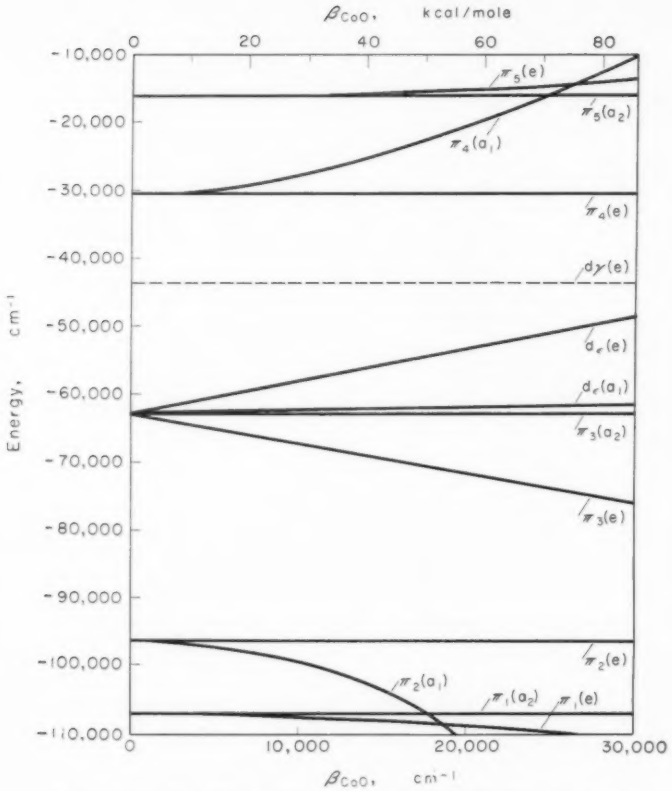

FIG. 3.—Effect of metal–oxygen π-bonding on the energy levels of $Co(acac)_3$.

argument, the d_γ-orbitals must lie below the π_4-orbitals. In $Mn(acac)_3$ and $Fe(acac)_3$ there are respectively one and two d_γ-electrons. If the π_4-orbitals were lower than the d_γ-orbitals then electrons would spontaneously fall into the ligand orbitals and the metal ions would be oxidized. This does not occur.

TABLE 2.—ELECTRONIC CONFIGURATION IN SOME ACETYLACETONATO COMPLEXES

Complex	No. of *d*-electrons	Configuration	References
$Ti(acac)_3$	1	d_ϵ^1	—
$V(acac)_3$	2	d_ϵ^2	—
$Cr(acac)_3$	3	d_ϵ^3	16
$Mn(acac)_3$	4	$d^3 d_\gamma^1$	16, 17
$Fe(acac)_3$	5	$d_\epsilon^3 d_\gamma^2$	18
$Co(acac)_3$	6	d_ϵ^6	16, 19

[16] H. S. JARRETT, *J. Chem. Phys.* **27**, 1298–1304 (1957).
[17] L. C. JACKSON, *Proc. Phys. Soc.* **47**, 1029–31 (1935).
[18] L. C. JACKSON, *Proc. Roy. Soc.* A **140**, 695–713 (1933).
[19] R. O. WHIPPLE, R. WEST and K. EMERSON, *J. Chem. Soc.* 3715 (1953).

Effect of π-bonding on the energy levels

The effect of increasing metal–ligand π-bonding is shown in Fig. 3 using $Co(acac)_3$ as the example. It will be seen that the d_ε and all of the π-orbitals are split into their e and a_1 or a_2 components. Formation of the direct products readily shows that only $a_1 \rightarrow a_1$ and $a_1 \rightarrow a_2$ transitions are forbidden. Therefore, when π-bonding is strong it is seen that four different $\pi_3 \rightarrow \pi_4$ transitions and three different $d_\varepsilon \rightarrow \pi_4$ transitions are possible. These are described below:

$\pi_3 \rightarrow \pi_4$ Transitions	
$\pi_3(e) \rightarrow \pi_4(a_1)$	Highest in energy. Shifts rapidly to higher energy with increasing metal–ligand π-bonding.
$\pi_3(e) \rightarrow \pi_4(e)$ $\pi_3(a_2) \rightarrow \pi_4(a_1)$	Both have about the same energy and are expected to overlap. π-Bonding shifts both to higher energy at about the same rate.
$\pi_3(a_2) \rightarrow \pi_4(e)$	Lowest in energy. Energy is independent of metal–oxygen π-bonding.
$d_\varepsilon \rightarrow \pi_4$ Transitions	
$d_\varepsilon(a_1) \rightarrow \pi_4(a_1)$	Forbidden.
$d_\varepsilon(a_1) \rightarrow \pi_4(e)$ $d_\varepsilon(e) \rightarrow \pi_4(a_1)$	Both have about the same energy and are expected to overlap. The transition energy is nearly independent of metal–ligand π-bonding.
$d_\varepsilon(e) \rightarrow \pi_4(e)$	Lowest in energy. Shifts to lower energy with increasing metal–ligand π-bonding.

Thus, one may expect to observe three $\pi_3 \rightarrow \pi_4$ transitions and two $d_\varepsilon \rightarrow \pi_4$ transitions in favorable cases.

The calculated transition energies were tested by choosing a value of β_{MO}, the energy of metal–oxygen π-bonding, which gave a good fit to the observed $\pi_3 \rightarrow \pi_4$ transition energies. In all cases it was possible to choose a value which gave very good agreement between the calculated and observed energies, not only for the $\pi_3 \rightarrow \pi_4$ transitions but also for the $d_\varepsilon \rightarrow \pi_4$ transitions. These data are obtained in Table 3. It will be seen that in most cases the agreement is within 1,500 cm^{-1}. In view of the rather drastic approximations made in these calculations, such good agreement is surprising and it must be, at least partly, fortuitous. It bears repeating however, that the Coulomb and exchange integrals were estimated from independent data, and β_{MO} is the only variable parameter.

The values of β_{MO} that were used are interesting in themselves in that they are a rough estimate of the energy of metal–oxygen π-bonding. It is seen in Table 3 that these energies range from near zero in $Ti(acac)_3$ to about 40 kcal per mole per bond

in $Co(acac)_3$. This may be compared with 63·2 kcal/mole for the π-contribution to the energy of a C=C double bond, and 94 kcal/mole for a C=O double bond.

In the first paper of this series[1] it was suggested that two possible types of π-interaction were occurring simultaneously in $M(acac)_3$ complexes. The first type involves

TABLE 3.—COMPARISON OF CALCULATED AND OBSERVED TRANSITION ENERGIES IN SOME tris(ACETYLACETONATO) COMPLEXES

Absorption curves have been presented in a preceding paper.[1] Calculated transition energies are in parenthesis.

Transition \ Complex, β_{MO}, cm^{-1}	$Ti(acac)_3$ $\beta_{MO} > -2000$	$V(acac)_3$ $\beta_{MO} = -6000$	$Cr(acac)_3$ $\beta_{MO} = -11000$	$Mn(acac)_3$ $\beta_{MO} = -12000$	$Fe(acac)_3$ $\beta_{MO} = -12500$	$Co(acac)_3$ $\beta_{MO} = -14000$
$\pi_3(e) \rightarrow \pi_4(a_1)$	32400 (32400)	~35900 (35600)	39300 (40600)	39500 (42400)	42500 (41800)	43900 (44000)
$\pi_3(e) \rightarrow \pi_4(e)$ $\pi_3(a_2) \rightarrow \pi_4(a_1)$		~34500 (34500) (33500)	37100 (37100) (37000)	~36800 (38300) (36400)	36800 (37200) (37400)	39000 (38800) (37500)
$\pi_3(a_2) \rightarrow \pi_4(e)$		— (32500)	33900 (32600)	— (32300)	— (32500)	~33900 (32300)
$d_\varepsilon(a_1) \rightarrow \pi_4(e)$ $d_\varepsilon(e) \rightarrow \pi_4(a_1)$	27500 (30000)	29200 (30400) (29500)	30200 (30800) (29800)	31400 (32000) (30700)	28500 (30000) (29500)	31000 (31700) (31000)
$d_\varepsilon(e) \rightarrow \pi_4(e)$		— (28400)	26300 (26800)	~25000? (26700)	32300? (25000)	~25000? (25600)

interaction between the d_ε-orbitals and higher, empty, π_4-orbitals and tends to increase Δ, the ligand field splitting parameter. The second type involves interaction between the d_ε-orbitals and lower, filled, π_3-orbitals and tends to decrease Δ. This would explain why the behaviour of the $\pi_3 \rightarrow \pi_4$ transitions indicate strong metal–ligand π-bonding while the position of the acetylacetonate ion in the spectrochemical series indicates little or no π-bonding. It is seen in Fig. 3 that both types of π-interaction actually do exist. The lower, filled, $\pi_3(e)$-orbitals are depressed in energy and the higher, empty, $\pi_4(a_1)$-orbitals are raised. The d_ε-orbitals are split, however, into the $d_\varepsilon(a_1)$ and $d_\varepsilon(e)$-orbitals. Only the $d_\varepsilon(a_1) \rightarrow d_\gamma(e)$ transition is independent of π-bonding as observation requires. The $d_\varepsilon(e) \rightarrow d_\gamma(e)$ transition would be expected at lower energy, in the red or near infra-red region. Since no new or unusual bands are found in this region the latter transition must be forbidden.

In all of the complexes considered in this paper except $Co(acac)_3$ four $\pi_3 \rightarrow d_\varepsilon$ transitions are possible with energies on the order of 2000–15000 cm^{-1}. Again, no unusual bands are observed in this region and it is assumed that these transitions are also forbidden.

The statement is often seen in the literature that the chelate ring with metal–ligand π-bonding is analogous to benzene. Resonance structures such as the following are usually written in order to illustrate this:

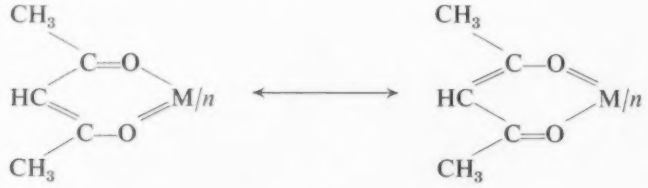

However, the metal–oxygen π-bond in the above structure occurs mainly through overlap of the metal d_ε-orbitals with the π-system of the acetylacetonate ion rather than through a p_z-orbital as it does in benzene or pyridine. Since the three d_ε-orbitals are orthogonal to one another (i.e., they do not interact), π-electrons cannot move freely in a circular path around the ring. Instead, there is a barrier at the metal ion, and it is therefore *not* analogous to benzene. The barrier is not expected to be infinitely high, however, since the orthogonality of the d_ε-orbitals is partially removed by strain in the chelate ring, and the metal $4p$-orbitals, which offer no such potential barrier, also take part in metal–ligand π-bonding.

VOL.
22
1961

VO
2
19

J. Inorg. Nucl. Chem., 1961, Vol. 22, pp. 193 to 197. Pergamon Press Ltd. Printed in Northern Ireland

THE COMPLEXES OF SOME 5-SUBSTITUTED TETRAZOLES WITH NICKEL(II)

N. A. DAUGHERTY and C. H. BRUBAKER, JR.
Kedzie Chemical Laboratory, Michigan State University, East Lansing, Michigan

(*Received* 11 *May* 1961; *in revised form* 24 *May* 1961)

Abstract—Unlike copper, nickel(II) forms only impure and poorly characterized compounds when its salts react with various 5-substituted tetrazoles in water, alcohols, dimethylformamide and other solvents.

However in solutions, particularly in dimethylformamide, complexation is clearly indicated by studies of absorption spectra. In some cases, such as 5-aminotetrazole, 2:1 complexes are formed, but with others, such as 5-phenyltetrazole, only $[C_7H_6N_4]/[Ni^{2+}] = 3/2$ is indicated. Nickel spectra suggest only octahedral co-ordination.

VOL.
22
1961

As part of a study[1,2] of metal complexes of tetrazoles, the reactions of nickel ion with some 5-substituted tetrazoles were investigated. Previous work with copper(II) indicated that 5-substituted tetrazoles coordinate as the anions, that the maximum number of tetrazoles bound per metal ion is two, and that the anion of the metal salt used influences the course of the reaction in a manner which is not well understood.

EXPERIMENTAL

Materials

Reagent grade chemicals were used throughout the investigation. Tetrazoles were obtained from R. M. HERBST* or were synthesized by use of the method of FINNEGAN and HENRY[3] The equivalent weights of the tetrazoles were determined by titration with standard base and were in good agreement with the calculated values.

Sodium salts of the tetrazoles were prepared by potentiometric titration of aqueous solutions, or suspensions of the tetrazoles, with NaOH solution. The aqueous solutions of the sodium salts were evaporated nearly to dryness; the solid was removed by filtration and recrystallized twice from ethanol or isopropyl alcohol. The sodium salts were dried at 110° before being used.

Analytical methods

Nickel. Samples of solid, nickel complexes were analysed for nickel by dissolving the samples in ammoniacal KCN solution and titrating the excess cyanide with standard $AgNO_3$ using KI as an indicator. The KCN was standardized each time a nickel analysis was made, by titration with standard $AgNO_3$.

Solutions of $Ni(NO_3)_2 \cdot 6H_2O$ in water or dimethylformamide were standardized gravimetrically with dimethylglyoxime.

Tetrazolate. The tetrazolate content of solid nickel complexes was determined by the method described[2] for copper-tetrazole complexes.

Carbon, hydrogen and nitrogen. Samples of complexes were analyzed for C, H, N by commercial analytical houses. The results often were unsatisfactory due to explosion of the samples.

Solid tetrazole complexes of nickel

Nickel complexes of several 5-substituted tetrazoles were obtained as poorly-characterized, amorphous, hygroscopic, blue or purple solids. With a few exceptions, the solids were insoluble or

* Department of Chemistry, Michigan State University.

[1] C. H. BRUBAKER, *J. Amer. Chem. Soc.* **82,** 82 (1960.)
[2] N. A. DAUGHERTY and C. H. BRUBAKER. *J. Amer. Chem. Soc.*, **83,** in press, and N. A. DAUGHERTY. Ph.D. Dissertation, Michigan State Univ. (1961).
[3] W. FINNEGAN and R. HENRY, *J. Amer. Chem. Soc.* **80,** 3908 (1958).

very slightly soluble in a variety of solvents such as, water, dioxane, ethanol, chloroform, benzene, ethylacetate, dimethylformamide and acetonitrile. Purification of the solids generally could not be accomplished by recrystallization or sublimation. The preparation of solid complexes of two tetrazoles will be described briefly.

Solid 5-aminotetrazole complex. Mixing aqueous solutions of $NiCl_2$ or $Ni(NO_3)_2$ with aqueous CN_5H_3 produces purple solutions which can be stored for over a year without separation of a solid phase. On the other hand, if $NiSO_4$ is used in place of the $Ni(NO_3)_2$, the purple solution, first produced, rapidly becomes cloudy and a purple solid precipitates. The gelatinous purple solid cannot be washed free of SO_4^{2-}.

Nickel, C, H and N, analyses indicate that the solid contains 1·5–1·7 tetrazoles per nickel.

A solid nickel–5-aminotetrazole complex also was obtained by slowly adding 50 ml of 0·10 M $Ni(NO_3)_2 \cdot 6H_2O$ in absolute ehtanol to 100 ml of 0·10 M CN_5H_3 in absolute alcohol. A gelatinous solid precipitated at once. The solid was separated by centrifugation and was washed several times with ethanol. After drying *in vacuo* over $Mg(ClO_4)_2$, the solid contained 23·9% Ni and 56·0% $CN_5H_2^-$ which corresponds to a tetrazole to nickel molar ratio of 1·6.

Comparison of the infra-red spectra of the complexes, in KBr disks, with the spectra of CN_5H_3 and $NaCN_5H_2$ suggests that the tetrazole has co-ordinated as the anion.

The magnetic susceptibility of the solid obtained from ethanol was determined by the Gouy method. Susceptibility measurements give a magnetic moment of 3·9 Bohr magnetrons. The value is somewhat doubtful because the exact formula of the complex (assumed to be $Ni(CN_5H_2)_2$) is not known. However, there seems to be little doubt that the solid is paramagnetic.

Solid nickel-5-phenyltetrazole complex. When isopropyl alcohol solutions of $Ni(NO_3)_2 \cdot 6H_2O$ and $C_7H_6N_4$ were mixed, a dark blue solution resulted. The blue solution turned cloudy within a few seconds and after 24 hr a gelatinous precipitate had separated. The solid was separated and washed several times with isopropyl alcohol, but the solid could not be washed free of nitrate. The light blue solid was dried and analysed for Ni and $C_7H_6N_4^-$. The results indicated 1·76 tetrazoles per nickel.

A second method of preparation involved the use of $NaC_7H_6N_4$ and $Ni(NO_3)_2 \cdot 6H_2O$. When dimethylformamide solutions of $Ni(NO_3)_2 \cdot 6H_2O$ and $NaC_7H_5N_4$ were mixed, a dark blue solution was produced. Evaporation of the solvent yielded a dark blue, acetone soluble, solid and a white, acetone insoluble solid (probably $NaNO_3$). The residue was extracted with dry acetone and the acetone solution was filtered. The acetone solution was evaporated to dryness, and the extraction, filtration, evaporation process was repeated three times. After drying *in vacuo* over $Mg(ClO_4)_2$, the light blue solid contained 16·8% Ni and 76·5% $C_7H_6N_4^-$ indicating a composition of 1·84 tetrazoles per nickel.

Infra-red spectra of the complexes prepared from isopropyl alcohol and dimethylformamide are nearly identical and indicate that the tetrazole has coordinated as the anion.

Other nickel–tetrazole complexes obtained as solids. Solid complexes of nickel and tetrazole, 5-*p*-nitrophenyltetrazole, 5-*p*-methoxyphenyltetrazole, and 5-methyltetrazole were obtained by mixing ethanol solutions of $Ni(NO_3)_2 \cdot 6H_2O$ and the tetrazoles. All of the complexes were amorphous, poorly characterized, solids containing 1·5–1·9 tetrazolate anions per nickel. Such materials may contain some solvent of crystallization, which was not removed by the vacuum drying procedure.

Complexes in solution

5-Aminotetrazole. The addition of CN_5H_3 to an aqueous solution of $NiCl_2$, changes the colour of the solution from green to purple. The visible spectra of solutions containing $NiCl_2$ and CN_5H_3 show absorption maxima at 930, 725, 740 and 385 mμ.

A continuous variation study of mixtures of $Ni(NO_3)_2$ and CN_5H_3 was made by means of spectrophotometric measurements at 540 mμ. A graph of excess absorbancy vs. $[CN_5H_3]/[Ni^{2+}]$ exhibits a broad maximum extending from a $[CN_5H_3]/[Ni^{2+}]$ ratio of 0·80 to a ratio of 2·40 (possibly meaning 2:1 complexing).

Attempts were made to carry out a continuous variation study in both water and dimethylformamide using $NaCH_5H_2$ in place of CN_5H_3 in order to obtain a higher degree of complex formation. However, all samples having a $[CN_5H_2^-]/[Ni^{2+}]$ 1·5 or greater rapidly became turbid.

5-Phenyltetrazole. In dimethylformamide solution, $Ni(NO_3)_2 \cdot 6H_2O$ and $C_7H_6N_4$ react to give blue–purple solutions. Continuous variation studies give results similar to those obtained for $Ni(NO_3)_2$ and CN_5H_3.

However, in contrast to CN_5H_3 and its sodium salt, the sodium salt of 5-phenytletrazole and $Ni(NO_3)_2 \cdot 6H_2O$ react in dimethylformamide to yield stable purple solutions.

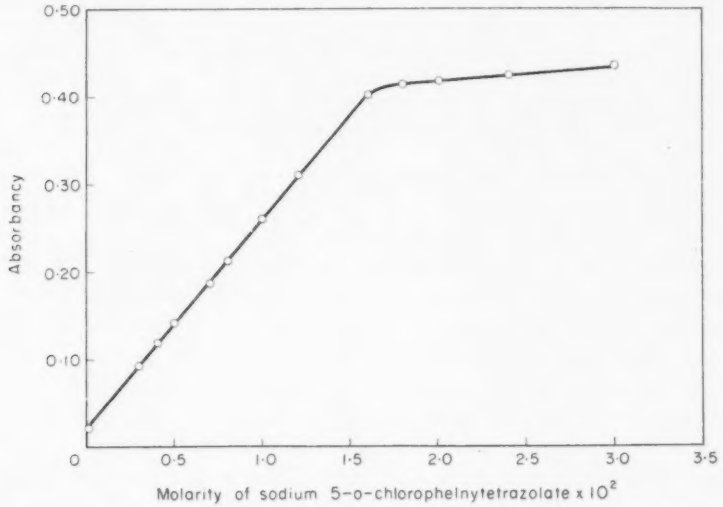

FIG. 1.—Absorbancy of $1{\cdot}03 \times 10^{-2}$ M $Ni(NO_3)_2 \cdot 6H_2O$ in dimethylformamide with various concentrations of sodium 5-*o*-chlorophenyltetrazolate. 570 mμ.

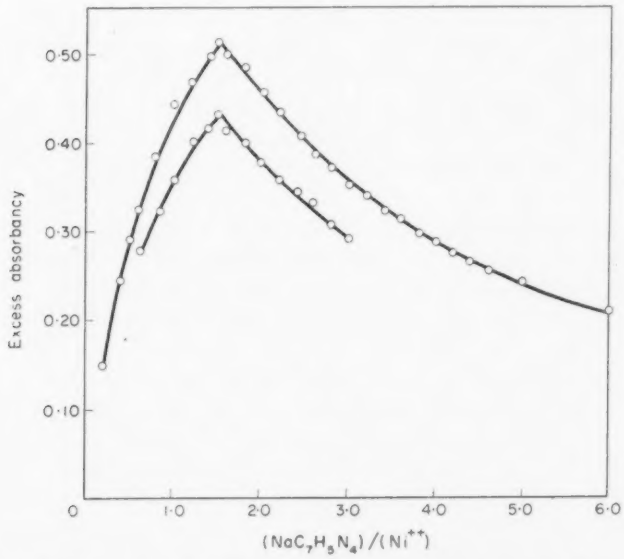

FIG. 2.—Continous variation study of $Ni(NO_3)_2 \cdot 6H_2O$ and sodium 5-phenyltetrazolate. Total molarity = $3{\cdot}44 \times 10^{-3}$. Upper curve, anhydrous dimethylformamide as solvent. Lower curve, dimethylformamide + 4% H_2O. 570 mμ.

A continuous variation study was made using $NaC_7H_5N_4$ and $Ni(NO_3)_2 \cdot 6H_2O$. Spectrophotometric measurements were made at 570 mμ. A graph of excess absorbancy vs. $[C_7H_5N_4^-]/[Ni^{2+}]$ show a rather sharp, single maximum at a $[C_7H_5N_4^-]/[Ni^{2+}]$ ratio of 1·5. A similar study was carried out in 96% (4% H_2O) dimethylformamide. The position of the maximum remained at a $[C_7H_5N_4^-]/[Ni^{2+}]$ ratio of 1·5.

A series of solutions was prepared (in dimethylformamide) in which the concentration of $Ni(NO_3)_2 \cdot 6H_2O$ was $1{\cdot}03 \times 10^{-2}$ and the concentration of $NaC_7H_5N_4$ was varied.

The absorbancies of the samples at 570 mμ were measured using 5 cm cells in a Beckman DU spectrophotometer. The absorbance increased linearly with tetrazole concentration until a mole ratio of 1·5/1 was reached and then leveled off to a constant value. The data from this spectrophotometric titration as well as the continuous variation data point to the existence of a species $[Ni_2(C_7H_5N_4)_3]_x^+$ in solution, c.f. Fig. 1, for the 5-phenyltetrazolate, and Fig. 2, for the 5-*o*-chlorophenyltetrazolate.

Other 5-aryltetrazoles. Spectrophotometric titration of $Ni(NO_3)_2 \cdot 6H_2O$ in dimethylformamide with standard solutions of the sodium salts of 5-*o*-chlorophenyltetrazole (Fig. 1) 5-*p*-chlorophenyltetrazole and 5-*p*-methoxyphenyltetrazole gives results similar to those obtained with $NaC_7H_5N_4$.

RESULTS AND DISCUSSION

The nickel complexes of several 5-substituted tetrazoles were obtained as poorly characterized solids from the reaction of nickel salts and tetrazoles in alcohols or from the reaction of nickel salts and, the sodium salt of the tetrazole in dimethylformamide. Analyses of the solids indicate that 1·5–1·9 tetrazoles are bound per nickel ion. Analtyical results, as well as comparison of the infra-red spectra of the complexes with the spectra of the tetrazoles and their sodium salts, indicate that the tetrazoles studied co-ordinate as tetrazolate anions. As in the case of copper ion, the maximum number of tetrazoles that can co-ordinate to the metal ion appears to be two.

Crystalline copper complexes of fairly high purity can be obtained by mixing solutions of the reactants to form a highly coloured solution from which the solid complex slowly crystallizes. However, in the case of nickel, mixing solutions of the reactants in methanol, ethanol, water or dimethylformamide produced highly coloured solutions from which the complex would not separate or resulted in the immediate formation of gelatinous precipitates which could not be washed free of impurities. Evaporation of the coloured solutions yielded heterogeneous mixtures of solids. Perhaps a solvent could be found from which crystalline nickel complexes can be isolated.

Continuous variation studies of $Ni(NO_3)_2 \cdot 6H_2O$ and $NaC_7H_5N_4$ in dimethylformamide point to the existence of a species $[Ni_2(C_7H_5N_4)_3]^+$ in solution. A titration curve for the spectrophotometric titration of $Ni(NO_3)_2 \cdot 6H_2O$ with $NaC_7H_5N_4$ shows a sharp break at a $[C_7H_5N_4^-]/Ni^{2+}$ ratio of 1·5 which also indicates the existence of a $[Ni_2(C_7H_5N_4)_3]^+$ species in solution (Fig. 1).

Spectrophotometric titration (in dimethylformamide) of $Ni(NO_3)_2 \cdot 6H_2O$ with the sodium salts of other 5-aryletrazoles also suggest that a species $Ni_2Y_3^+$ (T = a tetrazolate anion) is formed in solution. LEUSSING[4,5] has recently used spectrophotometric titration data to demonstrate the existence of nickel complexes of 1,2 ethandithiol and 2,3 dimercapto-1-propanol having the general formula $Ni_2X_3^{2+}$ where X represents the anion of the ligand.

If polymeric species also exist in the solid state, tetrazole/nickel ratios other than the expected 2:1 ratio are easily explained.

The visible spectra of the nickel complexes of 5-aminotetrazole and 5-phenyltetrazole indicate that the complexes are octahedral in solution. The number, position and intensities of the absorption bonds are in good agreement with those of known octahedral complexes (Table 1).

[4] D. LEUSSING and G. ALBERTS, *J. Amer. Chem. Soc.* **82**, 4458 (1960).
[5] D. LEUSSING, *J. Amer. Chem. Soc.* **81**, 4208 (1959).

TABLE 1.—SPECTRA OF OCTAHEDRAL NICKEL COMPLEXES

Compound of ligand	Absorption band	mμ	ν_i (cm^{-1})	Molar absorbancy index‡	ν_3/ν_1
$CN_5H_2^-$* $+Ni^{2+}$	ν_1	930	10740	3·3	1·73
	ν_2	725	13800	1·7	
	ν_3	540	18540	3·8	
	ν_4	385	26000	4·9	
$C_7H_5N_4^-$† $+Ni^{2+}$	ν_1	940	10630	10·2	1·66
	ν_2	770	13000	3·1	
	ν_3	565	17700	9·8	
	ν_4	356	28100	19·7	
$Ni(H_2O)_6^{2+}$ [6]	ν_1	1175	8500	2·0	1·81
	ν_2	740	13500	1·8	
	ν_3	650	15400	1·5	
	ν_4	396	25300	5·2	
$Ni(NH_3)_6^{2+}$ [6]	ν_1	930	10750	4·0	1·63
	ν_2	760	13150	5·0	
	ν_3	572	17500	4·8	
	ν_4	355	28200	6·3	

* Obtained from $NiCl_2$ and 5-aminotetrazole in H_2O
† Obtained from $Ni(NO_3)_2 \cdot 6H_2O$ and $NaC_7H_5N_4$ in dimethylformamide.
‡ Absorbancy in 1.00 cm cell (Total Ni concentration)

The number, positions and intensities of the bonds are not in agreement with those reported for square planar complexes by MAKI[7] or for the tetrahedral complexes reported by COTTON[8].

Acknowledgement—The authors wish to thank the Atomic Energy Commission, which supported this work under contract AT(11-1)-399.

[6] C. JORGENSEN, *Acta Chem. Scand.* **10**, 887 (1956).
[7] G. MAKI, *J. Chem. Phys.* **28**, 651 (1958).
[8] F. COTTON and D. GOODGAME, *J. Amer. Chem. Soc.* **82**, 5771 (1960).

VOL. 22 1961

VO
2
19

J. Inorg. Nucl. Chem., 1961, Vol. 22, pp. 199 to 204. Pergamon Press Ltd. Printed in Northern Ireland

PHOSPHONITRILIC BROMIDES

K. JOHN and T. MOELLER
Noyes Chemical Laboratory, University of Illinois, Urbana, Illinois

(*Received* 28 *April* 1961; *in revised form* 5 *June* 1961)

Abstract—The reaction between phosphorus(III) bromide, bromine, and ammonium bromide in either *sym*-tetrachloroethane or *sym*-tetrabromoethane yields, depending upon the temperature and the time of reaction, either the compound $NPBr_2PBr_n$ or members of the homologous series, $(NPBr_2)_n$. Conditions for the synthesis and separation of these compounds in good yields and certain of their properties are described.

VOL. 22 1961

ALTHOUGH a phosphonitrilic bromide was isolated at the time H. N. STOKES first recognized the phosphonitrilic chlorides as an homologous series, very little information dealing with the bromides has appeared in subsequent years. This is undoubtedly a reflexion of the difficulties of synthesis and separation that characterize these compounds. A few crystals of the trimer, $(NPBr_2)_3$, were obtained by BESSON[1] as a result of treatment of the ammonolysis product of phosphorus(V) bromide with excess phosphorus(V) bromide in a sealed tube at elevated temperature. A somewhat better yield of the trimer and the first synthesis of the tetramer resulted from an adaptation of SCHENK and RÖMER's procedure[2] for the phosphonitrilic chlorides to the reaction of phosphorus(V) bromide with ammonium bromide in *sym*-tetrachloroethane.[3] Unfortunately, the thermal decomposition of phosphorus(V) bromide and the consequent loss of bromine at the optimum reaction temperatures seriously reduce the yield. In a measure, this has been compensated for either by addition of bromine during the reaction[3,4] or at the beginning of the reaction.[5]

It has been shown,[6] however, that by allowing phosphorus(III) bromide to react with ammonium bromide and excess bromine at above 130°C in either *sym*-tetrachloroethane or *sym*-tetrabromoethane one can obtain the phosphonitrilic bromides in yields comparable to the best reported for the chlorides.[7,8] The best yields (ca. 50–60 per cent) of trimeric and tetrameric phosphonitrilic bromide are obtained when the temperature is maintained at 140–145°C for a period of 11 days. Troublesome sublimation of phosphorus(V) bromide in the initial stages of the reaction is avoided by raising the temperature to this range over a 3 day period. Under these conditions, formation of certain amounts of the oily higher homologues is unavoidable. The percentage of higher homologues in the reaction product increases with increasing reaction temperature. At 143°C, the reaction product was 58 per cent trimer and tetramer with ca. 8 per cent of tetramer in this mixture. At 175°C, the product

[1] A. BESSON, *C.R. Acad Sci. Paris* **114**, 1479 (1892).
[2] R. SCHENK and G. RÖMER, *Ber. Dtsch. Chem. Ger.* **57** B, 1343 (1924).
[3] H. BODE, *Z. Anorg. Chem.* **252**, 113 (1943).
[4] W. GRIMME, Dissertation, Münster (1926).
[5] N. E. BEAN and R. A. SHAW, *Chem. and Industr.* 1189 (1960).
[6] K. JOHN and T. MOELLER, *J. Amer. Chem. Soc.* **82**, 2647 (1960).
[7] L. G. LUND, N. L. PADDOCK, J. E. PROCTOR and H. T. SEARLE, *J. Chem. Soc.* 2542 (1960).
[8] M. L. NIELSEN and G. CRANFORD, *Inorganic Syntheses*, Vol. 6 pp. 94–97, (Edited by E. G. ROCHOW). McGraw-Hill, New York (1960).

contained only 33 per cent of trimer and tetramer, but ca. 50 per cent of this mixture was tetramer.

Separation of the trimer–tetramer fraction from the higher polymers can be effected by either solvent extraction with benzene or n-heptane or direct vacuum sublimation. During sublimation, the higher oily homologues are polymerized to greater or lesser degree to phosphonitrilic bromide rubber.[9] This rubber resembles the corresponding chloride rubber in hydrolyzing in moist air and in losing its plasticity at higher temperatures as a result of depolymerization.

Separation of the trimer from the tetramer is best effected by crystallization from solvents such as n-heptane or petroleum ether (b.p. 95–110°C). Although solubility determinations indicate the bromides to be less soluble than their chlorine analogues, they demonstrate substantial useful differences between trimer and tetramer (Table 1).

TABLE 1.—SOLUBILITY DATA FOR $(NPBr_2)_3$ AND $(NPBr_2)_4$ AT 25°C

Solvent	Solubility (g/100 g of solvent)	
	$(NPBr_2)_3$	$(NPBr_2)_4$
Carbon disulphide	24·50	7·40
Benzene	18·60	3·85
Chloroform	12·10	1·85
Diethyl ether	6·65	0·90
Carbon tetrachloride	5·50	0·95
Cyclohexane	4·00	0·80
Petroleum ether (90–110°C)	2·30	0·27
n-Heptane	1·45	0·15

TABLE 2.—NUCLEAR MAGNETIC RESONANCE SPECTRA OF $(NPBr_2)_3$ AND $(NPBr_2)_4$

Compound	Chemical Shift (p.p.m., reference 85% H_3PO_4)	Solvent	r.f. frequency (Mc/s)
$(NPBr_2)_3$	+49·5	CS_2	16·2
$(NPBr_2)_4$	+71·8	CS_2	16·2

TABLE 3.—INFRA-RED SPECTRA OF PHOSPHONITRILIC BROMIDES

Compound	NaCl Region		CsBr Region	
	P–N Frequency (cm^{-1})	Medium	Frequency* (cm^{-1})	Medium
$NPBr_2PBr_5$	1276	Nujol	509 (broad)	Nujol
$NPBr_2PBr_7$	1256	Nujol	494 (broad)	Nujol
$(NPBr_2)_3$	1175, 1126	CS_2	526, 437	Nujol
$(NPBr_2)_4$	1272	CS_2	517, 447, 415	Nujol
$(NPBr_2)_n$ (oil)	ca. 1302	CS_2		

* All very strong (v.s.).

[9] D. L. HERRING, *Chem. and. Industr.* 717 (1960).

The nuclear magnetic resonance spectra indicate the same positive shift with the tetramer as compared with the trimer noted with other phosphonitrilic halides (Table 2).[7] Similarly, the infra-red spectra show the same general differences in P-N stretching frequency (NaCl region) characteristic of other trimeric and tetrameric phosphonitrilic compounds (Table 3).[10] A general increase in this frequency parallels increase in degree of polymerization. Both trimer and tetramer give characteristic and different X-ray diffraction patterns (Table 4).

TABLE 4.—X-RAY DIFFRACTION POWDER DATA ($2D$ IN CM.)

$(NPBr_2)_3$	$(NPBr_2)_4$	$NPBr_2PBr_5$	$NPBr_2PBr_7$
3·64 *vw*	5·48 *m*	4·95 *w*	4·71 *s*
4·48 *vw*	6·14 *s*	5·56 *s*	5·52 *s*
5·60 *vw*	6·50 *m*	5·81 *w*	5·78 *m*
5·74 *s*	6·78 *m*	7·21 *m*	6·79 *s*
6·06 *m*	7·04 *m*	7·57 *s*	7·14 *s*
6·64 *s*	7·22 *m*	8·21 *w*	7·81 *s*
6·80 *s*	7·81 *s*	8·71 *w*	8·30 *m*
6·94 *s*	8·22 *s*	9·32 *w*	8·73 *m*
7·45 *m*	8·50 *w*	9·68 *w*	9·06 *m*
8·31 *s*	8·74 *w*	9·97 *m*	9·70 *vw*
8·41 *s*	9·36 *w*	11·02 *w*	10·11 *m*
9·48 *s*	9·96 *m*	11·34 *w*	10·73 *m*
9·85 *w*	10·40 *w*	12·24 *w*	11·43 *m*
10·17 *w*	10·66 *w*	12·52 *m*	11·91 *w*
10·60 *w*	11·18 *vw*	12·84 *w*	12·23 *m*
10·93 *m*	11·28 *w*	13·22 *w*	12·67 *w*
11·31 *vw*	11·70 *w*	13·76 *w*	13·18 *w*
11·61 *m*	12·08 *w*	14·22 *m*	13·64 *w*
11·81 *m*	12·52 *m*	14·57 *m*	14·05 *vw*
12·14 *m*	12·62 *w*		
12·34 *m*	12·84 *m*		
13·64 *w*	13·22 *w*		
14·10 *w*			
15·30 *m*			

vw = very weak; *w* = weak; *m* = medium; *s* = strong

If the reaction temperature is decreased below 130°C, the yield of cyclic phosphonitrilic bromides is decreased sharply. At between 115 and 120°C, no cyclic compounds are obtained. Rather, large quantities of reddish, crystalline $NPBr_2PBr_{5+n}$ ($n \geqslant 0$) result,

$$2PBr_3 + (2 + n)Br_2 + NH_4Br \rightarrow NPBr_4PBr_{5+n} + 4HBr$$

This rather indefinite species loses bromine reversibly in steps, as

$$\underset{\text{red}}{NPBr_2PBr_{5+n}} \xrightleftharpoons[Br_2]{\text{room temperature}} \underset{\text{red}}{NPBr_2PBr_7} \xrightleftharpoons[Br_2]{80\text{–}100^\circ C} \underset{\text{yellow}}{NPBr_2PBr_5}$$

Both $NPBr_2PBr_7$ and $NPBr_2PBr_5$ appear to be true compounds and not mixtures containing the cyclic phosphonitrilic bromides. Thus, each gives a distinctive X-ray diffraction pattern which contains no lines of the trimer or tetramer (Table 4), both

[10] N. L. PADDOCK and H. T. SEARLE, *Advances in Inorganic Chemistry and Radiochemistry*, (Edited by H. J. EMELÉUS and A. G. SHARPE) Vol. 1, pp. 347–383. Academic Press, New York (1959).

VOL. 22 1961

are insoluble in or decomposed by organic solvents, each hydrolyses much more rapidly than the trimer or tetramer, and extraction of either with organic solvents yields no trimer or tetramer. The two compounds dissolve readily in liquid bromine and add bromine by reversal of the above equilibria. All of these materials polymerize above 120°C to small quantities of trimer and tetramer and somewhat larger quantities of the higher homologues. The infra-red spectra of the compounds where $n = 0$ and 2 are somewhat less sharply defined than those of the trimer and tetramer, but they do indicate the presence of the P-N group (NaCl region). Nuclear magnetic resonance data could be obtained only with liquid bromine solutions of the samples. Although well-defined four-line and one-line spectra were obtained for the $n=0$ and 2 samples, respectively, they cannot be considered definitive because the reversible reaction with bromine previously indicated undoubtedly leads to mixtures.

These compounds resemble closely similar compounds isolated in the chloride series[7] and proposed to have linear structures.* It is reasonable to regard them as intermediates in the formation of the phosphonitrilic halides from the phosphorus(V) halides by analogy to the compound $Cl\phi_2[PNP(NH_2)_2\phi_2$ isolated from the reaction of diphenylphosphorus trichloride and ammonia and polymerizable to diphenylphosphonitrile.[11]

EXPERIMENTAL

Materials

All chemicals were of the highest purity commercially available. Phosphorus(III) bromide and bromine were used without further purification. Ammonium bromide was dried over phosphorus(V) oxide and ground. *Sym*-tetrachloroethane and *sym*-tetrabromoethane were dried over phosphorus(V) oxide and distilled. The n-heptane used for fractional crystallization and the benzene used for extraction were dried with sodium. Solvents used for solubility studies were distilled.

Synthesis of compounds

All syntheses were carried out with standardized quantities of reactants; namely 300 g (1 mole) of phosphorus(III) bromide, 350 g (2·19 mole) of bromine, 300 g (3·06 mole) of ammonium bromide, and ca. 600 ml of solvent. The temperature recorded for each synthesis is that of the oil bath used for heating. All yields are based upon the quantity of phosphorus(III) bromide used.

1. *Reaction at low temperatures—synthesis of* $NPBr_2PBr_5$ *and* $NPBr_2PBr_n$ ($n > 5$). To the standard mixture of phosphorus(III) bromide and ammonium bromide in *sym*-tetrachloroethane, approximately 150 g of bromine was added. The mixture was shaken thoroughly and then heated slowly to 115–118°C. The remaining bromine was then added. After the mixture had been held at this temperature range for 12–14 hr, the excess ammonium bromide was removed without cooling. The solution was then cooled slowly to 0°C to yield 290 g of dark red, crystalline $NPBr_2PBr_n$ ($n > 5$). Upon evaporation of excess bromine from the filtrate and concentration of the resulting solution, an additional 50 g of the product was obtained. The compound is insoluble in cold organic solvents, decomposed by hot organic solvents, readily soluble in liquid bromine, and very easily hydrolysed. On standing in a dry atmosphere at room temperature, it loses bromine slowly and reversibly to give red crystalline $NPBr_2PBr_7$. (Found: N, 1·81; P, 8·09; Br, 90·70. Calcd. for P_2NBr_9: N, 1·76; P, 7·79; Br, 90·45%).

Seventeen and twenty-one hundredths grammes of $NPBr_2PBr_7$ was heated at 85°C for 2 days under a vacuum of 0·25 mm with the loss of 3·44 g (3·46 g theoretical) of bromine. The resulting bright orange compound is similar in properties to $NPBr_2PBr_7$ but has a different X-ray diffraction

* The notations $NPBr_2PBr_5$ and $NPBr_2PBr_7$ are not intended to suggest structures. Although it is possible to formulate a number of simple or polymeric structural arrangements that preserve the indicated P–N bonding and do not violate the accepted concepts of electronic configuration and covalency, the available experimental data do not permit one to distinguish among them. It is apparent that a detailed structural analysis by X-ray methods is essential.

[11] I. I. BEZMAN and J. H. SMALLEY, *Chem. and Industr.* 839 (1960).

pattern (Table 4). When heated above 110°C, it polymerizes. (Found: N, 2·28; P, 9·94; Br, 87·53. Calcd. for P_2NBr_7: N, 2·21; P, 9·75; Br, 88·04%).

The compound $NPBr_2PBr_5$ was treated with bromine, either as such or in an inert solvent, to yield $NPBr_2.PBr_n$ ($n = 7$ or >7). Extraction with benzene or carbon disulphide removed no cyclic trimer or tetramer. Attempts to determine molecular weights in bromine by cryoscopic methods gave indeterminate results because of equilibrium addition and loss of bromine. An analogous behaviour has been observed for PBr_5 itself in bromine.[12,13]

2. *Reactions at medium temperatures—synthesis of* $(NPBr_2)_3$ *and* $(NPBr_2)_4$. As a normal procedure, the standard mixture of phosphorus(III) bromide and ammonium bromide in *sym*-tetrachloroethane with 200 g of bromine was heated to 140–142°C over a period of 5 days. The temperature was maintained at ca. 142°C for two days, and the remaining 150 g of bromine was added. The reaction was then stopped and the unreacted ammonium bromide removed by filtration. Evaporation of the solvent permitted recovery of 255·2 g of crude product. This was extracted with hot benzene to remove the trimeric and tetrameric phosphonitrilic bromides. After evaporating the benzene and subliming twice, 119·0 g (52·5 per cent yield) of trimer-tetramer mixture was obtained. In addition, 126·2 g (35·9 per cent yield) of $NPBr_2PBr_5$ resulted.

A similar experiment employing the same initial conditions but maintaining the reaction mixture at 142°C for 6 days, yielded no $NPBr_2PBr_5$, 131·8 g (58·1 per cent) of trimer-tetramer mixture, and 73·5 g (32·4 per cent) of a mixture of higher homologous.

In each instance, about 8 per cent of the tetramer was found in the trimer-tetramer mixture. A similar experiment carried out at 150–157°C (or 160–167°C) for 6 days decreased the yield of trimer-tetramer mixture to 49·6 per cent (or 45·7 per cent), but increased the tetramer content to 14 per cent (or 20 per cent) while increasing the yield of higher homologues to 40 per cent (or 45 per cent).

As an alternative, 300 g of ammonium bromide in 600 ml of *sym*-tetrachloroethane was heated to 132–134°C, and a mixture of 300 g of phosphorus(III) bromide and 250 g of bromine was added dropwise over a period of 14 hr. The mixture was then maintained at this temperature for 9 days, during which period the remaining 100 g of bromine was added. The procedure outlined above yielded 89·5 g (39·5 per cent yield) of trimer-tetramer mixture containing 5 per cent of the tetramer. The major product of the reaction was $NPBr_2PBr_5$. A similar experiment, differing only in the fact that the mixture was heated initially to 142°C and then maintained at 142–144°C for ten days, yielded 89·9 g (39·6% yield) of trimer-tetramer mixture containing ca. 14% of the tetramer. A large quantity of higher homologues resulted.

3. *Reactions at higher temperatures in* sym-*tetrabromoethane*. The normal procedure outlined under (2) was repeated with substitution of *sym*-tetrabromoethane as solvent, increase of the temperature to 160°C over a period of 6 days, and maintenance of this temperature for an additional 5½ days. After removal of unreacted ammonium bromide and evaporation of the solvent at 90°C (2 mm), a black, buttery residue was obtained. Penta-bromoethane resulting in the reaction was removed from this residue with small quantities of benzene, leaving 215 g (94·5 per cent yield) of crude product. Two sublimations yielded 72·9 g (32·1 per cent) of trimer-tetramer mixture containing 32–35 per cent of the tetramer.

A similar experiment, differing only in that the temperature was raised to 175°C and maintained there for 6 days, yielded 74·5 g (32·8 per cent) of trimer-tetramer mixture containing 43–46 per cent of the tetramer. Another experiment at 180°C (10 days) gave 58·1 g (25·7 per cent) of trimer–tetramer mixture containing about 50 per cent of the tetramer.

Extensive bromination and decomposition of the solvent prevent the use of still higher temperatures and the probable further enhancement of the tetramer content.

Separation of $(NPBr_2)_3$ *from* $(NPBr_2)_4$

By fractional sublimation, mixtures of trimeric and tetrameric phosphonitrilic bromides can be separated into trimer-rich (90–100°C at 0·025 mm) and tetramer-rich (130–150°C at 0·025 mm) fractions, but the method is too time-consuming to effect complete separation. The same can be said of chromatographic separation on alumina with benzene or diethyl ether as solvent.

Fractional crystallization from n-heptane or petroleum ether, b.p. 90–110°C (Table 1), gives the most efficient separation. The usual technique of fractional crystallization is employed. (Found: N, 6·87; P, 15·29; Br, 78·37 ($n = 3$). N, 6·79; P, 15·40; Br, 78·20 ($n = 4$). Calcd. for $(PNBr_2)_n$:

[12] W. Plotnikow, *Z. Phys. Chem.* **48,** 220 (1904).
[13] W. Finkelstein, *Z. Phys. Chem.* **105,** 10 (1923).

VOL. 22 1961

N, 6·84; P, 15·13; Br, 78·03%. Mol. wt. (cryoscopic in benzene). Found: 598. Calcd. for $n = 3$: 614·46. Found: 824. Calcd. for $n = 4$: 819·28).

Polymerization of $NPBr_2PBr_n$ ($n \geqq 5$)

All polymerization reactions were carried out at temperatures between 130°C and 170°C. Because of the bromination–debromination equilibrium, results obtained with all compounds of this type were comparable.

1. *In the presence of ammonium bromide in* sym-*tetrachloroethane*. A mixture of 103·2 g (0·13 mole) of $NPBr_2PBr_7$ and 50·7 g (0·51 mole) of ammonium bromide in 400 ml of *sym*-tetrachloroethane was heated slowly to 140–145°C and maintained at this temperature for 4–5 days. Filtration permitted recovery of nearly all of the added ammonium bromide. Evaporation of the solvent showed the presence of some phosphorus(III) bromide. These observations indicate that whatever the nature of the additional phosphorus in the compound, it is not present as adducted phosphorus(V) bromide. The dark brown. viscous liquid (87 g) remaining after evaporation of the solvent was shown by infrared examination to contain small quantities of trimeric and tetrameric phosphonitrilic bromides as well as the higher homologues in the series. The material was heated in a sublimation apparatus at 200°C and 0·25 mm. Some 9·9 g of trimer–tetramer mixture containing about 10% of the tetramer together with small quantities of phosphorus(V) bromide was collected as a volatile fraction. The higher homologues were converted to phosphonitrilic bromide rubber.

2. *In the presence or absence of ammonium bromide in a sealed tube*. An intimate mixture of 5 g of $NPBr_2PBr_5$ with 1 g of ammonium bromide was covered with a thick layer of ammonium bromide and sealed in a thick-walled tube. The tube was heated to 170°C over a period of 24 hr. The mixture turned brown and liquefied partially. The tube was opened and the lower homologues were extracted with carbon disulphide. Repeated sublimation gave 0·95 g of trimer–tetramer mixture containing 7–8 per cent of the tetramer. A similar experiment with the same quantity of $NPBr_2PBr_7$ yielded 0·93 g of trimer–tetramer mixture of the same composition. No trimer or tetramer could be detected in experiments carried out at 130–140°C.

Comparable experiments at 170°C using 10 g quantities of $NPBr_2PBr_5$ and $NPBr_2PBr_7$ in the absence of ammonium bromide gave 0·91 g and 0·92 g, respectively, of trimer–tetramer mixture, containing 7–8 per cent of tetramer, together with some phosphorus(V) bromide.

Solubility determinations

Saturated solutions of the phosphonitrilic bromides were prepared by allowing the required solvent to equilibrate for two days at 25°C with an excess of the bromide. Tared aliquots of the solution were withdrawn, and the solvent was removed under vacuum. The residue was then weighed directly.

Instrumental studies

The infra-red spectra in the sodium chloride region were obtained with a Model 21 Perkin-Elmer spectrometer, using a sodium chloride prism. The infra-red spectra in the cesium bromide region were obtained with a Perkin-Elmer Model 12 spectrometer modified to double pass action, using CsBr optics. The nuclear magnetic resonance spectra of phosphorus-31 were measured with a Model V–4300B Varian instrument, employing a Model V–4012–HR Varian magnet with a 16·2 Mc/s radiofrequency oscillator and a field of 9395 G. The X-ray diffraction powder patterns were obtained with a Hayes unit using nickel-filtered copper K°C radiation and a camera of 7·0 cm radius.

Analyses

Microanalytical determinations of phosphorus, nitrogen, and bromine were carried out by the Clark Microanalytical Laboratory, Urbana, Illinois. Trimer–tetramer compositions were established either by infra-red spectroscopy or by molecular weight-determination.

Acknowledgements—The authors are particularly indebted to Dr. C. F. CALLIS, Mr. J. J. YODER III, and Mr. M. M. CRUTCHFIELD of the Inorganic Chemicals Division, Monsanto Chemical Company, St. Louis, Missouri, for the measurement of the nuclear magnetic resonance spectra. This investigation was supported by Contract AF 33(616)–5486 with the Materials Laboratory of Wright Air Development Command, Wright-Patterson Air Force Base, Ohio. Reproduction of this communication in whole or in part is permitted for any purpose of the United States Government.

J. Inorg. Nucl. Chem., 1961, Vol. 22, pp. 205 to 212. Pergamon Press Ltd. Printed in Northern Ireland

THE PREPARATION AND PROPERTIES OF SOME INORGANIC ISOTHIOCYANATES

D. B. SOWERBY*
W. A. Noyes Laboratory, University of Illinois, Urbana, Illinois

(*Received* 24 *April* 1961; *in revised form* 20 *June* 1961)

Abstract—Reaction between ammonium or potassium thiocyanate and various phosphorus, silicon and arsenic chlorides in acetonitrile or liquid sulphur dioxide solution leads to complete substitution of the chlorine atoms by thiocyanate groups. The infra-red spectra of these products are discussed and indicate that the compounds are isothiocyanates rather than normal thiocyanates.

VOL. 22 1961

SÖDERBÄCK[1] in 1919 showed that oxidation of elemental arsenic and antimony with thiocyanogen in carbon disulphide solution produced the corresponding trithiocyanates. More general procedures for the preparation of non-metallic thiocyanates involve the reaction between the corresponding non-metal chloride and lead[2,3] mercury(II)[4] or silver thiocyanates either in benzene suspension or in the absence of solvent. The use of silver thiocyanate in benzene suspension has been extensively applied by FORBES and ANDERSON.[5] More recently, alkali metal or ammonium thiocyanates in acetone or acetonitrile solution have been employed as substituting agents, taking advantage of the solubility of the ionic thiocyanates and the essential insolubility of the resulting alkali metal or ammonium chlorides.

As it is possible for the thiocyanate group to be bonded by either the sulphur atom or the nitrogen, a question arises as to whether such reactions yield normal or isothiocyanates. The preparation of typical addition compounds indicates that the products from the reaction of potassium thiocyanate with substituted phosphorus chlorides,[6,7,8] acyl and aroyl chlorides[9] are isothiocyanates. Analogous reactions between alkyl halides and potassium thiocyanate in ethanol on the other hand, yield the corresponding normal thiocyanates.[10,11] Molar refraction measurements showed that phosphorus trichloride, phosphoryl chloride[12] and the methyl chlorosilanes[13] gave compounds with the isothiocyanate structure on treatment with metallic thiocyanates.

The experiments reported here and previously[14] are part of a program to test the

* Now at, Department of Chemistry, University College, London, W.C.1.

[1] E. SÖDERBÄCK, *Ann.* **419**, 217 (1919).
[2] A. E. DIXON, *J. Chem. Soc.* **79**, 541 (1901).
[3] J. E. REYNOLDS, *J. Chem. Soc.* **89**, 397 (1906).
[4] P. MIQUEL, *Ann. chim. phys.* [V] **11**, 289 (1877).
[5] H. H. ANDERSON, "Silicon, Sulphur and Phosphates". *Colloquium of the Section for Inorganic Chemistry of the International Union of Pure and Applied Chemistry*, *p.* 37 *and* 235. Münster, 1954.
[6] G. TESI, R. J. A. OTTO, F. G. SHERIF and L. F. AUDRIETH, *J. Amer. Chem. Soc.* **82**, 528 (1960).
[7] D. T. ELMORE and J. R. OGLE, *J. Chem. Soc.* 2286 (1959).
[8] J. MICHALSKI, H. STRZELECKA and J. WIECZORKOWSKI, *Roczniki Chem.* **31**, 879 (1957).
[9] D. T. ELMORE, J. R. OGLE, W. FLETCHER and P. A. TOSELAND, *J. Chem. Soc.* 4458 (1956).
[10] R. RIEMSCHNEIDER and G. ORLICK, *Monatsh. Chem.* **84**, 313 (1953).
[11] A. P. TERENTYEV and A. I. GERSHENOVICH, *J. Gen. Chem. USSR.* **23**, 209 (1953).
[12] A. E. DIXON and J. TAYLOR, *J. Chem. Soc.* **93**, 2148 (1908).
[13] H. H. ANDERSON, *J. Amer. Chem. Soc.* **69**, 3049 (1947).
[14] B. S. GREEN, D. B. SOWERBY and K. I. WIHKSNE, *Chem. and Industr.* 1306 (1960).

general application of soluble ionic thiocyanates as agents for the substitution of halogen atoms in nonmetallic compounds.

EXPERIMENTAL

Essentially the same procedure was employed in the preparation of the compounds listed in Table 1, except that liquid sulphur dioxide replaced acetonitrile as the reaction medium in the synthesis of phosphorus and arsenic triisothiocyanates. As the products are sensitive to moisture, the reactions were carried out with minimum contact with the atmosphere. The following preparations are typical.

TABLE 1

Compound	Yield (%)	b.p. (°C/mm)	Calcd.			Found		
			C	H	N	C	H	N
$Si(NCS)_4$	87	146*	18·43	—	21·50	18·01	—	21·18
$CH_3Si(NCS)_3$	85	73*	22·09	1·38	80·15†	22·01	1·36	79·6†
$(CH_3)_2Si(NCS)_2$	83	55/0·08	27·54	3·44	16·06	27·72	3·49	16·10
$(CH_3)_3SiNCS$	51	75–7/80	36·58	6·86	10·67	36·54	6·74	10·76
$PO(NCS)_3$	61	106–7/0·5	16·27	—	18·98	16·17	—	19·08
$C_6H_5PO(NCS)_2$	58	146–8/0·3	39·97	2·09	11·66	39·81	1·98	11·79
$PS(NCS)_3$	86	121–3/0·3	15·16	—	17·69	14·98	—	17·58
$C_6H_5PS(NCS)_2$	83	128–30/0·08	37·46	1·95	10·92	37·33	1·99	11·02
$P(NCS)_3$	64	87–8/0·08	17·54	—	20·46	17·30	—	20·52
$As(NCS)_3$	69	—	14·45	—	16·85	13·97	—	16·30

* Melting point.
† NCS content.

Tetraisothiocyanatosilane

A solution of 17 g (0·1 mole) of silicon tetrachloride in 50 ml of carbon tetrachloride was added dropwise with stirring to a solution–slurry of 30·4 g (0·4 mole) of ammonium thiocyanate in 200 ml of anhydrous acetonitrile. The reaction is exothermic and an immediate white precipitate of ammonium chloride formed. The solution was stirred for a further 30 min after the silicon tetrachloride solution had been added. Filtration gave 19·5 g of ammonium chloride (calc. 21·4 g). The filtrate was evaporated to dryness and the pale yellow residue was dissolved in the minimum quantity of warm acetonitrile. Cooling gave 22·6 g of the desired compound.

Arsenic tri-isothiocyanate

To a well-stirred solution of 9·2 g (0·12 mole) of ammonium thiocyanate in 150 ml of anhydrous liquid sulphur dioxide cooled to −25°, there was added dropwise 7·2 g (0·04 mole) of arsenic trichloride dissolved in 20 ml of benzene. After stirring for a further 10 min, the precipitated ammonium chloride was filtered off and washed with carbon disulphide. The combined filtrates were reduced to one half the original volume, and on cooling to −70°, 6·9 g of white crystalline arsenic tri-isothiocyanate separated. The substance decomposes at room temperature, and although it dissolves readily in carbon disulphide, ether, benzene and chloroform, these solutions rapidly deposit red-brown solids.

Infra-red spectra

Spectra in the sodium chloride region were obtained using a Perkin-Elmer Model 21 Spectrometer. Liquids were examined as capillary films and in carbon disulphide or carbon tetrachloride solution. Solids were mulled with Nujol. The measurements at longer wavelengths were made with a Perkin-Elmer Model 12 single beam spectrometer (modified to double pass action) with cesium bromide optics. The instrument was calibrated against atmospheric water vapor and other standards.[15]

[15] R. N. JONES, D. K. FAURE, W. ZAKARIAS, *Revue Univ. Mines*, **15**, 417 (1959). cf F. W. BENKE, Perkin-Elmer Corp. Reprint MPL-5603, 10505.

DISCUSSION

The methods of preparation used here in general require shorter reaction time and give at least comparable yields to those previously used for phosphoryl isothiocyanate,[16] phosphorus triisothiocyanate,[17,18] arsenic triisothiocyanate[1,16] and the isothiocyanatosilanes.[13] The reduced yield in the case of trimethylisothiocyanatosilane results from difficulties in separating the compound from the acetonitrile solvent. In addition the method has been applied in the preparation of the new compounds thiophosphoryl isothiocyanate, phenylphosphonic and phenylphosphonothionic diisothiocyanates. No definite compound was isolated from the reaction between arsenic trichloride and ammonium thiocyanate in acetonitrile; orange-red insoluble products were precipitated in addition to the ammonium chloride. Similar behaviour was noted in previous attempts to replace the chlorine atoms in arsenic trichloride[16] and monosubstituted chloroarsines[19] with thiocyanate groups. As disubstituted chloroarsines reacted smoothly in acetone solution, it was concluded that compounds containing two thiocyanate groups attached to an arsenic atom were not sufficiently stable for isolation. The preparation of arsenic tri-isothiocyanate described above using liquid sulphur dioxide as solvent indicates that the reaction with organo-dichloroarsines in this medium would give the desired products.

VOL. 22 1961

All the isothiocyanates prepared here, with the possible exception of the phenyl substituted phosphorus compounds are markedly unstable in the presence of atmospheric moisture. Consequently, they were handled only in a dry-box. Many of the liquids underwent some decomposition, indicated by progressive yellowing, even when sealed in glass ampoules. This may be due to the decomposition products of thiocyanic acid resulting from hydrolysis by traces of moisture. Phosphorus tri-isothiocyanate was the most unstable and on standing the originally colourless liquid darkened through yellow to brown and deposited a brown solid.

Infra-red spectroscopy, discussed below, indicates that in all the compounds prepared, the thiocyanate radical is attached to the central nonmetal by way of the nitrogen atom giving rise to isothiocyanates. Although analogous reactions with alkyl and substituted alkyl halides lead to the formation of normal thiocyanates, on distillation or suitable treatment at higher temperatures, these compounds isomerize to what are presumably the thermodynamically more stable isothiocyanate derivatives. Also pertinent is the fact that compounds involving the cyanate radical are invariably bonded through the nitrogen atom; the isomeric normal cyanates do not appear to be stable. Stable compounds containing the normal thiocyanate group are found in the case of aromatic thiocyanates and in thiocyanate complexes with metals such as mercury(II) and platinum. These latter elements show a marked tendency toward bond formation with sulphur, involving back donation of electrons from filled metal *d* orbitals to unfilled sulphur orbitals.

The fact that the nitrogen, rather than the sulphur atom of the thiocyanate radical is attached to the central nonmetal in the compounds reported here, can probably be rationalized on the basis of the smaller size and greater electronegativity of the nitrogen. In addition to the formation of a stronger σ-bond with nitrogen, additional π-bonding can also occur by overlap between the *d*-orbitals of the central atom and a

[16] H. H. ANDERSON, *J. Amer. Chem. Soc.* **64**, 1757 (1942).
[17] A. E. DIXON, *J. Chem. Soc.* **85**, 350 (1904).
[18] H. GALL and J. SCHÜPPEN, *Ber. Dtsch. Chem. Ges.* **63B**, 482 (1930).
[19] W. STEINKOPF and W. MEG, *Ber. Dtsch. Chem. Ges.* **53B**, 1013 (1920).

filled nitrogen *p*-orbital. The sulphur atom, on the other hand, being larger and the available orbitals more diffuse, overlap with the *d*-orbitals of the central atom would be much less important.

Infra-red spectra

The linear thiocyanate ion ($N\equiv C-S^-$) gives three fundamental vibrations active in the infra-red,[20] i.e. two stretching vibrations at 2066 cm^{-1} and 743 cm^{-1} associated with the $C\equiv N$ and C—S bonds respectively, and a deformation vibration at 470 cm^{-1}. When the thiocyanate group is covalently bonded through the nitrogen atom, the angle formed between the linear thiocyanate group and the central atom in general will be less than 180° and the positions of these maxima will be modified. CHAMBERLAIN and BAILAR[21] discussed the infra-red spectra of metal complexes involving co-ordinated isothiocyanate groups in terms of the loss of triple bond character of the N—C linkage (resulting in absorption at frequencies lower than that characteristic of the $C\equiv N$ group) and concomitant increase in the bond order of the C—S linkage (causing an increase in the frequency of the C—S absorption).

HAM and WILLIS[22], however, consider that in organic isothiocyanates (R—N=C=S), strong interaction between the cumulative double bonds will give rise to a pseudo-asymmetric vibration at higher frequencies than that characterized by the C=N bond and a symmetric NCS vibration lower than that expected for a C=S bond. Compounds containing the normal thiocyanate radical ($R-S-C\equiv N$) are expected to show absorptions essentially characteristic of the $C\equiv N$ and C—S bonds.

Recently reported spectra[23–27] of various iso and normal thiocyanates substantiate these postulates. Isothiocyanates all exhibit a very intense, broad absorption band between 2000 cm^{-1} and 2100 cm^{-1} (asymmetric stretch) which in dilute solution often shows fine structure. In addition, a second, strong band at ~1090 cm^{-1} for aliphatic compounds and at ~930 cm^{-1} for the aromatic analogs has been correlated with the symmetric stretching vibration. On the other hand, the spectra of organic thiocyanates show a sharp, moderately strong band at ~2175 cm^{-1} but no absorption in the region between 900 cm^{-1} and 1000 cm^{-1}. Absorption at ~460 cm^{-1} in both normal and isothiocyanates appears to be correlated with the NCS deformation vibration. In metal compounds containing co-ordinated thiocyanate groups, absorption in the 2000 cm^{-1} region generally occurs at lower frequencies if the thiocyanate is present in the iso configuration.[28,29]

Strong Raman lines in the spectra of trimethylisothiocyanatosilane and dimethyldiisothiocyanatosilane at ~2060 cm^{-1}, ~1000 cm^{-1} and ~460 cm^{-1} have been assigned, respectively, to the asymmetric, symmetric and deformation vibrations of the NCS group.[30] On the basis of these correlations, differentiation between compounds

[20] L. H. JONES, *J. Chem. Phys.* **25,** 1069 (1956).
[21] M. M. CHAMBERLAIN and J. C. BAILAR, JR. *J. Amer. Chem. Soc.* **81,** 6412 (1959).
[22] N. S. HAM and J. B. WILLIS, *Spectrochim. Acta* **16,** 279 (1960).
[23] N. S. HAM and J. B. WILLIS, *Spectrochim. Acta* **16,** 393 (1960).
[24] E. LIEBER, C. N. R. RAO and J. RAMACHANDRAN, *Spectrochim. Acta* **13,** 296 (1959).
[25] E. SVATEK, R. ZAHRADNIK and A. KJAER, *Acta Chem. Scand.* **13,** 442 (1959).
[26] G. L. CALDOW and H. W. THOMPSON, *Spectrochim. Acta* **13,** 212 (1958).
[27] L. S. LUSKIN, G. E. GANTERT and W. E. CRAIG, *J. Amer. Chem. Soc.* **78,** 4965 (1956).
[28] P. C. H. MITCHELL and R. J. P. WILLIAMS, *J. Chem. Soc.* 1912 (1960).
[29] A. TRAMER, *C.R. Acad. Sci., Paris* **250,** 3150 (1960).
[30] J. GOUBEAU and J. REYHING, *Z. Anorg. Chem.* **294,** 96 (1958).

containing the thiocyanate group in either the normal or the iso configuration is possible.

Silicon compounds

The infra-red spectra of tetraisothiocyanatosilane and the related methylisothiocyanatosilanes are summarized in Table 2. The assignments given were made using the known correlations for the methylchlorosilanes[31,32,33] and the Raman data cited previously.[30] The spectrum of tetraisothiocyanatosilane, here from a nujol mull differs from that obtained previously using the KBr disk technique.[30] The two most intense absorptions (in the regions 1950–2100 cm^{-1} and 950–1075 cm^{-1}) which appear in the spectra of the isothiocyanates but not in those of the corresponding chlorides

TABLE 2.

$Si(NCS)_4$	$CH_3Si(NCS)_3$		$(CH_3)_2Si(NCS)_2$		$(CH_3)_3SiNCS$		
Nujol mull	Nujol mull	CS_2 solution	Capillary film	CS_2 solution	Capillary film	CS_2 solution	
			303 *w*				
			435 *m*		432 *m*		
475 *m**	483 *w*		485 *s*		478 *w*		NCS deformation
553 *m*	535 *m*						
591 *s*			635 *vw*				
			683 *s*	678 *m*	633 *s*		Si-C symmetric stretch
715 *w*	725 *w*			760 *sh*	698 *w*	700 *w*	
	762 *m*	760 *m*					Si-C stretch
			800 *s*	800 *s*	760 *m*	758 *m*	Si-C asymmetric stretch
	790 *s*	785 *s*	830 *s*	825 *sh*	835 *s*	828 *s*	CH_3 rocking
948 *m*	965 *m*	960 *m*	960 *m*	958 *m*			
1075 *s*	1050 *s*	1050 *s*	1015 *s*	1017 *s*	952 *s*	952 *s*	Symmetric NCS stretch
					985 *w*	990 *w*	
	1100 *w*	1094 *w*	1075 *m*	1070 *w*	1050 *w*	1045 *w*	
1150 *w*							
	1273 *s*	1272 *s*	1262 *s*	1263 *s*	1255 *s*	1258 *s*	Symmetric CH_3 deformation
					1330 *w*	1330 *w*	
	1397 *w*	1403 *w*	1400 *m*	1400 *m*	1410 *m*	1408 *m*	Asymmetric CH_3 deformation
					1450 *w*		
2000 *vs*	2005 *vs*	1998 *vs*	2000 *vs*	2005 *vs*	1950 *s*	1960 *s*	Asymmetric NCS stretch
2135 *s*	2095 *vs*	2100 *vs*	2055 *vs*	2070 *vs*	2070 *vs*	2060 *vs*	
2160 *sh*							
2360 *w*		2250 *vs*			2290 *w*		
	2440 *w*	2410 *w*					
2580 *w*	2560 *w*	2550 *w*	2540 *w*	2500 *w*	2500 *w*	2500 *w*	
2620 *w*							
		2910 *w*	2908 *w*		2900 *w*	2900 *w*	Symmetric CH_3 stretch
		2960 *w*	2960 *m*	2960 *m*	2960 *m*	2960 *m*	Asymmetric CH_3 stretch
3470 *w*	3470 *w*	3450 *w*	3350 *w*				

* Abbreviations used: *w*, weak; *m*, medium; *s*, strong; *v*, very; *sh*, shoulder; *br*, broad.

[31] A. L. SMITH, *J. Chem. Phys.* **21**, 1997 (1953).
[32] K. SHIMIZU and H. MURATA, *J. Mol. Spect.* **4**, 201 (1960).
[33] K. SHIMIZU and H. MURATA, *J. Mol. Spect.* **4**, 214 (1960).

VOL. 22 1961

have been assigned to the asymmetric and symmetric NCS vibrations respectively. In dilute solution (carbon tetrachloride or carbon disulphide), the broad high frequency bands can be resolved into at least two maxima. In addition, all the compounds have a band of medium intensity at ~480 cm^{-1} assignable to the NCS deformation mode.

Absorptions associated with the methyl groups occur at essentially the same positions in the corresponding chlorides and isothiocyanates. The methyl stretching (2960 cm^{-1} and 2900 cm^{-1}) and deformation vibrations (1400 cm^{-1} and 1260 cm^{-1}) exhibit the same intensity relationships in both series of compounds.[34] The bands in the region between 760 cm^{-1} and 850 cm^{-1}, arising from Si—C stretching and CH_3 rocking vibrations, have been correlated with the number of methyl groups attached to a silicon atom.[34] These correlations are borne out in the spectra reported here. Bands of medium intensity occur in the region between 950 cm^{-1} and 985 cm^{-1} in the isothiocyanates, while the corresponding chlorides, this region contains only weak combination bands. These may be associated with Si—N vibrations but few compounds containing this structure have been examined to make the correlation with any certainty. A series of methyl silylamines show absorption in the 870–920 cm^{-1} region ascribed to a Si—N stretching mode.[35]

Phosphorus compounds

The data on these compounds, together with arsenic tri-isothiocyanate, is recorded in Tables 3 and 4. For the compounds in Table 3, the asymmetric NCS stretch gives rise to the intense, broad band in the 1900–2000 cm^{-1} region. The bands between 1000 cm^{-1} and 1065 cm^{-1} for the phosphorus compounds can then be correlated with

TABLE 3.

$P(NCS)_3$	$PO(NCS)_3$		$PS(NCS)_3$		$As(NCS)_3$	
Capillary film	Capillary film	CCl_4 solution	Capillary film	CCl_4 solution	CS_2 solution	
			330 *w*			
	380 *s*					P═O deformation (?)
	493 *s*		485 *s*			NCS deformation
620 *s**	630 *s*		622 *s*			
					710 *sh*	
			750 *s*			P═S stretch
750 *m*	750 *m*				750 *s*	
920 *m*	980 *m*	948 *m*	935 *m*	940 *m*	920 *s*	
1005 *vs*	1065 *vs*	1068 *vs*	1045 *vs*	1045 *vs*	960 *m*	Symmetric NCS stretch
1055 *m*						
1300 *w*	1280 *vs*, *br*	1310 *s*				P═O stretch
			1300 *w*	1300 *w*		
					1875 *sh*	
1950 *vs*, *br*	1950 *vs*, *br*	1950 *vs*	1940 *vs*, *br*	1940 *s*	1920 *vs*, *br*	Asymmetric NCS stretch
2600 *w*	2570 *w*	2570 *w*	2540 *w*	2550 *w*	2460 *w*	
3010 *w*	3000 *w*		2900 *w*		2860 *w*	
					3430 *w*	

* Abbreviations used: *w*, weak; *m*, medium; *s*, strong; *v*, very; *sh*, shoulder; *br*, broad.

[34] A. L. SMITH, *Spectrochim. Acta* **16**, 87 (1960).
[35] J. GOUBEAU and J. JIMÉNEZ-BARBERA, *Z. Anorg. Chem.* **303**, 217 (1960).

the symmetric vibration. With arsenic tri-isothiocyanate, the only bands in this general region are at 920 cm^{-1} and 960 cm^{-1}. Although the 920 cm^{-1} is of greater intensity, the higher frequency absorption has been correlated with the symmetric NCS vibration. Of these compounds, only phosphoryl and thiophosphoryl isothiocyanates were examined in the CsBr region; both show the expected absorption, 493 cm^{-1} and 483 cm^{-1} respectively, due to the isothiocyanate deformation.

The phosphoryl stretching vibration in phosphoryl isothiocyanate gave a strong broad band at 1280 cm^{-1} as a capillary film, but in 5 per cent carbon tetrachloride solution, the maximum was shifted to 1310 cm^{-1}. Using this latter value for the phosphoryl stretching frequency, calculation[36] of the "electronegativity" of the isothiocyanate group gives a relatively high value of 3·16. The spectrum of phosphoryl isothiocyanate shows a band of medium intensity at 380 cm^{-1}, which may be attributed to the phosphoryl bending vibration. In trimethyl phosphine oxide,[37] this vibration gives rise to a strong Raman line at 369 cm^{-1}.

VOL. 22 1961

The P═S stretching vibration leads to a strong band at 760 cm^{-1} in the spectrum of thiophosphoryl isothiocyanate. Although the position of this band is not as susceptible to the electronegativity of the attached atoms or groups as that due to the phosphoryl vibration, the position is comparable to those previously determined[38] for thiophosphoryl chloride (745 cm^{-1}) and thiophosphoryl bromide (718 cm^{-1}). A weak absorption at 1300 cm^{-1} appeared in some of the spectra of phosphorus tri-isothiocyanate and probably arises from air oxidation of this compound. Further correlations are uncertain, but the bands at 750 cm^{-1} and between 620 cm^{-1} and 630 cm^{-1} are probably associated with asymmetric and symmetric P—N stretching vibrations.

Table 4 contains a summary of the spectra of phenylphosphonic di-isothiocyanate, phenylphosphonothionic di-isothiocyanate and the chlorine analogs obtained using capillary films. The spectra of the chlorides are similar to those reported previously.[39] The major difference between the chlorides and isothiocyanates is the appearance of the two absorption bands associated with the isothiocyanate group, at 1040 cm^{-1} and 1940 cm^{-1} for the phosphoryl compound and at 1025 cm^{-1} and 1940 cm^{-1} for the sulphur analogue. The bands due to the monosubstituted phenyl group were assigned following the convention of WHIFFEN.[40] In general, only very small shifts were observed on substituting the chlorine atoms by isothiocyanate groups. An exception occurred with the strong absorption at 1105 cm^{-1} in the spectrum of phenylphosphonic dichloride which was shifted to higher frequencies (1123 cm^{-1}) on substitution with isothiocyanate. A similar situation holds in the case of the sulphur analogues where the corresponding maximum was shifted from 1095 cm^{-1} to 1113 cm^{-1} in the isothiocyanate. The absorption bands at ~1440 cm^{-1} are considered characteristic of the presence of the P-phenyl group[41] but absorption at this position also occurs in many monosubstituted benzene compounds.[40] Strong absorption at 1272 cm^{-1} in the phosphoryl compounds can be correlated with the phosphorus–oxygen stretching vibration, but the only absorptions in the region characteristic of the P═S linkage can be correlated with the vibrations of the phenyl

[36] J. V. BELL, J. HEISLER, H. TANNENBAUM and J. GOLDENSON, *J. Amer. Chem. Soc.* **76**, 5185 (1954).
[37] L. W. DAASCH and D. C. SMITH, *J. Chem. Phys.* **19**, 22 (1951).
[38] T. N. HOOGE and P. J. CHRISTEN, *Rec. Trav. Chim.* **77**, 911 (1958).
[39] L. W. DAASCH and D. C. SMITH, *Analyt. Chem.* **23**, 853 (1951).
[40] D. H. WHIFFEN, *J. Chem. Soc.* 1350 (1956).
[41] L. J. BELLAMY, *The Infra-red Spectra of Complex Molecules*, (2nd Ed). Methuen, London (1958).

ring. However, absorption due to this group is reported as being of variable intensity and in some cases, the band is absent.

TABLE 4.

$C_6H_5POCl_2$	$C_6H_5PO(NCS)_2$	$C_6H_5PSCl_2$	$C_6H_5PS(NCS)_2$	
683 *s**	688 *s*	683 *s*	690 *s*	Out of plane ring deformation (v)†
715 *s*	725 *s*	720 *w*	720 *w*	
745 *s*	750 *s*	745 *s*	750 *s*	C—H out of plane deformation (f)
	785 *w*	780 *w*	780 *w*	
838 *vw*	845 *w*	835 *w*		C—H out of plane deformation (g)
915 *w*		918 *w*		C—H out of plane deformation (i)
940 *w*	940 *w*		935 *w*	
995 *m*	995 *w*	995 *m*	995 *w*	Ring breathing (p)
1020 *w*		1025 *w*		C—H in plane deformation (b)
	1040 *vs*		1025 *vs*	Symmetric NCS stretch
1063 *w*				C—H in plane deformation (d)
1105 *s*	1123 *s*	1095 *s*	1113 *s*	
		1112 *sh*	1130 *sh*	
1138 *w*				
1160 *w*	1160 *w*	1158 *w*	1158 *w*	C—H in plane deformation (c)
1180 *w*	1182 *w*	1182 *w*	1182 *w*	C—H in plane deformation (a)
1273 *vs*	1272 *vs*			P═O stretch
		1278 *w*	1278 *w*	C—H in plane deformation (e)
1308 *w*		1305 *m*	1305 *m*	
1335 *w*		1335 *w*	1335 *w*	C—C stretch (o)
1385 *vw*	1390 *vw*	1388 *w*	1388 *w*	
		1398 *vw*		
1440 *vs*	1440 *vs*	1438 *vs*	1440 *s*	C—C stretch (n) and/or P-phenyl
1465 *vw*		1460 *w*	1460 *w*	
1485 *w*	1485 *w*	1480 *m*	1480 *m*	C—C stretch (m)
	1575 *sh*		1570 *m*	
1585 *m*	1588 *m*	1580 *m*	1585 *m*	C—C stretch (k, l)
1605 *vw*		1605 *vw*		
1675 *w*	1675 *w*	1668 *w*		
	1725 *vw*			
1765 *w*	1770 *w*	1760 *w*	1760 *w*	Aromatic combinations and overtones
1815 *w*		1805 *w*	1805 *w*	
		1892 *w*		
		1915 *w*		
	1940 *vs, br*		1940 *vs, br*	Asymmetric NCS stretch
		1968 *w*		
	2270 *w*	2190 *w*		
	2570 *m*		2430 *w*	
3070 *m*	3060 *m*	3065 *m*	3060 *m*	C—H stretch

* Abbreviations used: *w*, weak; *m*, medium; *s*, strong; *v*, very; *sh*, shoulder; *br*, broad.
† WHIFFEN's notation (see Reference 40).

Acknowledgements—The author thanks Dr. T. L. BROWN of the University of Illinois for help in the interpretation of the infra-red spectra. Mr. B. S. GREEN and Miss K. I. WIHKSNE carried out preliminary studies on the preparation of some of the compounds. Thanks are also due to Mr. J. NEMETH and his staff for analyses and to the Victor Chemical Company and General Electric Company for chemicals.

J. Inorg. Nucl. Chem., 1961, Vol. 22, pp. 213 to 229. Pergamon Press Ltd. Printed in Northern Ireland

EQUILIBRIUM PRESSURES AND PHASE RELATIONS IN THE URANIUM OXIDE SYSTEM

L. E. J. ROBERTS and A. J. WALTER
Atomic Energy Research Establishment, Harwell, England

(*Received* 11 *May* 1961)

Abstract—Equilibrium oxygen pressures have been directly determined by tensimetric experiments at 1000°–1450°C over the composition range $UO_{2\cdot00}$–$UO_{2\cdot30}$. An invariant point has been found at 1123 ± 5°, at which the three solid phases UO_{2+x}, U_4O_9 and $UO_{2\cdot61}$ are in equilibrium. The U_4O_9 phase does not extend to compositions richer in oxygen than $UO_{2\cdot25}$ in this temperature range. The tensimetric results are used to construct the relevant parts of the phase diagram and to calculate ΔG, ΔH and ΔS for the formation of all phases intermediate between UO_2 and U_3O_8 from $UO_{2\cdot00}$.

VOL. 22 1961

PREVIOUS studies of the uranium–oxygen system have shown that the phases stable at high temperatures are the UO_{2+x} phase, with a structure based on the fluorite structure of UO_2, the cubic or pseudo-cubic U_4O_9 phase and the orthorhombic U_3O_{8-y} phase.

Crystallographic studies[1] have shown that the limiting value of x in the annealed UO_{2+x} phase increases from nearly zero at 300° to 0·17 at 900°. BILTZ and MÜLLER studied the decomposition of U_3O_8 by tensimetric methods[2] at 750°–1160°; they showed that the limiting composition of the U_3O_{8-y} phase was $UO_{2\cdot61}$ at 1160° and that this was in equilibrium with a phase of composition about $UO_{2\cdot2}$, but their technique did not allow of the precise determination of oxygen pressures below 1 mm. BLACKBURN[3] made measurements between 950° and 1150° by the Knudsen effusion technique, estimating the change in composition by the change in weight of the effusion cell. ARONSON and BELLE[4] studied equilibria between 880° and 1080° by determining the e.m.f. of a cell reversible to oxygen ions only, with one electrode a uranium oxide of known composition and the other a mixture of iron and wustite which served as the standard electrode. These studies indicated that a single, non-stoicheiometric phase exists from $UO_{2\cdot0}$ to $UO_{2\cdot26}$ at 1130°. We have extended these studies to 1450°, using a tensimetric technique with direct measurement of oxygen pressures, and also studied in greater detail the region $UO_{2\cdot20}$–$UO_{2\cdot25}$ between 1000° and 1200°.

EXPERIMENTAL

(1) *Apparatus.* The sample was contained in a tube, 12·5 mm diameter and 45 cm long, of recrystallized pure alumina, obtained from Morgans Crucible Co. About 16 cm of this tube fitted inside a tube furnace consisting of platinum or platinum–rhodium alloy wire wound on an alumina tube. An 8 cm zone of this furnace was at a constant temperature to ±5° at 1200°. The alumina tube was connected with Apiezon 'W' wax to a Pyrex system consisting of a McLeod gauge, a liquid air trap and a Pirani gauge through 11 mm tubing; the section could be isolated by a stopcock lubricated with silicone grease. The stopcock led to a conventional gas-dosing system, consisting of a gas-burette and constant-volume mercury manometer, a gas-purification train and pumps.

(1) F. GRONVOLD, *J. Inorg. Nucl. Chem.* **1**, 357 (1955).
(2) W. BILTZ and H. MÜLLER, *Z. Anorg. Chem.* **163**, 257 (1927).
(3) P. E. BLACKBURN, *J. Phys. Chem.* **62**, 897 (1958).
(4) S. ARONSON and J. BELLE, *J. Chem. Phys.* **29**, 151 (1958).

Two thermocouples were strapped to the alumina tube at the same level as the samples; one was a Pt–13% Rh–Pt and the other a 5% Rh–Pt–20% Rh–Pt couple and both had been calibrated against a standard thermocouple calibrated by the National Physical Laboratory. The controlling thermocouple of a Kent controller-recorder was situated close to the measuring thermocouples. Crude control of the temperature was effected by a Variac transformer and the controller switched in a resistance which reduced the current by 10 per cent; the temperature could be held constant to $\pm 3^\circ$ at 1450°.

(2) *Materials*. Three samples of urania were used: (i) *M*. A pure grade of commercial dioxide, (ii) *C*4. A sample made from the pure grade of "ammonium diuranate" available in the U.K.A.E.A. This was roasted in air at 850°, forming U_3O_8, and reduced in hydrogen at 760°. (iii) *P*. A specimen made from sample M by heating in a vacuum-furnace to 2200°, crushing the sintered mass and taking only the coarse particles.

The characteristics of these specimens were as follows:

	M	*C*4	*P*
Density (g/cm³) (Helium disp.)	10·15	10·76	10·65
Surface area (m^2/g)	0·63	1·2	—
Crystallite size (μ)	0·18	0·53	>1

Samples were submitted for spectrographic analysis after the completion of some experiments—i.e. after the urania had been heated in contact with alumina for many hours. The samples contained 0·05–0·2 per cent of Al and 10–40 p.p.m. of Si; the only other major impurity detected was 1·1 per cent of Ta in specimen *P*, which had been heated in a vacuum furnace with Ta radiation shields.

(3) *Procedure*. In a typical experiment, a sample of urania was weighed into the furnace tube, either directly or in an alumina boat or crucible. It was outgassed at a high temperature and reduced to the stoicheiometric composition in several batches of pure carbon monoxide at 800°, and then outgassed at 1200°–1400° until the rise in pressure on isolating the system was small. Both gas condensible at −183°, probably CO_2, and permanent gas, either H_2 or N_2, were pumped off during this outgassing. The sample was then cooled to room temperature and a measured quantity of oxygen admitted. The temperature was raised until the oxidation rate was reasonably fast, but maintained below 300° so that U_3O_8 would not be formed immediately, and oxidation continued until the desired composition had been reached; any excess oxygen was pumped away. The sample was again outgassed at 850°, or at some other suitable temperature at which there was no risk of loss of oxygen, the system isolated and the temperature raised.

Equilibrium oxygen pressures were determined at a number of temperatures, on heating and again on cooling. The Pirani was used for determining that the pressure was constant; actual readings were made on the McLeod. Higher pressures than could be determined with the McLeod were read on the mercury manometer; to determine accurately pressures in the mm range, the gas-burette was put in connection with the furnace tube, then isolated and the gas in it compressed by a known ratio and the pressure measured.

Equilibrium was attained rapidly and the pressures could be seen following slightly behind the temperature rise and fall through the $\pm 3^\circ$ cycle of the controller. It was usually possible to take pressure readings at a precise point of the temperature cycle. The attainment of equilibrium was also checked at some points by admitting a little extra oxygen to the system at 1200°. The pressure fell to the previous equilibrium value in a few minutes. After some temperature cycles, the composition was sometimes changed by adding more oxygen, and the procedure repeated.

No correction to the composition of the oxide due to O_2 in the gas-phase were necessary until the pressure was higher than ~0·02 cm, for a 3 g sample of oxide; the composition loss at higher pressures was calculated from the known volumes of the various parts of the system.

At the end of the experiment, the oxide was recovered from the tube and analysed, either by the ignition of duplicate samples to U_3O_8 or by reduction to $UO_{2\cdot00}$ with CO and measurement of the CO_2 produced. Analyses of duplicate samples usually agreed to within ±·002 O/U.

VOL. 22 1961

THERMOMOLECULAR FLOW CORRECTION

The pressure (p_1) at the hot end of a tube at a temperature T_1 (°K) is equal to the measured pressure p_2 at room temperature T_2 (°K) only if the mean free path (λ) of the gas is less than $0{\cdot}01r$, where r is the radius of the tube. In the limiting case for very low pressures, when $\lambda/r \to \infty$, $p_1/p_2 = \sqrt{(T_1/T_2)}$. The mean free path of oxygen is 7·6 mm at 900° and 5×10^{-3} cm pressure. Since the alumina tube which contained the sample had an internal diameter of 12·5 mm it was necessary to estimate the thermomolecular flow correction for the intermediate case of $\lambda \sim r$.

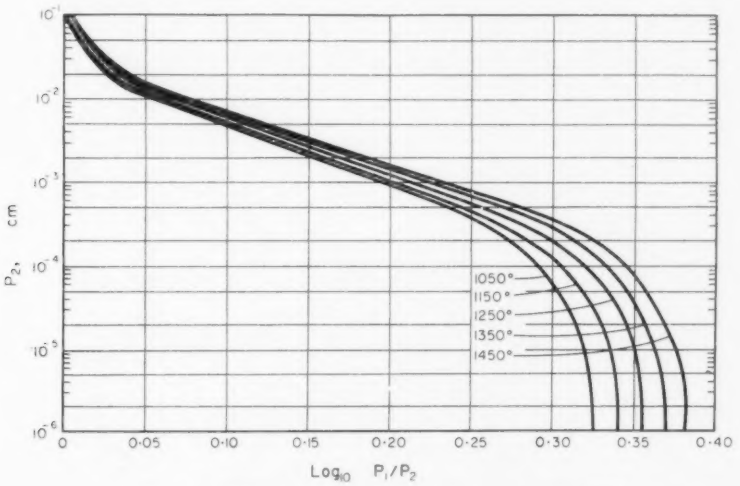

FIG. 1.—Thermomolecular flow corrections actually used.

No experimental determinations of this correction at high temperatures could be found in the literature. Recent appraisals of a general equation proposed by WEBER have been made by VAN ITTERBECK and DE GRANDE[5] and by LOS and FERGUSON[6], and of another equation proposed by LIANG by BENNETT and TOMPKINS[7]. The most appropriate equation for our conditions seemed to be that deduced by LOS and FERGUSON for argon, using the molecular constants known for oxygen. The equation used was

$$\log_{10}\frac{p_1}{p_2} = \tfrac{1}{2}\log_{10}\frac{T_1}{T_2} + 0{\cdot}09864\log_{10}\frac{y_1 + 0{\cdot}1468}{y_2 + 0{\cdot}1468} + 0{\cdot}1267\log_{10}\frac{y_1^2 + 5{\cdot}651\,y_1 + 9{\cdot}999}{y_2^2 + 5{\cdot}651\,y_2 + 9{\cdot}999} + 0{\cdot}2235\left(\tan^{-1}\frac{y_1 + 2{\cdot}825}{1{\cdot}420} - \tan^{-1}\frac{y_2 + 2{\cdot}825}{1{\cdot}420}\right).$$

In this equation, $y = r/\lambda$ and y_1, y_2 refer to T_1 and T_2 at the mean pressure $\frac{1}{2}(p_1 + p_2)$ in the tube. The mean free path λ can be calculated from the equation

$$\frac{1}{\lambda} = \frac{p}{(p\lambda)_0}\left(\frac{T_0}{T}\right)^{1+n}$$

[5] VAN ITTERBECK and E. DE GRANDE, *Physica* **13**, 422 (1947).
[6] J. M. LOS and R. R. FERGUSSON, *Trans. Faraday Soc.* **48**, 730 (1952).
[7] M. J. BENNETT and F. C. TOMPKINS, *Trans. Faraday Soc.* **53**, 185 (1957).

where p is expressed in microbars and $T_0 = 273{\cdot}2°K$. For oxygen, $(p\lambda)_0 = 6{\cdot}36$ and $n = 0{\cdot}42$.

It was convenient to express the results as a plot of p_2, the measured pressure, against $\log_{10}(p_1/p_2)$; the curves obtained for five temperatures are given in Fig. 1, assuming $T_2 = 295{\cdot}0°K$.

The best justification of the use of the correction factors in Fig. 1 is the internal consistency of the results so obtained. This is illustrated in Fig. 2, in which are plotted

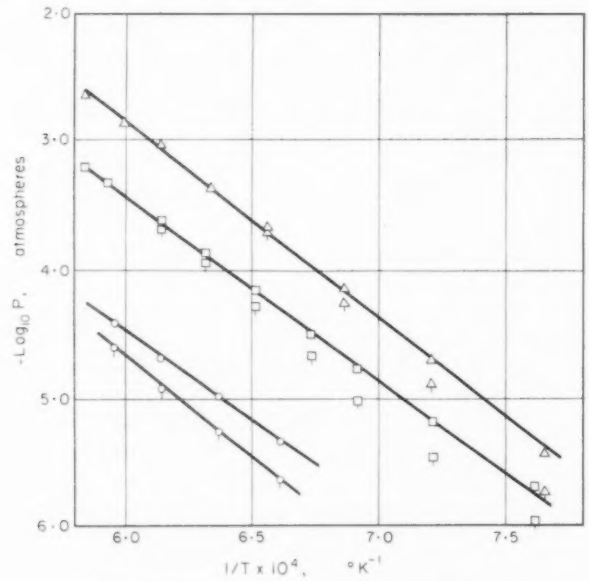

FIG. 2.—Application of thermomolecular flow corrections.
Compositions O/U: 2·141, ⊙ Uncorrected, ○ Corrected.
: 2·206, △ Uncorrected, △ Corrected.
: 2·186, ⊡ Uncorrected, □ Corrected.

the logarithms of observed pressures (p_2) and the corrected pressures (p_1) for three compositions in the non-stoicheiometric range. At the higher pressures, $p_1 \sim p_2$ and the slope of the $\log p$ vs. $1/T$ plots can be defined from those points where the thermomolecular flow correction is negligible. It can be seen that the corrected points at low pressures, where the correction is large, fall quite well on the same straight lines. This was thought to justify the use of the factors given in Fig. 1 in other cases where the higher pressure points were not obtained.

RESULTS AND DISCUSSION

(1) *Volatility*

A major experimental difficulty was the volatilization of a uranium oxide species, presumably UO_3,[8] at high temperatures. This caused the deposition of a sublimate in the cooler parts of the furnace tube which analysed as about $UO_{2{\cdot}5}$ and which consisted of a mixture of the U_4O_9 and $UO_{2{\cdot}61}$ phases. This caused a decrease in the

[8] R. J. ACKERMANN, R. J. THORN, C. ALEXANDER and M. TETENBAUM. *J. Phys. Chem.* **64**, (1960) 350.

O/U ratio of the specimen remaining at a higher temperature. The amounts of sublimate varied widely from run to run, as can be seen from the summary of all the experiments given in Table 1. The "calculated composition", given in column (3) of

TABLE 1.—LOSS OF WEIGHT DUE TO VOLATILITY

Run	Wt. of oxide (g)	Calculated composition O/U	Heating cycles	Final composition O/U	Sublimate calc. (mg)	Sublimate obs. (mg)
*C*4/2 to *C*4/10	6·279	2·097 to 2·405	21	—	—	Heavy
P/1 to *P*/7	4·180	2·311	15	—	—	Heavy
M/1 to *M*/7	4·055	2·05 to 2·315	20	2·303	89*	Slight
2/*M*/1 to 2/*M*/2	2·359	2·185 to 2·249	9	2·179	459	>200
Mp	4·388	2·184	4	2·184	0	Slight
2/*C*4	3·320	2·242	4	2·237	37	Slight
3/*C*4	2·680	2·195	3	2·170	182	—
4/*C*4	3·007	2·271	3	2·229	432	—
*H*1/*C*4	2·880	2·194	3	2·183	89	100
*H*2/*C*4	2·984	2·272	2	2·253	215	130
*H*3/*C*4	2·940	2·221 to 2·250	11†	2·247		Slight

* Calculated from reducing sublimate in tube to $UO_{2\cdot0}$.
† In this case alone the temperature did not rise above 1200°.

Table 1, is the O/U ratio computed from the original weight of the sample and the amounts of oxygen added to the stoicheiometric UO_2. The total number of heating cycles, usually between 800° and 1450°, before the sample was taken out, is given in column (4) and the amount of sublimate in column (7). The "final composition" recorded in column (5) is thought to be typical of the solid remaining at the highest temperature at the end of the heating cycles on the sample. This cannot be given for samples C_4 or P; the final analysis in these cases agreed quite closely with the calculated composition despite evidence that considerable volatility had occurred. The oxide samples C_4 and P were weighed directly into the tube and it is evident that the sublimate was non-adherent and mixed with the oxide from the bottom of the tube when the tube was opened. This difficulty was circumvented in runs *H*1/*C*4, *H*2/*C*4 and *H*3/*C*4 by using a horizontal furnace tube with the oxide sample in an alumina boat; the final composition was then the O/U ratio of the material in the boat at the end of the experiment. In all the other runs, the furnace tube was vertical but the oxide was contained in an alumina crucible and the final composition was estimated by analysing the sintered block of oxide always found in the crucible after the heating cycles; any loose scale that might have been removed as the crucible was taken out was thus not included in the specimen used for analysis. Samples of oxide were usually loose-packed at the start; sample M_p was a compressed pellet of oxide previously oxidized to the composition O/U = 2·184.

The weight of sublimate of composition $UO_{2\cdot55}$ necessary to account for the change in composition observed is given in Table 1 (column 6) and observations on the sublimate which could be removed from the tube are in column (7). In general, more volatilization occurred the higher the O/U ratio, particularly at compositions with O/U > 2·25, when the $UO_{2\cdot6}$ structure was formed, as might be expected. Very little volatilization occurred from the compressed pellet (*Mp*) and little from M samples

except from the 2M/1–2 runs, which were carried out using an alumina crucible from a different source; this type of crucible seemed to be more completely penetrated by the uranium oxide than the usual sort and this may have aided sublimation. The sublimation in runs on sample 2/*C*4 was less than expected. Very little sublimation occurred when the temperature was kept below 1200° (*H*3/*C*4).

It is probable that the amount of sublimation varied with the rate of heating, the extent to which the oxide sample was sintered and the oxygen pressure generated. It is by no means certain that the equilibrium pressure of UO_3 gas was ever attained.

From the maximum amount of sublimation that occurred in our experiments (run 4/*C*4), we calculated a UO_3 pressure of 10^{-3} atm at 1720°K, assuming that the specimen was at the highest temperature for a total of 1·5 hr and that one-third of the total sublimation occurred during that time. Towards the end of this study, an experimental determination of the free energy of formation of gaseous UO_3 was published.[8] Using this information, the known heats of formation of UO_2 and U_3O_8[9,10] and our own values for the heats of formation of intermediate phases, it was possible to calculate the pressures of UO_3(g) in equilibrium with the oxide samples in these experiments. The results of these calculations are collected below, together with the values of the oxygen pressures actually observed (atm).

Composition	1396°K		1695°K	
	$\log P_{UO_3}$	$\log P_{O_2}$	$\log P_{UO_3}$	$\log P_{O_2}$
$UO_{2\cdot2}$	−7·2	−4·8	−4·5	−2·8
$UO_{2\cdot61}$	−6·9	−3·7	−4·3	−1·5

The pressure of UO_3(g) is usually less than 1 per cent of the pressure of O_2. We have therefore applied no correction for UO_3 pressure, which means that the oxygen pressure may have been overestimated at the highest temperatures. No deviation in this sense from the expected law at high temperatures has been observed.

(2) *Corrections applied due to volatility*

All O/U ratios were corrected for loss of oxygen due to the volatility effect discussed above. In single-phase, non-stoicheiometric regions of the phase diagram, the occurrence of an appreciable loss of oxygen from the sample in the hottest zone of the furnace could be experimentally diagnosed since it caused a decrease in the oxygen pressure at any temperature on successive heating cycles or on cooling from the highest temperatures, at which most sublimation took place. Generally, the $\log p$ vs. $1/T$ plots of successive runs were closely parallel, and it seemed that more sublimation may have taken place the first time an oxide of a given composition was heated than on subsequent temperature cycles. The composition change that took place between successive heating cycles could be estimated from the fall in pressure once the isotherms of pressure against composition had been established. This could be done assuming that the composition determined by analysis at the end of the last heating run was typical of the last heating cycle; reference to Table 1 shows that this assumption could be made for specimens *Mp*, 2/*C*4, 3/*C*4, *H*1/*C*4, *H*2/*C*4, and *H*3/*C*4. Corrections for oxygen loss made using these approximate isotherms were accurate enough so long

as they were small, and the mean composition during the final heating cycle of some of these runs was corrected in this way. In addition, there was no evidence of sublimation from specimen *M* after the third run *M*3 and the final O/U ratio for this specimen was lower than the "calculated" value only by 0·01 O/U. The first two runs on specimen *C*4 (at O/U = 2·097 and 2·121) and the first run on specimen *P* at which measurable pressures were obtained (*P*/2, O/U = 2·114) showed only small volatility effects. The O/U ratios for later runs on these two specimens, *C*4/3–*C*4/10 and *P*/3–*P*/7, had to be estimated from the measured pressures and the isotherms constructed from the other experiments; there was thus no internal check on these values and, where they are used, the compositions in these runs are enclosed in brackets.

The final analyses, nominal compositions calculated from the oxygen added to $UO_{2\cdot00}$ and corrected compositions for all runs except *H*3/*C*4 are collected here; *H*3/*C*4 runs are discussed in detail below. Some explanation of the numbering of runs will enable the sequence of experiments to be followed. The symbols *C*4, *M* and *P* refer to the three specimens, described above, and *Mp* refers to a pressed pellet of *M*; the numbers before these symbols identify the particular sample and *H* refers to runs made with a horizontal furnace tube; the numbers following the sample symbol give the number of oxidation stages the sample has undergone and the final small letters *a*, *b*, *c* etc. identify the particular heating cycle at which measurements were made.

VOL. 22 1961

Run:	*C*4/2*c*	*C*4/3*c*	*P*/2*a*,*b*	*M*2*c*	*M*3	*M*4	*M*5
Calculated O/U:	2·097	2·121	2·114	2·145	2·218	2·249	2·269
Analysis O/U:	—	—	—				
Corrected O/U:	2·094	2·114	2·114	2·141	2·206	2·237	2·257
Run:	*M*6	*M*7	2/*M*/1	2/*M*/2*b*	*Mp*	2/*C*4*b*,*c*	3/*C*4*c*.
Calculated O/U:	2·291	2·315	2·185	2·249	2·184	2·242	2·195
Analysis O/U:		2·303		2·179	2·184	2·237	2·170
Corrected O/U:	2·279	2·303		2·179*	2·184	2·239	2·172
Run:	4/*C*4*c*	*H*1/*C*4*c*		*H*2/*C*4*b*			
Calculated O/U:	2·271	2·194		2·272			
Analysis O/U:	2·229	2·183		2·253			
Corrected O/U:	2·229*	2·186		2·262			

* Owing to large volatility, this composition is doubtful.

(3) *The phase diagram*

It is convenient to describe first the general features of the U—O_2 phase-diagram which have been established as a result of this work. In common with other authors, we have found (i) two regions in which the equilibrium pressure at any temperature does not vary with composition and in which two solid phases must co-exist; these are the UO_{2+x}–U_4O_{9-y} region below 1123° and the $UO_{2\cdot25}$–$UO_{2\cdot6}$ region at all temperatures, (ii) two ranges in which the pressure varies continuously with composition and in which only one solid phase can be present; these are the UO_{2+x} region ($0 < x < 0{\cdot}26$ above 1123°) and the U_4O_{9-y} region below 1123°.

The experimental results which establish this phase diagram are mainly the results on H_3/*C*4, shown in detail in Fig. 3. This specimen was oxidized successively to the compositions O/U = 2·221, 2·230, 2·239, 2·245 and 2·250 and pressure readings taken at temperatures of 900°–1200°. The agreement between successive runs at the same composition was good until the highest composition was reached, showing that no

appreciable volatility of UO_3 occurred until the composition O/U = 2·250. At lower temperatures the pressures recorded during the second heating run at this composition were appreciably below the first, and the final analysis was O/U = 2·247 ± 0·002; this is taken as the composition for the second heating run, and O/U = 2·250 assumed for the first.

The line *AB* represents the pressures in the two-phase region $UO_{2\cdot6}$–UO_{2+x} and is extrapolated from results at higher temperatures (see §4); the line *BC* also represents a two-phase region since pressures for the compositions from O/U = 2·262–2·303

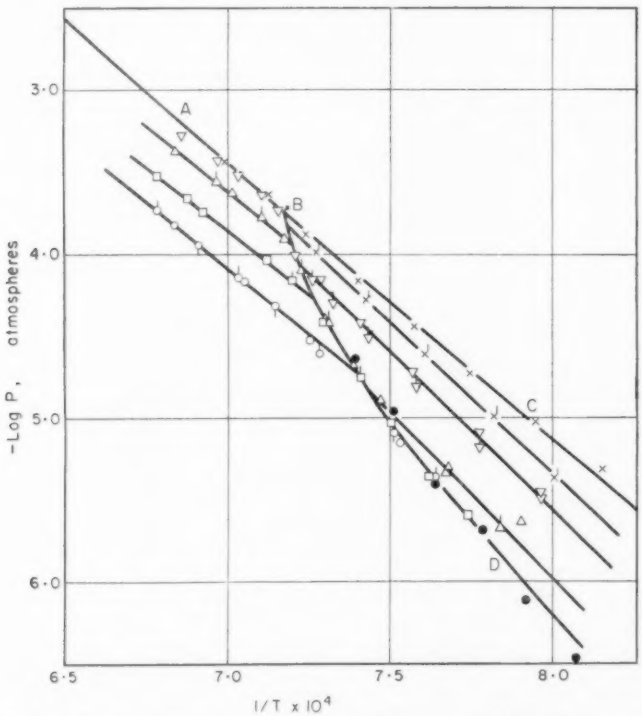

FIG. 3.—Equilibrium Oxygen Pressures below 1200°C. Compositions O/U: ⊙ 2·221; ⊡ 2·230; △ 2·239; ▽ 2·245; ⨯ 2·247; × 2·250: ● Blackburn's results.

agree with those for O/U = 2·250. The fact that pressures for a number of compositions fall along the curved line *BD* shows that this line represents pressures in the two phase region UO_{2+x}–U_4O_{9-y}. The logarithm of the pressures in the single-phase regions are a linear function of $1/T$ and the limiting values of the UO_{2+x}, U_4O_{9-y} phases are given by the points at which these lines in the non-stoicheiometric regions cut the line *BD*.

Some results from other runs can be compared with those in Fig. 3. The agreement with results from run *M*4 (O/U = 2·237) was good; the pressures for runs 4/*C*4 and 2/*C*4 are rather higher than those of *H*3/*C*4 runs at comparable compositions. Because of the difficulty of deciding exact compositions for runs carried to higher temperatures, the results on *H*3/*C*4 should be the more accurate.

Some results taken from BLACKBURN's paper[3] are shown in Fig. 3; the agreement with our results is reasonably good except that BLACKBURN's pressures in the two-phase

region U_4O_9–$UO_{2\cdot6}$ are lower than ours. The phase diagram constructed from the results in Fig. 3 and some results at higher temperatures described in §4 is given in Fig. 4. BLACKBURN's results for the phase boundaries are given also. Again, agreement is good except for two points in the UO_{2+x}–U_4O_{9-y} region but we cannot agree with BLACKBURN that the U_4O_9 phase extends much beyond the composition $UO_{2\cdot250}$. BLACKBURN estimated this phase boundary by using extrapolation procedures that may not have been very accurate.

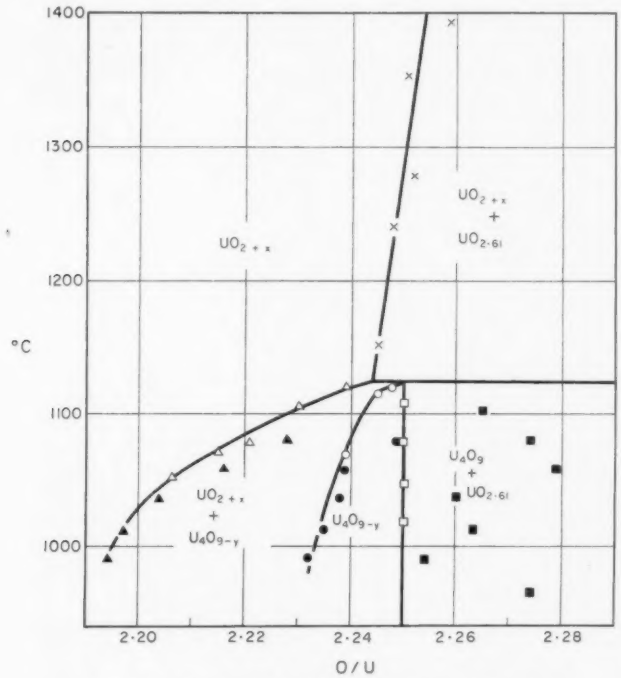

FIG. 4.—Portion of the Uranium-Oxygen Phase Diagram.
Open symbols—our results; full symbols—Blackburn's results. △ and ×: limit of UO_{2+x} phase; ○ and ⊡: limits of U_4O_{9-y} phase.

Special interest attaches to the temperature $1123 \pm 5°$, at which we show an invariant point with the three phases $UO_{2\cdot245}$, $UO_{2\cdot250}$ and $UO_{2\cdot6}$ in equilibrium. The evidence for this is that the pressures for *H*3/*C*4/4 (O/U = 2·245) *H*3/*C*4/5 *a* (O/U = 2·250) and *H*3/*C*4/5*b* (O/U = 2·247) all reach the two-phase line *AB* from 1123° to 1140° (Fig. 3). The *H*3/*C*4/4 and *H*3/*C*4/5*b* points are definitely below *BC*, and it is probable, though not completely certain, that the *H*3/*C*4/4 points begin to fall below the line *AB* at 1140°.

Thus below *B*, the two phase region *BC* should be regarded as U_4O_9–$UO_{2\cdot6}$, while above *B* it is correctly formulated as UO_{2+x}–$UO_{2\cdot6}$, but in fact the limiting value of x is close to 0·25 in the temperature range studied. This is referred to below.

(4) *The* $UO_{2\cdot6}$–$UO_{2\cdot25}$ *region*

The results for this two-phase region obtained on three specimens of *C*4 (runs *C*4/10, *H*2/*C*4, *H*3/*C*4), specimen *M* and specimen *P* are given in Fig. 5. The results were in

good agreement except that the pressures given by specimen *P* were systematically lower than the others; specimen *P* was the least pure specimen. Neglecting these, the results from 1123° to 1450° can be expressed by the equation:

$$\log_{10} p\,(\text{atm}) = 8{\cdot}78 - \frac{17{\cdot}460}{T} \qquad (1)$$

As discussed above, the U_4O_9 phase below 1123° is not precisely the same as the UO_{2+x}

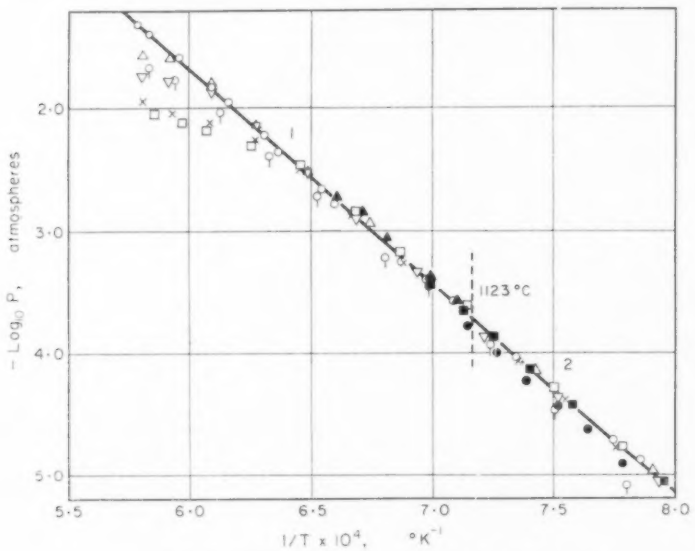

FIG. 5.—Oxygen equilibria involving the $UO_{2\cdot6}$ phase.
Original Compositions O/U : × 2·257; ▽ 2·279; △ 2·303; ⊡ 2·262; ○ >2·250; ♀ (2·29); ■ 2·250. ▲ results from Biltz and Müller; ●—results from Blackburn.

phase above that temperature despite the similarity of composition. The results in Fig. 5 below 1123° can best be fitted by

$$\log_{10} p\,(\text{atm}) = 8{\cdot}27 - \frac{16{,}760}{T} \qquad (2)$$

It must be pointed out, however, that the divergence of line (2) from line (1) at lower temperatures is barely more than the experimental error, and the uncertainty due to the thermo-molecular flow correction is largest at the lowest pressures.

BLACKBURN[3] gives the equation $\log p = 8{\cdot}425 - (17{,}100/T)$ for his measurements, made with a Knudsen cell from 960° to 1140°C; some of his results are plotted in Fig. 5. Results from ARONSON and BELLE[4] and BILTZ and MÜLLER[2] are also plotted in Fig. 5. Equations (1) and (2) satisfactorily express the mean of all these observations.

The O/U ratio at the upper limit of the two-phase region was found by BILTZ and MÜLLER[2] to be 2·607 from 1160° to 1214° and by BLACKBURN to be 2·607 from 850° to 1103°, with one value of 2·616 at 1126°. This is the lower limit of the U_3O_8 homogeneity range, called by BLACKBURN U_5O_{13}. The volatility effect made it difficult for us to determine this limit at higher temperatures, but it seems safe to assume that the limit remains close to 2·607.

The O/U ratio characteristic of the lower limit of the two-phase region was determined from the composition of the solid when the oxygen pressure began to fall below the value given by equation (1). This occurred as the solid was heated since the O/U of the solid fell due to the increasing quantities of oxygen in the gas-phase; the corrections to the original composition due to this loss of oxygen could be accurately computed since the volumes of the different parts of the apparatus were known.

The results for four runs which showed the behaviour characteristic of the lower limit of the two-phase region and for which the O/U ratio of the solid could be accurately estimated are shown in Fig. 5. From the composition and temperature at which the pressure fell below the limiting two-phase pressure, the lower limit of the two-phase region is as follows:

Run no:	*M5*	*H2/C4*	*M6*	*M7*
Temperature (°C):	1241	1276	1352	1393
O/U ratio:	2·248 ± 0·01	2·250 ± 0·01	2·254 ± 0·01	2·259 ± 0·01

VOL. 22 1961

In addition, the results for *H3/C4* (see §3) show that the phase limit is O/U = 2·250 ± 0·003 from 1123° to 950°; the behaviour in the region near 1120° has already been discussed. These results suggest that the boundary of the UO_{2+x} phase above 1123° gradually moves to higher O/U values, but do not definitely prove this.

(5) *The two-phase* U_4O_{9-y}–UO_{2+x} *region*

The evidence for the limits of this region have been discussed in §3 and the results given in Fig. 4. It is not surprising that the plot of $\log p$ versus $1/T$ for this region (line *BD*, Fig. 3) is curved since the composition of the two phases in equilibrium is continuously changing with temperature. Numerical values, read from the smoothed curve, are as follows:

$10^4/T$:	7·70	7·50	7·30	7·20	7·170
$-\log_{10} p$ (atm):	5·540	5·050	4·43	3·97	3·75

(6) *The non-stoicheiometric regions*

The best results for equilibria in the U_4O_{9-y} range are those for run *H3/C4* (Fig. 3). Isotherms of $\log p$ against composition are linear, as far as can be seen from the limited number of results. Partial molal quantities may be calculated as follows:

$$\bar{G} = RT \log_e p(O_2)$$

$$\bar{H} = R \frac{d(\log_e p)}{d\left(\frac{1}{T}\right)}$$

$$T\bar{S} = \bar{H} - \bar{G}$$

Some results are summarized in Table 2.

Isotherms for the UO_{2+x} region at 1220° and 1422° are shown in Fig. 6. The plotted points refer to runs for which the composition was known with reasonable accuracy (§2). Log p is a linear function of composition between $UO_{2\cdot14}$ and $UO_{2\cdot25}$; although there are few results at lower compositions, the deviation from linearity shown is

probably real, since this was found also at lower temperatures by ARONSON and BELLE[4]. The values of $\bar{G}$, $\bar{H}$ and $\bar{S}$ for all the experiments are collected in Table 3, together with the results of ARONSON and BELLE[4]. The actual pressures recorded in Table 3 were taken from straight lines drawn through the points on a log p versus $1/T$ plot. In general, these plots were satisfactorily linear, after due correction was made

TABLE 2.—EQUILIBRIA IN THE U_4O_{9-y} REGION

Composition	$\text{Log}_{10}\ p$ (atm)		$\bar{G}$ kcal		$\bar{H}$ kcal	$\bar{S}$ e.u.
O/U	1059°	1009°	1059°	1009°		
2·239	−4·96	−5·59	−24·00	−25·80	−96·2	−54·6
2·245	−4·60	−5·18	−22·25	−24·90	−88·4	−49·5
2·247	−4·41	−4·96	−21·35	−22·95	−84·0	−47·3

at the higher pressures for loss of oxygen from the solid to the gas phase; the composition change could be calculated and a corrected pressure at the same original composition calculated from the slope of the log p-composition isotherm at the particular temperature.

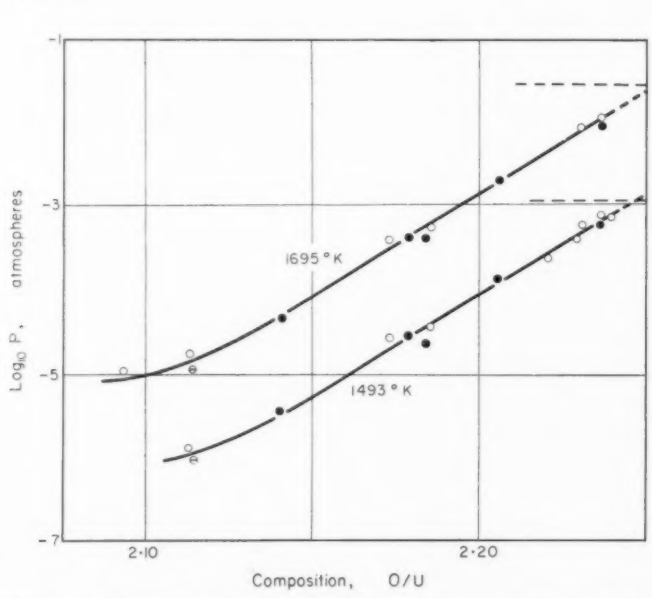

FIG. 6.—Oxygen Pressure Isotherms over UO_{2+x}. Specimens: ○—C4; ●—M; ⊖—P; – – – – limiting pressures.

We agree with ARONSON and BELLE that $\bar{H}$ numerically increases as the O/U ratio increases; our values agree well with theirs above O/U = 2·18 but are lower than theirs at lower compositions. Our results indicate that $\bar{H}$ does not change above O/U = 2·20; there may, in fact, be a slight decrease at higher compositions, but the accuracy of the results is insufficient to establish this. The numerical value of $\bar{S}$ also increases regularly and nearly linearly with increasing O/U ratio.

CALCULATION OF THERMODYNAMIC QUANTITIES

The direct calculation of the partial molal quantities $\bar{G}$, $\bar{H}$ and $\bar{S}$ for oxygen in UO_{2+x} or U_4O_{9-y} has been outlined above. The method of calculating $\bar{H}$, or ΔH in the two-phase regions, from the slope of the plots of $\log p$ vs. $1/T$, ignores the variation of

TABLE 3.—EQUILIBRIA IN THE UO_{2+x} REGION

Sample	Composition O/U	$-\text{Log}_{10} p$ (atm) 1493°K	1600°K	1695°K	$-\bar{G}$ kcal 1493°K	1600°K	1695°K	$-\bar{H}$ kcal.	$-\bar{S}$ e.u.
*C*4/2	2·094	—	5·450	4·965	—	39·90	38·42	63·0	14·4
*	2·112							69	18·3
*C*4/3	2·113	5·900	5·262	4·760	40·25	38·52	36·90	65·0	16·6
P/2	2·114	6·010	5·402	4·925	41·02	39·52	38·20	62·2	14·2
M/2	2·141	5·445	4·808	4·317	37·20	35·02	33·48	64·3	18·2
*	2·142							74	25·3
*C*4/4	(2·158)	5·110	4·420	3·882	34·88	32·35	30·10	69·8	23·4
*	2·164							74	27·0
3/*C*4	2·172	4·595	3·925	3·400	31·38	28·72	26·37	68·4	24·8
2/*M*/2	2·179	4·580	3·910	3·390	31·28	28·62	26·30	68·5	24·9
P/3	(2·180)	4·595	3·897	3·352	31·38	28·52	26·00	71·0	26·6
Mp	2·184	4·660	3·960	3·410	31·80	29·00	26·43	71·2	26·4
*	2·184							72	27·6
*H*1/*C*4	2·186	4·430	3·760	3·235	30·23	27·52	25·09	68·7	25·8
*C*4/5	(2·191)	4·330	3·625	3·070	29·57	26·55	23·81	71·0	27·8
*C*4/6	(2·198)	4·165	3·455	2·900	28·42	25·30	22·49	71·8	29·0
P/4	(2·199)	4·130	3·422	2·872	28·20	25·05	22·30	72·1	29·4
*C*4/7	(2·201)	4·072	3·365	2·810	27·80	24·62	21·80	72·1	29·7
*	2·203							74	29·4
M/3	2·206	3·896	3·218	2·690	26·60	23·57	20·87	68·7	28·2
*C*4/8	(2·215)	3·715	3·010	2·463	25·37	22·02	19·10	72·6	31·6
*H*3/*C*4	2·221	3·605	—	—	24·60	—	—	73·1	32·5
*P*5	(2·224)	3·490	2·805	2·268	23·82	20·53	17·58	70·0	30·9
*H*3/*C*4	2·230	3·395	—	—	23·20	—	—	70·5	31·7
4/*C*4	2·231	3·215	2·550	2·030	21·93	18·67	15·75	67·7	30·7
2/*C*4	2·237	3·112	2·450	1·932	21·25	17·94	14·99	67·4	30·9
*M*4	2·237	3·167	2·495	1·965	21·62	18·26	15·24	68·6	31·5
*H*3/*C*4	2·239	3·138	—	—	21·43	—	—	72·5	34·3
2/*C*4	2·239	3·035	2·362	1·840	20·72	17·30	14·27	68·2	31·8

* Results taken from Aronson and Belle (1150–1350°K).

ΔC_p with temperature. This is justified so long as the temperature range is small; estimates made by KUBASCHEWSKI and RAND[9] show that the values of ΔH would not be expected to alter by more than 3 kcal/g mole from 1000° to 1450°, and the individual values were actually estimated from pressure readings taken over a much smaller range of temperature; the errors in values of ΔH due to the scatter of the experimental points are greater than any caused by neglect of the specific heat term. However, this correction would become important in any attempt to extrapolate H values to room temperature.

The calculation of the complete thermodynamic functions G, H and S for the limiting compositions of each phase in the phase diagram from UO_2 to U_3O_8 was carried out at two temperatures, 1300° and 1396°K; the lower temperature was chosen

[9] O. KUBASCHEWSKI and M. H. RAND, *Thermodynamics of U compounds.* To be published.

VOL. 22 1961

for direct comparison with BLACKBURN[3] and 1396°K is the highest temperature at which the U_4O_9 phase can exist. Full thermodynamic quantities were calculated from partial molar quantities by using equations such as:

$$\Delta G = N_1 \int_0^z \Delta \bar{G}_2 \, dz$$

where ΔG represents the change in G on oxidizing UO_2 (phase 1) with O_2 (phase 2) through a non-stoicheiometric range to a composition where N_1 is the mole fraction of UO_2 and $z = N_2/N_1$ ($= x/2$ for the composition UO_{2+x}).

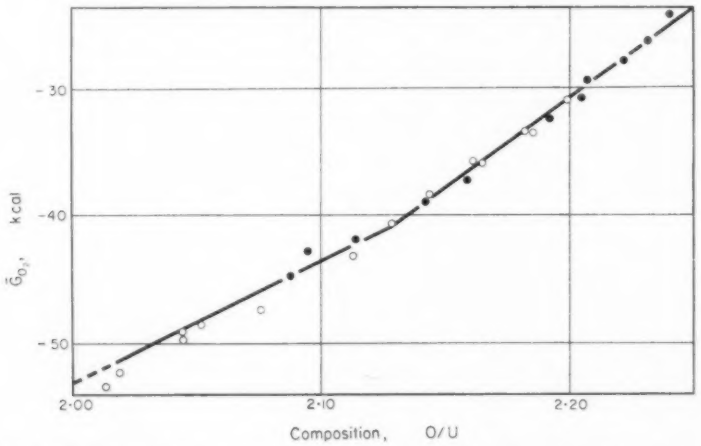

FIG. 7.—Partial molal free energy of O_2 in UO_{2+x} at 1396°K. ●—our results; ○—calc. from Aronson and Belle.

To apply such an equation, $\bar{G}_2$ must be known as a function of z from $z = 0$ to $z = z$. Our own measurements of $\bar{G}_2$ for the UO_{2+x} phase did not extend below $UO_{2\cdot1}$. However, the agreement between our results and those of ARONSON and BELLE was sufficiently close to permit combining the results; Fig. 7 is a plot of our values for $\bar{G}_2$ at 1396°K together with values extrapolated from the results of ARONSON and BELLE. The data are best represented by two straight lines, as shown. At 1300°K, we fixed the limit of the UO_{2+x} phase as $UO_{2\cdot199}$ (Fig. 4) and calculated ΔG for UO_2–$UO_{2\cdot199}$ from the results of ARONSON and BELLE.

The partial molal quantities in the homogeneity range U_4O_{9-y} (Fig. 3) were integrated in a similar fashion. ΔG and ΔH for the conversion of one limiting composition of a two-phase region to the other were directly calculated from the equilibrium pressures; it was assumed that the lower composition limit of the U_3O_{8-z} phase was $UO_{2\cdot61}$. BILTZ and MÜLLER's results[2] on the tensimetric degradation of U_3O_8 were used for the calculation of the U_3O_{8-z} phase; over narrow composition ranges, their results show a linear dependence of $\log p$ on composition at any temperature, with $\bar{H}$ approximately 68 kcal/mole at all compositions. BLACKBURN[3] gives an equation for $\bar{G}$, calculated from BILTZ and MÜLLER's data, which gives values in satisfactory agreement with ours.

The results of the calculations are collected in Tables 4 and 5. ΔH for the reaction

TABLE 4.—THERMODYNAMIC FUNCTIONS AT 1300°K

Reaction	ΔG kcal.	ΔH kcal.	ΔS e.u.	ΔS/mole O_2	ΔH/mole O_2
$UO_2 + 0{\cdot}0995\ O_2 = UO_{2{\cdot}199}$[4]	−4·49	−6·56	−1·59	−16·0	−66
$UO_{2{\cdot}199} + 0{\cdot}0185\ O_2 = UO_{2{\cdot}236}$	−0·619	−2·09	−1·13	−61	−118
$UO_{2{\cdot}236} + 0{\cdot}007\ O_2 = UO_{2{\cdot}250}$	−0·217	−0·631	−0·32	−46	−86
$UO_2 + 0{\cdot}125\ O_2 = UO_{2{\cdot}25}$	−5·33	−9·28	−3·04	−23	−69·5
$UO_{2{\cdot}25} + 0{\cdot}18\ O_2 = UO_{2{\cdot}61}$	−5·06	−13·80	−6·71	−37·4	−77
$UO_{2{\cdot}61} + 0{\cdot}03\ O_2 = UO_{2{\cdot}67}$[2]	−0·23	−2·00	−1·36	−45·3	−66
$UO_{2{\cdot}25} + 0{\cdot}21\ O_2 = UO_{2{\cdot}67}$	−5·29	−15·8	−8·07	−38	−75
$UO_2 + 0{\cdot}335\ O_2 = UO_{2{\cdot}67}$	−10·62	−25·08	−11·13	−33	−73·5
cf. Blackburn's data:					
$UO_2 + 0{\cdot}125\ O_2 = UO_{2{\cdot}25}$	−5·50	−8·50			
$UO_{2{\cdot}25} + 0{\cdot}21\ O_2 = UO_{2{\cdot}67}$	−5·30	−15·3			
$UO_2 + 0{\cdot}335\ O_2 = UO_{2{\cdot}67}$	−10·8	−23·8			
cf. Ackermann and Coughlin's data:					
$UO_2 + 0{\cdot}335\ O_2 = UO_{2{\cdot}67}$	−10·7	−22·6			

TABLE 5.—THERMODYNAMIC FUNCTIONS AT 1396°K

Reaction	ΔG kcal.	ΔH kcal.	ΔS e.u.	ΔS/mole O_2	ΔH/mole O_2
$UO_2 + 0{\cdot}122\ O_2 = UO_{2{\cdot}244}$	−4·89	−7·8	−2·08	−17·0	−64
$UO_{2{\cdot}244} + 0{\cdot}003\ O_2 = UO_{2{\cdot}250}$	−0·071	−0·8	−0·52	−173	−270
$UO_2 + 0{\cdot}125\ O_2 = UO_{2{\cdot}25}$	−4·96	−8·6	−2·60	−20·8	−69
$UO_{2{\cdot}25} + 0{\cdot}18\ O_2 = UO_{2{\cdot}61}$	−4·28	−13·8	−6·80	−37·8	−77
$UO_{2{\cdot}61} + 0{\cdot}03\ O_2 = UO_{2{\cdot}67}$	−0·147	−2·0	−1·32	−43	−66
$UO_{2{\cdot}25} + 0{\cdot}21\ O_2 = UO_{2{\cdot}67}$	−4·43	−15·8	−8·12	−39	−75
$UO_2 + 0{\cdot}335\ O_2 = UO_{2{\cdot}67}$	−9·39	−24·4	−10·7	−32	−73
cf. Ackermann and Coughlin's data:					
$UO_2 + 0{\cdot}335\ O_2 = UO_{2{\cdot}67}$	−10·06	−22·6			

$UO_{2{\cdot}244} + 0{\cdot}003\ O_2 = UO_{2{\cdot}250}$ at 1396°K was calculated (a) from the slope of the tangent to line *BD* in Fig. 3 at *B*, and (b) from the difference in ΔH for the reactions

$$UO_{2{\cdot}244} + 0{\cdot}183\ O_2 = UO_{2{\cdot}61} \quad \text{and}$$
$$UO_{2{\cdot}25} + 0{\cdot}18\ O_2 = UO_{2{\cdot}61}$$

which could be estimated from the slope of the log p vs. $1/T$ plots above and below 1396°K. (Fig. 5).

VOL. 22 1961

For comparison, BLACKBURN's data at 1300°K is included in Table 4 and values for ΔG and ΔH for the overall reaction $UO_2 + 0{\cdot}335\ O_2 = UO_{2{\cdot}67}$ based on thermal data are given in both Tables.

We accepted COUGHLIN's[10] values for the heat of formation and free energy of formation of UO_2 and took values for U_3O_8 from an assessment of recent data made by ACKERMANN *et al.*[8]; all these values were based on calorimetric measurements and specific heat data. The agreement between our results and BLACKBURN's at 1300°K is very good, considering the different techniques involved; the agreement between the ΔG values for the overall reaction calculated from the oxygen pressures with those derived from thermal data is also close enough to remove serious uncertainty arising from the extrapolation of the $\bar{G}_{O_2}$ plots for UO_{2+x} to $UO_{2{\cdot}00}$. There must be a rapid change of $\bar{G}_{O_2}$ with x at very low values of x, since the pressure of oxygen in equilibrium with UO_2 and U metal at 1396°K is 10^{-32} atm, which compares with 10^{-8} atm in equilibrium with $UO_{2{\cdot}01}$ (Fig. 7). If values for $\bar{G}_{O_2}$ at 1396°K decrease from −52 kcal at $UO_{2{\cdot}01}$ linearly to −202 kcal at $UO_{2{\cdot}000}$, then the ΔG value for the reaction $UO_2 + 0{\cdot}0050_2 = UO_{2{\cdot}01}$ is −0·37 kcal more negative than has been allowed, and this should be added to the ΔG values listed in Table 5 for $UO_{2{\cdot}244}$, $UO_{2{\cdot}250}$ and $UO_{2{\cdot}67}$. However, any UO_2 powder which has been handled in air, even at room temperature, is oxidized to a small extent[11] and the heat of formation of UO_2 has been determined for powders which have probably been non-stoicheiometric; it is therefore not certain to what precise composition the thermal data refers.

The entropy changes during the various stages of the formation of the U_4O_9 phase show clearly that this is a highly ordered phase compared to the UO_{2+x} phase. The unique nature of the U_4O_9 phase is also emphasised by the very high value of $\bar{H}$ for O_2 in the U_4O_{9-y} region, 84–96 kcal/g mole, much larger than $\bar{H}$ for O_2 in the UO_{2+x} or U_3O_{8-z} phases. The form of the isotherms in the UO_{2+x} region has been discussed by ARONSON and BELLE[4]. They showed that the observed variation of partial molal entropy with composition is in approximate agreement with the predicted change using a model in which the additional oxygen enters interstitial sites in a UO_2 lattice with the production of positive holes. Further discussion of the isotherms in this region is reserved to a later date.

Preliminary values for the oxygen pressures in equilibrium with different compositions which have been published previously[12] have to be somewhat corrected. Fig. 8 is a plot of the function $RT \ln p$, where p is the pressure of oxygen in atm, in equilibrium with (1) the U_4O_9–$UO_{2{\cdot}61}$ or UO_{2+x}–$UO_{2{\cdot}61}$ phases, (2) $UO_{2{\cdot}206}$ (3) $UO_{2{\cdot}094}$, (4) $UO_{2{\cdot}01}$—from ARONSON and BELLE's results, (5) the U_4O_{9-y}–UO_{2+x} region; this is uncertain at lower temperatures since the X-ray data indicate that the U_4O_{9-y} region contracts below 900°C.[1] The lines 6, 7, 8 and 9 on Fig. 8 are plots of the same function, $RT \ln p\ (O_2)$ for oxygen in equilibrium with CO/CO_2 mixtures having compositions 1/1, $1/10^3$, $1/10^6$, $1/10^9$ respectively. It can be seen that a $1/10^3$ mixture of carbon monoxide in carbon dioxide is reducing towards all compositions richer in oxygen than $UO_{2{\cdot}01}$ at temperatures below 900°C. This contrasts sharply with results obtained by BURDESE who reported that compositions between $UO_{2{\cdot}05}$ and U_4O_9 were

[10] J. P. COUGHLIN, Bureau of Mines Bulletin 542 (Washington, 1954).
[11] J. S. ANDERSON, L. E. J. ROBERTS and E. A. HARPER. *J. Chem. Soc.* 3946 (1955).
[12] L. E. J. ROBERTS, A. G. ADWICK, M. H. RAND, L. E. RUSSELL, A. J. WALTER. *Proceedings of the Second International Conference on the Peaceful Uses of Atomic Energy, Geneva* 1958. United Nations (1959). A/CONF/15/P/26.

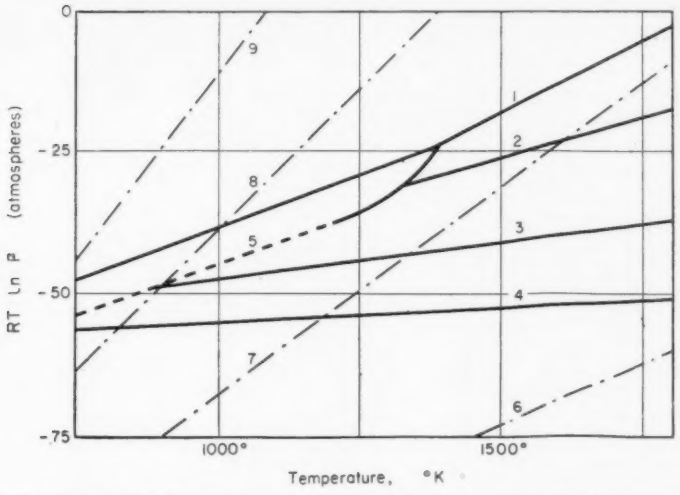

FIG. 8.—Plot of RT ln p for oxygen in equilibrium with uranium oxides and CO—CO_2 mixtures. Line 1 — $UO_{2\cdot25}$ + $UO_{2\cdot6}$; 2—$UO_{2\cdot206}$; 3—$UO_{2\cdot097}$; 4—$UO_{2\cdot01}$; 5—U_4O_{9-y} + UO_{2+x}; 6,7,8,9—CO_2/CO = 1/1, 10^3, 10^6, 10^9.

in equilibrium with CO/CO_2 mixtures containing 4–12 per cent of carbon monoxide at temperatures of 700–900°C.[13] The equilibrium oxygen pressures calculated by BURDESE from his results are many orders of magnitude lower than those extrapolated from our results or from those of BLACKBURN or ARONSON and BELLE. BURDESE's results cannot be accepted, nor can the phase diagram deduced from them, which showed a single UO_{2+x} region above 950°C.

Acknowledgement—We are indebted to Mr. F. T. BIRKS, A.E.R.E., for the spectrographic analyses of the samples and to Dr. M. H. RAND for a discussion of the thermodynamic results.

[13] A. BURDESE. *Gazz. Chim. Ital.* **89**, 718 (1959).

VOL. 22 1961

J. Inorg. Nucl. Chem., 1961, Vol. 22, pp. 231 to 239. Pergamon Press Ltd. Printed in Northern Ireland

A DIFFERENTIAL THERMAL ANALYSIS STUDY OF THE RARE EARTH ETHYL SULPHATES*

M. W. NATHANS
Lawrence Radiation Laboratory, University of California
Livermore, California

(*Received* 22 *January* 1961; *in revised form* 5 *June* 1961)

Abstract—Differential thermal analysis (DTA) curves were obtained for all rare earth ethyl sulphates in a stationary air atmosphere at an upheat rate of about 10°C per min. The effects of particle size, upheat rate and the conditions of the surrounding atmosphere were investigated. A partial interpretation of the peaks was made by a modified thermogravimetric method and other analytical means.

The decomposition of the salts follows more or less the following general pattern:

$$M(C_2H_5SO_4)_3 \cdot 9H_2O \rightarrow M(C_2H_5SO_4)_3 \cdot 5H_2O \rightarrow M(C_2H_5SO_4)_3 \rightarrow M(HSO_4)_3 \rightarrow \text{intermediates} \rightarrow M_2(SO_4)_3,$$

where M represents any rare earth metal. The first three steps all occur below 200°. The last step is certainly completed at 500°. The intermediates are possible double salts of the sulphates and the bisulphates or have the composition $pM_2(SO_4)_3 \cdot qH_2SO_4$.

The dehydration and the decomposition of the organic radical have activation energies of the order of 12 and 16 kcal/mole, respecrively. The bisulphate decomposition may have an activation energy of something like 8·5 kcal/mole. The reactions are first order, with one exception, which appears to be of fractional order.

THE thermal decomposition of rare earth salts has been studied in some detail only during the past five years. The principal aim of these studies was to determine the minimum temperature range in which a particular composition would be stable. This is of interest for gravimetric analysis. A secondary aim was the comparison of the behaviour of the different rare earths. Thus studies have been made, by DTA or with the thermobalance, of the oxalates,[1] 8-hydroxyquinolates and related salts,[2] cupferrates and neocupferrates,[3] chlorides,[4] fluorides,[5] sulphamates[6] and others. The ethyl sulphates, although not of analytical interest, are of some spectroscopic interest, and it appeared worth while to obtain a comparison of rare earth behaviour in this salt. They have the composition $M(C_2H_5SO_4)_3 \cdot 9H_2O$ and are crystallographically isostructural.

EXPERIMENTAL

Cerium ethyl sulphate was prepared from the sulphate as obtained from the G. Frederick Smith Chemical Co., by a double decomposition reaction with the stoicheiometric amount of barium ethyl sulphate. All other ethyl sulphates were prepared by converting the oxides obtained frrom Lindsay Chemical Corp. (Er_2O_3 from Research Chemicals Corp.) to the sulphates and subsequent conversion to the ethyl sulphates as with the cerium salt. The barium ethyl sulphate was "electronic grade"

* Work was performed under the auspices of the U.S. Atomic Energy Commission.

[1] W. W. WENDLANDT, *Analyt. chem.* **30,** 58 (1958); **31,** 408 (1959).
[2] W. W. WENDLANDT, *Analyt. Chim. Acta* **15,** 109 (1956); **17,** 274 428, (1957).
[3] (a) W. W. WENDLANDT and J. BRYANT, *Analyt. Chem.* **27,** 1277 (1955);
(b) W. W. WENDLANDT, *Analyt, Chim. Acta* **13,** 550 (1955); **21,** 116 (1959).
[4] W. W. WENDLANDT, *J. Inorg. Nucl. Chem.* **5,** 118 (1957); **9,** 136 (1959).
[5] W. W. WENDLANDT, *Science* **129,** 842 (1959).
[6] A. CHRETIEN and M. CAPESTAN, *C.R. Acad. Sci., Paris* **248,** 3176 (1959).

reagent from City Chemical Corp. Potassium ethyl sulphate was reagent-grade chemical from Eastman. All starting materials were at least 99 per cent pure. Most ethyl sulphates appeared slightly wet. The weights of the pyrolysis residues showed, however, that the compositions did not differ significantly from the theoretical ones.

The DTA furnace assembly was the Robert L. Stone Co. model CS-2. The samples are placed in cups which allow weighings. Auxiliary equipment included a Leeds and Northrup model-G potentiometer recorder with a Beckman model-14 breaker preamplifier and an L and N model-H cam-type programmer-recorder with a CAT proportional control and a Fidelity saturable reactor.

The thermobalance used for the lanthanum salt was a modified Ugine-Eyraud continuous recording thermobalance with an L and N Speedomax type-G X_1–X_2 recorder having a range of 20 mg $\pm$ 2 per cent full scale.

Some samples of the lanthanum salt which were heated in a muffle oven at different temperatures were analysed. The products of pyrolysis below 500°C were soluble in water, the 1100° product was dissolved in hydrochloric acid. Sulphate was determined by precipitation as $BaSO_4$, filtering the next day, dissolution of the precipitate in a known amount of ammonical EDTA and back titration with standard $MgCl_2$ with Eriochrome T as the indicator. Hydrogen ion was determined by titration with standard base.

Samples of about 100 mg were used in all experiments. Standard particle size was $-100/+200$ mesh. Standard upheat rate was about 10°C per min. These conditions were modified for a few experiments. Calcined alumina was used as the reference material. After a complete DTA curve was obtained a new sample was run, but with interruptions shortly after a peak in order to weigh the sample. The samples were removed from the furnace and weighed as rapidly as possible in order to keep the uptake of water from the air to a minimum. Occasionally some fumes were still coming off when the furnace was removed.

RESULTS

The DTA curves under standard conditions are shown in Fig. 1. Below about 250°C the curves are all similar, showing only endothermic reactions. There are

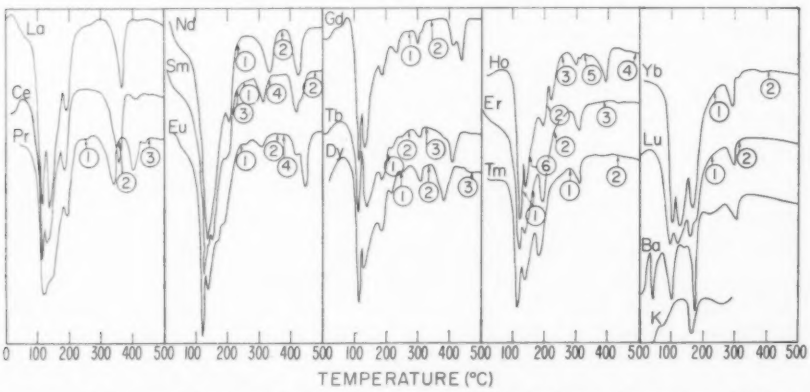

FIG. 1.—DTA curves for the ethyl sulphates of the rare earths, barium and potassium. Upheat rate 10°C/min nominal. 100 mg samples, $-100/+200$ mesh.

basically three peaks which are in nearly all cases well resolved. Sometimes additional structure can be seen. Between 250° and 500° there is varying behaviour. The lanthanum and cerium salts show one sharp peak between 300° and 400° and one or two weak ones at higher temperatures. The salts from praseodymium through holmium have at least two well defined peaks, which sometimes show structure. The remaining rare earth salts show only one peak of medium intensity just above 300°. For comparison the curves of barium and potassium ethyl sulphate are included.

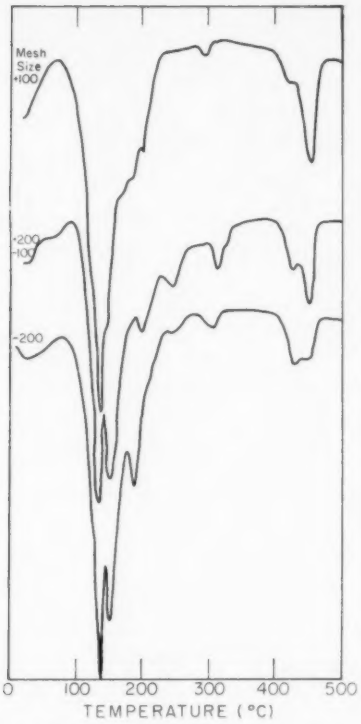

FIG. 2.—Effect particle size on the DTA of $Md(C_2H_5SO_4)_3 \cdot 9H_2O$.

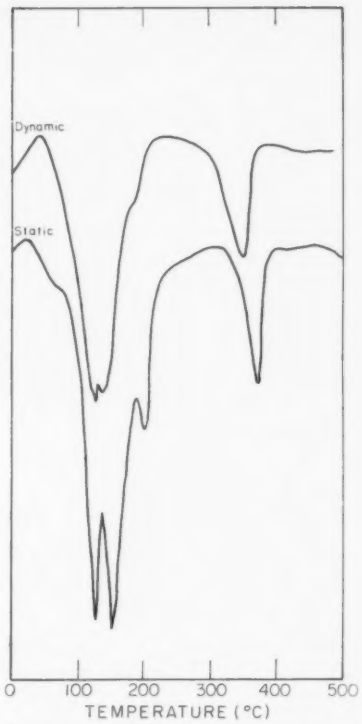

FIG. 3.—Comparison of DTA of $La(C_2H_5SO_4)_3 \cdot 9H_2O$ in static air and dynamic argon atmospheres.

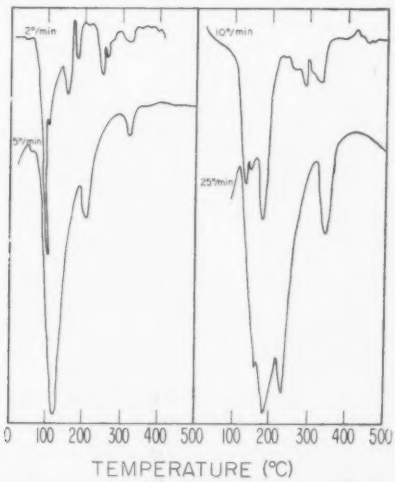

FIG. 4.—Effect of upheat rate on the DTA of $Er(C_2H_5SO_4)_2 \cdot 9H_2O$.

Fig. 2 shows the effect of particle size on the DTA of the gadolinium salt. The best resolution is obtained for the −100/+200 mesh fraction. Fig. 3 shows the DTA curves obtained in air and in a dynamic argon atmosphere with the lanthanum salt.

VOL. 22 1961

Changing the upheat rate was investigated with the erbium salt with an unexpected effect on the resolution (Fig. 4). The two lowest temperature peaks are better resolved at the higher upheat rates. The other peaks show considerable structure at the lowest heating rates. A more detailed study of the kinetics would clarify this.

TABLE 1.—WEIGHT DATA FOR RARE-EARTH ETHYL SULPHATES HEATED TO DIFFERENT TEMPERATURES*

	1 Bisulphate		2 2/1†		3 1/1†		4 1/2†		5 Sulphate	
	Theor.	Found	Theor.	Found	Theor.	Found	Theor.	Found	Theor.	Found
La	63·6	—	56·4	56·4	52·8	—	49·1	42·6 49·0	41·9	42·6
Ce	63·7	61·8	56·4	—	52·8	—	49·2	—	41·9	42·9 40·6
Pr	63·7	64·6 60·0	56·5	—	52·8	—	49·2	50·2 49·1	42·0	40·6 45·1
Nd	64·0	62·6	56·8	—	53·1	—	49·5	50·0	42·3	45·4 45·3
Sm	64·2	60·7 61·2	57·1	—	53·5	—	49·9	51·9	42·8	44·2
Eu	64·3	64·0	57·2	—	53·6	54·9 53·7	50·1	—	43·0	47·3 44·2
Gd	64·6	‡	57·5	55·8	54·0	—	50·5	50·3	43·4	43·3
Tb	64·7	64·6	57·6	(56·9)	54·1	—	50·6	50·9	48·5	42·9
Dy	64·9	60·0	57·9	—	54·4	—	50·9	50·6	43·9	43·0
Ho	64·9	63·1	57·9	—	54·4	53·5	51·0	—	44·0	46·7
Er	65·1	66·2	58·1	—	54·6	—	51·1	—	44·1	47·6 43·5
Tm	65·2	65·5	58·2	—	54·6	—	51·1	—	44·1	48·6
Yb	65·4	—	58·4	58·1	54·9	—	51·4	—	44·4	48·5
Lu	65·4	64·4	58·5	—	54·9	—	51·4	50·9	44·5	—

* Temperatures where samples were taken varied with the peak positions. The first column was obtained at about 230°, the second, third and fourth columns between 230° and 350°, and the fifth column at 450°. Values are reported as per cent weight remaining.

† (Equivalents of rare earth in bisulphate)/(equivalents of rare earth in sulphate).

‡ No data taken.

The interpretation of the peaks is based on measurements of the weights of samples at points indicated by numbers in Fig. 1. Compositions were calculated from these weighings and compared with theoretical compositions. The results are tabulated in Table 1. The numbers listed are weight per cent left after heating. Additional weighings were made of the lanthanum and holmium salts after the first and second peaks (Table 2). Chemical analyses were carried out on some of the decomposition products of the lanthanum salt after heating in a muffle oven (Table 3). The pyrolysis products of the potassium and barium salts were also weighed or analysed as a partial check (Table 4).

The data lead to the following interpretation. The decomposition of the rare earth ethyl sulphates starts with dehydration. Besides the enneahydrate which is stable at room temperature at least one other hydrate exists, probably the pentahydrate. The

TABLE 2.—EVIDENCE FOR THE EXISTENCE OF RARE-EARTH ETHYL SULPHATE PENTAHYDRATES

Compound	Weight (g)	Heating Temp (°C)	Wt left (%)	Theor. for pentahydrate (%)
$La(C_2H_5SO_4)_3 \cdot 9H_2O$	1·000	145	88·8	89·4
	0·0655	135	90·5	
$Ho(C_2H_5SO_4)_3 \cdot 9H_2O$	0·0780	135	88·1	88·7

TABLE 3.—ANALYSES OF LANTHANUM ETHYL SULPHATE SAMPLES HEATED TO DIFFERENT TEMPERATURES

Sample	Temp (°C)	Heating time (min)	Millimoles in original sample				
			La^{3+}(calc)	H^+	SO_4^{2-}	SO_4/La	H/SO_4
1	225	15	0·77	1·58	1·80	2·34	0·88
2	375	15	0·77	0·218	1·18	1·53	0·18
3	410	15	0·76	0·128	1·17	1·54	0·11
4	510	15	0·88	(0·02)	1·27	1·44	(~0)
5	510	30	0·80	(0·04)	1·18	1·48	(~0)
6	1050	15	0·76	—	0·40	0·52	—

Theoretical SO_4/La for 4 $La(HSO_4)_3 + La_2(SO_4)_3$ is 15/6 or 2·50; for $La_2(SO_4)_3$: 3/2 or 1·50; for $La_2O_2(SO_4)$: 1/2 or 0·50.
Theoretical H/SO_4 for 4 $La(HSO_4)_3 + La_2(SO_4)_3$ is 12/15 or 0·80; at 350° and 410° small amounts of bisulphate are still left.

TABLE 4.—ANALYSES OF BARIUM AND POTASSIUM ETHYL SULPHATES HEATED TO DIFFERENT TEMPERATURES

Sample	Temp (°C)	Wt of initial sample (%)	Theor. wt of initial sample (%)	Product
$Ba(C_2H_4SO_4)_2 \cdot 2H_2O$	100	98·7	—	—
	170	90·6	91·5	$Ba(C_2H_5SO_4)_2$
	250	75·3	78·0	$Ba(HSO_4)_2$
	1050	(X-ray analysis)		$BaSO_4$
$K_2C_2H_5SO_4$	250	85·9	82·9	$KHSO_4$*

*SO_4 found 4·04 mmole in 0·6775 g
theor: 4·14 mmole in 0·6775 g
H found 4·12 mmole in 0·6775 g
theor: 4·13 mmole in 0·6775 g

anhydrous ethyl sulphates are rather unstable and decompose below 200°C to the bisulphates. The bisulphates decompose either directly or in steps to the anhydrous sulphates. In some cases (La, Ce, Pr, Gd, Dy, Yb) the bisulphate starts to decompose before the decomposition of the ethyl group is complete. The intermediate compositions shown in Table 1 are given with some reserve. The DTA curves indicate the existence of double salts of the bisulphates with the sulphates. The most consistently

occurring composition is $M(HSO_4)_3 \cdot M_2(SO_4)_3$. It is likely that such a double salt has independent existence. Other compositions suggested by the table as having independent existence are $4M(HSO_4)_3 \cdot M_2(SO_4)_3$ and perhaps $2M(HSO_4)_3 \cdot M_2(SO_4)_3$. These compositions certainly are in need of confirmation. A few X-ray diffraction patterns obtained from pyrolysis products of the lanthanum salt were inconclusive.

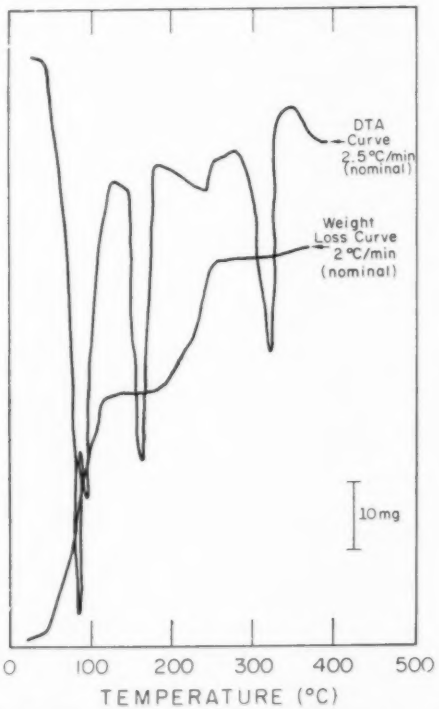

FIG. 5.—Comparison of weight loss curve (2°/min) with DTA (2·5°/min) of $La(C_2H\text{-}SO_4)_3 \cdot 9H_2O$.

Confirmation of the interpretation of the peak just below 200° was found from the potassium and barium salts. The former has only one endothermic peak corresponding to the reaction.

$$K(C_2H_5SO_4) \rightarrow KHSO_4 + C_2H_4.$$

The latter has two low temperature peaks, which correspond to dehydration. The third sharp peak, results from the reaction

$$Ba(C_2H_5SO_4)_2 \rightarrow Ba(HSO_4)_2 + 2\,C_2H_4.$$

The last peak, at about 300° corresponds to the reaction

$$Ba(HSO_4)_2 \rightarrow BaSO_4 + H_2O + SO_3.$$

This peak occurs at about the same temperature as a similar peak for the erbium, thulium, ytterbium and lutecium peaks, which have been interpreted the same way.

An attempt was made to establish the stability ranges of some of the low temperature pyrolysis products. The weight of lanthanum ethyl sulphate was followed with the thermobalance in a flow of about 100 cm^3 of nitrogen per minute (at room temperature) at a heating rate of about 2°/min. Fig. 5 shows both the weight loss curve

and the DTA curve at 2·5°/min. There is little positive correlation between the two curves. It is clear, however, that there is no stability range for the intermediate hydrate.

The results of isothermal experiments with the ethyl sulphates of La, Pr, Tb, Dy, Er,

TABLE 5.—STATIC WEIGHT LOSS OF SOME RARE-EARTH ETHYL SULPHATES AT 106°C

Salt of	Weight % after									
	0*	24	34	144	195	217	318	481	648	1008 (hr)
Pr	72·06†	62·00	61·23	60·37	60·42	60·23	60·58	59·83	59·58	58·97
Tb	71·35†	59·72	59·15	56·50	56·43	55·56	54·66	50·17	47·82	46·06
Dy	75·64†	64·81	64·95	63·74	63·82	63·36	63·56	61·82	61·17	59·94
Er	76·02†	66·43	65·68	59·23	57·15	55·83	52·44	50·48	50·26	50·74
Tm	76·86†	68·34	67·42	63·00	61·88	61·16	59·51	52·82	50·81	51·77
Yb	74·90†	65·13	64·37	57·34	(58·22)	54·18	53·25	44·47	—	44·41
	0	12	17	21	36	60	161	324	492	(hr)
La	100‡	64·7	62·8	62·2	60·5	60·0	60·0	58·6	(62·6)	

* Time started after 3 days at 50°, 1 day at 73°.
† Weight per cent left after previous heating at 50° and 73°.
‡ Heating started at 106°.

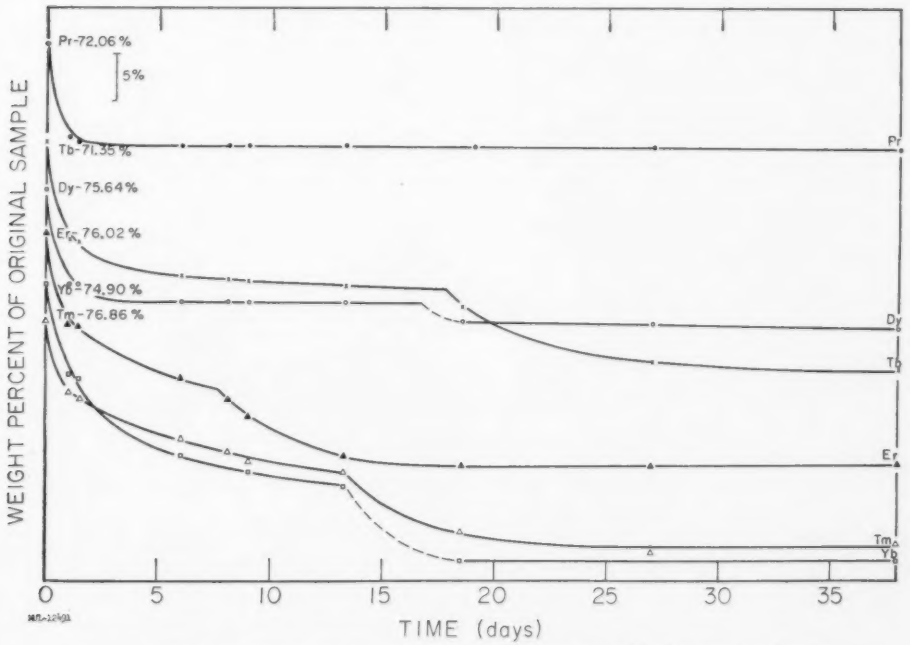

FIG. 6.—Weight loss-time curves for various ethyl sulphates at 106°C after previous heating at 50° and 73°C.

Tm, and Yb are shown in Table 5 and Fig. 6. The samples (except the La salt) were held at 50° for three days, at 73° for one day, and at 105° for 42 days. The lanthanum salt was heated at 106° only. At 50° constant weight appears to be reached after only a few hours at about 80 per cent, indicating perhaps the existence of a mono- or dihydrate,

VOL. 22 1961

although the Pr and Tb salts may have reached the anhydrous form already. After further heating the weight increased a little. This suggests that the constant weight composition is very sensitive to the humidity of the atmosphere. Yet there is no indication of a stable pentahydrate. No constant weight was reached at 73°, except perhaps with the Dy salt. Yet the Dy, Er, Tm, and Yb salts may have a stability region at about the

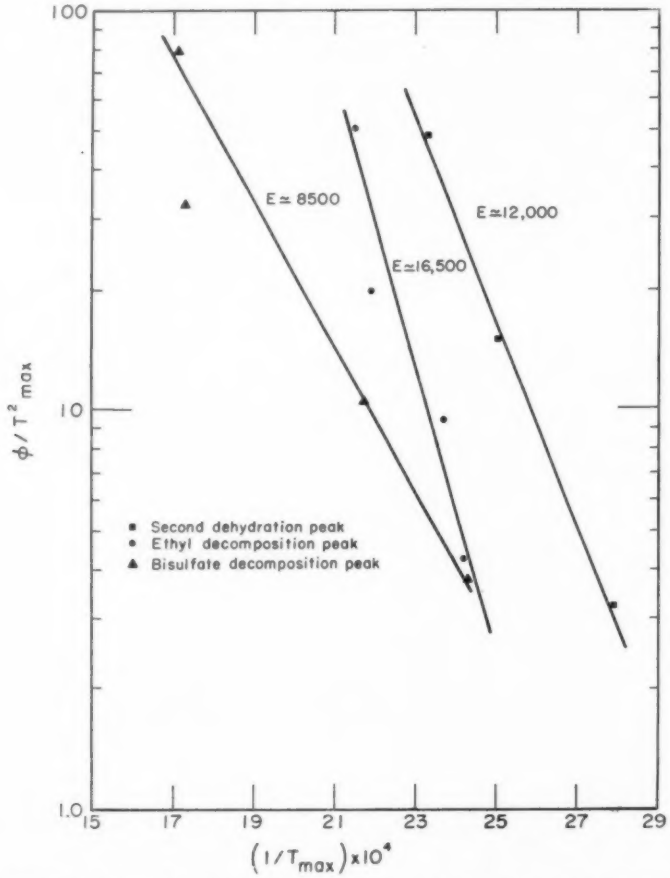

FIG. 7.—Calculation of activation energies of decomposition reactions of $Er(C_2H_5SO_4)_3 \cdot 9H_2O$.

composition of the anhydrous salt (about 77 per cent). The other two salts lost additional weight at 73°. The behaviour at 106° is very interesting. The lanthanum, praseodymium and dysprosium salts appear to have a stable composition at about 60 per cent, in accordance with weight data obtained from the dynamic measurements of the last two. The erbium and thulium salts have stable products at about 50 per cent weight loss, that is, at the composition $Er(HSO_4)_3 \cdot Er_2(SO_4)_3$. This composition was not found in the dynamic experiments. Finally, the terbium and ytterbium salts did not reach a stable composition at all. They both tend to yield the anhydrous sulphate at this temperature. The break in the curves may be explained by assuming two consecutive reactions.

An estimate was made of the activation energy of some of the reactions of the erbium salt. According to KISSINGER[7] the activation energy, E, is given by

$$E = -R \frac{d \ln (\phi/T_m^2)}{d(1/T_m)},$$

where R is the constant, ϕ the heating rate, and T_m the peak temperature in degrees K. Values of E were calculated with the data obtained from Fig. 4 for the first dehydration peak, the 200° peak, and the bisulphate decomposition peak. For the last calculation the average of the doublet was taken. The results are shown in Fig. 7. The activation

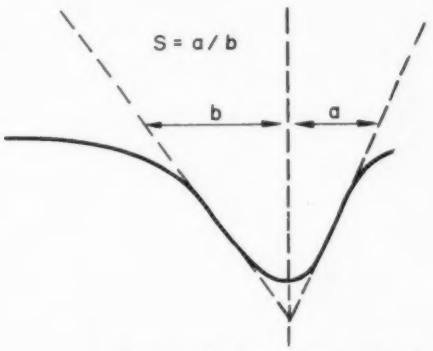

FIG. 8.—Definition of the shape factor S.

energies were found to be about 12,000 cal/mole for the dehydration, about 16,500 cal/mole for the ethyl decomposition, and about 8500 cal/mole for the bisulphate decomposition. These values must be considered tentative, however.

The empirical reaction order can be estimated from the peak shape.[8] The order is given by $n = 1{\cdot}26\, S^{\frac{1}{2}}$, where S is the shape factor defined by KISSINGER.[8] All peaks are sufficiently symmetric to allow the conclusion of a first order reaction for all decomposition steps, except a peak at about 300° for the majority of the ethyl sulphates where n is about 0·4.

Acknowledgements—I wish to thank Mr. C. L. Little, summer trainee and teacher at Manteca High School, for his great help in getting the equipment set up and in making the initial experiments. I also want to acknowledge the help of Mr. F. MCMURPHY during the later stages of this research, Mrs. G. STEPHAS for her help with the analyses, Mr. V. SILVEIRA for obtaining the X-ray diffraction patterns, and Mr. G. F. RYNDERS for making the run in his thermobalance and for several suggestions.

[7] H. E. KISSINGER, *J. Research Natl. Bur. Standards* **57**, 217 (1956).
[8] H. E. KISSINGER, *Analyt. Chem.* **29**, 1702 (1957).

VOL. 22 1961

J. Inorg. Nucl. Chem., 1961, Vol. 22, pp. 241 to 245. Pergamon Press Ltd. Printed in Northern Ireland

OBSERVATIONS ON THE OXIDATION AND REDUCTION OF PLATINUM(II) NITRO COMPLEXES

BADAR-UD-DIN and JOHN C. BAILAR, JR.
Department of Chemistry and Chemical Engineering, University of Illinois, Urbana, Illinois

(*Received* 13 *June* 1961)

Abstract—In the course of some experiments on the polarographic reduction of the nitro group in $[Pt(NH_2CH_2CH_2NHCH_2CH_2NH_2)(NO_2)]Br$, two interesting observations have been made.

(1) The original material, when allowed to stand in dilute aqueous perchloric acid, yielded crystals of the polymeric substance $[\{Pt(dien)NO_2\}Br_2]n$; this was apparently formed by oxidation of the starting material by nitrite ion, which was formed by aquation.

(2) The reduction product, $[Pt(dien)(NH_3)]^{2+}$, when treated with either $PtCl_4^{2-}$ or $PtCl_6^{2-}$, yielded crystals of the composition $[Pt(dien)(NH_3)][PtCl_4]$. Evidently, the $PtCl_6^{2-}$ is reduced to $PtCl_4^{2-}$ by the complex platinum(II) ammine cation.

VOL. 22 1961

THE reduction of a nitro group coordinated to a metal has been the subject of considerable interest and has been studied both chemically and polarographically. CHERNYAEV[1] studied the reduction of nitro groups in platinum(II) complexes by means of zinc and hydrochloric acid. He reduced several compounds such as *trans*-$[Pten(NH_3)(NO_2)]Cl$* and $[Pt(NH_3)_3NO_2]Cl$, and found the final products to be $[Pten(NH_3)_2]Cl_2$ and $[Pt(NH_3)_4]Cl_2$, respectively. Precipitation of these compounds by potassium chloroplatinate(II) gave long, dark red needles of the Magnus salts $[Pten(NH_3)_2][PtCl_4]$ and $[Pt(NH_3)_4][PtCl_4]$. CHERNYAEV obtained similar results with dinitro and tetranitro compounds. These results were used to show that the nitro group is bonded to the metal through nitrogen.† SELBIN[2] has suggested that the nitro group in such compounds is reduced first to co-ordinated hydroxylamine and then to co-ordinated ammonia. The work reported by him was undertaken to show the possible stages to which $-NO_2$ can be reduced in platinum complexes. If the $-NO_2$ group is reduced to the $-NH_2OH$ stage, only four electrons are involved, but to carry the reduction to $-NH_3$, six electrons are necessary. It was hoped that the number of electrons involved in such a reduction could be determined by polarographic studies. SELBIN's study was of a preliminary nature only, and the present work was undertaken in an attempt to make the results more definite. Several factors have combined to prevent the full realization of this goal; however, some interesting observations have been made during the course of the study, and are reported here.

One of the compounds used in SELBIN's work, nitro-diethylenetriamine platinum(II) bromide, was used. It was soon found that the apparent value of n (the number of electrons used in the reduction) increases with increasing concentration of the solution.

* The symbol "en" represents a molecule of ethylenediamine.

† CHERNYAEV refers to the complexes as "nitrites", but since they are bonded to the metal through nitrogen, English nomenclature would refer to them as "nitro" compounds.

[1] I. I. CHERNYAEV, *Ann. Inst. Platine, Léningr.* No. 7, 52–72 (1929); *Chem. Abstr.* **24**, 2684 (1930).
[2] J. SELBIN. Thesis, University of Illinois (1957).

If the value of D in the ILKOVIC equation is assumed to be $1{\cdot}0 \times 10^{-5}$ cm^2/sec, which is close to the known value for similar complexes, the calculated value of n varies from 3·88 at 5×10^{-5} M to 5·56 at $1{\cdot}0 \times 10^{-3}$ M. This variation is due to catalytic reduction of hydrogen ion, the extent of which is not proportional to concentration. To avoid this difficulty, the complex was studied coulometrically, the applied potential being controlled with the help of a manual potentiostat. As soon as the current was started in the coulometric cell, the mercury cathode became black and powdery. This behaviour can be attributed to the oxidation of mercury in the presence of bromide ion, a trace of the platinum complex being reduced.

A solution of nitro-diethylenetriamine platinum(II) bromide (10^{-2} M), when dissolved in 0·1 M perchloric acid, slowly precipitated needle-like crystals of very dark colour.

Analyses of the new compound gave the following results: Found: C, 9·37; H, 2·71; N, 10·76; Pt, 37·42; Br, 31·4. Calcd. for $([Pt(C_4H_{13}N_3)(NO_2)]Br_2)_n$: C, 9·53; H, 2·60; N, 11·1; Pt, 38·4; Br, 31·7%. This compound, which is water soluble, explodes when heated. It seems that the nitro-diethylenetriamine platinum(II) bromide has been partially oxidized to the platinum(IV) complex, probably by nitrite ion which has escaped from the complex. Dark coloured complexes of platinum and palladium in which the metal seems to be in the tripositive state were mentioned in the literature many years ago[3] but were assigned the correct structures only fairly recently. DREW and coworkers[4] postulated a metal–metal bond for compounds of this type. MANN and PURDIE[5] were nearer the truth when they suggested a complex structure resulting from the union of compounds in the dipositive and tetrapositive states. For example, they proposed that "$Pd(NH_3)_2Cl_3$" should be represented as

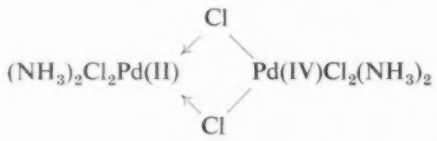

BROSSET's[6] X-ray study of such compounds showed that they are polynuclear complexes composed of infinite chains of alternating divalent and tetravalent metal atoms, which are oriented along the c(needle) axis. According to BROSSET, for example, the compound "$Pt(NH_3)_2Br_3$" is actually $Pt(II)(NH_3)_2Br_2{\cdot}Pt(IV)(NH_3)_2Br_4$, in which the metal atoms are bonded together through single bromine bridges; the intense coloration of the complex is associated with the presence of platinum in two different oxidation states. This view has been supported by COHEN and DAVIDSON[7]. Furthermore, SYRKIN and BELOVA[8] have reported that substances like $PtCl_3$, $PtenCl_3$, and $Pt(NH_3)_2Cl_2OH$ are diamagnetic, although they are formally compounds of tripositive platinum. These findings suggest that the nitro-diethylenetriamine platinum(II) bromide has been oxidized to the polynuclear chain

$$--Pt^{II}--Br—Pt^{IV}Br--Pt^{II}--Br—Pt^{IV}Br---$$

[3] H. ST. CLAIRE-DEVILLE and H. DEBRAY, *C.R. Acad. Sci, Paris* **87**, 926 (1878).
[4] H. D. K. DREW, F. W. PINKARD, G. H. PRESTON and W. WARDLAW, *J. Chem. Soc.* 1895 (1932).
[5] F. G. MANN and D. PURDIE, *J. Chem. Soc.* 873 (1936).
[6] C. BROSSET, *Arkiv Kemi, Mineral, Geol.* **25** A, No. 19 (1948).
[7] A. J. COHEN and N. R. DAVIDSON, *J. Amer. Chem. Soc.* **73**, 1955 (1951).
[8] VA. K. SYRKIN and V. I. BELOVA, *Zh. Fiz. Khim.* **23**, 664 (1949).

Since nitro-diethylenetriamine platinum(II) bromide could not be used in the coulometric experiment because of the formation of the polynuclear complex, it was converted to the sulphate, and this was subjected to coulometric electrolysis, using 0·1 M $HClO_4$ as the electrolyte. The potential was controlled at −0·55V; the current, which was initially about 9 mA, fell only slightly, its final value being 6 mA after 18 hr. The mercury cathode became coated with a scum which was shown to contain platinum. During the course of the electrolysis, this free platinum catalysed the electrolytic reduction of hydrogen ion. On this account, it was impossible to calculate the value of *n* from this experiment.

The nitro-diethylenetriamine platinum(II) sulphate was then subjected to simple polarographic study using a calomel reference electrode, but it was observed that the wave initially formed merged with that for the reduction of hydrogen ion as the concentration of the complex was increased. Evidently some reducible substance is formed when the complex salt is allowed to stand in dilute solution. Qualitative tests indicated that this is nitrite ion, liberated from the complex by aquation. However, the reduction of the nitro group in $[Pt(C_4H_{13}N_3)(NO_2)]_2SO_4$ was readily effected by the technique of CHERNYAEV. When a solution of the complex was reduced with zinc and hydrochloric acid and then treated with a saturated solution of potassium chloroplatinate(II), it immediately gave violet-red needle-like crystals of $[Pt(C_4H_{13}N_3)(NH_3)][PtCl_4]$. But, peculiarly enough, the same compound was precipitated when potassium chloroplatinate(IV) was used instead of the chloroplatinate(II). It seems that in the latter case the reaction proceeds by the reduction of K_2PtCl_6 to K_2PtCl_4 by part of the complex platinum(II) cation; this, in turn, is oxidized to some intermediate compound which remains in solution. REIHLEN and FLOHR[9], while discussing the possible structure of WOLFFRAM's salt,[10] the empirical formula of which is

$$Pt(C_2H_5NH_2)_4Cl_3 \cdot 2H_2O,$$

showed that this compound, when treated with a cold aqueous solution of chloroplatinic acid, gives a mixture of $[Pt^{II}(C_2H_5NH_2)_4]Cl_2$ and $[Pt^{IV}(C_2H_5NH_2)_4Cl_2]Cl_2$.

The platinum(II) complex can be crystallized from this mixture as the chloroplatinate(II) salt when the solution is acidified with dilute hydrochloric acid. According to Reihlen and Flohr, the reaction mechanism is:

(i) $[Pt(C_2H_5NH_2)_4]Cl_2 + Na_2PtCl_6 \rightarrow [Pt(C_2H_5NH_2)_4][PtCl_6] + 2NaCl$

(ii) $2[Pt(C_2H_5NH_2)_4][PtCl_6] \rightarrow [Pt^{II}(C_2H_5NH_2)_4][PtCl_4] + [Pt^{IV}(C_2H_5NH_2)_4Cl_2][PtCl_6]$

Using the reaction mechanism given by REIHLEN and FLOHR, the precipitation of $[Pt(C_4H_{13}N_3)(NH_3)][PtCl_4]$ both by K_2PtCl_4 and K_2PtCl_6 can be explained in the following manner:

(a) $[Pt^{II}(C_4H_{13}N_3)(NO_2)]^+ + \xrightarrow[HCl]{Zn} [Pt^{II}(C_4H_{13}N_3)(NH_3)]^{2+}$

(b) $[Pt^{II}(C_4H_{13}N_3)(NH_3)]^{2+} + PtCl_4^{2-} \rightarrow [Pt^{II}(C_4H_{13}N_3)(NH_3)][PtCl_4]$ (Magnus type salt. Reddish violet needles.)

(c) $2[Pt^{II}(C_4H_{13}N_3)(NH_3)]^{2+} + PtCl_6^{2-} \rightarrow [Pt^{II}(C_4H_{13}N_3)(NH_3)][PtCl_4] + [Pt^{IV}(C_4H_{13}N_3)(NH_3)Cl_2]^{2+}$

[9] H. REIHLEN and E. FLOHR, *Ber. Dtsch. Ges. Chem.* **67**, 2010 (1934).
[10] H. WOLFFRAM. Dissertation, Königsberg (1900).

The platinum(II) complex precipitated within a few minutes when either $PtCl_4^{2-}$ or $PtCl_6^{2-}$ was added to a solution of the reduced complex. The oxidation of *cis* and *trans*diglycine platinum(II)[11] by potassium chloroplatinate(IV) furnishes another example in support of this mechanism:

$$[Pt^{II}(NH_2{\cdot}CH_2{\cdot}COO)_2] + K_2PtCl_6 \rightarrow [Pt^{IV}(NH_2(CH_2COO)_2Cl_2] + K_2PtCl_4.$$

EXPERIMENTAL

1. *Preparation of potassium chloroplatinate(II).* This was prepared according to the method described by COOLEY[12].

2. *Bromo-diethylenetriamine platinum(II) bromide.* The method used was essentially that described by MANN[13]: A solution of 5 g of K_2PtCl_4 (0·01205 mole) in 100 ml of water was treated with 3·86 g of diethylenetriamine trihydrochloride (50 per cent excess) and the mixture was refluxed for about 4 hr. During refluxing some platinum mirror was deposited on the sides of the flask and the colour of the solution changed from red to pale-orange. The solution was filtered and its volume reduced to nearly half by evaporating in an air stream. It was again filtered and to the filtrate was added solid ammonium bromide after the addition of several drops of hydrobromic acid. In a few minutes diethylenetriamine platinum(II) bromide came down; the crystals were filtered, washed with alcohol and ether, and air dried. Yield: 45 per cent based on K_2PtCl_4. (Found, C, 10·63; H, 2·85; N, 9·24; Pt, 42·68; 34·83. Calcd. for $[Pt^{II}(C_4H_{13}N_3)Br]Br$: C, 10·48; H, 2·83; N, 9·17; Pt, 42·6; Br, 34·9%).

3. *Preparation of nitro-diethylenetriamine platinum(II) bromide.* The method used was that employed by SELBIN.[2] A solution of 0·3 g of $[Pt^{II}(C_4H_{13}N_3)Br]Br$ (·000655 mole) in 15 ml of water was treated with 0·101 g of silver nitrite (0·000655 mole). The silver bromide was removed and the clear, colourless filtrate was concentrated under vacuum, whereupon crystals of $[Pt^{II}(C_4H_{13}N_3)(NO_2)]Br$ were obtained in quantitative yield. (Found, C, 11·22; H, 3·03; N, 13·43; Pt, 45·2; Br, 18·6). Calcd. for $[Pt(C_4H_{13}N_3)(NO_2)]Br$: C, 11·3; H, 3·06; N, 13·4; Pt, 45·0; Br, 18·8%.

4. *Preparation of nitro-diethylenetriamine platinum(II) sulphate.* A solution of 1·64 g of nitro-diethylenetriamine platinum(II) bromide was treated with 0·6034 g of Ag_2SO_4 and the mixture was heated with stirring on a water bath for about 15 min. After this, it was cooled in ice and filtered. The filtrate was evaporated to crystallization in a vacuum. The crystals were washed with alcohol and ether and air dried. Yield, quantitative. (Found, C, 12·51; H, 3·36; N, 14·34; Pt, 49·73; S, 3·92. Calcd. for $[Pt(C_4H_{13}N_3)(NO_2)]_2SO_4$, C, 12·24; H, 3·32; H, 14·3; Pt, 50·0; S, 4·1%).

5. *Polarographic Reduction of the Nitro Group.* For the study of the polarographic reduction of the nitro group coordinated to platinum metal, varying amounts of nitro-diethylenetriamine platinum(II) bromide were added to 25 ml of 0·01 M $HClO_4$, which was used as the supporting electrolyte in the cell. Nitrogen was bubbled through to remove oxygen and the value of n was calculated from the ILKOVIC equation[2]. Assuming, with SELBIN, that the value of D is near $1{\cdot}0 \times 10^{-5}$ cm²/sec, which is close to the value for many ions of this size, the calculated value of n was found to increase as the amount of the complex in the cell was increased.

Concentration of $[Pt(C_4H_{13}N_3)(NO_2)]Br$ (mmole/l.)	Calculated value of n
0·05	3·88
0·0992	4·41
0·197	4·43
0·293	4·57

[11] A. A. GRINBERG, *Dokl. Akad. Nauk SSSR* **32,** 57 (1941).
[12] W. E. COOLEY, *Inorganic Synthesis*, Vol. 5, page 208. McGraw-Hill, New York (1957).
[13] F. G. MANN, *J. Chem. Soc.* 456 (1934).

In another experiment, when the concentration of $HClO_4$ was 0·1 M (i.e., ten times higher than in the above case), nitrogen was bubbled after each addition of the solution of the platinum complex.

Concentration of the complex in the cell (mmole/l.)	Calculated value of n
0·24	4·2
0·47	4·68
0·700	4·80
0·901	4·90
1·00	5·56

6. *Coulometric Reduction.* In the coulometric experiments, the electrode $\left|\begin{matrix}(AgCl)\\NaCl\end{matrix}\right| NaNO_3$ was used as a reference. The potential applied was −0·55 V. One hundred and fifty millilitres of 0·1 M $HClO_4$ was used in the electrolysis cell. The coulometer contained 0·1 M hydrazine sulphate solution, and 0·60 g of the nitro-diethylenetriamine platinum(II) sulphate was used in the $HClO_4$ solution. Nitrogen was used to remove oxygen.

7. *Preparation of Magnus salt.* To a solution of 0·2 g of nitro-diethylenetriamine platinum(II) sulphate in about 50 ml of water, 0·5 g of zinc dust and 1 ml of concentrated hydrochloric acid were added. When no more gas was evolved, the solution was filtered. A saturated solution of K_2PtCl_4 or K_2PtCl_6 was added slowly to the filtrate with stirring. The colour of the solution changed to violet-red and after some time, reddish crystals of $[Pt(C_4H_{13}N_3)(NH_3)][PtCl_4]$ were precipitated. The yield was 35 per cent based on the nitro-platinum complex when K_2PtCl_4 was used and even less when K_2PtCl_6 was employed. (Found with (a) K_2PtCl_4 solution: C, 7·35; H, 2·44; N, 8·71; Pt, 59·66; Cl, 21·7. (b) K_2PtCl_6 solution: C, 7·63; H, 2·66; N, 8·70; Pt, 59·39; Cl, 21·68. Calcd. for $[Pt(C_4H_{13}N_3)(NH_3)][PtCl_4]$ C, 7·51; H, 2·45; N, 8·59; Pt, 59·8; Cl, 21·8%).

Acknowledgement—The authors wish to express their thanks to Dr. T. B. Reddy and Prof. H. A. Laitinen for their generous help with the electrochemical experiments, and for their counsel. One of the authors (B. D.) wishes to thank the International Cooperation Administration (Pakistan Project) for financial assistance.

VOL. 22 1961

VO
2
19

J. Inorg. Nucl. Chem., 1961, Vol. 22, pp. 247 to 251. Pergamon Press Ltd. Printed in Northern Ireland

EXCHANGE PROPERTIES OF AMMONIUM SALTS OF 12-HETEROPOLYACIDS–III

THE SORPTION OF STRONTIUM AND YTTRIUM ON AMMONIUM PHOSPHOTUNGSTATE AND THEIR SEPARATION FROM CAESIUM

J. KRTIL

Institute of Nuclear Research, Czechoslovak Academy of Sciences, Řež u Prahy

(*Received* 10 *May* 1961)

Abstract—Both the static and dynamic sorption and elution of strontium and yttrium on ammonium phosphotungstate have been studied, and conditions for the separation of Sr and Y from Cs were determined

VOL. 22 1961

THE use of ammonium phosphotungstate as an ion exchanger for separating ^{137}Cs ions from fission products requires a knowledge of the behaviour of multivalent fission products such as Sr, Y, Ru, Zr and Nb on this sorbent, and of the conditions for minimum adsorption of these ions. The aim of this work was to study the sorption and elution of Sr and Y on ammonium phosphotungstate under static and dynamic conditions and to develop a convenient method for the separation of Sr and Y from Cs.

There is little information in the literature concerning the alkaline earth salts of heteropolyacids, which are much more soluble than those of some univalent metals (Hg, Ag, Tl, of the alkali metals). The alkaline earth salts of the heteropolyacids have been studied for their theoretical importance in relation to the Miolati-Rosenheim theory.[1,2] Their analytical importance is negligible, but they may be used to prepare free heteropolyacids without using the etherate, as reported by NIKITINA and co-workers[3] for silicotungstic acid. The adsorption of alkaline earths on ammonium phosphomolybdate was first studied by Buchwald and Thistlethwaite,[4] who found that one mole of sorbent contained 0·2 equivalents of Sr. SMIT and co-workers[5] mentioned the sorption of Sr and Y on a column of ammonium phosphomolybdate and asbestos, and assumed these ions to be adsorbed as univalent hydrolysed species. BROADBANK and co-workers[6] described the sorption of Sr, Ba and Y on ammonium phosphomolybdate from the analytical view point.

EXPERIMENTAL

The material used was ammonium phosphotungstate, $(NH_4)_{2\cdot26}H_{0\cdot72}(PW_{12}O_{40})\cdot12\cdot6\ H_2O$ (abbreviated to NH_4PW), prepared and analysed by the method described previously.[7] Dynamic experiments were carried out on ammonium phosphotungstate freshly precipitated on asbestos.[8] Tracer $^{90}Sr + {}^{90}Y$ was used for analysis. The chemicals used were of analytical grade.

[1] E. A. NIKITINA and N. E. KULAKOVA, *Zh. Neorg. Khim.* **4**, 3,564 (1959).
[2] E. A. NIKITINA and N. A. KULAKOVA, *Zh. Neorg. Khim.* **4**, 3,571 (1959).
[3] E. A. NIKITINA, N. P. PJATNICKAJA and I. I. ANGELOV, *Zh. Obshch. Khim.* **26**, 10 (1956).
[4] H. BUCHWALD and W. P. THISTLETHWAITE, *J. Inorg. Nucl. Chem.* **5**, 341 (1958).
[5] J. VAN R. SMIT, W. ROBB and J. JACOBS, *Nucleonics* **17**, 116 (1959).
[6] R. W. C. BROADBANK, S. DHABANANDANA and R. D. HARDING, *Analyst* **85**, 365 (1960).
[7] J. KRTIL and V. KOUŘIM, *J. Inorg. Nucl. Chem.* **12**, 367 (1960).
[8] J. KRTIL, *J. Inorg. Nucl. Chem.* To be published.

Static experiments: 0·2 g NH_4PW was weighed into a 10 ml polythene bottle, and 7 ml of 10^{-6} M ($^{90}Sr + {}^{90}Y$) carrier-free solution of appropriate pH were added. In further experiments carrier $Sr(NO_3)_2$ was added. After shaking until equilibrium was attained, NH_4PW was centrifuged, the distribution of Sr and Y between the phases was determined radiometrically, and the pH was measured. The Sr activity was measured at equilibrium and the Y activity was measured immediately after the separation of the phases, using an Al filter of 184 mg/cm², which absorbs the β-radiation of Sr and attenuates that of Y. The Y coefficient of attenuation was determined separately using pure Y under identical condition. The samples were measured on Al foils using a GM tube with mica window. The error in measurement was ± 3 per cent. Exchanged ammonium ion was determined colorimetrically by Nessler's reagent and the pH was measured with a quinhydrone electrode and Multoscop pH-meter.

RESULTS AND DISCUSSION

The dependence of the sorption of carrier-free Sr and Y on pH between 0 and 5·7 was first examined. pH values from 0 to 3·3 were obtained using HNO_3 at various

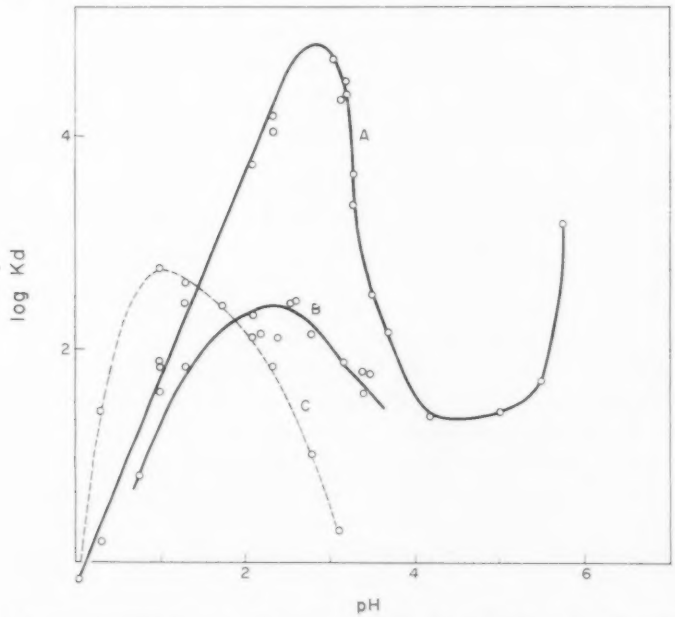

FIG. 1.—Dependence of log K_D for Sr and Y on pH.—*A*: Tracer Sr.—*B*: 1·72 μmoles Sr/ml—*C*: Tracer Y.

concentrations, and those between 3·3 and 5·7 by addition of known amounts of 0·1 N NH_4OH. The pH-dependence of log K_D for Sr and Y is shown in Fig. 1. The amount of adsorbed Sr increases with increasing pH, and reaches 100 per cent between pH 2·1 and 3·3. The latter corresponds to the pH of the suspension of NH_4PW in water, and in achieving higher pH values the sorption is influenced by the concentration of ammonium ions as well as by the pH. The influence of other ions, e.g. Na^+ and NH_4^+, on Sr and Y sorption at pH 2·1 was also examined and the experiments indicated that sorption was substantially lowered by both ions at micro concentrations. The influence of Na ions is smaller than that of ammonium ions and the sorption of Y is lowered to a lesser extent than that of Sr in the presence of other ions. Sr sorption decreases from pH 3·3 to 4, obviously due to the presence of NH_4^+ ion,

and thereafter increases due to sorption on the decomposition products of NH_4PW and to the existence of Sr bicarbonates in this pH range. Y sorption is similar to that of Sr, the former being not completely adsorbed and the maximum being shifted to lower pH values (pH 1). The dependence on pH of the distribution coefficient K_D, defined as β-activity per gram of NH_4PW/β-activity per ml of solution at equilibrium has a maximum at pH 2·5–3 for Sr and at pH 1 for Y. The dependence of log K_D on pH is linear to pH 3 for Sr, with a slope of 2, indicating that one Sr is exchanged for two H ions in this range. Since the sorption of trace amounts of Sr only leads to qualitative conclusions, and does not allow us to determine the maximum amount of Sr entering into the NH_4PW molecule or to describe the exchange mechanism, we have also carried out the sorption of weighable amounts of Sr and have measured the amount of exchanged ammonium ions corresponding to the Sr uptake. The dependence on pH is shown in Fig. 1 and in Table 1.

VOL. 22 1961

TABLE 1

pH	Sorbed Sr (%)	Sr/NH_4PW (mole ratio)	Exchanged NH_4^+, (mole)
1·0	54·4	0·10	0·26
1·3	67·4	0·14	0·26
2·1	85·9	0·18	0·24
2·6	88·9	0·17	0·26
3·1	69·3	0·13	0·30
3·5	62·3	0·12	0·29

The results indicate that one mole of NH_4PW absorbs a maximum of 0·18 mole of Sr; the Sr content in the molecule decreases with decreasing pH to 0·025 mole in 0·5 N HNO_3 and in the presence of ammonium salts. The ammonium ion exchanged remains almost constant at 0·3 mole. BROADBANK and co-workers[6] reported a maximum dynamic exchange capacity of 0·8 moles of Sr per mole of NH_4PMo. Our static experiments at similar concentrations indicate a maximum sorption of 0·25 mole Sr/mole NH_4PW.*

The amount of Sr per mole of sorbent is much smaller than that of Cs (1·8 moles in static experiments and 2 in dynamic experiments) and the dependence on pH indicate that the sorption of Sr in acid media is small. Sr may be exchanged in the crystal lattice for ammonium ion, and also (Table 1, pH 2·1 and 2·6) for hydrogen ion. The decrease in pH during the sorption of weighable amounts of Sr confirms that the process is one of ion exchange. The bonding between Sr and Y on the one hand and NH_4PW on the other is slight with respect to replacement by H ions, in contrast to the case of Cs and Rb adsorbed on NH_4PW.[7]

Dynamic experiments

Sr and Y sorption on asbestos alone was examined by absorbing micro-amounts on a column filled with asbestos, followed by elution with various electrolytes. The results indicated that strontium and yttrium are easily washed out by ammonium salts (0·3 M) or by acids (1 N HCl or HNO_3). Glass-wool and asbestos gave similar

* Mole ratio Sr: NH_4PW = 200:63

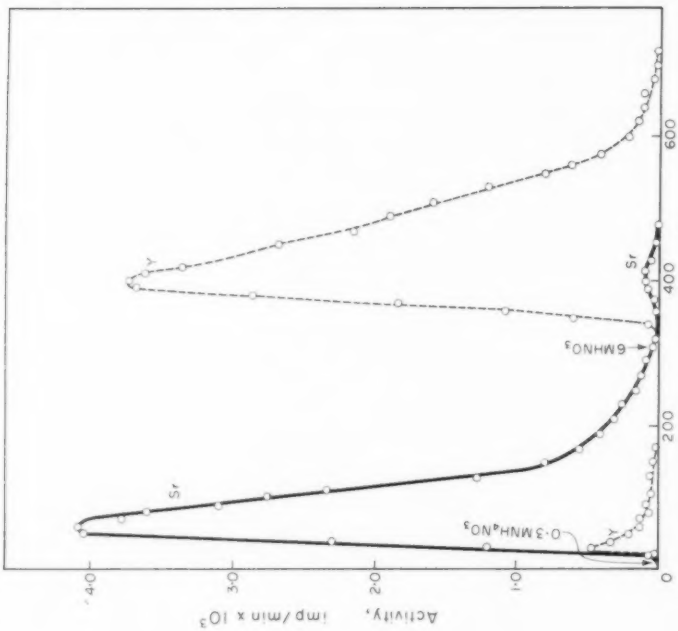

FIG. 3.—Separation of trace ^{90}Sr from trace ^{90}Y. 3 cm bed (0·2 g NH_4PW + 0·2 g asbestos), drop interval 17 sec.

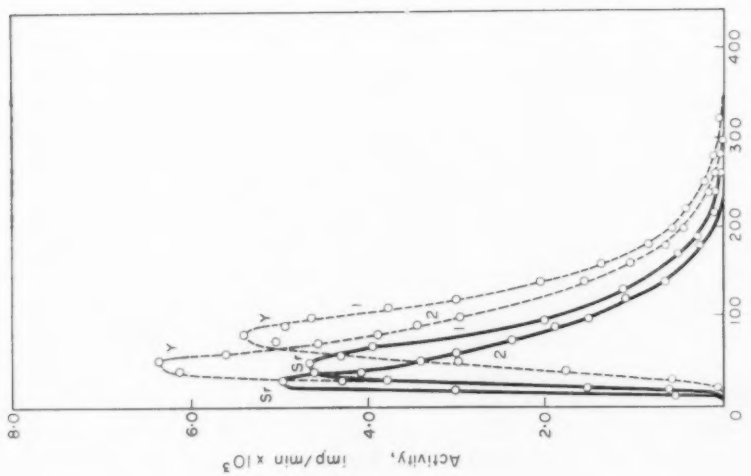

FIG. 2.—Elution of ^{90}Sr and ^{90}Y with nitric acid. 3 cm bed (0·2 g NH_4PW + 0·2 g of asbestos), drop interval 15 sec. 1: 1 N HNO_3, 2: 6 N HNO_3. Full line—Sr, dashed line – – Y.

results, indicating that asbestos possesses negligible sorption capacity for Sr and Y. Na ions were less effective than ammonium ions or acids, part of the Sr and Y remaining on the column. In further experiments Sr and Y were adsorbed on NH_4PW from 0·5 N acid and neutral (0·4 N $NaNO_3$) solution and then eluted with HCl, HNO_3 or NH_4NO_3. Fig. 2 shows that both elements are eluted together, with Sr tending to precede Y, which is more acidic than Sr, in agreement with the static experiments.

The difference between elution with 1 N and with 6 N HNO_3 is unimportant, and

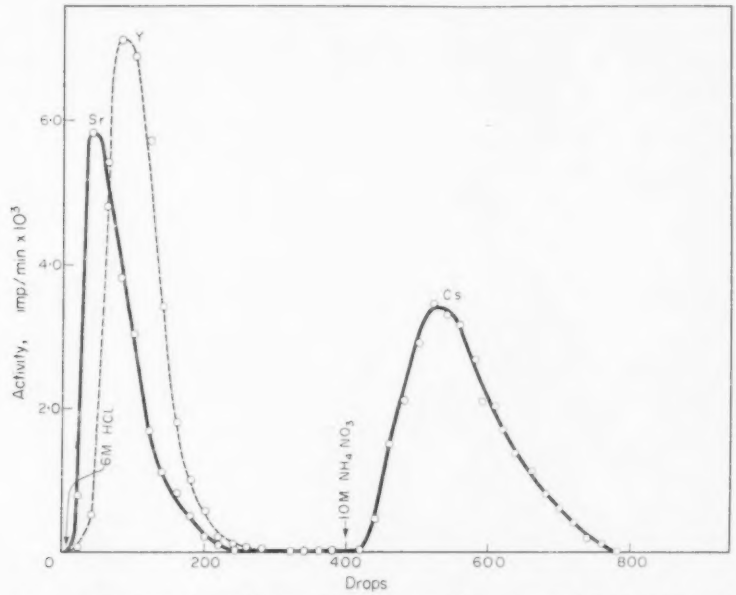

FIG. 4.—Separation of trace ^{90}Sr and ^{90}Y from trace ^{137}Cs. 3 cm bed (0·2 NH_4PW + 0·2 g of asbestos), drop interval 20 sec.

no difference was observed in the behaviour of HCl and HNO_3, or between sorption from acid or neutral solution provided that acid elution followed. Sr and Y may be separated by sorption from neutral solution followed by elution with 0·3 N NH_4NO_3 and 6 N HNO_3 (Fig. 3). Microamounts of Cs, Sr and Y were adsorbed from neutral or acid solution and were eluted first with 3 N or 6 N acid and after that with 6 N or 10 N ammonium nitrate, as shown in Fig. 4. Two peaks for Sr and Y were first obtained, and Cs was then eluted with ammonium salts. The exchange capacity for Cs decreases only slightly in 0·5 N HNO_3.

VOL. 22 1961

VO
2
19

J. Inorg. Nucl. Chem., 1961, Vol. 22, pp. 253 to 257. Pergamon Press Ltd. Printed in Northern Ireland

AN ION EXCHANGE STUDY OF COPPER PYROPHOSPHATE COMPLEXES IN SOLUTION

C. HEITNER-WIRGUIN and J. KENDY
Department of Inorganic and Analytical Chemistry, The Hebrew University of Jerusalem, Jerusalem, Israel

(*Received* 16 *May* 1961)

Abstract—The ion exchange method was used to investigate the complexes of copper and pyrophosphate which exist in solution in the range of pH values 1–10. The complex formed is

$$[CuH_q(P_2O_7)_2]^{(6-q)-},$$

and depending upon the pH of the solution the following species were obtained:

$[Cu(H_3P_2O_7)(H_2P_2O_7)]^{1-}$, $[Cu(HP_2O_7)(H_2P_2O_7)]^{3-}$ $[Cu(HP_2O_7)_2]^{4-}$ and $[Cu(HP_2O_7)(P_2O_7)]^{5-}$.

VOL. 22 1961

DURING the last ten years, a series of papers have appeared on the complexes of copper and pyrophosphate in solution. ROGERS and REYNOLDS,[1] HALDAR[2] and BOBTELSKY and KERTES[3] studied these complexes by potentiometric, conductometric, thermometric and ion transport methods, and concluded that two complexes were obtained, i.e. $[Cu(P_2O_7)]^{2-}$ and $[Cu(P_2O_7)_2]^{6-}$. The dissociation constants were determined from polarographic[1,4] solubility product[5] and other measurements,[6] but the results obtained by these authors do not agree. ONSTOTT and LAITINEN,[7] using the polarographic and potentiometric methods, studied the formation of these complexes as a function of the pH of the solution, and according to this study, the following equilibria exist:

$$[Cu(HP_2O_7)_2]^{4-} \overset{OH^-}{\rightleftharpoons} [Cu(HP_2O_7)(P_2O_7)]^{5-} \overset{OH^-}{\rightleftharpoons} [Cu(P_2O_7)_2]^{6-} \rightleftharpoons [Cu(OH)(P_2O_7)]^{3-}.$$

The anionic species with charges −5 and −6 exist at pH values 7–10, while the hydroxy-complex exists only in strongly alkaline solutions. According to these authors, when no pyrophosphate is available for formation of the 1:2 complex a complex is formed with one $HP_2O_7^{3-}$ group at pH values 3·6–5·3. A spectrophotometric investigation of this system was made by WATTERS and AARON,[8] who found some evidence for the existence of $[Cu(P_2O_7)_2]^{6-}$ and $[CuP_2O_7]^{2-}$ above pH 5·5. In the range of pH 2–5·5 they obtained a precipitate of $Na_2Cu_3(P_2O_7)_2$. The same authors also mention that in very dilute solutions two other compounds, $[Cu_2P_2O_7]^0$ and $[Cu_4P_2O_7]^{4+}$, are formed. In the present study an attempt was made to use the ion exchange method to investigate this complex system, as was done in previous work

[1] L. B. ROGERS and C. A. REYNOLDS, *J. Amer. Chem. Soc.* **71**, 2081, 1949.
[2] B. C. HALDAR, *Science and Culture*, **14**, 340–1 (1949), cf. *Chem. Abstr.* 6103 (1949).
[3] M. BOBTELSKY and S. KERTES, *J. Appl. Chem.* **5**, 675 (1955).
[4] E. ERIKSSON, *Kgl. Lantbruks, Högskol Ann* **16**, 39 and 72, 1949; *Chem. Abstr.* 3392 (1950).
[5] K. B. YATSIMIRSKA and P. VASIL'EV, *Zh. Anal. Khim.* **11**, 534 (1956); *Chem. Abstr.* 8570 (1957).
[6] Z. UKSHE and Z. LEVA, *Zh. Fiz. Khim.* **27**, 1396 (1953); *Chem. Abstr.* 3166 (1954).
[7] E. I. ONSTOTT and H. A. LAITINEN, *J. Amer. Chem. Soc.* **72**, 4729 (1950).
[8] J. I. WATTERS and A. AARON, *J. Amer. Chem. Soc.* **75**, 611 (1953).

on the copper triphosphate complexes.[9,10] As pyrophosphoric acid is more stable than triphosphoric acid, the present study was extended to include the whole range of pH values at which soluble complex species were obtained. An attempt was further made to ascertain whether chloride ion participates in the formation of some complexes and whether the water regain of the resin affects the sorption of the different species. To determine the charges of the complex ionic species obtained, a preliminary study of the sorption of the pyrophosphate ion alone was made in the whole pH range, and the mean charges of the sorbed pyrophosphate ions calculated.

EXPERIMENTAL

Ion Exchange

The batch technique described by SALMON[11] was employed, using 50 ml of solution and 0·500 g of the anion exchanger Deacidite FF–X (X = Cl^- or NO_3^-) having various values of water regain (0·6–0·9, 1·0–1·5 and 1·5–2·0). Elution and analysis were carried out as described previously.[10]

Reagents

The reagents were of analytical grade. Pyrophosphoric acid was prepared by passing a solution of tetra-sodium pyrophosphate through the cation exchanger Zeokarb 225–H^+. To obtain higher concentrations (0·25 M), the solution was evaporated under reduced pressure. The solutions thus obtained were shown to be free from sodium by flame-photometric measurements, and from orthophosphate by adding a solution of $AgNO_3$ acidified with HNO_3, when no precipitation was observed.

RESULTS

Table 1 shows the sorption of pyrophosphate ions on an ion exchange resin of medium water regain at various pH values. Similar experiments were carried out on a high and low water regain resin and showed that the equilibria are less dependent on the water regain of the resin than in the case of the triphosphate.[10] At lower pH values fairly large quantities of chloride ions remain on the resin at equilibrium owing

TABLE 1.—SORPTION OF PYROPHOSPHATE IONS BY DEACIDITE FF–Cl

Aqueous phase			Resin phase			
Initally		Finally				
$Na_4P_2O_7$ (M)	pH*	pH	N_{Cl}†	N_{Pyro}†	Charge on P_2O_7 ions sorbed‡	Water regain of the resin
0·036	1·42	1·53	0·09	0·54	1·7	0·6–0·9
0·04	1·55	1·55	0·62	0·20	1·9	1·0–1·5
0·04	5·00	4·85	0·42	0·26	2·2	1·0–1·5
0·04	6·08	6·12	0·35	0·26	2·4	1·0–1·5
0·04	6·48	6·52	0·29	0·25	2·8	1·0–1·5
0·04	7·05	7·18	0·28	0·27	2·7	1·0–1·5
0·04	7·50	7·57	0·21	0·28	2·8	1·0–1·5
0·04	7·75	7·82	0·21	0·28	2·8	1·0–1·5
0·04	9·95	9·22	0·05	0·28	3·4	1·0–1·5

* Obtained by addition of 1 M HCl except in the first case, where $H_4P_2O_7$ was used.
† N in this and following Tables indicates the number of moles of X sorbed per equivalent of resin.
‡ Derived from $(1-N_{Cl})N_{Pyro}$

[9] C. HEITNER-WIRGUIN, J. E. SALMON and E. B. MAYER, *J. Chem. Soc.* 460 (1960).
[10] C. HEITNER-WIRGUIN, *Bull. Res. Counc. Israel*, **9** A, 37 (1960).
[11] J. E. SALMON, *Rev. Pure Appl. Chem.* **6**, 24 (1956).

to the use of high concentrations of hydrochloric acid to acidify the solutions. At some pH values, when pyrophosphoric acid was used, relatively small quantities of chloride ions remained on the resin at equilibrium.

The mean charges obtained at different pH values agree with the dissociation constants of pyrophosphoric acid ($pK_1 = 0{\cdot}85$, $pK_2 = 1{\cdot}96$, $pK_3 = 6{\cdot}54$ and $pK_4 = 8{\cdot}44$). In the presence of nitrate ions the mean charges obtained were somewhat lower than in the presence of chloride ions, due to the different swelling of the resin in the chloride and nitrate form.[10]

TABLE 2.—SORPTION OF COPPER AND PYROPHOSPHATE FROM SOLUTIONS CONTAINING COPPER CHLORIDE (OR NITRATE) AND PYROSPHATE AT VARIOUS pH VALUES ON DEACIDITE FF–Cl (OR NO_3)

Aqueous phase					Resin phase					Water regain of the resin
Initally				Finally						
$CuCl_2$ (M)	$H_4P_2O_7$ (M)	Mole ratio P_2O_7:Cu	pH*	pH	N_{Cu}	N_{Pyro}	N_{Cl}	$\frac{N_{Pyro}}{N_{Cu}}$	q	
0·04	0·05	1·25	1·20	1·20	0·03	0·24	0·66	8	4·8	
0·02	0·05	2·54	1·20	1·25	0·04	0·41	0·43	10	5·2	Cl^-
0·02	0·10	5·08	1·20	1·10	0·04	0·54	0·21	13·5	5·2	0·6–0·9
0·02	0·152	7·62	1·22	1·0	0·04	0·56	0·17	14·0	5·2	
0·02	0·01	5	1·68	1·65	0·05	0·45	0·24	9	2·7	
0·02	0·01	5	6·20	5·90	0·14	0·33	0·29	2·4	1·8	
0·02	0·01	5	7·11	6·88	0·14	0·32	0·22	2·3	1·05	
0·02	0·01	5	7·80	7·60	0·13	0·29	0·23	2·2	0·8	Cl^-
0·02	0·06	3	9·52	9·30	0·14	0·30	0·18	2·1	0·9	1·5–2·0
0·02	0·08	4	9·92	9·52	0·13	0·30	0·22	2·3	1·1	
0·02	0·12	6	10·15	9·68	0·10	0·30	0·22	3·0	1·2	
0·02	0·16	8	10·25	9·65	0·085	0·29	0·22	4·0	0·9	
†										
0·02	0·06	3	9·52	8·9	0·10	0·29	0·25	2·8	1·5	
0·02	0·08	4	9·92	9·25	0·13	0·31	0·25	2·4	1·6	NO_3^-
0·02	0·12	6	10·15	9·25	0·09	0·27	0·25	3·2	1·7	1·5–2·0
0·02	0·16	8	10·25	9·45	0·09	0·26	0·25	3·1	1·2	

* Adjusted by addition of HCl to $Na_4P_2O_7$ or NaOH to $H_4P_2O_7$.
† Second part of the Table: read nitrate instead of chloride.

A qualitative study made by the extraction method showed that no extractable species exist in the whole complex system. There was also no pyrophosphate sorption on a cation exchanger from solutions containing various ratios of copper and pyrophosphate at various pH values. It can be concluded from these experiments that there is no evidence for the existence of either neutral or cationic complex species. The present study was therefore made solely on anion exchangers having various water regain values. Table 2 summarizes the results obtained at equilibrium from solutions containing various ratios of pyrophosphate to copper in the pH range of 1–10. The pH range 2–6 cannot be studied by this method because a precipitate is formed.

This table shows that the sorption of copper from acid solutions is very small. This may be due either to the instability of the complex formed, or to the low anionic charge of the complex and preferential sorption of the free pyrophosphate ion. At pH $>$ 6 the sorption of copper is much larger and the equivalents of complex sorbed are comparable with the equivalents of free pyrophosphate ions sorbed; the ratios of pyrophosphate to copper in the resin phase are always higher than 2:1. A few experiments were made in solutions containing nitrate instead of chloride and with a nitrate form of the exchanger (last four rows of Table 2). The results obtained are similar to those obtained in chloride solutions, so that the possibility of the participation of chloride ion in complex formation can be excluded.

Table 3 shows some results for the sorption of copper and pyrophosphate ions from very dilute solutions in the pH range 6–10. Even from solutions containing one pyrophosphate to one copper, the ratio of the ions sorbed is two pyrophosphate to one copper. The results obtained in these experiments cannot be accounted for in terms of the formation of the complex species $[Cu_2P_2O_7]^0$ and $[Cu_4P_2O_7]^{4+}$ mentioned by WATTERS and AARON.[8] There is a small decrease in the sorption of copper with an increase of the pyrophosphate concentration in solution, but this was also observed to some extent in more concentrated solutions (Table 2).

TABLE 3.—SORPTION OF COPPER AND PYROPHOSPHATE FROM DILUTED SOLUTIONS OF COPPER CHLORIDE AND SODIUM PYROPHOSPHATE ON DEACIDITE FF–Cl (WATER REGAIN 1·0–1·5).

Aqueous phase					Resin phase				
Initially				Finally					
$CuCl_2$ M	$H_4P_2O_7$ M	P_2O_7:Cu	pH	pH	N_{Cu}	N_{Pyro}	N_{Cl}	$\frac{N_{Pyro}}{N_{Cu}}$	q
0·002	0·002	1	6·75	6·15	0·04	0·08	0·91	2·0	2·1
0·002	0·004	2	8·75	8·0	0·07	0·14	0·70	2·0	1·7
0·002	0·006	3	9·30	8·9	0·07	0·20	0·46	2·9	1·1
0·002	0·008	4	9·55	8·85	0·06	0·25	0·28	4·1	1·1
0·002	0·02	10	9·90	9·68	0·06	0·28	0·18	4·7	1·1
0·002	0·04	20	9·95	9·95	0·05	0·29	0·15	5·8	1·3

DISCUSSION

According to the results previously published, two kinds of complexes are particularly mentioned, i.e. $1Cu:1P_2O_7$ and $1Cu:2P_2O_7$. An attempt was made to interpret the results obtained here in terms of the formation of two complexes $[CuH_qP_2O_7]^{(2-q)-}$ and $[CuH_q(P_2O_7)_2]^{(6-q)-}$. The first has a very low charge, and it does not seem probable that such a species is sorbed; furthermore, the capacity of the resin cannot be accounted for by the sorption of this complex. The ratio of pyrophosphate to copper on the resin is always greater than two, leading to the conclusion that the complex is formed, i.e. $[CuH_q(P_2O_7)_2]^{(6-q)-}$.

The charge on the complex species formed was calculated by accounting for the capacity of the resin in terms of the ions sorbed. If $[CuH_q(P_2O_7)_2]^{(6-q)-}$ is the formula of the complex sorbed, and

N_{Cu} = moles of complex sorbed, then

$N_{pyro} - 2N_{Cu}$ = moles of free pyrophosphate ($H_bP_2O_7^{(4-b)-}$) sorbed.

$(4 - b)$ = charge on the pyrophosphate ion when sorbed in absence of copper (Table 1).
$N_{Cu}^{(6-q)}$ = equivalents of complex sorbed.
$(4 - b)(N_{pyro} - 2N_{Cu})$ = equivalents of free pyrophosphate sorbed.
N_{Cl} = equivalents chloride sorbed.
Total equivalents sorbed =

$$1 = N_{Cu}(6 - q) + (4 - b)(N_{pyro} - 2N_{Cu}) + N_{Cl}$$

The values of q thus calculated are given in Tables 2 and 3, and show the number of hydrogen ions remaining on the complex at each pH value. This number varies from five at pH 1–2 to 1 at pH 9–10, and thus the following equilibria should be taken into consideration:

$$Cu^{2+} + 2H_4P_2O_7 \rightleftharpoons [Cu(H_3P_2O_7)(H_2P_2O_7)]^{1-} + 3H^+ \text{ (pH 1–1·5).} \quad (1)$$

$$[Cu(H_3P_2O_7)(H_2P_2O_7)]^{1-} + 2OH^- \rightleftharpoons [Cu(HP_2O_7)(H_2P_2O_7)]^{3-} + 2H_2O \text{ (pH 1·5–2).} \quad (2)$$

$$[Cu(HP_2O_7)(H_2P_2O_7)]^{3-} + OH^- \rightleftharpoons [Cu(HP_2O_7)_2]^{4-} + H_2O \text{ (pH 6–7)} \quad (3)$$

$$[Cu(HP_2O_7)_2]^{4-} + OH^- \rightleftharpoons [CuHP_2O_7)(P_2O_7)]^{5-} + H_2O \text{ (pH 7–10).} \quad (4)$$

No values of q less than one were obtained, so that probably no complex of the form $[Cu(P_2O_7)_2]^{6-}$ is sorbed.

The values of q obtained in nitrate solutions are higher than in chloride solutions, and seem to indicate that at the same pH value, the degree of hydrogen ions dissociation is less than in the chloride system. While in the chloride system a charge of five is found at pH 7–10, in the nitrate system the charge is 4·5, which could be accounted for by a nearly equal mixture of $[Cu(HP_2O_7)_2]^{4-}$ and $[Cu(HP_2O_7)(P_2O_7)]^{5-}$. There are practically no differences between the q values calculated in concentrated or dilute solutions (Tables 2 and 3).

In all cases it can be assumed that the pyrophosphate ion acts as a bidentate ligand, and thus two pyrophosphate ions satisfy the co-ordinated number 4 of copper.

VOL. 22 1961

J. Inorg. Nucl. Chem., 1961, Vol. 22, pp. 259 to 268. Pergamon Press Ltd. Printed in Northern Ireland

THE KINETICS OF ION EXCHANGE ON ZIRCONIUM PHOSPHATE AND HYDRATED THORIA

G. H. NANCOLLAS and R. PATERSON
Chemistry Department, The University, Glasgow, W.2

(*Received* 31 *May* 1961)

Abstract—The rates of sodium-hydrogen exchange on thoria and on zirconium phosphate in two particle sizes have been measured both by titration and potentiometrically in limited bath experiments over a sodium ion concentration range 0·01–1·0 M. The rate is independent of sodium ion concentration within this range, and the results indicate that the rate-controlling process is the diffusion of ions through the exchanger particles. Further evidence in support of particle diffusion is afforded by infinite bath caesium–potassium exchange experiments on zirconium phosphate using a tracer technique. The effective diffusion coefficient for the sodium and hydrogen ions in the thoria exchanger ranges from about 4–15 $\times$ 10^{-8} cm²/sec.

VOL.
22
1961

THE use of thoria and zirconium phosphate as ion exchange materials has been described by AMPHLETT and KRAUS.[1–4] Adsorbed anions and cations are rapidly and reversibly exchangeable for the ions present in the equilibrating solution and the hydrated oxide exhibits amphoteric properties, being capable of exchanging both anions and cations depending upon the pH of the medium.

It is important to have information about the kinetics of the exchange reaction and the present paper describes such a study with carefully prepared materials. A cation exchange reaction such as

$$XR + Y^+ = YR + X^+,$$

may be regarded as taking place through a number of steps;

(1) Film diffusion of Y ions through the solution up to the surface of the exchanger particle,
(2) diffusion of Y^+ ions to an exchange site XR within the particle,
(3) Chemical exchange between Y^+ and XR,
(4) diffusion of X^+ ions in the solid to the surface, and
(5) film diffusion of X^+ ions through the solution away from the particle.

The kinetics of the exchange will be governed by the slowest step in the process. CONWAY *et al.*[5] have shown that if (1) and (5) were rate controlling, the rate of exchange would be dependent upon stirring characteristics and upon the concentration of Y^+ ions in the solution. For particle diffusion (2) and (4) on the other hand, the rate should be independent of these factors but vary with particle size. A chemically controlled process would have a rate independent of particle size.

[1] C. B. AMPHLETT, *Proceedings of the Second International Conference on the Peaceful uses of Atomic Energy, Geneva*, (1958), vol. 28, p. 17 United Nations.
[2] C. B. AMPHLETT, L. A. MCDONALD and M. J. REDMAN, *J. Inorg. Nucl. Chem.* **6**, 220, 236 (1958).
[3] K. A. KRAUS, H. O. PHILLIPS, T. A. CARLSON and J. S. JOHNSON, *Proceedings of the Second International Conference on Peaceful uses of Atomic Energy, Geneva*, 1958, vol. 28, p. 3 United Nations.
[4] K. A. KRAUS and H. O. PHILLIPS, *J. Amer. Chem. Soc.* **78**, 249, 694 (1956).
[5] D. E. CONWAY, J. H. S. GREEN and D. REICHENBERG, *Trans. Faraday Soc.* **50**, 511 (1954).

Much work on the kinetics of ion exchange with organic resins e.g. references (5) and (6) has shown that diffusion through a solution film at the particle surface is the rate-controlling mechanism in very dilute solutions, whilst diffusion within the solid particles operates at higher concentrations. Preliminary results of AMPHLETT[2] on the effect of stirring rate and particle size on exchange rates in zirconium phosphate indicate a similar behaviour.

EXPERIMENTAL

Preparation of thoria

Thoria was precipitated by the slow addition of 0·5 M ammonium hydroxide to a well-stirred solution of 0·5 M thorium nitrate maintained at 70°. The gel was digested for several days at the same temperature to remove any excess ammonium hydroxide and to allow desorption of trapped ions. After washing and air drying at 50°, the glassy product was allowed to break down in water, air dried, and sieved to the required particle size. The product showed a well defined X-ray powder photograph indicating crystallinity. Two batches were prepared, *A* and *B*. Batch *B* was digested for a considerably longer period and showed evidence of greater crystallinity.

The complete conversion of thoria into the hydrogen form was made difficult by its amphoteric exchange properties, the normal treatment with mineral acid producing the corresponding anionic form. The method used was to wash in a column with distilled water for prolonged periods, the hydrogen form being produced by a hydrolytic reaction; batches *A* and *B* were prepared in this way. In addition, the hydrogen form of batch *B* was made by

(i) treating with hydrochloric acid and washing free from acid with distilled water (Batch B_2);

(ii) shaking an aqueous suspension for several days with a mixture of the organic ion exchange resins Amberlite IRA 400 in the hydroxyl form and Amberlite IR 120 in the hydrogen form. The organic resins, removed subsequently by flotation, were shown to replace quantitatively by OH^- and H^+ ions any anion or cation held by the thoria. (Batch B_3)

Preparation of zirconium phosphate

LARSEN *et al.*[7] describe the preparation of a well defined crystalline phosphate, diphosphatozirconic acid and a similar method was used. The product formed by the slow addition of 10 per cent v/v sulphuric acid solutions containing stoicheiometric proportions of zirconyl chloride and orthophosphoric acid to 10 per cent sulphuric acid at 75° was digested for several days, washed thoroughly, and dried in an air oven at 50°. Crystallinity was confirmed by microscopic examination and by X-ray powder photographs. Since the particle size was less than 200 B.S.S., far too small for normal column operation and the uses envisaged, the powder was compressed into pills under a pressure of about 5000 lb/in², allowed to break down in water for several days, air dried, and sieved as required. The resulting material of various particle sizes was very stable in water and showed no breakdown after several days in a stirred solution or prolonged immersion in boiling water. Likewise, there was no evidence of breakdown at the end of extensive exchange studies. Before use, the exchanger was transferred to columns and washed for several days with distilled water to remove any chloride or sulphate ions adsorbed during precipitation.

Analysis of the zirconium phosphate was made by dissolving in an alkaline solution of sodium peroxide at 0–10° and digesting at 70°, whereupon zirconia was precipitated. It was filtered and washed with ammonium hydroxide to convert into the ammonium form, which, when ignited to constant weight at 1000°, lost ammonia and yielded pure anhydrous zirconia. This precaution was not taken by LARSEN *et al.* Phosphate was determined by precipitation as ammonium phosphomolybdate, which was ignited at 500° and weighed as the anhydride. Trace amounts of phosphate in solution were determined as molybdovanadophosphoric acid using the spectrophotometric method of MICHELSON.[8]

Thermobalance studies

Weight loss characteristics of both exchangers, of importance in deciding upon drying temperatures, were studied in an automatic Stanton thermobalance over a temperature range 20° to 800°.

[6] T. R. E. KRESSMAN and J. A. KITCHENER, *Discuss. Faraday Soc.* **7**, 90 (1949).
[7] E. M. LARSEN, W. C. FERNELIUS and L. L. QUILL, *Industr. Engng. Chem.* **15**, 512 (1943).
[8] O. B. MICHELSON, *Analyt. Chem.* **29**, 60 (1957).

Confirmation that equilibrium conditions were maintained during the experiments was obtained by heating a number of separate samples to constant weight at various temperatures.

Particle sizes

A knowledge of the ratio of the radii of the exchanger particles was necessary for the interpretation of the dependence of the rate of exchange upon particle size. An optical microscope was used to measure 100 particle diameters of each sample and the average taken. In view of the non-uniform nature of the particles of many of the samples, it was thought desirable to use an independent estimate of the effective areas. The method used was similar to that of KOLTHOFF and O'BRIEN.[9] Weighed samples of exchanger were equilibrium with solutions of a dyestuff, Brilliant Cresyl Blue, having a pK value well outside the range of pH likely to be encountered. Concentrations of dyestuff were determined spectrophotometrically at 630 mμ after verifying Beer's Law. The ratio of the surface areas per gramme solid was obtained from the amounts adsorbed.

Rates of exchange

(i) *Limited bath experiments.* In batch experiments using thoria, 0·1 g samples of exchanger were added to 30 or 50 ml of 0·01 N NaOH solution containing 0·01 N, 0·1N or 1·0 N NaCl, and shaken mechanically in a thermostat at 25°. The procedure was similar to that of CONWAY *et al.*[5] and the amount of NaOH used was in all cases larger than the ion exchange capacity of the thoria sample. After a given time, the amount of exchange was determined by titrating portions of supernatant liquid against standard 0·01 N hydrochloric acid. For periods shorter than about 5 min, the technique described by AMPHLETT[2] was used. Reaction was carried out in a sintered-glass funnel which could be connected to suction for rapid removal of solution samples for analysis, or to a slight air pressure to prevent drainage.

Rates of exchange at 25° were also followed potentiometrically using the cell

Glass electrode	Solution under study	Sat. KCl	Calomel electrode

incorporating an efficient stirrer. E.m.f. measurements were made with a Pye potentiometer and Vibron electrometer (E.I.L. model 33B) as a null indicator. Electrode systems were standardised with 0·05 M potassium hydrogen phthalate, pH = 4·005,[10] B.D.H. tabloid phosphate buffer, pH = 6·99, and 0·05 M sodium borate, pH = 9·18 at 25°.[10] In thoria experiments, the cell incorporated a device for the rapid addition of 0·5 g samples of exchanger slurried with 5 ml of distilled water to the sodium hydroxide/chloride mixture. Nitrogen was bubbled through the solution during an experiment. "Alki" glass electrodes showed a small but reproducible drift in e.m.f. at the high pH's studied, and corrections derived from blank experiments were applied where appropriate.

In experiments with zirconium phosphate, a stronger acid exchanger, 0·5 g samples were added to carbonate-free water in the cell, and after an initial rapid fall in e.m.f. due to hydrolysis the reading became steady. Sodium chloride solution was added from a fast delivery pipette and the change in e.m.f. with time noted. With the smaller-sized fraction the rate of change of e.m.f. was too fast for manual operation and was recorded by rapidly photographing Vibron and time scales.

(ii) *Infinite bath experiments.* A number of caesium–potassium experiments were made using a shallow-bed method similar to that described by BOYD *et al.*[11] A 50 or 100 mg sample of exchanger was introduced into a small glass cell of 6 mm diameter, covered at each end with 200 B.S.S. nylon gauze. The cell was connected to three reservoirs by Quickfit joints, any of which could be selected by three-way taps. After flushing with distilled water to remove air bubbles, the exchanger was conditioned by passing an inactive solution consisting of 5×10^{-5} M CsCl + 0·1 M KCl through it for 3 hr. After this pre-treatment a solution of the same bulk concentration but containing ^{137}Cs as tracer was forced through the shallow exchanger bed for a pre-determined time followed immediately by a water wash. The exchanger was then flushed from the cell, filtered, and dried with acetone before placing on a counting planchette. No activity was removed from the exchanger during these operations. The amount of ^{137}Cs in the solid was obtained by standard counting techniques using an

[9] I. M. KOLTHOFF and A. S. O'BRIEN, *J. Amer. Chem. Soc.* **61**, 3409 (1939).
[10] Brit. Stand., 1647 (1950).
[11] G. E. BOYD, A. W. ADAMSON and L. S. MYERS, *J. Amer. Chem. Soc.* **69**, 2836 (1947).

VOL. 22 1961

I.D.L. scaler (type 1700). Uniform distribution of solid on the planchettes reduced self absorption errors which were, however, considered to be negligible since even the poorest deliberate distribution of sample resulted in a counting loss of less than 5 per cent.

RESULTS AND DISCUSSION

Thermobalance studies on thoria showed four distinct regions in the weight loss curve shown in Fig. 1 (curve i), (a) probably corresponds to the loss of surface and interstitially adsorbed water, (b) and (c) may be due to the loss of chemically bound

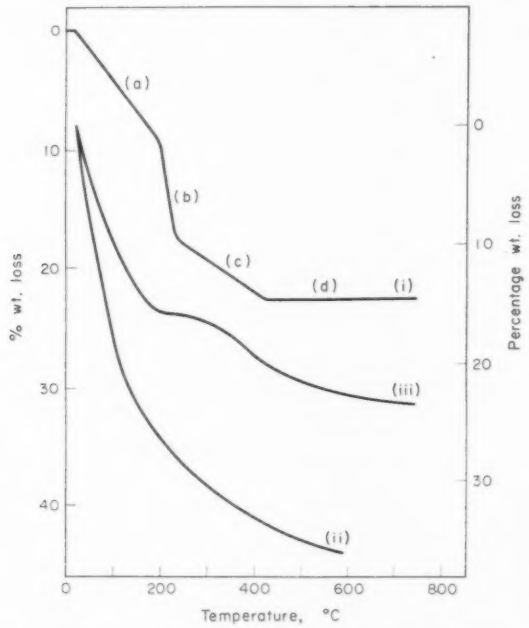

FIG. 1.—Per cent weight-loss curves. Curve (i) thoria (left-hand ordinates). Curve (ii) and (iii) zirconia and zirconium phosphate respectively (right-hand ordinates).

water molecules and (d) is the equilibrium value of the anhydrous material. It is interesting to compare these results with those of SIMON and FISCHER[12] who, using hydrated zirconia, found no discontinuities in the vapour pressure-temperature curves and concluded that it contained no chemically bound water molecules. A similar result has been obtained in this work in a thermobalance study of hydrated zirconia [Fig. 1 curve (ii)]. The curve for zirconium phosphate (curve iii) showed a steady weight loss up to 200° probably corresponding to the loss of interstitial water, followed by a plateau from 200 to 300° and a further slow loss up to the temperature limit of the thermobalance. The second weight loss is due to chemical rearrangement of phosphate to pyrophosphate.

Analysis of a zirconium phosphate sample which had been used extensively in rate experiments and column washed with about 10 l. of water, gave a ratio $PO_4/Zr = 1{\cdot}86$. In a freshly prepared sample the ratio was 1·88, confirming reproducibility of the method of preparation. The small difference corresponds to hydrolytic release of phosphate which was detected by trace analysis.

[12] A. SIMON and O. FISCHER, *Z. anorg. Chem.* **185**, 130 (1929).

pH titration curves obtained by batch equilibration showed only one inflexion indicating monofunctionality of exchange. This contrasts the behaviour of the gel zirconium phosphate of AMPHLETT[2] which possesses several dissociable hydrogen atoms. In view of the greater phosphate release at higher pH, however, the interpretation of such curves is rather uncertain.[13]

Thoria rate experiments

Data for two particle sizes, 60–100 B.S.S. and 160–200 B.S.S. are given in Table 1 in which subscripts T and P refer to titration and potentiometric experiments respectively. Within experimental error, both B_1 and B_2 showed the same exchange

TABLE 1.—SODIUM–HYDROGEN EXCHANGE ON HYDRATED THORIA
0·01 M SODIUM HYDROXIDE, 0·1 AND 1·0 M SODIUM CHLORIDE

Experiment number	Batch	Sodium chloride (Molar)	Particle size			B (min^{-1})	$D_i \times 10^8$ cm^2/sec.
			Sieve (B.S.S.)	Mean diameter (μ)	Radius from dye (Arbitrary)		
1_T	A	1·00	60–100	250	1·84	0·17	4·4
2_T	A	0·10	60–100	250	1·84	0·17	4·4
5_P	A	0·10	60–100	250	1·84	0·17	4·4
3_T	A	0·10	160–200	134	1·00	0·51	4·9
4_T	A	1·0	160–200	134	1·00	0·51	4·9
14_T	B_1	0·01	60–100	250	1·84	0·58	15·3
12_T	B_1	0·10	60–100	250	1·84	0·58	15·3
15_T	B_1	0·01	60–100	250	1·84	0·58	15·3
11_T	B_3	0·10	60–100	250	1·84	0·12	3·2

rates but B_3, the sample prepared by equilibrating with organic resins, appeared to be considerably slower. On washing with acid, however, its original rate of exchange was regained. It is not easy to explain the reason for this slow rate, but it may be partly due to adsorption of organic material on the surface of the particles, although the concentration of such material must be very small.

The extent of reaction, F, is expressed as[5]

$$F = \frac{\text{The amount of exchange at time } t}{\text{the amount of exchange at infinite time}}$$

and F is plotted against time in Figs. 2 and 3. It is seen that there is good agreement between titration and potentiometric results and the rate is, within experimental error, independent of sodium ion concentration between 0·01 M and 1·0 M, and markedly dependent upon particle size. Different methods of agitation, rotary stirring in the potentiometric experiments and mechanical shaking in titration experiments, were without effect on the rate of exchange. All this evidence points to particle diffusion being the rate-controlling mechanism and, following CONWAY *et al.*[5] we may apply

[13] E. M. LARSEN and D. R. VISSERS, *J. Phys. Chem.* **64**, 1732 (1960).

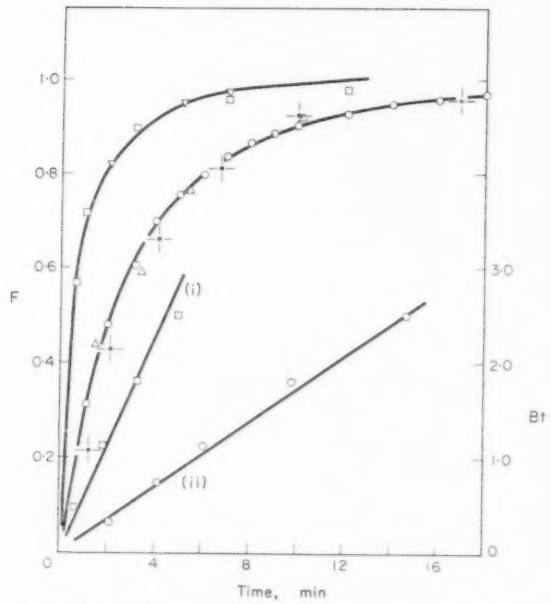

FIG. 2.—Plots of F and Bt against time for sodium–hydrogen exchange on thoria. ⊙, Expt. 5_P; △, 1_T; —•—, 2_T; ⊡, 3_T; ▽, 4_T. Curve (i) refers to upper F plot and (ii) to the lower.

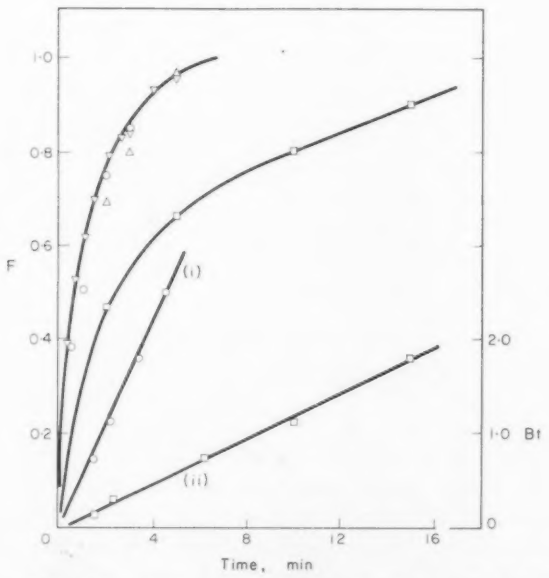

FIG. 3.—Plots of F and Bt against time for sodium–hydrogen exchange on thoria. ⊡, expt. 11_T; ⊙, 14_T; △, 12_T; ▽, 15_P. Curve (i) refers to upper F plot and (ii) to the lower.

the theory of BOYD *et al.*[11] describing diffusion into spherical particles of radius r by the expression

$$F = 1 - \frac{6}{\pi^2} \sum_{n=1}^{\infty} \frac{\exp(-n^2 Bt)}{n^2} \tag{1}$$

where

$$B = \pi^2 D_i / r^2 \tag{2}$$

D_i is the effective diffusion coefficient of sodium and hydrogen ions within the exchanger. F is a calculable mathematical function of Bt and to check equation (2) it is most convenient to obtain Bt for each F value from REICHENBERG's tables of Bt and F,[14] and to plot against the experimental time. Provided D_i is independent of F, the result should be a straight line of slope B and passing through the origin. Table 1 summarizes the results of the experiments and good linear Bt–t plots are shown in Figs. 2 and 3. Equation (2) confirms that for particle diffusion, F is dependent only upon D_i/r^2 and is independent of the concentration of ingoing ions.

VOL. 22 1961

The mean radius of the particles, measured optically, was 134 μ for the smaller-sized fraction and 250 μ for the larger-sized fraction. The ratio of the squares of the radii is thus 3·48, which agrees within experimental error with the inverse ratio of the B values, 3·10 as required by equation (2). Since many of the particles were irregular in shape, dye adsorption measurements were made in order to provide an independent value of the ratio of the surface areas. Assuming the particles to be spherical, the ratio of the squares of the radii was $3{\cdot}2 \pm 0{\cdot}2$, again in good agreement. Within experimental error, therefore, the proportionality of B to r^{-2} is confirmed and an effective diffusion coefficient can be calculated; the values are given in Table 1. It is seen that the diffusion coefficient for batch B is higher than for batch A. This reflects the difficulty of exactly reproducing a particular sample of exchanger and is probably due to the observed greater crystallinity of batch B.

The main criterion of infinite bath conditions for which equation (1) is strictly applicable is that the ionic composition of the surface of the exchanger should remain constant during a kinetic experiment, allowing diffusion of ions into the particle from a constant concentration of the surface.[15] In the present series of experiments these conditions prevail, since the hydrogen ions emerging from the exchanger after exchange by sodium ions are immediately neutralized by the excess hydroxyl ions. The exchange sites in the surface must therefore have been saturated with sodium ions throughout the experiment.

Zirconium phosphate rate experiments

Sodium–hydrogen experiments. This was followed by the e.m.f. method and the results for two particle sizes 60–100 and 160–200 B.S.S. are summarized in Table 2. Plots of F against time are given in Fig. 4. The very fast experiments with smaller-sized particles using the photographic technique for following the e.m.f. show somewhat greater scatter of points due to the larger experimental error. The rate of sodium–hydrogen exchange is again independent of stirring and of the concentration of sodium ions. Time plots of Bt in Fig. 3 agree very well at each ionic strength. The good linearity implies that the effective diffusion coefficient for this pair of ions remains

[14] D. REICHENBERG, *J. Amer. Chem. Soc.* **75**, 589 (1953).
[15] D. REICHENBERG, Private communication (1961).

TABLE 2.—SODIUM–HYDROGEN EXCHANGE ON ZIRCONIUM PHOSPHATE

Experiment number	Sodium chloride (Molar)	Particle size			B (min^{-1})
		Sieve (B.S.S.)	Mean diameter (μ)	Radius from dye (Arbitrary)	
17_P	0·01	60–100	360	1·9	2·6
18_P	0·10	60–100	360	1·9	2·6
24_P	0·10	160–200	119	1·0	6·7
25_P	0·01	160–200	119	1·0	6·7

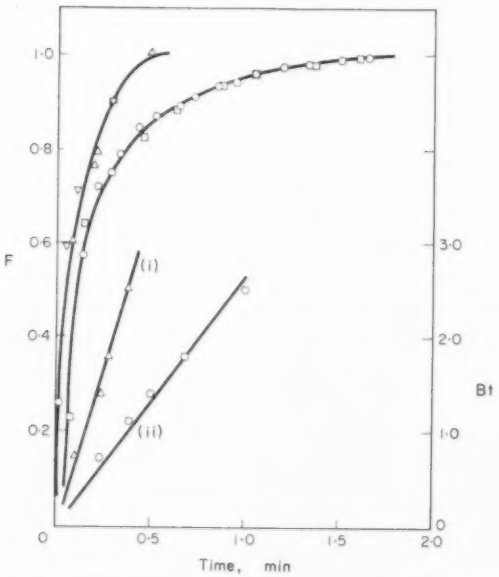

FIG. 4.—Plots of F and Bt against time for sodium–hydrogen exchange on zirconium phosphate. △, expt. 25_P; ▽, 24_P; ○, 17_P; □, 18_P. Curve (i) refers to upper F plot and (ii) to the lower.

TABLE 3.—CAESIUM–POTASSIUM EXCHANGE ON ZIRCONIUM PHOSPHATE

Infinite bath experiments. 5×10^{-5} M Caesium chloride + 0·1 M potassium chloride.

Experiment number	Sieve (B.S.S.)	Mean diameter (μ)	Radius from dye (Arbitrary)	$B \times 10^2$ (min^{-1})
27	60–100	360	1·9	1·8
28	60–100	119	1·9	7·5

constant over a range of exchanger composition. SOLDANO and BOYD[16] have shown this to be the case in a study of sodium–hydrogen exchange on Dowex 50. Self diffusion coefficients for sodium ions varied by only about 6 per cent over a range of hydrogen ion composition of the resin from 0 to 93 per cent.

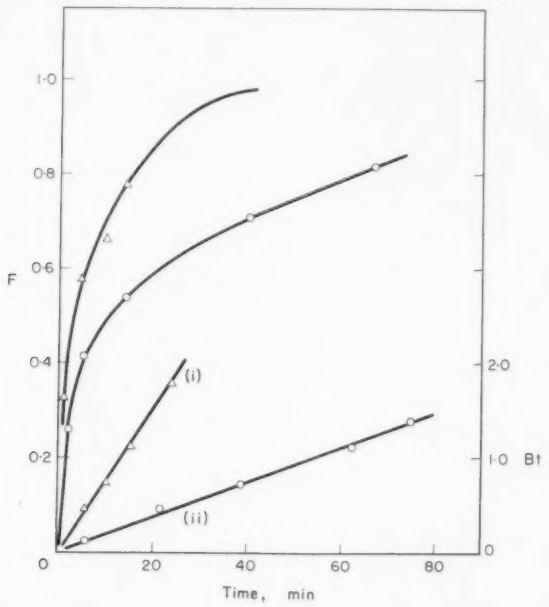

FIG. 5.—Plots of F and Bt against time for caesium–potassium exchange on zirconium phosphate. ○, expt. 27; △, expt. 28. Curve (i) refers to upper F plot and (ii) to the lower.

Results of Cs^+/K^+ exchange experiments on both particle sizes using the infinite bath techniques are given in Table 3. Time plots of F and Bt are given in Fig. 5. The latter show good linearity and provide further evidence that particle diffusion is the rate-controlling mechanism. Particle sizes, determined microscopically, are given in Table 3; the ratio of the squares of the apparent radii is 9. This differs widely from the inverse ratio of the B values which for Cs^+/K^+ exchange is 4 and for Na^+/H^+ exchange, c.a. 2·5. Each particle of exchanger produced by compression consists of a conglomeration of fine particles, the channels between which provide easy access to exchange sites. It is to be expected, therefore, that the rates of exchange interpreted on the basis of solid diffusion will be relatively faster in the larger-sized particles than in the smaller. This leads to the disagreement noted above. Dye adsorption measurements were made to obtain a more realistic ratio of surface areas. Assuming spherical particles, the ratio of the squares of the radii became 3·6, in very good agreement with the Cs^+/K^+ inverse ratio of B values. Poor agreement with the Na^+/H^+ value is probably due to the uncertainty in B for the smaller-sized fraction, with which the rate of exchange was very fast.

Throughout the present work, the main criteria of particle diffusion, i.e. a rate of exchange independent of the concentration of in-going ion and of stirring rate, are

[16] B. A. SOLDANO and G. E. BOYD, *J. Amer. Chem. Soc.* **75**, 6107 (1953).

closely followed. Errors due to hydrolysis become important at very low concentration and it has not been possible to reach the region observed with the organic ion exchange resins at which film diffusion is involved. The effective diffusion coefficient of 4–15 $\times$ 10^{-8} for Na^+/H^+ exchange on thoria may be compared with values from 10^{-6} to 10^{-5} cm^2/sec for sulphonic acid resins and 3·92 $\times$ 10^{-9} cm^2/sec for the weak acid exchanger Amberlite IRC 50.[5]

Acknowledgements—We thank Dr. C. B. Amphlett for many helpful discussions and the United Kingdom Atomic Energy Authority for an extra-mural contract in support of this work and for a maintenance grant to R. P.

J. Inorg. Nucl. Chem., 1961, Vol. 22, pp. 269 to 277. Pergamon Press Ltd. Printed in Northern Ireland

THE ADSORPTION OF MONOVALENT AND DIVALENT CATIONS BY DIALLYL PHOSPHATE AND STYRENE METHYLENE PHOSPHONATE POLYMERS

J. KENNEDY, J. MARRIOT and V. J. WHEELER
Atomic Energy Research Establishment, Harwell, Didcot, Berks.

(*Received* 2 *June* 1961)

Abstract—The adsorption of monovalent and alkaline earth cations by ionic phosphorylated resins has been investigated. Adsorption sequences under acidic conditions are Li < Na < K < Rb < Cs ≪ Ag and Sr < Ca ≪ Be, and with dibasic resins in alkaline media Na > K > Rb. The sequences for the alkali metal cations are in accord with those obtained by other investigators.

VOL. 22 1961

PREVIOUS investigations into the ion exchange properties of polymeric diallyl phosphate [HDAP = $(C_3H_5O)_2POOH$][1,2] indicated a marked selectivity for uranyl and beryllium ions, and the use of the sodium form of the resin (NaDAP) in conjunction with disodium EDTA presented methods of purifying these metals which at least on a laboratory scale have marked advantages over other ion exchange methods. Wells, in co-operation with workers at the National Chemical Laboratories, Teddington, and with the U.K. Atomic Energy Authority, has investigated ion adsorption by phosphorylated cellulose pulp—a polymer with a functionality which is mainly due to $PO(OH)_2$ groups—and has adapted it to the extraction of thorium from leach liquors on a pilot plant scale.[3,4] Using phosphorylated paper, the N.C.L. team have also effected a chromatographic separation of transitional elements.[5] Prior to their investigations, BREGMAN and MURATA[6,7] reported a reversal of the normal or "lyotropic" affinity sequence for the alkali metals with the difunctional phosphonic acid resin Nalcite X-219($-\underset{|}{CH}\cdot C_6H_4\ PO(OH)_2$[7]*) under alkaline conditions, and the normal order for the same resin under acidic conditions.

The high relative affinities of HDAP for Be^{2+} and UO_2^{2+} ions are in marked contrast to those of sulphonic acid resins, the affinities of which are lower for these ions than for most other polyvalent cations. These features, together with a behaviour parallel to that of the phosphorylated solvent analogues (e.g. butyl and octyl phosphoric acids) in the extraction of ions into a liquid organic phase,[8,9,10] suggest that adsorption by

* Prepared by reacting a styrene–8 per cent divinylbenzene copolymer with PCl_3 in presence of a Friedel-Crafts catalyst and subsequent oxidation of the product.[7b]

(1) J. KENNEDY, R. V. DAVIES, H. SMALL and B. K. ROBINSON, *J. Appl. Chem.* **9**, 32 (1959).
(2) J. KENNEDY and V. J. WHEELER, *Analyt. Chim. Acta* **20**, 412 (1959).
(3) A. J. HEAD, N. F. KEMBER, R. P. MILLER and R. A. WELLS, *J. Chem. Soc.* 3418).
(4) J. H. BUDDERY, W. D. JAMRACK and R. A. WELLS, *Chem. & Ind. (Rev.)* 235 (1959).
(5) N. F. KEMBER and R. A. WELLS, *Nature, Lond.* **175**, 512 (1955).
(6) J. I. BREGMAN and Y. MURATA, *J. Amer. Chem. Soc.* **74**, 1867 (1952).
(7) (a) J. I. BREGMAN, *Ann. N.Y. Acad. Sci.* **57**, 125 (1953); (b) Private communication (1961).
(8) C. A. BLAKE, C. F. BAES, K. B. BROWN, C. F. COLEMAN and J. C. WHITE, *Proceedings of the International Conference on the Peaceful Uses of Atomic Energy, Geneva*, 1958 15/P/1550 (1958).
(9) D. F. PEPPARD, G. W. MASON, W. J. DRISCOLL and S. MCCARTY, *J. Inorg. Nucl. Chem.* **12**, 141 (1959).
(10) D. DYRSSEN, *J. Inorg. Nucl. Chem.* **8**, 291 (1958).

polymeric phosphorylated resins occurs via complex or ion pair formation between the more highly charged cations and the functional groups ($PO\overline{O}$ and $PO\overline{O}_2$) rather than via coulombic attraction between the latter and hydrated cations as is generally the case with sulphonic acid resins.

It should be emphasized however that these conclusions with reference to HDAP for a number of polyvalent cations are based on qualitative or at most semi-quantitative experiments, and although there is no reason to doubt the affinity series $Th^{4+} > UO_2^{2+} >$ rare earths^{3+} [1] which can be demonstrated in column displacement tests, and which in any case is a normal behaviour for ligands possessing only oxygen donor atoms, much further work would be required to place this sequence on a quantitative basis.

The experimental difficulties involved in carrying out the necessary quantitative tests are in many cases far greater than those encountered in the case of the fully ionized conventional cation and anion exchangers. To quote an example, attainment of equilibrium between UO_2^{2+} and a given particle size of HDAP is extremely slow, and although a moderately large percentage uptake can be obtained after short contact periods in batch experiments in 0·1 N aqueous acid, and although the uptake does not increase appreciably when the contact time is extended to five weeks, a further large increase in distribution ratios is however experienced when the particle size is reduced.[11] In the case of UO_2^{2+} this slow attainment of equilibrium is due to a low rate of particle diffusion and probably also to the formation of a hydrophobic layer of UO_2-resin complex on the surface of the resin, though rates of chemical reaction may also be important in the case of other ions. Furthermore, by analogy with monomeric dialkyl phosphoric acids[8,9,10] the functional groups in HDAP may be associated thus:–

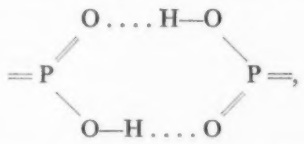

and the metal species M^{n+} in the resin phase at low loading may exist in the form $M(DAP)_n \cdot nHDAP$ rather than as $M(DAP)_n$. Finally, where the displacing cation is much more strongly adsorbed than that initially on the exchanger, large volume changes occur in the resin phase as the equivalent fraction N_M of the adsorbed metal is varied from 0 to 1. These features of HDAP and other phosphorylated resins would necessitate considerable additional experimentation in order to evaluate practical selectivity coefficients at high and even at trace loadings for equilibria involving certain cations (Th, UO_2^{2+}, Fe^{3+} etc.)

In contrast to UO_2^{2+} adsorption, it is found that equilibria between phosphorylated resins and the monovalent alkali metal cations and the divalent cations Ca^{2+} and Sr^{2+} (all of which are bound weakly relative to UO_2^{2+}) are rapidly established, and percentage uptake after a few hours' contact in batch experiments with a constant ratio of resin to solution is independent of contact time and of particle size. In view of the interest in separations of these cations a test of the efficiency of organic phosphorylated resins relative to other resins was desirable. If adsorption tests for these ions are carried out at trace equilibrium loading of the resin phase and at constant aqueous phase ionic strength, changes in the resin capacity and in its thermodynamic activity are negligible,

[11] J. KENNEDY, V. J. WHEELER and M. TOFT. Unpublished work.

and although uncertainties may still exist as to the nature of the adsorbed species it is unlikely that different modes of adsorption would prevail with ions of the same valency and same periodic group at loadings less than 2% of the resin capacity. If we represent exchange between a monovalent cation $A(R)^+$ in the resin phase and a monovalent ion P^+ in one case and a divalent ion Q^{2+} in another by the reactions.

$$P^+ + A(R)^+ \rightleftharpoons P(R)^+ + A^+ \quad (1)$$

$$\tfrac{1}{2}Q^{2+} + A(R)^+ \rightleftharpoons \tfrac{1}{2}Q(R)^{2+} + A^+ \quad (2)$$

and if the ion exchange process is considered as a Donnan membrane equilibrium,[12] then the practical affinity coefficient (k) for reaction (1) is

$$k_A{}^P = \frac{[P(R)][A]}{[P][A(R)]} = \frac{f_{A(R)} \cdot f_{PX}^2}{f_{P(R)} \cdot f_{AX}^2} \quad (3)$$

and for reaction (2)

$$k_A{}^Q = \frac{[Q(R)]^{\frac{1}{2}}[A]}{[Q]^{\frac{1}{2}}[A(R)]} = \frac{f_{A(R)} \cdot f_{QX}{}^{\frac{3}{2}}}{f_{Q(R)}^{\frac{1}{2}} \cdot f_{QX_2}^2} \quad (4)$$

Here f represents the molar activity coefficient and X is a permeable monovalent anion.

A preliminary account of some of the results in this publication has been given elsewhere.[13]

EXPERIMENTAL

Resins

HDAP was prepared in accordance with previous specifications[14] and ZeoKarb 225 was obtained from the Permutit Co. Ltd., London. Polystyrene–methylenephosphonic acid [H_2PMP,—$\underset{|}{CH}\cdot C_6H_4\cdot CH_2PO(OH)_2$] was also supplied by the Permutit Co., and is a hydrolytic product of the corresponding diethyl ester, which was obtained by an Arbuzov reaction[15] between triethyl phosphite [$(EtO)_3P$] and the chloromethylated product of a co-polymer of styrene and 1 per cent nominal divinyl benzene (1% DVB).[16]

Salt solutions

Solutions of inactive metal ions at concentrations $< 10^{-2}$ N were made up in standard solutions of perchloric acid, sodium perchlorate and potassium hydroxide, and except for Li, were spiked with radioactive isotopes (^{24}Na, ^{42}K, ^{86}Rb, ^{137}Cs, ^{110}Ag, ^{45}Ca, ^{89}Sr, ^{140}La, ^{91}Y and ^{7}Be obtained from the Radiochemical Centre, Amersham and/or the Isotope Division, A.E.R.E.) to give suitable counting rates in aliquots of the solutions taken for radiometric assay. With the exception of ^{7}Be and inactive Li, assay of the other solutions was carried out by liquid and/or solid (end window) β-counting. ^{7}Be was estimated using a γ-scintillation counter and Li by flame photometry. Perchlorate did not precipitate alkali metal cations at the concentrations used in these tests, and in instances where tests on Cs and Rb adsorption on HDAP and ZeoKarb 225 were carried out in the presence of HCl (0·1 and 0·001 N), distribution ratios did not differ significantly from those obtained in the presence of $HClO_4$ at the same concentrations, as would be expected from the relation $f_{ACl} \approx f_{AClO_4}$ (equation 3) at $\mu < 0{\cdot}1$.

Resin pretreatment and capacity determinations

Phosphorylated resins were recycled twice between 1 N NaOH, 1 N $HClO_4$ and water in that order and except for the use of 5 N $HClO_4$ pretreatment of ZeoKarb 225 was the same as for the phosphorylated resins. In the case of resins intended for equilibration with cations in $HClO_4$ solutions

[12] W. C. Bauman and J. Eichorn, *J. Amer. Chem. Soc.* **69**, 2830 (1947).
[13] J. Kennedy and V. J. Wheeler, *Chem. & Ind. (Rev.)* 1577 (1959).
[14] J. Kennedy, E. S. Lane and B. K. Robinson, *J. Appl. Chem.* **8**, 459 (1958).
[15] G. M. Kosolapoff, *Organophosphorus Compounds*, J. Wiley, New York (1950).
[16] J. R. Miller, CON/HAR 64, (1956); private communication (1956).

VOL. 22 1961

the resins (in acid form after recycling) were finally washed with standard $HClO_4$ of the same strength as that used in the equilibration tests. Batches of NaDAP and K_2PMP (obtained by treating the acid resins after recycling with excess NaOH and KOH) were similarly pretreated with standard $NaClO_4$ and KOH respectively. This stage of the pretreatment was essential, owing to appreciable changes in resin water contents with varying acidity and ionic strength (μ) of the equilibrating solutions, and also to prevent changes in μ due to loss of water from the resin phase. After pretreatment the resins were centrifuged to constant weight over porous glass filters in centrifuge tubes to remove the adhering solution[17,18] and the water content ($\simeq$ imbibed water) determined from the loss in weight of samples dried in vacuo at 60°C for two days. The water contents of the pretreated resins are therefore those of the latter in equilibrium with solutions used in the equilibration tests, and as the ion concentrations of the pretreating solutions were 0·1 N, errors in water content from residual acid or salt in the resin are negligible. Exchange capacities for pretreated resins were determined by washing a known weight of the moist pretreated resin (of known water content) with water to remove free acid, and then shaking overnight with excess standard alkali followed by filtration and acid titration of the filtrate using phenolphthalein. In the cases of NaDAP and K_2PMP pretreated samples of known weight and water content were converted to the acid forms and washed with water, and their capacities determined as before. A potentiometric titration curve for HDAP is given elsewhere,[14] and the Na/H exchange capacity of the batch under investigation was 4·64 milliequivalents (meq)/g of dry resin. A similar curve for H_2PMP was obtained by shaking eighteen accurately weighed samples of wet resin with varying quantities of 0·1 N NaOH in separate flasks for 24 hr, diluting to 100 ml, and measuring the pH of the solution. This "batch" titration method is necessary in the case of H_2PMP owing to the rather slow neutralization rate of the weakly acidic resin between its first and second inflection points, and the procedure is similar to that recommended elsewhere[19] for titration of carboxylic acid resins. Its exchange capacities at the equivalence points are 4·2 and ~8·2 meq/g.

Equilibration and distribution measurements

Resin samples of known total exchange capacity (0·5–1·0 meq), water content and mesh range ($\frac{1}{24}$–$\frac{1}{40}$ in.) were shaken for 12 hr with varying concentrations of salts in solutions of constant volume (50 ml), i.e. with a solution to solid ratio of >200 ml/dry g. To test if equilibrium had been attained, equal weights of the same resin of reduced particle size ($\frac{1}{80}$–$\frac{1}{100}$ in.) were contacted with the same solutions for much longer periods (~one week), and unless otherwise stated (see results) equilibria were found to be attained in <6 hr. The metal ion content of the resin after equilibration was estimated from the difference between the total initial and final concentrations of metal present in solution. In cases of low adsorption ($D < 50$), the activity of the resin was checked by eluting the adsorbed metal with acid after washing the resin with water, and determining the metal content of the acid eluent, and also in some cases by assaying the liquid residue remaining after wet oxidation of the resin with sulphuric and nitric acids. Distribution coefficients are defined as

$$D = \frac{\text{weight of cation in resin phase/dry g}}{\text{weight of cation in solution phase/ml}}$$

RESULTS

Table 1 gives distribution coefficients D for various resins and cations at trace resin loadings and trace aqueous phase concentrations (except in the case of zirconium phosphate) in solutions of stated ionic strength (μ), and a solution to dry resin ratio > 200 ml/g.

In addition to the values in Table 1 a value of $D = 205$ has been obtained for Ag^+ at trace loading on HDAP in 0·1N $HClO_4$. A value of 142 for Li at $6{\cdot}7 \times 10^{-5}$ N Li in 0·001 N $HClO_4$ would appear from Fig. 1 to be a limiting ratio. Values for Be^{2+} of > 4000 and 980 were obtained with HDAP and ZeoKarb 225 respectively at trace concentrations in 0·1 N $HClO_4$. Values of 21,280 and 3840 were obtained for Y^{3+} and

[17] K. W. PEPPER, *J. Appl. Chem.* **1**, 124 (1951).
[18] D. REICHENBERG and D. J. MCCAULEY, *J. Chem. Soc.* 2741 (1955).
[19] R. KUNIN, *Ion Exchange Resins*, (2nd Ed.) J. Wiley, New York (1958).

La^{3+} with HDAP in 0·1N $HClO_4$ after one week's contact using a mesh range of $\frac{1}{24}$–$\frac{1}{40}$ in., but these are not equilibrium values, as D increased to 29, 160 and 5400 respectively in the same contact period with a reduced particle size ($\frac{1}{80}$–$\frac{1}{100}$ in.). Apart from the latter results, those of Li and Be, and those with zirconium phosphate, the listed values are the averages of the experimental results for different aqueous phase concentrations of cation in the range where D is independent (mean deviation ± 6·0 per cent) of concentration (Figs. 1 and 2).

TABLE 1.—DISTRIBUTION COEFFICIENTS FOR VARIOUS RESINS AND MONOVALENT AND BIVALENT CATIONS

Resin	Capacity (meq/dry g)	DVB (%)	μ	H_2O in equilibrated resin (%)	D					
					Na^+	K^+	Rb^+	Cs^+	Ca^{2+}	Sr^{2+}
HDAP	4·64	0	0·001 N $HClO_4$	55·3	271	340	351	510		
			0·1 N $HClO_4$	34·0				4·6	61	26
NaDAP	3·95	0	0·001 N $NaClO_4$	81·0			4686	4780		
H_2PMP	8·2	1	0·001 N $HClO_4$	56·9	175		287	403		
			0·01 N $HClO_4$	48·0					1870	1287
K_2PMP	6·3	1	0·1 N KOH	80·0	79		49			
ZeoKarb 225 Commercial	5·06	ca. 8	0·1 N $HClO_4$	53·0	93	172	232	276	7250	8900
Zirconium Phosphate*	1·3	—	0·014 N Cl^-	—	36	84	182	200	56	63

* K_d values for zirconium phosphate are quoted from Amphlett *et al.*[20] and correspond to loading variations between 70 per cent in the case of Cs and 30 per cent in the case of Na. The initial aqueous phase concentrations were ~0·014 N in salt.

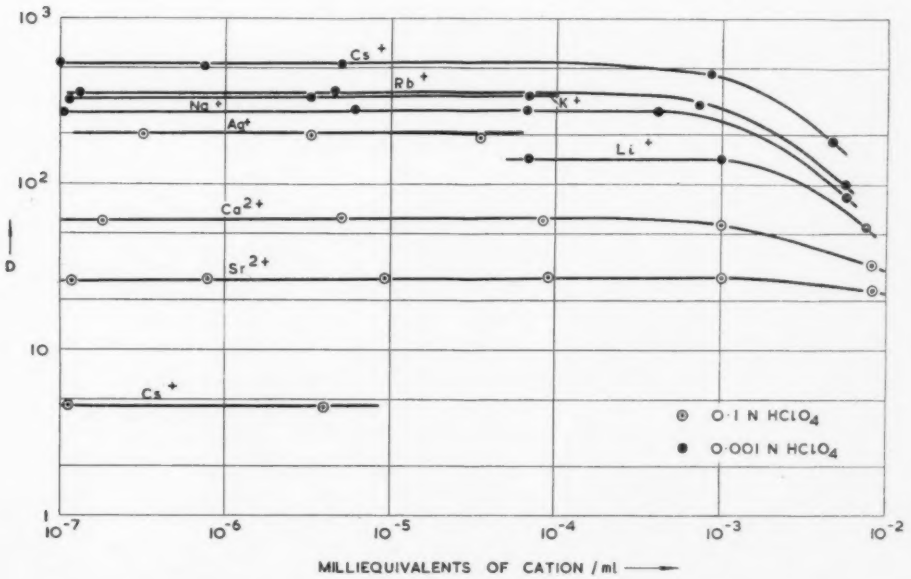

FIG. 1.—Adsorption of cations by HDAP from 0·1 N and 0·001 N $HClO_4$ as a function of concentration.

[20] C. B. AMPHLETT, L. A. MCDONALD and M. J. REDMAN, *J. Inorg. Nucl. Chem.* **6**, 220 (1958).

VOL. 22 1961

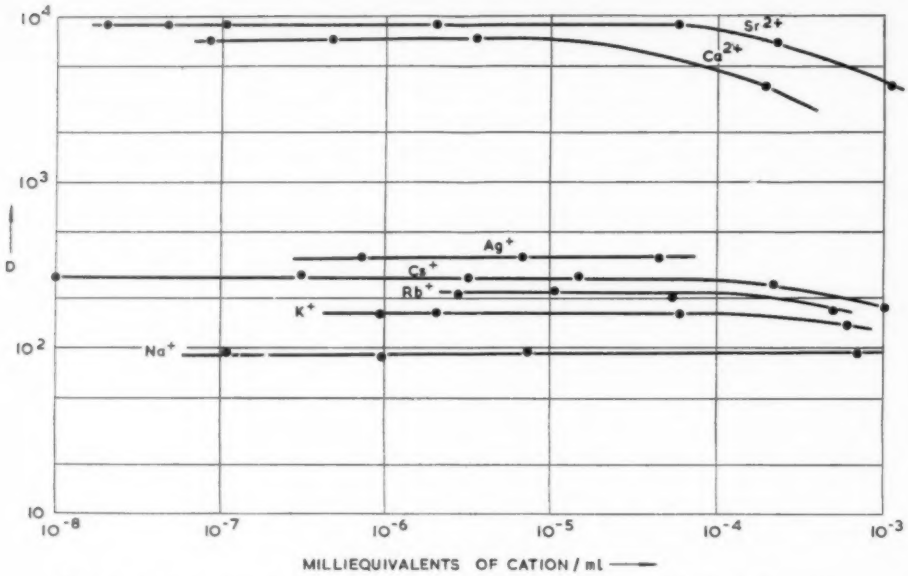

FIG. 2.—Adsorption of cations by ZeoKarb 225 from 0·1 N $HClO_4$ as a function of concentration.

DISCUSSION

From equations (3) and (4) the distribution coefficients are given by

$$D_P = \frac{P(R)}{[P]} = \frac{[A(R)]f_{A(R)} \cdot f_{PX}^{\ 2}}{[A] \cdot f_{P(R)} \cdot f_{AX}^{\ 2}} \tag{5}$$

and

$$D_Q = \frac{[Q(R)]}{[Q]} = \frac{[A(R)]^2 \cdot f_{A(R)}^{\ 2} \cdot f_{AX_2}^3}{[A]^2 \cdot f_{A(R)} \cdot f_{AX}^{\ 4}} \tag{6}$$

Values of D (Figs. 1 and 2) begin to decrease from a constant limit at metal ion solution concentrations $> 5 \times 10^{-5}$ N; as would be expected from (5) and (6) the lower the values, and therefore the lower the metal/resin loading ratios for a particular adsorption isotherm, the higher the aqueous phase concentration at which D begins to decrease. Furthermore, in cases where the initial acid ($HClO_4$) concentration is lower than or equal to the initial metal ion concentration, values of D in these regions will be affected by the appreciable increase in H^+ ion concentration at equilibrium. As both activity coefficient ratios and the value of [A] in the solution phase are either constant or may be estimated, any variation in D from a constant value (or from a predicted value based on mass action data in which only aqueous phase activities are considered) at relatively high loading will be a function both of [A(R)] and of the activity coefficient ratio of the resin cations as shown in equations (5) and (6).

In the case of the fully ionized sulphonic acid resins [A(R)] can be estimated by difference,[12,18,21] but the possibility of functional group association in HDAP polymer renders the resin concentration less than that based on its total acidic hydrogen content.

[21] T. R. E. KRESSMAN and J. A. KITCHENER, *J. Chem. Soc.* 1190 et seq. (1949); O. D. BONNER and L. L. SMITH, *J. Phys. Chem.* **61**, 326 (1957).

In addition HDAP is a relatively weak acid [pK_a of the monomeric analogue $(BuO)_2POOH = 1{\cdot}0$[22]] compared to sulphonic acids, and the ionic hydrogen [H(R) = A(R)] resulting from acidic dissociation is unknown, though from its neutralization curve [$pH_{\frac{1}{2}} \simeq 2{\cdot}2$[14]], its pK_a is probably $>1{\cdot}0$, as also values of pK_a for resins derived from acrylic acid are greater than that of the monomer.[19] At trace metal loadings however, and at constant aqueous phase acidity and ionic strength, all these quantitatively unknown attributes of the resins are constant.

As activity coefficient ratios in solution can be obtained either from data already available, or from experiments designed to obtain them, it is customary to define selectivity coefficients (K) in terms of equations that allow for these solution variables, i.e.

$$K_A^P = D_P \cdot \frac{[A] \cdot f_{AX}^2}{[A(R)] \cdot f_{PX}^2} = \frac{f_{A(R)}}{f_{P(R)}} \tag{7}$$

$$K_A^Q = D_Q \cdot \frac{[A]^2 \cdot f_{AX}^4}{[A(R)] \cdot f_{QX_2}^3} = \frac{f_{A(R)}^2}{f_{Q(R)}} \tag{8}$$

In the aqueous phase f_{PX} and f_{QX_2} for trace salt concentrations will be those of the pure salt solutions at the ionic strength of the mixed components (Harned Rule), and for $\mu < 0{\cdot}1$, $f_{AX}^2/f_{PX}^2 \simeq 1$. In the case of divalent cations at $\mu < 0{\cdot}1$, f_{AX}^4/f_{QX}^3, although not unity, will be approximately the same for the cations Ca^{2+} and Sr^{2+}. At trace concentrations and low ionic strength selectivity coefficients for cations of the same charge will therefore vary directly as their respective D values, and (as $f_{A(R)}$ is now constant) inversely with $f_{P(R)}$ and $f_{Q(R)}$. Taking the lowest selectivity coefficient in each sequence as standard (1·0), the relative selectivities for monovalent cation adsorption with HDAP in 0·001N $HClO_4$ are Li(1·0) < Na(1·81) < K(2·39) < Rb(2·47) < Cs(3·59), and Na(1·0) < Rb(1·19) < Cs(1·21) with NaDAP in 0·001N $NaClO_4$. Similarly the relative sequence for cation adsorption in HDAP in 0·1N $HClO_4$ is Sr(1·0) < Ca(2·31) < Be(> 154), and Cs(1·0) < Ag(44·6). In the case of H_2PMP in 0·001N $HClO_4$ the sequences are Na(1·0) < Rb(1·64) < Cs(2·3), and in 0·01N $HClO_4$ Sr(1·0) < Ca(1·45), and Rb(1·0) < K(1·27) < Na(1·58) for K_2PMP in 0·1N KOH. We have quoted ionic strengths in conjunction with relative sequences in these cases as [A(R]) and $f_{A(R)}$ would change appreciable with μ in the case of phosphorylated resins, as is evident from their water contents at different μ values (Table 1). Variations in acid strength were however desirable in order to obtain measurable distributions, but while the relative magnitudes of D may depend on μ, changes in the latter from 0·001 to 0·1 would hardly reverse the order of adsorption with these resins. In the case of ZeoKarb 225 the relative selectivity sequences are Na(1·0) < K(1·85) < Rb(2·5) < Cs(3·0) and Be(1·0) < Ca(7·4) < Sr(9·2). These relative sequences for sulphonated resins are well known from the work of others at higher resin loadings.[12,18,21,23]

From the ratios of the respective D values for different cations, relatively good separations may be expected with acidic phosphorylated resins. In the case of alkali metal separations however, any advantages in selectivities gained in separations with HDAP and H_2PMP compared to ZeoKarb 225 would be offset by their lower loadings under acidic conditions. Furthermore, while Cs/Rb separations with these resins appear to be slightly superior to that with zirconium phosphate, separations with the

[22] D. Dyrssen, *Acta Chem. Scand.*, **11**, 1277 (1957).
[23] G. E. Boyd, J. Schubert and A. W. Adamson, *J. Amer. Chem. Soc.* **69**, 2818 (1947).

VOL. 22 1961

latter as deduced from D ratios are those for high loadings and would be greater at trace ion concentrations where in fact $D_{Cs}/D_{Rb} \simeq 4$.[24] Better separations of silver can however be expected with HDAP than with zirconium phosphate[20] and sulphonated resins.[21]

The observation of BREGMAN that a dibasic phosphorylated resin gives the normal adsorption sequence for alkali metals under acidic conditions and the reversed sequence under alkaline conditions is confirmed. Russian workers[25,26] using the dibasic phosphorylated resin Cationite RF (a co-polymer of formaldehyde and resorcinol phosphoric acid) have also observed normal adsorption sequences for alkali cations under acidic eluting conditions, although their erroneous conclusion that this is not in accordance with Bregman's observations is probably due to them not having access to BREGMAN's full publications on the subject.[6,7] Although STEPHIN *et al.*[26] conducted experiments with Rb and K at pH 11·3 their results are difficult to interpret, due to the degradation of Cationite RF in alkaline media. Furthermore, unphosphorylated phenolic groups, if present in the resin, would also exchange to some extent at this pH. As in our experiments D and K values would vary as $1/f_{P(R)}$, the prevailing sequences with phosphorylated resins, including the reversal of the normal adsorption orders with Nalcite X-219[6] and K_2PMP under alkaline conditions, are in fact only to be expected from comparisons of the solution activity coefficient series for the monomeric salts, viz.

$$\gamma \pm KH_2PO_4 < \gamma \pm NaH_2PO_4 \text{ and } \gamma \pm K_2HPO_4 > \gamma \pm Na_2HPO_4.^{[27]}$$

The theory underlying cation exchange phenomena has been extensively discussed in recent years[18,21,23,28,29] and the subject has been critically assessed in recent review articles.[30,31,32] BREGMAN was however the first to point out[6,7] that the polarizability of the resin functional groups would have an important bearing on the order of adsorption of cations, and that the normal order with sulphonated resins and its reversal with carboxylated resins and with Nalcite X-219 under alkaline conditions was due to the polarizability sequence PO_2^{2-}, $COO^- > H_2O > SO^-_3$. On account of this, PO_2^{2-} and COO^- would displace H_2O from the cations, resulting in an adsorption sequence governed by the charge density of the unhydrated alkali cation. With more polarizing cations (H^+ and alkaline earths) the functional groups POO^- in HDAP and NaDAP and that from the first dissociation of H_2PMP (an analogue of Nalcite X-219) also interact more strongly than H_2O, implying a polarizability order $POO^- > H_2O$. On the other hand, the interaction sequence with the less polarizing alkali metal cations is $H_2O > POO^-$. The inability of POO^- to displace H_2O from alkali metal cations while displacing H_2O from H^+ parallels the interaction orders $H_2O > NH_3$ and $H_2O < NH_3$ respectively towards the same cations, which have been attributed[33] to

[24] C. B. AMPHLETT. Private communication (1961).
[25] N. K. SHCHIPAKINA, N. NEMIROVSKAYA and M. M. SENYAVIN, *Zhur. Anal. Khim.* **12**, 70 (1957).
[26] B. D. STEPIN, A. M. TARTAKOVSKAYA and V. E. PLYUSCHEV, *Russ. J. Inorg. Chem.* **5**, 781 (*Eng. Trans., Chem. Soc.*) (1960).
[27] G. SCATCHARD and P. C. BRECKENBRIDGE, *J. Phys. Chem.* **58**, 596 (1954).
[28] H. P. GREGOR, *J. Amer. Chem. Soc.* **70**, 1293 (1948); **73**, 643 (1951).
[29] E. GLUECKAUF, *Proc. Roy. Soc.*, **214** A, 207 (1952).
[30] J. A. KITCHENER, *Symposium on Ion Exchange and Its Application*, Society of Chemical Industry, London, 1955; J. A. KITCHENER, *Modern Aspects of Electro-Chemistry* No. 2, p. 87 (Edited by J. O'M. BOCKRIS), Butterworths (1959).
[31] C. B. AMPHLETT, *Metallur. Rev.* **1**, 419 (1956).
[32] D. REICHENBERG, *Chemische Technik*, **10**, 454 (1958).
[33] A. E. VAN ARKELL and J. H. DE BOER, *Rec. Trav. Chim.* **41**, 593 (1928).

the higher polarizability of NH_3 (refractivity = 5·6 cm^3) compared to water (3·7 cm^3) on the one hand, resulting in a higher induced dipole due to H^+ in NH_3 than in H_2O, the latter being displaced to form the solvation shell; on the other hand the high permanent dipole of H_2O ($1{\cdot}9 \times 10^{-18}$ c.s.u.) compared with NH_3 ($1{\cdot}5 \times 10^{-18}$ c.s.u.) results in greater interaction between H_2O and the slightly polarizing alkali metal cations. It is reasonable to assume that similar interaction forces are operative in cation exchange, although in the adsorption of polyvalent cations on weakly acidic resins chelate formation between metal and functional groups, and other factors operative in the coordination of metals, would also be important in determining affinity sequences.

Even in the case of sulphonic acid resins the normal adsorption order is reversed at high cross linking,[20,31] and reversals also occur with resins of moderate crosslinking (Dowex 50) under conditions of high ionic strength,[35] the effect in both cases being primarily due to the dehydration of the cations. It is interesting to speculate that the same primary cause, i.e. removal of solvating water (salting out) at high LiCl and HCl molarities may also contribute to the rather unexpected phenomenon of the high adsorption of the anionic species MCl_4^- by the cation exchanger Dowex 50,[36] in that the species $HMCl_4$ may under these conditions solvate as an oxonium salt (e.g. $RHSO_3{\cdot}HMCl_4$) with the sulphonic acid groups in the resin. It is probably on account of this mode of extraction that the resin selectivity is closely paralleled by the selectivity of ethers and other oxygenated compounds in the extraction of metal species under similar aqueous phase conditions.[37] At low aqueous acid concentrations trivalent lanthanides and actinides are adsorbed as the hydrated species by sulphonated resins, as can be inferred from the normal adsorption order. The "normal" sequence $Th^{4+} > U(IV) > Np(IV) > Pu(IV)$ has also been observed[38] for four-valent cations in 6N HCl, but as this would also be the order of increasing strength of the chloro-complexes, it would be interesting to determine the affinity sequences in more dilute acid, in view of the possibility of a reversal of this adsorption sequence due to the greater ion-pairing tendency of four-valent cations.

[34] H. P. Gregor and J. I. Bregman, *J. Coll. Sci.* **6**, 323 (1951).
[35] R. M. Diamond, *J. Amer. Chem. Soc.* **77**, 2981 (1955).
[36] K. A. Kraus, D. C. Michelson and F. Nelson, *J. Amer. Chem. Soc.* **81**, 3204 (1959).
[37] E. B. Sandell, *Colorimetric Determination of Trace Metals*, (2nd. Ed.), p. 34, Interscience New York (1950); G. H. Morrison and H. Freiser, *Solvent Extraction in Analytical Chemistry*. Wiley, New York (1957).
[38] R. M. Diamond, K. Street and G. T. Seaborg, *J. Amer. Chem. Soc.* **76**, 1468 (1954).

VOL. 22 1961

J. Inorg. Nucl. Chem., 1961, Vol. 22, pp. 279 to 284. Pergamon Press Ltd. Printed in Northern Ireland

POLAROGRAPHIC EVIDENCE FOR THE STABILITY OF COPPER(I) ION IN SOME NON-COMPLEXING NONAQUEOUS SOLVENTS

I. V. NELSON, R. C. LARSON and R. T. IWAMOTO
Department of Chemistry, University of Kansas, Lawrence, U.S.A.

(*Received* 16 *May* 1961)

Abstract—The polarographic behaviour of Cu(II) ion in methanol, ethanol, 1-propanol, 2-propnol, allyl alcohol, acetone, mesityl oxide, acetylacetone, acetic anhydride, nitromethane and pyridine is discussed. Stability of Cu(I) ion in a number of these solvents appears to be due to lower solvation energy of Cu(II) ion and not to higher solvation energy of Cu(I) ion than in water.

VOL. 22 1961

THE following potentials[1]*:

$$Cu^{2+} + 2e = Cu; \qquad E^\circ = +0{\cdot}095 \text{ V vs. S.C.E.}$$
$$Cu^{+} + e = Cu; \qquad E^\circ = +0{\cdot}279 \text{ V vs. S.C.E.}$$
$$Cu^{2+} + e = Cu^{+}; \qquad E^\circ = -0{\cdot}089 \text{ V vs. S.C.E.}$$
$$Cu^{2+} + 2e + Hg = Cu(Hg); \qquad E^\circ_a = +0{\cdot}035 \text{ V vs. S.C.E.}$$
$$Cu^{+} + e + Hg = Cu(Hg); \qquad E^\circ_a = +0{\cdot}146 \text{ V vs. S.C.E.}$$

account for the behaviour of *hydrated* copper ions in aqueous medium, i.e., *hydrated* cuprous ion is unstable, disproportionating into cupric ion and metallic copper, and *hydrated* cupric ion is polarographically reduced in one step to metallic copper. According to the potentials above, the polarographic reduction of cupric ion to cuprous should not take place until the potential of the electrode approaches −0·089 V vs. S.C.E. Because the potential to bring about reduction of hydrated cuprous ion, +0·146 V vs. S.C.E., is, however, more positive (easier for reduction to occur), *hydrated* cuprous ion is reduced immediately to metallic copper. Furthermore the small equilibrium concentration of cuprous ion shifts the potential necessary to bring about reduction of cupric ion to the more positive value +0·035 V vs. S.C.E. The polarographic $E_{\frac{1}{2}}$ value for the one two-electron step for the reduction of cupric ion is +0·03 V vs. S.C.E.

In the presence of complexing agents, such as Cl^- and NH_3, which form more stable complexes with Cu(I) ion than Cu(II) ion, the reduction potential for the Cu(I), Cu(Hg) couple is more negative than that for the Cu(II), Cu(I) couple, and the reduction of Cu(II) takes place in two one-electron steps.[2]

Polargraphic studies indicate that Cu(I) is stable in several nitrile solvents.[3–5]

* The saturated calomel reference electrode and normal calomel reference electrode are taken to have values of +0·242 V and +0·280 V, respectively, vs. the standard hydrogen electrode.

[1] W. M. LATIMER, *Oxidation Potentials*, (2nd Ed.) p. 185. Prentice-Hall New York (1952); J. J. LINGANE, *Electroanalytical Chemistry*, (2nd Ed.) p. 27. Interscience New York (1958); I. M. KOLTHOFF and J. J. LINGANE, *Polarography*, (2nd. Ed.) p. 227. Interscince New York (1952).

[2] G. THANHAUSER and G. MAASEN, Mitt. Kaiser-Wilhelm Inst. Eisenforsch. Disseldorf **19**, 27 (1937); G. MAASEN, *Angew. Chem.* **50**, 375 (1937); M. VORISKOVA, *Collection Czechslov. Chem. Communs.* **11**, 588 (1939); M. VON STACKELBERG and H. VON FREYHOLD, *Z. Elektrochem.* **46**, 120 (1940).

[3] I. M. KOLTHOFF and J. F. COETZEE, *J. Amer. Chem. Soc.* **79**, 870, 1825 (1957).

[4] A. I. POPOV and D. H. GESKE, *J. Amer. Chem. Soc.* **79**, 2074 (1957).

[5] R. C. LARSON and R. T. IWAMOTO, *J. Amer. Chem. Soc.* **82**, 3239, 3526 (1960).

KOLTHOFF and COETZEE[3] attribute this behaviour of copper to two factors: the relatively high solvation energy of the cuprous ion and the low solvation energy of the cupric ion. Examination of the potentials for the copper couples in acetonitrile,[3]

$$Cu^{2+} + e = Cu^{+};\ E_{\frac{1}{2}} = +1{\cdot}0\ V \text{ vs. S.C.E.}$$

$$Cu^{+} + e + Hg = Cu(Hg);\ E_{\frac{1}{2}} = -0{\cdot}36\ V \text{ vs. S.C.E.}$$

and the corresponding potentials in water indicates the relative contribution of these two factors to the stability of Cu(I) in acetonitrile. The potential shift of 0·51 V of $E_{Cu(I),Cu(Hg)}$ from $+0{\cdot}15\ V_{aq}$ to $-0{\cdot}36\ V_{aceto}$ must indeed be the result of Cu(I) being more highly solvated in acetonitrile (assuming that $E_{\frac{1}{2}}$ is approximately E°_{a} or E° and neglecting liquid–junction potential).* This means $E_{Cu(II),Cu(I)aceto}$ should mirror a similar shift of 0·51 V, from $-0{\cdot}09\ V_{aq}$ to $+0{\cdot}42\ V_{aceto}$ if the solvation energies of Cu(II) ion in water and in acetonitrile were similar. The more positive value of +1·0 V vs. S.C.E. in acetonitrile, however, indicates that this is not the case, but that the solvation energy for Cu(II) ion is lower in acetonitrile. It appears that both factors, higher solvation energy of Cu(I) ion and lower solvation energy of Cu(II) ion, contribute significantly to the stability of Cu(I) in acetonitrile. The potentials $E_{Cu(II),Cu(I)}$ +0·42 V (calc.) and $E_{Cu(I),Cu(Hg)}$ −0·36 V, however, indicate that the higher solvation energy of Cu(I) alone would be sufficient to stabilize Cu(I) in acetonitrile. The decrease in

* The first assumption is based on the following information:

$$E_{\frac{1}{2}}\ Cu(II),\ Cu(Hg) = +0{\cdot}03\ V \text{ vs. S.C.E.}$$

$$E^{\circ}_{a}\ Cu(II),\ Cu(Hg) = +0{\cdot}03\ V \text{ vs S.C.E.}$$

Assuming that solvent effects on the redox potential of the ferrocene-ferricinium ion couple are small and attributing the differences, therefore, in $E_{\frac{1}{2}}$ values to differences in liquid–junction potentials, we find from the data (unpublished) below that the uncertainty in the potential values reported for the copper couples in this article because of liquid junction effects when S.C.E. is the reference, except for pyridine, is ca. 0·1 V or less.

Solvents	(Ferricinium ion, Ferrocene)[a] $E_{\frac{1}{2}}$ 2 vs. S.C.E. (V)	Slope $\left(\frac{0{\cdot}059}{n}\right)$
Methanol	+0·37	0·065
Ethanol	+0·41	0·065
Acetylacetone	+0·35	0·100
1-Propanol	+0·42	0·050
2-Propanol	+0·44	0·058
Allyl Alcohol	+0·36	0·059
Acetone	+0·46	0·054
Mesityl Oxide	+0·45	0·062
Acetic Anhydride	+0·38	0·062
Pyridine	+0·50	0·083
Nitromethane	+0·31[b]	0·057
Acetonitrile	+0·35[a], +0·38[b]	0·056, 0·058

[a] 0·1 M $LiClO_4$ supporting electrolyte
[b] 0·1 M Et_4NClO_4 supporting electrolyte

$E_{\frac{1}{2}}$ vs. S.C.E. for the reduction of the large, slightly polarizable rubidium ion is −2·03 V, in water and −1·95 V in acetonitrile.[3] The 0·08 V difference is due to both lower solvation energy of rubidium ion in acetonitrile and difference in liquid–junction potentials between the solutions and the saturated calomel electrode. Difference in $E_{\frac{1}{2}}$ values in water and in acetonitrile due to liquid–junction effect, therefore, must be less than 0·08 V.

Interionic effects, expecially ion association, are important in solvents of low dielectric constant such as pyridine; it does not appear from our data, however, that in the solvents of dielectric constant 20 and larger that ion association breaks up the important primary solvation sphere of the copper ions.

solvation energy of Cu(II) ion from aqueous medium to acetonitrile being about as large as the increase in solvation energy of Cu(I), it appears that it too is sufficient by itself to stabilize Cu(I) in acetonitrile—$E_{Cu(II),Cu(I)}$ +0·49* V (calc.) and $E_{Cu(I),Cu(Hg)}$ +0·15 V. Increase in solvation energy of Cu(I), therefore, is not necessary for stabilizing Cu(I) in nonaqueous solvents provided there is an appreciable decrease in solvation energy of Cu(II). The results of the investigation reported here bear this out.

EXPERIMENTAL

The organic solvents were purified by treatment with appropriate reagents and fractional distillation:[6] Absolute methanol and absolute ethanol were treated with magnesium activated with iodine and fractionally distilled. Highest available purity 1-propanol was dried with anhydrous potassium carbonate, treated with magnesium activated by iodine, and fractionally distilled. Highest available purity 2-propanol, practical grade acetylacetone, technical grade mesityl oxide and highest available purity allyl alcohol were dried with anhydrous potassium carbonate and fractionally distilled after filtration from the potassium carbonate. Reagent grade acetone was treated with potassium permanganate, dried over anhydrous potassium carbonate and distilled from phosphorus pentoxide. Reagent grade acetic anhydride was fractionally distilled from anhydrous sodium acetate. Reagent grade pyridine was treated with a mixture of ceric sulphate and anhydrous potassium carbonate for 24 hr, filtered, refluxed over sodium hydroxide, and fractionally distilled. Highest available purity nitromethane was passed slowly through a column of activated alumina. The water content of the polarographic solutions (containing $LiClO_4$ supporting electrolyte) was determined by Karl Fischer titration to be ca. 5×10^{-3} M. Anhydrous lithium perchlorate and cupric perchlorate hexahydrate (G. Frederick Smith Chemical Co.) were dried in a vacuum oven at 60° and used without any pretreatment.

Polarograms were recorded with a Leeds and Northrup Type E Electrochemograph at 25°. An H-type cell was used; the dropping mercury electrode was placed in one side arm and a slowly bleeding, H-type, aqueous saturated calomel electrode in the other. Solutions were deoxygenated with purified nitrogen. Polarograms were corrected for the iR drop across the cell. An Industrial Instrument Co. Conductivity Bridge Model RC 16B2 was used to make the resistance measurements. Solutions were 1–0·1 millimolar in cupric perchlorate and 0·1 molar in lithium perchlorate.

RESULTS AND DISCUSSION

Table 1 summarizes the polarographic behaviour of Cu(II) in the solvents studied.

The slopes in Table 1 indicate that most of the polarographic waves are close to being reversible and that the Nernst expression can, therefore, be used in discussing the current–voltage curves.

The values of essentially one for $i_{d(1)}/i_{d(2)}$ and the close to 0·06 values, in most cases, for the slopes suggest that the two-step polarograms are the result of two-step electrochemical processes with each step involving one electron.

Although the solvation energies of Cu(II) and Cu(I) ions are lower in less basic methanol and ethanol than in water, that of Cu(II) ion, it appears, is still high enough that the reduction of Cu(I) ion remains easier than the reduction of Cu(II) to Cu(I). Consequently, the reduction of Cu(II) ion proceeds as it does in water, via a one two-electron step.

Acetylacetone forms a stable complex with Cu(II) ion.[7] With the resulting increase in solvation energy of the Cu(II) ion, one would expect the $E_{\frac{1}{2}}$ to be more

* Difference between observed $E_{\frac{1}{2}}$ value + 1·0 V for the Cu(II), Cu(I) couple and + 0·42 V, calculated by assuming no change in solvation energy of Cu(II), reflects the decrease in solvation energy of Cu(II) ion. This difference, 0·58 V, added to $E^{\circ}_{Cu(II),Cu(I)aq}$ −0·09 V gives +0·49 V.

[6] A. W. Weissberger and E. S. Proskauer, *Organic Solvents*, (2nd Ed.), Interscience, New York (1955). A. I. Vogel, *Practical Organic Chemistry*, (3rd Ed). Longmans, London (1956).

[7] M. Calvin and K. W. Wilson, *J. Amer. Chem. Soc.* **67**, 2003 (1945); **68**, 949 (1946).

VOL. 22 1961

negative than that in water. This effect, however, appears to be offset by a considerable decrease in the solvation energy of Cu(I) in acetylacetone, resulting in an $E_{\frac{1}{2}}$ value similar to those obtained in methanol and ethanol, although the increase and decrease in solvation energies of Cu(II) and Cu(I) ions, respectively, are probably considerably greater than in the two alcohols.

TABLE 1.—POLAROGRAPHIC DATA FOR Cu(II) IN NONAQUEOUS MEDIA

Solvent	$E_{\frac{1}{2}}$ *vs* S.C.E.[a,e] (*V*)	Slope $\left(\frac{0{\cdot}059 \text{ value}}{n}\right)$	$i_{d(1)}/i_{d(2)}$
Water	+0·03	0·037	
Methanol	+0·15	0·042	
Ethanol	+0·28	0·064	
Acetylacetone	+0·22	0·052	
1-Propanol	+0·39 (1st step)	0·059	1·00
	+0·25 (2nd step)	0·078	
2-Propanol	+0·46 (1st step)	0·082	0·94
	+0·25 (2nd step)	0·089	
Allyl alcohol	> +0·55[b] (1st step)	—	1·00
	−0·04 (2nd step)	0·079	
Acetone	+0·52 (1st step)	0·063	1·02
	+0·33 (2nd step)	0·065	
Mesityl oxide	+0·20 (1st step)	0·088	0·8
	−0·30 (2nd step)	0·105	
Acetic anhydride	ca. +0·51 (1st step)	[c]	ca. 0·9
	−0·16 (2nd step)	0·082	
Pyridine	> +0·1 [b](1st step)	—	0·88
	−0·64 (2nd step)	0·093	
Nitromethane	> +0·8 [b,d](1st step)	—	0·95
	+0·22 (2nd step)	0·068	

[a] 0·1 M $LiClO_4$ supporting electrolyte. [b] dissolution potential for Hg. [c] drawn-out wave [d] 0·1 M Et_4NClO_4 supporting electolyte. [e] Approximate corrections for differences in liquid-function potential may be made by using the data in footnote on page 3.

The $E_{\frac{1}{2}}$ values of +0·25 — +0·33 V for the reduction of Cu(I) ion in 1-propanol, 2-propanol, acetone and nitromethane and the E°_{a} value of +0·15 V for the Cu(I), Cu(Hg) couple in water indicate that the solvation energies of Cu(I) ion in these five solvents are nearly similar. The solvation energies of Cu(II) ion in the propanols acetone and nitromethane however, are so much less than in water that $E_{Cu(II),Cu(I)}$ shifts to a more positive value than $E_{Cu(I),Cu(Hg)}$ in the four nonaqueous solvents. The result is the observed two-step reduction of Cu(II) in these solvents which indicates that Cu(I) ion is stable with respect to disproportionation in these four solvents. The potentials for the two copper couples are not in the reverse order as they are in water.

The > +0·8 V value for $E_{\frac{1}{2}Cu(II),Cu(I)}$ in nitromethane indicates that Cu(II) ion is very poorly solvated. This is not surprising in view of the structural features of the solvent. Because of the poor solvating power of nitromethane, addition of water resulted, through highly selective solvation of Cu(II) ion by water, in a large increase in the solvation energy of the Cu(II) ion. The $E_{\frac{1}{2}}$ of the Cu(II), Cu(I) couple was > +0·8 V with 2×10^{-3} and 2×10^{-2} M water, +0·68 V with 2×10^{-1} M water, +0·56 V with 0·5 M water, and +0·38 V with ca. 1 M water. Comparison of these values with those reported by KOLTHOFF and COETZEE for the effect of water on the $E_{\frac{1}{2}}$ value for

the Cu(II), Cu(I) couple in acetonitrile, +1·0 V in water-free acetonitrile and +0·8 V with 4 per cent water (ca. 2 M), furnishes a good indication of the poor solvating ability of nitromethane. It is interesting to note that $E_{\frac{1}{2}}$ of the Cu(I), Cu(Hg) couple in nitromethane was hardly affected by addition of water; in ca. 1 M water it was +0·21 V. This fact lends support to our suggestion that the solvation energies of Cu(I) ion in the propanols, acetone, and nitromethane are not much different from that for Cu(I) ion in water.

Mesityl oxide with the carbonyl group in conjugation with the carbon–carbon double bond is expected to be more basic than acetone. The more negative $E_{\frac{1}{2}}$ values, +0·20 V and −0·30 V, therefore, are not unexpected. In order to obtain well-defined polarograms of Cu(II) in mesityl oxide, it was found necessary either to heat the solution or let it stand for ca. six days. The poor value for $i_{d(1)}/i_{d(2)}$ is undoubtedly associated with this difficulty.

The more negative potential for the Cu(I), Cu(Hg) couple in allyl alcohol than in 1-propanol, −0·04 V compared to +0·25 V, is in accord with the fact that Cu(I) ion forms a 1:1 complex with allyl alcohol.[8] In addition to shifting the potential of the Cu(I), Cu(Hg) couple more negative, the increase in solvation energy of Cu(I) ion, resulting from Cu(I) ion coordinating with the double bond, shifts the potential of the Cu(II), Cu(I) couple more positive. If the solvation energies of Cu(II) ion in both solvents are assumed to be the same, $E_{Cu(II),Cu(I)}$ in allyl alcohol should be +0·68 V, 0·29 V more positive than the value +0·39 V in 1-propanol.* Because $E_{Cu(II),Cu(I)}$ is more positive than +0·55 V, it appears that the solvation energy of Cu(II) ion in allyl alcohol is not much greater than in 1-propanol if it is at all. The same type of interaction between Cu(I) ion and the double bond could also account for the behaviour of Cu(I) ion in mesityl oxide; however, it appears unlikely from two standpoints: (1) the presence of the conjugated C=O group decreases the electron density of the double bond and, therefore, coordination at the double bond, (2) the presence of the two methyl groups at the β-position presents a steric barrier to co-ordination.

The more negative value of −0·16 V for $E_{Cu(I),Cu(Hg)}$ and the more negative than expected value of +0·51 V for $E_{Cu(II),Cu(I)}$ in acetic anhydride in comparison with the $E_{\frac{1}{2}}$'s in acetone suggest that copper (II) and (I), ions are, in line with the structural difference between the solvents, somewhat more strongly solvated in acetic anhydride than in acetone.

The $E_{\frac{1}{2}}$ for the reduction of Cu(I) ion in pyridine suggests very high solvation energy for Cu(I) ion in pyridine. The value is somewhat surprising in that when compared to the $E_{\frac{1}{2}}$ of −0·14 V vs. S.C.E. reported by LAITINEN and SHOEMAKER[9] for Cu(I) reduction in liquid ammonia, it indicates that Cu(I) ion has a much higher solvation energy in pyridine than in liquid ammonia. Part of this increase in solvation energy could be due to more pronounced interionic effects in this low dielectric constant medium.

The explanation offered for the stability of Cu(I) ion in 1-propanol, 2-propanol, acetone and nitromethane is substantiated by the fact that nitromethane solutions of Cu(I) ion can be prepared by (1) reduction of Cu(II) ion (cupric perchlorate) with copper foil and (2) anodic dissolution of metallic copper. Cu(I) solutions prepared as

* 0·29 V reflects the difference in the solvation energies of Cu(I) ion in allyl alcohol and 1-propanol.

[8] R. M. KEEFER, L. J. ANDREWS and R. E. KEPNER, *J. Amer. Chem. Soc.* **71**, 3906 (1949).
[9] H. A. LAITINEN and C. E. SHOEMAKER, *J. Amer. Chem. Soc.* **72**, 4975 (1950).

VOL. 22 1961

described above gave one-step polarograms with $E_{\frac{1}{2}}$ values of 0·22 V vs. S.C.E. and slopes of 0·059–0·063. Even after several days of standing, these solutions showed no indication (polarographic) of the presence of Cu(II) ion.

In summary it can be said (1) that the behaviour of copper ions is indeed sensitive to the nature of the solvent, (2) that the Cu(I) ion is stable with respect to disproportionation in the following non-complexing solvents: 1-propanol, 2-propanol, acetone, and nitromethane, and (3) that nonaqueous solvents can be used to bring about changes in the behaviour of copper ions which are, at present, being secured by complex formation.

Acknowledgement—The authors gratefully acknowledge the financial support from the American Chemical Society—Petroleum Research Fund (Grant No. 662-A) and the University of Kansas—General Research Fund which made this study possible.

J. Inorg. Nucl. Chem., 1961, Vol. 22, pp. 285 to 291. Pergamon Press Ltd. Printed in Northern Ireland

MOLECULAR WEIGHT STUDIES OF SEVERAL ORGANOPHOSPHORUS ACIDS*

J. R. FERRARO, G. W. MASON and D. F. PEPPARD
Argonne National Laboratory, Argonne, Illinois

(*Received* 14 *June* 1961)

Abstract—Molecular weight studies of several organophosphorus acids of the types $(GO)_2PO(OH)$, $(GO)G'PO(OH)$ and $(GO)PO(OH)_2$ have been made in several solvents, using an isothermal distillation method. In general, the monobasic acids are dimers in solvents such as n-hexane, cyclohexane, benzene and carbon tetrachloride; monomers in methyl alcohol; and intermediate in chloroform and acetone. Mono-(2-ethylhexyl)phosphoric acid is highly polymeric in n-hexane and cyclohexane, the molecular weight being 8–14·5 times the formula weight; hexameric in benzene and carbon tetrachloride; dimeric in acetone; and monomeric in methyl alcohol. The change in state of aggregation, for both the mono and dibasic acids, as the diluent is varied, parallels the predicted variation in solute–solvent interaction.

VOL. 22 1961

A VARIETY of organophosphorus acids have become important in solvent extraction, and several lanthanide and actinide separation flow-sheets are based upon systems consisting of these extractants in a carrier diluent vs. an aqueous mineral acid phase.[1,2] These extractants are generally used in a diluent and it is of interest to know their states of aggregation in these diluents. Cryoscopic measurements are impossible in many of these instances, therefore the SIGNER[3,4] method of determining molecular weights was used. This method offers the advantage that molecular weights may be determined in a moisture-free atmosphere in any solvent that is volatile.

The effects of water on the cryoscopic molecular weights were also determined.

EXPERIMENTAL

The cryoscopic studies were made according to procedures discussed in a previous publication.[5]

The SIGNER studies were made in Signer tubes (2-ml and 3-ml capacity) obtained from Scientific Glass Apparatus Company, Bloomfield, N.J. The procedure used is that described in the literature.[3,4] The standards employed were triphenyl methane (TPM) and tributyl phosphate (TBP), the latter proving monomeric (Signer method) against TPM as a standard in benzene. Errors are estimated to be in the range 5–10 per cent.

The various organophosphorus acids have been prepared and purified according to published procedures.[5,6]

The organic solvents were obtained from the following sources: n-hexane, b.p. 68–69°C and cyclohexane, spectroscopic grade, (Matheson, Coleman and Bell Co.); benzene and carbon tetrachloride, spectroscopic grades, (Eastman Organic Chemicals); chloroform, Reagent Grade (Merck and Co.); acetone, Reagent Grade (Fisher Scientific Co.), dried over anhydrous $CaCl_2$ and methyl alcohol, anyhdrous, analytical reagent grade (Mallinckrodt Chemical Works).

* Based on work performed under the auspices of the U.S. Atomic Energy Commission.

[1] D. F. PEPPARD, G. W. MASON and R. J. SIRONEN, *J. Inorg. Nucl. Chem.* **10**, 117 (1959); **7**, 276 (1958).
[2] D. F. PEPPARD, G. W. MASON and S. MCCARTY, *J. Inorg. Nucl. Chem.* **13**, 138 (1960); **12**, 141 (1959).
[3] R. SIGNER, *Liebigs. Ann.* **477**, 246 (1930).
[4] E. P. CLARK, *Analyt. Ed.* **13**, 820 (1941).
[5] D. F. PEPPARD, J. R. FERRARO and G. W. MASON, *J. Inorg. Nucl. Chem.* **7**, 231 (1958).
[6] D. F. PEPPARD, J. R. FERRARO and G. W. MASON, *J. Inorg. Nucl. Chem.* **12**, 60 (1959); **16**, 246 (1960).

RESULTS AND DISCUSSION

It has been demonstrated that the monobasic and dibasic organophosphorus acids are strongly intermolecularly hydrogen bonded.[5,6] Freezing-point depressions in benzene showed that the mono-basic acids, $(GO)_2PO(OH)$, and $(GO)G'PO(OH)$ were generally dimeric and the dibasic acids $(GO)PO(OH)_2$ were hexameric, or of even higher states of aggregation. In the case of the monobasic acids, where G is aryl or

TABLE 1.—CRYOSCOPIC MOLECULAR WEIGHTS FOR SEVERAL ORGANOPHOSPHORUS ACIDS IN BENZENE

	Formal conc.*	Mol. wt.	Mol. wt./ formula wt η
Bis[*p*(1,1,3,3-tetramethyl butyl)phenyl]phosphoric acid (F.W. 483)	0·15	975	2·0
Bis(phenyl)phosphoric acid (F.W. 250)	0·31	626	2·5
2(ethylhexyl) hydrogen phenylphosphonate (F.W. 270)	0·19	591	2·2
Benzyl hydrogen phenylphosphonate (F.W. 248)	0·12	543	2·2
n-butyl hydrogen phenylphosphonate (F.W. 224)	0·16	441	2·0
Tridecyl hydrogen phenylphosphonate (F.W. 306)	0·16	656	2·1
Bis(*p*-tolyl)phosphoric acid (F.W. 278)	0·18	618	2·2
Bis(*o*-tolyl)phosphoric acid (F.W. 278)	0·28	574	2·1
Bis(β-naphthyl)phosphoric acid (F.W. 350)	0·06	706	2·0
Bis(*p*-isopropyl)phosphoric acid (F.W. 334)	0·08	703	2·1
Bis(β-phenylethyl)phosphoric acid (F.W. 306)	0·16	648	2·1
Bis(γ-phenylpropyl)phosphoric acid (F.W. 334)	0·19	716	2·1

* Defined as (wt./formula wt.)/1000 g solvent

TABLE 2.—THE EFFECTS OF WATER ON THE CRYOSCOPIC MOLECULAR WEIGHTS OF SEVERAL ORGANOPHOSPHORUS ACIDS

Acid	Formality*	H_2O (%)	ΔT (°C)	Cryoscopic (Mol. wt.) In Benzene	Mol. wt./ formula wt. η
Bis(phenyl)phosphoric	0·21	0·86	0·072	3666	14·7
	0·21	0·71	0·128	1837	7·3
	0·21	0·51	0·266	909	3·6
	0·21	0·14	0·393	682	2·7
	0·21	nil	0·388	644	2·6
Bis(2-ethylhexyl) phosphoric	0·21	0·15	0·574	629	1·9
	0·21	0·01	0·574	620	1·9
Mono(2-ethylhexyl) phosphoric	0·24	0·89	0·078	3184	15·2
	0·24	0·31	0·118	2105	10·0
	0·24	0·16	0·142	1824	8·7
	0·24	0·01	0·163	1561	7·4
Mono[p(1,1,3,3-tetra-methylbutyl)phenyl] phosphoric	0·18	0·37	0·068	4049	14·2
	0·18	0·42	0·066	3779	13·2

VOL. 22 1961

TABLE 3.—MOLECULAR WEIGHTS OF BENZOIC ACID* AND SEVERAL ORGANOPHOSPHORUS ACIDS† IN BENZENE AND CARBON TETRACHLORIDE BY THE SIGNER METHOD

Solute	Solvents					
	Benzene			Carbon tetrachloride		
	Molarity at‡ equilibrium	Mol. wt.	Mol. wt./formula wt. η	Molarity at* equilibrium	Mol. wt.	Mol. wt./formula wt. η
Benzoic acid (F.W. 122)	0·058	233	1·9	0·015	239	2·0
				0·019	239	2·0
				0·065	247	2·0
Bis(phenyl)phosphoric acid (F.W. 250)	0·014	504	2·0	0·014	541	2·2
	0·058	589	2·4	0·061	652	2·6
	0·061	573	2·3	0·067	646	2·6
Phenyl hydrogen phenylphosphonate (F.W. 234)	0·012	447	1·9			
	0·013	449	1·9			
	0·047	523	2·2			
(2-ethylhexyl) hydrogen phenylphosphonate (F.W. 270)	0·010	477	1·8	0·010	533	2·0
	0·064	533	2·0	0·055	582	2·2
n-decyl hydrogen n-decylphosphonate (F.W. 362)	0·016	723	2·0	0·017	743	2·1
	0·066	703	1·9	0·080	690	1·9
n-butyl hydrogen n-butylphosphonate (F.W. 194)	0·024	380	2·0	0 020	418	2·2
	0·075	406	2·1	0·051	400	2·1
				0·070	416	2·2

* Tri n-butyl phosphate (TBP) was the standard for the organophosphorus acids.
† Tri phenyl methane (TPM) was the standard for benzoic acid.
‡ Defined as equal to the equilibrium molarity of the standard.

a variant thereof, cryoscopic molecular weights in benzene ran slightly higher than twice the formula weights (Table 1). With the monobasic acids where G is alkyl, the molecular weights were more nearly dimeric. Preliminary results had suggested that water might be causing the higher molecular weights in the aryl monobasic acids and could similarly affect the results for the dibasic acids. Water appeared to have no such effect upon the alkyl monobasic acids.

TABLE 4.—MOLECULAR WEIGHTS OF BIS(2-ETHYLHEXYL)PHOSPHORIC ACID* IN VARIOUS SOLVENTS BY THE SIGNER METHOD

Solvent	Molarity at† equilibrium	Mol. wt.	Mol. wt./formula wt. η
n-hexane	0·013	716	2·2
	0·078	661	2·1
Cyclohexane	0·015	695	2·1
	0·063	685	2·1
Benzene	0·012	578	1·8
	0·063	619	1·9
	0·065	633	2·0
	0·069	611	1·9
Carbon tetrachloride	0·010	630	2·0
	0·066	625	2·0
Chloroform	0·015	527	1·6
	0·057	597	1·9
Acetone	0·013	502	1·6
	0·039	537	1·7
	0·044	518	1·6
	0·049	547	1·7
Methyl alcohol	0·055	328	1·0

* F.W. = 323; TBP = Standard.
† Defined as equal to the equilibrium molarity of the standard.

Water effects on the cryoscopic molecular weights of several organophosphorus acids

The effects of water on the cryoscopic molecular weight of several organophosphorus acids in benzene are illustrated in Table 2. In the cases of bis-(phenyl)phosphoric acid, mono-(2-ethylhexyl)phosphoric and mono[*p*(1,1,3,3-tetramethylbutyl)-phenyl]phosphoric acids, water increases the molecular weight several fold. A possible explanation is that water, through hydrogen bonding, ties smaller polymeric aggregates into larger aggregates. Other examples of such water effects are known.[7] The molecular weights of the alkyl monobasic phosphorus acids are not increased by the action of water. It should be noted, in this connection, that in general, the monobasic aryl compounds form hydrates, whereas the monobasic alkyl ones do not.[8]

[7] E. N. LASSETTRE, *Chem. Rev.* **20**, 259 (1937).
[8] J. R. FERRARO and D. F. PEPPARD, Unpublished data (1962).

Molecular weights by the Signer method

The molecular weights of several organophosphorus acids as determined by the Signer method are shown in Tables 3–6. Most of the monobasic acids tend to exhibit a dimeric molecular weight in solvents such as n-hexane, cyclohexane, benzene and carbon tetrachloride. In solvents capable of hydrogen bonding or of interaction, the

TABLE 5.—MOLECULAR WEIGHTS OF 2-ETHYLHEXYL HYDROGEN 2-ETHYLHEXYL-PHOSPHONATE* IN VARIOUS SOLVENTS BY THE SIGNER METHOD

Solvent	Molarity at† equilibrium	Mol. wt.	Mol. wt./formula wt. η
n-hexane	0·017	466	1·5
	0·060	594	1·9
	0·064	591	1·9
Cyclohexane	0·009	412	1·4
	0·015	519	1·7
	0·128	543	1·8
	0·144	549	1·8
Benzene	0·012	425	1·4
	0·016	463	1·5
	0·066	578	1·9
	0·068	577	1·9
Carbon tetrachloride	0·025	587	1·9
	0·066	565	1·9
	0·086	551	1·8
Chloroform	0·015	351	1·2
	0·017	447	1·5
	0·052	500	1·6
	0·058	529	1·7
	0·061	509	1·7
	0·078	694	2·3
Acetone	0·015	395	1·3
	0·034	517	1·7
	0·058	531	1·7
	0·058	527	1·7
Methyl alcohol	0·060	292	1·0

* F.W. = 307 TBP = Standard.
† Defined as equal to the equilibrium molarity of the standard.

molecular weights show a decrease from the dimeric state. The decrease in experimental molecular weights in solvents such as chloroform, acetone and methyl alcohol parallels the predicted increase in solute–solvent interaction in these solvents. Both the monobasic phosphoric acids and the monobasic hydrogen phosphonates are monomeric in methyl alcohol.

There appears to be some difference in the stability of the dimers when comparing the phosphates with the phosphonates. In a comparison of 2-ethylhexyl hydrogen

VOL. 22 1961

2-ethylhexylphosphonate and of bis(2-ethylhexyl)phosphoric acid at low concentrations (about 0·01 molar) in n-hexane, cyclohexane and benzene, the 2-ethylhexyl hydrogen 2-ethylhexylphosphonate tends to reduce its degree of aggregation to

TABLE 6.—MOLECULAR WEIGHTS OF MONO(2-ETHYLHEXYL)PHOSPHORIC ACID* IN VARIOUS SOLVENTS BY THE SIGNER METHOD

Solvent	Molarity at† equilibrium	Mol. wt.	Mol. wt./formula wt. η
n-hexane	0·018	1973	9·4
	0·062	3039	14·5
	0·067	3051	14·5
	0·069	2721	13·0
	0·070	3078	14·5
Cyclohexane	0·013	2040	9·7
	0·053	1932	9·2
	0·057	2115	10·1
	0·069	1836	8·7
	0·074	1801	8·5
	0·086	2208	10·5
	0·097	2521	12·0
Benzene	0·014	1230	5·9
	0·036	1228	5·9
	0·037	1304	6·2
	0·084	1737	8·3
	0·089	1630	7·8
Carbon tetrachloride	0·014	1151	5·5
	0·052	1398	6·7
	0·058	1365	6·5
	0·060	1447	6·9
Chloroform	0·016	735	3·5
	0·068	952	4·5
	0·070	1047	5·0
Acetone	0·020	368	1·8
	0·036	399	1·9
	0·041	402	1·9
	0·067	413	2·0
	0·119	525	2·0
Methyl alcohol	0·052	211	1·0
	0·053	210	1·0

* F.W. = 210; TBP = Standard.
† Defined as equal to the equilibrium molarity of standard.

somewhere between a dimer and monomer, whereas bis(2-ethylhexyl)phosphoric acid appears to remain predominantly a dimer. Recently, THOMAS has studied compounds related to the hydrogen phosphonates and has obtained evidence for the presence of a free hydroxyl absorption.[9]

[9] L. C. THOMAS. Personal communication (1961).

Mono(2-ethylhexyl)phosphoric acid demonstrates very high molecular weights in n-hexane and cyclohexane, and its state of aggregation appears to be strongly concentration dependent (Table 6). The measured molecular weight decreases as the diluent employed ranges through the series: n-hexane, cyclohexane, benzene, carbon tetrachloride, chloroform, acetone and methyl alcohol. The ordering is consistent with predicted increasing solute–solvent interaction (e.g. hydrogen bonding). In acetone, the compound is a dimer and, in methyl alcohol, a monomer.

VOL.
22
1961

VO
2
19

J. Inorg. Nucl. Chem., 1961, Vol. 22, pp. 293 to 296. Pergamon Press Ltd. Printed in Northern Ireland

LIQUIDUS RELATIONS IN THE SYSTEM LITHIUM METAPHOSPHATE–LITHIUM PYROPHOSPHATE

M. M. MARKOWITZ, R. F. HARRIS and W. N. HAWLEY
Foote Mineral Co., Research and Engineering Center, P.O. Box 513, West Chester, Pa.

(*Received* 10 *May* 1961; *in revised form* 22 *June* 1961)

Abstract—Lithium metaphosphate and pyrophosphate are suggested as possible components for fused salt nuclear breeder blankets because of the relatively high thermal stability of these compounds and of the very low absorption of thermal neutrons exhibited by phosphorus. The phase system $LiPO_3$–$Li_4P_2O_7$ was studied by means of high temperature microscopy and differential thermal analysis. At liquidus temperatures, the system was determined to be of the simple eutectic type with the eutectic at 84·5 mole % $LiPO_3$ and 603°. An arrest occurring at 569° might indicate the existence of a polyphosphate higher than the pyrophosphate in the solidus region; however, the origin of this halt has not been identified. The $LiPO_3$–$Li_4P_2O_7$ system in contrast to other metaphosphate-pyrophosphate systems appears to be unique due to the absence of higher polyphosphates in the liquidus region.

VOL. 22 1961

GRUEN[1] has pointed out some of those factors significant to the application of a lithium-based fused salt system as a breeder blanket for the deuterium-tritium fusion reactor.[2] The relatively thermally unstable compounds lithium nitrite and nitrate have been considered as possible components.[1,3] Further thought indicates that molten mixtures of lithium metaphosphate and pyrophosphate might be of value as blanket materials because of the high intrinsic thermal stability of the component salts and of the low nuclear reactivity to thermal neutrons of the phosphorus-containing oxyanions.[4] Accordingly, a phase study of the system lithium metaphosphate–lithium pyrophosphate at liquidus temperatures was undertaken as a preliminary to further characterization of mixtures of these salts.

EXPERIMENTAL PROCEDURES AND RESULTS

Lithium metaphosphate was prepared by dehydration of lithium dihydrogen orthophosphate.[5] The latter compound was partially dehydrated at 200° for 4 hr to yield substantially lithium dihydrogen pyrophosphate; after grinding, this salt was heated at 300° for 4 hr and then for 4 hr at 800° in a platinum dish. Rapid cooling of the melt resulted in a clear glass which was crystallized after grinding by heating at 500° for 2 hr. This crystalline material was used in the preparation of all the samples for the phase studies. (Phosphorus:[6] Found, 36·06; Calcd. for $LiPO_3$, 36·06%).

Lithium pyrophosphate was prepared by reaction of anhydrous lithium hydroxide with pyrophosphoric acid. A mixture of 139·1 g (0·781 mole) pyrophosphoric acid,[7]

[1] D. M. GRUEN, Report ANL-5840 (1958).
[2] R. F. POST, *Rev. Mod. Phys.* **28,** 338 (1956).
[3] A. S. BISHOP, *Project Sherwood: The U.S. Program in Controlled Fusion*, pp. 42–43, Anchor Books, Doubleday, New York (1960).
[4] R. STEPHENSON, *Introduction of Nuclear Engineering*, p. 375. McGraw-Hill, New York (1954).
[5] R. K. OSTERHELD and M. M. MARKOWITZ, *J. Phys. Chem.* **60,** 863 (1956).
[6] L. T. JONES, *Industr. Engng. Chem., Analyt. Ed.* **14,** 536 (1942).
[7] J. E. MALOWAN, *Inorganic Syntheses*, Vol. 3, pp. 96–97. (Edited by L. F. AUDRIETH) McGraw-Hill New York (1950).

68·0 g (2·839 mole) anhydrous lithium hydroxide, and 1000 ml absolute ethanol was refluxed with vigorous stirring for three days. The insoluble material was filtered, washed with ethanol and dried for 5 hr at 160° under vacuum. This solid was then heated in air at 800° for 12 hr. (Phosphorus:[6] Found, 30·36; Calcd. for $Li_4P_2O_7$, 30·72%. Pyrophosphate group:[8] Found, 84·44°; Calcd. for $Li_4P_2O_7$, 86·24%). Lithium pyrophosphate has also been prepared in this laboratory by thermal treatment

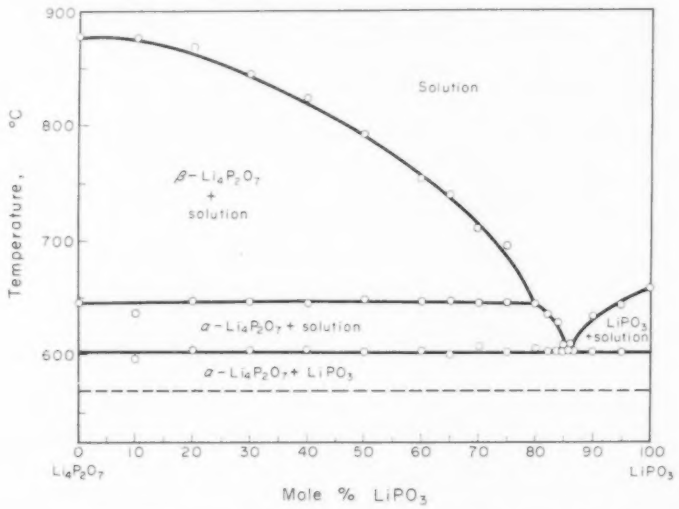

FIG. 1.—The system lithium metaphosphate–lithium pyrophosphate

of the reaction mixtures: $2LiH_2PO_4 + Li_2CO_3$, $2LiPO_3 + Li_2CO_3$, and Li_2CO_3, + $(NH_4)_2HPO_4$. The small weight losses engendered during heating the pure metaphosphate and pyrophosphate salts in platinum dishes in air for two days at 900° are indicative of the considerable thermal stability of these compounds. Thus, 10·0992 g $LiPO_3$ lost 0·0581 g and 9·5452 g $Li_4P_2O_7$ lost 0·0011 g under these conditions.

The phase relationships of the components and of mixtures thereof were studied by the techniques of high temperature microscopy[9] and of differential thermal analysis (DTA). The sample compositions are indicated by the experimental points in Fig. 1.

A high temperature hot stage was used for the microscopic investigations (1000°C Microscope Heating Stage, No. HATII, E. Leitz, Inc., 468 Fourth Ave., N.Y. 16, N.Y.). In this manner, the first formation of liquid in all samples was found to occur at about 603° over the entire range of sample compositions. The temperatures corresponding to the last disappearance of solid were determined to be unique functions of sample composition. Three separate determinations were made on each sample composition of intimately mixed crystalline materials. These combined observations resulted in the liquidus and eutectic portions of the curves of Fig. 1.

The DTA runs were performed using the instrumentation described elsewhere[10] in conjunction with bare platinum/10 per cent rhodium-platinum thermocouples. A

[8] R. N. BELL, *Analyt. Chem.* **19**, 97 (1947).
[9] W. C. MCCRONE, JR., *Fusion Methods in Chemical Microscopy*, pp. 22–24, 142–171. Interscience, New York (1957).
[10] M. M. MARKOWITZ, *J. Phys. Chem.* **62**, 827 (1958).

smaller version of the furnace arrangement of GORDON and CAMPBELL was used.[11] A sample size of 1·5 g contained in a Vycor test-tube was adopted with a heating rate of 10° per min; alumina was used as the reference standard. Each sample was subjected to three to five heating and cooling cycles during the DTA experiments. Dissolution of the Vycor container by the phosphate melts was judged to be slight. Thus, a loss in weight of about 10 mg was found for a typical Vycor test-tube (0·5 in. diam. × 3·6 in. length, 8·81 g) containing 1·5 g of a mixture of 50 wt.% $LiPO_3$–50 wt.% $Li_4P_2O_7$ maintained at 920° for 5 hr. Samples rich in lithium metaphosphate were found to supercool to glassy materials which recrystallized exothermally upon reheating. The behaviour of pure lithium metaphosphate during DTA has already been detailed;[12] melting of the crystalline material occurs at 658°. Lithium pyrophosphate was found to exhibit a reversible crystallographic transition at 646° and to melt at 878°. Those salt mixtures displaying this characteristic transition, as determined by DTA, are indicated in Fig. 1.

VOL. 22 1961

The DTA curves for mixtures of the components showed the presence of an endothermic break at about 569°. This break was only found to appear clearly after the first heating cycle and would thus indicate that intimate mixing of the components, through solution formation, facilitates the occurrence of the process giving rise to the thermal effect. No consistent order was found for the intensity of the break at 569° either as a function of sample composition or during successive DTA runs on the same sample. Apparently, the phenomenon occurring at 569° is of some incompletely reproducible type. This arrest is shown by the dashed line in Fig. 1. Some thermal interaction between the endotherm at 569° and the endothermic eutectic break at 603° was also found. This resulted in a somewhat irregular variation of the magnitude of the eutectic break. The liquidus temperatures determined by DTA were in close agreement with those found by microscopic observations.

Inspection of Fig. 1 shows the system to be of the simple eutectic type at liquidus temperatures, with the eutectic at 84·5 mole% $LiPO_3$ and 603°.

DISCUSSION

Attempts at identifying the origin of the DTA break at 569° were unsuccessful. Mixtures of lithium metaphosphate and lithium pyrophosphate in 10 mole% increments were fused at 900°, cooled rapidly, powdered, and tempered at 450° for three weeks. This was done to determine if a new crystalline polyphosphate phase would form. X-ray powder patterns of these annealed mixtures evidenced lines attributable only to the original crystalline components. This might indicate that if a crystalline polyphosphate ($M^{I}_{n+2}P_nO_{3n+1}$) higher than the pyrophosphate[13] ($n = 2$) is capable of formation in this system, its rate of formation must be very low at temperatures appreciably below its decomposition temperature (569°). The formation and decomposition of the postulated polyphosphate can probably be represented by the equation: $Li_4P_2O_7 + (n-2)LiPO_3 \rightarrow Li_{n+2}P_nO_{3n+1}$, $n \geq 3$. Lithium metaphosphate is expressed simply as $LiPO_3$ for ease of representation; like the other water-insoluble alkali metal metaphosphates, the lithium compound is undoubtedly a salt of highly polymeric, long-chain structure.[14]

[11] S. GORDON and C. CAMPBELL, *Analyt. Chem.* **27**, 1102 (1955).
[12] M. M. MARKOWITZ and D. A. BORYTA, *Analyt. Chem.* **32**, 1588 (1960).
[13] M. M. MARKOWITZ, *J. Chem. Educ.* **33**, 36 (1956).
[14] J. R. VAN WAZER, *Phosphorus and Its Compounds*, Vol. 1, pp. 672–678. Interscience, New York (1958).

It is of interest to note that in each of the phase systems for which extensive studies have been made between the metaphosphate and pyrophosphate compositions, polyphosphates ($n \geqslant 3$ existing within the liquidus region have been found. This includes the systems

$NaPO_3$–$Na_4P_2O_7$ ($n = 3$),[15]
KPO_3–$K_4P_2O_7$ ($n = 3$),[16,17]
$Ca(PO_3)_2$–$Ca_2P_2O_7$ ($n = 5$),[18,19]
and $Pb(PO_3)_2$–$Pb_2P_2O_7$ ($n = 4$).[20,21]

On the basis of the present studies, no polyphosphate higher than the pyrophosphate has been found to exist within the liquidus region of the lithium metaphosphate–lithium pyrophosphate system.

[15] E. P. PARTRIDGE, V. HICKS and G. V. SMITH, *J. Amer. Chem. Soc.* **63**, 454 (1941).
[16] R. K. OSTERHELD and L. F. AUDRIETH, *J. Phys. Chem.* **56**, 38 (1952).
[17] G. W. MOREY, *J. Amer. Chem. Soc.* **76**, 474 (1954).
[18] W. L. HILL, G. T. FAUST and D. S. REYNOLDS, *Amer. J. Sci.* **242**, 457 542 (1944).
[19] J. R. VAN WAZER and S. OHASHI, *J. Amer. Chem. Soc.* **80**, 1010 (1958).
[20] R. K. OSTERHELD and R. P. LANGGUTH, *J. Phys. Chem.* **59**, 76 (1955).
[21] R. P. LANGGUTH, R. K. OSTERHELD and E. F. KARL-KROUPA, *J. Phys. Chem.* **60**, 1335 (1956).

J. Inorg. Nucl. Chem., 1961, Vol. 22, pp. 297 to 304. Pergamon Press Ltd. Printed in Northern Ireland

SYNTHESIS AND PROPERTIES OF MONO- AND POLY-METHYLENE-DIPHOSPHONIC ACIDS AND ESTERS

K. MOEDRITZER and R. R. IRANI
Monsanto Chemical Company, Inoganic Chemicals Divison, St. Louis, Missouri

(*Received* 4 *May* 1961; *in revised form* 25 *May* 1961)

Abstract—A series of methylenediphosphonic acids, $(HO)_2OP(CH_2)_nPO(OH)_2$, (n = 1, 2, 3, 4, 5, 6 and 10) have been prepared by hydrolysis of the corresponding tetra-ethyl esters. The esters with $n \geqslant 3$ were obtained by either a Michaelis-Becker or an Arbuzov-Michaelis type reaction. For $n = 1$ or 2, a modified Michaelis-Becker reaction was utilized. The ^{31}P nuclear magnetic resonance chemical shifts as well as the infra-red spectra show that as n increases the effect of the two end phosphorus atoms on one another decreases, and becomes very small for $n > 3$. The X-ray diffraction patterns of the diphosphonic acids are reported.

VOL. 22 1961

MANY members of the series of the methylenedicarboxylic acids, $HOOC(CH_2)_nCOOH$, as well as their esters have been known for some time and their physical properties have been well defined. However, for the methylenediphosphonic acids, $(HO)_2OP(CH_2)_nPO(OH)_2$, and their esters, only some members[1–4] have been prepared and no extensive comparison of their physical constants is available.

This paper describes the synthesis of homologues of methylenediphosphonic acid and corresponding tetra-alkyl esters. Comparison and discussion of physical constants as well as infra-red absorption, X-ray diffraction and nuclear magnetic resonance (n.m.r) is presented.

RESULTS AND DISCUSSION

Preparation. Mono- and polymethylenediphosphonic acids can be prepared in nearly quantitative yield by the hydrolysis of the corresponding tetra-alkyl esters with conc. HCl:

$$(RO)_2OP(CH_2)_nPO(OR)_2 + 4HCl \rightarrow (HO)_2OP(CH_2)_nPO(OH)_2 + 4RCl \quad (1)$$

Recrystallization from water usually yields the acids in a very pure state. The tetra-alkyl esters of mono- and polymethylenediphosphonic acids required for the above hydrolysis reaction can be prepared by either one of the two general reactions (X = halogen, M = alkali metal):

$$X(CH_2)_nX + 2MOP(OR)_2 \rightarrow (RO)_2OP(CH_2)_nPO(OR)_2 + 2MX \quad (2)$$

$$X(CH_2)_nX + 2P(OR)_3 \rightarrow (RO)_2OP(CH_2)_nPO(OR)_2 + 2RX \quad (3)$$

Equation (2) is a Michaelis-Becker-type reaction and equation (3) is an Arbuzov-Michaelis reaction.

[1] A. H. FORD-MOORE and J. H. WILLIAMS, *J. Chem. Soc.* 1465 (1947).
[2] G. SCHWARZENBACH and J. ZURC, *Monatsh.* **81**, 202 (1950).
[3] G. M. KOSOLAPOFF, *J. Chem. Soc.* 3092 (1955).
[4] N. P. BOGONOSTSEVA, *Chem. Abstr.* **51**, 6581 (1957).

Both types of reactions work about equally well for alkylene dihalides with $n \geqslant 3$. However, for alkylene dihalides with $n = 1$ or 2 the Michaelis-Becker and the Arbuzov-Michaelis reactions either yield the expected esters in low yield or give side products only. Methylenedi-iodide and sodium diethyl phosphite have not been found to yield the expected ester ($n = 1$) according to equation (2),[5] whereas the reaction of methylenedi-iodide with trialkyl phosphite according to equation (3) gave the expected ester ($n = 1$) in only 26 per cent yield.[3] SCHWARZENBACH and ZURC[2] could not prepare the diphosphonate for $n = 2$ when reacting ethylenedibromide with sodium diethyl phosphite according to equation (2), but the Arbuzov-Michaelis reaction according to equation (3) yielded the expected ester in only 27 per cent yield.

For the preparation of methylenediphosphonates with $n = 1$ or 2 a variation of the Michaelis-Becker is applicable. This method is based on a stepwise synthesis of

TABLE 1.—PHYSICAL PROPERTIES AND ANALYTICAL DATA OF TETRA-ETHYL METHYLENEDIPHOSPHONATES $(C_2H_5O)_2OP(CH_2)_nPO(OC_2H_5)_2$

n	b.p. (°C/mm)	n_D^{25}	Yield (%)	Carbon (%)		Hydrogen (%)		Phosphorus (%)	
				Calc.	Found	Calc.	Found	Calc.	Found
1	130/1	1·4398	55*	37·50	37·54	7·69	7·54	21·49	21·17
2	160/2	1·4359	60†	39·74	38·81	8·00	7·69	20·50	20·60
3	178–180/1	1·4425	50‡	41·77	41·71	8·27	8·51	19·59	19·98
4	171/0·1	1·4455	55§	43·63	42·65	8·55	8·82	18·76	19·76
5	180–181/0·1	1·4464	60§	45·34	45·10	8·78	8·97	17·99	17·79
6	185/0·1	1·4462	48‡	46·92	46·52	9·00	9·20	17·29	16·79
10	225/0·8	1·4453	54‡	52·16	49·35	9·73	9·86	14·95	15·04

* Prepared according to equation (4), M = Na.
† Prepared according to equation (4), M = K.
‡ Prepared according to equation (2), M = Na.
§ Prepared according to equation (2), M = K.

the molecule. Suitable compounds are first made with one P—C bond in the molecule, which are subsequently reacted with dialkyl phosphite salts to give the desired diphosphonates. The compounds containing one P—C bond, dialkyl α-halomethyl- ($n = 1$) and β-halo-ethylphosphonate ($n = 2$), react in a Michaelis-Becker type reaction:

$$(RO)_2POM + X(CH_2)_nPO(OR)_2 \rightarrow (RO)_2OP(CH_2)_nPO(OR)_2 + MX \qquad (4)$$

to give the diphosphonates in 50–60 per cent yield.

The compounds for $n = 1$ or 2 were prepared according to equation (4) and the compounds for $n = 3$, 4, 5, 6 and 10 according to equation (2). In certain cases the use of potassium diethyl phosphite instead of sodium diethyl phosphite increased the yield of diphosphonate. For example the yield of dimethylene diphosphonate when sodium diethyl phosphite was used was only 8 per cent but increased to 60 per cent with potassium diethyl phosphite.

Table 1 lists the boiling point, refractive index, yield and analysis of the tetra-ethyl esters of the prepared mono- and polymethylene diphosphonic acids. In Table 2 physical properties and analytical data of the corresponding mono- and polymethylene-diphosphonic acids are compiled.

[5] P. NYLEN, *Diss. Uppsala* pp. 77–84 (1930).

Nuclear magnetic resonance spectra. The ^{31}P n.m.r. spectra of the methylene-diphosphonic esters, acids, di- and tetrasodium salts exhibit a single peak. For the compounds with $n = 1$ the resolution of the magnetic field was high enough to show

TABLE 2.—PHYSICAL PROPERTIES AND ANALYTICAL DATA OF METHYLENE-DIPHOSPHONIC ACIDS $(HO)_2OP(CH_2)_nPO(OH)_2$

n	m.p. (°C)	Yield* (%)	Equiv. wt.		Carbon (%)		Hydrogen (%)		Phosphorus (%)	
			Calc.	Found	Calc.	Found	Calc.	Found	Calc.	Found
1	200	92	88	90	6·82	6·87	3·44	3·25	35·20	34·11
2	220–223	94	95	97	12·63	12·08	4·24	4·24	32·60	31·94
3	178	87	102	105	17·67	17·89	5·29	5·26	30·36	30·40
4	217–220	98	109	111	22·03	21·99	5·55	5·44	28·41	27·66
5	155	95	118	116	25·87	23·89	6·08	6·04	26·09	25·91
6	206–208	98	123	125	29·27	29·12	6·55	6·39	25·17	25·23
10	208–209	81	150	151	39·74	39·57	8·00	8·12	20·50	20·22

* From ester hydrolysis

VOL. 22 1961

the 1-2-1 splitting due to the interaction of the two hydrogen atoms attached to the bridging carbon atom.

Table 3 lists the ^{31}P n.m.r. chemical shifts of the investigated compounds. Three general trends are obvious:

TABLE 3.—^{31}P n.m.r. CHEMICAL SHIFTS IN p.p.m. RELATIVE TO 85% H_3PO_4 OF METHYLENE-DIPHOSPHONIC ACIDS, SOME PHOSPHONIC ACIDS AND THEIR DERIVATIVES; RELIABILITY ±1 p.p.m.

Compound $(YO)_2OP(CH_2)_nPO(OY)_2$*	Diethyl ester	Acid†	Mono-sodium salt†	Disodium salt†	Tetra-sodium salt†
$n = 1$	−19·0	−16·7		−15·2	−13·6
$n = 2$	−26·8	−27·4		−23·3	−22·4
$n = 3$	−29·3	−28·2		−24·8	−22·2
$n = 4$	−31·5	−31·6		−26·9	−23·1
$n = 5$	−30·8	−31·9		−25·6	−23·8
$n = 6$	−29·6	−30·6		−26·5	−23·5
$n = 10$	−30·9	−28·6‡		−27·7	−22·6
$ClCH_2PO(OY)_2$	−18·1	−17·8	−14·0	−12·3	
$Cl(CH_2)_2PO(OY)_2$	−24·4	−24·6	−24·3	−22·0	
$CH_3(CH_2)_{11}PO(OY)_2$	−29·9	−29·9	−28·0§	−21·9	

* Y = H, Na or C_2H_5
† In water
‡ In tetrahydrofuran
§ In dioxane-water

(1) With increasing number of CH_2 groups between the two phosphorus atoms the chemical shift becomes more negative and finally reaches a limiting value for $n > 3$. In the compounds with $n = 1$ the two phosphorus atoms are identical and each

phosphorus atom behaves with respect to its electronic environment like a phosphorus atom connected to a carbon atom with a strongly electro-negative ligand attached to the latter. This shielding effect[6] of one phosphorus atom with respect to the other in the molecule is approximately the same as if one of the phosphorus atoms were replaced by chlorine, as illustrated in Table 3 also. The same argument can be extended for the compounds with $n = 2$, except that the shielding effect of the second phosphorus atom is less because it has to act over a distance of three bond lengths. Again, the chemical shifts of corresponding P—C—C—P and P—C—C—Cl compounds are equal. The shielding effect seems to drop off quite rapidly with increasing number of CH_2 groups between the two phosphorus atoms. For $n > 3$ the phosphorus atoms do not shield one another, and the electron environment of each single P atom is the same as if the second P atom were not present in the molecule at all. As shown in Table 3 the chemical shift of the compounds with $n > 3$ is of the same order of magnitude as the shift of corresponding compounds with only one phosphorus atom, such as long chain phosphonate derivatives.

(2) The chemical shifts of the methylenediphosphonic acids are very close to those of their tetra-alkyl esters. This has been found to be true for other alkyl esters of quadruply connected phosphorus compounds, e.g. $OP(OEt)_3$: +1 p.p.m., $OP(OH)_3$: 0 p.p.m. Apparently, the electronic environment of the phosphorus atom in the acids and esters is solely determined by the oxygen atoms.

(3) The sodium salts of phosphonic and methylenediphosphonic acids show chemical shifts which are more positive than the corresponding acids. The chemical shifts of the disodium and tetrasodium salts are displaced +2 to+4 and +4 to +8 p.p.m. relative to the corresponding acids respectively. This positive shift upon salt formation is in opposite direction to that observed with the sodium salts of phosphoric acid: H_3PO_4: 0 p.p.m., NaH_2PO_4: −0·5 p.p.m., Na_2HPO_4: −3·5 p.p.m., Na_3PO_4: −6 p.p.m.[7]

Infra-red Spectra. The infra-red absorption bands of the tetra-alkyl mono- and polymethylenediphosphonates are recorded in Table 4. The frequency of the phosphoryl group generally appears in a rather wide range, from 1350 to 1200 cm^{-1}.[8] The variation of the position of the band depends mainly on the electronegativity of the substituents on the phosphorus. The phosphoryl stretching frequency shifts towards smaller wave numbers with decreasing electronegativity of the substituents. As the influence of the two phosphorus atoms in the diphosphonates on each other becomes weaker with an increase in the number of CH_2 groups separating them, the P=O frequency shifts to lower wave numbers. This is shown in the compounds with $n = 1$, 2 and 3. From $n \geqslant 3$ the phosphoryl absorption remains at a constant wavenumber, indicating the vanished influence of the electronegative phosphonate groups on each other.

The bands at 1171–1166 and 1049–1031 cm^{-1} remain fairly constant throughout the whole series. They have been identified[9] as the independent stretching motions of the C—O and P—O portion of the P—O—C link. The band at 1104–1100 cm^{-1} which appears in all compounds of this series has been found[9] to occur in all EtO—P

[6] J. R. VANWAZER, C. F. CALLIS, J. N. SHOOLERY and R. C. JONES, *J. Amer. Chem. Soc.* **78**, 5715 (1956).
[7] R. A. Y. JONES and A. R. KATRITZKI, *J. Inorg. Nucl. Chem.* **15**, 193 (1960
[8] L. J. BELLAMY, *The Infra-red Spectra of Complex Molecules*, Methuen, London (1958).
[9] R. A. MCIVOR, G. A. GRANT and C. E. HUBLEY, *Canad. J. Chem.* **34**, 1611 (1956).

compounds, with the exact nature of this absorption being still unknown. In agreement with previous work,[10] phosphonates were found to have a characteristic band in the range of 971–959 cm^{-1}.

TABLE 4.—INFRA-RED ABSORPTION BANDS (cm^{-1}) OF TETRA-ETHYL METHYLENE-DIPHOSPHONATES $(C_2H_5O)_2OP(CH_2)_nPO(OC_2H_5)_2$*

(a) NaCl region

$n = 1$	$n = 2$	$n = 3$	$n = 4$	$n = 5$	$n = 6$	$n = 10$	
2985 *s*	2994 *s*	3012 *s*	2976 *s*	2985 *s*	2985 *s*	2976 *s*	CH stretching
2941 *m*	2949 *m*	2976 *m*	2923 *m*	2941 *m*	2958 *m*	2967 *m*	
1492 *w*	1492 *w*	1492 *w*					C—H deformation
1453 *m*	1453 *m*	1453 *m*	1449 *m*	1453 *m*	1470 *m*	1470 *m*	
	1432 *m*						
1404 *m*	1404 *s*	1404 *s*	1398 *s*	1398 *s*	1404 *s*	1404 *s*	
1379 *m*	1383 *m*	1379 *m*	1369 *w*	1375 *w*	1379 *w*	1379 *w*	
1266 *vs*	1261 *vs*	1250 *vs*	1250 *vs*	1253 *vs*	1252 *vs*	1253 *vs*	P=O stretching
1201 *w*	1201 *m*	1201 *m*	1193 *w*				
1168 *m*	1172 *s*	1171 *m*	1167 *s*	1166 *s*	1170 *s*	1171 *s*	C—O—(P) vibration
1031 *vs*	1049 *vs*	1049 *vs*	1045 *vs*	1042 *vs*	1047 *vs*	1047 *vs*	P—O—(C) vibration
971 *vs*	971 *vs*	967 *vs*	962 *vs*	959 *vs*	965 *vs*	965 *vs*	
830 *vs*	840 *m*	855 *m*	855 *w*	822 *s*	818 *s*	818 *s*	P—C vibration
808 *s*	801 *vs*	787 *vs*	752 *s*	741 *w*	809 *s*	790 *s*	

(b) KBr region

830 *vs*	800 *vs*	797 *vs*	787 *vs*	790 *vs*	794 *vs*	790 *vs*	P—C vibration
	738 *m*		735 *w*		735 *vw*	730 *vw*	
		704 *m*	702 *m*	704 *s*	702 *w*		
546 *w*	552 *m*	549 *vs*	556 *s*	542 *vs*	546 *s*		
		530 *m*		532 *w*			
515 *vs*	498 *vs*	493 *m*	500 *m*	500 *vw*			
			488 *m*		488 *m*	493 *vw*	

* *w* = weak, *m* = medium, *s* = strong, *v* = very.

The infra-red absorption bands of mono- and polymethylene-diphosphonic acids are recorded in Table 5. The P—OH stretching vibration which usually is reported to be at 2700–2560 cm^{-1} is found in the range 2695–2660 cm^{-1}. A very strong absorption band has been observed in the region 2336–2272 cm^{-1} throughout the whole series of compounds. This band probably is connected with the P—OH frequency. Further substantiation could be obtained by deuteration studies. The bands at 1466–1460 cm^{-1}

[10] L. W. DAASCH and D. C. SMITH, *Analyt. Chem.* **23**, 853 (1951).

VOL. 22 1961

represent C—H deformation frequencies arising from CH_2 groups. Due to strong hydrogen bonding with the P—OH groups the phosphoryl frequency is in the range 1220–1170 cm^{-1}, considerably lower than found in the corresponding tetra-ethyl

TABLE 5.—INFRA-RED ABSORPTION BANDS (cm^{-1}) OF METHYLENE-DIPHOSPHONIC ACIDS $(HO)_2OP(CH_2)_nPO(OH)_2$

$n = 1$	$n = 2$	$n = 3$	$n = 4$	$n = 5$	$n = 6$	$n = 10$	
(a) NaCl region							
2899 *vs*	2874 *vs*	2817 *vs*	2899 *vs*	2899 *vs*	2874 *vs*	2899 *vs*	C—H stretching
2695 *m*	2690 *m*	2660 *m*	2690 *m*	2625 *m*	2675 *m*	2660 *m*	P—OH stretching
2273 *vs*	2272 *vs*	2336 *vs*	2326 *vs*	2326 *vs*	2309 *vs*	2326 *vs*	
1639 *m*		1613 *m*		1639 *m*			
1562 *m*							
1515 *m*							
		1460 *m*	1460 *m*	1466 *m*	1466 *m*	1466 *m*	C—H deformation
1404 *w*	1404 *m*	1414 *m*	1403 *m*	1399 *m*	1408 *m*	1408 *m*	C—H bending
1374 *m*		1370 *m*	1342 *m*				
		1290 *s*	1299 *s*	1312 *m*	1299 *s*	1307 *m*	
						1279 *s*	
1272 *m*		1256 *s*		1253 *n*	1258 *m*	1255 *m*	
1215 *vs*	1220 *s*	1208 *vs*	1205 *vs*	1212 *m*	1170 *s*	1176 *s*	P=O stretching
	1183 *m*	1176 *s*		1167 *m*			
1163 *m*	1143 *m*	1130 *m*		1142 *m*			
1116 *m*	1116 *m*				1114 *s*	1116 *s*	
1104 *m*							
1092 *m*	1092 *m*	1087 *s*	1075 *s*	1081 *s*	1082 *s*	1071 *m*	
	1064 *w*						
1020 *m*	1020 *m*	1020 *m*	1005 *s*	1000 *vs*	1005 *vs*	1005 *vs*	
997 *m*	1000 *m*	994 *m*					
966 *s*	952 *m*	966 *m*	955 *s*	949 *vs*	949 *vs*	940 *vs*	
918 *vs*	934 *s*	931 *s*	925 *s*	931 *s*		930 *sh*	
845 *s*							P—C—P
815 *vs*							
808 *w*							
766 *s*		774 *m*	773 *m*	785 *s*	785 *vs*	778 *vs*	
	748 *s*	750 *m*	764 *m*	770 *m*	748 *m*	763 *sh*	
720 *s*	708 *s*	713 *s*	711 *s*	713 *s*	716 *m*	715 *vs*	
(b) KBr region							
772 *m*	770 *m*		774 *s*	777 *m*	794 *vs*	778 *vs*	P—C stretching,
	757 *m*	753 *s*	769 *s*		749 *s*		CH_2 rocking,
710 *w*	709 *m*	715 *m*	713 *vs*	717 *s*	720 *m*	718 *s*	skeletal vibrations
564 *vs*						557 *m*	
		529 *m*	534 *vs*	545 *vs*	538 *s*	540 *s*	
508 *vs*		514 *s*		500 *vs*			
472 *vs*	483 *vs*	487 *s*	459 *s*		463 *vs*	476 *s*	
	447 *s*	461 *s*					

esters. As with the esters, a decrease of the wave number of the P=O frequency with increasing number of CH_2 groups between the two phosphorus atoms in the molecule occurs.

Unlike phosphonates and many other phosphorus compounds giving many absorptions in the 900–700 cm^{-1} region which could not be accounted for[10] it is fairly simple to correlate absorption bands for the P—C stretching frequency in diphosphonic acids due to the absence of interfering bonds. With the rock salt as well as with the potassium bromide optics, three distinct absorption bands at 780–770, 750–760 and 720–708 cm^{-1} were found in all compounds. Some of these bands apparently are attributable to the P—C stretching mode. Another set of absorptions connected with the P—C bond is found in the 550–500 cm^{-1} region.

In connection with these assignments it was of special interest to attribute a frequency for the P—C—P linkage. Methylene-diphosphonic acid gives three distinct bands at 845 (*s*), 815 (*vs*) and 808 cm^{-1} (*w*) which do not appear in the spectra of higher homologues. It is therefore assumed that these frequencies result from the P—C—P linkage.* Due to overlapping absorptions found in the whole series, these frequencies could not be resolved in the spectra of the corresponding tetra-alkyl esters.

X-ray diffraction pattern. In Table 6 the interplanar spacings and relative intensities of the ten strongest peaks of mono- and polymethylenediphosphonic acids are listed. The *d*-spacing of the most intense line increases with increasing number of CH_2 groups between the phosphorus atoms.

VOL. 22 1961

TABLE 6.—X-RAY DIFFRACTION PATTERNS OF METHYLENE-DIPHOSPHONIC ACIDS $(HO)_2OP(CH_2)_nP(OH)_2$*

$n = 1$		$n = 2$		$n = 3$		$n = 4$		$n = 5$		$n = 6$		$n = 10$	
d[Å]	I/I_1	*d*[Å]	I/I_1	*d*[Å]	I/I_1	*d*[Å]	I/I_1	*d*[Å]	I/I_1	*d*[Å]	I/I_1	*d*[Å]	I/I_1
2·70	100	4·50	100	4·30	100	7·16	100	9·45	100	11·18	100	17·66	100
4·48	59	3·90	66	4·27	47	3·57	70	4·39	78	4·77	59	4·00	6
4·07	24	5·75	17	4·37	30	4·48	29	3·73	36	3·66	56	3·37	6
3·83	21	3·74	16	3·49	29	2·38	16	3·02	34	4·19	51	4·67	6
3·37	13	2·88	13	4·15	24	1·91	9	3·09	24	5·18	50	5·00	6
5·12	6	3·83	10	4·19	17	3·95	9	4·31	22	3·69	49	4·62	5
3·52	6	2·79	10	6·46	17	1·42	7	3·83	18	4·84	44	7·37	5
2·70	6	2·40	9	3·85	15	4·32	7	10·39	15	4·46	42	3·70	5
2·55	5	2·57	8	3·86	15	2·31	7	4·50	14	3·54	42	2·67	4
3·50	5	2·46	6	3·91	10	1·71	4	4·09	14	2·74	28	3·23	4

* This table contains only the 10 most intense lines

EXPERIMENTAL

The measurements of the ^{31}P n.m.r. chemical shifts were made with a Varian Model V–4300B n.m.r. high resolution spectrometer, utilizing a Varian Magnet, Model V–4012–HR, and were reproducible to ±1 p.p.m. The ^{31}P spectra were obtained with a 16·2 mc/s radio-frequency oscillator using a field of about 9395 G.

The infra-red spectra were recorded from 5000 to 660 cm^{-1} (NaCl region) and 1000 to 400 cm^{-1} (KBr region) with a Beckman IR-4 Double Beam spectrometer. The liquid materials were examined as film between NaCl(KBr) disks and the solids as KBr pellets.

The X-ray patterns were recorded with a Norelco X-Ray Diffractometer with copper K-α radiation (nickel filter), wavelength $\lambda = 1{\cdot}541$ Å; I/I_1 was recorded by a scintillation counter diffractometer.

* RICHARD *et al.*[11] attribute a band at 800 cm^{-1} to the P–C–P linkage in diphosphine dioxides.

[11] J. J. RICHARD, K. E. BURKE, J. W. O'LAUGHLIN and C. V. BANKS, *J. Amer. Chem. Soc.* **83**, 1722 (1961).
[12] A. M. KINNEAR and E. A. PERREN, *J. Chem. Soc.* 3437 (1952).

Preparation of methylenediphosphonic acid. Tetra-ethyl methylenediphosphonate and the corresponding acid were prepated according to the procedure given by SCHWARZENBACH and ZURC[2]. The use of potassium diethylphosphate instead of sodium diethylphosphite had no effect on the yield.

Preparation of dimethylenediphosphonic acid. Diethyl β-chloro-ethylphosphonate was obtained by esterification of β-chloro-ethylphosphonic dichloride. The latter was prepared by the method of KINNEAR and PERREN[12] in 78 per cent yield. In a three-necked flask fitted with reflux condenser, dropping funnel and stirrer 183 g (0·92 mole) of diethyl β-chloro-ethylphosphonate was slowly added to an ether solution of potassium diethyl phosphite (prepared from 35·7 g (0·90 mole) potassium and 127 g (0·93 mole) of diethyl phospite in 750 ml of diethyl ether). After refluxing for 1 hr and separating the potassium chloride the solution was fractionally distilled, yielding 166 g (0.55 mole) tetra ethyl dimethylenediphosphonate. The latter gave the correponding acid on refluxing with conc. HCl.

Preparation of tri- to decamethylenediphosphonic acid. One mole of α,ω-dibromo-alkane, $Br(CH_2)_n Br$, $n = 3, 4, 5, 6$ and 10, was added through a dropping funnel to a stirred solution of two moles of sodium(potassium) diethyl phosphite in diethyl ether (diglyme). After refluxing for 2 hr and removing of the sodium (potassium) bromide the residual solution was fractionally distilled in vacuo yielding the tetra-ethyl polymethylenediphosphonate as colourless liquid. Refluxing of the latter ester with conc. HCl gave the corresponding acid which could be recrystallized from water (the acid $n = 10$ crystallized from ethyl alcohol water mixtures).

Acknowledgement—This research was supported in part by the Air Research and Development Command, United States Air Force, under contract AF33(616)–6950 monitored by the Materials Laboratory, Wright Air Development Centre, Wright Patterson Air Force Base, Ohio. We are also indebted to Mr. D. BISNO for some of the experimental work and Mr. J. T. Yoder for the n.m.r. measurements.

J. Inorg. Nucl. Chem., 1961, Vol. 22, pp. 305 to 323. Pergamon Press Ltd. Printed in Northern Ireland

REACTIONS OF CO-ORDINATED LIGANDS—II

PREPARATION OF A NEW CLASS OF IRON ISONITRILE COMPLEXES, $(RCH_2NC)_5Fe^{II}CNX$

W. Z. HELDT
E. I. du Pont de Nemours and Company, Inc.
Explosives Department, Experimental Station Laboratory
Wilmington, Delaware

(*Received* 20 *December* 1960; *in revised form* 9 *March* 1961)

VOL. 22 1961

Abstract—A convenient method for the preparation of a new class of iron isonitrile complexes, $(RCH_2NC)_5Fe^{II}CNX$(I), from alkali ferrocyanides and alkyl halides activated in the α-position by a carbon–carbon double bond is described. The structure proof for $(C_6H_5CH_2NC)_5FeCNBr$ is given by its conversions to $(C_6H_5CH_2NC)_4Fe(CN)_2$ and $(C_6H_5CH_2NC)_6FeBr_2$; hydrolysis to benzylamine; reduction to benzylamine and N-methylbenzylamine, and oxidation to benzoic acid. The preparation of $(RCH_2NC)_4Fe(CN)_2$(II) and $(RCH_2NC)_6FeBr_2$(III) complexes from (I) or directly from alkali ferrocyanides is given. The probable reaction mechanism of this reaction is the displacement of halide from the alkyl halide by the ferrocyanide anion or the partially alkylated ferrocyanide anion. Both the ionization of the alkyl halide and the nucleophilicity of the anion appear to influence the rate of the reaction.

IN a previous communication[1] we have described attempts to displace the isonitrile group in an iron isonitrile complex by hydrogen cyanide. The decomposition of the iron isocyanide–cyanide complex was a complex reaction which appeared to be catalysed by impurities deposited on the walls of the reaction vessel. Since iron isonitriles are reported to be stable compounds,[2] it is the purpose of this paper to develop a reliable synthesis of iron isonitrile complexes for the study of their reactions. This paper describes the synthesis of the heretofore unknown class of iron isonitrile complexes, $(RCH_2NC)_5Fe^{II}CNX$ and their conversion to $(RCH_2NC)_4Fe^{II}(CN)_2$ and $(RCH_2NC)_6Fe^{II}Br_2$.

EXPERIMENTAL

Preparation of $(C_6H_5CH_2NC)_5FeCNBr\cdot H_2O$ (*Procedure A*)

Potassium ferrocyanide trihydrate (General Chemical Division, Allied Chemical and Dye Corp., New York, N.Y.) was dried at 150°C/24 mm Hg for 4 hr. (Found: (Karl Fischer) = 0·27% H_2O. Calc. for the monohydrate = 4·66).

Potassium ferrocyanide, 61·5 g (= 0·166 mole) and benzyl bromide, 171 g (= 1·0 mole) were stirred and heated on a steambath for 55 hr in a three neck flask closed by a calcium chloride drying tube. The brown, viscous reaction mixture was washed with 2 l. of petroleum ether, and the petroleum ether-insoluble brown oil was extracted with 2 × 500 ml of boiling chloroform; the last chloroform extracts were only slightly yellow. The chloroform-insoluble material, 144 g, was neglected. The chloroform extracts were evaporated to dryness under vacuum, without heating. The brown residue was dissolved in 150 ml of boiling methyl ethyl ketone; upon cooling yellow crystals of $[(C_6H_5CH_2NC)_5FeCN]Br\cdot H_2O$ crystallized out. (In several cases when the reaction time was

[1] W. Z. HELDT, *J. Org. Chem.* In press.
[2] L. MALATESTA, *Progress in Inorganic Chemistry* (Edited by F. A. Cotton) Vol. 1, p. 320. Interscience, New York (1959).

extended beyond 55 hr, the brown oil could not be crystallized from methyl ethyl ketone. It was then pressed on porous plate and allowed to dry overnight. The brown semisolid then always crystallized from methyl ethyl ketone). After 5–10 recrystallizations from methyl ethyl ketone and drying at 0·1 mm/25°C, m.p. 101–104°C, 109 g of slightly yellowish long needles were obtained. (Found: C, 64·36, 63·76; H, 4·98, 4·79; N, 10·63, 10·88, 10·80; Fe, 7·30, 7·39; Br, 10·50, 9·65. Calc. for $(C_6H_5CH_2NC)_5FeCNBr{\cdot}H_2O$: C, 64·33; H, 4·87; N, 10·98; Fe, 7·30; Br, 10·44%).

The infra-red spectrum of this compound is recorded in Fig. 1b; prolonged (71·2 hr) drying at 0·1 mm/25°C, removed the water of crystallization in the above complex and the melting point increased to 111–112°C. (Found: C, 65·78; H, 5·15; N, 11·27; Fe, 7·83; Br, 9·66, 11·35. Calc. for $(C_6H_5CH_2NC)_5FeCNBr$: C, 65·87; H, 4·72; N, 11·24; Fe, 7·47; Br, 10·69%).

Distillation of the pet. ether extracts at 10 mm Hg yielded 13 g of benzylbromide and 1·5 g of an amide, b.p. 140–163°C/10 mm, probably N-benzyl formamide.

Molecular weight determinations of the anhydrous compound (mol. wt. = 747) in nitrobenzene (20 g) by the freezing point method indicate dissociation into two ions:

mg of (I)	94	161	308	495	525
mol. wt.	380	350	371	565	500

Cryoscopic molecular weight determinations in diphenyl amine or bromoform indicated a mol. wt. of 642 ± 12, or 729 ± 9 respectively; as expected, this was a much lower dissociation than in nitrobenzene.

Conductivity determinations in purified nitrobenzene, using a dip-type cell and bright Pt electrodes,[3] gave the following results:

TABLE A.—CONDUCTIVITY DETERMINATIONS IN NITROBENZENE AT 25°C

Concentration		Specific conductance in nitrobenzene (Ω^{-1})
$[(C_6H_5CH_2NC)_5FeCN]Br$	5×10^{-5} molar	$1{\cdot}48 \times 10^{-6}$
$[(C_6H_5CH_2NC)_5FeCN]Br$	5×10^{-4} molar	$1{\cdot}44 \times 10^{-5}$
$[(C_6H_5CH_2NC)_5FeCN]Br$	1×10^{-3} molar	$2{\cdot}58 \times 10^{-5}$
$(CH_3CH_2)_4NCl$	5×10^{-5} molar	$1{\cdot}74 \times 10^{-6}$
$(CH_3CH_2)_4NCl$	1×10^{-3} molar	$3{\cdot}6 \times 10^{-5}$

These data are in agreement with specific conductance in nitrobenzene as reported for other univalent: univalent ions.[3,4] Therefore, the complex must be a 1 : 1 electrolyte in nitrobenzene.

No decomposition of the complex took place over a period of three years when it was exposed to sunlight and "atmospheric conditions" in the laboratory. A single crystal of the complex was also stable during extensive exposure to X-rays.[5]

Preparation of $(C_6H_5CH_2NC)_5FeCNBr$ *and* $(C_6H_5CH_2NC)_4Fe(CN)_2$ (*Procedure B*)

To 184 g (= 0·5 moles) of $K_4Fe(CN)_6$ were added 342 g (2·0 moles) of benzyl bromide and the heterogeneous reaction mixture was stirred on a steambath for 47 hr in a vessel closed by a calcium chloride drying tube. The reaction mixture was then treated with 500 ml of petroleum ether to remove the non-reacted benzyl bromide and the petroleum ether extracts were neglected. The petroleum ether insoluble material was extracted with 3 × 500 ml of boiling chloroform. The chloroform extracts were then evaporated to near dryness, yielding a yellow solid FI 152 g m.p. 165–200°C, and a viscous brown oil as the filtrate (FII). The crystalline material (FI) was boiled with 500 ml of methyl ethyl ketone and was filtered hot. The material, soluble in hot methyl ethyl ketone, crystallized upon evaporation of the solvent to about 100 ml, yielding 60 g of yellow crystals. After drying at 25°C/1·0

[3] R. S. NYHOLM and A. KABESH, *J. Chem. Soc.* 38 (1951).
[4] C. R. WISCHONKE and C. A. KRAUS, *J. Amer. Chem. Soc.* **69**, 2472 (1947).
[5] A. G. SCOTT. Private communication (1958).

mm Hg for several hours, the substance melted at 100–102°C. (Found: C, 63·73; H, 4·99; N, 10·90; Fe, 7·46. Calc. for $(C_6H_5CH_2NC)_5FeCNBr\cdot H_2O$: C, 64·33; H, 4·87; N, 10·98; Fe, 7·30%).

The infra-red spectrum of this material was identical with the infra-red spectrum with the previously prepared $(C_6H_5CH_2NC)_5FeCNBr\cdot H_2O$.

The methyl ethyl ketone insoluble fraction, 95 g, was recrystallized twice from chloroform and carbon tetrachloride; after drying at 25°C/1·0 mm Hg for 3 hr, it melted at 229·5–230·0°C.

(Found C, 70·88, 70·64; H, 4·93, 5·14; N, 13·69, 13·70; Fe, 9·82, 9·60; Br, 0%; mol. wt., 520,

Infrared spectra in $CHCl_3$ of $(C_6H_5CH_2NC)_6FeBr_2$ (a); $(C_6H_5CH_2NC)_5FeCNBrH_2O$ (b); $(C_6H_5CH_2NC)_4Fe(CN)_2$ (c)

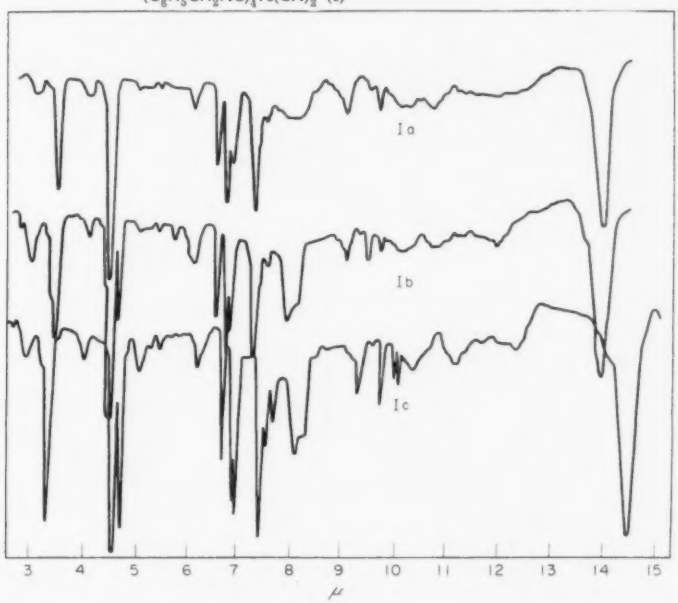

FIG. 1.

530 (cryoscopic). Calc. for $(C_6H_5CH_2NC)_4Fe(CN)_2$: C, 70·96; H, 4·90; N, 14·60; Fe, 9·71%; mol. wt., 576).

The infra-red spectrum of this compound is recorded in Fig. 1c; the filtrates FII were evaporated to dryness and were crystallized partially from ethylene glycol dimethyl ether. The crystalline material, 61 g, was recrystallized from chloroform and carbon tetrachloride. After several recrystallizations from methyl ethyl ketone, the material had a m.p. 100–102°C. This material did not depress the melting point of $(C_6H_5CH_2NC)_5FeCNBr\cdot H_2O$ upon admixture, and the infra-red spectra of both samples were superimposable.

Preparation of $(p\text{-}ClC_6H_4CH_2NC)_5FeCNBr$ (*Procedure C*)

p-Chlorobenzyl bromide was prepared by the bromination of *p*-chlorotoluene at 160°C according to the procedure of SHOESMITH[6] in 70 per cent conversion, b.p. 91–129°C/10 mm. This material yielded the pure *p*-chlorobenzyl bromide after recrystallization from petroleum ether, m.p. 43–45°C. *p*-Chlorobenzyl bromide, 51·2 g (0·25 mole) and 18·3 g (0·05 mole) of $K_4Fe(CN)_6$ were heated on a steambath for 60 hr. The brown reaction mixture was then extracted with 3 × 100 ml of petroleum ether and the petroleum ether-insoluble brown oil was extracted with 3 × 150 ml of boiling chloroform, the last extracts being only slightly yellow. The chloroform insoluble material, 23 g, was neglected. The chloroform extracts were evaporated to dryness to yield 19 g of brown oil, which failed to crystallize. The chloroform extract residues were dissolved then in the least amount of chloroform and were chromatographed on 200 g of alumina.

[6] J. B. SHOESMITH and R. H. SLATER, *J. Chem. Soc.* 219 (1926).

TABLE 1.—REACTION OF $K_4Fe(CN)_6$

Alkylhalide (moles)	$K_4Fe(CN)_6$ (moles)	Solvent	Time (hrs)	Temp. (°C)	Isonitrile complex isolated Formula	Conv. crude (g)	M.P.[1]
$C_6H_5CH_2Br$ (2·0)	(·334)	none	(a) 48 (b) 120	100 25	$(C_6H_5CH_2NC)_5FeCNBr$	35	110–112
					$(C_6H_5CH_2NC)_6FeBr_2\cdot H_2O$	30	119–121·2
$C_6H_5CH_2Br$ (2·0)	(0·5)	none	47	100	$(C_6H_5CH_2NC)_4Fe(CN)_2$	95	229·5–230
					$(C_6H_5CH_2NC)_5FeCNBr\cdot H_2O$	121	100–102
$oCH_3C_6H_4CH_2Br$ (0·5)	(0·1)	none	45	100	$(oCH_3C_6H_4CH_2NC)_4Fe(CN)_2\cdot H_2O$	33	247–249·5
					$(oCH_3C_6H_4CH_2NC)_5FeCNBr$	37	143·4–145·6
$mCH_3C_6H_4CH_2Br$ (0·5)	(0·1)	none	45	100	$(mCH_3C_6H_4CH_2NC)_5FeCNBr\cdot H_2O$	39	oil
$pCH_3C_6H_4CH_2Br$ (0·5)	(0·1)	none	45	100	$(pCH_3C_6H_4CH_2NC)_5FeCNBr\cdot H_2O$	72	147·8–149·8
$pClC_6H_4CH_2Br$[2] M.P. 43–45°C (0·25)	(0·05)	none	60	100	$(pClC_6H_4CH_2NC)_5FeCNBr$	12·4	160·2–162·6
$pCH_3CO_2C_6H_4CH_2Br$[3] M.P. 44–48°C (0·25)	(0·05)	none	48	100	$(pCH_3CO_2C_6H_4CH_2NC)_5FeCNBr\cdot H_2O$	2·95	185–186·2
$(C_6H_5)CHBr$[4] M.P. 28°C (0·5)	(0·1)	none	10	100	$[(C_6H_5)_2CHNC]_4Fe(CN)_2$	102·0	242–244
					$[(C_6H_5)_2CHNC]_4FeCNBr$	8·5	122–123·5
$(C_6H_5)_3CBr$ (0·05)	(0·01)	$CHCl_3$ 100 ml	18	reflux	$[(C_6H_5)_3CNC]_5FeCNBr$	6·07	298–300
$CH_2=CHCH_2Br$ (1·0)	(0·17)	none	48	reflux	$(CH_2=CHCH_2NC)_5FeCNBr\cdot H_2O$	85·0	56–58
3-Thenyl Br[5] (0·5)	(0·1)	$CH_3COCH_2CH_3$	48	reflux	$(C_4H_3SCH_2NC)_5FeBr_2\cdot H_2O$ (?)	48·1	oil

(1) Uncorrected. (2) SHOESMITH and SLATER, *J. Chem. Soc.* 219 (1926). (3) FUSAN and COOKE, *J. Amer. Chem. Soc.* 62, 1180 (1940) (4) FRIEDEL, *Bull. Soc. Chim., (France)* series 2, 33, 337 (1880). (5) CAMPAIGNE, *J. Amer. Chem. Soc.* 70, 1555 (1949). (6) Methyl ethyl ketone insoluble, recrystallized from $CHCl_3$–CCl_3. (7) I 6 × 50 ml, 9·65 g; II 6 × 50 ml, 11·69 g; III 4 × 50 ml, 6·26 g; IV 6 × 50 ml, 6·26 g; I and II were rechromatographed but failed to crystallize; after drying at 25°C/0·1 mm Hg submitted to analysis; recrystallized from methyl ethyl ketone. (9) I 10 × 50 24·46 g; II 4 × 50, 0·426 g; III 3 × 50, 0·103 g; IV 3 × 50, 0·347 g; V 4 × 50, 2·95 g. Fraction V was recrystallized several times from methyl ethyl ketone and was dried at 35°C/0·1 mm Hg. (10) Crystallized from chloroform-acetone and dried at 56°C/0·1 mm Hg. (11) Reduce filtrates of (1) to dryness and crystallize residue from $CHCl_3$–CCl_3 by slowly allowing the solvent to evaporate. Recrystallized from $CHCl_3$–CCl_3 and dried at 56°C/0·1 mm

Alumina was prepared by suspending 1 kg (F = 20 mesh alumina; Aluminum Company of America) in 2 l. of water and then adding to this suspension 50 per cent sulphuric acid until the pH of the supernatant liquor stayed at pH = 6·70–7·00 after two hours of rapid stirring. The alumina was then filtered off and was dried at 120–150°C/24 mm in a vacuum oven for 12–14 hr. The dried alumina (10–15 times the weight of the material to be chromatographed) was placed in chloroform. The column was washed with (I) 5 × 50 ml of chloroform, (II) 2 × 50 ml of 50 per cent chloroform acetone, (III) 4 × 50 ml of acetone, (IV) 6 × 50 ml 50 per cent acetone-methanol and 7 × 50 ml of methanol. (All solvents used in this chromatography were "analytical grade".) From fraction I there crystallized 4·45 g of starting material, and FIII yielded on slow evaporation of the solvent and addition of ethyl methyl ketone 12·4 g (27 per cent conversion) of an isonitrile complex. After three recrystallizations from methyl ethyl ketone and drying at 25°C/0·1 mm, the compound melted at 160·2–162·6°C. (Found C, 53·48; H, 3·50; N, 10·34; Fe, 6·65; Cl, 18·84. Calc. for $(p\text{-}ClC_6H_4CH_2NC)_5FeCNBr$: C, 53·54; H, 3·29; N, 9·14; Fe, 6·07; Cl, 19·17%).
Infra-red spectrum ($CHCl_3$): 3·42 (*m*), 4·55 (*vs*), 4·72 (*m*), 6·25 (*w*), 6·68 (*s*), 6·95 (*m*), 7·10 (*m*), 7·45 (*m*) 8·80 (broad), 9·85 (*m*), 13·80 (broad) (μ).

The compounds described in Table 1 were synthesized by either of these three procedures. Details are given in the footnotes to Table 1.

WITH ALKYL BROMIDES

Procedure (see expt.)	Specific magnetic susceptibility $\times 10^6$	Carbon Calcd.	Carbon Found	Hydrogen Calcd.	Hydrogen Found	Nitrogen Calcd.	Nitrogen Found	Iron Calcd.	Iron Found	Bromide Calcd.	Bromide Found	Sulphur or chlorine Calcd.	Sulphur or chlorine Found
B	−0·48	65·87	65·74	4·72	5·08	11·24	11·28	7·47	7·41	10·69	11·35		
B[6]		61·55	61·81	4·74	4·84	8·98	9·09	5·96	6·64	17·07	17·23		
B	−0·39	70·96	70·88 70·64	4·90	4·93 5·14	14·60	13·69 13·70	9·71	9·82 9·60				
B		64·33	63·73	4·87	4·99	10·98	10·00	7·30	7·46				
B[6]		70·15	69·33 69·36	5·89	6·11 6·12	12·91	12·37 12·42	8·54	8·40 8·56				
B		67·62	67·18 67·12	5·55	5·65 5·85	10·28	11·67	6·83	7·07	9·77	8·44 8·67		
C[7]		66·11	66·02	5·67	5·92	10·06	9·44	6·68	6·09	9·56	10·14 10·15		
A[8]	−0·32	66·11	66·78	5·67	5·67	10·06	10·26	6·68	6·98	9·56	9·29		
C		53·54	53·48	3·29	3·50	9·14	10·34	6·07	6·65	8·64	6·95	Cl 19·17	Cl 18·84
C[9]		58·01	57·29	4·48	4·72	7·95	8·22	5·28	5·28	7·56	7·95		
B[10]		79·08	78·63 78·69	5·04	5·27 5·21	9·54	8·90 9·42	6·34	6·66				
B[11]		73·24	74·29	4·74	4·95	7·49	7·22	5·96	6·23	8·55	8·49		
C[12]		80·41	80·90	5·01	5·25	6·57	6·71	3·70	3·89	5·29	4·08		
A[13]		50·72	50·35	5·07	5·46	16·91	16·23	11·23	10·58	16·07	15·85		
C[14]		42·40	42·14	3·20	3·23	8·24	8·36 8·20	6·57	6·94			S 18·87	S 17·19

Hg. (12) I 6 × 50, 7·894 g; II 6 × 50, 3·33 g; III 4 × 50, 0·022 g; IV 2 × 50, 0·005 g; V 4 × 50, 1·415 g. Fraction II was recrystallized about 5 times from $CHCl_3$–CCl_3 and was dried at 56°C/0·1 mm Hg. (13) Evaporate $CHCl_3$ extract to dryness; crystallized from acetone at 0°C after about 2–4 months. (14) I 20 × 50, 1·2 g; II 20 × 50, 0·979 g; III 20 × 50, 7·03 g; IV 40 × 50, 28·5 g; V 40 × 50, 28·5 g. Fractions III–V contained the isonitrile complex; the chromatography was repeated, whereby the purest isonitrile fraction was isolated in IV but which failed to crystallize. This material was dried for analysis 25°C/0·1 mm. IR (CHCl) 3·38 (s), 350 (m), 4·56 (vs), 4·72 (m), 5·60 (w), 5·80 (vw), 6·72 (w), 6·95 (w), 7·08 (w), 7·24 (m), 7·42 (m), 7·55 (m), 8·72 (m), 9·05 (s), 9·70 (m), 11·68 (m), 12·05 (m).

Permanganate oxidation of $(C_6H_5CH_2NC)_5FeCNBr{\cdot}H_2O$

To a solution of 24·0 g (= 0·6 mole) of sodium hydroxide in 300 ml of water were added 15·8 g (= 0·1 mole) of potassium permanganate. The solution was cooled to room temperature, 7·3 g (= 0.0095 mole) of $[(C_6H_5CH_2NC)_5FeCN]Br{\cdot}H_2O$ were added and the reaction mixture was heated to 100°C for 15 min. The heating mantle was then removed and when the reaction mixture reached 60°C, methyl alcohol was added until the excess permanganate decolorized. The reaction mixture was filtered from the MnO_2 and the filtrate was cooled to 10°C and acidified with 50 ml of concentrated HCl. After the filtrate had stood for one hour on ice the benzoic acid was filtered off. The benzoic acid filtrate was reduced to one-fourth of its volume; upon cooling a little more benzoic acid crystallized out. The total amounts of benzoic acid isolated, after drying at 25°C/1·0 mm Hg were 5·0 g (0·041 mole) or 86 per cent conversion. The benzoic acid was identified by mixed melting point of an authentic sample and by its infra-red spectrum.

Catalytic hydrogenation of $[(C_6H_5CH_2NC)_5FeCN]Br{\cdot}H_2O$

To a solution of 54 g (= 0·07 mole) of $(C_6H_5CH_2NC)_5FeCNBr{\cdot}H_2O$ in 200 ml of methanol in a stainless steel pressure tube were added two teaspoons of Raney-Nickel catalyst and the reaction mixture was kept at 130°C and 195–210 atm pressure of hydrogen for 15 hr. The total hydrogen

absorbed was about 83 atm. To ensure complete hydrogenation two more teaspoons of Raney-Nickel were added and the reaction mixture was kept at 130°C and 480–500 atm pressure for 4·5 hr. The pressure drop was only about 20 atm. The reaction mixture was filtered from the Raney-Nickel catalyst and the catalyst was washed with 5 × 20 ml of methanol. The filtrates were reduced to about 50 ml under vacuum at 20 mm/35°C, whereby a solid residue remained (F A). The liquid portion of the filtrate was distilled through a short distillation column (ca. 10 plates) and all material boiling below 65°C/760 mm was neglected. The higher boiling residue was designated (F B). Fraction A was washed with 3 × 100 ml of ether, then was treated with 2 × 200 ml of boiling chloroform. The chloroform extracts were allowed to come to room temperature, whereby 523 mg of a blue precipitate separated out, which evolved $HCN(H_4Fe(CN)_6$ or polymerization products?) The organic extracts of Fraction A were combined with Fraction B. The chloroform-insoluble portion of Fraction A, 6 g, m.p. 208–215°C, formed a precipitate with silver nitrate, i.e., it was apparently an amine hydrobromide.

When one gramme of this bromide was made alkaline with 30 ml of 20% NaOH and reacted with 1·6 g of *p*-toluenesulphonyl chloride, a tosylate formed. After two recrystallizations from 95 per cent ethyl alcohol and drying, the product melted at 113·5–114·5°C. (Found: C, 64·80; H, 5·95; N, 5·30. Calc. for $C_6H_5CH_2NHSO_2C_6H_4$-p-CH_3: C, 64·34; H, 5·79; N, 5·36%)

A mixed melting point with an authentic sample did not give a melting point depression.

Fraction B was washed 6 × 100 ml with 2N HCl. The organic layer was dried with $MgSO_4$ and was distilled first at 760 mm and subsequently under reduced pressure.

DISTILLATION

Fraction	Boiling point (°C)	Pressure (mm)	Wt distilled (mg)
I	45–69	20	74
II	113–119	20	390
III	121	20	120
			Total 584 mg

The infrared spectra of FII and FIII were identical, indicating the presence of an amide (2·95 μ, 5·95–6·01 μ), presumably N-benzyl formamide.

The HCl extracts were made alkaline; the alkaline solution was extracted with 3 × 300 ml of ether, the ether layers were dried with $MgSO_4$ and distilled through a fractionating column, first under 760 mm and subsequently under reduced pressure.

DISTILLATION

Fraction	b.p. (°C)	Pressure (mm)	Wt. (g) distilled	Analysis (%) Found	Calculated
1	36–61	760	11·8	Note: Contains no amine No ppt. with HCl–ether.	
2	61–183	760	6·9	Note: Yields 7·1 g of amine hydrochloride.	
3	83–88	20	8·0		
4	88–173	20	4·2		
5	173–170	20	4·5	C, 84·00; H, 8·26; N, 7·00	$(C_6H_5CH_2)_2NH$ C, 85·23; H, 7·66; N, 7·10
6	165–175	7	1·5		
7	Residue		2·2	*Note*: No amine, no tosylate, no picrate.	
		Total 27·3			

Fraction 3 was an amine, from this amine only one base-insoluble tosylate could be prepared, m.p. 94·0–94·7°C, which was identical with N-methyl-N-benzyl *p*-toluenesulphonamide. No traces of α-phenyl ethyl amine were detected in Fractions 2, 3, and 4 when these were analysed by vapour phase chromatography.

Hydrolysis of $(C_6H_5CH_2NC)_5FeCNBr\cdot H_2O$ *with* 20 *per cent sulphuric acid in acetic acid*

To a solution of 52·4 g (= 0·5 mole) concentrated sulphuric acid in 160 ml of water was added a solution of 54 g (= 0·07 mole) of $(C_6H_5CH_2NC)_5FeCNBr\cdot H_2O$ dissolved in 100 ml of glacial acetic acid and the heterogeneous solution was refluxed for 49 hr. The mixture became homogeneous after about one day. The reaction mixture was then cooled to room temperature and was poured into a slurry of 70 g (= 0·524 mole) of barium oxide in 100 ml of water. The barium sulphate, which precipitated out, was filtered through a fine fritted funnel. The filtrate was then freeze-dried, the distillate of water and glacial acetic acid being neglected. There remained a residue, which was extracted with 200 ml of acetone and subsequently with 200 ml of absolute ethyl alcohol in a soxhlet extractor. Each extraction was run for three days (Extract A). To ensure the removal of any entrapped organic material in the $BaSO_4$ precipitate, the $BaSO_4$ was extracted with 2 × 500 ml acetone and then with 1 × 500 ml absolute ethanol in a soxhlet, each extraction running for three days; finally the $BaSO_4$ was steam distilled, the distillate being extracted with 3 × 150 ml of ether. All organic extracts were combined with Extract A and were reduced under 5 mm/25°C vacuum to a semi-solid mass (benzylamine boils at about 5 mm/50°C therefore, little or no benzylamine was lost). The semi-solid brown residue was dissolved in 400 ml of chloroform and the chloroform layer was extracted with 3 × 10 ml of 4 N hydrochloric acid. The chloroform layer was then washed with water, dried with $MgSO_4$ and was chromatographed on 500 g of alumina. The column was washed with (I) 800 ml of chloroform, (II) 100 ml 50 per cent chloroform-acetone, (III) 200 ml acetone, (IV) 100 ml 50 per cent acetone–methanol (V) 1200 ml of methanol. Fractions I–VI yielded upon evaporation of the solvent 28·33 g (= 54 per cent) of starting material. Evaporation of FV yielded 8·79 g of a yellow oil which failed to crystallize. Infra-red ($CHCl_3$): 3·00(*s*), 3·40(*s*), 4·52(*vs*), 5·85(*s*), 6·25(*w*), 6·38(*s*), 6·68(*s*), 6·88(*s*), 6·95(*s*), 7·42(*s*), 8·10(*broad*), 8·50(*w*), 9·28(*s*), 9·73(*s*), 11·00(*w*), 14·42(*s*). No traces of an organic acid were detected. The hydrochloric acid extracts were made strongly basic and were extracted with 3 × 200 ml of ether. After being dried with $MgSO_4$, the ether extracts were distilled first at 760 mm and then at reduced pressure.

DISTILLATION

Fraction	b.p. (°C)	Pressure (mm)	Wt. distilled (g)	Remarks
a	96–97	38	0·55	Infra-red indicates an amine
b	97–106	38	1·735	with traces of an amide.
c	106–128	38	1·88	Redistillation (spinning
d	128–141	38	0·25	band column, ca. 50 plates)
e	141	38	0·30	
1	35–98	38	0·20	
2	98–101	38	6·90	
3	101–138	38	4·90	
4	132–135	38	1·40	
5	Residue		1·20	

Fraction 2 yielded only one *p*-toluenesulphonamide, m.p. 114·5–114·9°C.

(Found: C, 63·87; H, 5·92; N, 5·35; S, 12·07. Calc. for $C_6H_5CH_2NHSO_2C_6H_4(p\text{-}CH_3)$: C, 64·34; H, 5·79; N, 5·36; S, 12·27%). The admixture of this sample did not depress the m.p. of an authentic sample of N-benzyl-*p*-toluene sulphonamide. Fractions 3a and 3b consisted only of benzylamine, which was identified as the *p*-toluene sulphonamide. The infra-red spectra of Fractions 3c and3d

VOL. 22 1961

TABLE 2.—SYNTHESIS OF VARIOUS

$(C_6H_5CH_2NC)_5FeCNBr\cdot H_2O$ (mole)	MeX (mole)	Procedure	CH_3OH (ml)	H_2O (ml)	Time (hrs)	Temp. (°C)	M.P.
(0·005)	NaCl (0·05)	E[1]	(100)	(50)	1	25	106–108·5
(0·005)	KI (0·05)	E[2]	(100)	—	1	25	119·2–119·6
(0·009)	KSCN (0·1)	E[2]	(10)	(25)	1	25	110–111·2
(0·009)	$LiClO_4$ (0·1)	E[3]	(50)	(100)	1	25	139–140
(0·009)	$C_6H_5CO_2K$ (0·05)	E[4]	(60)	(25)	1	25	114·5–117
(0·009)	CF_3CO_2Ag (0·01)	D	(40)	(50)	1	25	113–115
(0·005)	Ag_2SO_4 (0·0025)	D[5]	(50)	(150)	5	100	122–124
(0·05)	H_2SO_4 80%, 104 ml	F	—		4	100	156·8–157·8

(1) Column was eluted with I 4 × 50 methyl ethyl ketone, 0·148 g; II 4 × 50 ml 50% methyl ethyl ketone-methanol, 3·01 g; III 4 × 50 ml methanol, 0·083 g, III was recrystallized several timed for methyl ethyl ketone and was dried at 25°C/0·1 mm Hg.

(2) Organic filtrates reduced to dryness and recrystallized from methyl ethyl ketone and dried at 25°C/0·1 mm Hg for analysis.

were identical with N-benzyl formamide; Fractions 3c and 3d were hydrolysed with 90% H_2SO_4 for 2 hr on a steambath yielding only benzylamines, identified as the *p*-toluene sulphonamides.

Anion exchanges in $(C_6H_5CH_2NC)_5FeCNBr$ (*Procedure D, Table* 2)

$[(C_6H_5CH_2NC)_5FeCN]NO_3\cdot H_2O$ was prepared by the addition of a solution of 7·86 g (= 0·01 mole) of $[(C_6H_5CH_2NC)_5FeCN]Br\cdot H_2O$ dissolved in 40 ml of absolute ethyl alcohol to 1·69 g (= 0·01 mole) of silver nitrate dissolved in 10 ml of distilled water. The silver bromide was filtered off and the filtrate was evaporated to dryness under vacuum. The solid residue was dissolved in acetone and CCl_4 was added until the solution became just cloudy. The solution was cooled on dry-ice and was then allowed to stand at room temperature for several days. Two types of rosettes crystallized out, which were separated mechanically: (a) m.p. 85–87°C, (b) m.p. 105–107°C. Fraction (a), 665 mg, was then chromatographed on alumina and eluted in the manner described in Procedure C above. The column was washed with 14 × 50 ml of $CHCl_3$. Fractions 12–14 were recrystallized from $CHCl_3$–CCl_4 and subsequently from methyl ethyl ketone: m.p. 85·5–87·5°C after drying at 0·4 mm/25°C. (Found: C, 66·28, 66·72; H, 4·95, 4·43; N, 12·79; Fe, 7·90. Calc. for $[(C_6H_5CH_2NC)_5FeCN]NO_3\cdot H_2O$: C, 65·89; H, 4·99; N, 13·12; Fe, 7·47%).

Fraction (b), 1·5 g, was dissolved in methyl ethyl ketone and was filtered through alumina suspended in methyl ethyl ketone. The main fraction crystallized from methyl ethyl ketone melted at 106–108°C after drying at 0·4 mm/25°C. Found: C, 67·38, 66·75; H, 4.95, 5·05; N, 13·31, 13·35; Fe, 7·70. Calc. for $[(C_6H_5CH_2NC)_5FeCN]NO_3$: C, 67·50; H, 4·83; N, 13·44; Fe, 7·66%.

Infra-red ($CHCl_3$): 2·98(*w*), 3·37(*m*), 4·62(*vs*), 4·78(*m*), 6·22(*w*), 6·68(*m*), 6·87(*s*), 6·95(*s*), 7·42(*vs*), 8·12(*w*), 9·28(*w*), 9·72(*w*), 9·98(*w*), 12·06(*w*), 14·40(*vs*), 15·15(*s*), (μ).

Procedure E

A compound assumed to be $[(C_6H_5CH_2NC)_5FeCN]SCN$ was prepared by the addition of a solution of 7·1 g (= 0·009 mole) of $[(C_6H_5CH_2NC)FeCN]Br\cdot H_2O$ in 10 ml of methanol to a solution

$(C_6H_5CH_2NC)_5FeCNx\cdot XH_2O$ COMPLEXES

Isonitrile complex isolated	Carbon calcd.	Carbon found	Hydrogen calcd.	Hydrogen found	Nitrogen calcd.	Nitrogen found	Iron calcd.	Iron found	Miscellaneous calcd.	Miscellaneous found
$(L_5FeCN)Cl\cdot 2H_2O$ (?)	66·62	65·24	5·32	4·77	11·37	11·21	7·55	7·57	Cl 4·80	6·39
$(L_5FeCN)I\cdot H_2O$ (?)	60·58	60·65	4·59	4·44	10·34	8·91	6·87	6·87	I 15·62	18·22
$(L_5FeCN)SCN$	69·51	68·91	4·86	4·97	13·51	13·40	7·70	8·07	S 4·42	4·52
$(L_5FeCN)ClO_4$	64·19	64·32	4·60	4·46	10·96	10·81	7·28	7·48	Cl 4·62	4·26
$(L_5FeCN)OH\cdot 5H_2O$	63·56	63·71	5·98	5·15	10·85	11·09	7·21	7·39	Br 0	0
$(L_5FeCN)CO_2CF_3$	66·16	66·49	4·51	5·09	10·75	10·79	7·15	7·63		
$(L_5FeCN)_2SO_4\cdot 2H_2O$	64·28	63·83	4·90	4·99	11·36	11·60	9·06	8·86	S 2·60	2·77
$(L_5FeCN)HSO_4\cdot H_2O$	62·99	63·26	4·88	4·82	10·74	10·61	7·14	7·57	S 4·10	3·90

(3) I 4 × 50 ml chloroform, 6·049 g; II 4 × 50 ml 50% chloroformacetone, 0·580 g; III 4 × 50 ml acetone, 0·874 g; IV 4 × 50 ml 50% acetone-methanol, 0·250 g; V 2 × 50 ml methanol, 0·05 g. I was crystallized several times from methyl ethyl ketone and was dried at 25°C/0·1 mm.

(4) Column eluted with 10 × 50 ml of 90% methyl ethyl ketone-methanol; F 3–4 were recrystallized from methyl ethyl ketone and were dried at 25°C/0·1 mm Hg.

(5) Recrystallized from methyl ethyl ketone and dried at 25°C/0·1 mm Hg.

of 10 g (0·1 mole) of KSCN in 25 ml of water. After 14 days at room tempreature (a slight pinkish colour developed after this time) the solution was evaporated to dryness under vacuum and the residue was extracted with chloroform (3 × 50 ml). The chloroform extracts were washed with water, dried with $MgSO_4$, evaporated to dryness and crystallized from cold methyl ethyl ketone. After several recrystallizations from methyl ethyl ketone, the product melted at 110–111·2°C after drying at 0·1 mm/25°C. (Found: C, 68·91, 68·70; H, 5·15, 4·97; N, 13·40, 12·65; S, 4·52; Fe, 8·07. Calc. for $[(C_6H_5CH_2NC)_5FeCN]SCN$: C, 69·51; H, 4·86; N, 13·51; S, 4·42; Fe, 7·70%.)

Infra-red ($CHCl_3$): 3·38(*s*), 4·62(*vs*), 4·72(*s*), 4·87(*s*), 6·24(*w*), 6·68(*s*), 6·87(*s*), 6·95(*s*), 7·42(*s*), 8·25 (*broad*), 9·30(*w*), 9·75(*w*), 14·40(*s*), 15·15(*m*), (μ).

Procedure F

To 105 ml of 81 per cent sulphuric acid solution cooled to 25°C were added 36 g (0·05 moles) of $(C_6H_5CH_2NC)_5FeCNBr\cdot H_2O$ and the reaction mixture was heated on the steambath for 4 hr. The reaction mixture was then cooled to room temperature and was poured onto 400 ml of water. Forty-two grammes of a yellow, water insoluble oil separated out, which solidified after two washings with about 100 ml fresh batches of water. After three recrystallizations from methyl ethyl ketone and drying at 56°C/0·1 mm Hg, the compound melted at 156·8–157·8°C. (Found: C, 63·26; H, 4·82; N, 9·93; Fe, 7·57; S, 3·90. Calc. for $(C_6H_5CH_2NC)_5FeCNHSO_4\cdot H_2O$: C, 62·99; H, 4·88; N, 10·74; Fe, 7·14; S, 4·10%).

Infra-red ($CHCl_3$): 2·95(*w*), 3·12(*m*), 3·40(*s*), 4·55(*vs*), 4·72(*s*), 6·25(*w*), 6·68(*s*), 6·89(*s*), 6·95(*s*), 7·10(*w*), 7·42(*s*), 8·30(*broad*), 9·50(*s*), 11·65(*broad*), 14·40(*s*), (μ).

Preparation of $(C_6H_5CH_2NC)_4Fe(CN)_2$ *from* $(C_6H_5CH_2NC)_5FeCNBr$

Forty-six grammes (= 0·06 moles) of $(C_6H_5CH_2NC)_5FeCNBr$ were placed into a small still equipped with a graduate cylinder as a receiver and the system was evacuated to 0·4 mm Hg. The

reaction vessel was placed on a steambath and the progress of the reaction was followed by measuring the amount of benzyl bromide collected in the still.

DISTILLATION (100°C/0·4 mm Hg)

Time (min)	Wt. distilled (g)	Reaction (%)
0	0	0
93	0·34	3
140	1·02	10
228	2·37	23
408	4·94	48
618	5·31	51
1000	7·00	68

The yellow residue from the distillation was extracted with 3 × 150 ml of boiling methyl ethyl ketone and the solution was filtered hot. The methyl ethyl ketone insoluble material, 25 g, (70 per cent conversion melted at 245–249°C. After one recrystallization from $CHCl_3$–CCl_4, the material had a m.p. 228–230°C. The specimen did not depress the melting point of $(C_6H_5CH_2NC)_4Fe(CN)_2$ prepared above and their infra-red spectra (Fig. 1c) were identical.

Reaction of $(C_6H_5CH_2NC)_5FeCNBr$ *with an excess of benzyl bromide*

A mixture of 3·6 g (= 0·005 mole) of $(C_6H_5CH_2NC)_5FeCNBr$, m.p. 111–112°C, was heated with 10 g (= 0·06 mole) of benzyl bromide on a steambath for 12 hr. The brown reaction mixture was then washed with petroleum ether (2 × 50 ml) and ether (1 × 50 ml) in order to remove the excess benzyl bromide. The oily residue was taken up in boiling methyl ethyl ketone and was filtered from a trace of insoluble material (I). Upon cooling there crystallized in two crops 3·85 g of a solid (II) m.p. 120–125°C. Fraction I was recrystallized from chloroform yielding ~700 mg of yellowish crystals, m.p. 130–135°C. The second band present in the starting material at 4·72 μ almost disappeared in this complex, and the infra-red spectrum was almost identical with $(C_6H_5CH_2NC)_6FeBr_2$. Fraction II was chromatographed on 30 g of alumina suspended in chloroform. Elution of the column with chloroform and 50 per cent chloroform acetone yielded 1·8 g of starting material. Further elution of the column with 50 per cent acetone-methanol yielded 1·7 g of a material, m.p. 120–130. After several recrystallizations from methyl ethyl ketone, the material melted at 134·2–135·2°C, after drying at 25°C/0·1 mm Hg. (Found: C, 61·84; H, 4·75; Br, 17·40; Fe, 6·64; N, 9·09. Calc. for $(C_6H_5CH_2NC)_6FeBr_2$: C, 62·76; H, 4·61; N, 9·15; Fe, 6·08; Br, 17·40%).

The infra-red spectrum of this material was identical with $(C_6H_5CH_2NC)_6FeBr_2$. Although the melting point was different from the $(C_6H_5CH_2NC)_6FeBr_2$ prepared above, probably these two materials represent two dimorphic forms of the same compound.

Hydrogenation of $(C_6H_5CH_2NC)_6FeBr_2$ *with Raney-nickel*

$(C_6H_5CH_2NC)_6FeBr_2$, m.p. 119–121·2°C, 10 g (0·011 mole), prepared from benzyl bromide and potassium ferrocyanide, was dissolved in 70 ml of absolute methanol, and then one half teaspoon Raney-Nickel catalyst was added to this solution. The reaction mixture was pressurized in a stainless steel vessel with 600 atm H_2 and was heated for 6 hr at this pressure. A total of 35 atm H_2 was consumed after this time. The stainless steel vessel was washed thoroughly with methanol and the organic liquors were filtered from the catalyst and were evaporated to dryness under vacuum. In the residue there remained a compound, 3·8 g, which crystallized when washed with ether and after chromatography on alumina melted at 167·5–168°C. (Found: C, 47·75; H, 5·99; N, 7·00. Calc. for $C_6H_5CH_2NHCH_3 \cdot HBr$: C, 47·54; H, 5.98; N, 6·93%).

The distillate and the ether wash of the residue were combined and were distilled at 15 mm Hg. Fractions a–c reacted with *p*-toluenesulphonyl chloride to yield only one *p*-toluenesulphonate, after several recrystallizations, m.p. 94·0–94·5°C. (Found: C, 65·00; H, 6·45; N, 4·99. Calc. for $C_{15}H_{17}NSO_3$: C, 65·42; H, 6·22; N. 5·09%).

The sample did not give any melting point depression with an authentic sample of N-benzyl N-methyl *p*-toluenesulphonamide. The total material accounting in this experiment was about 90 per cent.

DISTILLATION

Fraction	b.p. (°C)	Wt. distilled (g)	n_D^{29}
a	70–75	1·89	1·5180
b	75–90	1·29	1·5238
c	90–100	0·39	1·5272
		3·57	

Reaction of $(C_6H_5CH_2NC)_6FeBr_2$ *with* $LiClO_4$

To a solution of 3·0 g (= 0·0033 mole) of $(C_6H_5CH_2NC)_6FeBr_2$, m.p. 119–121·2°C, in 50 ml of absolute methanol were added 5·3 g (0·05 mole) of $LiClO_4$ and the reaction mixture was evaporated to dryness. The residue was extracted with $CHCl_3$ several times, was filtered and the filtrate was chromatographed on 100 g of alumina (see above) suspended in $CHCl_3$. The first three fractions, 150 ml, eluted with $CHCl_3$, 3·184 g, m.p. 160–165°C were recrystallized several times from methyl ethyl ketone. After drying at 25°C/0·1 mm Hg, the compound melted at 163·5–164°C. (Found: C, 60·57; H, 4·86; N, 8·14; Fe, 5·68; Cl, 7·06. Calc. for $(C_6H_5CH_2NC)_6Fe(ClO_4)_2$: C, 60·19; H, 4·42; N, 8·77; Fe, 5·83; Cl, 7·41%).

Infra-red ($CHCl_3$): 3·39(*m*), 4·52(*vs*), 6·25(*w*), 6·72(*m*), 6·92(*m*), 7·00(*m*), 7·45(*m*), 9·18(*vs*), 14·45(*vs*), (μ).

Reaction of benzyl isonitrile with $Fe(ClO_4)_2 \cdot 6H_2O$

Benzyl isonitrile was prepared according to the procedure of HOFMAN[7], from benzyl amine and chloroform, b.p. 122–125°C/50 mm, infra-red strong band at 4·55 μ.

To a solution of 3·6 g (= 0·01 mole) of $Fe(ClO_4)_2 \cdot 6H_2O$ in 50 ml of absolute methanol was added at room temperature with stirring a solution of 8·4 g (0·072 mole) of benzylisonitrile in 50 ml of methanol. Immediately the yellow reaction mixture turned red but no precipitate appeared. The solvent was reduced to about one quarter of its volume and was placed in the refrigerator. After about one week, yellow crystals separated out, 8·2 g or 90 per cent. After two recrystallizations from methyl ethyl ketone and drying at 25°C/0·1 mm, the compound melted at 163·2–165·3°C. (Found: C, 60·50; H, 4·72; N, 8·73; Fe, 6·19; Cl, 7·35. Calc. for $(C_6H_5CH_2NC)_6Fe(ClO_4)_2$: C, 60·19; H, 4·42; N, 8·77; Fe, 5·83; Cl, 7·40%).

This sample did not give a melting point depression with the diperchlorate prepared above.

Reaction of $K_3Fe(CN)_6$ *with trityl bromide*

To 3·38 g (0·01 mole) of $K_3Fe(CN)_6$ (dried at 150°C/0·1 mm) in 100 ml of dry chloroform were added 16·15 g (0·05 mole) of trityl bromide and the reaction mixture was refluxed for 66 hr. The reaction mixture was cooled and was filtered from the chloroform insoluble material. The residue was extracted with 100 ml of boiling chloroform, the organic extracts were combined and were placed on a column prepared from 250 g of alumina (see above) suspended in chloroform. The column was eluted with 4 × 100 ml of chloroform (I), 4 × 100 ml of 50 per cent chloroform–acetone (II), 5 × 100 ml acetone (III) and finally with 2 × 100 ml of 50 per cent acetone–methanol (IV). Only one fraction was isolated from (I) and (II), 18·4 g (wet) which crystallized from chloroform–carbon tetrachloride and dried at 25°C/0·1 mm Hg, m.p. 291–303°C. Two recrystallizations from methyl ethyl ketone and drying at 80°C/0·1 mm Hg yielded a compound with a m.p. 303–306·5°C. (Found: C, 76·10; H, 4·77; N, 6·90; Fe, 4·52; Br, 6·32. Calc. for $[(C_6H_5)_3CNC]_4Fe^{III}(CN)_2Br$: C, 77·84; H, 4·78; N, 6·64; Fe, 4·41; Br, 6·33%).

Specific magnetic susceptibility $\chi = (+)\ 1{\cdot}46 \times 10^{-6}$ c.g.s. at 26°C.

[7] A. W. HOFMANN, *Ann*, **144**, 114 (1867).

RESULTS AND DISCUSSION

A. *Physical properties of* $(C_6H_5CH_2NC)_5FeCNBr$

When a mixture consisting of 1 mole of anhydrous potassium ferrocyanide and 5 mole of benzyl bromide is vigorously stirred on a steambath for 40–55 hr, a brown, semisolid product is formed (see Fig. 2 and Table 1). When the reaction mixture is processed, a greenish-white solid is obtained. This material is insoluble in benzene and water but dissolves readily in chloroform acetone and alcohol. Ultimate analysis

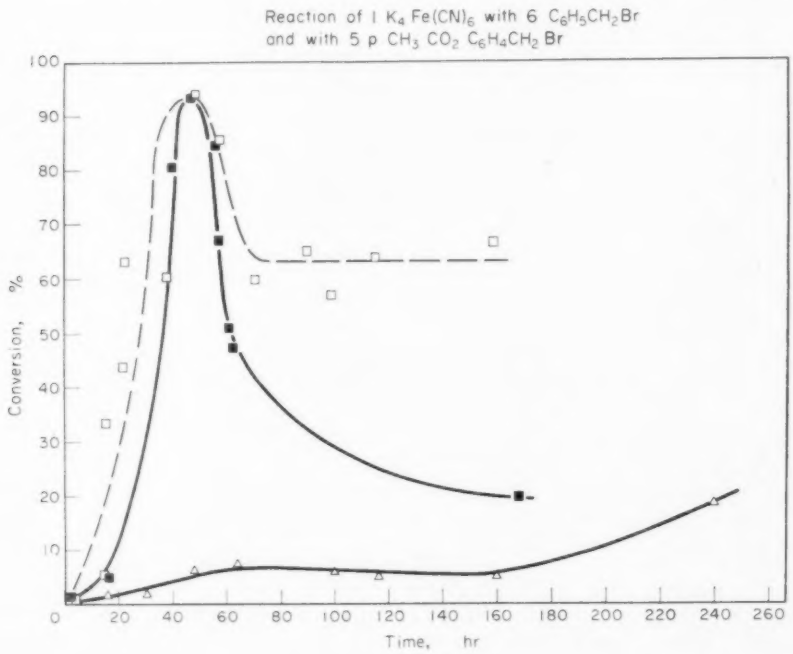

FIG. 2.

of this material corresponds to the empirical formula $[(C_6H_5CH_2NC)_5Fe^{II}CN]Br$(I). Molecular weight determinations of the monohydrate of I (mol. wt. 765·5) by the single crystal X-ray diffraction method indicated a molecular weight of 775.[5] Molecular weight determinations and conductivity measurements in nitrobenzene indicated that I dissociates into two univalent ions in this solvent.

The infra-red spectrum of the hydrate of I (Fig. 1b) exhibits peaks at 3·00, 4·56 and 4·72 μ. These may be interpreted as OH stretching frequency (3·00 μ)[8], C≡N stretching frequency for either a nitrile or an isonitrile ligand[8,9] (4·56 μ) and a C≡N stretching frequency for an inorganic cyanide (4·72 μ)?

Complex I is diamagnetic; the specific magnetic susceptibility χ is (−) 0·48 × 10^{-6} c.g.s. at 26°C (see also Table 1).

B. *Structure proof for* $(C_6H_5CH_2NC)_5FeCNBr$

The structure proof for $(C_6H_5CH_2NC)_5FeCNBr$ is summarized in Fig. 3.

[8] L. J. BELLAMY, *The Infra-red Spectra of Complex Molecules*. J. Wiley, New York (1958).
[9] I. UGI and R. MEYR, *Ber. Dtsch. Chem. Ges.* **93**, 239 (1960).

When I was dissolved in methanol and an excess of a foreign anion was added a metathetical reaction took place in which the bromide ion was exchanged with the foreign anion added.

$$[(C_6H_5CH_2NC)_5FeCN]Br{\cdot}H_2O + NaX \rightarrow [(C_6H_5CH_2NC)_5FeCN]X{\cdot}H_2O + NaBr$$
$$= Cl, I, SCN, ClO_4, OH, HSO_4X$$

The bromide ion must therefore serve as anion for the monopositive

$$[(C_6H_5CH_2NC)_5FeCN]^{\oplus}$$

complex ion. The products of metathesis are crystalline materials, which may or may not contain water of hydration. The presence of water in the complexes was shown by ultimate analysis, infra-red spectra, nuclear magnetic resonance spectra and, in case of $X = NO_3$ and Br, by preparation of both the anhydrous and hydrated complexes. Potassium benzoate yielded the corresponding hydroxide ($X = OH$) as the only product of metathesis, instead of the expected benzoate ($X = C_6H_5CO_2$).

VOL. 22 1961

The relatively high water content of these compounds suggests a clathrate structure for these compositions. POWELL and BARTINDALE found earlier that a similar compound, $(CH_3NC)_6Fe^{II}Cl_2$, forms a clathrate complex with water.[10]

Alternative methods for replacement of the bromide were (a) addition of the silver salt of an anion or (b) heating I with slightly diluted strong acids, such as 80% H_2SO_4 at 100°C. The preparations of various $(C_6H_5CH_2NC)_5FeCNX{\cdot}xH_2O$ salts are summarized in Table 2 and the three methods employed are described in some detail in the Experimental Part.

Oxidation of I with alkaline permanganate yielded 4·3 moles of benzoic acid per mole of I. This evidence is in agreement with the formula assigned to I.

The cyano penta-benzylisonitrile iron (II) cation is extremely stable toward acids such as warm conc. H_2SO_4 and in 80% H_2SO_4 to about 120°C. At higher temperatures decomposition of the complex takes place. Partial hydrolysis of I (about 30 per cent) took place when I was refluxed with 20% H_2SO_4 in aqueous acetic acid for 49 hr. When the reaction mixture was processed 28·23 g of I were recovered, benzyl amine and N-benzyl formamide were identified in about 30 per cent conversion and a new isonitrile complex was formed in about 10–15 per cent conversions. This new isonitrile complex has only one cyanide band at 4·55 μ, the second cyanide peak present in the starting material at 4·72 μ and tentatively assigned to the inorganic cyanide group having disappeared.

A potentiometric titration of I in liquid ammonia with a standard solution of potassium in liquid ammonia, an experiment performed by WATT of the University of Texas,[11] clearly indicated only a one-electron reduction. This reduction could yield two distinctly different types of complexes (assuming no reduction of double bonds takes place):

$$[(C_6H_5CH_2NC)_5Fe^{II}CN]Br + K \rightarrow (C_6H_5CH_2NC)_5Fe^{I}CN + KBr$$

or
$$[(C_6H_5CH_2NC)_5Fe^{II}CN]Br + K \rightarrow (C_6H_5CH_2NC)_5Fe^{I}Br + KCN$$

[10] H. M. POWELL and G. W. R. BARTINDALE, *J. Chem. Soc.* 799 (1945).
[11] G. W. WATT. Private communication (1957).

A larger scale reduction in dried liquid ammonia with potassium in a closed system yielded an oil, which after chromatography on alumina, yielded a reddish material which thus far could not be crystallized. Qualitative tests with $AgNO_3$ indicate that little or no bromine is present in this material.

Provided that no isomerization precedes the hydrogenation, the hydrogenation of benzyl isonitrile would yield the following compounds as main constituents:

$$C_6H_5CH_2NC + H_2 \xrightarrow{\text{catalyst}} C_6H_5CH_2NHCH_3 + C_6H_5CH_2NH_2$$

On the other hand, hydrogenation of the benzyl cyanide should yield β-phenylethylamine as the only product of hydrogenation.

Hydrogenation of I with Raney-Nickel catalyst at 200 atm and 130°C yields only products which are derived from benzyl isonitrile, i.e., benzylamine and N-methylbenzylamines and N,N-dibenzylamine. The materials were identified by ultimate analysis and preparation of their corresponding *p*-toluenesulphonamides. The total material accounting in this experiment was 76–80 per cent. This experiment indicates that the complex does not contain benzylcyanide as a ligand and that the isomerization of complexed benzylisocyanide to benzylcyanide does not take place below 130°C.

Dry distillation of I under reduced pressure yielded $(C_6H_5CH_2NC)_4Fe(CN)_2$ in nearly quantitative conversion. Tetrabenzyl isonitrile iron^{II} cyanide had two cyanide bands at 4·58 μ and 4·78 μ a slight shift of both bands toward higher wave length as compared to I. The higher wave length band assigned tentatively to the inorganic cyanide increased in intensity as compared to the same peak in I (Fig. 1c).

Alkylation of I with benzyl bromide yielded the expected $(C_6H_5CH_2NC)_6FeBr_2$. The structure of this compound has been proven by ultimate analysis; by reduction to the expected benzyl amine and N-methyl benzyl amine; by an independent synthesis (see Experimental Part), and by metathesis to hexabenzyl isocyano iron^{II} diperchlorate. The same compound was prepared independently by the addition of benzyl isonitrile to iron perchlorate hexahydrate according to the method of MALATESTA.[12] (See Fig. 3.) The second cyanide peak at 4·72 μ, characteristic of the

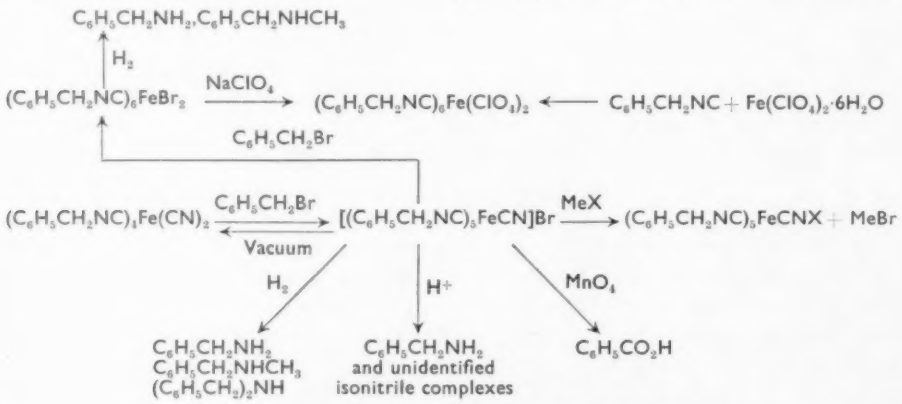

FIG. 3.—Structure proof for $(C_6H_5CH_2NC)_5Fe^{II}CNBr$

inorganic cyanide in I, is no longer present in this compound (Fig. 1a), and the coordinated isonitrile stretching vibration is shifted to 4·50 μ.

[12] L. MALATESTA, A. SACCO and G. PADOA, *Ann. Chim.* (*Rome*) **43**, 622 (1953).

It is perhaps important to point out that most of the isonitrile complexes described in this paper could be isolated in forms having different melting points depending on the solvent used for recrystallization. $(C_6H_5CH_2NC)_6Fe^{II}Br_2$ for example showed polymorphism. When prepared directly from benzyl bromide and $K_4Fe(CN)_6$ and recrystallized from $CHCl_3$–CCl_4 the salt melted at 119–121·2°C. The same compound prepared from I and benzyl bromide and recrystallized from methyl ethyl ketone melted, on the other hand, at 134·2–135·2°C.

C. *Comments on the reaction mechanism*

The alkylation of $K_4Fe(CN)_6$ with alkyl halides is a heterogeneous reaction. All attempts to study this reaction under homogeneous conditions failed. Some of the variables investigated in this reaction are summarized in Table 3. The stirring rate, an important variable in a heterogeneous reaction, was not investigated but was kept constant at approximately 400 rev/min.

Benzyl bromide yields highest conversions to isonitrile complexes if Me in $Me_4Fe^{II}(CN)_6$ is potassium: K > Na = (CH_4) N > Li. No isonitrile complexes are formed with Ca, Ba and Pb^{II} ferrocyanides under similar conditions.

Solvents of high solvolytic power[13] (which favour ionization) have relatively little influence on this reaction (Table 3). Good conversions to I were obtained when the solvent was benzyl bromide, acetonitrile and methyl ethyl ketone, solvents of widely different solvolytic powers. The alkylation of $K_4Fe(CN)_6$ takes place also in nucleophilic solvents[14] such as dimethyl sulphoxide and alcohols (Table 3). The yields are rather poor since the solvent appears to compete with the ferrocyanide for the intermediate carbonium ion. Isonitrile complex formation took place fastest when the alkylating agent was benzyl bromide:

$$C_6H_5CH_2Br > C_6H_5CH_2OSO_2C_6H_4pCH_3 > C_6H_5CH_2Cl$$

Under corresponding conditions, benzyl chloride gave only very small conversions (1 per cent) to $(RCH_2NC)_5FeCNCl$. No isonitrile complexes were isolated in the reaction of benzyl iodide with $K_4Fe(CN)_6$, since under these conditions the rate of decomposition of benzyl iodide appears to be faster than the rate of isonitrile complex formation.

The alkylation of complex ferrocyanide with an alkylating agent may be summarized in the following equation:

$$K_4[Fe(CN)_6]^{4-} \underset{k_{-1}}{\overset{k_1}{\rightleftharpoons}} K_3[(LNC)Fe(CN)_5]^{3-} \underset{k_{-2}}{\overset{k_2}{\rightleftharpoons}} \cdots \underset{k_{-4}}{\overset{k_4}{\rightleftharpoons}}$$

$$(LNC)_4Fe(CN)_2 \underset{k_{-5}}{\overset{k_5}{\rightleftharpoons}} [(LNC)_5FeCN]Br \underset{k_{-6}}{\overset{k_6}{\rightleftharpoons}} [(LNC)_6Fe]Br_2$$

At the beginning of the reaction, the alkyl halide reacts with tetra-valent anion but in the last stage with a univalent cation. Furthermore, whereas at the beginning stages of the reaction the nucleophile is quite insoluble in the alkylhalide, toward the end of the reaction its solubility should be increased considerably. There is thus present a multiplicity of nucleophiles reacting with the alyklating agents.

[13] E. M. Kosower, *J. Amer. Chem. Soc.* **80**, 3233 (1958).
[14] S. Winstein, E. Grunwald and H. W. Jones, *J. Amer. Chem. Soc.* **73**, 2700 (1951).

TABLE 3.—THE SYNTHESIS OF IRON ISONITRILE COMPLEXES: INFLUENCES OF REACTANTS AND REACTION CONDITIONS

Alkylating agent (mole)	Metalferro cyanide (mole)	Solvent (Ml)	Reaction conditions Time (hrs)	Temp. (°C)	Conversion to products % Total isonitrile complex	$(RCH_2NC)_5Fe(CN)Br$
$C_6H_5CH_2Br$ (05)	$[(CH_3)_4N]_4Fe(CN)_6$[1] (0·046)	none	48	100	36	
$C_6H_5CH_2Br$ (0.26)	$Li_4Fe(CN)_6$ (0·04)	none	48	100		10
$C_6H_5CH_2Br$ (0·6)	$Na_4Fe(CN)_6$ (0·3)	none	48	100		26
$C_6H_5CH_2Br$ (5·5)	$K_4Fe(CN)_6$ (1·0)	none	48	100	78	47
$C_6H_5CH_2Br$ (0·05)	$Ca_2Fe(CN)_6$ (0·05)	none	48	100	none	
$C_6H_5CH_2Br$ (0·26)	$Ba_2Fe(CN)_6$ (0·04)	none	48	100	none	
$C_6H_5CH_2Br$ (0·5)	$Pb_2Fe(CN)_6$ (0·1)	none	48	100	none	
$C_6H_5CH_2Cl$ (1·0)	$K_4Fe(CN)_6$ (0·7)	none	4	reflux		about 1
$C_6H_5CH_2Br$ (2·0)	$K_4Fe(CN)_6$ (0·3)	none	12	100	43	

$C_6H_5CH_2I$ (0·20)	$K_4Fe(CN)_6$ (0·05)	none	12	100	none	
$C_6H_5CH_2OSO_2C_6H_4(pCH_3)$[2] (0·15)	$K_4Fe(CN)_6$ (0·03)	$CH_3COCH_2CH_3$ (200)	96	reflux		35
$C_6H_5CH_2Br$ (0·3)	$K_4Fe(CN)_6$ (0·047)	$CHCl_3$ (150)	48	reflux	none	
$C_6H_5CH_2Br$ (0·3)	$K_4Fe(CN)_6$ (0·047)	dioxane (150)	48	reflux	none	
$C_6H_5CH_2Br$ (2·0)	$K_4Fe(CN)_6$ (0·33)	CH_3CN (300)	66	reflux	43	
$C_6H_5CH_2Br$ (0·3)	$K_4Fe(CN)_6$ (0·047)	CH_3CH_2OH (150)	48	reflux	14	
$C_6H_5CH_2Br$ (0·3)	$K_4Fe(CN)_6$ (0 047)	CH_2OHCH_2OH (150)	48	100	23	
$C_6H_5CH_2Br$ (0·5)	$K_4Fe(CN)_6$ (0·09)	$(CH_3)_2NCHO$ (100)	48	100	46	
$C_6H_5CH_2Br$ (0·5)	$K_4Fe(CN)_6$ (0·1)	$(CH_3)_2SO$ (100)	48	100	6·5	
$C_6H_5CH_2Br$ (0·5)	$K_4Fe(CN)_6$ (0·09)	C_5H_5N (100)	48	80	none	
$C_6H_5CH_2Br$ (2·92)	$K_4Fe(CN)_6$ (0·33)	$CH_3COCH_2CH_3$ (500)	92	reflux	47	

(1) Prepared from $(CH_3)_4NOH$ and $H_4Fe(CN)_6$.
(2) Prepared according to the procedure of TIPSON, *J. Org. Chem.* **9**, 235 (1944).

A typical reaction-profile for an alkylation reaction is represented in Fig. 2, for the reaction of six moles of benzyl bromide with one mole of $K_4Fe(CN)_6$ at 100°C with no solvent employed. (Each reaction mixture was processed according to Procedure A (see Experimental Part) in order to determine the amount of I formed.) There is a distinct induction period of about 16 hr followed by a maximum conversion to I of 93 per cent, at 48 hr and a subsequent sharp decline of the conversion to I. The induction period is probably determined by the sum of the initial rate constants $(k_1/k_{-1} + k_2/k_{-2} + k_3/k_{-3})$. Following the induction period is the formation of $(RCH_2NC)_4Fe(CN)_2$ which in turn at 48 hr is completely converted to I. After this time, a decomposition of I to $(RCH_2NC)_6FeBr_2$ and unknown products (See Experimental) takes place. All of the substituted benzyl bromides investigated in any detail exhibited similar behavior. The induction periods for the following compounds were:

$$p\text{-}CH_3C_6H_4CH_2Br = 8 \text{ hr}; \; o\text{-}CH_3C_6H_4CH_2Br \cong 12 \text{ hr}$$

$$p\text{-}ClC_6H_4CH_2Br = 35 \text{ hr}; \; p\text{-}CH_3CO_6C_6H_4CH_2Br = 220 \text{ hr}$$

$$\text{and } p\text{-}NO_2C_6H_4CH_2Br = \gg 400 \text{ hr}$$

Isonitrile complexes, very probably the total of $(RCH_2NC)_4Fe(CN)_2$ and $(RCH_2NC)_5FeCNBr$, were formed in maximum conversions after the following times of reaction with the given halides:

$p\text{-}CH_3C_6H_4CH_2Br$ and $o\text{-}CH_3C_6H_4CH_2Br = 25$ hr, $p\text{-}ClC_6H_4CH_2Br = 63$–$80$ hr and $p\text{-}CH_3CO_2C_6H_4CH_2Br \gg 240$ hr

The approximate rate of reaction of one mole of $(C_6H_5CH_2NC)_4Fe(CN)_2$ and one mole of I with two moles of benzyl bromide at 100°C in a sealed tube was studied briefly. These rates are not strictly comparable with the rates in the original heterogeneous reaction since the mixing due to shaking of the heterogeneous solution in the tube is not comparable to the stirring in the heterogeneous system in a reaction vessel. The benzyl bromide consumed was determined by an infra-red spectroscopic method. Fifty per cent of $(RCH_2NC)_4Fe(CN)_2$ was converted to I (i.e. k_5/k_{-5}) in 8–10 hr and 50 per cent of I was converted into $(RCH_2NC)_6FeBr_2$ (i.e. k_6/k_{-6}) in 35–40 hr. This experiment indicated that there are differences in the reactivity of the different nucleophiles present toward $C_6H_5CH_2Br$. It would be expected that if the reaction is at all ionic $(RCH_2NC)_4Fe(CN)_2$, a neutral species, should react faster with $C_6H_5CH_2Br$ than $[(RCH_2NC)_5FeCN]^{\oplus}Br^{\ominus}$, a positive cation. The experiment also showed that diffusion in these reactions is of lesser importance than is the nucleophilicity of the anions.

When the $C_6H_5CH_2Br/K_4Fe(CN)_6$ ratio was decreased from five to four, the formation of $(C_6H_5CH_2NC)_4Fe(CN)_2$ was favoured, but a considerable amount of I was nevertheless isolated (see Experimental and Table 1).

The qualitative rate of reaction of RCH_2Br with $K_4Fe(CN)_6$ under comparable conditions decreases in the following sequence:

$$(C_6H_5)_3CBr > (C_6H_5)_2CHBr > p\text{-}CH_3C_6H_4CH_2Br \cong o\text{-}CH_3C_6H_4CH_2Br >$$
$$C_6H_5CH_2Br \cong CH_2{=}CH{-}CH_2Br > p\text{-}ClC_6H_4CH_2Br >$$
$$pCH_3CO_2C_6H_4CH_2Br > p\text{-}NO_2C_6H_4CH_2Br \cong (CH_3)_3CBr$$

In the case of triphenyl bromoethane the reaction proceeded even in chloroform as the solvent, whereas no reaction of benzyl bromide with $K_4Fe(CN)_6$ was observed in this solvent. Only trace-quantities of an isonitrile complex were isolated in the reaction of tert-butyl bromide with $K_4Fe(CN)_6$. The above sequence coincides with the sequence for carbonium ion stability, the most stable carbonium ion being the triphenylmethyl carbonium ion.[15] The resonance stabilization of the carbonium ion facilities both the S_{N_1} and S_{N_2} mechanism of the reaction but particularly strongly the S_{N_1} mechanism. If in this series the rate-determining step is the ionization of the alkyl halide (S_{N_1}) then the reaction of triphenyl bromomethane with $K_4Fe(CN)_6$ should certainly be determined by the rate of triphenyl bromomethane ionization.

Attempts to form ferricyanide complexes by the reaction of benzyl bromide and $K_3Fe(CN)_6$ failed. This difference between the $Fe(CN)_6^{3-}$ and $Fe(CN)_6^{4-}$ anion seems to be due to the greater basicity or nucleophilicity of the latter anion.[16] The solubility of both salts in benzyl bromide is very small. If there is a difference the less charged ferricyanide complex would be expected to show a greater solubility and mobility.[17] Triphenyl bromomethane, on the other hand, reacted with $K_3Fe^{III}(CN)_6$ to yield the expected ferricyanide complex $[(C_6H_5)_3CNC]_4Fe^{III}(CN)_2Br$, although at a slower rate than with $K_4Fe(CN)_6$. It must therefore be inferred that the nucleophilic power of the anion is of some importance even in the reaction of triphenyl bromomethane, provided that the rate of diffusion of both anions is comparable. Therefore, triphenyl bromomethane and most certainly alkylating agents forming carbonium ions of lesser stability will react with the ferrocyanide complex by the S_{N_2} mechanism in nonpolar solvents.

In a series of para-substituted benzyl bromides the "initiation" period (see above) and maximum conversion to isonitrile complexes is related to the σ value of the para-substitutent. This effect is due to (a) the ionization of the alkyl halide and (b) to differences in the nucleophilicity of the cyanides in the partially substituted ferrocyanide complex, i.e. $K_3[RNCFe(CN)_5]$ etc. This last hypothesis requires that the effect of the para-substituent be transmitted through a ten atom chain ($NC\check{F}eCNCH_2C_6H_4pX$) containing a methylene group, and therefore this effect is probably mainly inductive in origin.[18]

Acknowledgement—The author wishes to thank Dr. G. R. Coraor for many helpful discussions and suggestions.

[15] C. K. INGOLD, *Structure and Mechanism in Organic Chemistry*, p. 326, Cornell University Press, New York (1953).
[16] (a) I. M. KOLTHOFF and W. J. TOMSICEK, *J. Phys. Chem.* **39**, 955 (1935).
(b) B. V. NEKRASOV and G. V. ZOTOV, *J. Applied Chem.* (USSR) **14**, 264 (1941). *Chem. Abstr.* **36**, 18349 (1941).
(c) J. BRIGANDO, *Bull. Soc. Chim. France*, 503 (1957).
[17] S. PLESNIEWICZ, *Roczniki Chem.* **14**, 764 (1934); *Chem. Abstr.* **29**, 6126[7] (1935); *Roczniki Chem.*, **16**, 223 (1936); *Chem. Abstr.* **30**, 7423[7] (1936).
[18] J. CHATT, L. A. DUNCANSON and L. M. VENANZI, *J. Chem. Soc.* 4456, 4461 (1955); 3203 (1958).

VOL. 22 1961